NOVEL TECHNOLOGIES FOR MICROALGAE UTILIZATION TO ACHIEVE GLOBAL SUSTAINABLE DEVELOPMENT GOALS (SDGS)

EDITED BY: Norio Nagao, Tatsuki Toda, Fatimah MD. Yusoff, Raul Muñoz and Sandric Chee Yew Leong

PUBLISHED IN: Frontiers in Bioengineering and Biotechnology

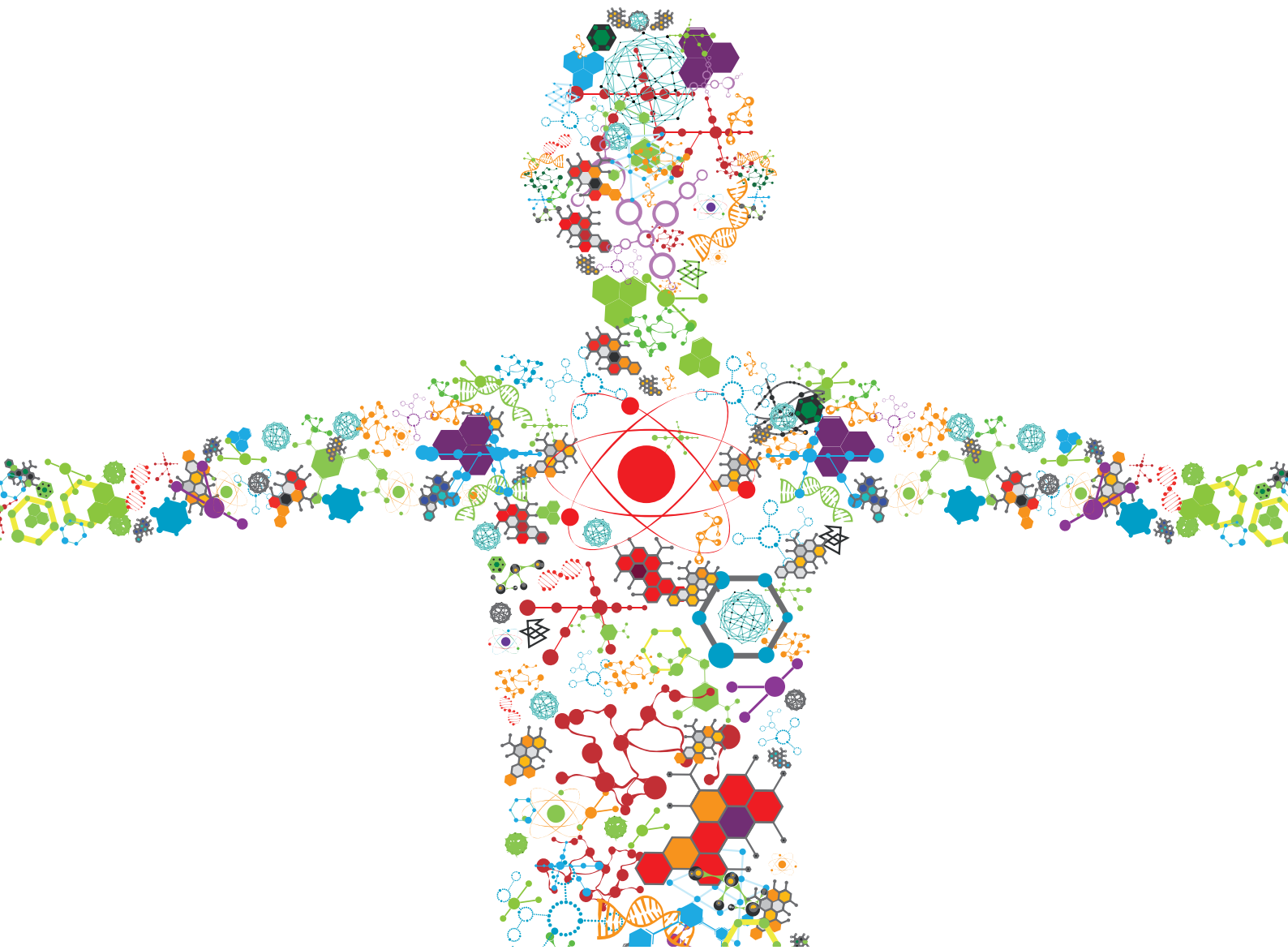

frontiers Research Topics

frontiers

ISSN 1664-8714
ISBN 978-2-88966-886-1
DOI 10.3389/978-2-88966-886-1

About Frontiers

Frontiers is more than just an open-access publisher of scholarly articles: it is a pioneering approach to the world of academia, radically improving the way scholarly research is managed. The grand vision of Frontiers is a world where all people have an equal opportunity to seek, share and generate knowledge. Frontiers provides immediate and permanent online open access to all its publications, but this alone is not enough to realize our grand goals.

Frontiers Journal Series

The Frontiers Journal Series is a multi-tier and interdisciplinary set of open-access, online journals, promising a paradigm shift from the current review, selection and dissemination processes in academic publishing. All Frontiers journals are driven by researchers for researchers; therefore, they constitute a service to the scholarly community. At the same time, the Frontiers Journal Series operates on a revolutionary invention, the tiered publishing system, initially addressing specific communities of scholars, and gradually climbing up to broader public understanding, thus serving the interests of the lay society, too.

Dedication to Quality

Each Frontiers article is a landmark of the highest quality, thanks to genuinely collaborative interactions between authors and review editors, who include some of the world's best academicians. Research must be certified by peers before entering a stream of knowledge that may eventually reach the public - and shape society; therefore, Frontiers only applies the most rigorous and unbiased reviews.
Frontiers revolutionizes research publishing by freely delivering the most outstanding research, evaluated with no bias from both the academic and social point of view. By applying the most advanced information technologies, Frontiers is catapulting scholarly publishing into a new generation.

What are Frontiers Research Topics?

Frontiers Research Topics are very popular trademarks of the Frontiers Journals Series: they are collections of at least ten articles, all centered on a particular subject. With their unique mix of varied contributions from Original Research to Review Articles, Frontiers Research Topics unify the most influential researchers, the latest key findings and historical advances in a hot research area! Find out more on how to host your own Frontiers Research Topic or contribute to one as an author by contacting the Frontiers Editorial Office: frontiersin.org/about/contact

NOVEL TECHNOLOGIES FOR MICROALGAE UTILIZATION TO ACHIEVE GLOBAL SUSTAINABLE DEVELOPMENT GOALS (SDGS)

Topic Editors:
Norio Nagao, Blue Scientific Shinkamitgoto Co., Ltd., Japan
Tatsuki Toda, Sōka University, Japan
Fatimah MD. Yusoff, Putra Malaysia University, Malaysia
Raul Muñoz, University of Valladolid, Spain
Sandric Chee Yew Leong, National University of Singapore, Singapore

Citation: Nagao, N., Toda, T., Yusoff, F. M., Muñoz, R., Leong, S. C. Y., eds. (2021). Novel Technologies for Microalgae Utilization to Achieve Global Sustainable Development Goals (SDGs). Lausanne: Frontiers Media SA.
doi: 10.3389/978-2-88966-886-1

Table of Contents

frontiers in Bioengineering and Biotechnology

ORIGINAL RESEARCH
published: 06 December 2019
doi: 10.3389/fbioe.2019.00396

Microalgal Protein Extraction From *Chlorella vulgaris FSP-E* Using Triphasic Partitioning Technique With Sonication

*Shir Reen Chia[1], Kit Wayne Chew[2], Hayyiratul Fatimah Mohd Zaid[3], Dinh-Toi Chu[4], Yang Tao[5] and Pau Loke Show[1]**

[1] Department of Chemical and Environmental Engineering, Faculty of Science and Engineering, University of Nottingham Malaysia, Semenyih, Malaysia, [2] Faculty of Science and Engineering, School of Mathematical Sciences, University of Nottingham Malaysia, Semenyih, Malaysia, [3] Fundamental and Applied Sciences Department, Centre of Innovative Nanostructures & Nanodevices (COINN), Institute of Autonomous System, Universiti Teknologi PETRONAS, Bandar Seri Iskandar, Malaysia, [4] Faculty of Biology, Hanoi National University of Education, Hanoi, Vietnam, [5] College of Food Science and Technology, Nanjing Agricultural University, Nanjing, China

OPEN ACCESS

Edited by:
Fatimah Md Yusoff, Putra Malaysia University, Malaysia

Reviewed by:
Ankush Karemore, Georgia Institute of Technology, United States
Helen Treichel, Universidade Federal da Fronteira Sul, Brazil

***Correspondence:**
Pau Loke Show
Pauloke.show@nottingham.edu.my; showpauloke@gmail.com

Specialty section:
This article was submitted to Bioprocess Engineering, a section of the journal Frontiers in Bioengineering and Biotechnology

Received: *26 August 2019*
Accepted: *21 November 2019*
Published: *06 December 2019*

Citation:
Chia SR, Chew KW, Zaid HFM, Chu D-T, Tao Y and Show PL (2019) Microalgal Protein Extraction From Chlorella vulgaris FSP-E Using Triphasic Partitioning Technique With Sonication. Front. Bioeng. Biotechnol. 7:396. doi: 10.3389/fbioe.2019.00396

Green microalgae containing various bioactive compounds and macronutrients such as lipids, carbohydrates, and proteins, have attracted much attention from the global community. Microalgae has the potential to be applied in food industries due to its high protein content, rapid growth rate, and ability to survive in harsh conditions. This study presents a simple yet efficient technique of sonication-assisted triphasic partitioning process, also known as ultrasonic-assisted three phase partitioning (UATPP), for the extraction of proteins from *Chlorella vulgaris* FSP-E. Comparison studies between three phase partitioning (TPP) and UATPP was conducted to investigate the feasibility of the enhanced technique on proteins extraction. Types of salt, ratio of slurry to t-butanol, salt saturation, sonication frequency, power, irradiation time, and duty cycle as well as biomass loading were studied. UATPP was found to be an improved technique compared to TPP. An optimum separation efficiency and yield of 74.59 ± 0.45 and 56.57 ± 3.70% was obtained, respectively, with the optimized conditions: salt saturation (50%), slurry to t-butanol ratio (1:2), sonication power (100%), irradiation time (10 min), frequency (35 kHz), duty cycle (80%) and biomass loading (0.75 wt%). A scaled-up study was performed to validate the reliability of UATPP for protein extraction. The outcome of the study revealed that UATPP is an attractive approach for downstream processing of microalgae.

Keywords: protein extraction, ultrasonic, triphasic partitioning technique, microalgae, bio-separation

INTRODUCTION

Nowadays, the growth of global human population is increasing at an incredible speed each year. An estimated 70% increase in food production will be needed for the growing human population (by around 2.3 billion) by the year 2050 (Tester and Langridge, 2010). The remarkable supply growth of food productions have reduced the proportion of global hunger, despite the world

population doubling over the last half-century (Bleakley and Hayes, 2017). Nevertheless, the world is facing a great challenge in sustaining adequate food production to meet the rising demands. Methods and techniques used conventionally to produce food will soon no longer be a solution due to the emission of greenhouse gases by these processes, nutrient run-off causing environmental pollutions, degradation of soil and disruption of ecosystem caused by over-harvesting of aquatic foods (Tester and Langridge, 2010). Specifically, protein is one of the macronutrients that will be in shortage at the near future. A substitution or alternative protein source and more efficient production techniques needs to be discovered and developed in order to meet the global demand.

Microalgae is well-known as a viable source of biological components such as carbohydrates, lipids, pigments, vitamins, and polyphenols, especially proteins (Hsieh and Wu, 2009; Chia et al., 2018). The protein quality in microalgae is known to be similar with some of the traditional protein sources like milk, meat, and egg (Bleakley and Hayes, 2017). In general, the protein content of microalgae constitutes a major portion compared to lipid and carbohydrate (Lavens and Sorgeloos, 1996). The total protein content from microalgae, especially *Chlorella* sp. is about 43–50% (Ramazanov and Ramazanov, 2006; Phukan et al., 2011). In the studies of Thompson et al. (1996) and Richmond (2017), the nutritive quality of *Chlorella sp.* was proved to be influenced by light environment during the microalgae cultivation stage (Thompson et al., 1996; Richmond, 2017). Higher protein production was obtained with the increment of light irradiance and longer photoperiod (Seyfabadi et al., 2011), since the efficiency of protein solubilization are influenced by the chemical composition, structural characteristics and the morphology of microalgae (Ursu et al., 2014). *Chlorella* protein are also proven to be safe for consumption through various clinical and animal studies, and positive health effects such as lower high blood pressure, glucose, and cholesterol levels are seen with the dietary of *Chlorella* protein (Waghmare et al., 2016).

Apart from that, there are several advantages of using microalgae as main source of proteins, for example, rapid growth rate, high productivity, can withstand harsh conditions, ability to be cultivated using exhaust industrial gases and indirectly reducing greenhouse gas emissions (Jeon et al., 2005; Chew et al., 2018a). The cultivation of microalgae does not require freshwater and it can be cultivated using non-arable land that does not affect the need for land to grow food crops. These advantages have attracted huge interests to further investigate the potential of microalgae in pharmaceutical, food, cosmeceutical, and bioenergy applications. Nevertheless, the production cost of biomolecules from microalgae in industrial-scale is relatively high and the commercialization of microalgae technology still remains a challenge to the current industry (Chia et al., 2018). Thus, the development of an efficient technique for scalable production is deemed vital in order to maximize the recovery of biomolecules as well as the industrial profitability.

Conventional separation techniques like membrane separation, column chromatography, precipitation and crystallization often consists of multiple unit operations and requires high consumption of toxic organic solvents. The multiple processing stages consequently contributes to more time consumption and product loss throughout the entire process, and this leads to lower concentrations of the end products. Currently, the industry is searching for alternative techniques to overcome the mentioned drawbacks using more greener and efficient techniques. Hence, three phase partitioning (TPP) was introduced as an efficient approach in extracting and purifying enzymes and biomolecules (Akardere et al., 2010; Gagaoua et al., 2014). TPP is easy to operate, efficient and scalable, where the salt is added to the aqueous solution containing the targeted product, followed by the addition of t-butanol to form three phases. The top phase of TPP is the t-butanol layer, middle phase is the protein precipitate layer and bottom phase is the aqueous layer where the solubility of t-butanol with water will change with the addition of salt. Since it is a three phase system, the targeted product may partition to either of the phases due to the operational conditions and physicochemical properties of targeted product (Avhad et al., 2014).

The partitioning behavior of targeted product depends on the mass transfer phenomenon, where the purification fold and partitioning of end-product can be improved through the increment of mass transfer (Niphadkar and Rathod, 2015). The utilization of ultrasound has been well applied in various processes such as extraction, absorption, bioremediation, and fermentation to improve the mass transfer of targeted products (Gogate and Kabadi, 2009; Sulaiman et al., 2011; Tay et al., 2016). The mass transfer of targeted products is intensified when the ultrasonic waves generate cavitational bubbles in the medium. The shock waves and mechanical shear will be imparted to the surrounding environment due to the collapsing of these bubbles (Avhad et al., 2014). The cavitational phenomenon caused by the difference in mechanical shear and local energy densities will speed up the mass transfer across the phases in the system. Therefore, the integrated approach for protein extraction was conducted to improve the purification and mass transfer of protein.

The aim of the present study was to achieve a maximum recovery of proteins from *Chlorella vulgaris* FSP-E through triphasic partitioning techniques, three phase partitioning (TPP) and ultrasound-assisted three phase partitioning (UATPP). The first attempt was performed using TPP and UATPP with similar operating conditions to extract and purify proteins from microalgae in a single unit operation. Several operating parameters like types of salt, salt saturation, slurry to t-butanol ratio, ultrasonic power, ultrasonic frequency and time, duty cycle and biomass loading were then studied and optimized.

MATERIALS AND METHODS

Chemicals and Reagents

T-butanol, ammonium sulfate ($(NH_4)_2SO_4$), sodium sulfate (Na_2SO_4), magnesium sulfate ($MgSO_4$), magnesium acetate ($Mg(CH_3COO)_2$), dipotassium hydrogen phosphate (K_2HPO_4), Bradford reagent, and tris-HCl buffer were purchased from R&M chemicals (Malaysia). Bovine serum albumin (BSA) standards were purchased from Merck (Malaysia). All chemicals used were of analytical grade.

Microalga

The microalga selected is the green microalgae, *C. vulgaris* (strain FSP-E). BG-11 medium was used for pre-culturing the selected microalgae for around 7 days and then the microalgae was cultivated in batch mode for 10–14 days by supplying 5% of CO_2 continuously. The BG-11 medium used was prepared with: 1.5 g/L of $NaNO_3$, 0.03 g/L of K_2HPO_4, 0.075 g/L of $MgSO_4.7H_2O$, 0.006 g/L of citric acid, 2 g/L of Na_2CO_3, 3.6 g/L of $CaCl_2.2H_2O$, 0.6 g/L of $H_8N_8CeO_{18}$, 0.1 g/L of EDTA, 2.86 g/L of H_3BO_3, 1.81 g/L of $MnCl_2.4H_2O$, 0.222 g/L of $ZnSO_4.7H_2O$, 0.39 g/L $Na_2MoO_4.2H_2O$, 0.079 g/L of $CuSO_4.5H_2O$, and 0.049 g/L of $Co(NO_3)_2.6H_2O$.

The microalgae were cultivated in batch mode using a 1 L indoor glass vessel photo-bioreactor (PBR) by inoculation from the pre-culture cultivated in a PBR (250 mL). Light source was provided continuously to illuminate the culture by mounting external LED lights on the both sides of the PBR. The initial culturing of microalgae and transfer of inoculum from the agar plate to the PBR were performed under a UV laminar flow chamber to prevent biological contamination. The biomass productivity, nitrate content, and pH values of the microalgae culture were monitored during the batch cultivation. The biomass was harvested when the growth of microalgae achieved a stationary phase. The harvested biomass was centrifuged at 6,000 rpm using a centrifuge (Eppendorf, 5430) for 5 min to remove liquid content. The remaining biomass paste was frozen at −20°C for 24 h before freeze-dried prior to the extraction experiments.

Determination of Protein Content

The proteins extracted were examined and quantified through modified Bradford method (Bradford, 1976). A total amount of sample containing proteins, 0.25 mL, was mixed with 2.5 mL of Bradford reagent and measured at the wavelength of 595 nm using a UV-Vis spectrophotometer. The readings obtained in absorbance unit were converted into protein concentration using the calibration curve performed while using BSA as standard. Calibration curve of proteins concentration was performed using standards in a range of 0–1 mgL^{-1}.

Determination of Separation Efficiency (*E*), Total Protein Content, and Yield (Y)

Separation efficiency of the extracted protein was calculated using Equation (1):

$$E = \frac{V_M C_M}{V_T C_T + V_M C_M + V_B C_B} \quad (1)$$

where V_T, V_M, and V_B are volume of top, middle and bottom phase, respectively; C_T, C_M, and C_B are concentration of top, middle and bottom phase, respectively.

The total protein content in microalgae biomass (P_T) was calculated using Equation (2) (Safi et al., 2013):

$$P_T = N_{ea} \times NTP \quad (2)$$

where N_{ea} is the total nitrogen (%) in *C. vulgaris* FSP-E and a value of 4.18% was obtained through elemental analysis; NTP is a constant value of nitrogen-to-protein conversion factor, which is 4.78 (Lourenço et al., 2004; Templeton and Laurens, 2015). Therefore, the final value of P_T used in this work is 19.98%. The elemental composition of microalga is carbon %: 49.32, hydrogen %: 8.24, nitrogen %: 4.18 and sulfur %: −0.15.

Yield of proteins (Y) from microalgae biomass was calculated using Equation (3):

$$Y = \frac{V_M C_M}{\frac{P_T}{100} \times W_i} \times 100\% \quad (3)$$

where W_i is the initial weight of biomass microalgae used in the study.

Three Phase Partitioning (TPP)

The study of TPP was conducted with a total working volume of 10 mL using the predetermined initial conditions. The system was prepared using 5 mL of 30% saturation $(NH_4)_2SO_4$, 5 mL of pure t-butanol and 0.5 wt% of freeze-dried microalgae biomass. Firstly, the microalgae biomass was dissolved in deionized water before mixing with salt solution. Five milliliters of t-butanol was then added to the mixture of microalgae biomass and salt solution in a small beaker. The mixture was stirred using a magnetic stirrer at 200 rpm for 1 h and was allowed to separate for 30 min at room temperature. Three phases were observed and separated carefully by pipetting them out from the beaker. The intermediate protein precipitate was dissolved in appropriate amount of tris-HCl buffer and analyzed for protein content. The separation efficiency and yield of proteins in all three phases were analyzed and compared with the ultrasound-assisted three phase partitioning process. All the experiments were repeated three times and the mean of the values were reported.

Ultrasound-Assisted Three Phase Partitioning (UATPP)

Ultrasound-assisted three phase partitioning of proteins was conducted using an ultrasonic water bath. The initial conditions of UATPP such as the working volume, saturation of salt solution, and weight of biomass were similar with TPP for the comparison study. The preparation and mixing procedure of UATPP was similar with TPP, but a glass vial was used for ultrasonic treatment. The initial volume ratio used is 1:1. The glass vial containing the mixture was placed into the ultrasonic water bath, operating with 35 kHz and 100% sonication power for 5 min. The glass vial was then taken out and allowed to separate for 30 min at room temperature. The intermediate protein precipitate was dissolved with tris-HCl and proteins in all three phases were analyzed through the modified Bradford method. All the experiments were done in triplicate and the mean values were reported.

Optimization of Operating Parameters

The optimization of UATPP was applied for proteins extraction, where the system composed of t-butanol and salt solution with sonication effect. Operating parameters of UATPP which includes the type and saturation of salt, ratio of slurry to t-butanol, sonication power, frequency, irradiation time, duty cycle, and biomass loading, were studied in the optimization step.

Initial conditions and subsequent variables for each parameter were shown in **Table 1**. Types of salt was set as the first parameter to determine the interaction of different salts with t-butanol in order to precipitate out the protein from the biomass. Optimum salt saturation was investigated to reduce the usage of salt in the whole system, where the highest salt saturation studied was up to 60%. The third parameter, slurry to t-butanol ratio was studied before the optimization of sonication properties. The relationship between the volume of slurry and t-butanol used in experiment was studied as it is critical in optimizing the TPP process (Sharma et al., 2000). The sonication parameters were optimized to use energy more efficiently and save operating cost where possible while achieving optimum proteins extraction. The last parameter, biomass loading was examined due to possible change in equilibrium of three phases in the system. The effects of operating parameters were studied using one-factor-at-a-time (OFAT) approach.

Field Emission Scanning Electron Microscope FESEM

Field Emission Scanning Electron Microscope (FESEM, Quanta 400F) (FEI, USA) analysis was used to analyze the morphological structure of microalgae biomass before and after extraction (with and without UATPP).

Statistical Analysis

The data was subjected to one-way ANOVA (with significance $p \leq 0.05$) data analysis and the mean differences were compared using Tukey HSD *post-hoc* test. All studies were conducted in triplicate and the values were expressed as mean ± standard error. The statistical analysis was performed using IBM SPSS statistics software (SPSS version 26.0 for window; IBM Corporation; United States).

RESULTS AND DISCUSSION

Comparison Study

The study of TPP and UATPP showed that the addition of sonication resulted in better extraction of proteins from microalgae. The results obtained using both methods were tabulated in **Table 2**.

In both cases, the proteins favorably partitioned to the intermediate phase and less proteins partitioned to the top and bottom phase. These precipitated proteins formed in between the top and bottom phases created the three-phase formation (Chew et al., 2018b). Better results were obtained using UATPP compared to TPP due to the mechanism of ultrasonication which has helped to break the cell wall of microalgae. The cavitation bubbles induced by ultrasonic waves disrupts the microalgae cell wall, leading to the release of proteins from microalgae cells. In addition, TPP requires 1 h to partition proteins from microalgae biomass while UATPP only needs 10 min to achieve higher yield of proteins. This significant finding showed that higher yield and better separation efficiency of proteins could be achieved within shorter processing time by UATPP as supported by Pakhale and Bhagwat (2016). The findings are in agreement with Zhang et al.'s work, where the recovery of targeted product increased using UATPP compared to conventional TPP (Zhang et al., 2017). The reduced processing time subsequently leads to lower operating cost via UATPP.

Optimization of UATPP Process Parameters

Types of Salt

The first parameter that was optimized in this study is the compatibility of t-butanol with various types of salt for protein extraction. Salts type plays an important role in UATPP as the partitioning behavior of proteins is influenced through the interaction of salts and t-butanol depending on the ionic strength

TABLE 2 | Comparison study between TPP and UATPP.

Methods	Yield (Y, %)	Separation efficiency (E, %)
TPP	25.15 ± 1.04	49.78 ± 0.44
UATPP	40.01 ± 4.51	52.26 ± 2.47

TABLE 1 | Operating parameters for UATPP.

No.	Operating parameter	Initial setting	Variables	Unit	Justification
1.	Types of salt	$(NH_4)_2SO_4$	Na_2SO_4, $MgSO_4$, $Mg(CH_3COO)_2$, K_2HPO_4	N/A	First parameter to optimize the salt saturation
2.	Salt saturation	30	20, 40, 50, 60	%	–
3.	Slurry to t-butanol ratio	1:1	1:0.5, 1:1.5, 1:2, 1:2.5	N/A	The ratio of slurry is set as 1 (slurry : t-butanol)
4.	Sonication power	100	20, 40, 60, 80	%	–
5.	Sonication frequency and irradiation time	35 kHz and 10 min	Set A (35 kHz): 2.5, 5, 7.5, 12.5 min Set B (130 kHz): 2.5, 5, 7.5, 10, 12.5 min	kHz, min	–
6.	Duty cycle	100	20, 40, 60, 80	%	100% is continuous sonication
7.	Biomass loading	0.5	0.25, 0.75, 1.00, 1.25	wt%	–

of solution. All the systems showed a slight difference (around 9%) in separation efficiency, ranging from 45.48 ± 1.90 to 54.48 ± 2.58%, excluding the system consisting of $Mg(CH_3COO)_2$ from **Figure 1**. The protein yield for Na_2SO_4, $MgSO_4$, and K_2HPO_4 was comparable, falling in the range of 31.94 ± 0.24 to 32.63 ± 4.04%, while $(NH_4)_2SO_4$ obtained the highest yield of proteins. Based on the statistical analysis, the yield of protein was significantly affected by the types of salt ($p < 0.05$).

The combination of selected salts with t-butanol have formed a distinct three phase except for $Mg(CH_3COO)_2$, where only two phases were observed with a blur separation interface. This phenomenon may be due to the salting-in effect by $Mg(CH_3COO)_2$ at a particular molality. However, the salting-out effect of $Mg(CH_3COO)_2$ with IL was stronger than K_2HPO_4 as stated by Neves et al. (2015), proving that every combination of salt and solvent have to be investigated for their suitability to extract specific products (Neves et al., 2015). $(NH_4)_2SO_4$ obtained the highest yield of proteins as it has higher hydration capacity and affinity of water compared to other types of salt. The hydration energy of sulfate ions has increased its effective radius by involving large proportions of water molecules and promoting the stability of proteins through hydrophobic interactions. Large ions gather together and isolate the proteins through precipitating the proteins out of the water phase. Besides that, the sulfate ions are positioned in the front part of the Hofmeister series. They interact well with water molecules as they act as dehydrating agent, forming H-bonds as well as dehydrate proteins (Pakhale and Bhagwat, 2016). T-butanol with the presence of high $(NH_4)_2SO_4$ concentration acts in more lipophilic manner, increasing the hydrophobicity and exclusion from water due to the higher effective dielectric constant of water (Waghmare et al., 2016). Various studies have utilized $(NH_4)_2SO_4$ in both TPP and UATPP for its salting out ability, and have successfully extracted the desired products (Pakhale and Bhagwat, 2016; Gagaoua et al., 2017). Therefore, the system of $(NH_4)_2SO_4$ and t-butanol was chosen for further studies.

Effect of $(NH_4)_2SO_4$ Saturation

Saturation of $(NH_4)_2SO_4$ is a significant parameter on UATPP due to the salting-out phenomenon. The effect of $(NH_4)_2SO_4$ saturation was investigated from 20 to 60% (w/v). **Figure 2** showed that increasing $(NH_4)_2SO_4$ saturation enhanced the separation efficiency and yield of proteins due to the salting out effect. The protein yield showed an increasing trend along with the increased saturation of salt up to 50% saturation, where it starts to decrease, this is in agreement with results reported by previous research (Niphadkar and Rathod, 2015). The yield of proteins decreased at higher saturation of $(NH_4)_2SO_4$ (>50%) due to the irreversible denaturation of proteins with too much salt concentration. The maximum separation efficiency was obtained using 60% saturation of $(NH_4)_2SO_4$ while maximum yield was obtained using 50% saturation of salt. The protein was more likely to be partitioned at higher $(NH_4)_2SO_4$ saturation which leads to higher separation efficiency due to the stronger salting-out effect. Higher saturation of $(NH_4)_2SO_4$ will cause water from the solvation layer around proteins to be dissipated more easily. This will lead to the exposure of hydrophobic patches of protein surfaces, causing the interaction with hydrophobic patches of other protein surfaces to occur. As a result, aggregation and precipitation of proteins would be observed in the intermediate phase (Niphadkar and Rathod, 2015). The results obtained by Niphadkar and Rathod (2015) was slightly lower than the result from this experiment, which is 40% $(NH_4)_2SO_4$. The experiment was conducted under 1:0.5 of crude extract to t-butanol ratio, pH 6, 60% duty cycle with 25 kHz frequency and 3 min irradiation time (Niphadkar and Rathod, 2015). However, it was found that the result obtained was in agreement with the study of Zhang et al. (2017), 50% of $(NH_4)_2SO_4$ was the optimized $(NH_4)_2SO_4$ concentration to recover phycocyanin from *Spirulina* (Zhang et al., 2017). The conditions performed for the phycocyanin extraction was 1:1 crude extract to t-butanol ratio, pH7 at 25 kHz frequency with 50% duty cycle. The statistical analysis showed that the yield of protein was significantly affected ($p < 0.05$) by the salt saturation parameter. Lower protein yield was observed in lower $(NH_4)_2SO_4$ saturation (20%) as it is insufficient to modify the hydrophobic patches surfaces of proteins. Similar results have been observed in the work of Avhad et al. (2014) where lower recovery and purification fold was found at lower $(NH_4)_2SO_4$ saturation (20% w/v) (Avhad et al., 2014). The highest yield was obtained using 50% saturation of $(NH_4)_2SO_4$, therefore it was selected for the next study.

Effect of Slurry to T-butanol Ratio

The alcohol used for UATPP was set as t-butanol as it is commonly used in past studies (Yadav et al., 2017; Patil and Yadav, 2018). Dhananjay and Mulimani (2009) have stated that at room temperature, t-butanol tends to be kosmotropic, contributing to enzyme-t-butanol co-precipitates that floats above the bottom phase (Dhananjay and Mulimani, 2009). Another unique characteristic of t-butanol is that it could not permeate into folded proteins due to its structure and size, which can avoid protein denaturation (Dennison, 2000). The effect of slurry to t-butanol ratio on UATPP of protein was examined by altering the working volume of t-butanol while the slurry remained constant throughout the experiment. The ratio of slurry to t-butanol such as 1:0.5, 1:1, 1:1.5, 1:2, and 1:2.5, was studied with the optimized $(NH_4)_2SO_4$ saturation. The working volume of t-butanol was chosen to be adjusted rather than $(NH_4)_2SO_4$ because previous studies stated that the inherent properties of t-butanol have offered great advantages in partitioned enzyme (Avhad et al., 2014), as it aids in enhancing the protein yield through UATPP.

It was observed that the separation efficiency and yield of proteins were rising with increasing slurry to t-butanol ratio from **Figure 3**. However, both separation efficiency and yield has decreased at the highest ratio (1:2.5). The denaturation of protein was more likely to occur if the volume of t-butanol is high (>1:2), where this was also observed in extraction of enzymes (Narayan et al., 2008). The increment of surface tension caused by high concentration of t-butanol also leads to lower yield and separation efficiency. This is due to the high surface tension that has decreased cavitation (Santos et al., 2008). Kulkarni and Rathod (2014) have reported similar trends where the yield of

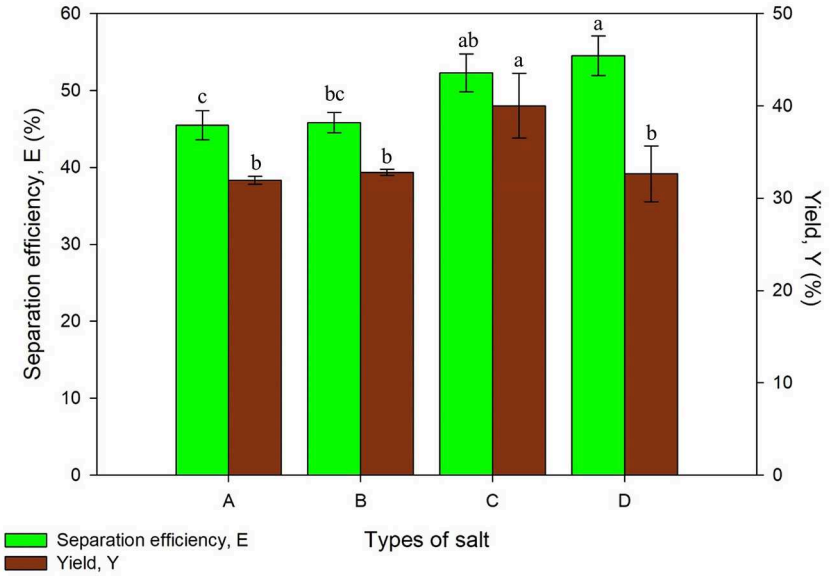

FIGURE 1 | Effect of types of salt on separation efficiency (E) and yield of protein (Y) where A is Na_2SO_4, B is $MgSO_4$, C is $(NH_4)_2SO_4$, and D is K_2HPO_4. Means with the same letter are not significantly different (One-way ANOVA followed with Tukey's test).

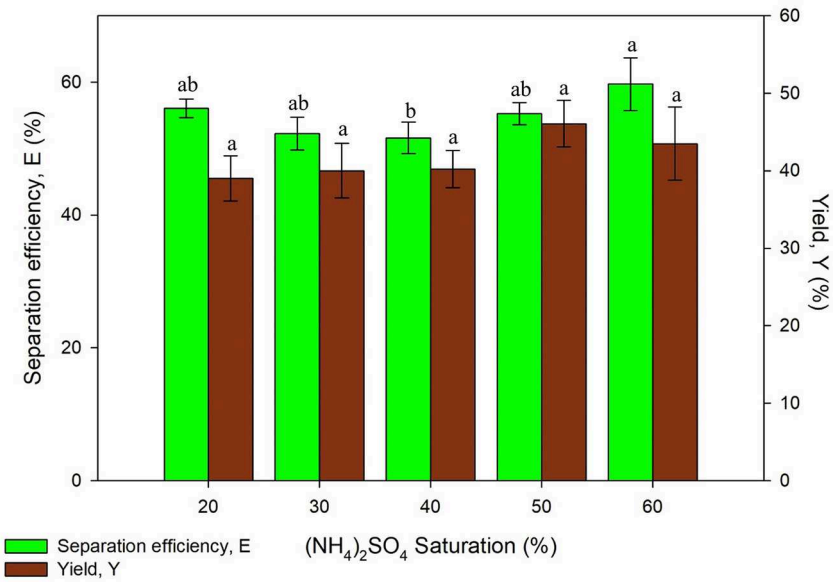

FIGURE 2 | Effect of $(NH_4)_2SO_4$ saturation on separation efficiency (E) and yield of protein (Y). Means with the same letter are not significantly different (One-way ANOVA followed with Tukey's test).

mangiferin decreased with the increasing ratio of slurry to t-butanol (Kulkarni and Rathod, 2014). The separation efficiency of protein using all systems was more than 50% except from the ratio of 1:0.5, in which the synergistic effect of $(NH_4)_2SO_4$ to recover proteins could not be achieved since the volume of t-butanol is much less. On the other hand, the yield obtained was varied through different ratios. The protein yield obtained falls in the range of 35.28 ± 1.16–49.50 ± 0.89%, with the highest yield obtained being 1:2 of slurry to t-butanol ratio. Chew et al. (2019) have reported a 1:1 ratio of slurry to t-butanol as the optimum ratio for protein extraction from *Chlorella* sp. which was not in agreement with the obtained result due to different TPP conditions, for example, the optimized salt concentration was 30% in the work by Chew et al. (2019). Thus, the appropriate ratio of slurry to t-butanol should be determined for specific optimized extraction. The ratio of slurry to t-butanol significantly

affected the protein yield ($p < 0.05$). The optimum value of separation efficiency and yield were obtained using the ratio of 1:2 and this was selected for next study.

Effect of Ultrasonic Power

The ultrasonic power was studied as part of the optimization of sonication in the system. This study was conducted with the optimum values from previous experiments and initial settings of other parameters by varying the power of the ultrasonic bath. The ultrasonic power is an important factor that affects the cost of the process when operated at industrial scale (Niphadkar and Rathod, 2015; Zhang et al., 2017). On top of that, the ultrasonic power has to be optimized to avoid denaturation of proteins. Generation of large amplitude ultrasonic waves may produce more cavitation bubbles through higher ultrasonic power. The higher cavitation effect may result in denaturation of proteins although higher mass transfer can be achieved.

As illustrated in **Figure 4**, the results obtained has shown an increasing trend in the separation efficiency and yield of proteins along with higher ultrasonic power. This is because the collapsing of cavitation bubbles has imparted vicious mechanical shear to the system. The mechanical shear induced resulted in the better disruption of microalgae cell wall and subsequently enhanced the mass transfer and protein yield (Zhang et al., 2017). The statistical analysis also showed that the recovery of protein was significantly affected ($p < 0.05$) by the ultrasonic power. The difference of separation efficiency obtained using 20–100% of ultrasonic power did not vary beyond 4%, which was a considerably small difference in values. The separation efficiency obtained indicates that the partitioning behavior of proteins was not influenced much by the ultrasonic power. However, the yield of proteins considerably increased around 10% using 100% of ultrasonic power compared to the lowest yield obtained, which is more favorable in the process. Thus, 100% of ultrasonic power was chosen for further studies due to the highest yield obtained.

Effect of Ultrasonic Frequency and Irradiation Time

The study on ultrasonic frequency and time was categorized into two sets, Set A and Set B as listed in **Table 1**. Set A consists of irradiation time ranging from 2.5 to 12.5 min with the constant frequency of 35 kHz while Set B consisted of same time range with the frequency of 35 and 130 kHz, both the results obtained are illustrated in **Figures 5**, **6**, respectively. Ultrasonic frequency and duration of ultrasonic irradiation was altered as the former regulates power dissipated to the system and the dose of ultrasound was quantified by the latter. The results for yield obtained in 35 kHz shown an increasing trend from 5 to 10 min of irradiation and reduced significantly at 12.5 min.

As for 130 kHz, the yield was in an increasing trend as irradiation time increased and later decreased after 10 min of irradiation time. The reduction of yield at longer irradiation time may be resulted from the excessive ultrasonic irradiation time that altered the protein conformation and led to the degradation of proteins. Furthermore, the increment of temperature from the long irradiation time would contribute to the degradation and activity loss of proteins. The findings were in agreement with previous studies where UATPP of fibrinolytic enzyme and polyphenol oxide were performed (Avhad et al., 2014; Niphadkar and Rathod, 2015). It was observed that the shorter the irradiation period, lower yield was obtained. This is possibly due to insufficient ultrasonic irradiation to disrupt the rigid microalgae cell wall. If the ultrasonic irradiation is not sufficient, the agitation could not lead to the formation of large turbulence in the solvent phase, thus the mass transfer could not be enhanced (Niphadkar and Rathod, 2015). In all sets of experiment, the highest yield was obtained at 10 min of irradiation time for lower frequency, 35 kHz. Higher frequency of ultrasonic has decreased the cavitation yield due to formation of smaller and less energetic cavitation bubbles compared to low frequency, leading to lower yield of products (Kirpalani and McQuinn, 2006). As compared to the study performed by Zhang et al. (2017), the higher frequency (40 kHz) obtained lower purity and recovery of phycocyanin compared to the lower frequency (25 kHz) (Zhang et al., 2017), supporting as well the statement of Kirpalani and McQuinn (2006). The frequency of sonication and irradiation time significantly affected the protein recovery through the statistical analysis ($p < 0.05$). There have been reports that concluded low frequency was favorable for biomolecules extraction (Capote and de Castro, 2007; Kulkarni and Rathod, 2014). Therefore, 10 min of irradiation time with 35 kHz of ultrasonic frequency was selected for the next study.

Effect of Duty Cycle

Duty cycle was varied by switching the ON and OFF time of ultrasonic process at 35 kHz. Higher percentage of duty cycle has higher fraction of ultrasonic irradiation in one period. It was found that the separation efficiency and yield has increased up to 80% of duty cycle (48 s ON and 12 s OFF) and thereafter it decreases as shown in **Figure 7**. This is probably a result of the excessive ultrasonic dose of UATPP. The degradation of protein structure could occur at higher duty cycle as the temperature rose along with the mechanical shear caused by the implosion of cavitation bubbles. The results obtained were in agreement with previous studies, where the phycocyanin recovery decreased after 90% of duty cycle (Zhang et al., 2017). However, the purification of serratiopeptidase from *Serratia marcescens* NRRL B 23112 using UATPP only required 40% duty cycle for 5 min to obtain highest purity and recovery (Pakhale and Bhagwat, 2016). The decrement was caused by excessive sonication dose toward the system. Based on the statistical analysis, the duty cycle of sonication significantly affected the protein yield ($p < 0.05$). Sonication can be operated in continuous mode or pulse mode. The pulse mode of sonication to intensify bioprocesses shows great potential due to various advantages. It is preferable as the energy utilized in pulse mode is lower than in continuous mode and more energy efficient as unnecessary heat and energy loss can be avoided. It is stated that the pulse mode of sonication was able to intensify the recovery as well as reduce the occurrence of heat sensitive compounds degradation (Kulkarni and Rathod, 2014). On top of that, the lifespan of transducers can be prolonged in pulse mode compared to continuous mode (Dey and Rathod, 2013). Thus, the duty cycle of 80% was chosen as the optimized condition in this study.

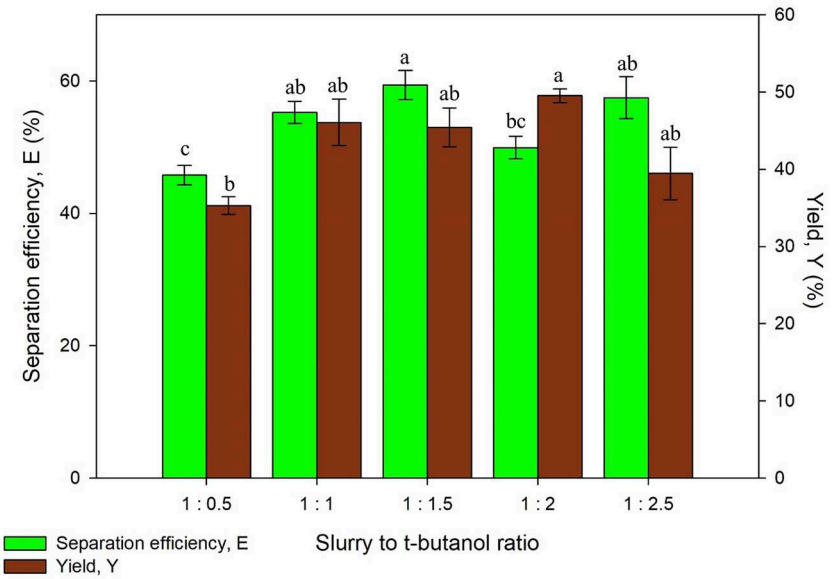

FIGURE 3 | Effect of slurry to t-butanol ratio on separation efficiency (E) and yield of protein (Y). Means with the same letter are not significantly different (One-way ANOVA followed with Tukey's test).

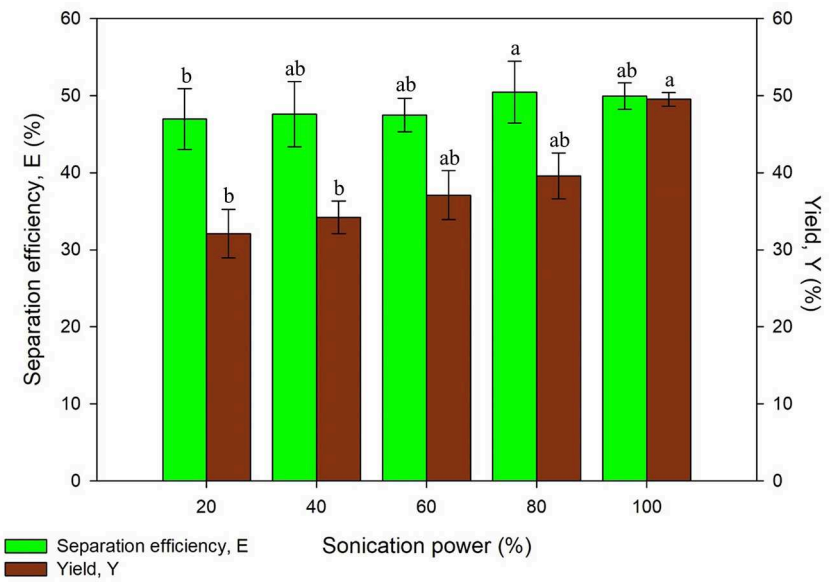

FIGURE 4 | Effect of sonication power on separation efficiency (E) and yield of protein (Y). Means with the same letter are not significantly different (One-way ANOVA followed with Tukey's test).

Effect of Biomass Loading

Apart from the optimization on sonication, the biomass loading was altered to study its effect on protein extraction via UATPP. The biomass loading in a range of 0.25–1.25 wt% were examined. It is known that the yield of proteins could be increased by increasing the biomass loading. The studies related to aqueous two phase system have proven that protein separation is saturated once the biomass loading has achieved the critical quantity (Selvakumar et al., 2010). However, there is no research reporting the effect of biomass loading on UATPP whereby the equilibrium between the three phases could possibly be affected by the weight of biomass loaded into the system.

From **Figure 8**, an increasing trend was observed from 0.25 to 0.75 wt% of biomass loading and the protein yield was decreased after 0.75 wt% of biomass. The highest yield was discovered at 0.75 wt% of biomass with moderate separation efficiency. It is

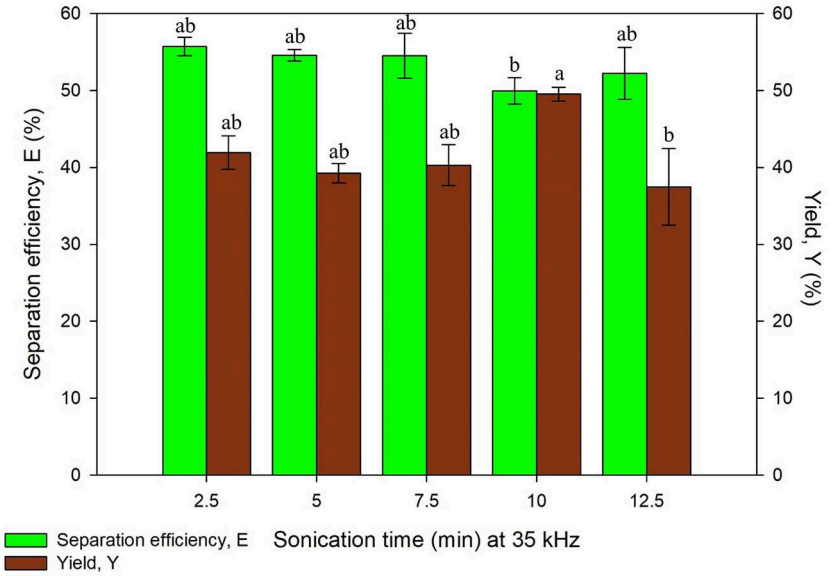

FIGURE 5 | Effect of sonication time at frequency, 35 kHz on separation efficiency (E) and yield of protein (Y). Means with the same letter are not significantly different (One-way ANOVA followed with Tukey's test). Analysis tests were performed with data in **Figure 6** (130 kHz frequency).

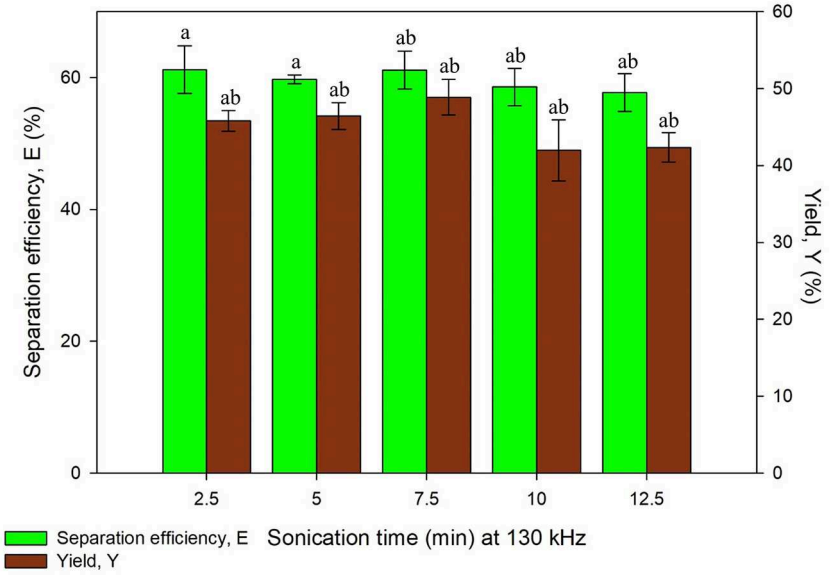

FIGURE 6 | Effect of sonication time at frequency, 130 kHz on separation efficiency (E) and yield of protein (Y). Means with the same letter are not significantly different (One-way ANOVA followed with Tukey's test). Analysis tests were performed with data in **Figure 5** (35 kHz frequency).

the optimum biomass loading because the sonication irradiation was fully utilized to disrupt the microalgae cells, and subsequently improved the protein recovery. Besides, it was observed that the lower protein yield has been obtained by lower biomass loading. This is due to the initial quantity of proteins that already exists in the biomass loading is low, such that the microalgae cell wall were fully disrupted by sonication, and the total amount of proteins present remain the same. It was observed that the proteins recovered at higher biomass loading (>0.75 wt%) was also decreased. The obtained results were found to be in agreement with work of Chew et al. (2019) where the recovery of protein decreased at higher microalgae percentage, 0.75 wt% (Chew et al., 2019). The biomass loaded to the system has influenced the separation efficiency and yield of protein such that higher loading of biomass into the system leads to uneven distribution of ultrasonic irradiation and may cause the incomplete breakage

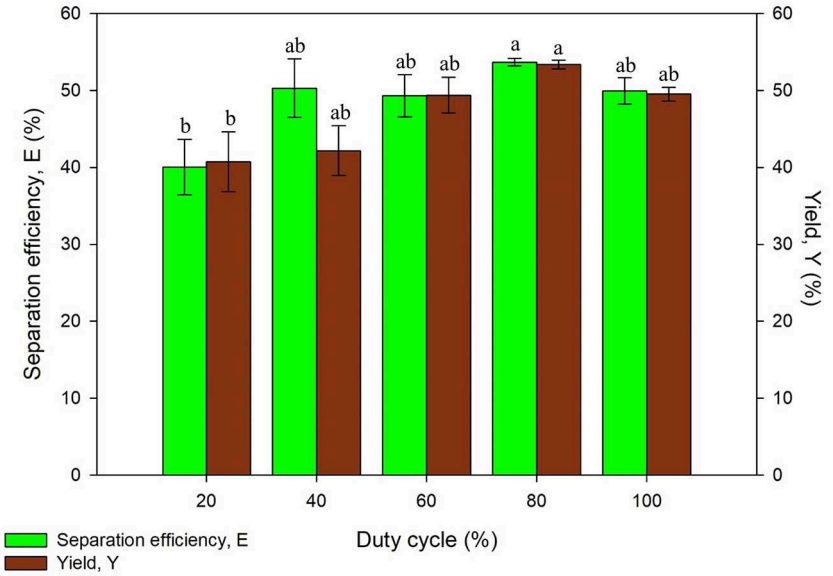

FIGURE 7 | Effect of duty cycle on separation efficiency (E) and yield of protein (Y). Means with the same letter are not significantly different (One-way ANOVA followed with Tukey's test).

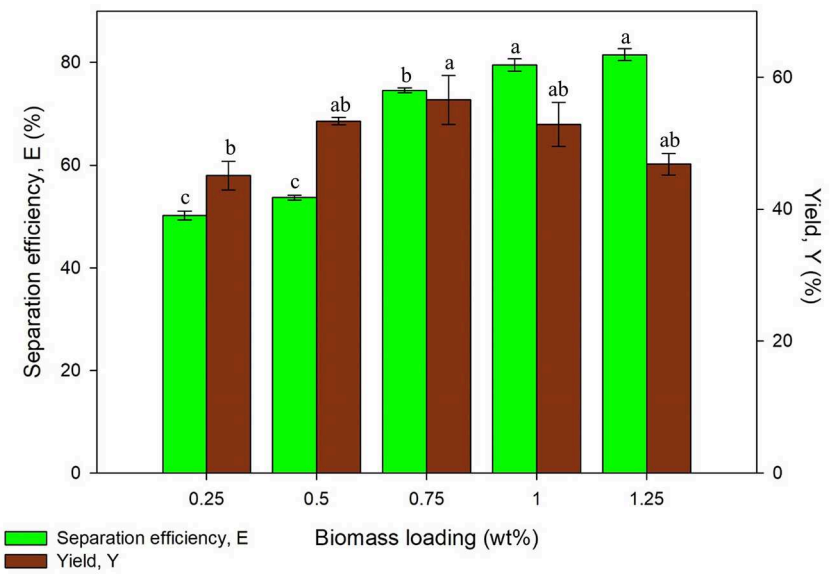

FIGURE 8 | Effect of biomass loading on separation efficiency (E) and yield of protein (Y). Means with the same letter are not significantly different (One-way ANOVA followed with Tukey's test).

of cell wall for protein extraction. Therefore, a biomass loading of 0.75 wt% was taken for further studies with the consideration of separation efficiency and yield obtained. The statistical analysis showed that biomass loading significantly affected ($p < 0.05$) the yield of proteins in the system.

Scale Up

The integrated system of sonication and TPP on protein extraction in a larger scale was examined and explored for its feasibility, reliability, as well as the possibility of this technique to be scaled-up. The system was conducted with all the optimized parameters such as 50% of $(NH_4)_2SO_4$ saturation, 1:2 of slurry to t-butanol ratio, 100% of power, 35 kHz of ultrasonic frequency, 10 min of irradiation time, 80% of duty cycle and 0.75 wt% of biomass loading. The large-scale study was performed with the total working volume of 10 times higher than the lab scale study. A total working volume of 150 mL with 50 mL of slurry and 100 mL of t-butanol were used. The yield obtained in larger

TABLE 3 | Comparative evaluation of other studies using TPP and ultrasound-assisted TPP.

Studies	Target compound	Findings	References
Extraction of protein from *Chlorella* sp. in lab-scale	Protein	A total yield of 56.57% ± 3.70 and 74.59% ± 0.45 separation efficiency were obtained	This study
Extraction of protein from *Chlorella* sp. in large-scale	Protein	A total yield of 57.03% ± 1.32 and 70.88% ± 1.02 separation efficiency were obtained	This study
Recovery of astaxanthin from *Paracoccus* NBRC 101723 using ultrasound-assisted three phase partitioning (UA-TPP)	Astaxanthin	Recovery of 428 μg/g of wet biomass was achieved using 40% $(NH_4)_2SO_4$, 1:0.75 biomass to t-butanol ratio assisted with sonication as pretreatment using 100% amplitude for 20 s	Chougle et al., 2014
Ultrasound-assisted three-phase partitioning of polyphenol oxidase from potato peel (*Solanum tuberosum*)	Polyphenol oxidase	70% recovery of polyphenol oxidase and 6.3 purification factor were obtained using 40% $(NH_4)_2SO_4$, 1:1 extract to t-butanol ratio, pH 7, 40% duty cycle with 25 kHz frequency	Niphadkar and Rathod, 2015
Concentration and characterization of microalgae proteins from *Chlorella pyrenoidosa* (three phase partitioning)	Protein	78.1% w/w protein concentration was obtained using 40% $(NH_4)_2SO_4$, pH 6, 1:1.5 of slurry to t-butanol ratio with enzymatic treatment (combination of Stargen and Carezyme)	Waghmare et al., 2016
Ultrasound-assisted three phase partitioning of phycocyanin from *Spirulina platensis*	Phycocyanin	94.3% recovery of phycocyanin with 6.69 purification factor were obtained using 50% $(NH_4)_2SO_4$, 1:1 crude extract to t-butanol ratio, pH 7, 50% duty cycle with 25 kHz frequency	Zhang et al., 2017

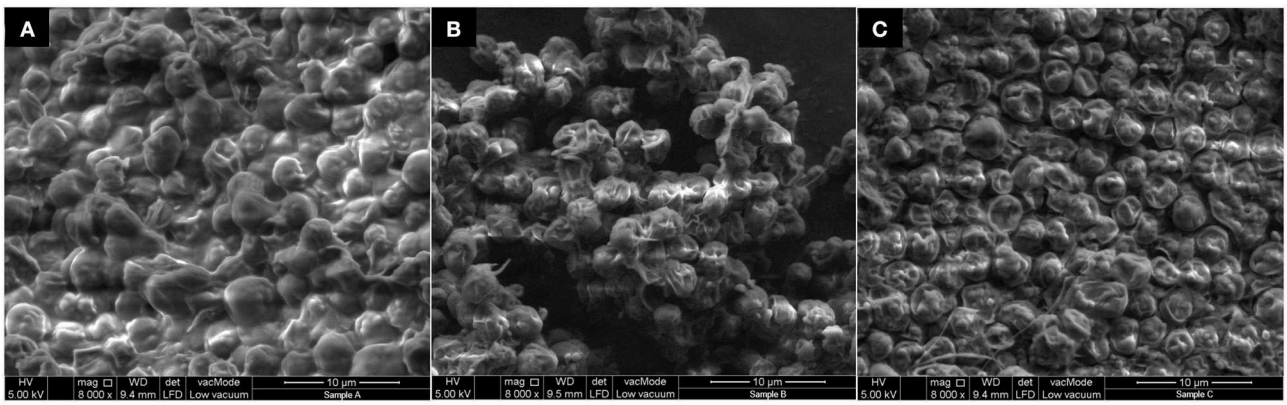

FIGURE 9 | FESEM images of microalgae cells **(A)** before sonication treatment; **(B)** after ultrasound with water as medium; **(C)** after ultrasound with UATPP medium.

scale system (56.57 ± 3.70%) was comparable with the yield obtained with the lab scale system (57.03 ± 1.32%). Relatively high separation efficiency of protein was obtained in large scale as well. Based on the results shown in **Table 3**, the reliability of this technique in scale-up has been verified and could be further up-scaled toward an industrial scale.

A comparative study was performed using the results obtained in current study and literature from previous studies. There are three studies that found that 40% $(NH_4)_2SO_4$ was the suitable salt saturation % for recovering their targeted compounds (Chougle et al., 2014; Niphadkar and Rathod, 2015; Waghmare et al., 2016), which was not in agreement with our findings. It was found that most of the condition utilized in the mentioned studies was not similar with the current study and the recovery of compounds obtained was generally higher. The recovery of protein in Waghmare et al. (2016) was performed with enzymatic treatment which requires higher slurry to t-butanol ratio compared to this study in order to achieve optimum results. The results obtained in the study of Zhang et al. (2017) was similar with results obtained in current study, which requires 50% $(NH_4)_2SO_4$ and low irradiation frequency (25 kHz) to recover phycocyanin from microalgae, a different type of protein.

Field Emission Scanning Electron Microscopy (FESEM) Characteristics of Microalgae Surfaces

Figure 9 shows the FESEM images of the surface of microalgae before sonication treatment, after sonication treatment (with water as medium) and after UATPP treatment (with solvents of UATPP). In **Figure 9A**, the surfaces of microalgae before

any sonication treatment were observed to be smooth and round-shape cells that are clumped on the surface. After treatment with sonication, the microalgae cells shrunk and became rougher compared to the microalgae cells without ultrasonic treatment (**Figure 9B**). However, the structure of microalgae was more severely altered, and became flat and more shrunken after the treatment with UATPP (**Figure 9C**). This indicates that UATPP can deal more disruptive damage to the microalgae cell wall compared to treatment with sonication only, where the use of TPP solvents can further help to recover higher portions of the compounds in microalgae. The obtained results have proven that UATPP is very effective in disrupting the microalgae cells and leads to the enhancement of protein extraction.

CONCLUSIONS

In this work, proteins from *C. vulgaris* FSP-E was successfully extracted using sustainable bioprocessing technique, ultrasound-assisted three phase partitioning. The enhanced yield and separation efficiency with reduced processing time and capability to be scaled up, indicates that UATPP is an effective approach for future integrated bio-separation technique for biomolecules extraction from microalgae. The optimized conditions for protein recovery was identified and discussed to move towards the realization of producing low cost nutritional food for the society as well as to develop and improve the current downstream bioprocessing techniques.

DATA AVAILABILITY STATEMENT

All datasets analyzed for this study are included in the manuscript.

AUTHOR CONTRIBUTIONS

SC contributed to the writing of the manuscript, especially the original draft, methodology and the formal analysis of study. KC reviewed and edited the draft prior to the submission. PS contributed to the funding acquisition and supervised the project. HZ assisted in project administration and funding acquisition. D-TC was involved in the investigation of the study. YT contributed into funding acquisition of the research.

FUNDING

This work was supported by the Fundamental Research Grant Scheme, Malaysia [FRGS/1/2015/SG05/UNIM/03/1], International Cooperation Seeds Funding of Nanjing Agricultural University [Grant number: 2018-AH-04] and Yayasan Universiti Teknologi PETRONAS [Grant number: YUTP 015LC0-047].

REFERENCES

Akardere, E., Özer, B., Çelem, E. B., and Önal, S. (2010). Three-phase partitioning of invertase from Baker's yeast. *Sep. Purif. Technol.* 72, 335–339. doi: 10.1016/j.seppur.2010.02.025

Avhad, D. N., Niphadkar, S. S., and Rathod, V. K. (2014). Ultrasound assisted three phase partitioning of a fibrinolytic enzyme. *Ultrason. Sonochem.* 21, 628–633. doi: 10.1016/j.ultsonch.2013.10.002

Bleakley, S., and Hayes, M. (2017). Algal proteins: extraction, application, and challenges concerning production. *Foods* 6:33. doi: 10.3390/foods6050033

Bradford, M. M. (1976). A rapid and sensitive method for the quantitation of microgram quantities of protein utilizing the principle of protein-dye binding. *Anal. Biochem.* 72, 248–254. doi: 10.1016/0003-2697(76)90527-3

Capote, F. P., and de Castro, M. L. (2007). *Analytical Applications of Ultrasound, Vol. 26.* Amsterdam: Elsevier.

Chew, K. W., Chia, S. R., Lee, S. Y., Zhu, L., and Show, P. L. (2019). Enhanced microalgal protein extraction and purification using sustainable microwave-assisted multiphase partitioning technique. *Chem. Eng. J.* 367, 1–8. doi: 10.1016/j.cej.2019.02.131

Chew, K. W., Chia, S. R., Show, P. L., Yap, Y. J., Ling, T. C., and Chang, J. S. (2018a). Effects of water culture medium, cultivation systems and growth modes for microalgae cultivation: a review. *J. Taiwan Inst. Chem. Eng.* 91, 332–344. doi: 10.1016/j.jtice.2018.05.039

Chew, K. W., Ling, T. C., and Show, P. L. (2018b). Recent developments and applications of three-phase partitioning for the recovery of proteins. *Sep. Purif. Rev.* 48, 52–64. doi: 10.1080/15422119.2018.1427596

Chia, S. R., Chew, K. W., Show, P. L., Yap, Y. J., Ong, H. C., Ling, T. C., et al. (2018). Analysis of economic and environmental aspects of microalgae biorefinery for biofuels production: a review. *Biotechnol. J.* 1700618. doi: 10.1002/biot.201700618

Chougle, J. A., Singhal, R. S., and Baik, O. S. D. (2014). Recovery of astaxanthin from paracoccus NBRC 101723 using ultrasound-assisted three phase partitioning (UA-TPP). *Sep. Sci. Technol.* 49, 811–818. doi: 10.1080/01496395.2013.872146

Dennison, R. (2000). T-butanol: nature's gift for protein isolation. *S. Afr. J. Sci.* 96, 159–160.

Dey, S., and Rathod, V. K. (2013). Ultrasound assisted extraction of β-carotene from spirulina platensis. *Ultrason. Sonochem.* 20, 271–276. doi: 10.1016/j.ultsonch.2012.05.010

Dhananjay, S., and Mulimani, V. (2009). Three-phase partitioning of α-galactosidase from fermented media of *Aspergillus oryzae* and comparison with conventional purification techniques. *J. Ind. Microbiol. Biotechnol.* 36, 123–128. doi: 10.1007/s10295-008-0479-6

Gagaoua, M., Boucherba, N., Bouanane-Darenfed, A., Ziane, F., Nait-Rabah, S., Hafid, K., et al. (2014). Three-phase partitioning as an efficient method for the purification and recovery of ficin from mediterranean fig (*Ficus carica* L.) latex. *Sep. Purif. Technol.* 132, 461–467. doi: 10.1016/j.seppur.2014.05.050

Gagaoua, M., Ziane, F., Rabah, S. N., Boucherba, N., El-Okki, A. A. K. E. H., Bouanane-Darenfed, A., et al. (2017). Three phase partitioning, a scalable method for the purification and recovery of cucumisin, a milk-clotting enzyme, from the juice of *Cucumis melo* var. reticulatus. *Int. J. Biol. Macromol.* 102, 515–525. doi: 10.1016/j.ijbiomac.2017.04.060

Gogate, P. R., and Kabadi, A. M. (2009). A review of applications of cavitation in biochemical engineering/biotechnology. *Biochem. Eng. J.* 44, 60–72. doi: 10.1016/j.bej.2008.10.006

Hsieh, C. H., and Wu, W. T. (2009). A novel photobioreactor with transparent rectangular chambers for cultivation of microalgae. *Biochem. Eng. J.* 46, 300–305. doi: 10.1016/j.bej.2009.06.004

Jeon, Y. C., Cho, C. W., and Yun, Y. S. (2005). Measurement of microalgal photosynthetic activity depending on light intensity and quality. *Biochem. Eng. J.* 27, 127–131. doi: 10.1016/j.bej.2005.08.017

Kirpalani, D., and McQuinn, K. (2006). Experimental quantification of cavitation yield revisited: focus on high frequency ultrasound reactors. *Ultrason. Sonochem.* 13, 1–5. doi: 10.1016/j.ultsonch.2005.01.001

Kulkarni, V. M., and Rathod, V. K. (2014). Extraction of mangiferin from *Mangifera indica* leaves using three phase partitioning coupled with ultrasound. *Ind. Crops Prod.* 52, 292–297. doi: 10.1016/j.indcrop.2013.10.032

Lavens, P., and Sorgeloos, P. (1996). *Manual on the Production and Use of Live Food for Aquaculture.* Charlottesville, VA: Food and Agriculture Organization (FAO).

Lourenço, S. O., Barbarino, E., Lavín, P. L., Lanfer Marquez, U. M., and Aidar, E. (2004). Distribution of intracellular nitrogen in marine microalgae: calculation of new nitrogen-to-protein conversion factors. *Eur. J. Phycol.* 39, 17–32. doi: 10.1080/0967026032000157156

Narayan, A., Madhusudhan, M., and Raghavarao, K. (2008). Extraction and purification of Ipomoea peroxidase employing three-phase partitioning. *Appl. Biochem. Biotechnol.* 151, 263–72. doi: 10.1007/s12010-008-8185-4

Neves, C. M., Held, C., Mohammad, S., Schleinitz, M., Coutinho, J. A., and Freire, M. G. (2015). Effect of salts on the solubility of ionic liquids in water: experimental and electrolyte perturbed-chain statistical associating fluid theory. *Phys. Chem. Chem. Phys.* 17, 32044–32052. doi: 10.1039/C5CP06166K

Niphadkar, S. S., and Rathod, V. K. (2015). Ultrasound-assisted three-phase partitioning of polyphenol oxidase from potato peel (*Solanum tuberosum*). *Biotechnol. Prog.* 31, 1340–1347. doi: 10.1002/btpr.2139

Pakhale, S. V., and Bhagwat, S. S. (2016). Purification of serratiopeptidase from *Serratia marcescens* NRRL B 23112 using ultrasound assisted three phase partitioning. *Ultrason. Sonochem.* 31, 532–538. doi: 10.1016/j.ultsonch.2016.01.037

Patil, P. D., and Yadav, G. D. (2018). Application of microwave assisted three phase partitioning method for purification of laccase from *Trametes hirsuta*. *Process Biochem.* 65, 220–227. doi: 10.1016/j.procbio.2017.10.006

Phukan, M. M., Chutia, R. S., Konwar, B. K., and Kataki, R. (2011). Microalgae chlorella as a potential bio-energy feedstock. *Appl. Energy* 88, 3307–3312. doi: 10.1016/j.apenergy.2010.11.026

Ramazanov, A., and Ramazanov, Z. (2006). Isolation and characterization of a starchless mutant of *Chlorella pyrenoidosa* STL-PI with a high growth rate, and high protein and polyunsaturated fatty acid content. *Phycol. Res.* 54, 255–259. doi: 10.1111/j.1440-1835.2006.00416.x

Richmond, A. (2017). *Handbook of Microalgal Mass Culture (1986)*. New York, NY: CRC Press.

Safi, C., Charton, M., Pignolet, O., Silvestre, F., Vaca-Garcia, C., and Pontalier, P. Y. (2013). Influence of microalgae cell wall characteristics on protein extractability and determination of nitrogen-to-protein conversion factors. *J. Appl. Phycol.* 25, 523–529. doi: 10.1007/s10811-012-9886-1

Santos, H. M., Lodeiro, C., and Capelo-Martínez, J. L. (2008). "Power ultrasound meets protemics," in *Ultrasound in Chemistry: Analytical Applications*, ed J. L. Capelo-Martínez (Weinheim: John Wiley & Sons), 107–127. doi: 10.1002/9783527623501.ch5

Selvakumar, P., Ling, T. C., Walker, S., and Lyddiatt, A. (2010). A practical implementation and exploitation of ATPS for intensive processing of biological feedstock: a novel approach for heavily biological feedstock loaded ATPS. *Sep. Purif. Technol.* 75, 323–331. doi: 10.1016/j.seppur.2010.08.022

Seyfabadi, J., Ramezanpour, Z., and Amini Khoeyi, Z. (2011). Protein, fatty acid, and pigment content of *Chlorella vulgaris* under different light regimes. *J. Appl. Phycol.* 23, 721–726. doi: 10.1007/s10811-010-9569-8

Sharma, A., Sharma, S., and Gupta, M. N. (2000). Purification of alkaline phosphatase from chicken intestine by three-phase partitioning and use of phenyl-Sepharose 6B in the batch mode. *Bioseparation* 9, 155–161. doi: 10.1023/A:1008195729472

Sulaiman, A. Z., Ajit, A., Yunus, R. M., and Chisti, Y. (2011). Ultrasound-assisted fermentation enhances bioethanol productivity. *Biochem. Eng. J.* 54, 141–150. doi: 10.1016/j.bej.2011.01.006

Tay, W. H., Lau, K. K., and Shariff, A. M. (2016). High frequency ultrasonic-assisted CO2 absorption in a high pressure water batch system. *Ultrason. Sonochem.* 33, 190–196. doi: 10.1016/j.ultsonch.2016.04.004

Templeton, D. W., and Laurens, L. M. L. (2015). Nitrogen-to-protein conversion factors revisited for applications of microalgal biomass conversion to food, feed and fuel. *Algal Res.* 11, 359–367. doi: 10.1016/j.algal.2015.07.013

Tester, M., and Langridge, P. (2010). Breeding technologies to increase crop production in a changing world. *Science* 327, 818–822. doi: 10.1126/science.1183700

Thompson, P. A., Guo, M. X., and Harrison, P. J. (1996). Nutritional value of diets that vary in fatty acid composition for larval Pacific oysters (*Crassostrea gigas*). *Aquaculture* 143, 379–391. doi: 10.1016/0044-8486(96)01277-X

Ursu, A. V., Marcati, A., Sayd, T., Sante-Lhoutellier, V., Djelveh, G., and Michaud, P. (2014). Extraction, fractionation and functional properties of proteins from the microalgae *Chlorella vulgaris*. *Bioresour. Technol.* 157, 134–139. doi: 10.1016/j.biortech.2014.01.071

Waghmare, A. G., Salve, M. K., LeBlanc, J. G., and Arya, S. S. (2016). Concentration and characterization of microalgae proteins from *Chlorella pyrenoidosa*. *Bioresour. Bioprocess.* 3:16. doi: 10.1186/s40643-016-0094-8

Yadav, N., Gupta, M. N., and Khare, S. K. (2017). Three phase partitioning and spectroscopic characterization of bioactive constituent from halophilic *Bacillus* subtilis EMB M15. *Bioresour. Technol.* 242, 283–286. doi: 10.1016/j.biortech.2017.04.090

Zhang, X. F., Wang, X., and Luo, G. H. (2017). Ultrasound-assisted three phase partitioning of phycocyanin from Spirulina platensis. *Eur. J. Pure Appl. Chem.* 4, 1–5.

Conflict of Interest: The authors declare that the research was conducted in the absence of any commercial or financial relationships that could be construed as a potential conflict of interest.

frontiers in Bioengineering and Biotechnology

REVIEW
published: 14 July 2020
doi: 10.3389/fbioe.2020.00790

Genetic Engineering Strategies for *Euglena gracilis* and Its Industrial Contribution to Sustainable Development Goals: A Review

Ryo Harada[1], Toshihisa Nomura[1,2], Koji Yamada[1,3], Keiichi Mochida[1,2] and Kengo Suzuki[1,3]**

[1] RIKEN Baton Zone Program, Yokohama, Japan, [2] RIKEN Center for Sustainable Resource Science, Yokohama, Japan, [3] Euglena Co Ltd, Tokyo, Japan

The sustainable development goals (SDGs) adopted at the 2015 United Nations Summit are globally applicable goals designed to help countries realize a sustainable future. To achieve these SDGs, it is necessary to utilize renewable biological resources. In recent years, bioeconomy has been an attractive concept for achieving the SDGs. Microalgae are one of the biological resources that show promise in realizing the "5F"s (food, fiber, feed, fertilizer, and fuel). Among the microalgae, *Euglena gracilis* has the potential for achieving the "5F"s strategy owing to its unique features, such as production of paramylon, that are lacking in other microalgae. *E. gracilis* has already been produced on an industrial scale for use as an ingredient in functional foods and cosmetics. In recent years, genetic engineering methods for breeding *E. gracilis* have been researched and developed to achieve higher yields. In this article, we summarize how microalgae contribute toward achieving the SDGs. We focus on the contribution of *E. gracilis* to the bioeconomy, including its advantages in industrial use as well as its unique characteristics. In addition, we review genetic engineering-related research trends centered on *E. gracilis*, including a complete nuclear genome determination project, genome editing technology using the CRISPR-Cas9 system, and the development of a screening method for selecting useful strains. In particular, genome editing in *E. gracilis* could be a breakthrough for molecular breeding of industrially useful strains because of its high efficiency.

Keywords: *Euglena gracilis*, SDGs, bioeconomy, genetic engineering, CRISPR-Cas9

OPEN ACCESS

Edited by:
Raul Muñoz,
University of Valladolid, Spain

Reviewed by:
Pau Loke Show,
University of Nottingham, United Kingdom
Changhong Yao,
Sichuan University, China

****Correspondence:***
Ryo Harada
ryo.harada@riken.jp
Kengo Suzuki
suzuki@euglena.jp

Specialty section:
This article was submitted to Bioprocess Engineering, a section of the journal Frontiers in Bioengineering and Biotechnology

Received: *28 April 2020*
Accepted: *22 June 2020*
Published: *14 July 2020*

Citation:
Harada R, Nomura T, Yamada K, Mochida K and Suzuki K (2020) Genetic Engineering Strategies for Euglena gracilis and Its Industrial Contribution to Sustainable Development Goals: A Review. Front. Bioeng. Biotechnol. 8:790. doi: 10.3389/fbioe.2020.00790

SUSTAINABLE DEVELOPMENT GOALS (SDGs) AND THE BIOECONOMY

The SDGs have taken over the millennium development goals (MDGs) established in 2001, and have been listed in the "2030 Agenda for Sustainable Development" adopted at the United Nations Summit in September 2015. The SDGs are international goals, which consist of 17 interconnected goals and 169 targets (United Nations, 2016) for the period from 2016 to 2030. These universal goals

Abbreviations: SDGs, sustainable development goals; MDGs, millennium development goals.

apply to all countries and aim at issues, such as inequality, sustainable consumption and production, and climate change, that need to be addressed, especially by developed countries. As the SDGs are designed to solve problems at a global level, there is the need for not only governments, but also private companies to work together (Scheyvens et al., 2016).

Bioeconomy is a concept to utilize materials, chemicals, and energy derived from renewable biological resources and is therefore closely associated with the SDGs (McCormick and Kautto, 2013). Hence, the expansion of the bioeconomy will contribute to the achievement of the SDGs. The European government has led several movements to popularize bioeconomy since the mid-2000s (McCormick and Kautto, 2013). Achieving the bioeconomic vision requires the active participation of the general public and the commitment of governments and industries to drive concerted efforts on the sustainable development of the bioeconomy (McCormick and Kautto, 2013).

CONTRIBUTION OF MICROALGAE TO THE SDGs

Microalgae are organisms that grow in a variety of environments, including freshwater, seawater, wet soils, and rocks and form the basis of aqueous food chains (Dittami et al., 2017). They are known to produce useful physiologically active compounds for use as functional foods as well as lipids for use in biofuels. Therefore, they are considered to have a potential to realize the goals of the bioeconomy. In many countries, microalga-related developments require substantial investments and have successfully progressed from the research phase to the demonstration phase (Su et al., 2017). The major commercial areas where microalgae can be used are food (Christaki et al., 2011), fuel (Mofijur et al., 2019), cosmetics (Ariede et al., 2017), healthcare (Nethravathy et al., 2019), and feed (Dineshbabu et al., 2019). In addition, microalgae show promise in their application in wastewater treatment (De Francisci et al., 2018) and the reduction of carbon dioxide (CO_2) emissions (Klinthong et al., 2015). Utilization of algae for wastewater treatment and CO_2 emission reduction contributes to the "SDG-6: ensure availability and sustainable management of water and sanitation for all" and the "SDG-13: take urgent action to combat climate change and its impacts."

INDUSTRIAL USES OF *E. gracilis*

Growth Advantages of *E. gracilis* Compared to Other Euglena Species

The microalga *E. gracilis* has been used as a model organism in basic research for decades, especially to study photosynthesis. Besides *E. gracilis*, the genus *Euglena* includes more than 200 species, some of which have beneficial characteristics, such as the production of paramylon and several other biologically active substances, and are thus valuable for industrial use. Among these species, *E. gracilis* shows a much faster growth rate than other *Euglena* species under optimal conditions (Suzuki et al., 2015), making it more suited for mass culture and commercialization. Microalgae are known for their ability to take up toxic heavy metals from the environment, leading to the induction of a heavy-metal stress response in them (El-Esawi, 2019). Similar to other microalgae, *E. gracilis* is resistant to the stress caused by heavy metals such as Cd^{2+}, Cr^{3+}, Hg^{2+}, Cr^{6+}, Pb^{2+}, UO_2^{2+}, and Zn^{2+} (El-Esawi, 2019) and has good physical and metabolic adaptability (Rodríguez-Zavala et al., 2007; Lira-Silva et al., 2011; García-García et al., 2018; El-Esawi, 2019). This finding indicates that wastewater can be used to culture *E. gracilis* even on uncultivated land.

Characteristics of Paramylon Obtained From *E. gracilis*

Paramylon is a β-1,3-glucan synthesized by *E. gracilis*, which accumulates in the cells. These glucan crystals can be used in a wide range of industrial applications and be degraded to wax esters under anaerobic conditions. β-1,3-glucan is a polysaccharide abundant in fungi including mushrooms and is widely recognized as a useful component owing to its immune boosting properties (Nakashima et al., 2018b). Paramylon from *E. gracilis* has a similar effect and its role as a functional food has been long studied (Nakashima et al., 2018b; Barsanti and Gualtieri, 2019). The paramylon content in *E. gracilis* Z can be as high as 60–70% of the dry weight of the cell (Yasuda et al., 2018).

Characteristics of Wax Esters From *E. gracilis*

Euglena gracilis is capable of fermenting paramylon under anaerobic conditions and producing large amounts of wax esters (Inui et al., 1982; Zimorski et al., 2017). This reaction involves the anaerobic breakdown of paramylon into glucose units and an enzymatic metabolism to pyruvate, which is then oxidized by the O_2-sensitive enzyme pyruvate:NADP+ oxidoreductase to produce acetyl-CoA in the mitochondria (Rotte et al., 2001). Acetyl-CoA functions as the C2 donor in the reverse β-oxidation reaction to form acylated CoA (Inui et al., 1984). Next, acyl-CoA is exported to the endoplasmic reticulum, reduced to fatty alcohols, and esterified with another molecule of acyl-CoA to form a wax ester (Teerawanichpan and Qiu, 2010). This series of anaerobic processes constitute the wax ester fermentation. As wax esters can be commercialized as raw materials for biofuels, many genetic studies have focused on the analysis of metabolic pathways with the aim of increasing their production (Inui et al., 2017). The analysis of sulfur metabolites using LC/MS has shown that degradation of glutathione and proteins occurs as a secondary reaction during wax ester fermentation (Yamada et al., 2019). The secondary reaction in *E. gracilis* generates hydrogen sulfide,

which is empirically known to be accompanied by wax ester fermentation reactions.

Advantages of the Industrial Use of *E. gracilis* for "5F" Products

The use of *E. gracilis* in industry is expected to grow further due to the establishment of a mass culture technology. This large-scale commercial cultivation of *E. gracilis* began in 2007 after a successful mass cultivation in 2005, which focused on improving its yield and drying processes (Suzuki, 2017). Since then, *E. gracilis* has been actively studied to enhance further commercialization. Commercialization with *E. gracilis* is based on the strategy known as the "5F of biomass" or "5F"s, which represent food, fiber, feed, fertilizer, and fuel (Suzuki, 2017) (**Figure 1**). The "5F"s of biomass indicate biomass utilization listed in a descending order of added value; the products at the higher level are relatively more expensive than those positioned at the lower level. For example, "food" is located at the top of this list owing to its high unit price, which can be further increased using marketing- and supply strategies. On the other hand, the other "F"s, namely, feed, fertilizer, and fuel are of comparatively less value per unit in the commodity area. For example, price per weight of petroleum is low and is a competitor of biomass fuel. Therefore, it is necessary that biomass fuel be supplied at low cost. Food products derived from *E. gracilis*, ranking highest on the list of "5F"s, have already met with success (Suzuki, 2017), and the other "F"s will soon follow suit.

A variety of nutritional products for human and animal consumption are obtained from *E. gracilis*, leading to its commercial use as a food ingredient. Commercialization of *E. gracilis* as food is an established practice undertaken by many organizations in several countries including Japan and the United States (Gissibl et al., 2019). Studies evaluating the nutritional value of microalgae have been conducted for over 50 years, and these values have been well documented. *Chlorella* species are rich in amino acids, fatty acids, and vitamins (Morimura and Tamiya, 1954). The accurate analysis of cell components for each culture condition conducted using the *E. gracilis* Z strain (Kitaoka and Hosoya, 1977) revealed that *E. gracilis* has high levels of the amino acid, methionine, which is comparable to casein in terms of nutritional value, and is a rich source of proteins (**Table 1**) (Kitaoka and Hosoya, 1977). Although *E. gracilis* requires vitamins B1 and B12 as essential nutrients for growth, it is known to synthesize many of the other vitamins (Baker et al., 1981). The production of vitamins C and E can be increased by modifying the culture conditions (**Table 1**; Kitaoka, 1989). The fatty acids synthesized by *E. gracilis* are primarily highly unsaturated and their composition varies significantly depending on the culture conditions. When *E. gracilis* is grown under illumination, there is an increase in the unsaturated fatty acids including C16 and C18; under dark conditions, palmitic acid, abundant in phospholipids and long-chain fatty acids C20 and C21, is the primary product (Hulanicka et al., 1964).

Unlike other microalgae, *E. gracilis* lacks a cell wall, and is therefore easy to be digested when consumed. This is a desirable feature in nutritional supplements. Commercially, *E. gracilis* is made available as a dry powder intended to be added to beverages or to bakery products such as cookies. It is also sold as a supplement by Euglena Co,. Ltd., (Japan) in the form of capsules. *E. gracilis* can therefore be used as a nutritional supplement in various foods. In addition, Euglena Co., Ltd., obtained Halal certification for *E. gracilis* in 2013; therefore, a high demand for this microalga as a nutritional substitute for animal protein is anticipated from the vegetarian population and religious communities that follow Halal practices. As *E. gracilis* does not require agricultural land for production, the large-scale production does not compete with the production of crops, which will contribute to the remediation of the food problem. In developed nations, *E. gracilis* is in demand as an ingredient in functional foods depending on the function of paramylon. Studies on the immunomodulatory functions of paramylon have reported an amelioration of influenza symptoms (Nakashima

TABLE 1 | Compositions of *E. gracilis* Z (Based on Kitaoka and Hosoya, 1977).

		GL**	GD**	Autotrophic condition
General composition of *E. gracilis* Z*	Clude proteins	54.81	31.75	58.71
	True proteins	45.97	25.53	50.94
	Clude fats	15.19	8.71	15.5
	Ashes	4.96	2.13	6.8
	Paramylon	17.6	53.77	15.97
	Residues	7.44	3.64	3.02
	Water	3.49	2.54	6.81
Composition of essential amino acids† and amino acid values	Isoleucine	3.3	3.3	3.5
	Leucine	6.5	6.5	7.3
	Lysine	5.9	5.8	5.6
	Sulfur-containing amino acids	4.4	4.4	3.2
	Aromatic amino acids	7.2	7.2	7.6
	Threonine	4.1	4.4	4.3
	Tryptophan	1	1	1.1
	Valine	4.7	5.3	5
	Amino acid value	83	83	88
Compositions of vitamins in *E. gracilis* (mg/100 g and ‡ug/100 g)	Vitamin B1 ‡[a]	27.9	25.3	1
	Vitamin B2	5.6	4.3	4.5
	Vitamin B6	1.07		
	Vitamin B12 ‡[a]	10.1	30.5	36.6
	Nicotinic acid and Nicotinamide	37	41.4	28.3
	Biotin‡	79	88	14
	Pantothenic acid	3.4	2.9	3.6
	p-aminobenzoic acid			63
	Ascorbic acid	425	61	345
	Carotene	174	9.4	10.5
	Vitamin E	155	31	
	Vitamin K1		0.5	

**Freeze-dried sample, Except for water, values indicate parcentage of compositions per dry weight. **GL: Wild strain cultured under light condition, GD: Wild strain cultured under dark condition. †Grams of amino acids per 16 g of nitrogen. [a]Vitamin is added in the culture medium. ‡ug/100g.*

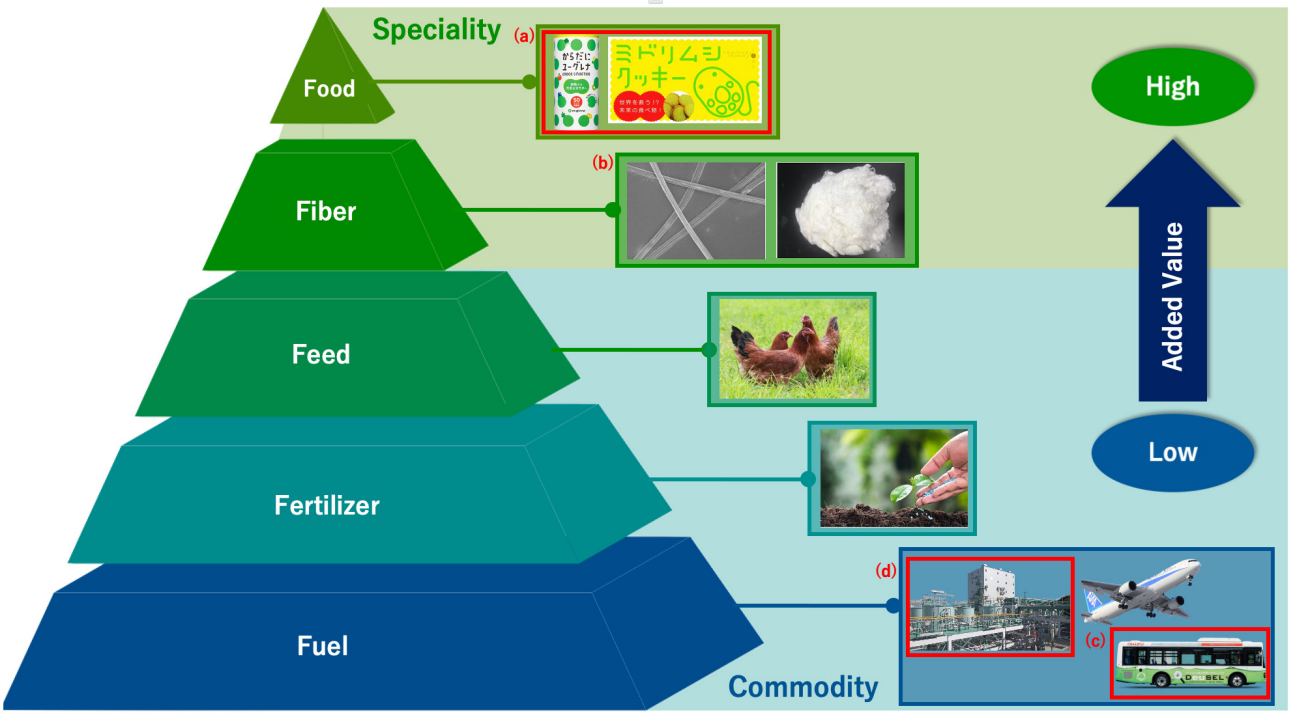

FIGURE 1 | Concept of 5F of biomass using *E. gracilis*. Each product is arranged from the top in the order of added value. Those marked in red are already in operation or commercialized. **(A)**: Foods are drink and cookie they include *E. gracilis*. **(B)**: Fiber include rayon which contains paramylon (Euglena Co Ltd and Omikenshi Co Ltd, 2020). **(C)**: Fuel derives from *E. gracilis* has already used for bio diesel. **(D)**: There is manufacturing plant for bio jet fuel and diesel fuel derives from *E. gracilis* in Japan.

et al., 2017), atopic dermatitis (Sugiyama et al., 2010), and rheumatic disorders (Suzuki et al., 2018). Furthermore, oral administration of paramylon inhibits hyperglycemia in type 2 diabetic OLETF rats (Shimada et al., 2016) and exhibits antifibrotic activity in NASH mice (Nakashima et al., 2018a). Paramylon also displayed anti-obesity and anti-inflammatory effects in mice fed a combination of *E. gracilis* and vegetables (Okouchi et al., 2019).

Paramylon is considered to be an alternative for petroleum-based plastics and a natural compound that does not compete with other petroleum products. The production of plastics is accompanied by a large emission of greenhouse gases and a consumption of enormous amounts of energy. Therefore, the use of biomaterials in the manufacture of plastics is an environmentally friendly approach. A study shows that paramylon functions as a filler in bioplastics and improves the final product by causing an increase in the maximum stress point and elasticity, and by decreasing the maximum displacement point (Suzuki et al., 2013). A plastic material composed of paramylon and the fats and oils derived from the shells of cashews has been developed. This material shows higher heat resistance than do traditional bioplastics such as polylactic acid and nylon 11 (AIST, 2013). Under anaerobic conditions, *E. gracilis* produces succinic and lactic acids, which can be used as ingredients for the manufacture of plastics (Tomita et al., 2016). Therefore, the *E. gracilis* biomass can be used in the manufacture of bioplastics owing to its environmentally friendly properties.

The role of *E. gracilis* in enhancing the properties of feed has also been studied. The addition of paramylon to the culture environment during the cultivation of *Artemia*, a raw fish feed, imparts a stress resistance property to this genus (Vismara et al., 2004). Moreover, *E. gracilis* biomass is being considered as a functional feed for livestock to reduce methane generation. Studies suggest that methane emissions from ruminant livestock, due to the presence of large amounts of methanogens in the rumen, have a major impact on global warming (Johnson and Johnson, 1995). It has also been reported that the addition of soybean oil to the feed significantly reduces the presence of methanogens in the rumen, which results in reduced methane emissions (Lillis et al., 2011). The wax esters of *E. gracilis* are rich in medium chain fatty acids, primarily myristic acid, which when mixed with feed might be responsible for the significant reduction of methane emissions (Aemiro et al., 2018). Moreover, hay mixed with *E. gracilis* has been shown to increase the nutritional value of feed for sheep (Aemiro et al., 2017), indicating the potential of *E. gracilis* as feed in livestock.

Microalgae including *E. gracilis* are of great value as fertilizers and can help increase agricultural output. High yields of crops are currently achieved using pesticides and inorganic fertilizers that make the sustainable use of arable land practically impossible (Vox et al., 2010). Therefore, an organic fertilizer that is safe

and induces high crop yields is necessary. The microalgae that have been studied for use as fertilizers include *Acutodesmus dimorphus* (Garcia-Gonzalez and Sommerfeld, 2015), *Chlorella spp.*, *Neochloris conjuncta*, *Botryococcus braunii* (Uysal et al., 2016), and *Nannochloropsis oculata* (Coppens et al., 2015). Microalgae are mainly used as fertilizers to supply nitrogen (Uysal et al., 2016). When used as a fertilizer, *N. oculata* improves the sugar and carotenoid contents of tomatoes, but decreases the crop yield (Coppens et al., 2015). It has been reported that paramylon produced by *E. gracilis* functions as a biostimulant in plants (Levine et al., 2014). Moreover, the use of fertilizers containing *E. gracilis* and paramylon stimulates growth, improves abiotic stress tolerance, and improves crop yield, thereby indicating *E. gracilis* potential as an adjuvant to fertilizer use (Levine et al., 2014).

The wax ester accumulated in *E. gracilis* is mainly composed of myristyl myristate (C28), which is categorized as a third-generation biofuel, indicating that *E. gracilis* may be appropriate for use as a biofuel (Inui et al., 2017). Fatty acid methyl ester and the hydrocracked alkane of the wax have lower freezing points than other microalgal biofuels that are rich in medium chain fatty acids such as palmitic- and stearic acids (Hu et al., 2008), and are therefore suitable as biojet fuels (Klopfenstein, 1985). In addition, wax esters have been shown to produce larger amounts of paraffins and olefins instead of flame-retardant aromatics than catalytic cracking of triacylglycerols. This indicates that the lipids from *E. gracilis* are suitable ingredients for biofuel production using catalytic cracking (Shimada et al., 2018).

RESEARCH CHALLENGES INVOLVED IN THE GENETIC MODIFICATION OF *E. gracilis*

Unlike other microalgae, the presence of paramylon and wax esters in *E. gracilis* imparts properties conducive to its industrial use. The auxotrophy of vitamins B1 and B12 is believed to be responsible for their limited yields by *E. gracilis*, even after technical optimization of cultivation techniques (Gissibl et al., 2019). Therefore, supplementation of these vitamins by scaling up cultivation, co-culturing *E. gracilis* and bacteria that produce the required nutrients, and production of transgenic *E. gracilis*, are a few solutions to overcome this problem (Gissibl et al., 2019). Co-culturing microalgae and microalga growth-promoting bacteria (MGPB) is known to increase biomass production (Fuentes et al., 2016; Ramanan et al., 2016; Toyama et al., 2019) *Emticicia sp.* EG3 was the first MGPB to be discovered and used in co-culture with *E. gracilis*, which enhanced the biomass production more than three-fold (Toyama et al., 2019).

Although co-culture with MGPB may be a solution for improving the yield of *E. gracilis*, breeding the strain is a more straightforward procedure to achieve high yields of the desired products. To achieve effective breeding aimed at improving the production of *E. gracilis* to suit individual purposes, technologies targeting classical mutant screening and targeted gene modification are needed, and some of these techniques have been developed. Using classical mutant screening, methods to effectively induce mutations in *E. gracilis* have been explored. In the next section, the history and prospects of technology development concerning gene regulation and breeding of *E. gracilis* are described.

Complete Nuclear Genome Sequencing

The complete genomes of chloroplast and mitochondria of *E. gracilis* were determined in 1993 and 2015 (Hallick et al., 1993; Dobáková et al., 2015), respectively. However, the complete nuclear genome sequence of *E. gracilis* has not been determined and only a draft genome is available (Ebenezer et al., 2017). The nuclear genome of *E. gracilis* is 1.4–2.0 Gbp (Ebenezer et al., 2017), which is approximately 10–50 times larger than that of other algae, and estimated to contain repetitive sequences at a high frequency. Therefore, it is necessary to obtain not only the short reads, but also the long read sequences using a sequencer (Ebenezer et al., 2017). There is also a need for new pipelines to be developed in bioinformatics to address the high ploidy of the nuclear genome of *E. gracilis* (Ebenezer et al., 2019).

For a large nuclear genome containing a high frequency of repetitive sequences, it may be useful to apply the techniques used to determine plant genomes. Plants amplify their genomes using transposon amplification during the process of evolution and domestication. Repetitive sequences, transposable elements, and gene duplication in particular have significantly increased in gymnosperm genome (Mackay et al., 2012). The similarity of these paralogs creates ambiguity during genome assembly using short-read next-generation sequencers. These ambiguities make it difficult to construct a complete genome and some sequences may be lost. In addition, short-read mapping requires a lot of computer resources. One way to solve these problems is to generate long reads beyond the region of the repetitive sequence and provide them to ambiguous regions. Long read sequences are provided by Sequencing Platforms such as TruSeq Synthetic Long Read (Illumina), SMRT (PacBio), and ONT (Oxford Nanopore), among which, the PacBio SMRT sequencer is most widely used. *De novo* assembly by PacBio is more continuous and complete than other approaches. The nuclear genome of *E. gracilis* is difficult to study owing to its large size, repetition, and complexity (Gumińska et al., 2018). Therefore, it is necessary to obtain high-quality DNA samples from the absorbance ratios point of view for enough data to provide adequate coverage to enable genome assembly (Gumińska et al., 2018). CTAB-based DNA purification methods are more efficient and accurate than commercial kits and methods using phenol-chloroform extraction (Gumińska et al., 2018).

Transient Gene Silencing Using RNA Interference

RNAi is a frequently tool used for transient gene regulation in several microorganisms including *E. gracilis*. This technique was first established in nematodes and trypanosomes (Fire et al., 1998; Ngô et al., 1998) and then applied to *E. gracilis* to regulate photoactivated adenylyl cyclase (Iseki et al., 2002). Knockdown of genes by RNAi using double-stranded RNA is only a transient method to elucidate gene function and therefore, cannot be used

to breed useful strains. However, RNAi has been an effective tool in knocking down genes such as redox-related enzymes in *E. gracilis* (Ozasa et al., 2017). RNAi has also been used in the knockdown of *EgSTD1* and *EgSTD2*, which are related to the wax ester fermentation pathway (Kimura and Ishikawa, 2018).

Transgene Introduction Techniques

Several transgenic technologies like particle gun, electroporation, and *Agrobacterium*-mediated transformation have been reported to introduce transgenes into *E. gracilis* cells (Ohmachi et al., 2016; Shigeoka et al., 2016; Khatiwada et al., 2019). Stable transgenic lines are claimed to have been produced by introducing a linear DNA gene expression cassette derived from T-DNA using the particle gun method (Shigeoka et al., 2016). Transgene introduction techniques have been used to study photosynthesis with the aim of enhancing wax ester production. Consequently, the transgenic *E. gracilis* (EpFS) line, which expresses fructose-1,6-bisphosphatase and sedoheptulose-1,7-bisphosphatase involved in the cyanobacterial Calvin cycle, has been created (Ogawa et al., 2015). Comparison of the photosynthetic capacity and wax ester productivity of the transgenic strain with that of the wild type showed that photosynthetic activity was significantly higher and the wax ester production was 13–100 times higher in the transgenic strain (Ogawa et al., 2015). Therefore, gene transfer may be a useful tool for artificial regulation of metabolic pathways. However, the culture of genetically modified *E. gracilis* may be prohibited by local laws pertaining to genetically modified organisms (GMOs) (Behera, 2014). Furthermore, the long-term stability of the introduced transgenes has not been evaluated, suggesting that the industrial use of these transgenic lines could possibly give rise to unforeseen problems such as impacts on the human body and environment. Therefore, there is a need for reliable methods with better stability.

Classical Breeding Methods for Creating Nuclear Mutants

Using nuclear mutant organisms other than GMOs for industry is not regulated by law in many countries. Therefore, various forward genetic approaches have been attempted to create nuclear mutants of *E. gracilis*. These approaches are described as classical breeding because they depend on the expression of new traits upon spontaneous mutations. Traditionally, UV and X-rays as physical mutagens, and NTG and EMS as chemical mutagens are used to produce *E. gracilis* mutants. However, many such mutants are thought to be derived from mutations in the chloroplast genome (Schiff et al., 1980). The production of *E. gracilis* mutants deriving its phenotype from the mutations in the nuclear genome is thought to be difficult due to its genomic redundancy or the highly efficient DNA repair mechanisms (Yamada et al., 2016a). Introduction of mutations using heavy ion beams efficiently induces mutations in higher plants (Kazama et al., 2013). Although the underlying mechanism is not fully understood, high-temperature tolerant mutants and lipid-rich mutants, whose phenotypes are probably derived from mutations of the nuclear genome, have been successfully produced by irradiating *E. gracilis* using a heavy ion beam (Yamada et al., 2016a,b).

Methods for Selecting Useful Strains

Mutants with useful traits need to be chosen for selective breeding. Selection of mutants of *E. gracilis* requires devising

TABLE 2 | Examples of RNP-based genome editing of microalgae.

Species	RNP type	Delivery	Exogenous DNA	Target gene	Selection	Efficiency	References
Chlamydomonas reinhardtii CC-124	SpCas9	Electroporation	Free, linearized Plasmid	*MAA7, CpSRP43, ChlM*	5-FI, Hygromycin and Clony color	0.17–40%	Shin et al., 2016
Chlamydomonas reinhardtii CC-4349	SpCas9	Electroporation	Free	*CpFTSY, ZEP*	Free	0.007–1.11%	Baek et al., 2016
Chlamydomonas reinhardtii CC-1883	LbCpf-1 (LbCas12a)	Electroporation	ssODN	*FKB12, CpFTSY, CpSRP43, PHT7*	Rapamycin, Clony color or size	0.5–16% (Scarless 0.1–10%)	Ferenczi et al., 2017
Coccomyxa sp. strain KJ	SpCas9	Electroporation	Free	*KJFTSY*	Free	0.01%	Yoshimitsu et al., 2018
Phaeodactylum tricornutum	SpCas9	Particle bombardment	Free	*PtAureo1a* with *PtUMPS, PtAPT*	5-FOA, 2-FA	65–100%	Serif et al., 2018
Nannochloropsis oceanica IMET1	SpCas9, FnCas12a, LbCas12a, AsCas12a	Electroporation	dsDNA	*NR*	Zeocin	0–93%	Naduthodi et al., 2019
Chlamydomonas reinhardtii CC-4533	SpCas9	Electroporation	dsDNA	*CrFzl*	Paromomycin	47.5%	Findinier et al., 2019
Euglena gracilis	SpCas9	Electroporation	Free	*EgGSL2*	Free	77.7–90.1%	Nomura et al., 2019

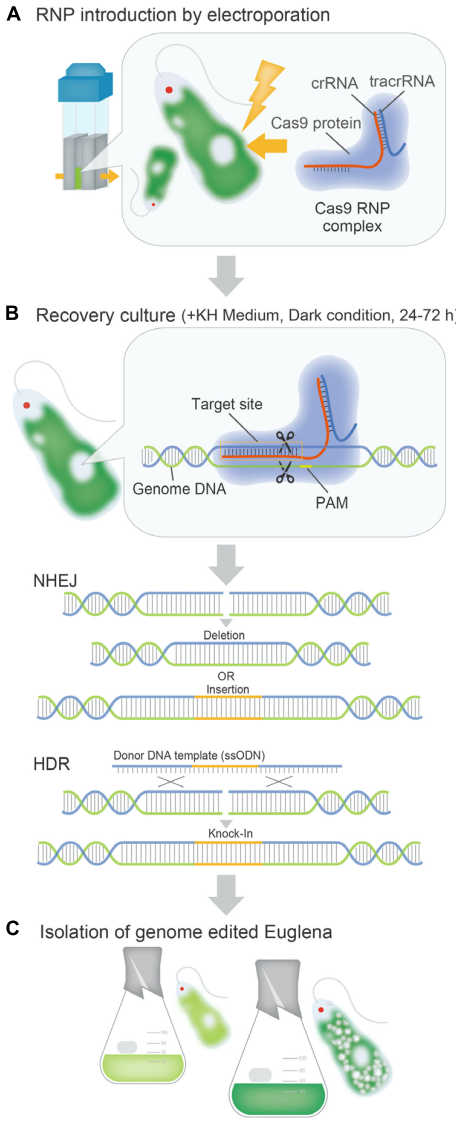

FIGURE 2 | Overview of the Cas9 RNP-based genome editing process in *E. gracilis*. **(A)**: Direct delivery of Cas9RNP complexes to *E. gracilis* cells by electroporation. **(B)**: Mutagenesis events during recovery culture after introduction of Cas9 RNPs into *E. gracilis* cells. **(C)**: Establishment and industrial use of functionally modified euglena strains.

and experimentation with classical screening methods, such as live- and a behavior-based selections. This is of particular importance in the commercial application of biofuel made from lipids obtained from *E. gracilis*, which necessitates the breeding of *E. gracilis* strains that can produce more wax esters. A study reported an improved fluorescence-activated cell sorting-based selection method for *E. gracilis* wherein BODIPY staining of the cellular lipids and large nozzles were used to sort live cells to obtain such mutants (Yamada et al., 2016a). Using this method, a strain containing 40% more lipids than the wild type was segregated from the Fe-ion-beam irradiated mutant population (Yamada et al., 2016a). In addition, a selection method using a microfluidic device has been successful in classifying *E. gracilis* based on the shape of individual cells (Li C. et al., 2017; Li M. et al., 2017). This method is expected to become a powerful screening technique when extended to and integrated with metabolic and genetic engineering technologies. In addition to these sorting techniques, non-staining imaging techniques for lipids and polysaccharides in live individual *E. gracilis* cells have been developed using Raman micro-spectroscopy, a technique helpful in determining the unique molecular information of *E. gracilis* by analyzing the wax ester fermentation (Iwasaki et al., 2019). At present, large-scale label-free single-cell analysis of paramylon in *E. gracilis* is possible (Hiramatsu et al., 2020).

Genome Editing of *E. gracilis* Using CRISPR-Cas9

The utilization of genome editing in *E. gracilis* could be a breakthrough for molecular breeding of industrially useful strains. Strains created using the genome editing technology employing the ribonucleoprotein (RNP) complex are transgene-free and are suitable for industrial use. At present, RNP-based genome editing of microalgae using CRISPR-Cas9 (Cong and Zhang, 2014) has been actively performed in various species, but many selection-free methods display a low mutation efficiency (∼1%) (**Table 2**; Baek et al., 2016; Shin et al., 2016; Ferenczi et al., 2017; Serif et al., 2018; Yoshimitsu et al., 2018; Findinier et al., 2019; Naduthodi et al., 2019; Nomura et al., 2019). In *E. gracilis*, a highly efficient genome editing method was recently established based on a Cas9-RNP introduction procedure, which does not depend on the expression of the transgene in the cell (**Figure 2**). In the first case, the Cas9 RNP targeting the gene *EgGSL2* involved in the biosynthesis of paramylon in *E. gracilis* (Tanaka et al., 2017) was introduced using electroporation. Direct delivery of Cas9 RNPs into the cell achieved a non-homologous end joining-mediated indel mutation rate of up to 90.1% (Nomura et al., 2019). This rate is much higher than the mutation efficiency of Chlamydomonas (∼10%) and other microalgae (∼1%) when using the RNP-based genome editing method (Jeon et al., 2017; Spicer and Molnar, 2018). In addition, using single-stranded oligodeoxynucleotide as donor DNA template, precise knock-in (∼70%) of 42 bp exogenous DNA sequences via homology-induced repair has been successfully achieved (Nomura et al., 2019). In many microalgae, except *E. gracilis*, the lower efficiency of genome editing is related to the presence of cell walls or structures on the cell surface (Jeon et al., 2017). It is speculated that the introduction of RNP is less inhibited in *E. gracilis* than in other microalgae, due to the lack of a cell wall in the former. The high efficiency of genome editing that cannot be achieved in other microalgae leads to the stable mutagenesis or the transformation of *E. gracilis*. This is one of the advantages of the industrial use of *E. gracilis* as a controllable microalga.

CONCLUSION

Euglena gracilis can produce commercially useful substances, such as paramylon and wax esters, that cannot be biosynthesized

by other microalgae. These products find use in several applications and contribute to the "5F of biomass." The commercial profitability of *E. gracilis* in the food industry has already been demonstrated. Prior to further industrial use of *E. gracilis*, it is necessary to control its production using genetic technology, especially complete nuclear genome sequencing and efficient gene technology. Complete nuclear genome sequencing has not yet been achieved and requires the development of efficient pipelines for long read acquisition and the assembly of acquired genes. For the latter, CRISPR-Cas9 has established itself as an efficient mutagenesis technology for *E. gracilis* as compared to its application in other microalgae. Techniques for selecting useful strains are constantly being developed and evaluated. These technologies have the potential to provide knowledge on *E. gracilis* gene function and achieve efficient breeding. We can thus expect obtaining products and services from *E. gracilis* for people and improving the environment to achieve the SDGs.

AUTHOR CONTRIBUTIONS

RH wrote this manuscript with support from TN, KY, and KS. TN aided in writing this manuscript and created **Figure 2**. KY and KM aided in writing this manuscript. KS aided in writing this manuscript and supervised this work. All authors contributed to the article and approved the submitted version.

ACKNOWLEDGMENTS

We thank Aya Ide for support in creating the figure illustration.

REFERENCES

Aemiro, A., Kiiru, P., Watanabe, S., Suzuki, K., Hanada, M., Umetsu, K., et al. (2017). The effect of euglena (*Euglena gracilis*) supplementation on nutrient intake, digestibility, nitrogen balance and rumen fermentation in sheep. *Anim. Feed Sci. Technol.* 225, 123–133. doi: 10.1016/j.anifeedsci.2017.01.017

Aemiro, A., Watanabe, S., Suzuki, K., Hanada, M., Umetsu, K., and Nishida, T. (2018). Effect of substituting soybean meal with euglena (*Euglena gracilis*) on methane emission and nitrogen efficiency in sheep. *Anim. Sci. J.* 90, 71–80. doi: 10.1111/asj.13121

AIST (2013). *Development of Euglena-Based Bioplastics*. Available online at: https://www.aist.go.jp/aist_e/list/latest_research/2013/20130228/20130228.html (accessed February 28, 2013).

Ariede, M. B., Candido, T. M., Jacome, A. L., Velasco, M. V., Carvalho, J. C., and Baby, A. R. (2017). Cosmetic attributes of algae - a review. *Algal Res.* 25, 483–487. doi: 10.1016/j.algal.2017.05.019

Baek, K., Kim, D. H., Jeong, J., Sim, S. J., Melis, A., Kim, J. S., et al. (2016). Dna-free two-gene knockout in *Chlamydomonas reinhardtii* via crispr-cas9 ribonucleoproteins. *Sci. Rep.* 6:30620.

Baker, E. R., Mclaughlin, J. J., Hutner, S. H., Deangelis, B., Feingold, S., Frank, O., et al. (1981). Water-soluble vitamins in cells and spent culture supernatants of poteriochromonas stipitata, *Euglena gracilis*, and *Tetrahymena thermophila*. *Arch. Microbiol.* 129, 310–313. doi: 10.1007/bf00414703

Barsanti, L., and Gualtieri, P. (2019). Paramylon, a potent immunomodulator from wzsl mutant of *Euglena gracilis*. *Molecules* 24:3114. doi: 10.3390/molecules24173114

Behera, K. K. (2014). "Phytoremediation, transgenic plants and microbes," in *Sustainable Agriculture Reviews* (Cham: Springer), 65–85.

Christaki, E., Florou-paneri, P., and Bonos, E. (2011). Microalgae: a novel ingredient in nutrition. *Int. J. Food Sci. Nutr.* 62, 794–799. doi: 10.3109/09637486.2011.582460

Cong, L., and Zhang, F. (2014). Genome engineering using crispr-cas9 system. *Chrom. Mutagen. Methods Mol. Biol.* 1239, 197–217. doi: 10.1007/978-1-4939-1862-1_10

Coppens, J., Grunert, O., Hende, S. V., Vanhoutte, I., Boon, N., Haesaert, G., et al. (2015). The use of microalgae as a high-value organic slow-release fertilizer results in tomatoes with increased carotenoid and sugar levels. *J. Appl. Phycol.* 28, 2367–2377. doi: 10.1007/s10811-015-0775-2

De Francisci, D., Su, Y., Iital, A., and Angelidaki, I. (2018). Evaluation of microalgae production coupled with wastewater treatment. *Environ. Technol.* 39, 581–592. doi: 10.1080/09593330.2017.1308441

Dineshbabu, G., Goswami, G., Kumar, R., Sinha, A., and Das, D. (2019). Microalgae-nutritious, sustainable aqua- and animal feed source. *J. Funct. Foods* 62:103545. doi: 10.1016/j.jff.2019.103545

Dittami, S. M., Heesch, S., Olsen, J. L., and Collén, J. (2017). Transitions between marine and freshwater environments provide new clues about the origins of multicellular plants and algae. *J. Phycol.* 53, 731–745. doi: 10.1111/jpy.12547

Dobáková, E., Flegontov, P., Skalickɹ, T., and Lukeš, J. (2015). Unexpectedly streamlined mitochondrial genome of the euglenozoan *Euglena gracilis*. *Genome Biol. Evol.* 7, 3358–3367. doi: 10.1093/gbe/evv229

Ebenezer, T. E., Carrington, M., Lebert, M., Kelly, S., and Field, M. C. (2017). *Euglena gracilis* genome and transcriptome: organelles, nuclear genome assembly strategies and initial features. *Cell Mol. Biol.* 979, 125–140. doi: 10.1007/978-3-319-54910-1_7

Ebenezer, T. E., Zoltner, M., Burrell, A., Nenarokova, A., Vanclová, A. M. N., Prasad, B., et al. (2019). Transcriptome, proteome and draft genome of *Euglena gracilis*. *BMC Biol.* 17:11. doi: 10.1186/s12915-019-0626-8

El-Esawi, M. A. (2019). "Genetic technologies and enhancement of algal utilization in wastewater treatment and bioremediation," in *Application of Microalgae in Wastewater Treatment*, eds S. Gupta and F. Bux (Cham: Springer), 163–175. doi: 10.1007/978-3-030-13913-1_9

Euglena Co Ltd and Omikenshi Co Ltd (2020). *Paramylon-Containing Rayon Fiber and Method for Producing Paramylon-Containing Rayon Fiber*. Japan patent number: 6654264. Japan Patent Office.

Ferenczi, A., Pyott, D. E., Xipnitou, A., and Molnar, A. (2017). Efficient targeted dna editing and replacement in *Chlamydomonas reinhardtii* using cpf1 ribonucleoproteins and single-stranded dna. *Proc. Natl. Acad. Sci. U.S.A.* 114, 13567–13572. doi: 10.1073/pnas.1710597114

Findinier, J., Delevoye, C., and Cohen, M. M. (2019). The dynamin-like protein fzl promotes thylakoid fusion and resistance to light stress in *Chlamydomonas reinhardtii*. *PLoS Genet.* 15:e1008047. doi: 10.1371/journal.pgen.1008047

Fire, A., Xu, S., Montgomery, M. K., Kostas, S. A., Driver, S. E., and Mello, C. C. (1998). potent and specific genetic interference by double-stranded rna in caenorhabditis elegans. *Nature* 391, 806–811. doi: 10.1038/35888

Fuentes, J., Garbayo, I., Cuaresma, M., Montero, Z., González-del-valle, M., and Vílchez, C. (2016). Impact of microalgae-bacteria interactions on the production of algal biomass and associated compounds. *Mar. Drugs* 14:100. doi: 10.3390/md14050100

García-García, J., Peña-sanabria, K., Sánchez-thomas, R., and Moreno-sánchez, R. (2018). Nickel accumulation by the green algae-like *Euglena gracilis*. *J. Hazard. Mater.* 343, 10–18. doi: 10.1016/j.jhazmat.2017.09.008

Garcia-Gonzalez, J., and Sommerfeld, M. (2015). Biofertilizer and biostimulant properties of the microalga acutodesmus dimorphus. *J. Appl. Phycol.* 28, 1051–1061. doi: 10.1007/s10811-015-0625-2

Gissibl, A., Sun, A., Care, A., Nevalainen, H., and Sunna, A. (2019). Bioproducts from *Euglena gracilis*: synthesis and applications. *Front. Bioeng. Biotechnol.* 7:108. doi: 10.3389/fbioe.2019.00108

Gumińska, N., Płecha, M., Walkiewicz, H., Hałakuc, P., Zakryś, B., and Milanowski, R. (2018). Culture purification and dna extraction procedures suitable for next-generation sequencing of euglenids. *J. Appl. Phycol.* 30, 3541–3549. doi: 10.1007/s10811-018-1496-0

Hallick, R. B., Hong, L., Drager, R. G., Favreau, M. R., Monfort, A., Orsat, B., et al. (1993). Complete sequence of *Euglena gracilis* chloroplast DNA. *Nucleic Acids Res.* 21, 3537–3544.

Hiramatsu, K., Yamada, K., Lindley, M., Suzuki, K., and Goda, K. (2020). Large-scale label-free single-cell analysis of paramylon in *Euglena gracilis* by high-throughput broadband raman flow cytometry. *Biomed. Opt. Exp.* 11, 1752–1759.

Hu, Q., Sommerfeld, M., Jarvis, E., Ghirardi, M., Posewitz, M., Seibert, M., et al. (2008). Microalgal triacylglycerols as feedstocks for biofuel production: perspectives and advances. *Plant J.* 54, 621–639. doi: 10.1111/j.1365-313x.2008.03492.x

Hulanicka, D., Erwin, J., and Bloch, K. (1964). Lipid metabolism of *Euglena gracilis*. *J. Biol. Chem.* 239, 2778–2787.

Inui, H., Ishikawa, T., and Tamoi, M. (2017). "Wax ester fermentation and its application for biofuel production," in *Euglena: Biochemistry, Cell and Molecular Biology. Advances in Experimental Medicine and Biology*, Vol. 979, eds S. Schwartzbach and S. Shigeoka (Cham: Springer), 269–283. doi: 10.1007/978-3-319-54910-1_13

Inui, H., Miyatake, K., Nakano, Y., and Kitaoka, S. (1982). Wax ester fermentation in *Euglena gracilis*. *FEBS Lett.* 150, 89–93. doi: 10.1016/0014-5793(82)81310-0

Inui, H., Miyatake, K., Nakano, Y., and Kitaoka, S. (1984). Fatty acid synthesis in mitochondria of *Euglena gracilis*. *Eur. J. Biochem.* 142, 121–126. doi: 10.1111/j.1432-1033.1984.tb08258.x

Iseki, M., Matsunaga, S., Murakami, A., Ohno, K., Shiga, K., Yoshida, K., et al. (2002). a blue-light activated adenylyl cyclase mediates photoavoidance in *Euglena gracilis*. *Nature* 415, 1047–1051. doi: 10.1038/4151047a

Iwasaki, K., Kaneko, A., Tanaka, Y., Ishikawa, T., Noothalapati, H., and Yamamoto, T. (2019). Visualizing wax ester fermentation in single *Euglena gracilis* cells by raman microspectroscopy and multivariate curve resolution analysis. *Biotechnol. Biofuels* 12:128.

Jeon, S., Lim, J. M., Lee, H. G., Shin, S. E., Kang, N. K., Park, Y. I., et al. (2017). Current status and perspectives of genome editing technology for microalgae. *Biotechnol. Biofuels* 10:267.

Johnson, K. A., and Johnson, D. E. (1995). Methane emissions from cattle. *J. Anim. Sci.* 73, 2483–2492. doi: 10.2527/1995.7382483x

Kazama, Y., Hirano, T., Nishihara, K., Ohbu, S., Shirakawa, Y., and Abe, T. (2013). Effect of high-LET Fe-ion beam irradiation on mutation induction in *Arabidopsis thaliana*. *Genes Genet. Syst.* 88, 189–197. doi: 10.1266/ggs.88.189

Khatiwada, B., Kautto, L., Sunna, A., Sun, A., and Nevalainen, H. (2019). Nuclear transformation of the versatile microalga *Euglena gracilis*. *Algal Res.* 37, 178–185. doi: 10.1016/j.algal.2018.11.022

Kimura, M., and Ishikawa, T. (2018). Suppression of dyrk ortholog expression affects wax ester fermentation in *Euglena gracilis*. *J. Appl. Phycol.* 30, 367–373. doi: 10.1007/s10811-017-1235-y

Kitaoka, S. (1989). *Euglena-Physiology And Biochemistry*. Japan: Conference publishing center.

Kitaoka, S., and Hosoya, K. (1977). Studies on culture conditions for the determination of the nutritive value of *Euglena gracilis* protein and the general and amino acid compositions of the cells. *J. Jpn. Soc. Agric. Chem.* 51, 477–482. doi: 10.1271/nogeikagaku1924.51.8_477

Klinthong, W., Yang, Y. H., Huang, C. H., and Tan, C. S. (2015). A review: microalgae and their applications in co2 capture and renewable energy. *Aerosol. Air Qual. Res.* 15, 712–742.

Klopfenstein, W. E. (1985). Effect of molecular weights of fatty acid esters on cetane numbers as diesel fuels. *J. Am. Oil Chem. Soc.* 62, 1029–1031. doi: 10.1007/bf02935708

Levine, R. B., Horst, G. P., and Lebrun, J. R. (2014). *Modulation of Plant Immune System Function*. U. S. Patent No:61/782.254. Washington, DC: U.S. Patent and Trademark Office.

Li, C., Lin, F., An, D., Wang, W., and Huang, R. (2017). Genome sequencing and assembly by long reads in plants. *Genes* 9:6. doi: 10.3390/genes9010006

Li, M., Muñoz, H. E., Goda, K., and Carlo, D. D. (2017). Shape-based separation of microalga *Euglena gracilis* using inertial microfluidics. *Sci. Rep.* 7:e010452-5. doi: 10.1038/s41598-017-10452-5

Lillis, L., Boots, B., Kenny, D. A., Petrie, K., Boland, T. M., Clipson, N., et al. (2011). The effect of dietary concentrate and soya oil inclusion on microbial diversity in the rumen of cattle. *J. Appl. Microbiol.* 111, 1426–1435. doi: 10.1111/j.1365-2672.2011.05154.x

Lira-Silva, E., Ramírez-lima, I. S., Olín-Sandoval, V., García-garcía, J. D., García-contreras, R., Moreno-sánchez, R., et al. (2011). Removal, accumulation and resistance to chromium in heterotrophic *Euglena gracilis*. *J. Hazard. Mater.* 193, 216–224. doi: 10.1016/j.jhazmat.2011.07.056

Mackay, J., Dean, J. F., Plomion, C., Peterson, D. G., Cánovas, F. M., Pavy, N., et al. (2012). Towards decoding the conifer giga-genome. *Plant Mol. Biol.* 80, 555–569. doi: 10.1007/s11103-012-9961-7

McCormick, K., and Kautto, N. (2013). The bioeconomy in europe: an overview. *Sustainability* 5, 2589–2608. doi: 10.3390/su5062589

Mofijur, M., Rasul, M., Hassan, N., and Nabi, M. (2019). Recent development in the production of third generation biodiesel from microalgae. *Energy Proc.* 156, 53–58. doi: 10.1016/j.egypro.2018.11.088

Morimura, Y., and Tamiya, N. (1954). Preliminary experiments in the use of chlorella as human food. *Food Technol.* 8:179.

Naduthodi, M. I. S., Mohanraju, P., Südfeld, C., D'adamo, S., Barbosa, M. J., and Van der oost, J. (2019). Crispr-cas ribonucleoprotein mediated homology-directed repair for efficient targeted genome editing in microalgae nannochloropsis oceanica imet1. *Biotechnol. Biofuels* 12:66.

Nakashima, A., Sugimoto, R., Suzuki, K., Shirakata, Y., Hashiguchi, T., Yoshida, C., et al. (2018a). Anti-fibrotic activity of *Euglena gracilis* and paramylon in a mouse model of non-alcoholic steatohepatitis. *Food Sci. Nutr.* 7, 139–147. doi: 10.1002/fsn3.828

Nakashima, A., Yamada, K., Iwata, O., Sugimoto, R., Atsuji, K., Ogawa, T., et al. (2018b). B-glucan in foods and its physiological functions. *J. Nutr. Sci. Vitaminol.* 64, 8–17. doi: 10.3177/jnsv.64.8

Nakashima, A., Suzuki, K., Asayama, Y., Konno, M., Saito, K., Yamazaki, N., et al. (2017). Oral administration of *Euglena gracilis* z and its carbohydrate storage substance provides survival protection against influenza virus infection in mice. *Biochem. Biophys. Res. Commun.* 494, 379–383. doi: 10.1016/j.bbrc.2017.09.167

Nethravathy, M. U., Mehar, J. G., Mudliar, S. N., and Shekh, A. Y. (2019). Recent advances in microalgal bioactives for food, feed, and healthcare products: commercial potential, market space, and sustainability. *Comprehens. Rev. Food Sci. Food Saf.* 18, 1882–1897.

Ngô, H., Tschudi, C., Gull, K., and Ullu, E. (1998). doublestranded rna induces mrna degradation in trypanosoma brucei. *Proc. Natl. Acad. Sci. U.S.A.* 95, 14687–14692. doi: 10.1073/pnas.95.25.14687

Nomura, T., Inoue, K., Uehara-yamaguchi, Y., Yamada, K., Iwata, O., Suzuki, K., et al. (2019). Highly efficient transgene-free targeted mutagenesis and single-stranded oligodeoxynucleotide-mediated precise knock-in in the industrial microalga *Euglena gracilis* using cas9 ribonucleoproteins. *Plant Biotechnol. J.* 17, 2032–2034. doi: 10.1111/pbi.13174

Ogawa, T., Tamoi, M., Kimura, A., Mine, A., Sakuyama, H., Yoshida, E., et al. (2015). Enhancement of photosynthetic capacity in *Euglena gracilis* by expression of cyanobacterial fructose-1,6-/sedoheptulose-1,7-bisphosphatase leads to increases in biomass and wax ester production. *Biotechnol. Biofuels* 8:e0264-5. doi: 10.1186/s13068-015-0264-5

Ohmachi, M., Fujiwara, Y., Muramatsu, S., Yamada, K., Iwata, O., Suzuki, K., et al. (2016). A modified single-cell electroporation method for molecule delivery into a motile protist, *Euglena gracilis*. *J. Microbiol. Methods* 130, 106–111. doi: 10.1016/j.mimet.2016.08.018

Okouchi, R., Yamamoto, K., Ota, T., Seki, K., and Imai, M. (2019). Simultaneous intake of *Euglena gracilis* and vegetables exerts synergistic anti-obesity and anti-inflammatory effects by modulating the gut microbiota in diet-induced obese mice. *Nutrients* 11:204. doi: 10.3390/nu11010204

Ozasa, K., Won, J., Song, S., Tamaki, S., Ishikawa, T., and Maeda, M. (2017). Temporal change of photophobic step-up responses of *Euglena gracilis* investigated through motion analysis. *PLoS One* 12:e0172813. doi: 10.1371/journal.pgen.172813

Ramanan, R., Kim, B., Cho, D., Oh, H., and Kim, H. (2016). Algae-bacteria interactions: evolution, ecology and emerging applications. *Biotechnol. Adv.* 34, 14–29. doi: 10.1016/j.biotechadv.2015.12.003

Rodríguez-Zavala, J. S., García-garcía, J. D., Ortiz-cruz, M. A., and Moreno-sánchez, R. (2007). Molecular mechanisms of resistance to heavy metals in the protist *Euglena gracilis*. *J. Environ. Sci. Health Part A* 42, 1365–1378. doi: 10.1080/10934520701480326

Rotte, C., Stejskal, F., Zhu, G., Keithly, J. S., and Martin, W. (2001). Pyruvate:nadp oxidoreductase from the mitochondrion of *Euglena gracilis* and from the apicomplexan cryptosporidium parvum: a biochemical relic linking pyruvate metabolism in mitochondriate and amitochondriate protists. *Mol. Biol. Evol.* 18, 710–720. doi: 10.1093/oxfordjournals.molbev.a003853

Scheyvens, R., Banks, G., and Hughes, E. (2016). The private sector and the sdgs: the need to move beyond 'business as usual'. *Sustainab. Dev.* 24, 371–382. doi: 10.1002/sd.1623

Schiff, J. A., Lyman, H., and Russell, G. K. (1980). [2] isolation of mutants of *Euglena gracilis*: an addenum. *Methods Enzymol. Photosynth. Nitrogen Fixat. Part C* 69, 23–29. doi: 10.1016/s0076-6879(80)69004-

Serif, M., Dubois, G., Finoux, A. L., Teste, M. A., Jallet, D., and Daboussi, F. (2018). One-step generation of multiple gene knock-outs in the diatom phaeodactylum tricornutum by dna-free genome editing. *Nat. Commun.* 9, 1–10.

Shigeoka, S., Tamoi, M., Suzuki, K., and Yoshida, E. (2016). U.S. Patent Application No. 14/770,715. Washington, DC: U.S. Patent and Trademark Office.

Shimada, I., Nakamura, Y., Kato, S., Mori, R., Ohta, H., Suzuki, K., et al. (2018). Catalytic cracking of wax esters extracted from *Euglena gracilis* for hydrocarbon fuel production. *Biomass Bioenergy* 112, 138–143. doi: 10.1016/j.biombioe.2018.03.004

Shimada, R., Fujita, M., Yuasa, M., Sawamura, H., Watanabe, T., Nakashima, A., et al. (2016). Oral administration of green algae, *Euglena gracilis*, inhibits hyperglycemia in oletf rats, a model of spontaneous type 2 diabetes. *Food Funct.* 7, 4655–4659. doi: 10.1039/c6fo00606j

Shin, S. E., Lim, J. M., Koh, H. G., Kim, E. K., Kang, N. K., Jeon, S., et al. (2016). Crispr/cas9-induced knockout and knock-in mutations in *Chlamydomonas reinhardtii*. *Sci. Rep.* 6, 1–15.

Spicer, A., and Molnar, A. (2018). Gene editing of microalgae: scientific progress and regulatory challenges in Europe. *Biology* 7:21. doi: 10.3390/biology7010021

Su, Y., Song, K., Zhang, P., Su, Y., Cheng, J., and Chen, X. (2017). Progress of microalgae biofuel's commercialization. *Renew. Sustain. Energy Rev.* 74, 402–411.

Sugiyama, A., Hata, S., Suzuki, K., Yoshida, E., Nakano, R., Mitra, S., et al. (2010). Oral administration of paramylon, a β-1,3-d-glucan isolated from *Euglena gracilis* z inhibits development of atopic dermatitis-like skin lesions in nc/nga mice. *J. Vet. Med. Sci.* 72, 755–763. doi: 10.1292/jvms.09-0526

Suzuki, K. (2017). "Large-scale cultivation of euglena," in *Euglena: Biochemistry, Cell and Molecular Biology. Advances in Experimental Medicine and Biology*, Vol. 979, eds S. Schwartzbach and S. Shigeoka (Cham: Springer).

Suzuki, K., Mitra, S., Iwata, O., Ishikawa, T., Kato, S., and Yamada, K. (2015). Selection and characterization of euglena anabaena var. Minor as a new candidate euglena species for industrial application. *Biosci. Biotechnol. Biochem.* 79, 1730–1736.

Suzuki, K., Nakano, R., Yamaguchi, H., Maruta, A., and Nakano, Y. (2013). Function of paramylon from *Euglena gracilis* as filler. *J. Soc. Powder Technol. Jpn.* 50, 728–732. doi: 10.4164/sptj.50.728

Suzuki, K., Nakashima, A., Igarashi, M., Saito, K., Konno, M., Yamazaki, N., et al. (2018). *Euglena gracilis* z and its carbohydrate storage substance relieve arthritis symptoms by modulating th17 immunity. *PLoS One* 13:e0191462. doi: 10.1371/journal.pone.0191462

Tanaka, Y., Ogawa, T., Maruta, T., Yoshida, Y., Arakawa, K., and Ishikawa, T. (2017). Glucan synthase-like 2 is indispensable for paramylon synthesis in *Euglena gracilis*. *FEBS Lett.* 591, 1360–1370. doi: 10.1002/1873-3468.12659

Teerawanichpan, P., and Qiu, X. (2010). Fatty acyl-coa reductase and wax synthase from *Euglena gracilis* in the biosynthesis of medium-chain wax esters. *Lipids* 45, 263–273. doi: 10.1007/s11745-010-3395-2

Tomita, Y., Yoshioka, K., Iijima, H., Nakashima, A., Iwata, O., Suzuki, K., et al. (2016). Succinate and lactate production from *Euglena gracilis* during dark, anaerobic conditions. *Front. Microbiol.* 7:2050. doi: 10.3389/fmicb.2016.02050

Toyama, T., Hanaoka, T., Yamada, K., Suzuki, K., Tanaka, Y., Morikawa, M., et al. (2019). Enhanced production of biomass and lipids by *Euglena gracilis* via co-culturing with a microalga growth-promoting bacterium, emticicia sp. *Eg3*. *Biotechnol. Biofuels* 12:e01544-42. doi: 10.1186/s13068-019-1544-2

United Nations (2016). *The Sustainable Development Goals 2016*. New York, NY: United Nations.

Uysal, O., Uysal, F. O., and Ekinci, K. (2016). Determinationo fertilizing characteristics of three different microalgae cultivated in raceways in greenhouse conditions. *Agron. Ser. Sci. Res.* 59, 15–19.

Vismara, R., Vestri, S., Frassanito, A. M., Barsanti, L., and Gualtieri, P. (2004). Stress resistance induced by paramylon treatment in artemia sp. *J. Appl. Phycol.* 16, 61–67. doi: 10.1023/b:japh.0000019113.77013.0d

Vox, G., Teitel, M., Pardossi, A., Minuto, A., Tinivella, F., and Schettini, E. (2010). *Sustainable Greenhouse Systems, Sustainable Agriculture: Technology, Planning And Management*. New York, NY: Nova science publishers.

Yamada, K., Nitta, T., Atsuji, K., Shiroyama, M., Inoue, K., Higuchi, C., et al. (2019). Characterization of sulfur-compound metabolism underlying wax-ester fermentation in *Euglena gracilis*. *Sci. Rep.* 9:600. doi: 10.1038/s41598-018-36600-z

Yamada, K., Kazama, Y., Mitra, S., Marukawa, Y., Arashida, R., Abe, T., et al. (2016a). Production of a thermal stress resistant mutant *Euglena gracilis* strain using fe-ion beam irradiation. *Biosci. Biotechnol. Biochem.* 80, 1650–1656. doi: 10.1080/09168451.2016.1171702

Yamada, K., Suzuki, H., Takeuchi, T., Kazama, Y., Mitra, S., Abe, T., et al. (2016b). Efficient selective breeding of live oil-rich *Euglena gracilis* with fluorescence-activated cell sorting. *Sci. Rep.* 6:327. doi: 10.1038/srep26327

Yasuda, K., Ogushi, M., Nakashima, A., Nakano, Y., and Suzuki, K. (2018). Accelerated wound healing on the skin using a film dressing with β-glucan paramylon. *Vivo* 32, 799–805. doi: 10.21873/invivo.11310

Yoshimitsu, Y., Abe, J., and Harayama, S. (2018). Cas9-guide rna ribonucleoprotein-induced genome editing in the industrial green alga *Coccomyxa* sp. Strain kj. *Biotechnol. Biofuels* 11, 1–10.

Zimorski, V., Rauch, C., Hellemond, J. J., Tielens, A. G., and Martin, W. F. (2017). "The mitochondrion of *Euglena gracilis*," in *Euglena: Biochemistry, Cell and Molecular Biology. Advances in Experimental Medicine and Biology*, Vol. 979, eds S. Schwartzbach and S. Shigeoka (Cham: Springer), 19–37. doi: 10.1007/978-3-319-54910-1_2

Conflict of Interest: KY and KS are employees of Euglena Co Ltd, which is a private company selling *E. gracilis* products.

The remaining authors declare that the research was conducted in the absence of any commercial or financial relationships that could be construed as a potential conflict of interest.

frontiers in Bioengineering and Biotechnology

METHODS
published: 21 July 2020
doi: 10.3389/fbioe.2020.00746

A Simple and Non-destructive Method for Chlorophyll Quantification of *Chlamydomonas* Cultures Using Digital Image Analysis

Nicola J. Wood[1,2], *Alison Baker*[3], *Rupert J. Quinnell*[4] *and Miller Alonso Camargo-Valero*[2,5]*

[1] *Centre for Doctoral Training in Bioenergy, School of Chemical and Process Engineering, University of Leeds, Leeds, United Kingdom,* [2] *BioResource Systems Research Group, School of Civil Engineering, University of Leeds, Leeds, United Kingdom,* [3] *Centre for Plant Sciences and School of Molecular and Cellular Biology, Faculty of Biological Sciences, University of Leeds, Leeds, United Kingdom,* [4] *School of Biology, Faculty of Biological Sciences, University of Leeds, Leeds, United Kingdom,* [5] *Departamento de Ingeniería Química, Universidad Nacional de Colombia, Manizales, Colombia*

OPEN ACCESS

Edited by:
Raul Muñoz, University of Valladolid, Spain

Reviewed by:
Enrica Uggetti, Universitat Politecnica de Catalunya, Spain
Ankush Karemore, Georgia Institute of Technology, United States
Poonam Singh, Durban University of Technology, South Africa

***Correspondence:**
Miller Alonso Camargo-Valero
M.A.Camargo-Valero@leeds.ac.uk

Specialty section:
This article was submitted to Bioprocess Engineering, a section of the journal Frontiers in Bioengineering and Biotechnology

Received: *17 January 2020*
Accepted: *11 June 2020*
Published: *21 July 2020*

Citation:
Wood NJ, Baker A, Quinnell RJ and Camargo-Valero MA (2020) A Simple and Non-destructive Method for Chlorophyll Quantification of Chlamydomonas Cultures Using Digital Image Analysis. Front. Bioeng. Biotechnol. 8:746. doi: 10.3389/fbioe.2020.00746

Growing interest in the use of microalgae as a sustainable feedstock to support a green, circular, bio-economy has led to intensive research and development initiatives aimed at increasing algal biomass production covering a wide range of scales. At the heart of this lies a common need for rapid and accurate methods to measure algal biomass concentrations. Surrogate analytical techniques based on chlorophyll content use solvent extraction methods for chlorophyll quantification, but these methods are destructive, time consuming and require careful disposal of the resultant solvent waste. Alternative non-destructive methods based on chlorophyll fluorescence require expensive equipment and are less suitable for multiple sampling of small cultures which need to be maintained under axenic growth conditions. A simple, inexpensive and non-destructive method to estimate chlorophyll concentration of microalgal cultures *in situ* from digital photographs using the RGB color model is presented. Green pixel intensity and chlorophyll *a*, *b* and total chlorophyll concentration, measured by conventional means, follow a strong linear relationship (R^2 = 0.985–0.988). In addition, the resulting standard curve was robust enough to accurately estimate chlorophyll concentration despite changes in sample volume, pH and low concentrations of bacterial contamination. In contrast, use of the same standard curve during nitrogen deprivation (causing the accumulation of neutral lipids) or in the presence of high quantities of bacterial contamination led to significant errors in chlorophyll estimation. The low requirement for equipment (i.e., a simple digital camera, available on smartphones) and widely available standard software for measuring pixel intensity make this method suitable for both laboratory and field-based work, particularly in situations where sample, qualified personnel and/or equipment is limited. By following the methods described here it should be possible to produce a standard curve for chlorophyll analysis in a wide range of testing conditions including different microalga cultures, culture vessel and photographic set up in any particular laboratory.

Keywords: chlorophyll, digital image analysis, RGB color model, microalgae, *C. reinhardtii*

INTRODUCTION

Photosynthetic microalgae have gained attention for their ability to efficiently convert solar energy into biomass as a potential source of biofuels and high-value chemicals (Chisti, 2007; Wijffels and Barbosa, 2010; Liu and Benning, 2013; Goncalves et al., 2016). Chlorophylls *a* and *b* are the primary photosynthetic pigments in microalgae and are responsible for the characteristic green color of chlorophyte cultures. The quantity of these pigments is therefore related to biomass production and can provide an indication of the growth of the culture (Wood et al., 2005). Additionally, unlike growth measurements such as optical density or dry biomass weight, chlorophyll content can be used as a measurement of culture density without interference from non-photosynthetic organisms such as bacterial contaminants. In industrial applications the production of neutral lipids (i.e., triacylglycerols, TAGs), which are favored for use as a biodiesel starting product, has been linked to breakdown and recycling of membrane lipids including the chloroplast membrane (Moellering and Benning, 2010; Siaut et al., 2011). The rapid and accurate determination of changes in chlorophyll content can therefore be used as an indicator of possible neutral lipid production in microalgal cultures.

Conventional methods for chlorophyll quantification involve destructive solvent extraction and subsequent spectroscopic chlorophyll analysis (Porra et al., 1989). These methods are time consuming, require removal of sample from the culture vessel and subsequent destruction of the sample and require careful disposal of the resultant solvent waste. The removal and destruction of sample can be problematic, in particular for time course studies, where culture volume can limit the number of measurable parameters.

Fluorescence is widely used as a non-destructive method of chlorophyll detection and quantification in both plants (Buschmann et al., 2000) and algae (Vincent, 1983), including in environmental samples (Wang et al., 2018), and commercial products are available (Netto et al., 2005). However, these require specialized expensive equipment and may not be suited to small volumes and to maintaining culture sterility. There is a need for a simple, inexpensive, non-destructive method that does not require multiple sampling of small volume cultures which need to be maintained axenically.

Recently, digital imaging techniques have emerged as a means by which to rapidly and non-destructively measure chlorophyll content. In particular, the almost universal presence of smartphones has enabled the use of smartphone cameras in laboratory digital analysis (Rignon et al., 2016). A handful of studies have made use of the RGB color model for chlorophyll determination in plant leaves such as maize (Friedman et al., 2016), potato plants (Gupta et al., 2013) and in marine microalgal cultures (e.g., *N. oculta*; Su et al., 2008) via digital imaging. The RGB color scale represents the intensity of red, green and blue components of a pixel within a digital computer image. Intensity ranges on a scale from 0 to 255 for each color, where white has RGB values (255,255,255) and black has values (0,0,0). However, many methods published to date require the use of advanced modeling software or complex mathematical processing (Su et al., 2008; Dey et al., 2016; Friedman et al., 2016).

In this study, the microalga *Chlamydomonas reinhardtii* has been used to develop a simple and rapid method to quantify chlorophyll concentration of algal cultures non-destructively *in situ* using the RGB scale to quantify pixel color intensity from digital photographs. The effect of bacterial contamination, sample volume, pH and neutral lipid production on the accuracy and reproducibility of the method is also evaluated. The method presented here is much simplified compared with other digital analysis methods for chlorophyll determination. Furthermore, the method is non-destructive and can be conducted without removal of sample from the culture vessel. This method requires minimal data manipulation and the use of only easily accessible software packages.

The method used to make the standard curve presented here is for monitoring chlorophyll concentrations in cultures of *C. reinhardtii* grown in 7 ml Bijou flasks. Digital images have been acquired under constant light conditions at a specific location using a smartphone digital camera. By creating a standard curve for the specific organism, culture conditions and photographic set-up available in any individual laboratory, the method presented here could be used to determine chlorophyll concentration for a range of algal species or consortia grown in a range of culture vessels.

MATERIALS AND METHODS

Cultivation and Sample Preparation

Chlamydomonas reinhardtii strain CC-1690 (*wt, mt+*) was obtained from the Chlamydomonas Resource Center (2016) (University of Minnesota, USA; www.chlamycollection.org) and cultivated in sterile Tris-Acetate-Phosphate (TAP) media which contains 7.5 mM NH_4Cl as the only available nitrogen source; the composition is detailed in Gorman and Levine (1965), cited in www.chlamycollection.org. Starter cultures were grown statically in 5 ml TAP media contained within 7 ml plastic Bijou flasks fitted with screw-top lids (Medline Scientific, Product Code 129202) at 20°C with a 16-h photoperiod (∼50 μmol photons m^{-2} s^{-1}).

All cultures were grown to stationary phase before being aliquoted, with a range of sample volumes, into fresh 7 ml Bijou flasks. Unless otherwise stated, all samples were made up to a total of 5 ml with TAP media, to create cultures with a range of absorbance values at 600 nm (A_{600}) between 0.005 and 2.5, for chlorophyll analysis. The control dataset (sterile CC-1690, 5 ml, pH 7.0–8.5) samples were cultured as described and analyzed as described in sections Photographic Chlorophyll Analysis and Chlorophyll Analysis by Solvent Extraction, using 5 ml standard TAP media as a baseline.

In order to test the reproducibility of the analysis when environmental interference is present, a range of commonly encountered parameters were chosen for investigation; the altered culture and sample preparation methods are detailed in sections Testing the effect of sample volume, Testing the effect of high pH, Testing the effect of bacterial contamination, Testing the effect of induced lipid accumulation.

Testing the Effect of Sample Volume

"Low volume" samples (sterile CC-1690, 3.5 ml, pH 7.0–8.5) were cultured as described in section Cultivation and Sample Preparation but made up to a final volume of 3.5 ml with TAP media. Samples were analyzed as described in sections Photographic Chlorophyll Analysis and Chlorophyll Analysis by Solvent Extraction using 3.5 ml standard TAP media as a baseline.

Testing the Effect of High pH

"High pH" samples (sterile CC-1690, 5 ml, pH 9.5) were cultured as described in section Cultivation and Sample Preparation before being transferred in CAPS-Acetate-Phosphate media (TAP media containing 10 mM CAPS buffer in place of the Tris buffer, adjusted to pH 9.5 by addition of 1M KOH). Starter cultures were decanted into 1.5 ml Eppendorf tubes, pelleted (6,000 rpm, ∼3,400 g, 5 min) in a microcentrifuge, washed twice in new media and resuspended in CAPS-Acetate-Phosphate media (pH = 9.5) to a range of biomass concentrations. Analysis was conducted as described in sections Photographic Chlorophyll Analysis and Chlorophyll Analysis by Solvent Extraction using 5 ml CAPS-Acetate-Phosphate media as a baseline.

Absorbance spectra at pH 7.0 and 9.5 were obtained by pelleting 2 × 500 µl samples from a stationary phase culture grown as described above. The supernatant was removed, and the samples resuspended in 1.5 ml TAP or CAPS-Acetate-Phosphate media, respectively. The samples were left at room temperature for 30 min before measuring the absorbance spectra in the visible range (400–750 nm). 1 ml of each sample was then taken for chlorophyll quantification as described in section Chlorophyll Analysis by Solvent Extraction.

Testing the Effect of Bacterial Contamination

Contaminated samples (CC-1690 + *E. coli*, 5 ml, pH 7.0–8.5) were created by the addition of two different amounts of stationary phase *Escherichia coli* (*E. coli*) culture (A_{600} = 3.64). The *E. coli* culture was decanted into 1.5 ml aliquots contained within 1.5 ml Eppendorf tubes and pelleted (13,000 rpm, ∼16,000 g, 10 min) in a microcentrifuge, the supernatant removed and the cultures resuspended in TAP medium. Sixteen *C. reinhardtii* samples were prepared; each sample was prepared to one of eight optical densities (A_{600} 0.005–1.0) in duplicate. Each duplicate was spiked with 1.5 ml or 0.325 ml *E. coli* culture (approximate A_{600} = 1.0 and 0.25, respectively) to create a range of algal biomass concentrations containing two different *E. coli* contaminant concentrations. Analysis was conducted as described in sections Photographic Chlorophyll Analysis and Chlorophyll Analysis by Solvent Extraction using 5 ml TAP media as a baseline.

Testing the Effect of Induced Lipid Accumulation

Large quantities of neutral lipids are known to accumulate in microalgae under nitrogen starvation (Siaut et al., 2011; Valledor et al., 2014). "TAP-N" samples (sterile CC-1690, 5 ml, pH 7.0–8.5, TAP-N media) were created to test the effect of neutral lipid accumulation on photographic chlorophyll determination. Starter cultures were cultured as described in section Cultivation and Sample Preparation before being transferred into TAP-N media (TAP media omitting NH_4Cl). Starter cultures were decanted into 1.5 ml Eppendorf tubes, pelleted (6,000 rpm ∼3,400 g, 5 min) in a microcentrifuge, washed twice in new media and resuspended in TAP-N media to range of biomass concentrations. Analysis was conducted as described in sections Photographic Chlorophyll Analysis and Chlorophyll Analysis by Solvent Extraction using 5 ml TAP-N media as a baseline.

Photographic Chlorophyll Analysis

Analysis was first conducted via the photographic digital analysis method demonstrated here, followed by comparison with a standard analytical method for chlorophyll quantification of microalgal cultures. A simplified step by step protocol for creating the standard curve is presented in the **Supplementary Material**.

Photographic Set-Up

Photographic analysis was conducted by photographing each sample in triplicate (the three photographs were taken immediately one after another without disturbing the sample or camera position) using a smartphone (iPhone 5s, Apple Inc.) digital camera (8 megapixel, 1.5 µm pixels) mounted on a tripod. The camera was positioned at an angle of 30° from vertical at a height of 6.5 cm above the base of the sample flask and a horizontal distance of 8.5 cm from the flask edge; camera position was chosen to center the sample within the photograph and minimize shadowing. All measurements were taken from the center of the camera lens. Samples were shaken vigorously to resuspend any sedimented cells and positioned against a constant white background created by mounting white paper against a card box. The light concentration, measured at the sample position, was ∼10 ± 1 µmol photons m^{-2} s^{-1}. **Figure 1** shows the camera and sample set-up for photographic chlorophyll analysis.

FIGURE 1 | Set up showing the sample and tripod positioning for photographic chlorophyll analysis.

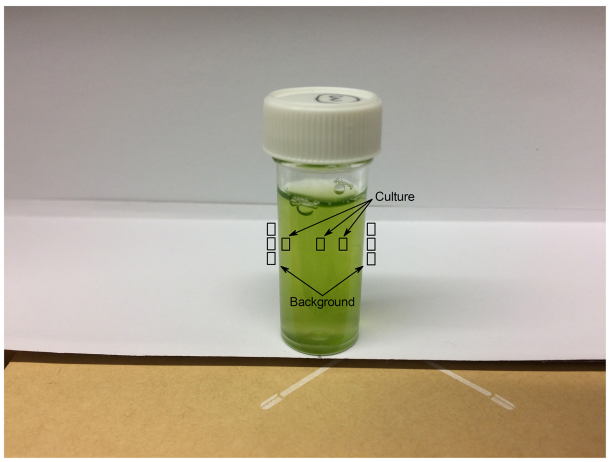

FIGURE 2 | Pixel selection regions within sample photographs for photographic RGB data analysis.

RGB Data Analysis

"Green Pixel Intensity" was determined from each photograph using Microsoft Paint software (MS Windows 7, version 6.1). Red, green and blue pixel intensities were obtained using the RGB color model; pixels were selected using the "color picker" tool and the RGB components extracted from the "edit colors" feature.

Three individual pixels were selected each from the culture and from the white paper both to the immediate left and right of the flask as a background. Given the shadow present from the flask lid in each image, pixel selections for the culture were made one each from the different shadowed and un-shadowed regions. The sampled regions are shown in **Figure 2**.

Green pixel intensity (*GPI*) was calculated for each pixel from RGB data according to Equation (1).

$$Green\ Pixel\ Intensity\ (GPI) = \frac{G}{R+G+B} \quad (1)$$

where R, G, and B are the red, green and blue pixel intensities, respectively.

For each photograph, *GPI* was calculated for each selected culture and background pixel and the mean *GPI* for each of the culture and background calculated. The mean background *GPI* was subtracted from the mean culture *GPI* such that:

$$GPI_{sample} = GPI_{culture} - GPI_{background} \quad (2)$$

where $GPI_{culture}$ is the mean *GPI* of three pixels selected from the culture and $GPI_{background}$ is the mean of six pixels taken from the white paper background to the immediate left and right of the culture (**Figure 2**).

On each day of sampling, a baseline green pixel intensity was obtained as described above from a sample vessel containing medium in the absence of culture and analyzed as above such that:

$$GPI_{baseline} = GPI_{media} - GPI_{background} \quad (3)$$

where GPI_{media} is the mean *GPI* of three pixels selected from the media and $GPI_{background}$ is the mean of six pixels taken from the white paper background to the immediate left and right of the media (**Figure 2**).

Once each photograph had been analyzed as above, the mean GPI_{sample} and mean $GPI_{baseline}$ were calculated from the corresponding GPI_{sample} and $GPI_{baseline}$ calculated values for each of the three photographs taken.

Final green pixel intensity (GPI_{final}) for each sample was obtained by subtracting the mean green pixel intensity of the baseline from that of the sample according to Equation (4).

$$Final\ Green\ Pixel\ Intensity\ \left(GPI_{final}\right) = mean\ GPI_{sample} - mean\ GPI_{baseline} \quad (4)$$

such that GPI_{final} represents the mean of the three photographs taken.

Chlorophyll Analysis by Solvent Extraction

Chlorophyll quantification was conducted spectrophotometrically via solvent extraction in 80% (v/v) acetone/20% (v/v) methanol. A known volume of sample was pelleted in a microcentrifuge (13,000 rpm, ∼16,000 g, 10 min) and the supernatant removed; sample volume was selected to maintain an absorbance <1.00 after chlorophyll extraction. The pellet was resuspended in 80% (v/v) acetone in methanol by vortexing before being further centrifuged (13,000 rpm, ∼16,000 g, 5 min) to remove cell debris. The absorbance of the supernatant was measured at 646.6, 663.6 and 750 nm in a glass cuvette against an 80% acetone/20% (v/v) methanol blank, using a Jenway 6715 UV/Vis spectrophotometer. Once chlorophyll extraction had taken place, all samples were kept in the dark until analysis to prevent chlorophyll degradation.

Chlorophyll content was calculated according to the extinction coefficients described in Porra et al. (1989) as follows:

$$Chl\ a\ (\mu g/ml) = \frac{12.25\ E_{663.6} - 2.55\ E_{646.6}}{sample\ volume\ (ml)} \quad (5)$$

$$Chl\ b\ (\mu g/ml) = \frac{20.31\ E_{646.6} - 4.91\ E_{663.6}}{sample\ volume\ (ml)} \quad (6)$$

$$Chl\ a+b\ (\mu g/ml) = \frac{17.76\ E_{646.6} + 7.34\ E_{663.6}}{sample\ volume\ (ml)} \quad (7)$$

where $E_{663.6}$ and $E_{646.6}$ represent absorbances at 663.6 nm and 646.6 nm minus absorbance at 750 nm, respectively.

Statistical Analysis

Power Analysis

G*power (version 3.1) (Faul et al., 2009), was used to conduct a sensitivity power analysis (two tailed; linear bivariate regression: two groups, difference between slopes; $\alpha = 0.05$; power $= 1 - \beta = 0.80$) to determine the detectable effect size ($|\Delta slope|$) between each environmental variable and the control dataset for the given sample sizes.

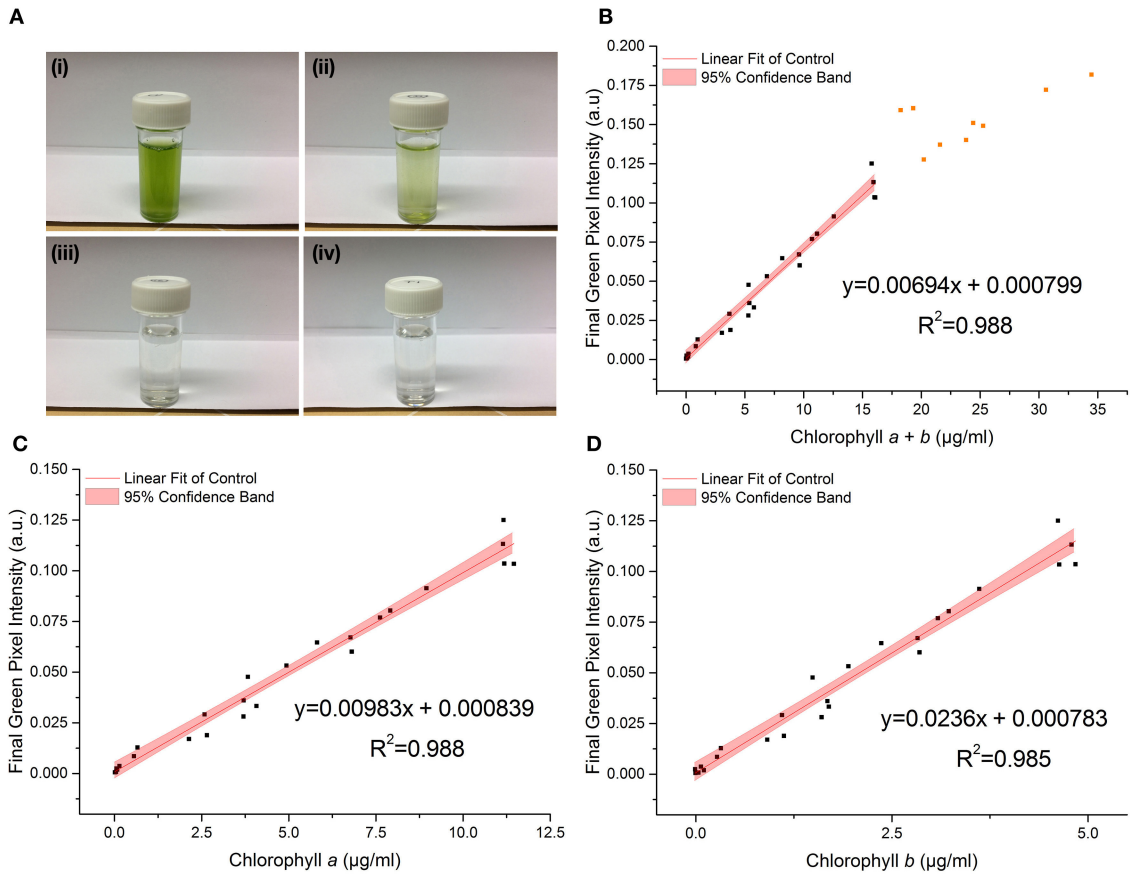

FIGURE 3 | (A) Photographs of *C. reinhardtii* samples for RGB digital analysis of chlorophyll concentrations: chlorophyll $a + b$ = (i) 18.2 µg/ml; (ii) 3.7 µg/ml; (iii) 0.1 µg/ml; (iv) 0 µg/ml (TAP blank). **(B–D)** The correlation between chlorophyll $a + b$, chlorophyll *a* and chlorophyll *b* concentrations respectively, as measured by standard extraction method in 80% acetone, and final green pixel intensity calculated from the RGB color model for a sterile culture of wild-type *C. reinhardtii* CC-1690 cultivated in TAP media under 50 µmol photons m^{-2} s^{-1} illumination (16 h photoperiod) and diluted to a range of biomass concentrations for analysis. Data points represent the mean green pixel intensity of three photographs (y) and the mean chlorophyll concentration of three sample aliquots (x). Orange points indicate those excluded from the fitting model due to lack of continued linearity.

General Linear Model Analysis

The relationship between Final Green Pixel Intensity (GPI_{final}), from photographic digital image analysis, and chlorophyll concentration, determined by extraction in 80% (v/v) acetone in methanol, for the control dataset was analyzed by linear regression. Microsoft Excel software was used to calculate the coefficient of determination (R^2) for the correlation assuming a linear relationship between total chlorophyll concentration and green pixel intensity. Data points were subsequently removed (starting with the highest chlorophyll concentration) and the R^2 value recalculated as each additional point was removed. The linear portion of the correlation was chosen as the range of points (>2 points) responsible for the R^2 closest to 1.00. Beyond this point there was also a noticeable increase in the scatter of the data resulting in additional uncertainty in the fit. Regressions for all potential environmental interferences were considered linear within the same region as that of the control dataset.

OriginPro (Origin® 9.1) software was used to compute the 95% confidence band for the linear portion of each curve. The 95% confidence band represents the region in which there is 95% certainty of the true linear fit residing. Analytical characteristics for determination of Chlorophyll *a*, *b* and total (Chlorophyll *a* and *b*) were determined using methodologies typically used in the development of spectrophotometric methods, for the assessment of key performance indicators including: Limit of Blank (LoB), Limit of Detection (LoD), Linear Interval and Precision, reported as the percent relative standard deviation (%RSD) from the samples used to make the standard curve (Horwitz et al., 1980; Armbruster and Pry, 2008).

IBM® SPSS Statistics® (version 22) was used to compare the slopes and intercepts of different standard curves using a univariate general linear model. A full model was fitted, with different slopes and intercepts for each fitted line. A significant difference between slopes was tested by examining the interaction term; if this was not significant, the interaction term was removed from the model and a significant difference between intercepts was tested. Normality of residuals was checked by visual inspection of Q-Q plots.

TABLE 1 | Regression parameters and analytical characteristics for the control dataset.

	Equation	R^2	$F_{(1,23)}$	p^a	LoB, μg/ml	LoD, μg/ml	Upper limit of linear interval, μg/ml	%RSD
Chl *a* + *b*	$y = 0.00694(\pm0.00029)\,x + 0.000799(\pm0.00198)$	0.988	0.162	0.691	0.05	0.12	16.00	5.75
Chl *a*	$y = 0.00983(\pm0.00032)\,x + 0.000839(\pm0.00193)$	0.988	0.190	0.667	0.06	0.10	16.00	4.74
Chl *b*	$y = 0.02361(\pm0.00086)\,x + 0.000783(\pm0.00217)$	0.985	0.129	0.722	0.05	0.08	16.00	4.98

[a]*p-values indicating whether the intercept is significantly different from zero in each case.*
LoB, Limit of Blank; LoD, Limit of Detection; %RSD, Mean Percent Relative Standard Deviation.

RESULTS

Validity of the RGB Model for Predicting Chlorophyll Content

To test the validity of the RGB method (Equation 1) to estimate the chlorophyll content of a microalgal culture, a series of sterile 5 ml *C. reinhardtii* samples were made to a range of optical densities in standard Tris-Acetate Phosphate (TAP) Media, pH 7.0–8.5. Samples were first photographed for digital analysis as described in methods before being aliquoted for standard spectroscopic chlorophyll quantification via extraction in 80% (v/v) acetone in methanol.

Figure 3 shows the relationship between the RGB method and chlorophyll concentration, as measured by the standard extraction method, for the control dataset.

The linear region of the correlation was determined from the correlation between the standard and RGB methods for total chlorophyll (chlorophyll $a + b$) concentration (**Figure 3B**). Adding points individually with increasing chlorophyll concentration resulted in a constant gradient up to a chlorophyll $a + b$ concentration (X) of 16 μg/ml (final green pixel intensity = 0.125). Including points above $X =$ 16 μg/ml resulted in the steady reduction of the gradient of the fitted line indicating that the plot tends toward a plateau at high chlorophyll concentrations. In addition, above $X =$ 16 μg/ml there is a noticeable increase in the scatter of the plot. The reduction in gradient as well as increased scatter beyond X = 16 μg/ml suggests a reduced sensitivity of the RGB method above this point; points above $X = 16$ μg/ml have therefore been excluded from the fitting model and all subsequent plots. For cultures of higher chlorophyll concentration, samples would need to be removed and diluted before analysis. The lower limit for the linear interval was determined by calculating the Limit of Detection (LoD) of the method (Armbruster and Pry, 2008); the resulting LoDs for the determination of total chlorophyll, chlorophyll *a* and chlorophyll *b* were 0.12, 0.10, 0.08 μg/ml, respectively.

There is a strong correlation between the RGB and standard methods for chlorophyll quantification for chlorophyll *a*, *b* and total chlorophyll as shown by the R^2 values of 0.988, 0.985, and 0.988 respectively. 95% confidence bands demonstrate a high level of precision in the slopes and intercepts of the fitted lines.

TABLE 2 | Detectable effect size (|Δslope|).

Sample set vs. control	Detectable effect size (|Δslope|)[a]
Low volume	0.00115
High pH	0.00106
+1.5 ml *E. coli*	0.00107
+0.325 ml *E. coli*	0.00122

[a]*between each measured variable and the control dataset as calculated from G*power software; α =0.05; power = 1 − β = 0.80.*

Data for the control dataset was acquired on three separate days and combined, there was no difference between days in the slopes [$F_{(2,16)} = 0.952$, $p = 0.407$] or intercepts [$F_{(2,16)} = 1.345$, $p =$ 0.285], thus demonstrating the reproducibility of the method over different sampling periods. The precision of the method was assessed by calculating the percent relative standard deviation (%RSD) from readings included in the standard curve within the linear interval of the method. For chlorophyll quantification for chlorophyll *a*, *b* and total chlorophyll the average %RSD values were 4.74, 4.98, and 5.75%, respectively.

The high *p*-values for the intercept show that the intercept is not significantly different from zero in each case, which is as expected given the green pixel intensity of the TAP blank has been subtracted from each data point. The regression parameters and analytical characteristics for the control dataset are given in **Table 1**.

Effect of Environmental Conditions on the Chlorophyll/RGB Correlation

To investigate whether a single standard curve, for the given experiment, could be used to estimate chlorophyll concentration from green pixel intensity in spite of potential environmental interference, four commonly encountered environmental variables were introduced and their effect on the correlation individually investigated. In each case, linear regression analysis was used to determine whether the slopes and intercepts of each correlation could be considered to be statistically similar to that of the control dataset (**Figure 3**). Owing to the loss of linearity

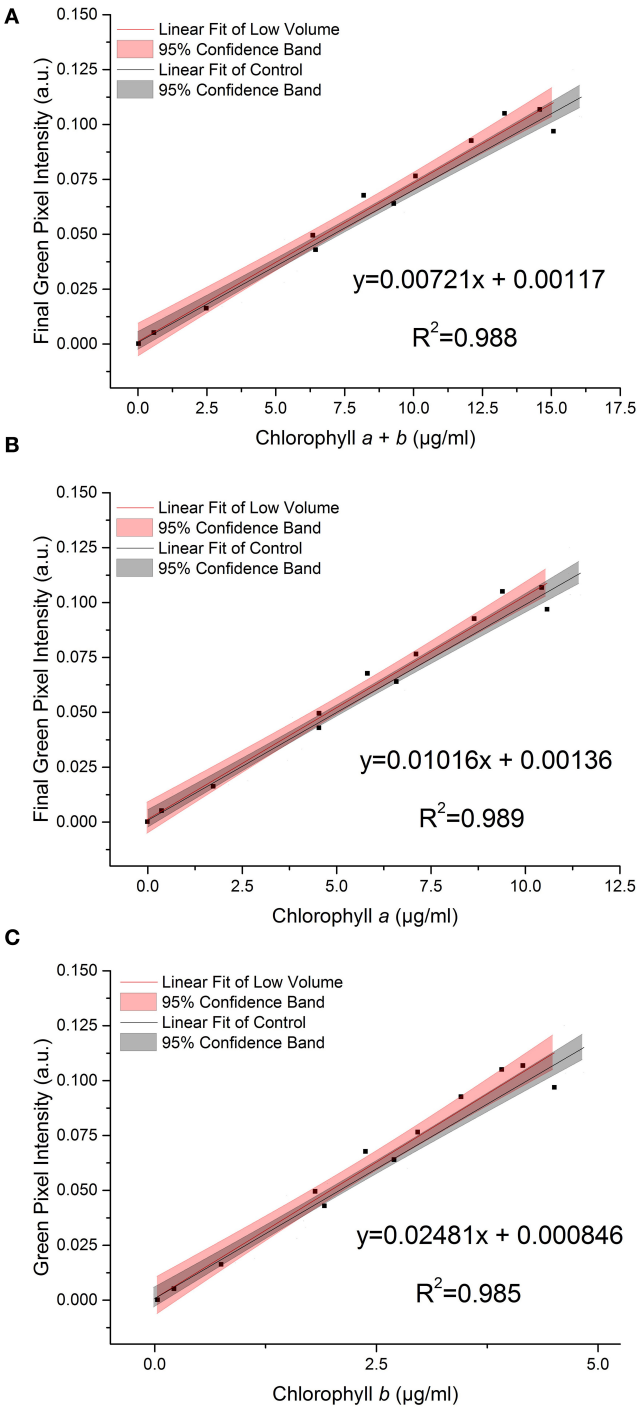

FIGURE 4 | The relationship between final green pixel intensity, calculated from the RGB color method, and **(A)** chlorophyll *a* + *b*, **(B)** chlorophyll *a* and **(C)** chlorophyll *b* concentrations, as measured by standard extraction method in 80% acetone, for a culture of *C. reinhardtii* photographed at two different culture volumes. Red = "low volume", 3.5 ml samples; Gray = control, 5 ml samples. Data points represent the mean green pixel intensity of three photographs (y) and the mean chlorophyll concentration of three sample aliquots (x).

in the correlation at concentrations above chlorophyll $a + b =$ 16 µg/ml (green pixel intensity = 0.125), correlations have only been compared up to green pixel intensity = 0.125; data points above this have been removed from the fitted lines.

Table 2 gives the minimum detectable effect size (|Δslope|) for the given sample sizes. The effect size, in this case, is the smallest difference in slope between the RGB/chlorophyll correlations for control and variable datasets that can be distinguished with the given sample sizes.

Figure 4 shows the effect on the relationship between green pixel intensity and chlorophyll *a*, *b* and total chlorophyll when the photographed sample volume is reduced from 5.0 to 3.5 ml. Samples were photographed at a volume of 3.5 ml for comparison with the control samples (5 ml) before being analyzed for chlorophyll concentration by extraction in 80% (v/v) acetone in methanol. In each case the linear fit for the low volume samples (red) is shown next to that of the control dataset (gray) with the 95% confidence bands of each fit. In each case the R^2 values of 0.988, 0.989 and 0.985 for total chlorophyll ($a + b$), chlorophyll *a* and chlorophyll *b*, respectively demonstrate a strong linear relationship between the green pixel intensity and chlorophyll concentration for the lower sample volume.

Comparing the low volume and control datasets, we found no significant difference between the slopes of the two lines ($p > 0.05$, **Table 3**); this is corroborated by the overlapping 95% confidence bands in each case.

Similarly, we found no significant difference between the intercepts of the low volume and control datasets ($p > 0.05$, **Table 3**).

During growth, even buffered cultures can vary in their pH owing to the consumption and release of carbon dioxide during photosynthesis and respiration. A selection of samples were transferred into high pH media (pH 9.5) immediately before being photographed in order to test the effect of pH on the RGB method. **Figure 5** shows the relationship between green pixel intensity and conventional chlorophyll quantification for high pH samples compared to the control dataset (7.0 < pH <8.5). The control dataset is present at a range of pH values owing to the increase in pH as the culture grows. The strong linear relationship is maintained despite the increase in pH as is evident from the high R^2 values ($R^2 > 0.995$ in each case).

We found a significant difference between the slopes of the high pH and control data for total chlorophyll and chlorophyll *a* ($p = 0.035$ and 0.009 respectively, **Table 4**). In contrast, for chlorophyll *b* there is no significant difference in the slope or intercept compared with that of the control data ($p = 0.383$) indicating that chlorophyll *b* concentration determined from the RGB color method is less sensitive to change in the culture pH. This can be seen clearly from the plots of the correlations against the control correlation (**Figure 5**). With the exception of chlorophyll *b*, the high pH correlation is steeper than the corresponding correlation for the control dataset.

E. coli was added at two different concentrations ($A_{600} \approx$ 1.0 and 0.25) to a range of *C. reinhardtii* samples to investigate the effect of bacterial contamination on the RGB method.

TABLE 3 | Regression parameters for "Low Volume" samples.

			Slope[a]		Intercept[b]	
	Equation	R^2	$F_{(1,33)}$	p	$F_{(1,34)}$	p
Chl $a + b$	$y = 0.00721(\pm0.00035)\,x + 0.00117(\pm0.00337)$	0.988	0.405	0.529	1.292	0.264
Chl a	$y = 0.01016(\pm0.00047)\,x + 0.00136(\pm0.00320)$	0.989	0.335	0.567	1.251	0.271
Chl b	$y = 0.02481(\pm0.00139)\,x + 0.00085(\pm0.00388)$	0.985	0.545	0.466	1.328	0.257

[a]*p-values indicating whether the slope of the fitted line is significantly different from that of the control dataset in each case.*
[b]*p-values indicating whether the intercept of the fitted line is significantly different from zero and from the control dataset in each case.*

TABLE 4 | Regression parameters for "High pH" samples.

			Slope[a]		Intercept[b]	
	Equation	R^2	$F_{(1,31)}$	p	$F_{(1,32)}$	p
Chl $a + b$	$y = 0.00782(\pm0.00021)\,x - 0.00316(\pm0.00186)$	0.997	4.868	0.035	–	–
Chl a	$y = 0.01137(\pm0.00026)\,x - 0.00204(\pm0.00154)$	0.998	7.890	0.009	–	–
Chl b	$y = 0.02493(\pm0.00104)\,x - 0.00530(\pm0.00292)$	0.993	0.783	0.383	1.825	0.186

[a]*p-values indicating whether the slope of the fitted line is significantly different from that of the control dataset in each case.*
[b]*p-values indicating whether the intercept of the fitted line is significantly different from zero and from the control dataset in each case.*

Figure 6 shows the relationship between the two methods for each concentration of *E. coli* (red) compared to the control dataset (gray). The clear linear relationship between the two methods is maintained despite the bacterial contamination ($R^2 >$ 0.995 in both cases). There was no significant difference between the slopes of the contaminated samples and control data for chlorophyll *a*, *b* or total chlorophyll concentration (**Table 5**).

However, when fitting two lines with the same slope, there was a significant difference between the intercepts of the contaminated and control datasets for both the high and low *E. coli* cases, except for low *E. coli* chlorophyll *b* (**Table 5**). This difference in the intercepts of the contaminated and control correlations can be clearly seen in **Figure 6**, indicating that the high *E. coli* contamination is causing a zero error in the intercept affecting the detection limit of the method. That can be easily corrected if the level of contamination is known.

When starved of nitrogen, microalgae typically accumulate neutral lipids and cellular chlorophyll content is seen to deplete; this is proposed to be due to recycling of the chloroplast membrane lipids in favor of neutral lipid accumulation as an energy store (Moellering and Benning, 2010; Valledor et al., 2014). Reduction in chlorophyll concentration therefore has the potential to be used in many cases as an early indicator of neutral lipid accumulation. To test the effect of this process on the RGB method, a series of samples at a three optical densities (A_{600} = 1.6 – 0.6) were transferred into TAP-N media and analyzed periodically, one sample per starting optical density over 8 days, as the chlorophyll content gradually decreased. **Figure 7** shows the effect of nitrogen starvation on the correlation between green pixel intensity and chlorophyll concentration; individual symbols represent different starting optical densities.

Decreasing initial culture absorbance (A_{600}) is shown to result in a decrease in the measured green pixel intensity at similar chlorophyll concentrations. Similarly, the green pixel intensity at zero chlorophyll concentration is shown to be dependent upon the initial optical density of the samples. For nitrogen starved *C. reinhardtii* there is a clear difference in the correlations between methods compared with that of the control dataset.

Table 6 gives the error generated, as a percentage of the actual value, if the standard curve for the control dataset is used to estimate chlorophyll concentration for each environmental variable; TAP-N correlations are not included owing to the poor similarity with the control. In each case, the green pixel intensity corresponding to the maximum and half maximum measurable chlorophyll concentrations for the control dataset are used to calculate the predicted and actual chlorophyll concentrations for each variable in order to calculate the generated errors.

For the low volume, high pH and low *E. coli* concentration the errors are typically $\leq$10% indicating only a relatively small overall error in the estimate of chlorophyll concentration. The standard curve for the control dataset could be used in each of these cases with relatively small errors. In contrast, there is a large error introduced when there is larger *E. coli* contamination,

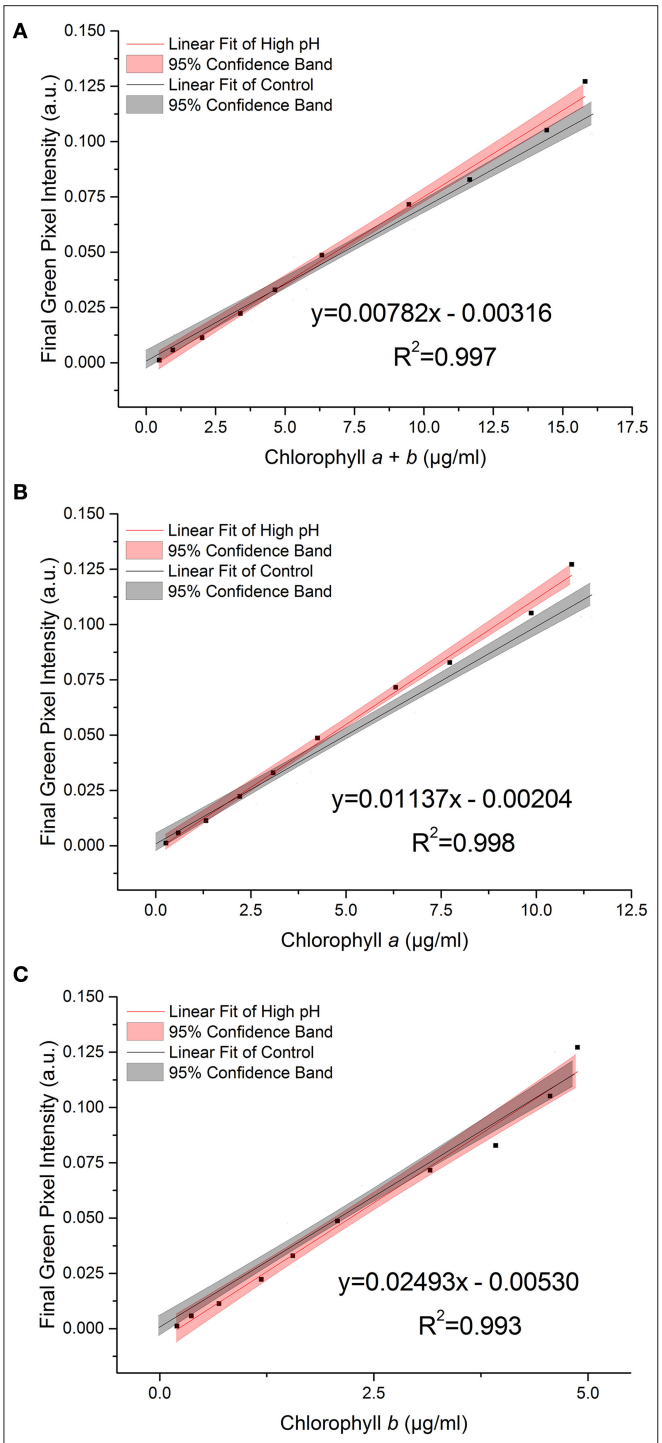

FIGURE 5 | The relationship between final green pixel intensity, calculated from the RGB color method, and **(A)** chlorophyll *a* + *b*, **(B)** chlorophyll *a* and **(C)** chlorophyll *b* concentrations, as measured by standard extraction method in 80% acetone, for a culture of *C. reinhardtii* photographed at two different culture pHs. Red = "high pH", pH 9.5 samples; Gray = control, pH 7.0–8.5 samples. Data points represent the mean green pixel intensity of three photographs (y) and the mean chlorophyll concentration of three sample aliquots (x).

with errors typically between 15 and 25%. Use of the standard curve of the control dataset would yield greater errors when high levels of contamination are present. The errors shown also corroborate that *E. coli* contamination induces a zero error in the intercept of the standard curve as can be seen from the increased percentage error at lower chlorophyll concentrations, while high pH results in an increased slope of the fit, seen from the reduced error at lower total chlorophyll and chlorophyll *a* concentrations.

DISCUSSION

This study presents a simple and non-destructive method by which the concentration of chlorophyll *a*, *b* and total chlorophyll of a microalgal culture can be estimated from the green pixel intensity of digital photographs using a standard calibration curve. The ability to determine chlorophyll *in situ* avoids repeated sampling, which is a problem with small culture volumes where there is insufficient material for repeated removal of sample, and which also risks introducing contamination. Compared with other digital image analysis methods (Su et al., 2008; Dey et al., 2016; Friedman et al., 2016), the method reported here needs only simple, easily available digital camera equipment and software and no complicated analysis. It should be easy to implement in different laboratory settings once a standard curve has been established for the specific experimental set up.

There is a strong linear relationship ($R^2 \geq 0.985$) between green pixel intensity, calculated from the tested method, and total chlorophyll concentration, as measured by a standard spectroscopic method with chlorophyll extraction in 80% (v/v) acetone/20% methanol (Porra et al., 1989) for a sterile culture of *C. reinhardtii* in TAP media (pH 7.0–8.5), photographed at a sample volume of 5 ml, up to a concentration of 16 µg/ml total chlorophyll (green pixel intensity = 0.125). Above this, the gradient of the slope decreases indicating the curve tends toward a plateau at high chlorophyll concentration. From this, the limit of sensitivity for the method has been estimated at a green pixel intensity of 0.125 and therefore samples with higher chlorophyll concentration (>16 µg/ml) should be diluted to fall within the linear interval of the RGB method.

A selection of commonly encountered environmental variables were chosen to investigate the sensitivity of the method to environmental interference. For each variable investigated, the excellent linear relationship between green pixel intensity and chlorophyll concentration was maintained.

Statistical analysis revealed no significant difference in the green pixel intensity/chlorophyll correlation when the photographed sample volume was decreased. This indicates that the method is insensitive to this factor and a single standard curve created could be used to estimate chlorophyll concentration. This is particularly important for time-course studies where the culture volume may be reduced gradually over time as a result of other analyses.

In contrast, we found that there is a statistically significant increase in the slope of the green pixel intensity/chlorophyll

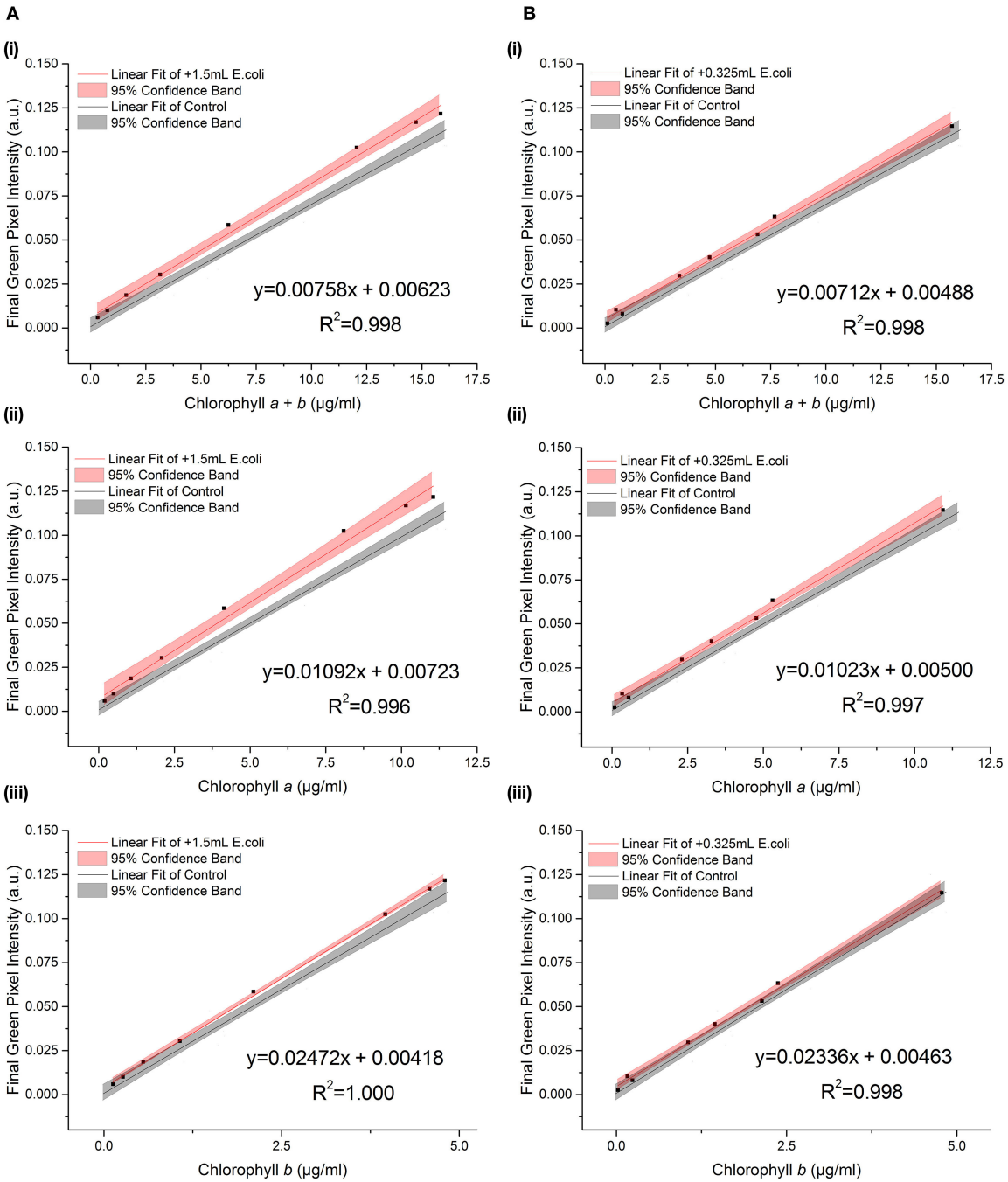

FIGURE 6 | The relationship between final green pixel intensity, calculated from the RGB color method, and (i) chlorophyll *a* + *b*, (ii) chlorophyll *a* and (iii) chlorophyll *b* concentrations, as measured by standard extraction method in 80% acetone, for a culture of *C. reinhardtii* contaminated with two different concentrations of *E. coli*. **(A)**: Red = addition of 1.5 ml E. coli ($A_{600} \approx 1.0$); Gray = control, sterile samples. **(B)**: Red = addition of 0.325 ml E. coli ($A_{600} \approx 0.25$); Gray = control, sterile samples. Data points represent the mean green pixel intensity of three photographs (y) and the mean chlorophyll concentration of three sample aliquots (x).

correlation for both total chlorophyll and chlorophyll *a* when pH is increased. **Figure 8** shows the visible range absorbance spectra for a culture of *C. reinhardtii* at pH 7.0 and 9.5. For the sake of comparison, the pH 9.5 spectrum has been adjusted to a total chlorophyll concentration equivalent to that of the pH 7.0 sample, assuming a directly proportional relationship between total chlorophyll concentration and biomass optical density. As can be seen from the spectra, the higher pH sample has a lower

TABLE 5 | Regression parameters for contaminated samples.

				Slope[a]		Intercept[b]	
		Equation	R^2	$F_{(1,29)}$	p	$F_{(1,30)}$	p
+1.5 ml *E. coli*	Chl *a* + *b*	$y = 0.00758(\pm0.00022)\,x + 0.00623(\pm0.00198)$	0.998	2.526	0.123	16.156	<0.001
	Chl *a*	$y = 0.01092(\pm0.00041)\,x + 0.00723(\pm0.00257)$	0.996	3.542	0.070	21.394	<0.001
	Chl *b*	$y = 0.02472(\pm0.00025)\,x + 0.00418(\pm0.00071)$	1.000	0.623	0.436	5.301	0.028
+0.325 ml *E. coli*	Chl *a* + *b*	$y = 0.00712(\pm0.00019)\,x + 0.00488(\pm0.00132)$	0.998	0.142	0.709	4.704	0.038
	Chl *a*	$y = 0.01023(\pm0.00029)\,x + 0.00500(\pm0.00139)$	0.997	0.395	0.535	6.233	0.018
	Chl *b*	$y = 0.02336(\pm0.00056)\,x + 0.00463(\pm0.00118)$	0.998	0.022	0.882	1.894	0.179

[a] *p-values indicating whether the slope of the fitted line is significantly different from that of the control dataset in each case.*
[b] *p-values indicating whether the intercept of the fitted line is significantly different from zero and from the control dataset in each case.*

TABLE 6 | Percentage error generated when using control data standard curve to estimate chlorophyll concentration in the presence of environmental interference*.

	Total chlorophyll		Chl *a*		Chl *b*	
	% error at max	% error at half max	% error at max	% error at half max	% error at max	% error at half max
Low volume	4.3	4.6	3.9	4.4	5.1	5.2
High pH	8.8	5.2	12.9	10.2	0.1	−4.8
+1.5 ml *E. coli*	14.9	21.1	17.8	25.3	7.9	11.4
+0.325 ml *E. coli*	6.4	10.7	8.1	12.4	2.4	6.2

**Percentages are calculated at the maximum measurable and half maximum measurable chlorophyll concentration from the control data standard curve.*

absorbance in the green region of the spectrum (∼520–560 nm) and higher absorbance in both the red (∼630–750 nm) and blue (∼450–490 nm) regions of the spectrum. These differences will result in the culture presenting with a stronger green color and are likely responsible for the increased green pixel intensity of the high pH samples at similar chlorophyll concentrations given that green pixel intensity is defined as the ratio of the green pixel component over the sum of red, green and blue components (Equation 1). This increase in green color at high pH may be as a result of chlorophyll conversion to chlorophyllin which occurs via the removal of a hydrocarbon side chain and replacement of the central magnesium ion with copper; copper chlorophyllin has a much more intense green color compared with non-copper chlorophyll (Kendrick, 2012).

Addition of *E. coli* ($A_{600} \approx 1.0$) revealed a significant increase in the intercept of the green pixel intensity/chlorophyll regression for total chlorophyll and chlorophyll *a*, as can be seen from **Figure 6**. It is likely that a zero error in the intercept is being induced by the opacity of *E. coli* even in the absence of algal biomass. The magnitude of this error was, as expected, higher for high levels of contamination. Given that there is no significant difference in the slope of the line with *E. coli* contamination, the zero error in the intercept could likely be corrected for where the level of contamination is known.

These observed differences in the lines for the *E. coli* and high pH cases were much lower, or absent, for chlorophyll *b* than total chlorophyll and chlorophyll *a*. The reason for this is not understood but indicates chlorophyll *b*, as calculated from the RGB method, is less sensitive to changing environmental conditions. The control correlation could be used as a standard curve to estimate chlorophyll *b* concentration from green pixel intensity despite the environmental interferences investigated.

In contrast to the other environmental interferences investigated, there is a very clear difference between the correlations for nitrogen starved samples compared with that of the control dataset. For each initial biomass concentration, the slope of the correlation is much shallower than that of the control dataset and there is a clear increase in the intercept of the correlation with increasing initial biomass concentration. Both these factors would result in a significant overestimation of the chlorophyll concentration from the green pixel intensity if the original standard curve is used. We propose that this is most likely due to the yellow color of the lipids as chlorophyll concentration decreases. Given the proximity of yellow and green within the visible spectrum, the residual yellow color will likely cause significant interference with the green pixel intensity. The green component of the RGB scale has previously

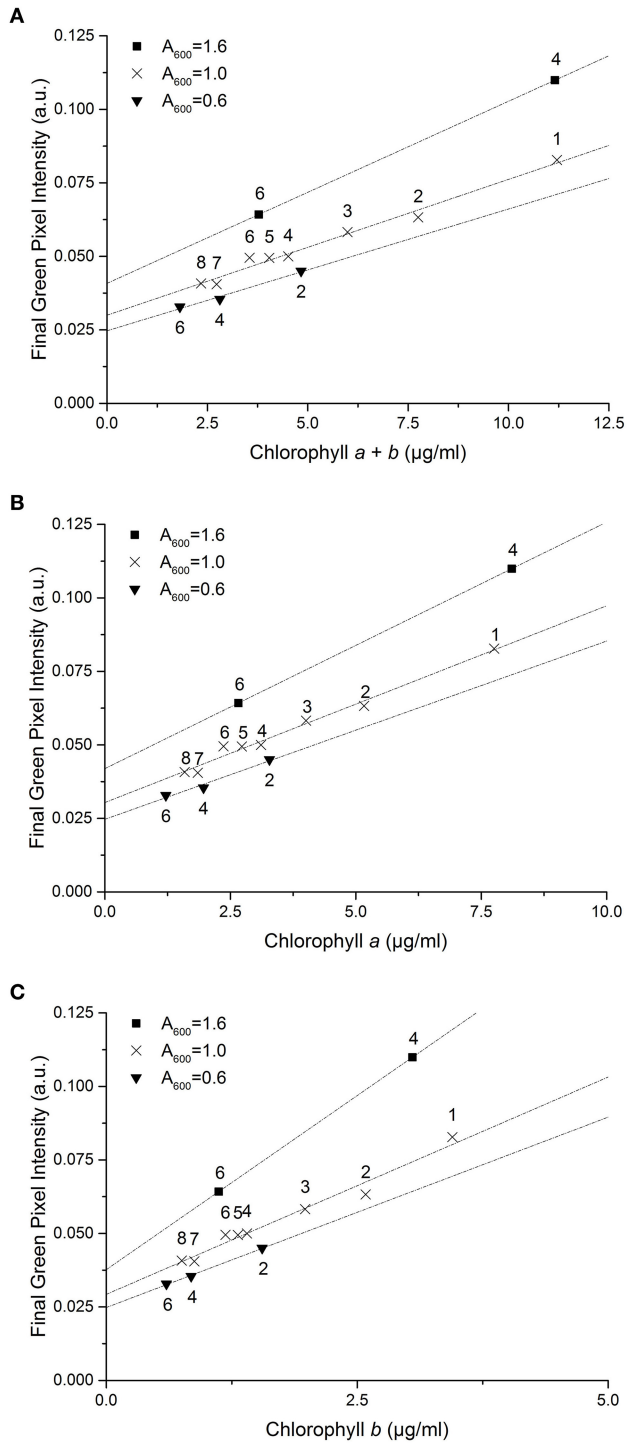

FIGURE 7 | The correlation between final green pixel intensity, calculated from the RGB color method, and **(A)** chlorophyll *a* + *b*, **(B)** chlorophyll *a* and (**C**) chlorophyll *b* concentrations, as measured by standard extraction method in 80% acetone, for a culture of *C. reinhardtii* in TAP-N media and photographed over 8 days with three initial starting biomass concentrations as indicated by the different A_{600} values. Numbers above data points represent the number of days after inoculation that analysis took place. Data points represent the mean green pixel intensity of three photographs (y) and the mean chlorophyll concentration of three sample aliquots (x) and lines represent linear fits through the points.

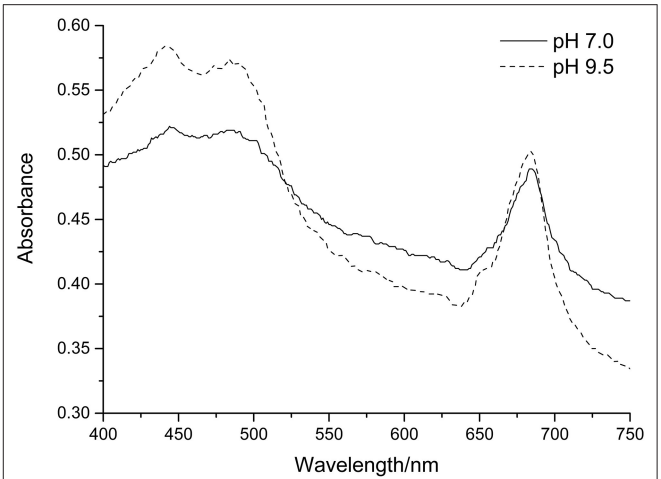

FIGURE 8 | Absorption spectra of *C. reinhardtii* in Tris-Acetate-Phosphate (pH 7.0) and CAPS-Acetate-Phosphate (pH 9.5) media. In each case spectra have been normalized to a chlorophyll *a* + *b* concentration = 7.5 μg/ml.

been shown to be significant when estimating the lipid content of a microalgal culture using digital image analysis (Su et al., 2008). Without a significant correction for lipid accumulation, the developed method is not suitable for estimating chlorophyll concentration when chlorophyll concentration is reduced as a result of nitrogen starvation due to interference from neutral lipid accumulation. Despite this, the method could be applied to qualitatively determine if chlorophyll concentration is increasing/decreasing.

This method extends other digital analysis methods by investigating its applicability over a wide range of commonly encountered environmental variables. The insensitivity of this method to small changes in sample volume and low concentrations of bacterial contamination means that the method could be used with a single standard curve in spite of these changes, making this method useful for a range of experimental investigations. The method is also shown to be useful when high levels of bacterial contamination are present or with a variable culture pH, however these conditions may lead to higher errors in the estimation of total chlorophyll and chlorophyll *a*. In addition, the method is unique in its minimal use of data processing all of which can be conducted through widely accessible software packages.

CONCLUSIONS

Digital image analysis has been used to develop an inexpensive and rapid method to estimate chlorophyll *a*, *b* and total chlorophyll concentration of an algal culture without sample destruction. Comparison of the Green Pixel Intensity (GPI) method described and a standard spectroscopic method for chlorophyll quantification of a culture of *C. reinhardtii* CC-1690 revealed a strong linear correlation ($R^2 > 0.985$) up to a green pixel intensity of 0.125, corresponding to a total chlorophyll

concentration of 16 μg/ml in this case. The standard curve created is robust despite changes in sample volume and small quantities of bacterial contamination and can therefore be used in these cases without modification. Increasing pH resulted in a small increase in the slope of the GPI/chlorophyll correlation but errors in chlorophyll estimation remained small. In contrast, large quantities of bacterial contamination result in an error in the intercept of the standard curve leading to overestimations of chlorophyll concentration. It is likely that correction factors could be found and applied where the level of contamination is known. Lipid accumulation, as a result of nitrogen deprivation, resulted in significant changes to the GPI/chlorophyll correlation proposed to be due to yellowing of the culture as chlorophyll was depleted and neutral lipids accumulated. As such the method, as it stands, is not appropriate for cultures with reduced chlorophyll concentrations as a result of significant lipid accumulation.

This method has the potential to be applied widely to different algal culture situations or even environmental samples, particularly in situations where sample and equipment availability may be limited. This could include, for example, field laboratories and laboratories in developing countries, school laboratories or citizen science projects. It would require following the methodology described to construct a standard curve relating chlorophyll content to GPI for the specific algal species, culture vessel and photographic set up. Although the experiments presented here used an iPhone 5S and Microsoft Paint, in principle any digital camera and software capable of analyzing RGB pixel intensity could be used as long as the conditions used for establishing the standard curve (growth, photographic set up, and software) are subsequently replicated precisely for the experimental samples. To the best of our knowledge, the simplicity and accessibility of this method is unique compared with other non-invasive chlorophyll quantification methods, requiring very little equipment, expertise or specialist software.

DATA AVAILABILITY STATEMENT

All datasets generated for this study are included in the article/**Supplementary Material**.

AUTHOR CONTRIBUTIONS

NW contributed to the conception and design of experimental work, collection, assembly and analysis of the data and produced the article draft. AB and MC-V contributed to the conception and design of experimental work and critically revised the article. RQ contributed to the statistical analysis and interpretation of the data, and critically revised the article. All authors read and approved the submitted manuscript.

FUNDING

NW was supported by UK Research and Innovation (UKRI) through the EPSRC Centre for Doctoral Training in Bioenergy, University of Leeds (grant number EP/L014912/1). Work in AB and MC-V laboratories is supported by a grant award from the Biotechnology and Biological Sciences Research Council - BBSRC (BB/N016033/ 1).

ACKNOWLEDGMENTS

We thank Dr. Brahim Achour for his advice on the statistical analyses and the presentation of figures, Dr. Travis Beddoe for providing *E. coli* for sensitivity analysis and Dr. Lili Chu for helpful discussion and advice.

SUPPLEMENTARY MATERIAL

The Supplementary Material for this article can be found online at: https://www.frontiersin.org/articles/10.3389/fbioe.2020.00746/full#supplementary-material

REFERENCES

Armbruster, D. A., and Pry, T. (2008). Limit of blank, limit of detection and limit of quantitation. *Clin. Biochem. Rev.* 29, S49–S52.

Buschmann, C., Langsdorf, G., and Lichtenthaler, H. (2000). Imaging of the blue, green, and red fluorescence emission of plants: an overview. *Photosynthetica* 38, 483–491. doi: 10.1023/A:1012440903014

Chisti, Y. (2007). Biodiesel from microalgae. *Biotechnol. Adv.* 25, 294–306. doi: 10.1016/j.biotechadv.2007.02.001

Chlamydomonas Resource Center. (2016). TAP and Tris-minimal (online). Available online at: https://www.chlamycollection.org/methods/media-recipes/tap-and-tris-minimal/ (accessed November 10, 2016).

Dey, A. K., Sharma, M., and Meshram, M. R. (2016). An analysis of leaf chlorophyll measurement method using chlorophyll meter and image processing technique. *Proc. Comput. Sci.* 85, 286–292. doi: 10.1016/j.procs.2016.05.235

Faul, F., Erdfelder, E., Buchner, A., and Lang, A.-G. (2009). Statistical power analyses using G*Power 3.1: tests for correlation and regression analyses. *Behav. Res. Methods* 41, 1149–1160. doi: 10.3758/BRM.41.4.1149

Friedman, J. M., Hunt Jr, E. R., and Mutters, R. G. (2016). Assessment of leaf color chart observations for estimating maize chlorophyll content by analysis of digital photographs. *Agron. J.* 108, 822–829. doi: 10.2134/agronj2015.0258

Goncalves, E. C., Wilkie, A. C., Kirst, M., and Rathinasabapathi, B. (2016). Metabolic regulation of triacylglycerol accumulation in the green algae: identification of potential targets for engineering to improve oil yield. *Plant Biotechnol. J.* 14, 1649–1660. doi: 10.1111/pbi.12523

Gorman, D. S., and Levine, R. P. (1965). Cytochrome F and plastocyanin: their sequence in the photosynthetic electron transport chain of *Chlamydomonas reinhardi*. *Proc. Natl. Acad. Sci. U.S.A.* 54, 1665–1669. doi: 10.1073/pnas.54.6.1665

Gupta, S. D., Ibaraki, Y., and Pattanayak, A. K. (2013). Development of a digital image analysis methods for real-time estimation of chlorophyll content in micropropagated potato plants. *Plant Biotechnol. Rep.* 7, 91–97. doi: 10.1007/s11816-012-0240-5

Horwitz, W., Kamps, L. R., and Boyer, K. W. (1980). Quality assurance in the analysis of foods and trace constituents. *J. Assoc. Off. Anal. Chem.* 63, 1344–1354. doi: 10.1093/jaoac/63.6.1344

Kendrick, A. (2012). *Natural Food Additives, Ingredients and Flavourings: 2 – Natural Food and Beverage Colourings*. Cambridge, UK: Woodhead Publishing Series in Food Science, Technology and Nutrition, 24–40. doi: 10.1533/9780857095725.1.25

Liu, B., and Benning, C. (2013). Lipid metabolism in microalgae distinguishes itself. *Curr. Opin. Biotechnol.* 24, 300–309. doi: 10.1016/j.copbio.2012.08.008

Moellering, E. R., and Benning, C. (2010). RNA interference silencing of a major lipid droplet protein affects lipid droplet size in *Chlamydomonas reinhardtii*. *Eukaryot. Cell* 9, 97–106. doi: 10.1128/EC.00203-09

Netto, A. T., Campostrini, E., de Oliveira, J. G., and Bressan-Smith, R. E. (2005). Photosynthetic pigments, nitrogen, chlorophyll a fluorescence and SPAD-502 readings in coffee leaves. *Sci. Hortic.* 104, 199–209. doi: 10.1016/j.scienta.2004.08.013

Porra, R. J., Thompson, W. A., and Kriedemann, P. E. (1989). Determination of accurate extinction coefficients and simultaneous equations for assaying chlorophylls a and extracted with four different solvents: verification of the concentration of chlorophyll standards by atomic absorption spectroscopy. *Biochem. Biophys. Acta* 975, 384–394. doi: 10.1016/S0005-2728(89)80347-0

Rignon, J. P. G., Capuani, S., Fernandes, D. M., and Guimarães, T. M. (2016). A novel method for the estimation of soybean chlorophyll content using a smartphone and image analysis. *Photosynthetica* 54, 559–566. doi: 10.1007/s11099-016-0214-x

Siaut, M., Cuiné, S., Cagnon, C., Fessler, B., Nguyen, M., Carrier, P., et al. (2011). Oil accumulation in the model green alga *Chlamydomonas reinhardtii*: characterisation, variability between common laboratory strains and relationship with starch reserves. *BMC Biotechnol.* 11:7. doi: 10.1186/1472-6750-11-7

Su, C.-H., Fu, C.-C., Chang, Y.-C., Nair, G. R., Ye, J.-L., Chu, I.-M., et al. (2008). Simultaneous estimation of chorophyll a and lipid contents in microalgae by three-color analysis. *Biotechnol. Bioeng.* 99, 1034–1039. doi: 10.1002/bit.21623

Valledor, L., Furuhashi, T., Recuenco-Muñoz, L., Wienkoop, S., and Weckwerth, W. (2014). System-level network analysis of nitrogen starvation and recovery in *Chlamydomonas reinhardtii* reveals potential new targets for increased lipid accumulation. *Biotechnol. Biofuels* 7, 171–187. doi: 10.1186/s13068-014-0171-1

Vincent, W. F. (1983). Fluorescence properties of the freshwater phytoplankton: three algal classes compared. *Br. Phycol. J.* 18, 5–21. doi: 10.1080/00071618300650021

Wang, H., Zhu, R., Zhang, J., Ni, L., Shen, H., and Xie, P. (2018). A novel and convenient method for early warning of algal cell density by chlorophyll fluorescence parameters and its application in a highland lake. *Front. Plant Sci.* 9:869. doi: 10.3389/fpls.2018.00869

Wijffels, R. H., and Barbosa, M. J. (2010). An outlook on microalgal biofuels. *Science* 329, 796–799. doi: 10.1126/science.1189003

Wood, A. M., Everroad, R. C., and Wingard, L. M. (2005). "Chapter 18: Measuring growth rates in microalgal cultures," in *Algal Culturing Techniques*, ed R. A. Andersen (Burlington, MA; San Diego, CA; London, UK: Elsevier Academic Press) 269–286.

Conflict of Interest: The authors declare that the research was conducted in the absence of any commercial or financial relationships that could be construed as a potential conflict of interest.

frontiers in Bioengineering and Biotechnology

ORIGINAL RESEARCH
published: 21 August 2020
doi: 10.3389/fbioe.2020.00978

Effect of Membrane Hydrophobicity and Thickness on Energy-Efficient Dissolved Oxygen Removal From Algal Culture

Masatoshi Kishi[1,2]*, *Kenta Nagatsuka*[1] and *Tatsuki Toda*[2,3]

[1] Faculty of Science and Engineering, Soka University, Tokyo, Japan, [2] Plankton Eco-Engineering Research Center, Soka University, Tokyo, Japan, [3] Graduate School of Science and Engineering, Soka University, Tokyo, Japan

Removal of dissolved oxygen from algal photobioreactors is essential for high productivity in mass cultivation. Gas-permeating photobioreactor that uses hydrophobic membranes to permeate dissolved oxygen (pervaporation) from its body itself is an energy-efficient option for oxygen removal. This study comparably evaluated the characteristics of various commercial membranes and determined the criteria for the selection of suitable ones for the gas-permeating photobioreactors. It was found that oxygen permeability is limited not by that in the membrane but in the liquid boundary layer. Membrane thickness had a negative effect on membrane oxygen permeability, but the effect was as minor as less than 3% compared with the liquid boundary layer. Due to this characteristic, the lamination of non-woven fabric with the microporous film did not significantly decrease the overall oxygen transfer coefficient. The permeability in the liquid boundary layer had a significantly positive relationship with the hydrophobicity. The highest overall oxygen transfer coefficients in the water-to-air and water-to-water oxygen removal tests were $2.1 \pm 0.03 \times 10^{-5}$ and $1.39 \pm 0.09 \times 10^{-5}$ m s^{-1}, respectively. These values were considered effective in the dissolved oxygen removal from high-density algal culture to prevent oxygen inhibition. Furthermore, hydrophobicity was found to have a significant relationship also with water entry pressure, which needs to be high to avoid culture liquid leakage. Therefore, these results suggested that a microporous membrane with strong hydrophobicity laminated with non-woven fabric would be suitable characteristics for gas-permeating photobioreactor.

Keywords: dissolved oxygen, gas-permeating, hydrophobicity, microporous membrane, thickness, pervaporation

OPEN ACCESS

Edited by:
Ao Xia,
Chongqing University, China

Reviewed by:
Zhanyou Chi,
Dalian University of Technology, China
Kit Wayne Chew,
Xiamen University Malaysia, Malaysia

***Correspondence:**
Masatoshi Kishi
masa-kishi@soka.gr.jp

Specialty section:
This article was submitted to Bioprocess Engineering, a section of the journal Frontiers in Bioengineering and Biotechnology

Received: *06 June 2020*
Accepted: *27 July 2020*
Published: *21 August 2020*

Citation:
Kishi M, Nagatsuka K and Toda T (2020) Effect of Membrane Hydrophobicity and Thickness on Energy-Efficient Dissolved Oxygen Removal From Algal Culture. Front. Bioeng. Biotechnol. 8:978. doi: 10.3389/fbioe.2020.00978

INTRODUCTION

Microalgal mass-cultivation techniques for the production of pharmaceuticals, cosmetics, nutritional supplements, biomaterials, and biofuels have been widely studied over the decades (Burlew, 1953; Behera et al., 2015; Woortman et al., 2020). For the improvement of algal productivity, various components of algal cultivation have been intensively studied, including control and optimization of pH, culture medium, temperature, nutrient supply, and reactor design (Yew et al., 2019). While the high-density microalgal culture in a closed reactor is advantageous for high-quality biomass and low harvesting cost (Richmond., 2013), photosynthetic oxygen easily

accumulates and inhibit the algal growth (Weissman et al., 1988; Kazbar et al., 2019). For example, the dissolved oxygen concentration exceeded 70 mg L^{-1} (more than 6 times the air saturation) in the outdoor *Arthrospira platensis* culture, at which the chlorophyll synthesis decreased to less than half (Torzillo et al., 1998). Prolonged exposure to high oxygen concentration can further lead to cell lysis (Vonshak et al., 1996). Especially in outdoor strong light conditions, the effect of oxygen inhibition increases owing to photorespiration (Shelp and Canvin, 1980; Molina et al., 2001). It is therefore necessary to reduce dissolved oxygen concentration. The most common and effective method of oxygen removal in a closed reactor is aeration. However, the aeration requires considerable high energy demand, and it may consist of 40% of the total cultivation and harvesting cost (Norsker et al., 2011). Low-cost oxygen removal is therefore a great concern in algal mass-cultivation.

A recently developed concept of gas-permeating photobioreactor has demonstrated that a bag reactor partially made of a microporous film enables non-aerated dissolved oxygen removal by diffusion through the surface through pervaporation process (Kishi, 2018). This reactor was constructed by attaching a transparent plastic film and a microporous gas-permeating film, so that accumulated oxygen escapes to the atmosphere through the membrane without extensive aeration (**Figure 1**). Furthermore, the white membrane reflects the irradiated light inside the reactor enabling efficient light utilization. Under low mixing and aeration frequency, a significantly higher cyanobacterial growth was observed in the gas-permeating reactor compared with that in the conventional plastic bag reactor. This gas-permeating reactor may reduce the culture energy by 80 to 90% according to the results (Kishi, 2018) and can potentially be effective especially for high-value algal products that require closed conditions.

There have been many studies that used membranes for gas exchange in algal reactors such as for carbon dioxide supply (Lee and Hing, 1989; Pörs et al., 2010; Kim et al., 2011; Thrane et al., 2015; Mortezaeikia et al., 2016; Shesh et al., 2019). A recent floating bag reactor used gas-permeable membrane as a part of the sealing for oxygen release (Zhu et al., 2018b), but the membrane was meant to support the gas-gas exchange between the reactor headspace and the atmosphere. If the gas-permeating membrane is used as an interface between algal culture and the atmosphere (or water in the case of the submerged reactor), the specific surface of the membrane can be made large enough to remove the excess amount of oxygen via pervaporation. While gas-gas permeation is relatively simple because of negligible gas-boundary resistance, liquid-gas pervaporation is more complex since the liquid boundary layer often exhibit large resistance (Carvalho and Malcata, 2001).

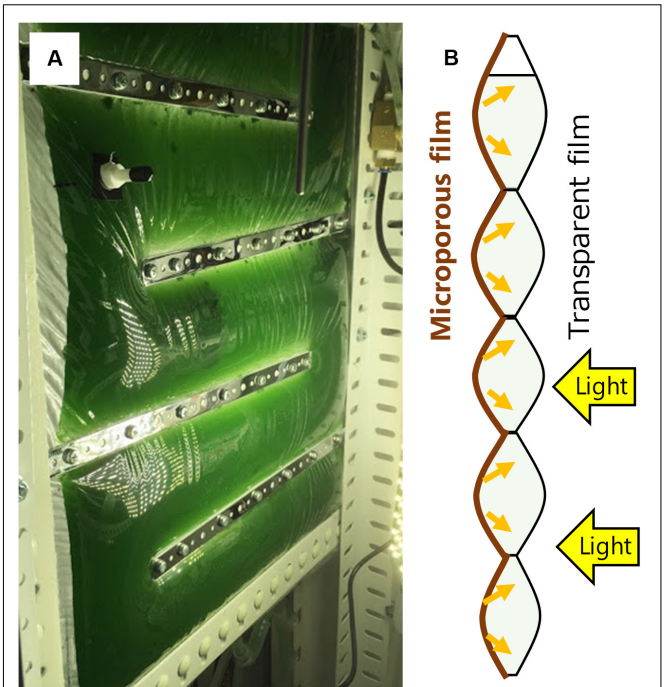

FIGURE 1 | Gas-permeating algal photobioreactor **(A)** photo of the reactor in *Arthrospira platensis* culture; **(B)** Side view of a schematic diagram of the reactor [modified from Kishi (2018)]. Oxygen is removed from the microporous film side by diffusion. Light enters from the transparent film and reflects at the microporous film.

Oxygen removal through pervaporation has been attempted for semiconductors, beverages, and pharmaceuticals (Ito et al., 1998), but only a few studies have attempted dissolved oxygen removal from algal reactors through a membrane. Furthermore, most previous studies focused on the hollow-fiber membrane (Jana et al., 2017; Bazhenov et al., 2018; Su and Wei, 2019), while the gas-permeating photobioreactor utilizes a simple film as a part of the bag reactor surface that sustains the culture liquid. This structural difference creates differences in necessary criteria of membrane characteristics, namely tensile strength and water entry pressure, which is not necessarily important in hollow-fiber reactors. Thus, there is a need to characterize and select suitable membranes that have both high oxygen permeability and physical strength.

The membrane characteristics (e.g., material, pore size, thickness, and hydrophobicity) influence properties important in gas-permeating reactors, including oxygen permeability, physical strength (tensile strength and water entry pressure), and optical characteristics. Some characteristics such as thickness have both positive and negative effects; for instance, thicker membranes possess higher strength while having lower gas permeability. To select suitable membranes for the gas-permeating reactor, a comprehensive characterization of various properties is needed. Therefore, this study aimed to characterize different commercially available membranes and to reveal their effects on the properties of the gas-permeating reactor so that

Abbreviations: k_A, oxygen transfer coefficient in the boundary layer in the Room A (low oxygen side) [m s^{-1}]; K_{AA}, K_{WA}, K_{WW}, overall oxygen transfer coefficient for Air-Air, Water-Air, and Water–Water permeation conditions, respectively, [m s^{-1}]; k_B, oxygen transfer coefficient in the boundary layer in the Room B (high oxygen side) [m s^{-1}]; k_M, oxygen transfer coefficient in the membrane [m s^{-1}]; MP, microporous films; NP, non-porous films; NW, microporous films with non-woven fabric support; PE, polyethylene; PP, polypropylene; PTFE, polytetrafluoroethylene; WP, woven porous films.

dissolved oxygen can be removed from a closed system without intensive energy.

MATERIALS AND METHODS

Tested Films

The tested commercial films differed in materials (polyethylene [PE], polypropylene [PP], polytetrafluoroethylene [PTFE], or nylon), pore characteristics, attachment of non-woven fabric, and structure (stretched or woven) (**Table 1**). The films were categorized into four groups: standard microporous films (MP), a microporous film with non-woven fabric support (NW), woven porous film (WP), and non-porous films (NP). Silicone rubber film (NP-S) and polypropylene film (NP-P) were included as a comparison with the porous films. The thickness of NW films was measured using the scanning electron microscope. For the other films, the thickness value was derived from product information.

Theory and Experimental Design of Oxygen Permeation

In gas permeation through the membrane, the permeability depends on the overall resistance ($1/K$) that is the sum of resistance at the membrane ($1/k_M$) and in the fluid boundary layers on both sides of the membrane ($1/k_A$ and $1/k_B$) (Carvalho and Meireles, 2006; Raisi and Aroujalian, 2011):

$$\frac{1}{K} = \frac{1}{k_A} + \frac{1}{k_M} + \frac{1}{k_B} \quad (1)$$

where K is the overall transfer coefficient, k_i is the transfer coefficients for respective layers. For the case of gas to gas permeation, the gas diffusivity is much larger than that in the membrane, and thus oxygen permeability depends on the membrane (Yamamoto and Nakajima, 1979; Côté et al., 1989). Based on this assumption, Air-Air gas permeation was assumed to solely rely on membrane resistance, and Eq. 1 can be simplified to:

$$\frac{1}{K_{AA}} = \frac{1}{k_M} \quad (2)$$

Similarly, in the case of Water-Air permeation, the resistance in the membrane and liquid boundary layer becomes the rate-limiting (Brüschke, 1990; Carvalho and Malcata, 2001; Raisi and Aroujalian, 2011). Thus, the overall resistance was assumed as the sum of the membrane and liquid boundary:

$$\frac{1}{K_{WA}} = \frac{1}{k_M} + \frac{1}{k_B} \quad (3)$$

On another hand, Water–Water permeability requires consideration of resistance in all three layers:

$$\frac{1}{K_{WW}} = \frac{1}{k_A} + \frac{1}{k_M} + \frac{1}{k_B} \quad (4)$$

In this estimation, k_M and k_B were assumed to remain constant throughout different permeation test conditions.

Upon the above presumptions, oxygen permeability of the membrane was evaluated under three conditions of Air-Air, Water-Air, and Water–Water phases (**Figure 2**). Oxygen permeability was measured using a hand-made acrylic device composed of two rooms (A and B). Room A was continuously flushed with water or air with an oxygen concentration of

TABLE 1 | Characteristics of the membranes used in this study.

ID	Material	Thickness (μm)	Pore size (μm)	Porosity (%)	Product name	Company	Model number
Microporous film							
MP1-1	PE	25	0.1	80	Miraim	Teijin	01–20
MP1-2	PE	30	0.2	80			02–35
MP1-3	PE	75	0.5	80			05–75
MP2	PP	38	0.3	21	Microporous Film	3M	–
MP3-1	PTFE	30	0.2	N.D.	Poreflon	Sumitomo	HP-020-30
MP3-2	PTFE	60	0.22	N.D.			FP-022-60
MP3-3	PTFE	80	0.2	N.D.			WP-020-80
Microporous film with non-woven fabric support							
NW1-1	PE	45*	N.D.	N.D.	Breathron	Nitto	BRN3000E1
	(Cloth: PET)	205*	N.D.	N.D.			
NW1-2	PE	50*	N.D.	N.D.			BRN-1860
	(Cloth: Nylon)	300*	N.D.	N.D.			
Woven porous film							
WP	Nylon	40	N.D.	N.D.	Silfine	Toyobo	EL1044PWR3
Non-porous film							
NP-S	Silicone	500	–	–	Silicone Rubber Sheet	Togawa Rubber	–
NP-PP	PP	50	–	–	Pylen	Toyobo	P8128

*PE: polyethylene; PET: polyethylene terephthalate; PP: polypropylene; PTFE: polytetrafluoroethylene. N.D. no data; – not applicable; *Data measured with scanning electron microscopy. Other data were obtained from the product datasheet.*

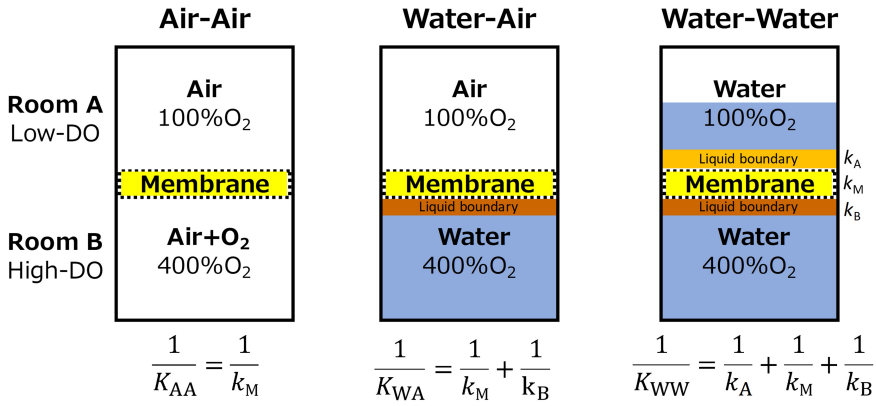

FIGURE 2 | Design of oxygen permeability tests. Overall oxygen transfer coefficient (K) of each condition was used to deduce the transfer coefficient within the membrane (k_M), upper liquid boundary (k_A), and lower liquid boundary (k_B). Transfer resistant between air and membrane was assumed to be negligible.

100%air-saturation, while Room B contained high oxygen concentration (400%air-saturation) water or air. Using Eq. 1–3, the overall mass transfer coefficients (K) of each three conditions were used to estimate the transfer coefficient of (1) membrane (k_M), (2) liquid boundary layer in Room B (k_B), and (3) liquid boundary layer in Room A (k_A).

The overall mass transfer coefficient K (m s^{-1}) was estimated from the change of the dissolved oxygen concentration in Room B (C_B; %air-saturation) using the following equation:

$$\log\frac{C_B(0) - C_A}{C_B(t) - C_A} = Kat \quad (5)$$

where t is the elapsed time (s); C_A is the dissolved oxygen concentration in Room A that was kept at 100%air-saturation; a is the specific surface of membrane over the volume of Room B (14.3 m^{-1}).

Analysis

Dissolved as well as gaseous oxygen concentration was measured using an optical oxygen sensor (FireStingO2, PyroScience) with contactless oxygen sensor spots (OXSP5, PyroScience). Film hydrophobicity was evaluated by a contact angle of 20 μL distilled water. Optical characteristics were measured using a spectrophotometer (UV-2450, Shimadzu) equipped with an integrating sphere. The absorption and reflection spectra of the wavelength between 400 and 700 nm were integrated to obtain total absorbance, transmittance, and reflectance of photosynthetically available radiations.

Tensile strength (N cm^{-1}) was measured for MP3-1, NW1-2, WP, and NP-P using a material analyzer (A&D). The films were cut into 10 × 100 mm test strip for both horizontal and vertical direction. The tensile strength values for MP1 series and MP2 were obtained from their product datasheets. For standardization purposes, the more durable direction of the film was annotated as the vertical direction. Water entry pressure is the minimum pressure required to force water through the pores of a hydrophobic membrane, and its data was derived from product information for data analysis.

Statistical Analysis

Linear regression analysis was used to determine relationships between membrane characteristics and functionality. All analyses were measured for at least three times except for the contact angle measurement, and average data was used for the regression analysis. $P < 0.05$ was considered significant.

RESULTS

Oxygen Permeability Test

Air–Air Permeability

The Air-Air permeability test was implemented to estimate membrane permeability k_M (Eq. (2)). The lowest membrane permeability was observed with polypropylene film (NP-P), which was about 10^4 smaller than microporous films (**Table 2**). Silicone rubber (NP-S) had nearly 5 times higher transfer coefficient than NP-P but was still a few magnitudes lower than microporous films. All microporous films had similar permeability despite different pore sizes, thickness, and material. Woven porous (WP) had significantly lower k_M than microporous films, and attachment of non-woven fabric support (NW) further decreased the membrane permeability. Within the NW products, the k_M of NW1-2 was approximately 5 times lower than NW1-1.

The membrane oxygen permeability k_M had a significant linear relationship with the thickness of permeable membranes excluding NP-P (**Figure 3**). Within the range of tested film, there was no correlation of k_M with pore size or porosity.

Water-Air Permeability

Compared with the Air-Air condition, the oxygen transfer coefficients decreased to nearly 1% (**Table 2**). While NW had lower transfer coefficients than MP series in Air-Air permeability, there was no significant difference among MP and NW series in Water-Air permeability. Compared to the other films, WP, NP-S, and NP-P were significantly lower. However, the difference

TABLE 2 | Overall oxygen transfer coefficients and contact angle of various films.

Film ID	Film type	Air-Air permeation K_{AA} ($\times 10^{-3}$ m s^{-1})	Water-Air permeation K_{WA} ($\times 10^{-5}$ m s^{-1})	Water-Water permeation K_{WW} ($\times 10^{-5}$ m s^{-1})	Contact angle (°)
MP1-1	Microporous; PE	2.00 ± 0.04	1.80 ± 0.13	1.26 ± 0.01	114
MP1-2	Microporous; PE	1.95 ± 0.04	1.90 ± 0.29	1.35 ± 0.04	122
MP1-3	Microporous; PE	1.90 ± 0.10	1.99 ± 0.06	1.39 ± 0.09	118
MP2	Microporous; PP	1.97 ± 0.01	1.96 ± 0.05	0.94 ± 0.06	100
MP3-1	Microporous; PTFE	2.01 ± 0.03	2.10 ± 0.03	1.16 ± 0.05	134
MP3-2	Microporous; PTFE	1.00 ± 0.02	2.00 ± 0.13	1.28 ± 0.10	116
MP3-3	Microporous; PTFE	0.21 ± 0.01	1.96 ± 0.12	1.34 ± 0.13	121
NW1-1	Nonwoven support	2.02 ± 0.01	1.76 ± 0.09	1.17 ± 0.04	110 [120]*
NW1-2	Nonwoven support	1.97 ± 0.06	1.70 ± 0.03	0.60 ± 0.03	108 [96]*
WP	Woven porous	1.67 ± 0.11	1.24 ± 0.14	0.43 ± 0.04	96
NP-S	Silicone	0.00075 ± 0.00008	1.16 ± 0.03	0.59 ± 0.04	94
NP-P	Dense PP film	0.00016 ± 0.00003	0.10 ± 0.04	0.05 ± 0.08	–

*PE: polyethylene; PP: polypropylene; PTFE: polytetrafluoroethylene. *Contact angles for nonwoven fabric support for the NW series was shown in parenthesis.*

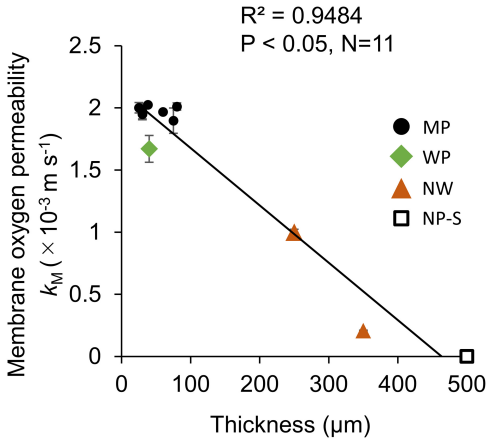

FIGURE 3 | The relationship between oxygen transfer coefficient at the membrane (k_M) and membrane thickness in the Air-Air permeation test. N = 3 for all the 11 films measured in this study. The error bar shows the standard deviation. MP: microporous; WP: woven porous; NW: microporous with a non-woven fabric; and NP-S: silicone films.

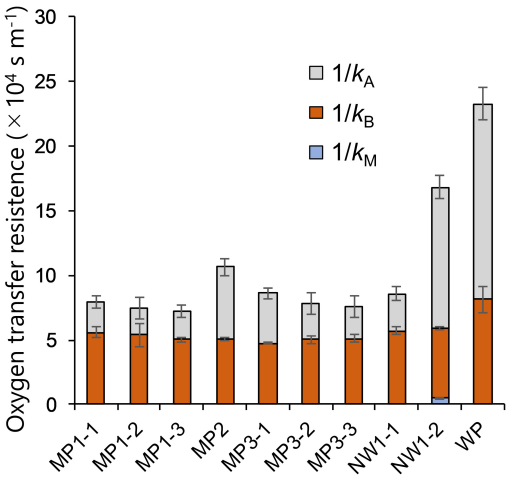

FIGURE 4 | Breakdown of mass transfer resistance in the Water–Water oxygen permeation test. N = 3 for all membranes. Error bars show the standard deviation of each breakdown.

between other films and NP-S became smaller compared to Air-Air permeation. The NP-S transfer coefficient increased from the Air-Air condition by 15 times.

Water–Water Permeability

The oxygen transfer coefficients were about half of the Water-Air permeability values for most of the films (**Table 2**). There was a clear difference in NW1-1 and NW1-2 in terms of reduction of *K;* although Water-Air transfer coefficients were comparable for the two, Water–Water permeability was lower by half for NW1-2.

The oxygen transfer coefficients of Air-Air, Water-Air, and Water–Water permeability tests were used to derive relative contributions of k_M, k_B, and k_A on the overall resistance of Water–Water permeation test (**Figure 4**). Membrane resistance consisted of less than 1% of the total resistance except for the NW series, which was still less than 3%. Liquid boundaries in both sides of the membrane exhibited the major resistance in the permeability of oxygen. For NP-S and NP-P, due to the higher permeability in Water-Air and Water–Water conditions (in which combined resistance of membrane and both sides of the liquid boundary were assumed) compared to Air-Air conditions (in which only membrane resistance was assumed), the relative contributions were not calculated.

Physicochemical Characteristics of Films and Their Effects

Tensile strength was measured for selected films (**Figure 5**). Dense polypropylene film (NP-P) had the highest strength, and the woven porous film was the next, showing about half of NP-P. Microporous films generally exhibited low strength although MP1 series had relatively stronger characteristics in one direction. Compared to the microporous film, attachment of non-woven

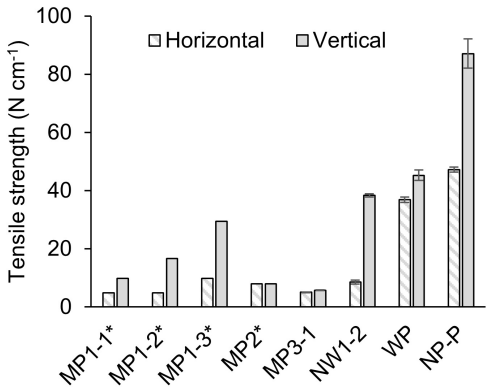

FIGURE 5 | Tensile strength of the films. The error bar shows the standard deviation of *N* = 3. The values with asterisks (*) were derived from the product datasheet. MP: microporous; WP: woven porous; NW: microporous with a non-woven fabric; and NP-P: non-porous polypropylene film.

fabric support improved the strength in one direction as much as woven film. There was no significant relationship between tensile strength and thickness or pore characteristics.

Contact angle that indicates hydrophobicity of films was in the range of 94 to 134°, indicating moderate to strong hydrophobicity (**Table 2**). PTFE and PET indicated relatively stronger hydrophobicity, while nylon was less water repellent.

The contact angle exhibited significant correlations with oxygen permeability in both sides of liquid boundary layers, k_B and k_A, across the various types of porous membranes (**Figures 6A,B**). Although transfer coefficients k_A was calculated by subtracting k_M and k_B from the overall coefficient of Water–Water permeation, a significant correlation was observed (**Figure 6B**). The effect of different non-woven fabric hydrophobicity was also taken into consideration for k_A. The contact angle also had a positive correlation with water entry pressure (**Figure 7**).

The optical characteristics of the tested membranes indicated that most porous membranes except WP, which is dyed with black paint, had high reflectance of approximately >80%. The reflectance rate of those white membranes correlated with the thickness (**Figure 8**). In the correlation analysis of NW, membrane thickness excluding non-woven fabric was applied.

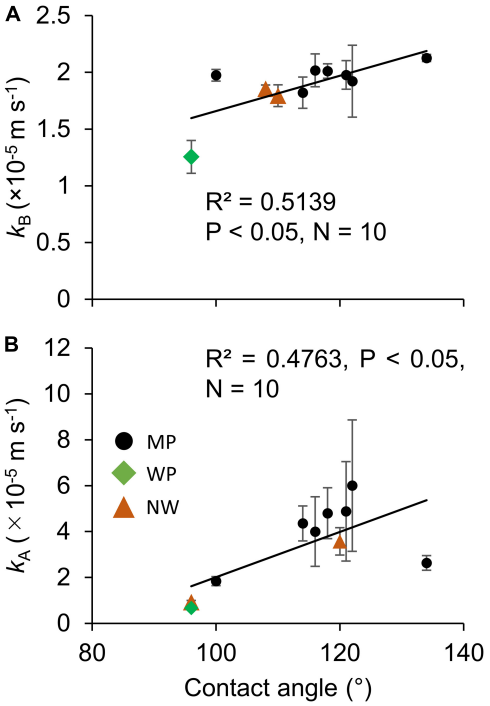

FIGURE 6 | The effect of hydrophobicity (contact angle) on the oxygen transfer coefficients in **(A)** Room B and **(B)** Room A. *N* = 3 for all the 10 microporous membranes measured in this study. The error bar shows the standard deviation. MP: microporous; WP: woven porous; and NW: microporous with a non-woven fabric.

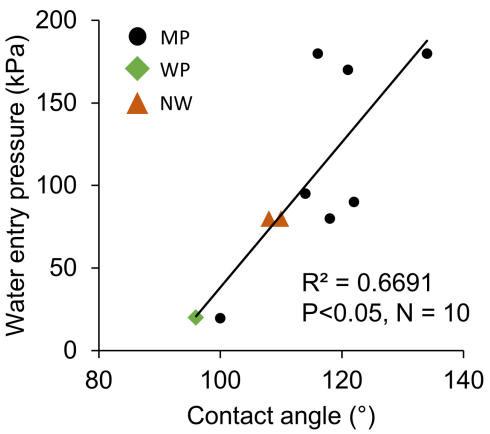

FIGURE 7 | The positive relation between water entry pressure and hydrophobicity (contact angle). *N* = 1 for all the 10 microporous membranes measured in this study. MP: microporous; WP: woven porous; and NW: microporous with a non-woven fabric.

DISCUSSION

Oxygen Transfer

The membrane permeability had little effect on the dissolved oxygen removal as k_M was only less than 3% of the overall oxygen resistance from water because of much higher resistance in the liquid layers (**Figure 4**). The reason behind the smaller resistance could be the relatively large pore size and the hydrophobicity that may have filled the pore with gas. This finding was similar to those of CO_2 supply (Carvalho and Malcata, 2001) in which the effect of membrane permeability was considered negligible when Henry's constant was high. This low contribution in resistance was the case even with a membrane laminated with non-woven fabric support. Although the membrane gas transfer coefficient of NW1-2 was less than 10% of MP membranes (**Table 2**) due to the increased thickness (**Figure 3**), this resistance did not affect much on the overall oxygen transfer from water to air (**Figure 4**).

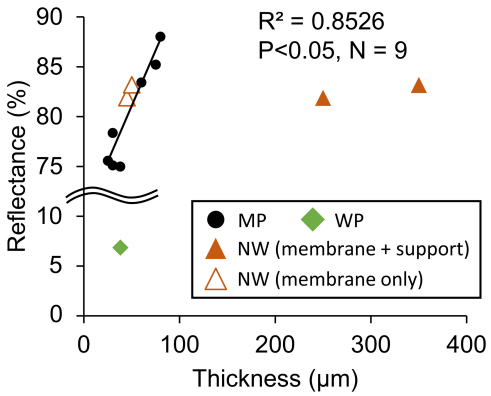

FIGURE 8 | Relationship between optical reflectance and membrane thickness. MP: microporous; WP: woven porous; and NW: microporous with non-woven fabric support. The thickness of the membrane only was adopted for NW in the regression line. WP was removed from the regression analysis due to its black dye.

This result was somewhat inconsistent with previous studies that stated increased modeling accuracy by the inclusion of the support layer in the estimation of pervaporation flux (Heintz and Stephan, 1994; Lipnizki et al., 2002). However, these studies dealt with a more accurate estimation of transfer using much smaller pore-size support (0.016 μm). In the rough estimation like this study, the liquid boundary transfer coefficient can be solely considered for dissolved oxygen removal. Thus, attachment of large-pore support like the non-woven fabric was found to be effective in increasing the membrane durability (**Figure 5**), while not negatively affecting dissolved oxygen removal properties.

Reduction in the liquid boundary transfer coefficient was found to be the most important factor in dissolved oxygen removal. The current study described that increasing hydrophobicity improves oxygen permeability (**Figure 6**), and the highest k_B of 2.13 × 10^{-5} m s^{-1} was achieved with MP3-1 of the highest hydrophobicity. This oxygen transfer coefficient was similar to a previous study of 1.2–2.5 × 10^{-5} m s^{-1} (Kishi, 2018), 0.052–0.77 × 10^{-5} m s^{-1} (Vladisavljević, 1999), 0.44–1.56 × 10^{-5} m s^{-1} (Su, 2018), 0.75–4.65 × 10^{-5} m s^{-1} (Bhaumik et al., 2004), and 1.1–3.4 × 10^{-5} m s^{-1} (Côté et al., 1989). This coefficient enables maintenance of dissolved oxygen at 200% with a gas-permeating reactor having 1 g L^{-1} d^{-1} of algal biomass productivity, based on the assumption of the gas-permeating bag reactor configuration (Kishi, 2018): specific membrane surface area of 87 m^{-1} and oxygen production to biomass production ratio of 1.1 g g^{-1}. These results suggested that an energy-efficient oxygen removal from a closed reactor is possible through the use of a hydrophobic membrane to prevent oxygen inhibition without intensive aeration.

The overall oxygen transfer coefficients in the Water–Water permeation test were in the range of 0.43 to 1.39 × 10^{-5} m s^{-1} (**Table 2**). Although this is a comparably smaller value than Water-Air permeation, 1.39 × 10^{-5} m s^{-1} of oxygen transfer, for example, can maintain dissolved oxygen at 250% with the same assumption as above. Considering over 600% oxygen concentration in a closed photobioreactor (Torzillo et al., 1998), this oxygen concentration maintenance can be considered effective. Therefore, this result suggests that gas-permeating photobioreactors can be operated facing water such as that of the Solix system where whole bag reactors are submerged within a water bath for effective temperature control (Morweiser et al., 2010). Care needs to be taken in choosing appropriate film support with hydrophobicity, since liquid boundary layer on the low-oxygen side matters in Water–Water oxygen permeation.

Interestingly, silicone rubber had K_{WA} and K_{WW} close to those of porous films despite distinctively lower K_{AA} ($\fallingdotseq k_M$), which was a few magnitudes lower than K_{WA} and K_{WW} (**Table 2**). The mechanism behind this characteristic is not clear as far as the authors' knowledge, but a relatively hydrophilic feature of dense silicone may have supported faster diffusion of gas through the membrane with the existence of water than without water.

Water Entry Pressure and Optical Properties

Water entry pressure was higher for increasingly hydrophobic films (**Figure 7**). The Young-Laplace equation states that water breakthrough pressure P (a similar index as the water entry pressure) (Scott and Barker, 2006) positively correlates with contact angle θ and inversely correlates with pore radius r (Di Felice, 2016; Bazhenov et al., 2018):

$$P = \frac{-2\sigma \cos\theta}{r} \quad (6)$$

where σ is liquid surface tension. Although the relationship between equation-based estimation and actual water entry pressure did not correspond well (R^2 = 0.26), the theory explains well that water repellency avoids water permeation through membrane pores. As a low water entry pressure leads to algal culture leakage through the membrane, a moderately high value is favorable. For example, solely considering the static pressure, water entry pressure of 20 kPa in MP2 can only sustain a 2-m water head, while 180 kPa in MP3-1 can sustain up to an 18-m water head. Considering the dynamic pressure due to culture mixing, a higher water entry pressure is demanded to prevent culture leakage.

Optical reflectance positively correlated with membrane thickness (**Figure 8**). The mechanisms for this correlation could be that the microstructure refracted light, and the thicker the film, the more potent light is backscattered. The reason for NW being out of the correlation could be because the non-woven fabric is much less dense than the microporous film, and light escaped through the large pores. Due to the high reflectance of most of the porous films, the gas-permeating photobioreactor was designed to utilize the reflectance of light (Kishi, 2018). Thus, the thicker film may be somewhat beneficial for the gas-permeating reactor, as an increase in membrane oxygen permeation does not deteriorate dissolved oxygen removal much.

Suggested Gas-Permeating System for Algal Photobioreactor

The results of this study indicated that there are favorable physicochemical properties and structure of membranes that are suitable for the gas-permeating photobioreactor (**Figure 9**). Firstly, for the improvement of oxygen permeability, hydrophobicity of membranes facing water needs to be high. Secondly, since the thickness of the membrane does not affect the overall dissolved oxygen transfer, attachment of porous support and increase in membrane thickness would be beneficial to increase the strength and optical reflectance. Such characteristics and structure would enable a durable oxygen-permeating photobioreactor.

The suggested gas-permeating membrane system can be applied to various types of algal photobioreactors. A bag reactor supported by iron frames (Sierra et al., 2008), hanged column-type bag reactors (Abomohra et al., 2014), and multi-folded reactors (Schreiber et al., 2017) are largely operated examples of bag reactors. A gas-permeable membrane can be added to such reactors for energy-efficient dissolved oxygen removal without interfering the productivity, as long as the membrane does not shade the algal culture. The recent development in submerged and floating bag reactors can be interesting applications of the membrane dissolved oxygen system. For example, Solix proposed a completely submerged flat-panel bag photobioreactor system for better temperature control (Morweiser et al., 2010). Another example is floating bag reactors such as that utilizes wave for mixing the algal culture (Zhu et al., 2018a,b). Since Water–Water oxygen permeability of hydrophobic membrane was found to be high enough for maintaining dissolved oxygen concentration of algal culture at an adequately low level, the membrane can be used as a part of the culture container for those submerged and floating reactors. However, if the surrounding water is an uncontrolled environment like the ocean, biofouling on the outer side can be a serious issue, as reported in Zhu et al. (2018b).

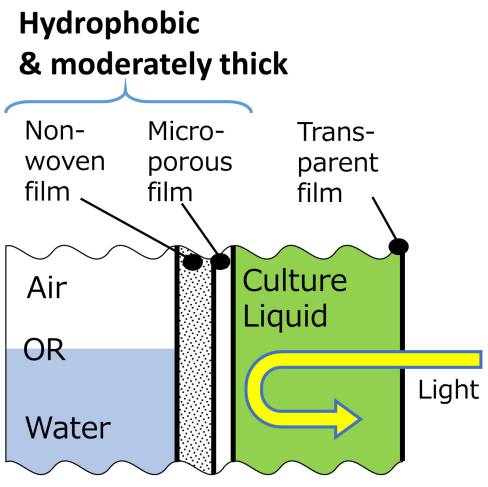

FIGURE 9 | Proposed schematic structure of a gas-permeating photobioreactor composed of three film layers for dissolved oxygen removal.

For the practical selection of the membrane, however, additional cost and technical analysis are required. For instance, although the highest hydrophobicity was achieved with PTFE membranes, its cost is relatively high, and the construction of a bag reactor may be challenging due to its difficulty in attaching with other materials. Recent developments in film surface hydrophobization (Tuteja et al., 2007; Xue et al., 2009, 2014) may make cheap and easily handleable microporous films suitable for the gas-permeating photobioreactor.

In addition, further long-term cultivation tests are needed to evaluate the formation of microbial biofilm on the surface of the hydrophobic membrane, as the hydrophobic surface tends to easily develop microbial adhesion (Mazumder et al., 2010). Although long-term durability (ca. 100 days) of a microporous film in a gas-permeating reactor was indicated in a previous study with *Arthrospira platensis* culture (Kishi, 2018), the culture condition of extremely high alkalinity may have majorly contributed to this favorable results.

CONCLUSION

This study compared the oxygen permeability of various films to clarify the suitable criteria for selecting membrane in an energy-efficient dissolved oxygen removal from algal reactors. The oxygen permeation test in Air-Air, Water-Air, and Water–Water conditions revealed the relative importance of liquid boundary layer resistance compared to the membrane resistance, which only consisted of less than 3% of the overall resistance. Membrane hydrophobicity was found to improve the liquid boundary oxygen transfer as well as water entry pressure. Moreover, since the oxygen transfer resistance in the membrane is neglectable, attachment of non-woven fabric support for improved strength was found to be a good option for gas-permeating bag reactor. Using the membrane with the highest hydrophobicity and oxygen permeability, the overall oxygen transfer coefficient was found to be high enough to maintain adequately low levels of dissolved oxygen in highly productive algal culture. Moreover, the overall oxygen transfer coefficients in both Water-Air and Water–Water conditions were high, indicating that the gas-permeating membrane can be also applied to floating and submerged conditions.

DATA AVAILABILITY STATEMENT

The raw data supporting the conclusions of this article will be made available by the authors, without undue reservation.

AUTHOR CONTRIBUTIONS

MK, KN, and TT contributed to the conception and design of the study. KN implemented most of the experimental works. MK performed the statistical analysis and wrote the first draft of the

manuscript. All authors contributed to the manuscript revision, read, and approved the submitted version.

FUNDING

This research was partially supported by the Sasakawa Scientific Research Grant from the Japan Science Society (29-229) and the Japan Science and Technology Agency (JST)/Japan International Cooperation Agency (JICA), Science and Technology Research Partnership for Sustainable Development (SATREPS) JPMJSA1509.

ACKNOWLEDGMENTS

Films were generously provided by the Teijin, Nitto, 3M, Sumitomo Electric, and Toyobo. Tensile strength was kindly measured by the A&D Inc. We express sincere gratitude to all who have contributed.

REFERENCES

Abomohra, A. E. F., El-Sheekh, M., and Hanelt, D. (2014). Pilot cultivation of the chlorophyte microalga Scenedesmus obliquus as a promising feedstock for biofuel. *Biomass Bioenergy* 64, 237–244. doi: 10.1016/j.biombioe.2014.03.049

Bazhenov, S. D., Bildyukevich, A. V., and Volkov, A. V. (2018). Gas-liquid hollow fiber membrane contactors for different applications. *Fibers* 6:76. doi: 10.3390/fib6040076

Behera, S., Singh, R., Arora, R., Sharma, N. K., Shukla, M., and Kumar, S. (2015). Scope of algae as third generation biofuels. *Front. Bioeng. Biotechnol.* 2:90. doi: 10.3389/fbioe.2014.00090

Bhaumik, D., Majumdar, S., Fan, Q., and Sirkar, K. K. (2004). Hollow fiber membrane degassing in ultrapure water and microbiocontamination. *J. Memb. Sci.* 235, 31–41. doi: 10.1016/j.memsci.2003.12.022

Brüschke, H. E. A. (1990). Removal of ethanol from aqueous streams by pervaporation. *Desalination* 77, 323–330. doi: 10.1016/0011-9164(90)85032-6

Burlew, J. S. (1953). "Current status of the large-scale culture of algae," in *Algal Culture, From Laboratory to Pilot Plant*, ed. J. S. Burlew (Washington, DC: Carnegie Institution of Washington), 3–23.

Carvalho, A. P., and Malcata, F. X. (2001). Transfer on carbon dioxide within cultures of micro algae: plain bubbling versus hollow-fibre modules. *Biotechnol. Prog.* 17, 265–272. doi: 10.1021/bp000157v

Carvalho, A. P., and Meireles, L. A. (2006). Microalgae reactors: a review of enclosed systems and performances. *Biotechnol. Prog.* 3, 1490–1506. doi: 10.1002/bp060065r

Côté, P., Bersillon, J. L., and Huyard, A. (1989). Bubble-free aeration using membranes: mass transfer analysis. *J. Memb. Sci.* 47, 91–106. doi: 10.1016/S0376-7388(00)80862-5

Di Felice, R. (2016). Breakthrough Pressure. *Encycl. Membr.* 279–280. doi: 10.1007/978-3-662-44324-8

Heintz, A., and Stephan, W. (1994). A generalized solution-diffusion model of the pervaporation process through composite membranes Part II. Concentration polarization, coupled diffusion and the influence of the porous support layer. *J. Memb. Sci.* 89, 153–169. doi: 10.1016/0376-7388(93)E0223-7

Ito, A., Yamagiwa, K., Tamura, M., and Furusawa, M. (1998). Removal of dissolved oxygen using non-porous hollow-fiber membranes. *J. Memb. Sci.* 145, 111–117. doi: 10.1016/S0376-7388(98)00068-4

Jana, A., Bhattacharya, P., Guha, S., Ghosh, S., and Majumdar, S. (2017). Application of a new ceramic hydrophobic membrane for providing CO_2 in algal photobioreactor during cultivation of Arthrospira sp. *Algal Res.* 27, 223–234. doi: 10.1016/j.algal.2017.08.030

Kazbar, A., Cogne, G., Urbain, B., Marec, H., Le-Gouic, B., Tallec, J., et al. (2019). Effect of dissolved oxygen concentration on microalgal culture in photobioreactors. *Algal Res.* 39, 101432. doi: 10.1016/j.algal.2019.101432

Kim, H. W., Marcus, A. K., Shin, J. H., and Rittmann, B. E. (2011). Advanced control for photoautotrophic growth and CO_2-utilization efficiency using a membrane carbonation photobioreactor (MCPBR). *Environ. Sci. Technol.* 45, 5032–5038. doi: 10.1021/es104235v

Kishi, M. (2018). *Oxygen Removal Efficiency from Microalgal Culture by Gas-Permeating Photobioreactor*. Ph.D. Dissertation. Soka University, Tokyo, Japan.

Lee, Y. K., and Hing, H. K. (1989). Supplying CO_2 to photosynthetic algal cultures by diffusion through gas-permeable membranes. *Appl. Microbiol. Biotechnol.* 31, 298–301. doi: 10.1007/BF00258413

Lipnizki, F., Olsson, J., Wu, P., Weis, A., Trägårdh, G., and Field, R. W. (2002). Hydrophobic pervaporation: influence of the support layer of composite membranes on the mass transfer. *Sep. Sci. Technol.* 37, 1747–1770. doi: 10.1081/SS-120003042

Mazumder, S., Falkinham, J. O., Dietrich, A. M., and Puri, I. K. (2010). Role of hydrophobicity in bacterial adherence to carbon nanostructures and biofilm formation. *Biofouling* 26, 333–339. doi: 10.1080/08927010903531491

Molina, E., Fernández, J., Acién, F. G., and Chisti, Y. (2001). Tubular photobioreactor design for algal cultures. *J. Biotechnol.* 92, 113–131. doi: 10.1016/S0168-1656(01)00353-4

Mortezaeikia, V., Yegani, R., Hejazi, M. A., and Chegini, S. (2016). CO_2 biofixation by *Dunaliella salina* in batch and semi-continuous cultivations, using hydrophobic and hydrophilic poly ethylene (PE) hollow fiber membrane photobioreactors. *Iran. J. Chem. Eng.* 13, 47–59.

Morweiser, M., Kruse, O., Hankamer, B., and Posten, C. (2010). Developments and perspectives of photobioreactors for biofuel production. *Appl. Microbiol. Biotechnol.* 87, 1291–1301. doi: 10.1007/s00253-010-2697-x

Norsker, N. H., Barbosa, M. J., Vermuë, M. H., and Wijffels, R. H. (2011). Microalgal production - a close look at the economics. *Biotechnol. Adv.* 29, 24–27. doi: 10.1016/j.biotechadv.2010.08.005

Pörs, Y., Wüstenberg, A., and Ehwald, R. (2010). A batch culture method for microalgae and cyanobacteria with CO_2 supply through polyethylene membranes. *J. Phycol.* 46, 825–830. doi: 10.1111/j.1529-8817.2010.00844.x

Raisi, A., and Aroujalian, A. (2011). Aroma compound recovery by hydrophobic pervaporation: the effect of membrane thickness and coupling phenomena. *Sep. Purif. Technol.* 82, 53–62. doi: 10.1016/j.seppur.2011.08.018

Richmond, A. (ed.). (2013). "Biological principles of mass cultivation of photoautotrophic microalgae," in *Handbook of Microalgal Culture: Applied Phycology and Biotechnology* (Arizona: Arizona State University)169–204. doi: 10.1002/9781118567166.ch11

Schreiber, C., Behrendt, D., Huber, G., Pfaff, C., Widzgowski, J., Ackermann, B., et al. (2017). Growth of algal biomass in laboratory and in large-scale algal photobioreactors in the temperate climate of western Germany. *Bioresour. Technol.* 234, 140–149. doi: 10.1016/j.biortech.2017.03.028

Scott, J. B. T., and Barker, R. D. (2006). Pore geometry of Permo-Triassic sandstone from measurements of electrical spectroscopy. *Geol. Soc. London Spec. Publ.* 263, 65–81. doi: 10.1144/GSL.SP.2006.263.01.03

Shelp, B. J., and Canvin, D. T. (1980). Photorespiration and oxygen inhibition of photosynthesis in chlorella pyrenoidosa. *Plant Physiol.* 65, 780–784. doi: 10.1104/pp.65.5.780

Shesh, T., Eustance, E., Lai, Y. J., and Rittmann, B. E. (2019). Characterization of CO_2 flux through hollow-fiber membranes using pH modeling. *J. Memb. Sci.* 592, 117389. doi: 10.1016/j.memsci.2019.117389

Sierra, E., Acién, F. G., Fernández, J. M., García, J. L., González, C., and Molina, E. (2008). Characterization of a flat plate photobioreactor for the production of microalgae. *Chem. Eng. J.* 138, 136–147. doi: 10.1016/j.cej.2007.06.004

Su, J. (2018). Effects of vacuum and flow rate on water deoxygenation through Tri-Bore PVDF hollow fiber membranes. *SF J. Mater. Chem. Eng.* 2018, 1010.

Su, J., and Wei, Y. (2019). Novel tri-bore PVDF hollow fiber membranes for the control of dissolved oxygen in aquaculture water. *J. Water Process Eng.* 30, 100584. doi: 10.1016/j.jwpe.2018.02.019

Thrane, J.-E., Kyle, M., Striebel, M., Haande, S., Grung, M., Rohrlack, T., et al. (2015). Spectrophotometric analysis of pigments: a critical assessment of a

high-throughput method for analysis of algal pigment mixtures by spectral deconvolution. *PLoS One* 10:e0137645. doi: 10.1371/journal.pone.0137645

Torzillo, G., Bernardini, P., and Masojídek, J. (1998). On-line monitoring of chlorophyll fluorescence to assess the extent of photoinhibition of photosynthesis induced by high oxygen concentration and low temperature and its effect on the productivity of outdoor cultures of *Spirulina platensis*. *J. Phycol.* 34, 504–510. doi: 10.1046/j.1529-8817.1998.340504.x

Tuteja, A., Choi, W., Ma, M., Mabry, J. M., Mazzella, S. A., Rutledge, G. C., et al. (2007). Designing superoleophobic surfaces. *Science* 318, 1618–1622. doi: 10.1126/science.1148326

Vladisavljević, G. T. (1999). Use of polysulfone hollow fibers for bubbleless membrane oxygenation/deoxygenation of water. *Sep. Purif. Technol.* 17, 1–10. doi: 10.1016/S1383-5866(99)00012-X

Vonshak, A., Torzillo, G., Accolla, P., and Tomaselli, L. (1996). Light and oxygen stress in *Spirulina platensis* (cyanobacteria) grown outdoors in tubular reactors. *Physiol. Plant.* 97, 175–179. doi: 10.1111/j.1399-3054.1996.tb00494.x

Weissman, J. C., Goebel, R. P., and Benemann, J. R. (1988). Photobioreactor design: mixing, carbon utilization, and oxygen accumulation. *Biotechnol. Bioeng.* 31, 336–344. doi: 10.1002/bit.260310409

Woortman, D. V., Fuchs, T., Striegel, L., Fuchs, M., Weber, N., Brück, T. B., et al. (2020). Microalgae a superior source of folates: quantification of folates in halophile microalgae by stable isotope dilution assay. *Front. Bioeng. Biotechnol.* 7:481. doi: 10.3389/fbioe.2019.00481

Xue, C. H., Jia, S. T., Zhang, J., and Tian, L. Q. (2009). Superhydrophobic surfaces on cotton textiles by complex coating of silica nanoparticles and hydrophobization. *Thin Solid Films* 517, 4593–4598. doi: 10.1016/j.tsf.2009.03.185

Xue, C. H., Li, Y. R., Zhang, P., Ma, J. Z., and Jia, S. T. (2014). Washable and wear-resistant superhydrophobic surfaces with self-cleaning property by chemical etching of fibers and hydrophobization. *ACS Appl. Mater. Interfaces* 6, 10153–10161. doi: 10.1021/am501371b

Yamamoto, M., and Nakajima, K. (1979). Gas Permeability and Pore Size Distribution on Porous Membrane -Effect of Metal Coating-. *Membrane* 4, 61–67. doi: 10.5360/membrane.4.61

Yew, G. Y., Lee, S. Y., Show, P. L., Tao, Y., Law, C. L., Nguyen, T. T. C., et al. (2019). Recent advances in algae biodiesel production: from upstream cultivation to downstream processing. *Bioresour. Technol. Reports* 7, 100227. doi: 10.1016/j.biteb.2019.100227

Zhu, C., Zhai, X., Wang, J., Han, D., Li, Y., Xi, Y., et al. (2018a). Large-scale cultivation of Spirulina in a floating horizontal photobioreactor without aeration or an agitation device. *Appl. Microbiol. Biotechnol.* 102, 8979–8987. doi: 10.1007/s00253-018-9258-0

Zhu, C., Zhu, H., Cheng, L., and Chi, Z. (2018b). Bicarbonate-based carbon capture and algal production system on ocean with floating inflatable-membrane photobioreactor. *J. Appl. Phycol.* 30, 875–885. doi: 10.1007/s10811-017-1285-1

Conflict of Interest: The authors declare that the research was conducted in the absence of any commercial or financial relationships that could be construed as a potential conflict of interest.

frontiers in Bioengineering and Biotechnology

REVIEW
published: 04 September 2020
doi: 10.3389/fbioe.2020.01004

Integration of Algae to Improve Nitrogenous Waste Management in Recirculating Aquaculture Systems: A Review

Norulhuda Mohamed Ramli[1,2], J. A. J. Verreth[1], Fatimah M. Yusoff[3,4], K. Nurulhuda[2], N. Nagao[5] and Marc C. J. Verdegem[1]*

[1] Aquaculture and Fisheries Group, Wageningen University & Research, Wageningen, Netherlands, [2] Department of Biological and Agricultural Engineering, Faculty of Engineering, Universiti Putra Malaysia, Serdang, Malaysia, [3] International Institute of Aquaculture and Aquatic Sciences, Universiti Putra Malaysia, Port Dickson, Malaysia, [4] Department of Aquaculture, Faculty of Agriculture, Universiti Putra Malaysia, Serdang, Malaysia, [5] Bluescientific Shinkamigoto Co. Ltd. (BSCIS), Nagasaki, Japan

This review investigates the performance and the feasibility of the integration of an algal reactor in recirculating aquaculture systems (RAS). The number of studies related to this topic is limited, despite the apparent benefit of algae that can assimilate part of the inorganic waste in RAS. We identified two major challenges related to algal integration in RAS: first, the practical feasibility for improving nitrogen removal performance by algae in RAS; second, the economic feasibility of integrating an algal reactor in RAS. The main factors that determine high algal nitrogen removal rates are light and hydraulic retention time (HRT). Besides these factors, nitrogen-loading rates and RAS configuration could be important to ensure algal performance in nitrogen removal. Since nitrogen removal rate by algae is determined by HRT, this will affect the size (area or volume) of the algal reactor due to the time required for nutrient uptake by algae and large surface area needed to capture enough light. Constraints related to design, space, light capture, and reactor management could incur additional cost for aquaculture production. However, the increased purification of RAS wastewater could reduce the cost of water discharge in places where this is subject to levees. We believe that an improved understanding of how to manage the algal reactor and technological advancement of culturing algae, such as improved algal reactor design and low-cost artificial light, will increase the practical and economic feasibility of algal integration in RAS, thus improving the potential of mass cultivation of algae in RAS.

Keywords: algal cultivation, nitrogen, recirculating aquaculture system, ammonia, nitrate, removal rates, HRT

OPEN ACCESS

Edited by:
Ken'ichiro Matsumoto, Hokkaido University, Japan

Reviewed by:
Eric M. Hallerman, Virginia Tech, United States
Shreeshivadasan Chelliapan, University of Technology, Malaysia, Malaysia

****Correspondence:***
Norulhuda Mohamed Ramli
m_nurulhuda@upm.edu.my; norul49huda@gmail.com

Specialty section:
This article was submitted to Bioprocess Engineering, a section of the journal Frontiers in Bioengineering and Biotechnology

Received: *17 April 2020*
Accepted: *31 July 2020*
Published: *04 September 2020*

Citation:
Ramli NM, Verreth JAJ, Yusoff FM, Nurulhuda K, Nagao N and Verdegem MCJ (2020) Integration of Algae to Improve Nitrogenous Waste Management in Recirculating Aquaculture Systems: A Review. Front. Bioeng. Biotechnol. 8:1004. doi: 10.3389/fbioe.2020.01004

INTRODUCTION

According to FAO (2019), aquaculture production increased steadily at an average of 4.8% per year from 2010 until 2017. In 2017, aquaculture contributed 46.4% of the world total fishery production, which is equivalent to 80.1 million metric tons (valued at USD 23.8 billion). This share is expected to reach 52% in 2025, which is equivalent to 102 million tons of production. This indicated that the aquaculture sector will be the main driver of the world fish supply (FAO, 2019).

Fish production systems can be categorized into three types: flow-through systems (cages and raceways), semi flow-through systems (ponds), and recirculating aquaculture systems (RAS) where either nutrients, water, or both are recycled. The highest water exchange rate is applied in the flow-through system (>50 m^3 kg^{-1} feed), medium exchange rate in the semi flow-through system (1–50 m^3 kg^{-1} feed) and minimum exchange rate in the conventional RAS (0.1–3 m^3 kg^{-1} feed) (Martins et al., 2010; Bregnballe, 2015). RAS has an advantage over the flow-through and semi flow-through systems because waste discharge into the environment can be controlled, a smaller volume of water per kilogram fish production is used, higher biosecurity standards can be applied, and in cases where antibiotics have to be applied, discharge to the environment can be prevented. Due to expected water scarcity, limited area for aquaculture (FAO, 2016), and increasingly strict environmental regulations, RAS has become more important for aquaculture activities.

Recirculating aquaculture systems are intensive systems, which rely on formulated feed to provide all the nutrient requirements for the cultured organisms. A RAS must consist of a self-cleaning-conditioning system, which the water is reused for culture (Timmons and Ebeling, 2007). Analyzing information in the literature, Schneider et al. (2005) concluded that between 50 and 70% of feed nitrogen (N) becomes waste in the culture system. Meanwhile, fish feeds usually contain a high percentage of crude protein, between 30 and 60%. According to Ebeling et al. (2006), when introducing 1 kg of feed containing 32% crude protein in a 1 m^3 RAS, 30 g ammonia-nitrogen (ammonia-N) will be released, which in this case will raise the ammonia-N concentration by 30 mg L^{-1}.

In a RAS, the concentration of ammonia-N must be maintained below 1 mg L^{-1} due to its harmful effect upon fishes (Greiner and Timmons, 1998; Timmons and Ebeling, 2007). Total ammonia nitrogen (TAN) consists of unionized ammonia (NH_3) and ammonium ion (NH_4^+). In this article, ammonia and ammonium are referred to the unionized and ionized species, respectively. Meanwhile, total ammonia is referred to as TAN. The toxicity of NH_3 is related to dissolved carbon dioxide (CO_2) concentration and pH of the water. As dissolved CO_2 decreases, the pH increases and increases the toxicity of NH_3 (Timmons and Ebeling, 2007). Dissolved CO_2 is continuously produced in RAS *via* fish and bacterial respiration, and bacterial decomposition. A degassing process is integrated into a RAS to control CO_2 concentration. Meanwhile, pH of water in RAS could decrease as a result of the nitrification process; therefore, bicarbonate is added to regulate pH in the system. Failure to manage dissolved CO_2, and pH could expose the fish to a higher risk of TAN toxicity. In nitrification, TAN is converted to nitrite and nitrite to nitrate. Nitrite is a toxic species of inorganic nitrogen at levels more than 1 mgL^{-1}, and nitrate is found harmful for many fresh water fish species at concentrations above 1,000 mgL^{-1} and for marine species at concentration more than 500 mgL^{-1} (Colt, 2006).

In a RAS, recycling reduces the amount of water use needed. In order to maintain the water quality in a RAS while keeping water renewal limited, a series of water purifying units can be installed, such as a solids removal unit, a biological filtration unit for inorganic nitrogen removal, and a reservoir where water conditioning may take place (likes heating, oxygenation, and disinfection) (Bregnballe, 2015). The biological filtration unit controls the concentration of total ammonia. The key process for controlling the total ammonia level is autotrophic nitrification, which converts total ammonia into nitrite and nitrite into nitrate. However, the product of nitrification, nitrate, accumulates in the RAS. Therefore, in recent RAS configurations, a denitrification reactor often is added to maintain a low level of nitrate in the system. The concentration of nitrate-N (NO_3-N) can be as high as 400 to 500 mg NO_3-N L^{-1} in a conventional RAS without the denitrification component (Van Rijn et al., 2006). The high nitrate concentration can have adverse effects on the growth of farmed organisms (Davidson et al., 2017).

However, denitrification is not a productive process in the sense that the inorganic nitrate-N is converted to N_2 gas, a non-readily useful form of nitrogen. At the same time, producing inorganic N fertilizers from N_2 gas is an energy-intensive process (Bartels, 2008). Therefore, to improve the sustainability of a RAS, alternative approaches for ammonia, nitrite, and nitrate conversion need to be explored, such as assimilation of nitrogen by organisms that can be subsequently harvested. An example is assimilation by algae. Recent studies show many benefits of integrating algae in an aquaculture production system. They improve the stability of water quality of a RAS (Ramli, 2018) and may help to control harmful bacteria in the culture water (Defoirdt et al., 2004; Natrah et al., 2011, 2014; Tendencia et al., 2013), or remove heavy metals and organic contaminants from the water (Muñoz and Guieysse, 2006; Matamoros et al., 2015; Suresh Kumar et al., 2015). Integration of algae in a RAS could be relatively easy and inexpensive, as demonstrated in a study by Valeta and Verdegem (2015), which used an algal-turf-scrubber in a RAS. On the other hand, anaerobic denitrification units are expensive and can prove finicky to operate. This statement is based on the authors' personal experiences working with an experimental setup of an up-flow sludge blanket manure denitrification reactor and from a study by Meriac et al. (2014a) that integrated a denitrification reactor in RAS.

Besides improving water quality, algae may be an important fish food because they contain high protein (between 40 and 70%), carbohydrate (between 10 and 65%) and lipid (between 5 and 45%) per unit dry weight and contain polyunsaturated fatty acids, such as docosahexaenoic acid (22:6 $n-3$), eicosapentaenoic acid (20:5 $n-3$) and arachidonic acid, which can be used by various fish and larvae (Sargent et al., 1997; Becker, 2013; Roy and Sen Pal, 2015). Recently the use of microalgae in fish feed has become more significant as microalgae can potentially reduce the need for inclusion of fish meal and fish oil in fish feeds (Shah et al., 2018). Neori (2011) reported that microalgae use as feed through the technique of green-water culture serves as an important driver to increase production of planktivorous species such as Nile tilapia (*Oreochromis niloticus*), rohu carp (*Labeo rohita*), bighead carp (*Hypophthalmichthys nobilis*), catla (*Catla catla*), and shrimps.

Many reviews have covered extensively the cultivation of algal in different environments such as open and closed microalgae production systems (Masojídek and Torzillo, 2008; Mata et al., 2010; Yusoff et al., 2019) and various wastewater systems (Larsdotter, 2006a; Pittman et al., 2011; Abdel-Raouf et al., 2012). These studies have demonstrated benefits of integration of algae in the systems for nitrogenous waste management. Works related to algae integration in RAS is limited, and no recent report was found except for studies by the authors (Ramli et al., 2018a,b) that deal with algae-bacteria interactions in a RAS. Van Rijn (2013) reported that integration of phototrophic organisms (such as algae) in a RAS was mainly restricted to outdoor RAS due to the large areas required for photosynthesis. Since the development has been rather slow, the state-of-the-art is limited to work presented in this review. Consequently, the potential and feasibility of integration of microalgae in a RAS, especially indoors, for nitrogenous waste removal remains unclear and must be explored. Therefore, the objective of this paper is to review nitrogen removal performance by algae subject to different configurations of RAS.

The review starts by indicating differences between RAS integrated with algae and integrated multi-trophic aquaculture (IMTA), which also integrates algae in the system (see Section "The Differences Between RAS Integrated With Algae and IMTA"). Next, this review examines how different RAS has exhibited different nitrogen removal rates by identifying variables or factors that might influence removal rates (see Section "Integrating RAS With Algal Reactor"). These identified factors are further discussed (see "Factors Affecting Nitrogen Removal Rates by Algae"). Some insights on cost-benefit analysis on integrating algae in RAS are discussed in Section "Cost-Benefit Analysis of RAS-Photobioreactor Integration." Information gathered in this review will give better insights into how nitrogen removal by algae in RAS could be optimized and assess whether RAS could be used for mass cultivation of algae.

THE DIFFERENCES BETWEEN RAS INTEGRATED WITH ALGAE AND IMTA

One of the aquaculture technologies which also uses algae for nitrogenous waste management is IMTA. According to Buck et al. (2018), in IMTA, fed species, mainly fish or shrimps, are co-cultivated with extractive species such as suspension-feeders (e.g., mussel or oyster), deposit-feeders (e.g., sea-cucumber or sea-urchin), and macroalgae (e.g., kelp). One of the main objectives of IMTA is to increase the productivity per unit of feed given to a system, thus increasing the sustainability of aquaculture activities (Neori et al., 2004). The concept of IMTA applies to coastal lagoons, bays, and inland aquaculture such as ponds and tanks. In ponds, the culture water could be partly or fully channeled to algae culture systems and recirculated, and thus can be considered as a RAS or semi-RAS for inland aquaculture (Neori et al., 2003, 2017; Schuenhoff et al., 2003; Abreu et al., 2011). However, in open systems such as coastal lagoons, sequestration of the wastes by algae, though promising, is difficult to measure due to dilution (Troell et al., 2003; Buck et al., 2018), and uncertainties in estimating the contribution of nutrients already present in the open production environment.

Recirculating aquaculture systems and IMTA were originally conceptually different in terms of nutrient recycling. RAS aims to maintain water quality for cultured species while removing waste products such as organic particles (sludge) coming from feces, remnant feed, and sloughed biofilm from biofilter media. In RAS, dissolved ammonia is not removed but converted into less toxic nitrate, while both ammonia and nitrate can also be taken up by algae. In addition, nitrogen can be removed through denitrification. In contrast, IMTA aims through co-cultivation of extractive species to trap as much nutrients as possible in commercially valuable species or products. As a result, in practice IMTA and RAS partially overlap. This review focuses on the integration of algae in RAS, not covering the nutrient trapping by algae and the fate of algae in open systems. Findings presented are, however, also relevant to land-based nearly-closed or semi-closed IMTA.

INTEGRATING RAS WITH ALGAL REACTOR

An RAS must include of a series of water purifying units, namely a solids removal unit and a biofiltration unit. The concept of a RAS was originally designed for indoor systems (Rakocy et al., 1992), and this concept has been broadened to include outdoor pond systems (Lazur and Britt, 1997; Bosma and Verdegem, 2011). In this review, for the outdoor ponds to be considered a RAS, the fish culture pond must be associated with a water purification pond or other unit for biofiltration. Meanwhile, RAS also are operated in greenhouses, as demonstrated in the study of Huang et al. (2013). The greenhouse offers protection from the environment, is easily controlled, and uses mainly natural light. For this review, RAS in a greenhouse is considered as indoor RAS because of the protection it receives.

The main processes for water treatment in a RAS are solids separation and biological treatment processes mainly for transforming inorganic nitrogenous wastes into nitrate or nitrogen gas through nitrification/denitrification or for ammonia assimilation into algae and bacteria. In an outdoor RAS, the biological processes may occur simultaneously in ponds, whereas, in an indoor RAS, bacterial and algal processes typically are compartmentalized and managed specifically to support the purification process in each compartment.

This review focuses on a RAS, which has at least one algae tank or pond as a bio-filtration unit separated from the main culture unit be it outdoor or indoor. Currently, there is a limited number of studies on RAS integrated with algae (**Table 1**) (Further descriptions of these systems can be found in **Supplementary Table 1**).

The different RASs that have been integrated with an algae unit (**Table 1**) could be classified according to the type of algae cultured (macroalgae or microalgae), the location of algae unit (indoor or outdoor), and the different configurations of the RAS. Different fish or invertebrate species, stocking densities, and feeds given affect the nutrients availability in the respective systems.

TABLE 1 | Rates of nitrogen removal by algae reactors in recirculating aquaculture systems (RAS).

System type	Cultured animal (stocking density, kg m^{-3})	Feeding	Nitrogen loading rate, g m^{-2} day^{-1}	Nitrogen removal rate, g m^{-2} day^{-1}	References
Microalgae (indoor)					
Valeta and Verdegem (2015) – Study 2 RAS + Periphyton turf scrubber, (PTS) which comprise microalgae and other micro-organisms	Tilapia (*Oreochromis niloticus* L) (28–70)	Commercial feed (CP was not given)	3.76–3.81 g TAN	0.302–0.656	Valeta and Verdegem, 2015
Huang et al. (2013) - Study 3 RAS + PTS	Rainbow mussels (*Villosa iris*) (245 animals m^{-2}, 17.3 mm length)	*Nannochloropsis* (0.02 ml L^{-1}) and mixture of *Isochrysis* sp., *Pavlova* sp., *Thalassiosira weissflogii*, and *Tetraselmis* sp. (0.007 ml L^{-1})	n.a	0.01	Huang et al., 2013
Microalgae (outdoor)					
SustainAqua (2009) – Study 4 RAS + outdoor PTS	Fishpond - common carp (*Cyprinus carpio*) (15) Periphyton pond-tilapia (*Oreochromis niloticus* L) (0.5)	Commercial feeding in fishpond (40% CP)	3.8	1	SustainAqua, 2009
Gál et al. (2003) – Study 7 Combined Intensive – extensive pond system	Extensive pond – 90% common carp (*Cyprinus carpio*) and 10% Chinese carp (*Hypophthalmichthys molitrix* and *Aristichthys nobilis*) (0.014–0.15) Intensive pond – common carp (*Cyprinus carpio*), African catfish (*Clarias gariepinus*) and tilapia (*Oreochromis niloticus*) (0.07–3.9)	Commercial feed (0.042–0.06 g N day^{-1}) (CP was not given)	0.87	0.26	Gál et al., 2003
Li et al. (2019) – Study 8 RAS- outdoor raceway (microalgae, multi species)	European sea bass (*Dicentrarchus labrax* L.) (30- initial density)	Commercial feed (*ad libitum*) estimate CP = 43%	0.435	0.391	Li et al., 2019
Macroalgae (indoor)					
Cahill et al. (2010) – Study 1a RAS + Algae tank (*Ulva lactuca*)	Rainbow abalone (*Haliotis iris*) (4.45)	Commercial feeding (0.75% body weight) CP not mentioned, but 35% used from reference	0.1134[1]	*0.135	Cahill et al., 2010
Cahill et al. (2010) – Study 1b RAS + Algae tank (*Ulva pinnatifida*)	Rainbow abalone (*Haliotis iris*) (0.004)	Commercial feed (0.75% body weight)	*0.1134	*0.135	Cahill et al., 2010
Macroalgae (outdoor)					
Pagand et al. (2000) – Study 5 RAS + HRAP - Mix of microalgae and macroalgae species (*Ulva* sp., *Enteromorpha* sp. *Ectocarpus* sp.)	European sea bass (*Dicentrarchus labrax* L.) (100)	Commercial feed (n.a) estimate CP = 40%	1.6	0.9 (winter) 2.79 (summer) (0.5 to winter; 0.9 summer) (0.1 g N g^{-1} algae day^{-1})	Pagand et al., 2000
Deviller et al. (2004) – Study 6 RAS + HRAP – Mix of microalgae and macroalgae species (*Ulva*, *Enteromorpha*, and *Cladophora*)	European sea bass (*Dicentrarchus labrax* L.) (10 ± 2; initial density, 82 ± 22; final density)	Commercial feed, 44–52% protein (1.5% body weight)	2	1.0 (0.5 ± 0.2 g N m^{-2} day^{-1})-summer (0.09) g N m^{-2} day^{-1}) winter	Deviller et al., 2004

The system configurations are detailed in ***Supplementary Table 1****. (Studies 1–8 refer to labels used in the main text,* ***Figures 1–4*** *and* ***Supplementary Table 1****). [1]When assuming depth of algae tank is 0.3 m (also for other information which is labeled with an *).*

These nutrients are partially digested by the cultivated organisms and became the nutrient source for the algae. In this review, only nitrogen is considered. The nitrogen-loading rate indicates the amount of nitrogen entering the algal reactor per area per day (g m^{-2} day^{-1}). The nitrogen removal rate indicates the amount of nitrogen removed by the algal reactor (g m^{-2} day^{-1}). Before

any comparison can be made between the respective studies, it is important to check how nitrogen loading rates and nitrogen removal rates were calculated in each study.

Estimation of Nitrogen Loading Rate

The nitrogen loading rate is the amount of nitrogen received per unit area of the algae reactor per unit of time (g N m^{-2} day^{-1}). The nitrogen loading rates in the eight studies are shown in **Figure 1**. In this review, Studies 1 through 8 as referred to **Figure 1** will be used in the text. Studies 1 (Cahill et al., 2010), 2 (Valeta and Verdegem, 2015), and 4 (SustainAqua, 2009) reported the nitrogen loading rates measured in their studies. However, Studies 5 (Pagand et al., 2000), 6 (Deviller et al., 2004), 7 (Gál et al., 2003), and 8 (Li et al., 2019) did not report the nitrogen loading rate, and therefore, the nitrogen loading rate was estimated by the authors in this review using the nitrogen concentration and flow rate into the algal reactor or using the percentage of nitrogen removal rate in the studies. Similarly, Study 3 did not report nitrogen loading rates. In this case, it was impossible to calculate the nitrogen loading rate since the mussels cultivated under Study 3 were fed live algae, and no information was given concerning the amount of microalgae fed.

Estimation of Nitrogen Removal Rate

There were three methods used to estimate the nitrogen removal rate in the respective studies. The first method estimated the nitrogen removal rate from algal growth or algal productivity (Brune et al., 2003). The basis for this method is that the rate of algal productivity (photosynthesis) reflects the rate of nitrogen assimilation of algae (g N m^{-2} day^{-1}). The nitrogen assimilation by algae reduces the nitrogen concentration in water, and thus is considered also as nitrogen removal. The nitrogen removal rate by algae is normally expressed per unit area considering the light distribution, which is expressed per unit area. During photosynthesis, inorganic carbon in the form of carbon dioxide (CO_2) or bicarbonate (HCO_3) is used as the carbon source and nitrogen in the form of ammonium (NH_4^+) (Equation 1) or nitrate (NO^-_3) (Equation 2) is used as an N source (Stumm and Morgan, 1995; Ebeling et al., 2006):

$$16NH_4 + 92CO_2 + 92H_2O + 14HCO_3^- + HPO_4 \rightarrow C_{106}H_{263}O_{110}N_{16}P + 106O_2 \quad (1)$$

$$16NO_3^- + 124CO_2 + 140H_2O + HPO_4^{2-} \rightarrow C_{106}H_{263}O_{110}N_{16}P + 138O_2 + 18HCO_3^- \quad (2)$$

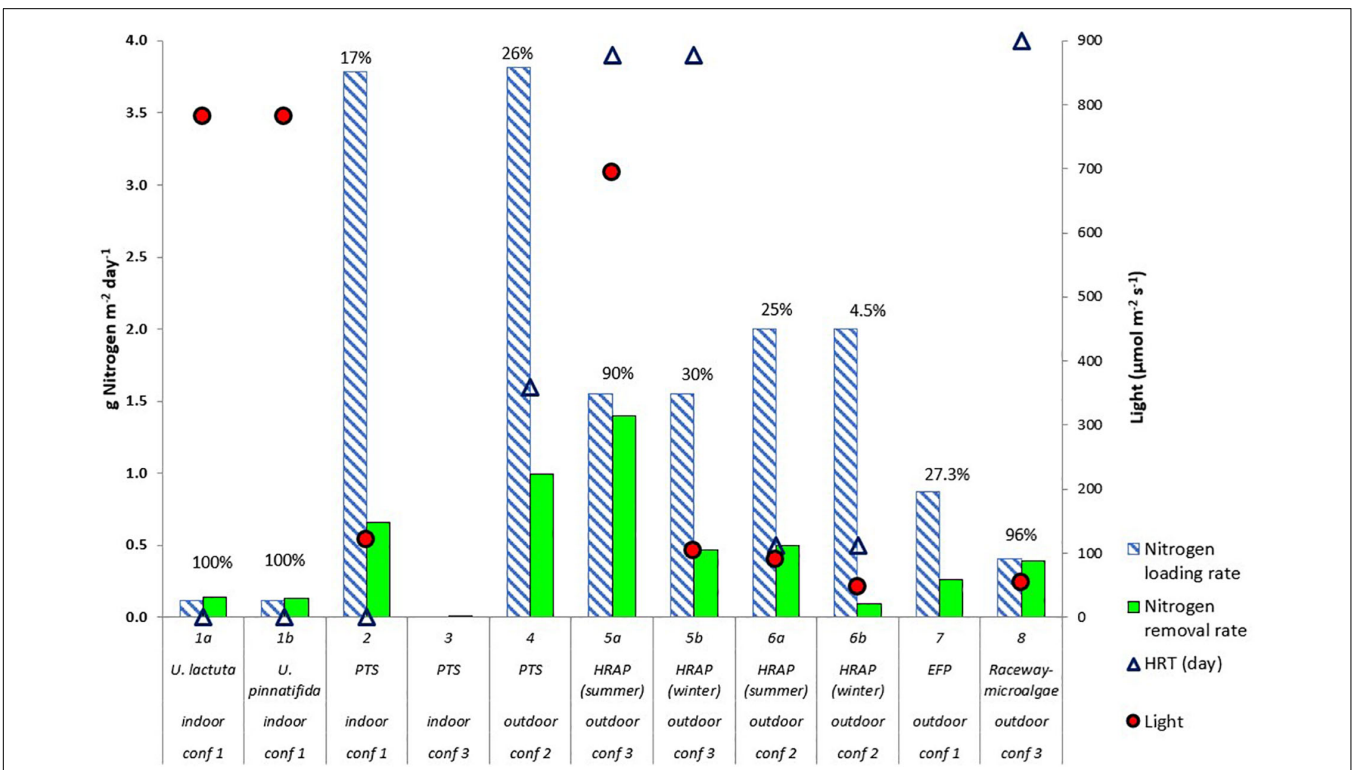

FIGURE 1 | Nitrogen removal and loading rate (g Nitrogen m^{-2} day^{-1}) by algal reactors in recirculating aquaculture systems (RAS).% value refers to the percentage of nitrogen removed. Maximum photosynthetic active radiation (light – µmol m^{-2} s^{-1}) used in the studies are shown by red circles. Hydraulic retention time (HRT) (days) are shown by triangles (primary axis). For Study 3, HRT was not given, for Study 7, HRT was 60 days (not included in figure) The RAS configurations of Studies 1–8 are shown in **Figure 4**. Indoor and outdoor labels in the figure indicate the location of the algae reactors. The algae reactor in Study 1 used two algal species (Cahill et al., 2010), *Ulva lactuca* and *Ulva pinnatifida*. Study 2 (Valeta and Verdegem, 2015), Study 3 (Huang et al., 2013), and Study 4 (SustainAqua, 2009) used a periphyton turf scrubber (PTS). Study 5 (Pagand et al., 2000) and Study 6 (Deviller et al., 2004) used high-rate macroalgal based algal ponds (HRAP), and Study 7 (Gál et al., 2003) used an extensive fish pond (EFP). Study 8 (Li et al., 2019) used outdoor microalgal based raceway as methods to integrate algae in the RAS.

According to Equation 1, 1 g of ammonium nitrogen assimilated by algae produces 15.84 g of algae biomass. Also, in this formula, carbon comprises 35% and nitrogen comprises 6% of the algal biomass; thus, the ratio of carbon to nitrogen (*C*/*N*) of algae biomass is 5.6:1. This formula can be used to estimate nitrogen assimilation when the algal biomass (given as dry weight or as carbon content) in a system is known. There is also another ratio used for carbon content in algae whereby from the measured algae dry solids, 50% is carbon (Chisti, 2007). Meanwhile, a *C*/*N* ratio of algae of 10:1 also is used (Boyd, 1985) as in Study 7 (Gál et al., 2003). The use of a *C*/*N* ratio of 5.6:1 could lead to a higher estimation of nitrogen removal by algae than using a *C*/*N* ratio of 10:1. The nitrogen content of algae also can be directly determined by nitrogen composition analysis of the algae (Study 4) (SustainAqua, 2009).

Where algal productivity is not available, standing algal biomass (g m^{-2} or g L^{-1}) is used as a metric of N removal. This method is normally used in combination with the calculation of the nitrogen budget of a system. A disadvantage is that by using the algal standing biomass, the nitrogen removal rate cannot be determined.

The second method used to determine the nitrogen removal was by measuring nitrogen difference between influent and effluent streams of an algal reactor (Pagand et al., 2000). In the third method, the nitrogen removal by an algal reactor was estimated by comparing difference of nitrogen between a system with algae and a system without algae.

The first method was reported in Study 1 (Cahill et al., 2010), Study 4 (SustainAqua, 2009), and Study 7 (Gál et al., 2003). The second method was reported in Studies 2 (Valeta and Verdegem, 2015), 5 (Pagand et al., 2000), and 8 (Li et al., 2019). The third method was reported in Studies 3 (Huang et al., 2013) and 6 (Deviller et al., 2004).

Nitrogen Removal Rate in Algae Reactors in RAS

Different nitrogen loading and removal rates as the result from different RAS configurations and culture practices is visualized in **Figure 1**. Based on **Figure 1**, variables presented with regards to nitrogen removal rate are nitrogen loading rate, light, hydraulic retention time (HRT) of algae reactors, type of algae, algae cultivation system [periphyton turf scrubber (PTS), high-rate algal pond (HRAP), extensive fish pond (EFP), and microalgal based raceway], location of algae reactor (indoor versus outdoor), and RAS configuration (1, 2, and 3). The concept of PTS in the mentioned studies is also termed as an algal turf scrubber (ATS), where microalgae and other types of microorganisms attach on a substrate prepared for the experiments (Adey, 1982, 1992, 1998; Adey and Purgason, 1998). Therefore, the term PTS will be used in this review. The HRAP term is used to describe the specific characteristics of a pond that is shallow, normally at 0.5 m deep, and intensively mixed (Benemann et al., 1977). The other variables were not plotted in **Figure 1**, either because the values were controlled by the fish requirement rather than algal requirement (e.g., pH) or because no quantitative data were provided in the studies (e.g., species composition and nutrient composition).

The above-mentioned system variables influenced nitrogen removal rates. From **Figure 1**, study 5a (Pagand et al., 2000) had the highest nitrogen removal by the algae (1.4 g N m^{-2} day^{-1}). This removal rate is comparable with removal rates achieved by algae in aerated pond systems (between 0.5 and 1.8 g N m^{-2} day^{-1}, considering the *C*/*N* ratio of algae between 5.6:1 and 10:1 as described in section "Estimation of Nitrogen Removal Rate") (Brune et al., 2003), and in IMTA systems (between 1.3 and 1.5 g N m^{-2} day^{-1}) (Abreu et al., 2011; Ben-Ari et al., 2014). Factors that could explain this high nitrogen removal and which were not demonstrated in other studies were the combination of high light intensity (694 μmol m^{-2} s^{-1}) and HRT (3.9 days). Study 5b (Pagand et al., 2000) had a lower nitrogen removal rate than 5a because of the low light intensity during winter. For Studies 1 (Cahill et al., 2010) and 8 (Li et al., 2019), even though the nitrogen removal rate was 100%, which might indicate the efficiency of the algae, the nitrogen loading rates were low compared to other studies. For Studies 2 (Valeta and Verdegem, 2015) and 6 (Deviller et al., 2004), either light intensity or HRT was low, which caused the low nitrogen removal rate. Meanwhile, in all studies, especially for outdoor algal ponds, Studies 4 (SustainAqua, 2009), 6 (Deviller et al., 2004), and 7 (Gál et al., 2003), nitrogen removal could be driven by heterotrophic bacteria, possibly due to high carbon, which was released by bacteria and algal decomposition in the system. This is related to the fact that even though nitrogen removal by algae was not 100%, inorganic nitrogen concentration in the RAS was low (**Supplementary Table 2**). The effects of algae type, algae cultivation system, location, and RAS configuration on nitrogen removal rate could not be quantified, although these factors might be important. Nevertheless, outdoor systems could be associated with high light intensity, which determines the high nitrogen removal rate by the algae.

From these examples, factors that may affect nitrogen removal rate can be categorized under five main factors: (1) algal biological characteristics (algal growth rate, algal species and species composition); (2) RAS configuration; (3) nutrient availability in RAS (nitrogen loading rate, nitrogen species and nutrient waste composition); (4) algal culture system (outdoor versus indoor algae culture), and algal cultivation technique (suspended or attached); and (5) algal reactor conditions (such as HRT, light, carbon dioxide, dissolved oxygen, and pH). These factors are further discussed in Section "Factors Affecting Nitrogen Removal Rates by Algae."

FACTORS AFFECTING NITROGEN REMOVAL RATES BY ALGAE

Algae Growth Rate

It is widely accepted that algae growth rate is expected to be correlated with nitrogen removal rate. A high algal biomass can be an indicator of a high growth rate. However, a high biomass does not guarantee a high nitrogen removal rate because other

environmental factors such as light and CO_2 in the culture system may become limiting.

When a comparison is made between macroalgae and microalgae (**Figure 2**), the macroalgae biomass (g algae m^{-2} algae reactor) was higher than the microalgae/periphyton biomass. Except for Study 8 (Li et al., 2019), a relatively high microalgal biomass was observed. This could be due to the HRAP technique used in that study that enhanced the growth of microalgae (Brune et al., 2003). However, the removal rate of nitrogen per g algae per day (mg N removed g^{-1} algae day^{-1}) by a mixture of microalgae and periphyton was higher than that by macroalgae (**Figure 3**). This was most likely because the periphyton biomass also comprised of microorganisms, which also took up nitrogen (Azim et al., 2005; Asaduzzaman et al., 2008; Levy et al., 2017). Moreover, Hein et al. (1995) reported that the nitrogen uptake kinetics by algae is size-dependent. The report suggested that small-sized algae could provide a higher surface area for the nitrogen uptake rates, which is why microalgae could have a higher uptake rate than macroalgae.

In most algal reactors in a RAS, multi-species algae were observed instead of mono-species (**Table 1**). Since algae have different tolerance levels for total ammonia and different affinities toward the respective nitrogen species, presence of multiple species can be beneficial to nitrogen removal in a RAS through niche separation by these species in the systems [please see more elaboration in section "Outdoor Versus Indoor Algae Reactor (Light and Temperature)"].

Meanwhile in mono-species cultures, growth factors are more easily controlled. For instance, in Study 1 (Cahill et al., 2010) a single species of alga (*Ulva lactuca* for treatment 1, *and Ulva pinnatifida* for treatment 2), was used in the reactor, and the culture conditions were set according to the species' requirements. The use of a mono-species culture for a specific function in a RAS, for example for nitrate removal, would be beneficial if the algae perform well under the RAS conditions.

Nitrogen Loading Rates and Waste Composition

One of the most striking differences between the respective studies is the nitrogen loading rate (**Figure 1**). Studies 1 (Cahill et al., 2010) and 8 (Li et al., 2019), which had a low loading rates (0.11 and 0.41 g N m^{-2} day^{-1}, respectively), had a 100% removal rate. However, other studies, which had nitrogen loading rates above 0.8 g N m^{-2} day^{-1}, had nitrogen removal rates of between 17 and 27%, except for two cases that received high light intensity (690 μmol m^{-2} s^{-1}) and low light intensity (46 μmol m^{-2} s^{-1}), exhibiting 90 and 5% nitrogen removal rates, respectively. Hence, the nitrogen loading rate and nitrogen removal rates vary greatly between systems. Before the effects of nitrogen loading rates are discussed, factors that determine the nitrogen loading rates will be elaborated first. Waste composition is also discussed under this topic because factors that determine the nitrogen loading rate also affect waste composition.

Factors Determine Nitrogen Loading Rates and Nutrient Composition of Waste

In a RAS, the nitrogen loading rate tends to be dependent on the types of culture, stocking density, and the RAS configuration.

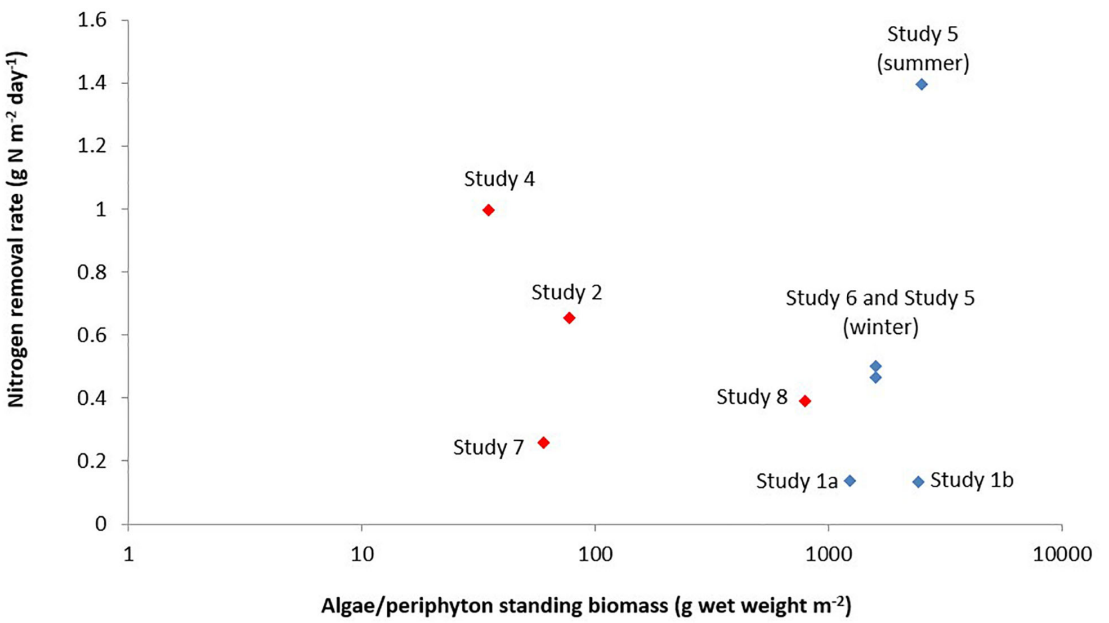

FIGURE 2 | Nitrogen removal rate versus algae/periphyton standing biomass in a recirculating aquaculture system. The red diamonds represent microalgae biomass for the studies of Gál et al. (2003) (Study 7) and Li et al. (2019) (Study 8), and periphyton biomass for the studies of SustainAqua (2009) (Study 4), and Valeta and Verdegem (2015) (Study 2). The periphyton biomass consisted of microorganisms such as phytoplankton, bacteria, fungi, protozoa, and range of invertebrates and detritus. The blue diamonds represent the macroalgae biomass from the studies of Cahill et al. (2010) (Study 1), Deviller et al. (2004) (Study 6), and Pagand et al. (2000) (Study 5). Information on algae for Study 3 was not part of the design of that study, thus, was not provided by those authors.

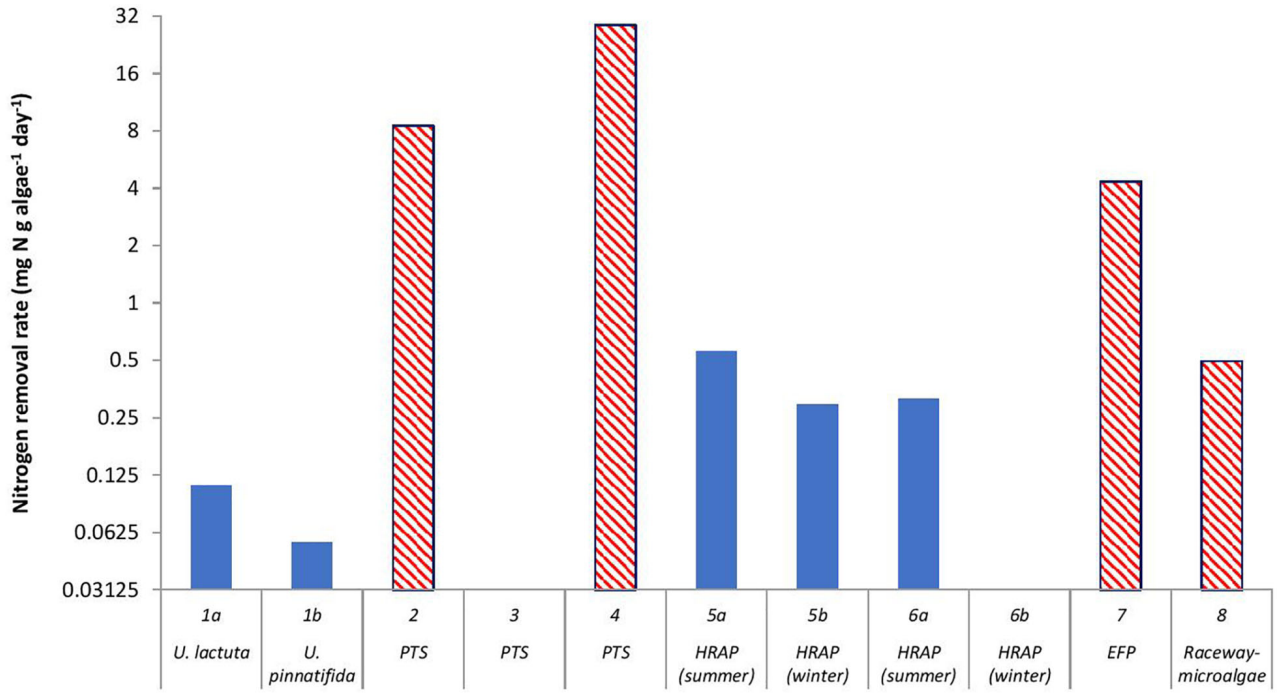

FIGURE 3 | Nitrogen removal rate by algae (mg N g algae dry weight^{-1} day^{-1}) in a recirculating aquaculture system. The algal reactor in Study 1 (Cahill et al., 2010) used two algal species, *Ulva lactuca* and *Ulva pinnatifida*. Study 2 (Valeta and Verdegem, 2015), Study 3 (Huang et al., 2013), and Study 4 (SustainAqua, 2009) used a periphyton turf scrubber (PTS), Study 5 (Pagand et al., 2000), and Study 6 (Deviller et al., 2004) used high-rate macroalgal based algal ponds (HRAP), Study 7 (Gál et al., 2003) used an extensive fish pond (EFP), and Study 8 (Li et al., 2019) used outdoor microalgal based raceway as methods to integrate algae in the RAS. The red bars with a diagonal pattern represent microalgae and the blue bars represent macroalgae. Information on algae for Studies 3 and 6b were not part of the design of those studies, thus, were not provided by those authors.

Metabolism, nutrient requirement, and husbandry of fish, crustaceans, and mollusks differ, and therefore different nutrient-loading rates are observed (Butterworth, 2010; Meriac et al., 2014b; Nunes et al., 2014). For example, the indoor RAS in Study 2 (Valeta and Verdegem, 2015) maintained tilapia at densities ranging between 30 and 70 kg m^{-3}, producing a nitrogen loading rate into the algae reactor of 3.79 g nitrogen m^{-2} day^{-1}. In Studies 5 (Pagand et al., 2000) and 6 (Deviller et al., 2004), indoor RASs contained sea bass and the maximum stocking densities used were 100 and 80 kg m^{-3}, respectively. Even though the algal reactors in these studies received only 6–10% input from the fish culture tank, the nitrogen loading was high (**Figure 1**). However, for Study 4 (SustainAqua, 2009), even though the stocking density in the carp pond was low (15 kg m^{-3}), a high nitrogen loading rate was observed in the algal reactor because it received 100% input from fishpond. In these studies, therefore, RAS configuration also played a role in determining the nitrogen loading into algae reactors, which will be discussed in the following section.

RAS configuration

Based on the studies of RAS, which included an algal reactor (**Table 1**), three different RAS configurations can be conceptualized to enhance the effectiveness of ammonia removal (**Figure 4**). In these configurations, only units supplying input to the algal reactor are considered. The first configuration comprises a fish culture unit and an algal reactor. The second configuration connects three components, a fish culture unit, a solids removal unit, and an algal reactor, and the third configuration is the same as the second except that a nitrification unit is integrated before the algal reactor.

The first RAS configuration uses an algal reactor as the only means to remove nitrogen. Since there is no nitrification unit installed, the algal reactor must be designed for a complete removal of the nitrogen excreted by the fish, as in Studies 1 (Cahill et al., 2010), 2 (Valeta and Verdegem, 2015), and 7 (Gál et al., 2003). The waste composition, that is, carbon to nitrogen (*C*/*N*) ratio of the waste entering the algal reactor, was expected to be high under this setup because particulate waste entered the algal reactor.

In the second configuration, the algal reactors served as a post-solids removal treatment unit since approximately 70–80% of the particulate waste was removed in the solids removal tank, as in Studies 4 (SustainAqua, 2009), 5 (Pagand et al., 2000), and 6 (Deviller et al., 2004). The solids removal process was performed in conventional RAS to support the biofilter, which requires a low *C*/*N* ratio (preferably between 0 and 1) (Zhu and Chen, 2001); therefore, under the second configuration, the algae reactor would receive a low *C*/*N* ratio. With the solids removal process, the *N*/*P* ratio of the waste entering the algae

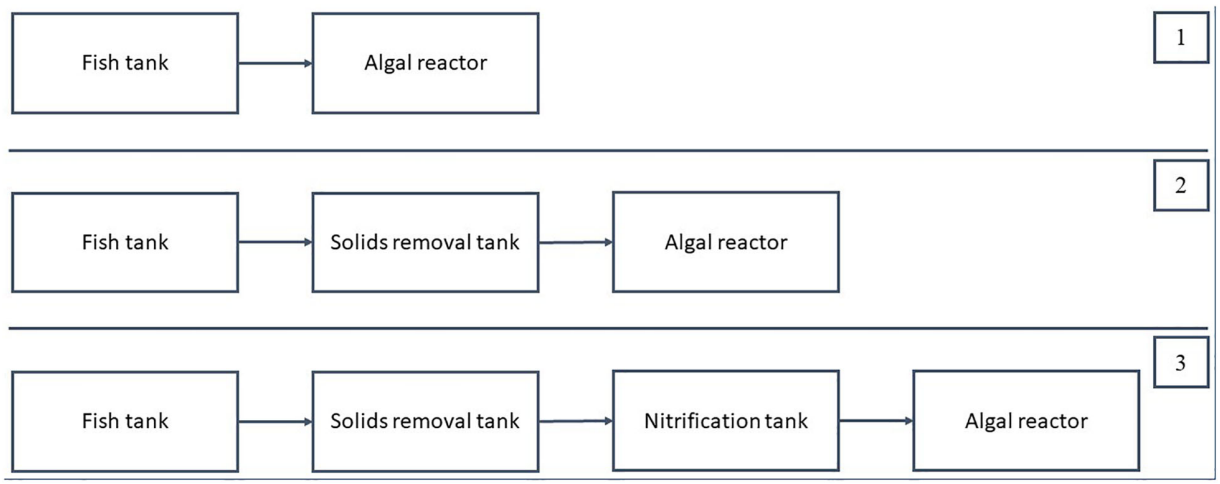

FIGURE 4 | Recirculating aquaculture system (RAS) configurations with algal reactors. After the algal reactors, the water was either fully recirculated back into the RAS, or partly discharged to the environment. Configuration 1 was used by Studies 1 (Cahill et al., 2010), 2 (Valeta and Verdegem, 2015), and 7 (Gál et al., 2003). Configuration 2 was used by Studies 4 (SustainAqua, 2009), 5 (Pagand et al., 2000), and 6 (Deviller et al., 2004). Configuration 3 was used by Studies 3 (Huang et al., 2013) and 8 (Li et al., 2019).

reactor would also be affected because particulate *P* would be removed in the solids removal unit. In this configuration, the amount of water channeled from the solids removal unit can be controlled. For example, in Study 4 (SustainAqua, 2009), 100% of the water was channeled into the algae pond. Meanwhile, for Study 6 (Deviller et al., 2004), only about 10% of the water was channeled into the algae pond.

For the third configuration, an algal reactor is located after the nitrification reactor. The nitrification reactor reduces the ammonia concentration and increases the nitrate concentration, allowing the algae to function specifically for the removal of nitrate-N. As reported in Studies 3 (Huang et al., 2013) and 8 (Li et al., 2019), which used this configuration, the nitrate level is significantly lower in the RAS with algae than in the control RAS without algae. Thus, the second and the third configurations allow the flexibility to control nitrogen loading and size of the algae reactor, including flow rates.

Effects of Nitrogen Loading Rate and Waste Composition on Nitrogen Removal Rate

Total ammonia tolerance of algae

Nitrogen loading rate determines the concentration of nitrogen in the water and affects algae growth. Generally, an ammonium-N concentration below 1.09 mg L^{-1} would not affect the growth of microalgae (Collos and Harrison, 2014). For the marine phytoplankton species, *Nephroselmis pyriformis*, unionized ammonia-N at 0.0328 mg L^{-1}, and ammonium-N at 3.14 mg L^{-1} were found to be toxic (Källqvist and Svenson, 2003). Meanwhile, Collos and Harrison (2014) reviewed 45 freshwater and 68 marine microalgae species and concluded that optimum and toxic levels of ammonium differ between microalgae species (**Table 2**). In these studies, unionized ammonia toxicity was observed mainly when the pH was >9, and ammonium toxicity occurred when the pH was <8. Collos and Harrison (2014) suggested *Nannochloropsis* sp. as a suitable candidate for aquaculture systems, since this species can tolerate total ammonia levels of 12 mg L^{-1} at pH 8 (Hii et al., 2011). Further, *Chlorella vulgaris*, which is a common species in aquaculture ponds, was reported to tolerate an ammonia-N concentration of 280 mg L^{-1} at pH 7.0 (Tam and Wong, 1996).

Preference of nitrogen species

The preference of algae for the reduced forms of nitrogen (ammonium, urea, dissolved free amino acids and adenine) or the oxidized form of nitrogen (nitrate) could affect the nitrogen removal rate by algae (Dortch, 1990; Yuan et al., 2012). Most algae prefer ammonium as the nitrogen source because less energy is needed compared to other forms of inorganic nitrogen, such as nitrate (Dortch, 1990; Hii et al., 2011). Only when ammonium was not detected was nitrate uptake positive, and correlated with phytoplankton cell size (Yuan et al., 2012). The common view of the nitrogen cycle is that bacteria decompose organic nitrogen and that algae use inorganic nitrogen. There is some overlap, as both bacteria and algae use both organic and inorganic nitrogen (Kirchman, 1994; Allen et al., 2002;

TABLE 2 | Toxic and optimum concentration of ammonium for different microalgae species [Collos and Harrison (2014) and references therein].

	Toxic	Optimum
	Ammonium level (mg L^{-1})	Ammonium level (mg L^{-1})
Chlorophyceae	702.4	136.9
Cyanophyceae	234.1	45.0
Prymnesiophyceae	41.4	25.2
Diatomophyceae	64.8	6.1
Raphidophyceae	45.0	4.7
Dinophyceae	21.6	1.8

Bronk et al., 2006). When inorganic nitrogen is limited, algae can use urea as a nitrogen source (Bradley et al., 2010). For example, *Prochlococcus* spp. was found to assimilate organic nitrogen in a low-nutrient environment (Zubkov et al., 2003). Yuan et al. (2012) found that after ammonium is depleted, algae would use organic N (including urea and amino acids) rather than nitrate. *Nannochloropsis oculata* and *Stigeoclonium nanum* prefer ammonium to nitrate, in contrast to *Chlorella vulgaris* that prefers nitrate (Podevin et al., 2015; Ramli et al., 2017).

While most green algae and cyanobacteria prefer ammonium to nitrate, diatoms, and dinoflagellates prefer nitrate over ammonium (Dortch, 1990; Domingues et al., 2011). In the Gulf of Riga, Latvia, only diatoms were able to use the oxidized form of nitrogen (nitrate), while other phytoplankton such as cryptophytes, dinoflagellates, and filamentous cyanobacteria were able to use reduced forms of nitrogen (Berg et al., 2003). There is mounting evidence that supports this finding (Glibert et al., 2014a,b, and references therein). For instance, the occurrence of harmful algal blooms was encouraged under an elevated *N*/*P* condition with a high concentration of ammonium or urea. This finding has led many researchers to recommend strategies that the effluent entering the San Francisco Bay Delta in California should have a high nitrate concentration through nitrification in order to encourage diatoms, which are more beneficial for fish and higher trophic level consumers (Glibert et al., 2014a,b). In a RAS, where the nitrate concentration can become too high, the use of diatoms to remove nitrate should be encouraged (Ramli, 2018). Diatoms are commonly found in aquaculture ponds (Yusoff et al., 2002; Khatoon et al., 2007; Shaari et al., 2011) and HRAP connected to RAS (Pagand et al., 2000). This proves that aquaculture waste is suitable for diatom culture. Nonetheless, Khatoon et al. (2007) observed that even though diatoms dominated the periphyton community at the beginning, after the 21 days of experiment, biofouling activities started to occur and dominated the substrate after 60 days of the experiment. However, for indoor RAS, no study on the use of substrate, except for Huang et al. (2013) and Valeta and Verdegem (2015), and no biofouling activities on algae substrate were reported. Besides biofouling, another important consideration for diatom culture is silicate concentration. Normally, in diatom cultures, silicate is added to support cell wall development (Bondoc et al., 2016). Therefore, experiments aiming to develop guidelines for silicate requirements to integrate diatom culture in RAS are needed.

Effects of waste composition (C/N and N/P ratio)

Nitrogenous waste composition may influence the nitrogen assimilation (nitrogen removal) by the algae (Glibert, 2012). In aquaculture systems, waste composition influences the contributions of heterotrophic, autotrophic, or phototrophic processes to waste removal (Avnimelech, 1999; Ebeling et al., 2006). A carbon to nitrogen (*C*/*N*) ratio of more than 10 will encourage heterotrophic processes, while a *C*/*N* ratio between 6 and 7 will encourage photosynthetic process by microalgae (Ebeling et al., 2006). When decomposition of microalgae is high, the *C*/*N* ratio in the water will increase, which favors heterotrophic processes. Sometimes, even though high microalgal abundance is observed, heterotrophic processes may dominate the removal of nitrogen, which has been observed in an intensive tank system receiving a high feed load (Rakocy et al., 2004).

The nitrogen to phosphorus ratio (*N*/*P*) affects the algal community composition (Heisler et al., 2008; Glibert, 2012). In turn, algal composition affects the nitrogen removal in an ecosystem. For example, in a community where cyanobacteria dominate then ammonium removal is high, whereas in a community where diatoms dominate then nitrate removal is high (Glibert et al., 2014b). A specific example of the *N*/*P* ratio affecting algal growth was reported for *Tisochrysis lutea* and *Nannochloropsis oculata*; a *N*/*P* ratio of 20 improved their growth while a *N*/*P* ratio of 120 reduced their growth (Rasdi and Qin, 2015). Increased or reduced algal growth under a certain nutrient composition will have a direct effect on the algal composition. In addition to the waste composition (*N*/*P* ratio), nutrient concentrations, especially of nitrogen, phosphorus and silica, influence the microalgal community structure in ponds (Yusoff and McNabb, 1989, 1997). For instance, Liu et al. (2011) showed that the effect of the *N*/*P* ratio is dependent on the nutrient concentration for *Microcystis aeruginosa*. When the initial nitrogen concentration was 10 mg L^{-1}, an *N*/*P* ratio of 16 was the optimum for their growth, but when the initial *P* was 1 mg L^{-1}, a *N*/*P* ratio of 40 was found to be optimum (Liu et al., 2011).

In aquaculture ponds, the microalgal community composition is highly dynamic; thus, an algae reactor connected to an aquaculture pond should experience similar dynamics. Shaari et al. (2011) reported that before shrimp were introduced into a culture pond, cyanobacteria dominated. After the shrimp had been introduced, diatoms dominated. In contrast, Yusoff et al. (2002) found that diatoms were dominant at the early and middle stages of shrimp culture: toward the end of the culture period, cyanobacteria were dominant. The result was supported by the study of Casé et al. (2008) who found that diatoms were replaced by cyanobacteria toward the end of the shrimp culture.

Outdoor Versus Indoor Algae Reactor (Light and Temperature)

From the RAS studies, the major practical differences between outdoor and indoor algae culture are the options to control light and temperature. Light is an important parameter affecting algal growth and influencing nitrogen assimilation by the algae. The saturation irradiance observed for many algae species was between 100 and 400 μmol photons per m^2 per second (Necchi, 2004). However, light availability in the water is limited by water turbidity; therefore, even though enough light might be provided, the light availability for algae might be restricted (Anthony et al., 2004; Tait et al., 2014).

During summer when light irradiance is high, an outdoor culture system that received sunlight had a higher nitrogen removal rate than an indoor algae reactor (**Figure 1**). On the other hand, the outdoor algae cultures are exposed to fluctuations in sunlight irradiance due to the day/night cycles and changes in weather conditions and seasons. A wide range of irradiance was

reported, between 46 and 1700 μmol photons per m^2 per second (**Figure 1** and **Table 1**). Quick changes in irradiance pose a high risk of culture collapse (Brune et al., 2003; Blanken et al., 2013).

Valeta and Verdegem (2015) (Study 2) applied artificial light with an intensity of 120 μmol photons per m^2 per second. When artificial light is supplied, no fluctuation of light intensity occurs. Microalgae can use all the photons in the photosynthetic active radiation (PAR), which have a wavelength between 400 and 700 nm (Blanken et al., 2013). However, red light (660 nm) is the optimum light for photosynthesis (Chen et al., 2010; Cuaresma et al., 2011). Therefore, by using artificial light, for example LED light, the specific wavelength required can be supplied (Schulze et al., 2014). However, it is well accepted that the costs of artificial light for culturing algae is high. Blanken et al. (2013) reported that the cost of artificial light is $25.3 per kg dry-weight biomass (at the time when the paper was published, 1.34 US dollars was equal to 1 €). From the point of biofuel production, this value would make the cost of algae production 25 times more expensive than using sunlight. Profitable biofuel production requires a cost under $1.3 per kg dry-weight biomass (Wijffels et al., 2010; Slade and Bauen, 2013). Therefore, the lighting cost could be an issue and impede integration of algae into a RAS.

Temperature is important because it influences the rates of enzymatic reactions that occur during photosynthesis. With a 10°C temperature increase, the enzymatic reactions are doubled (Goldman and Carpenter, 1974), thus doubling the nutrient uptake by the algae. In an outdoor culture where temperature cannot be controlled, minimizing the temperature fluctuation is a challenge, especially in areas that experience drastic temperature fluctuations (**Supplementary Table 1**). During winter, the water temperature can be sufficiently low that it results in a low nitrogen removal rate, as observed in Pagand et al. (2000) and Deviller et al. (2004) (Studies 5 and 6). Again, the advantage of an indoor reactor is that temperature can be controlled, enabling stable nitrogen removal all year round.

Effects of the Algae Cultivation Method

There are two algal culture methods that might be used in a RAS; namely, suspended or attached. From the comparison given (**Figure 1**), the method of cultivation did not seem to influence the nitrogen removal rate because of the interacting effects of other factors such as light and CO_2. Nonetheless, each method requires specific management, for example, reactor preparation or mixing, which have a direct impact on algae growth, and thus the nitrogen removal rate by the algae. For suspended culture, the preparation of the reactor is relatively simple, with a simple pond or a tank as enough. The HRAP is an intensive waste water treatment pond, which combines wastewater treatment, reclamation, and algal biomass production (Benemann et al., 1977). The pond is shallow and continuously aerated normally by paddle wheel to expose the algal cells to sunlight, to create a homogenous chemical environment and to avoid pond stratification (Brune et al., 2003). Meanwhile, in a raceway, algae are kept in suspension by a paddle wheel (Vonshak and Richmond, 1988). Reports on the use of suspended algae in an indoor algae reactor were not found.

The attached culture method refers to an ATS or PTS, which use substrates to support the growth of algae mats (Adey et al., 1993, 1996, 2013; Azim et al., 2005). In ponds, vertical poles, for example bamboo, fixed at the bottom often are used as a substrate (Azim et al., 2002; Richard et al., 2010). The substrates provide additional surface area for algae growth (Rahman et al., 2008; Asaduzzaman et al., 2010a,b). Air lifts or paddle wheels also are used to keep the water column mixed. The pond depth is also shallow, ranging between 0.5 and 1.0 m. This is unlike the suspension pond, where microalgae can have equal exposure to light through proper mixing. The bottom section of the water column receives less light than that close to the surface. Even so, the presence of substrate contributes to a large portion of autotrophic productivity by the periphyton community. Guiral et al. (1993) reported that a pond with a periphyton community realized 7.9 g C m^{-2} day^{-1} productivity, where this value was 4.5 times higher than in a pond with a phytoplankton community. Also reported in Azim et al. (2002), periphyton is accounted for 50% of the total primary productivity in a fishpond. In an indoor RAS, a flat wire mesh can be used as substrate and laid horizontally to provide an optimum surface area for the algae mats (Valeta and Verdegem, 2015) (Study 2). For mixing, a tipping bucket, which is located at the top section of the substrate, is filled and emptied continuously to create waves over the substrate in order to move nutrients across the substrate and facilitate gas exchange. In Huang et al. (2013), the ATS (60 cm long × 60 cm wide; mesh size = 1.3 cm × 1.3 cm) was made from plastic mesh. Water was pumped from the RAS over a vertically positioned ATS and returned through a sump to the RAS. This setup allowed light to easily illuminate the biofilm, promoted CO_2 and O_2 exchange, and facilitated homogenous distribution of nutrients passing through the ATS.

The major disadvantage for these two methods is that to capture enough light to control the ammonia, a larger surface area is needed. However, in many RAS, the surface area is of great concern. Since the surface area problem is not limited to the application of algae in a RAS, a recent innovation was made for the algae cultivation method where a solid-state biofilm method was applied (Naumann et al., 2013). The basic principle of this method is that algae were cultivated on vertically orientated twin-layer modules, which consisted of two ultrathin layers. The first layer is a macroporous layer where the algae culture medium passes through by the force of gravity, and the second layer is a microporous layer where the microalgae biofilm is attached (Naumann et al., 2013). The vertical arrangement of the biofilm substrates allows more efficient use of the surface area and exposure to light (Cuaresma et al., 2011). Blanken et al. (2014) used a very similar approach by applying a microalgal biofilm on a rotating Algadisk, which was vertically positioned and placed in a container. The disk rotated between the air (light) and water (dark) phase, and nutrients were supplied to the microalgal biofilm during the latter phase. When *Chlorella sorokiniana* was cultured using the Algadisk method, an algal productivity of 20.1 ± 0.7 g per m^2 disk surface per day was observed. This productivity would be equal to the removal of 1 g N m^{-2} day^{-1} [using the estimation method used in Gál et al. (2003)] (Study 7), which was higher than the nitrogen removal reported by

Valeta and Verdegem (2015), (Study 2) of 0.66 g N m^{-2} day^{-1} when using an indoor PTS. The Algadisk concept may be better than the PTS because of the optimum use of the surface area.

Effects of CO_2, O_2, and pH

Unlike light and temperature, the pH, carbon dioxide, and oxygen values are directly affected by the rate of photosynthesis and respiration in a RAS. In a RAS, the pH could become the least of the problems for algae, because the pH in a RAS is kept close to neutral for fish culture. Normally in a RAS relying on nitrification, the pH is kept above 6 by supplying bicarbonate to compensate for the loss in alkalinity due to nitrification. As shown in **Supplementary Table 1**, in all studies the pH was maintained between 6.5 and 8.4. By employing photosynthesis in a RAS, the annual amount of bicarbonate addition was reduced, despite low light irradiance during winter as in Study 6. In Study 5, the treated water had a higher pH level than the untreated water. The measurement was taken at midday when photosynthesis was at the highest rate. However, no pH value was reported during dark hours; therefore, the effect of pH on the algae during dark hours was unknown. Nonetheless, for a RAS set-up, the fish tank is separated from the algae tank, and the pH in the fish tank is controlled. Therefore, the fluctuation of pH in the algae reactor has minimal effect on the fish.

A RAS is a highly aerated system to supply enough oxygen for fish and bacterial respiration. Saturation higher than 100% is applied at the water inlet to prevent oxygen depletion (Bregnballe, 2015). In outdoor aquaculture systems such as ponds, diel oxygen fluctuations caused by photosynthesis are reported. Meanwhile, in an algal reactor, oxygen produced by algae could create super-saturation, which could negatively affect algae growth (Chisti, 2007). The oxygen is removed from an algal reactor by degassing through proper mixing. The different dissolved oxygen requirements of a RAS and an algal reactor should be taken into account when including an algae reactor in a RAS.

In addition, due to the highly aerated environment in a RAS, CO_2 insufficiency can become a serious problem for algae. Fish require oxygen, which can be produced by the algae, and in return, the CO_2 produced by fish respiration can be absorbed by the algae. How possible interactions between CO_2 and O_2 concentrations in RAS affect fish and algae production in RAS is insufficiently explored. The requirements of CO_2 by the algae and of oxygen by the fish should be a complementary process when algae are integrated in a RAS. The mass transfer of O_2 and CO_2 should be monitored to provide solid proof for the supposed mutual benefit and to develop management criteria, which guarantee optimization of this synergistic effect. Nonetheless, until any solution for the synergistic effects can be achieved by algae and fish, the CO_2 insufficiency in algal tank can be avoided by supplying pure CO_2 gas as normally practiced in commercial algal photobioreactors.

Effects of Hydraulic Retention Time

Generally, flow rates through fish tanks in a RAS are set to supply enough O_2 for the fish. Flow rates are also important to guarantee that solid and dissolved wastes (CO_2, total ammonia, dissolved organic carbon) are quickly transferred out of the culture tanks. This means that in general, short HRT prevail in the fish tanks of a RAS. For a culture tank less than 1 m^3, an HRT of 10 min is quite normal, but for culture tanks of more than 1 m^3, an HRT of 30 min or more is needed (Timmons and Ebeling, 2007). In addition, the type of the solid removal system used in a RAS sets different requirements for the HRT for proper solid waste removal. Normally the longest HRT applied in solid waste removal systems or settling basins is 15–30 min (Liao and Mayo, 1974). Further, fluidized bed sand biofilters that use fine sand particles require a longer HRT than other bio-filtration systems. However, fluidized bed sand biofilters are not commonly used because most RAS are operated under a short HRT in the culture tanks. In contrast, algae reactors require a longer HRT for the algae to grow.

The HRT of an algae reactor influences nutrient, CO_2, and O_2 transfer and therefore affects the algal growth rate (Inoue and Uchida, 2016). The applied HRT in the algal reactor will affect the gradients of nutrients, pH, CO_2, and O_2 along the reactor. An HRT that is too short will not ensure complete nutrient removal by the algae, whereas an HRT that is too long may cause starvation of the algal cells (Larsdotter, 2006b; Anbalagan et al., 2016). The HRT of an algae reactor should not exceed the time required to maintain the growth rates of algae in the photobioreactor (Larsdotter, 2006b). An HRT less than 0.5 days causes a washout of algae cells and a HRT of 2–3 days is recommended to obtain maximum biomass yield at 12–25°C and 190–450 μmol m^{-2} s^{-1} (Takabe et al., 2016). However, a relatively short HRT is normally used in algal reactors, which might explain the low nitrogen removal rates achieved (**Supplementary Table 1**). The HRT for the algal reactor will determine the size of the reactor. The longer the HRT, the larger the algal reactor required. Nonetheless, even for a short HRT, the size of the algae reactors used were one to two times the size of the fish culture vessel (**Supplementary Table 1**). The size of the algae reactor is expected to be one of the main factors influencing the farmers' choice of which type of algal reactor to install in their RAS.

COST-BENEFIT ANALYSIS OF RAS-PHOTOBIOREACTOR INTEGRATION

Culturing microalgae using aquaculture wastewater has been found to be efficient (Yusoff et al., 2001; Guo et al., 2013). In this way, the cost of nutrients and water for the algae can be eliminated. It was reported that the cost to produce microalgae using wastewater from a fish farm in a tubular photo bioreactor (PBR) was 36€ kg^{-1} dry weight (Michels, 2015) (for this estimation, microalgae were cultured in a tubular PBR with a total area of 1,000 m^2. Sunlight and a low-cost temperature controller were used. The average microalgae productivity was 0.3 g L^{-1} day^{-1} at an average biomass concentration of 0.7 g L^{-1} and PAR at 11.8 mole m^{-2} day^{-1}). Meanwhile, Oostlander et al. (2020) estimated a cost of €43- kg^{-1} cost production of microalgae in an aquaculture hatchery, which uses tubular reactors having a total

areas of 1,500 m^2. In this review, estimation of cost by Michels (2015) is used for the following analysis.

Current interest concerns how integration of microalgae in a RAS could affect the RAS total production cost. From Timmons et al. (2002), the cost of producing tilapia was 2.06 € kg^{-1} (1.76 $US kg^{-1}, 1 € = 1.17 US$). The tilapia were produced in a RAS facility producing 590,000 kg tilapia per year. The stocking density applied was 100 kg m^{-3}. It was assumed that the tilapia were fed at 2.5% body weight per day, with feed containing 32% crude protein. Therefore, for 100 kg m^{-3} production, 2.5 kg feed would be given per day. This would produce 62 g ammonia-N day^{-1}, using the same assumptions as in Section "INTRODUCTION." Considering that the nitrogen content in microalgae dry matter is 6% (Equation 1, see section "Integrating RAS With Algal Reactor"), then 1,033 g microalgae biomass is required to take up 62 g ammonia-N per day. For simplification, 1,000 g (1 kg) microalgae dry weight is taken as the final value.

At a production cost of 2.06 € kg^{-1}, 206 € is needed to produce 100 kg tilapia. One kg microalgae is needed to assimilate all the ammonia-N, and the cost of microalgae production was 36€ kg^{-1} dry weight. Therefore, the cost addition by microalgae is about 17.5% of the cost for producing tilapia. However, if artificial light is used, the algal production cost increases by 23€ kg^{-1}, raising the cost of tilapia production in the RAS by 29% (see section "Factors Affecting Nitrogen Removal Rates by Algae" on light).

From the aspect of water use, based on a productivity of 0.3 g L^{-1} day^{-1} achieved by Michels (2015), then 1,000 g algae dry weight would require 3,333 L (3.3 m^3) of photo bio-reactor. Therefore, 3.3 m^3 of microalgae culture capacity is needed to remove the ammonia-N produced by a 1 m^3 culture tank in a RAS.

From Ngoc et al. (2016), the cost of producing *Pangasius* was 97.92 € per 100 kg of fish. In this study, 608 tons of *Pangasius* ha^{-1} $year^{-1}$ was produced in a large-scale (>3 hectares) *Pangasius* pond-RAS. Integrating microalgae production would increase the cost for producing *Pangasius* by 37%. Therefore, in the setup used by Ngoc et al. (2016), PBR might not be a suitable method and hence, an outdoor HRAP or periphyton pond would be a more suitable alternative for reducing the cost for algae integration in the RAS.

Even though addition of an algal reactor into RAS could add to the production cost, it is important to note that some countries charges levy for every unit of pollution discharged to the environment. For example, in the Netherlands, the levies that are charged to farmers are based on unit of pollution (p.u.), which refers to oxygen-consuming substances discharged per year (Herman et al., 2017). One unit of pollution is equals to 49.6 kg O_2 per year, and the charge is €32/p.u. (Warmer and van Dokkum, 2002). Based on the prior estimation that 1033 g of microalgae are needed to assimilate 62 g ammonia-N per day ammonia produce in a one cubic meter of fish tank, the photosynthesis that will use 62 g ammonia-N per day will produce 940 g oxygen per day (based on Equation 1). Therefore, for 1 year, it can be estimated that 343.1 kg oxygen will be produced by the microalgae. This oxygen is equals to 6.9 p.u., which value at €221 per year.

The advantageous effect of algae integration on cost is also dependent on the value of the algae. For example, the market value of common microalgal species such as *Chlorella* and *Arthrospira* (formerly known as *Spirulina*) biomass are 44 and 42 USD kg^{-1}, respectively (Barkia et al., 2019). These values are higher than the algal production cost estimated above, and if the biomass can be produced in a RAS, it will increase the total revenue of the RAS. In terms of water volume, adding three times the volume of the fish culture tanks to culture algae in a RAS raises system and production costs. Therefore, the percentage of nitrogen immobilized in the algal biomass might be reduced to the level that is economically acceptable. Nonetheless, technological advancement in algae cultivation is moving toward higher algal productivity and lower cost. The same development is also occurring in a RAS. If cost reductions can be realized in algal systems and in RAS systems, then cost-effective integration of an algal reactor in a RAS might become feasible.

CONCLUSION

This review identifies two challenges related to algal integration in RAS: first, the practical feasibility for improving nitrogen removal performance by an algal reactor in RAS, and second, the economic feasibility of integrating an algal reactor in RAS. This review demonstrates that algae could be used to remove inorganic nitrogen in RAS. The maximum removal that was achieved by one of the RASs reviewed was 1.4 g N m^{-2} day^{-1}. The main factors that determine the high removal rates are light and HRT. Besides these factors, RAS configuration is important for the effectiveness of the algal reactor. RAS configuration relates directly to the HRT that can be applied for the algal reactor. When an algal reactor receives a fraction of wastewater and is placed after the solids waste removal unit or nitrification unit, this configuration could allow flexibility to determine the HRT of the algal reactor. Since the performance of nitrogen removal rates by algae is determined by HRT, this will affect the size (area or volume) of the algal reactor due to the time required for nutrient uptake by algae and large surface area needed to capture enough light. Another important factor that determines nitrogen removal rate is the nitrogen loading rate. From the review, the maximum nitrogen loading rate that allows the maximum nitrogen removal rate by algal reactor remains unknown. Therefore, the importance of these three factors (light, HRT, and nitrogen loading rate) for maximum nitrogen removal by the algal reactor in RAS warrants further investigation. Future work also should focus on implementing a practical and easy-to-manage algal reactor for RAS. The growth and efficiency of the algae in assimilating inorganic nitrogenous waste in RAS must be one of the top design priorities.

Regarding economic feasibility, current algae management and cost structure might hinder the integration of algae in a RAS. However, we believe that future technological advancements in algal cultivation methods (such as improved algal reactor designs and low-cost artificial light) will make algae integration more economically feasible. Advancement in algal cultivation

technology will continue, as algae is a high-value material, which are highly sought by the pharmaceutical, animal feed, and energy industries. Limited availability of natural resources such as land and water, as well as possible water discharge regulations will also be driving factors to integrate algae in fish farming activities including RAS.

Our work also can be used as a guideline for choosing many different available methods to ensure a high removal rate for nitrogen by integrating algae in the RAS. The authors suggest the following step-by step process for the integration of algae in a RAS:

(1) The role of the algae in a RAS should be specified, either to utilize total ammonia, or nitrate because this would determine the location of algal tank in the RAS, which is related to RAS configuration. For ammonia removal, the optimal location to integrate the algal reactor can be between the solids removal and biofiltration units where the ammonia concentration is high and the dissolved oxygen level is low. For nitrate removal, location of the algal reactor can be between the bio-filtration unit and the sump, where the nitrate concentration is high.
(2) Algae selection should be done according to their functions in the system, either to remove ammonia or nitrate only, or to be harvested as live feed or for other commercial purposes. A single-species or multiple species of algae can be integrated in the RAS for ammonia and nitrate removal, and for commercial purposes. For ammonia or nitrate removal only, a natural mixed population of algae is also an option.
(3) Algae cultivation technique (suspended or attached) can be chosen based on the algae selected; for example, the suspended technique is more suitable for planktonic algae while attached technique is more suitable for benthic algae.
(4) The operational conditions of an algal reactor, such as HRT, mixing rate, and light, should be optimized for algal growth.
(5) The algal reactor could be integrated as part of the RAS configuration or at the end of the RAS before the water is discharged to the environment. The benefit of having an algal reactor as a within-RAS component is that algae will increase the purification degree of RAS, thus decreasing the water exchange rate. Meanwhile, integrating an algal reactor as an end-of-pipe waste treatment could be easy and efficient to reduce waste discharge from RAS. This could reduce waste discharge fees where they are applied.

AUTHOR CONTRIBUTIONS

NR, MV, and JV conceived of the presented idea. NR wrote the manuscript with the help of MV, JV, FY, KN, and NN. All authors contributed to the article and approved the submitted version.

FUNDING

This work was supported by the Ministry of Higher Education, Malaysia (Skim Latihan Akademik IPTA), Universiti Putra Malaysia, International Foundation for Science grant number A/5348-1 and SATREPS-COSMOS Project No. JPMJSA1509 and the matching fund from the Ministry of Higher Education Malaysia.

ACKNOWLEDGMENTS

This research was conducted under the graduate school of the Wageningen Institute of Animal Science, Wageningen University and Research, Netherlands. The content of this manuscript was part of the thesis, "microalgae-bacteria interactions: a key for improving water quality in recirculating aquaculture systems?" published by the university. We wish to express our sincere appreciation to Universiti Putra Malaysia for the support we received. We thank reviewers for their insightful comments and suggestions.

SUPPLEMENTARY MATERIAL

The Supplementary Material for this article can be found online at: https://www.frontiersin.org/articles/10.3389/fbioe.2020.01004/full#supplementary-material

REFERENCES

Abdel-Raouf, N., Al-Homaidan, A. A., and Ibraheem, I. B. M. (2012). Microalgae and wastewater treatment. *Saudi J. Biol. Sci.* 19, 257–275. doi: 10.1016/j.sjbs.2012.04.005

Abreu, M. H., Pereira, R., Buschmann, A. H., Sousa-Pinto, I., and Yarish, C. (2011). Nitrogen uptake responses of Gracilaria vermiculophylla (Ohmi) Papenfuss under combined and single addition of nitrate and ammonium. *J. Exp. Mar. Bio. Ecol.* 407, 190–199. doi: 10.1016/j.jembe.2011.06.034

Adey, W., Luckett, C., and Jensen, K. (1993). Phosphorus removal from natural waters using controlled algal production. *Restor. Ecol.* 1, 29–39. doi: 10.1111/j.1526-100X.1993.tb00006.x

Adey, W. H. (1982). *Algal turf scrubber*. United States patent US 4;333;263 (Washington, DC: Smithsonian Institute).

Adey, W. H. (1992). "Water purification system and apparatus," in *United States Patent U.S* 5,097,795 (Washington, DC: Ecological Systems Tech LP).

Adey, W. H. (1998). *Algal Turf Water Purification Method*. United States patent US 5, 823 (Sugar Land, TX: Aquatic BioEnhancement Systems).

Adey, W. H., Laughinghouse, H. D., Miller, J. B., Hayek, L. A., Thompson, J. G., Bertman, S., et al. (2013). Algal turf scrubber (ATS) floways on the Great Wicomico River. Chesapeake Bay: productivity, algal community structure, substrate and chemistry1. *J. Phycol.* 49, 489–501. doi: 10.1111/jpy.12056

Adey, W. H., Luckett, C., and Smith, M. (1996). Purification of industrially contaminated groundwaters using controlled ecosystems. *Ecol. Eng.* 7, 191–212. doi: 10.1016/0925-8574(96)00008-0

Adey, W. H., and Purgason, R. (1998). *Method of Raising Fish by use of algal turf*. United States patent US 5,778,823 (Sugar Land, TX: Aquatic BioEnhancement Systems).

Allen, A. E., Howard-Jones, M. H., Booth, M. G., Frischer, M. E., Verity, P. G., Bronk, D. A., et al. (2002). Importance of heterotrophic bacterial assimilation of ammonium and nitrate in the Barents Sea during summer. *J. Mar. Syst.* 38, 93–108. doi: 10.1016/S0924-7963(02)00171-9

Anbalagan, A., Schwede, S., Lindberg, C. F., and Nehrenheim, E. (2016). Influence of hydraulic retention time on indigenous microalgae and activated sludge process. *Water Res.* 91, 277–284. doi: 10.1016/j.watres.2016.01.027

Anthony, K. R. N., Ridd, P. V., Orpin, A. R., Larcombe, P., and Lough, J. (2004). Temporal variation of light availability in coastal benthic habitats: effects of clouds, turbidity, and tides. *Limnol. Oceanogr.* 49, 2201–2211. doi: 10.4319/lo.2004.49.6.2201

Asaduzzaman, M., Rahman, M. M., Azim, M. E., Islam, M. A., Wahab, M. A., Verdegem, M. C. J., et al. (2010a). Effects of C/N ratio and substrate addition on natural food communities in freshwater prawn monoculture ponds. *Aquaculture* 306, 127–136. doi: 10.1016/j.aquaculture.2010.05.035

Asaduzzaman, M., Wahab, M. A., Verdegem, M. C. J. J., Adhikary, R. K., Rahman, S. M. S. S., Azim, M. E., et al. (2010b). Effects of carbohydrate source for maintaining a high C:N ratio and fish driven re-suspension on pond ecology and production in periphyton-based freshwater prawn culture systems. *Aquaculture* 301, 37–46. doi: 10.1016/j.aquaculture.2010.01.025

Asaduzzaman, M., Wahab, M. A., Verdegem, M. C. J., Huque, S., Salam, M. A., and Azim, M. E. (2008). C/N ratio control and substrate addition for periphyton development jointly enhance freshwater prawn Macrobrachium rosenbergii production in ponds. *Aquaculture* 280, 117–123. doi: 10.1016/j.aquaculture.2008.04.019

Avnimelech, Y. (1999). Carbon/nitrogen ratio as a control element in aquaculture systems. *Aquaculture* 176, 227–235. doi: 10.1016/s0044-8486(99)00085-x

Azim, M. E., Verdegem, M. C. J., Van Dam, A. A., and Beveridge, M. C. M. (2005). *Periphyton-Ecology, Exploitation and Management*. Wallingford: CABI Publishing.

Azim, M. E., Wahab, M. A., Verdegem, M. C. J., van Dam, A. A., van Rooij, J. M., and Beveridge, M. C. M. (2002). The effects of artificial substrates on freshwater pond productivity and water quality and the implications for periphyton-based aquaculture. *Aquat. Living Resour.* 15, 231–241. doi: 10.1016/s0990-7440(02)01179-8

Barkia, I., Saari, N., and Manning, S. R. (2019). Microalgae for high-value products towards human health and nutrition. *Mar. Drugs* 17:304. doi: 10.3390/md17050304

Bartels, J. R. (2008). *A Feasibility Study of Implementing An Ammonia Economy*. Graduate Theses and Dissertations, Iowa State University Iowa, doi: 10.31274/etd-180810-1374.

Becker, E. W. (2013). "Microalgae for Aquaculture: nutritional Aspects," in *Handbook of Microalgal Culture*, Ed. A. Richmond (Hoboken, NJ: John Wiley & Sons, Ltd), 671–691. doi: 10.1002/9781118567166.ch36

Ben-Ari, T., Neori, A., Ben-Ezra, D., Shauli, L., Odintsov, V., and Shpigel, M. (2014). Management of Ulva lactuca as a biofilter of mariculture effluents in IMTA system. *Aquaculture* 434, 493–498. doi: 10.1016/j.aquaculture.2014.08.034

Benemann, J. R., Weissman, J. C., Koopman, B. L., and Oswald, W. J. (1977). Energy production by microbial photosynthesis. *Nature* 268, 19–23. doi: 10.1038/268019a0

Berg, G. M., Balode, M., Purina, I., Bekere, S., Béchemin, C., and Maestrini, S. Y. (2003). Plankton community composition in relation to availability and uptake of oxidized and reduced nitrogen. *Aquat. Microb. Ecol.* 30, 263–274. doi: 10.3354/ame030263

Blanken, W., Cuaresma, M., Wijffels, R. H., and Janssen, M. (2013). Cultivation of microalgae on artificial light comes at a cost. *Algal Res.* 2, 333–340. doi: 10.1016/j.algal.2013.09.004

Blanken, W., Janssen, M., Cuaresma, M., Libor, Z., Bhaiji, T., and Wijffels, R. H. (2014). Biofilm growth of Chlorella sorokiniana in a rotating biological contactor based photobioreactor. *Biotechnol. Bioeng.* 111, 2436–2445. doi: 10.1002/bit.25301

Bondoc, K. G. V., Heuschele, J., Gillard, J., Vyverman, W., and Pohnert, G. (2016). Selective silicate-directed motility in diatoms. *Nat. Commun.* 7, 1–7. doi: 10.1038/ncomms10540

Bosma, R. H., and Verdegem, M. C. J. (2011). Sustainable aquaculture in ponds: principles, practices and limits. *Livest. Sci.* 139, 58–68. doi: 10.1016/j.livsci.2011.03.017

Boyd, C. E. (1985). Chemical budgets for channel catfish ponds. *Trans. Am. Fish. Soc.* 114, 291–298. doi: 10.1577/1548-86591985114<291:cbfccp<2.0.co;2

Bradley, P. B., Sanderson, M. P., Frischer, M. E., Brofft, J., Booth, M. G., Kerkhof, L. J., et al. (2010). Inorganic and organic nitrogen uptake by phytoplankton and heterotrophic bacteria in the stratified Mid-Atlantic Bight. *Estuar. Coast. Shelf Sci.* 88, 429–441. doi: 10.1016/j.ecss.2010.02.001

Bregnballe, J. (2015). A guide to recirculation aquaculture. *FAO Eurofish Rep* 100.

Bronk, D. A., See, J. H., Bradley, P., and Killberg, L. (2006). DON as a source of bioavailable nitrogen for phytoplankton. *Biogeoscie. Discuss.* 3, 1247–1277. doi: 10.5194/bgd-3-1247-2006

Brune, D. E., Schwartz, G., Eversole, A. G., Collier, J. A., and Schwedler, T. E. (2003). Intensification of pond aquaculture and high rate photosynthetic systems. *Aquac. Eng.* 28, 65–86. doi: 10.1016/S0144-8609(03)00025-6

Buck, B. H., Troell, M. F., Krause, G., Angel, D. L., Grote, B., and Chopin, T. (2018). State of the art and challenges for offshore Integrated multi-trophic aquaculture (IMTA). *Front. Mar. Sci.* 5:165. doi: 10.3389/fmars.2018.00165

Butterworth, A. (2010). Integrated Multi-Trophic Aquaculture systems incorporating abalone and seaweeds. *Glob. Focus* 39, 23–32.

Cahill, P. L., Hurd, C. L., and Lokman, M. (2010). Keeping the water clean - Seaweed biofiltration outperforms traditional bacterial biofilms in recirculating aquaculture. *Aquaculture* 306, 153–159. doi: 10.1016/j.aquaculture.2010.05.032

Casé, M., Leça, E. E., Leitão, S. N., SantAnna, E. E., Schwamborn, R., and de Moraes Junior, A. T. (2008). Plankton community as an indicator of water quality in tropical shrimp culture ponds. *Mar. Pollut. Bull.* 56, 1343–1352. doi: 10.1016/j.marpolbul.2008.02.008

Chen, H. B., Wu, J. Y., Wang, C. F., Fu, C. C., Shieh, C. J., Chen, C. I., et al. (2010). Modeling on chlorophyll a and phycocyanin production by Spirulina platensis under various light-emitting diodes. *Biochem. Eng. J.* 53, 52–56. doi: 10.1016/j.bej.2010.09.004

Chisti, Y. (2007). Biodiesel from microalgae. *Biotechnol. Adv.* 25, 294–306. doi: 10.1016/j.biotechadv.2007.02.001

Collos, Y., and Harrison, P. J. (2014). Acclimation and toxicity of high ammonium concentrations to unicellular algae. *Mar. Pollut. Bull.* 80, 8–23. doi: 10.1016/j.marpolbul.2014.01.006

Colt, J. (2006). Water quality requirements for reuse systems. *Aquac. Eng.* 34, 143–156. doi: 10.1016/j.aquaeng.2005.08.011

Cuaresma, M., Janssen, M., Vílchez, C., and Wijffels, R. H. (2011). Horizontal or vertical photobioreactors? How to improve microalgae photosynthetic efficiency. *Bioresour. Technol.* 102, 5129–5137. doi: 10.1016/j.biortech.2011.01.078

Davidson, J., Good, C., Williams, C., and Summerfelt, S. T. (2017). Evaluating the chronic effects of nitrate on the health and performance of post-smolt Atlantic salmon Salmo salar in freshwater recirculation aquaculture systems. *Aquac. Eng.* 79, 1–8. doi: 10.1016/j.aquaeng.2017.08.003

Defoirdt, T., Boon, N., Bossier, P., and Verstraete, W. (2004). Disruption of bacterial quorum sensing: an unexplored strategy to fight infections in aquaculture. *Aquaculture* 240, 69–88. doi: 10.1016/j.aquaculture.2004.06.031

Deviller, G., Aliaume, C., Nava, M. A. F., Casellas, C., and Blancheton, J. P. (2004). High-rate algal pond treatment for water reuse in an integrated marine fish recirculating system: effect on water quality and sea bass growth. *Aquaculture* 235, 331–344. doi: 10.1016/j.aquaculture.2004.01.023

Domingues, R. B., Barbosa, A. B., Sommer, U., and Galvao, H. M. (2011). Ammonium, nitrate and phytoplankton interactions in a freshwater tidal estuarine zone: potential effects of cultural eutrophication. *Aquat. Sci.* 73, 331–343. doi: 10.1007/s00027-011-0180-0

Dortch, Q. (1990). The interaction between ammonium and nitrate uptake in phyplankton. *Mar. Ecol. Prog. Ser.* 61, 183–201. doi: 10.3354/meps061183

Ebeling, J. M., Timmons, M. B., and Bisogni, J. J. (2006). Engineering analysis of the stoichiometry of photoautotrophic, autotrophic, and heterotrophic removal of ammonia-nitrogen in aquaculture systems. *Aquaculture* 257, 346–358. doi: 10.1016/j.aquaculture.2006.03.019

FAO (2016). *The State Of World Fisheries And Aquaculture 2016: Contributing To Food Security And Nutrition For All*. Rome: FAO, 160.

FAO (2019). *FAO Yearbook. Fishery and Aquaculture Statistics 2017*. Rome: FAO.

Gál, D., Szabó, P., Pekár, F., and Váradi, L. (2003). Experiments on the nutrient removal and retention of a pond recirculation system. *Hydrobiologia* 506–509, 767–772. doi: 10.1023/B:HYDR.0000008589.46810.af

Glibert, P. M. (2012). Ecological stoichiometry and its implications for aquatic ecosystem sustainability. *Curr. Opin. Environ. Sustain.* 4, 272–277. doi: 10.1016/j.cosust.2012.05.009

Glibert, P. M., Maranger, R., Sobota, D. J., and Bouwman, L. (2014a). The Haber Bosch-harmful algal bloom (HB-HAB) link. *Environ. Res. Lett.* 9:10. doi: 10.1088/1748-9326/9/10/105001

Glibert, P. M., Wilkerson, F. P., Dugdale, R. C., Parker, A. E., Alexander, J., Blaser, S., et al. (2014b). Phytoplankton communities from San Francisco Bay Delta respond differently to oxidized and reduced nitrogen substrates-even under conditions that would otherwise suggest nitrogen sufficiency. *Front. Mar. Sci.* 1:17. doi: 10.3389/fmars.2014.00017

Goldman, J. C., and Carpenter, E. J. (1974). A kinetic approach to the effect of temperature on algal growth. *Limnol. Oceanogr.* 19, 756–766. doi: 10.4319/lo.1974.19.5.0756

Greiner, A. D., and Timmons, M. B. (1998). Evaluation of the nitrification rates of microbead and trickling filters in an intensive recirculating tilapia production facility. *Aquac. Eng.* 18, 189–200. doi: 10.1016/S0144-8609(98)00030-2

Guiral, D., Arfi, R., Da, K. P., and Konan-Brou, A. A. (1993). Communautés, biomasses et productions algales au sein d'un recif artificiel (acadja) en milieu lagunaire tropical. *Rev. Hydro-biol. Trop.* 26, 219–228.

Guo, Z., Liu, Y., Guo, H., Yan, S., and Mu, J. (2013). Microalgae cultivation using an aquaculture wastewater as growth medium for biomass and biofuel production. *J. Environ. Sci.* 25, S85–S88. doi: 10.1016/S1001-0742(14)60632-X

Hein, M., Pedersen, M. F., and Sand Jensen, K. (1995). Size-dependent nitrogen uptake in micro- and macroalgae. *Mar. Ecol. Prog. Ser.* 118, 247–254. doi: 10.3354/meps118247

Heisler, J., Glibert, P. M., Burkholder, J. M., Anderson, D. M., Cochlan, W., Dennison, W. C., et al. (2008). Eutrophication and harmful algal blooms: a scientific consensus. *Harmful Algae* 8, 3–13. doi: 10.1016/j.hal.2008.08.006

Herman, H., Martin, K., Wijnand, D., Rob, U., Willem, W., and Walkier, R. (2017). *Water Governance. The Dutch Water Authority Model*. The Hague: Dutch Water Authorities.

Hii, Y. S., Soo, C. L., Chuah, T. S., Mohd-Azmi, A., and Abol-Munafi, A. B. (2011). Interactive effect of ammonia and nitrate on the nitrogen uptake by Nannochloropsis sp. *J. Sustain. Sci. Manag.* 6, 60–68.

Huang, Z., Jones, J., Gu, J., Hallerman, E., Lane, T., Song, X., et al. (2013). Performance of a recirculating aquaculture system utilizing an algal turf scrubber for scaled-up captive rearing of freshwater mussels (Bivalvia: Unionidae). *N. Am. J. Aquac.* 75, 543–547. doi: 10.1080/15222055.2013.826762

Inoue, K., and Uchida, T. (2016). Cultivation of microalgae using sewage and organic component evaluation. *Chem. Eng. Technol.* 39, 1662–1668. doi: 10.1002/ceat.201500099

Källqvist, T., and Svenson, A. (2003). Assessment of ammonia toxicity in tests with the microalga. Nephroselmis pyriformis, Chlorophyta. *Water Res.* 37, 477–484. doi: 10.1016/S0043-1354(02)00361-5

Khatoon, H., Yusoff, F., Banerjee, S., Shariff, M., and Bujang, J. S. (2007). Formation of periphyton biofilm and subsequent biofouling on different substrates in nutrient enriched brackishwater shrimp ponds. *Aquaculture* 273, 470–477. doi: 10.1016/j.aquaculture.2007.10.040

Kirchman, D. L. (1994). The uptake of inorganic nutrients by heterotrophic bacteria. *Microb. Ecol.* 28, 255–271. doi: 10.1007/bf00166816

Larsdotter, K. (2006a). *Microalgae for Phosphorus Removal from Wastewater in a Nordic climate*. Doctoral thesis, Royal Institute of Technology Stockholm.

Larsdotter, K. (2006b). Wastewater treatment with microalgae- A literature review. *Vatten* 62, 31–38.

Lazur, A. M., and Britt, D. C. (1997). Pond recirculating production systems. *SRAC Publ.* 455, 8.

Levy, A., Milstein, A., Neori, A., Harpaz, S., Shpigel, M., and Guttman, L. (2017). Marine periphyton biofilters in mariculture effluents: nutrient uptake and biomass development. *Aquaculture* 473, 513–520. doi: 10.1016/j.aquaculture.2017.03.018

Li, M., Callier, M. D., Blancheton, J. P., Galès, A., Nahon, S., Triplet, S., et al. (2019). Bioremediation of fishpond effluent and production of microalgae for an oyster farm in an innovative recirculating integrated multi-trophic aquaculture system. *Aquaculture* 504, 314–325. doi: 10.1016/j.aquaculture.2019.02.013

Liao, P. B., and Mayo, R. D. (1974). Intensified fish culture combining water reconditioning with pollution abatement. *Aquaculture* 3, 61–85. doi: 10.1016/0044-8486(74)90099-90094

Liu, Y., Li, L., and Jia, R. (2011). The optimum resource ratio (N:P) for the growth of Microcystis aeruginosa with abundant nutrients. *Procedia Environ. Sci.* 10, 2134–2140. doi: 10.1016/j.proenv.2011.09.334

Martins, C. I. M., Eding, E. H., Verdegem, M. C. J., Heinsbroek, L. T. N., Schneider, O., Blancheton, J. P., et al. (2010). New developments in recirculating aquaculture systems in Europe: a perspective on environmental sustainability. *Aquac. Eng.* 43, 83–93. doi: 10.1016/j.aquaeng.2010.09.002

Masojídek, J., and Torzillo, G. (2008). "Mass cultivation of freshwater microalgae," in *Encyclopedia of Ecology*, eds S. E. Jørgensen, and B. D. Fath (Amsterdam: Elsevier Science), 2226–2235. doi: 10.1016/b978-0-12-409548-9.09373-9378

Mata, T. M., Martins, A. A. A., and Caetano, N. S. (2010). Microalgae for biodiesel production and other applications: a review. *Renew. Sustain. Energy Rev.* 14, 217–232. doi: 10.1016/j.rser.2009.07.020

Matamoros, V., Gutiérrez, R., Ferrer, I., García, J., and Bayona, J. M. (2015). Capability of microalgae-based wastewater treatment systems to remove emerging organic contaminants: a pilot-scale study. *J. Hazard. Mater.* 288, 34–42. doi: 10.1016/j.jhazmat.2015.02.002

Meriac, A., Eding, E. H., Kamstra, A., Busscher, J. P., Schrama, J. W., and Verreth, J. A. J. (2014a). Denitrification on internal carbon sources in RAS is limited by fibers in fecal waste of rainbow trout. *Aquaculture* 434, 264–271. doi: 10.1016/j.aquaculture.2014.08.004

Meriac, A., Eding, E. H., Schrama, J., Kamstra, A., and Verreth, J. A. J. (2014b). Dietary carbohydrate composition can change waste production and biofilter load in recirculating aquaculture systems. *Aquaculture* 420–421. doi: 10.1016/j.aquaculture.2013.11.018

Michels, M. H. A. (2015). *Microalgae for Aquaculture*. Doctoral thesis, Wageningen University Wageningen.

Muñoz, R., and Guieysse, B. (2006). Algal-bacterial processes for the treatment of hazardous contaminants: a review. *Water Res.* 40, 2799–2815. doi: 10.1016/j.watres.2006.06.011

Natrah, F. M. I., Bossier, P., Sorgeloos, P., Yusoff, F. M., and Defoirdt, T. (2014). Significance of microalgal–bacterial interactions for aquaculture. *Rev. Aquac.* 6, 48–61. doi: 10.1111/raq.12024

Natrah, F. M. I., Defoirdt, T., Sorgeloos, P., and Bossier, P. (2011). Disruption of bacterial cell-to-cell communication by marine organisms and its relevance to aquaculture. *Mar. Biotechnol.* 13, 109–126. doi: 10.1007/s10126-010-9346-3

Naumann, T., Çebi, Z., Podola, B. B., Melkonian, M., Cebi, Z., Podola, B. B., et al. (2013). Growing microalgae as aquaculture feeds on twin-layers: a novel solid-state photobioreactor. *J. Appl. Phycol.* 25, 1413–1420. doi: 10.1007/s10811-012-9962-6

Necchi, O. (2004). Light-related photosynthetic characteristics of lotic macroalgae. *Hydrobiologia* 525, 139–155. doi: 10.1023/B:HYDR.0000038861.18999.7b

Neori, A. (2011). "Green water" microalgae: the leading sector in world aquaculture. *J. Appl. Phycol.* 23, 143–149. doi: 10.1007/s10811-010-9531-9

Neori, A., Chopin, T., Troell, M., Buschmann, A. H., Kraemer, G. P., Halling, C., et al. (2004). Integrated aquaculture: rationale, evolution and state of the art emphasizing seaweed biofiltration in modern mariculture. *Aquaculture* 231, 361–391. doi: 10.1016/j.aquaculture.2003.11.015

Neori, A., Msuya, F. E., Shauli, L., Schuenhoff, A., Kopel, F., and Shpigel, M. (2003). A novel three-stage seaweed (*Ulva lactuca*) biofilter design for integrated mariculture. *J. Appl. Phycol.* 15, 543–553. doi: 10.1023/b:japh.0000004382.89142.2d

Neori, A., Shpigel, M., Guttman, L., and Israel, A. (2017). Development of polyculture and integrated multi - trophic aquaculture (IMTA) in Israel: a review. *Isr. J. Aquac. - Bamidgeh* 69, 1–19.

Ngoc, P. T. A., Meuwissen, M. P. M., Cong Tru, L., Bosma, R. H., Verreth, J., and Lansink, A. O. (2016). Economic feasibility of recirculating aquaculture systems in Pangasius farming. *Aquac. Econ. Manag.* 20, 185–200. doi: 10.1080/13657305.2016.1156190

Nunes, A. J. P., Sá, M. V. C., Browdy, C. L., and Vazquez-Anon, M. (2014). Practical supplementation of shrimp and fish feeds with crystalline amino acids. *Aquaculture* 431, 20–27. doi: 10.1016/j.aquaculture.2014.04.003

Oostlander, P. C., van Houcke, J., Wijffels, R. H., and Barbosa, M. J. (2020). Microalgae production cost in aquaculture hatcheries. *Aquaculture* 525:735310. doi: 10.1016/j.aquaculture.2020.735310

Pagand, P., Blancheton, J. P., Lemoalle, J., and Casellas, C. (2000). The use of high rate algal ponds for the treatment of marine effluent from a recirculating fish rearing system. *Aquac. Res.* 31, 729–736. doi: 10.1046/j.1365-2109.2000.00493.x

Pittman, J. K., Dean, A. P., and Osundeko, O. (2011). The potential of sustainable algal biofuel production using wastewater resources. *Bioresour. Technol.* 102, 17–25. doi: 10.1016/j.biortech.2010.06.035

Podevin, M., De Francisci, D., Holdt, S. L., and Angelidaki, I. (2015). Effect of nitrogen source and acclimatization on specific growth rates of microalgae determined by a high-throughput in vivo microplate autofluorescence method. *J. Appl. Phycol.* 27, 1415–1423. doi: 10.1007/s10811-014-0468-2

Rahman, M. M., Verdegem, M., Nagelkerke, L., Wahab, M. A., Milstein, A., and Verreth, J. (2008). Effects of common carp *Cyprinus carpio* (L.) and feed addition in rohu Labeo rohita (Hamilton) ponds on nutrient partitioning among fish, plankton and benthos. *Aquac. Res.* 39, 85–95. doi: 10.1111/j.1365-2109.2007.01877.x

Rakocy, J. E., Bailey, D. S., Thoman, E. S., and Shultz, R. C. (2004). "Intensive tank culture of tilapia with a suspended, bacterial-based, treatment process," in *New Dimensions in Farmed Tilapia, Proceedings of the Sixth International Symposium on Tilapia in Aquaculture*, ed. R. B. Bolivar (Manila: AGRIS), 584–596.

Rakocy, J. E., Losordo, T. M., and Masser, M. P. (1992). Recirculating aquaculture tank production systems. *SRAC Publ. No.* 454, 1–7.

Ramli, N. M., Giatsis, C., Yusoff, F. M., Verreth, J., and Verdegem, M. (2018a). Resistance and resilience of small-scale recirculating aquaculture systems (RAS) with or without algae to pH perturbation. *PLoS One* 13:e195862. doi: 10.1371/journal.pone.0195862

Ramli, M. N., Yusoff, F. M. F. M., Giatsis, C., Tan, G. Y. A. G. Y. A., Verreth, J. A. J. J. A. J., and Verdegem, M. C. J. M. C. J. (2018b). Effects of Stigeoclonium nanum, a freshwater periphytic microalga on water quality in a small-scale recirculating aquaculture system. *Aquac. Res.* 49, 3529–3540. doi: 10.1111/are.13818

Ramli, N. M. (2018). *Microalgae-Bacteria Interactions: A Key for Improving Water Quality in Recirculating Aquaculture Systems?*. Doctoral thesis, Wageningen University The Netherlands.

Ramli, N. M., Verdegem, M. C. J., Yusoff, F. M., Zulkifely, M. K., and Verreth, J. A. J. (2017). Removal of ammonium and nitrate in recirculating aquaculture systems by the epiphyte Stigeoclonium nanum immobilized in alginate beads. *Aquac. Environ. Interact.* 9, 213–222. doi: 10.3354/aei00225

Rasdi, N. W., and Qin, J. G. (2015). Effect of N:P ratio on growth and chemical composition of Nannochloropsis oculata and Tisochrysis lutea. *J. Appl. Phycol.* 27, 2221–2230. doi: 10.1007/s10811-014-0495-z

Richard, M., Maurice, J. T., Anginot, A., Paticat, F., Verdegem, M. C. J., and Hussenot, J. M. E. (2010). Influence of periphyton substrates and rearing density on Liza aurata growth and production in marine nursery ponds. *Aquaculture* 310, 106–111. doi: 10.1016/j.aquaculture.2010.10.023

Roy, S., and Sen Pal, R. (2015). Microalgae in Aquaculture: a review with special references to nutritional value and fish dietetics. *Proc. Zool. Soc.* 68, 1–8. doi: 10.1007/s12595-013-0089-9

Sargent, J. R., McEvoy, L. A., and Bell, J. G. (1997). Requirements, presentation and sources of polyunsaturated fatty acids in marine fish larval feeds. *Aquaculture* 155, 117–127. doi: 10.1016/S0044-8486(97)00122-1

Schneider, O., Sereti, V., Eding, E. H., and Verreth, J. A. J. (2005). Analysis of nutrient flows in integrated intensive aquaculture systems. *Aquac. Eng.* 32, 379–401. doi: 10.1016/j.aquaeng.2004.09.001

Schuenhoff, A., Shpigel, M., Lupatsch, I., Ashkenazi, A., Msuya, F. E., and Neori, A. (2003). A semi-recirculating, integrated system for the culture of fish and seaweed. *Aquaculture* 221, 167–181. doi: 10.1016/s0044-8486(02)00527-6

Schulze, P. S. C., Barreira, L. A., Pereira, H. G. C., Perales, J. A., and Varela, J. C. S. (2014). Light emitting diodes (LEDs) applied to microalgal production. *Trends Biotechnol.* 32, 422–430. doi: 10.1016/j.tibtech.2014.06.001

Shaari, A. L., Surif, M., Latiff, F. A., Omar, W. M. W., and Ahmad, M. N. (2011). Monitoring of water quality and microalgae species composition of Penaeus Monodon ponds in Pulau Pinang. Malaysia. *Trop. Life Sci. Res.* 22, 51–69.

Shah, M. R., Lutzu, G. A., Alam, A., Sarker, P., Kabir Chowdhury, M. A., Parsaeimehr, A., et al. (2018). Microalgae in aquafeeds for a sustainable aquaculture industry. *J. Appl. Phycol.* 30, 197–213. doi: 10.1007/s10811-017-1234-z

Slade, R., and Bauen, A. (2013). Micro-algae cultivation for biofuels: cost, energy balance, environmental impacts and future prospects. *Biomass Bioenergy* 53, 29–38. doi: 10.1016/j.biombioe.2012.12.019

Stumm, W., and Morgan, J. J. (1995). *Aquatic Chemistry: Chemicals Equilibria and Rates in Natural Waters*. 3rd Edn. New York, NY: John Wiley and Sons, Inc.

Suresh Kumar, K., Dahms, H. U., Won, E. J., Lee, J. S., and Shin, K. H. (2015). Microalgae - A promising tool for heavy metal remediation. *Ecotoxicol. Environ. Saf.* 113, 329–352. doi: 10.1016/j.ecoenv.2014.12.019

SustainAqua (2009). *Integrated Approach for a Sustainable and Healthy Freshwater Aquaculture. SustainAqua Handbook - A Handbook for a Sustainable Aquaculture*. Bremerhaven: The EU project SustainAqua.

Tait, L. W., Hawes, I., and Schiel, D. R. (2014). Shining light on benthic macroalgae: Mechanisms of complementarity in layered macroalgal assemblages. *PLoS One* 9:e114146. doi: 10.1371/journal.pone.0114146

Takabe, Y., Hidaka, T., Tsumori, J., and Minamiyama, M. (2016). Effects of hydraulic retention time on cultivation of indigenous microalgae as a renewable energy source using secondary effluent. *Bioresour. Technol.* 207, 399–408. doi: 10.1016/j.biortech.2016.01.132

Tam, N. F. Y., and Wong, Y. S. (1996). Effect of ammonia concentrations on growth of Chlorella vulgaris and nitrogen removal from media. *Bioresour. Technol.* 57, 45–50. doi: 10.1016/0960-8524(96)00045-4

Tendencia, E. A., Bosma, R. H., Verdegem, M. C. J., and Verreth, J. A. J. (2013). The potential effect of greenwater technology on water quality in the pond culture of Penaeus monodon Fabricius. *Aquac. Res.* 46, 1–13. doi: 10.1111/are.12152

Timmons, M. B., and Ebeling, J. M. (2007). *Recirculating Aquaculture, 2nd ed. NRAC Publication. Northeastern Regional Aquaculture Center*. New York, NY: Cayuga Aqua Ventures.

Timmons, M. B., Ebeling, J. M., Wheaton, F. W., Summerfelt, S. T., and Vinci, B. J. (2002). *Recirculating Aquaculture Systems*, 2nd Edn. New York, NY: Cayuga Aqua Ventures.

Troell, M., Halling, C., Neori, A., Chopin, T., Buschmann, A. H., Kautsky, N., et al. (2003). Integrated mariculture: asking the right questions. *Aquaculture* 226, 69–90. doi: 10.1016/S0044-8486(03)00469-1

Valeta, J., and Verdegem, M. (2015). Removal of nitrogen by algal turf scrubber technology in recirculating aquaculture system. *Aquac. Res.* 46, 945–951. doi: 10.1111/are.12255

Van Rijn, J. (2013). Waste treatment in recirculating aquaculture systems. *Aquac. Eng.* 53, 49–56. doi: 10.1016/j.aquaeng.2012.11.010

Van Rijn, J., Tal, Y., and Schreier, H. J. (2006). Denitrification in recirculating systems: theory and applications. *Aquac. Eng.* 34, 364–376. doi: 10.1016/j.aquaeng.2005.04.004

Vonshak, A., and Richmond, A. (1988). Mass production of the blue-green alga Spirulina: an overview. *Biomass* 15, 233–247. doi: 10.1016/0144-4565(88)90059-5

Warmer, H., and van Dokkum, R. (2002). Water pollution control in the Netherlands. *Policy Pract.* 2001:77.

Wijffels, R. H., Barbosa, M. J., and Eppink, M. H. M. (2010). Microalgae for the production of bulk chemicals and biofuels. *Biofuels, Bioprod. Biorefining.* 4, 287–295. doi: 10.1002/bbb.215

Yuan, X., Glibert, P. M., Xu, J., Liu, H. H., Chen, M., Liu, H. H., et al. (2012). Inorganic and organic nitrogen uptake byphytoplankton and bacteria in Hong Kong waters. *Estuar. Coasts* 35, 325–334. doi: 10.1007/s12237-011-9433-3

Yusoff, F. M., Matias, H. B., Khalid, Z. A., and Phang, S.-M. (2001). Culture of microalgae using interstitial water extracted from shrimp pond bottom sediments. *Aquaculture* 201, 263–270. doi: 10.1016/s0044-8486(01)00673-1

Yusoff, F. M., and McNabb, C. D. (1989). Effects of nutrient availability on primary productivity and fish production in fertilized tropical ponds. *Aquaculture* 78, 303–319. doi: 10.1016/0044-8486(89)90108-7

Yusoff, F. M., and McNabb, C. D. (1997). The effects of phosphorus and nitrogen on phytoplankton dominance in tropical fish ponds. *Aquac. Res.* 28, 591–597. doi: 10.1111/j.1365-2109.1997.tb01079.x

Yusoff, F. M., Norio, N., Imaizumi, Y., and Toda, T. (2019). "Bioreactor for microalgal cultivation systems: strategy and development," in *Prospects of*

Renewable Bioprocessing in Future Energy Systems, eds e Ali A. Rastegari, A. N. Yadav, and A. Gupta (Switzerland: Springer Nature), 117–159. doi: 10.1007/978-3-030-14463-0

Yusoff, F. M., Zubaidah, M. S., Matias, H. B., and Kwan, T. S. (2002). Phytoplankton succession in intensive marine shrimp culture ponds treated with a commercial bacterial product. *Aquac. Res.* 33, 269–278. doi: 10.1046/j.1355-557x.2002.00671.x

Zhu, S., and Chen, S. (2001). Effects of organic carbon on nitrification rate in fixed film biofilters. *Aquac. Eng.* 25, 1–11. doi: 10.1016/S0144-8609(01)00071-1

Zubkov, M. V., Fuchs, B. M., Tarran, G. A., Burkill, P. H., and Amann, R. (2003). High rate of uptake of organic nitrogen compounds by *Prochlorococcus cyanobacteria* as a key to their dominance in oligotrophic cceanic waters. *Appl. Environ. Microbiol.* 69, 1299–1304. doi: 10.1128/aem.69.2.1299-1304.2003

Conflict of Interest: NN was employed by company Bluescientific Shinkamigoto Co. Ltd.

The remaining authors declare that the research was conducted in the absence of any commercial or financial relationships that could be construed as a potential conflict of interest.

frontiers in Bioengineering and Biotechnology

ORIGINAL RESEARCH
published: 08 September 2020
doi: 10.3389/fbioe.2020.550758

Design of Value Chains for Microalgal Biorefinery at Industrial Scale: Process Integration and Techno-Economic Analysis

Petronella M. Slegers[1,2,3†‡], Giuseppe Olivieri[4,5†], Elke Breitmayer[2], Lolke Sijtsma[6], Michel H. M. Eppink[4], Rene H. Wijffels[4,7] and Johannes H. Reith[4]*

[1] Biobased Chemistry and Technology, Wageningen University & Research, Wageningen, Netherlands, [2] Nova-Institute for Ecology and Innovation, Hürth, Germany, [3] Operations Research and Logistics, Wageningen University & Research, Wageningen, Netherlands, [4] Bioprocess Engineering – AlgaePARC, Wageningen University & Research, Wageningen, Netherlands, [5] Dipartimento di Ingegneria Chimica, dei Materiali e della Produzione Industriale, Università degli Studi di Napoli Federico II, Naples, Italy, [6] Wageningen Food & Biobased Research, Wageningen University & Research, Wageningen, Netherlands, [7] Faculty of Biosciences and Aquaculture, Nord University, Bodø, Norway

OPEN ACCESS

Edited by:
Fatimah Md Yusoff, Universiti Putra Malaysia, Malaysia

Reviewed by:
Changhong Yao, Sichuan University, China
Sergio Revah, Autonomous Metropolitan University, Mexico

***Correspondence:**
Petronella M. Slegers
ellen.slegers@wur.nl

[†] These authors have contributed equally to this work

[‡] Present address:
Petronella M. Slegers, Operations Research and Logistics, Wageningen University & Research, Wageningen, Netherlands

Specialty section:
This article was submitted to Bioprocess Engineering, a section of the journal Frontiers in Bioengineering and Biotechnology

Received: *10 April 2020*
Accepted: *14 August 2020*
Published: *08 September 2020*

Citation:
Slegers PM, Olivieri G, Breitmayer E, Sijtsma L, Eppink MHM, Wijffels RH and Reith JH (2020) Design of Value Chains for Microalgal Biorefinery at Industrial Scale: Process Integration and Techno-Economic Analysis. Front. Bioeng. Biotechnol. 8:550758. doi: 10.3389/fbioe.2020.550758

The objective of this work was to identify industrial scenarios for the most promising microalgal biorefinery value chains on the basis of product selection, yields, and techno-economic performance, using biological characteristics of algae species. The development, value creation, and validation of several new processing routes with applications in food, aquafeeds and non-food products were particularly considered in this work. The techno-economic performance of various single product value chains (SP) and multiproduct value chains (MP) was evaluated for four industrial microalgal strains. Cost-revenue optimization was done for a 10 kton microalgal dry weight y^{-1} simulated biorefinery plant, using flow sheeting software for equipment sizing, mass and energy flow modeling, and subsequent techno-economic evaluation. Data on yield, material and energy consumption were based on pre- and pilot size production plants (TRL 5–6). Revenue optimization was accomplished by first analyzing the performance of single product value chains of the microalgal strains. Subsequently, a strategy was developed to exploit almost all biomass based on the most promising microalgal strains. The cultivation costs are most of the time the major costs of the value chains. For the single product value chains common process bottlenecks are low product yields, especially for soluble proteins where only a small fraction of the biomass is leading to economic value. The biorefinery costs (excluding cultivation) vary significantly for various species, due to the species-specific operating conditions as well as differences in product yields. For the evaluated single product value chain scenarios the costs for utilities and other inputs were in general the highest contributing expenses. A biorefinery approach significantly increases the biomass utilization potential to marketable products from 7–28% to more than 97%. Although the cascading approach increases the total production costs of the multiproduct value chains significantly, this is more than compensated by the increased

overall biomass revenue. For all selected multiproduct chains there is a significant potential to become profitable at a relevant industrial scale of 10 kton per year. Additional insights in the product functionality, quality, and their market size are needed to narrow down the wide range of foreseen product revenues and resulting profits.

Keywords: microalgae, biorefinery, value chain, process design, techno-economic evaluation, revenue

HIGHLIGHTS

- Biomass cascading improves the biomass exploitation from $< 25\%$ to $> 95\%$.
- Cultivation costs are most of the time the major costs of the value chains.
- Biorefinery costs vary significantly for various microalgal species.
- Profitable biorefinery processes have been developed at relevant pilot scale.
- Multiproduct biorefinery can enhance profits in the microalgae value chain.

INTRODUCTION

Nowadays, the economy is changing from being fossil-based toward renewable and biobased. In a biobased economy, biomass is fully valorized and used for the sustainable production of food, feed, chemicals, fuels, power, and heat (International Energy Agency [IEA]2009)[1]. Microalgae have a huge potential as bioresource for food, (aqua)feed, chemicals, and materials. Microalgae have the advantage of high growth yields, low land requirements, and the ability to grow on salt water and waste water (Wijffels and Barbosa, 2010; Wijffels et al., 2010). Furthermore, microalgae contain various valuable components that can be processed into a versatile range of products (de la Noue and de Pauw, 1988; Buono et al., 2014), ranging from bulk product such as food commodities to specialty ingredients for food and non-food applications (Wijffels et al., 2010; Milledge, 2011; Draaisma et al., 2013; Ruiz et al., 2016). Well-known examples of microalgal products are pigments from *Dunaliella salina* and *Haematococcus pluvialis,* food supplements from *Chlorella* and *Spirulina*, and omega–3 rich oils from *Nannochloropsis gaditana, Schizochytrium* sp., and *Crypthecodinium cohnii*. A complete list of other potential products have been recently reviewed by Chew et al. (2017) and Chandra et al. (2019).

Currently, most applications of microalgal biomass are still for food, feed, and high value applications (Vandermeulen et al., 2012; Vigani et al., 2015; Rajesh Banu et al., 2020). The economic potential of various microalgae products has been studied previously by several authors (Davis et al., 2014; Gong and You, 2015; Quinn and Davis, 2015; Dong et al., 2016; Thomassen et al., 2016; Laurens et al., 2017; Asiedu et al., 2018; DeRose et al., 2019). Ruiz et al. (2016) gave an overview of the different market scenarios for a benchmark microalgal composition. The cost estimates for cultivation (including harvesting) are in the range of 3.20–11.00 € kg^{-1} biomass (100 ha cultivation system; Ruiz et al., 2016). Processing costs (excluding cultivation and harvesting) were estimated between 0.40–1.80 € kg^{-1} biomass for commodities and 2.30–4.30 € kg^{-1} biomass for speciality products in a biorefinery (both designed for 100 ha production scale; Ruiz et al., 2016). The cost estimates for biofuel production are currently ranging from an optimistic 0.55 to 9.00 € L^{-1} biodiesel corresponding to about 1.65–27.00 € kg^{-1} microalgal biomass (Quinn and Davis, 2015). The production of high value products shows more favorable economics. For omega-3 fatty acids, the production costs ranged between 2.35 and 8.10 € kg^{-1} microalgal biomass (based on 100 ha production scale) depending on the production system and location (Chauton et al., 2015). Pigment production from microalgae is also economically viable (Ruiz et al., 2016; Thomassen et al., 2016) with costs ranging from 12.50 to 107.95 € kg^{-1} biomass, depending on the cultivation and process technologies used, as well as type of pigments for market applications.

A biorefinery approach can be used to valorize all valuable biomass components by using a combination of several separation techniques and potentially leads to better economic performance (Eppink et al., 2019). The overall biorefinery costs (including cultivation and harvesting) are known to strongly depend on the cultivation location, cultivation system, biomass composition, and selected downstream processing technologies (Norsker et al., 2011; Delrue et al., 2013; Draaisma et al., 2013; Chauton et al., 2015; Quinn and Davis, 2015; Ruiz et al., 2016). Beal et al. (2015) provided an extensive techno-economic analysis of an energy-production focussed biorefinery chain (cultivation and downstream processing), including a diverse product portfolio (biodiesel, biocrude, animal feed, and ethanol), several process scenarios, two microalgal strains, two locations, and two cultivation conditions at 1 ha scale and projected to 100 ha scale. The scenario for commodities such as fuels is the least favorable option (Beal et al., 2015). Ruiz et al. (2016) and Beal et al. (2018) have extended the techno-economic analysis to more complete biorefineries, including various production scenarios associated to wider product portfolios (fuel, food and feed commodities, food additives, cosmetics, and pharma) and a larger variety of locations (Spain, Saudi Arabia, Netherlands, Turkey, Hawaii, and Thailand).

The recent analyses performed by Beal et al. (2015); Ruiz et al. (2016), and Beal et al. (2018) on the economics of the biorefinery are still limited by: (1) extrapolation of data on separation performances obtained at lab-scale and then scaled up to 100 ha production scale; (2) estimation of

[1]http://www.iea-bioenergy.task42-biorefineries.com/en/ieabiorefinery/Activities-1.htm

production cost based on extrapolation of data obtained at pre-pilot scale (for example from AlgaePARC, 25 m^2) to 1 and 100 ha scale; (3) analysis of potential market for microalgal components based on a survey of current commercially substitute products, (4) generic processing efficiencies that do not take into account the effect of biological characteristics of algae species (such as cell size, cell wall thickness, and biochemical composition) on the processing performance (Gupta et al., 2017; de Carvalho et al., 2020). Additionally, commercial implementation of microalgal biorefineries is limited due to: (1) a still unfavorable balance between costs and revenues, (2) lack of well-established biorefinery processes at relevant industrial scale, which have to be tailored to the features of the specific microalgal components, (3) lack of available, validated market applications for the microalgal components.

In the EU FP7 MIRACLES-project these issues were addressed by developing novel biorefinery processes incorporating mild cell disruption and environmentally sustainable extraction and fractionation processes, and by proofing the commercial viability of the products by testing their functionality and formulations based on established industrial microalgal strains and potential business and end-users (partners of the project: Chimar Hellas AE, CropEye, DSM Food specialties BV, EcoTreasures BVBA, Ewos innovations AS, Fitoplancton Marino SL, ImEnz Bioengineering BV, Natac biotech SL, Rodenburg Biopolymers BV, Sparos LDA, Unilever Research and Development Vlaardingen BV, Value for Technology BVBA).

The objective of this work is to identify industrial product scenarios for the most promising microalgal biorefinery value chains on the basis of product selection, product yield and techno-economic performance using biological characteristics of algae species. In particular, the development, value creation, and validation of several new processing routes with product applications in food, aquafeeds and non-food products were considered in this work. The chains are designed using processing techniques developed or improved in the MIRACLES-project, complemented with data from best practice techniques (when required) and based on the marketable products that were validated in the project. The techno-economic performance of various single and multiproduct value chains was evaluated for four benchmark industrial microalgal strains.

MATERIALS AND METHODS

First single product value chains were selected and for each chain a processing chain was designed and implemented in SuperPro Designer®. The processing chains integrate novel technologies with benchmark technologies, both developed and tested within the framework of the MIRACLES-project. A sensitivity analysis was applied to determine the range of processing cost. After economic evaluation of the single product value chains, four multiproduct value chains were designed and evaluated, taking advantage of a cascading principle and thereby valorizing almost all biomass.

Single Product Value Chains

Five single product value chains were selected and analyzed for identifying the most suitable microalgal biorefineries. Single product value chains are those that have one main valuable marketable product, the remainder of the biomass being regarded as residue for lower value applications. Four benchmark microalgal strains have been adopted: *Nannochloropsis gaditana* (marine), *Scenedesmus obliquus*[2] (freshwater), *Phaeodactylum tricornutum* (marine), and *Isochrysis galbana* (marine). A large variety of interesting products is reported for these strains: polyunsatured fatty acids (C18:3, C20:5, and C22:6), sterols, functional proteins, carotenoids/antioxidants, and specialty carbohydrates (Pulz and Gross, 2004; Milledge, 2011). The choice was made for the following main products:

- whole microalgae (SP-I).
- broken microalgae (SP-II).
- water-soluble native proteins (SP-III).
- pigments dissolved in lipids (SP-IV).
- triacylglyceride-rich oil (SP-V).

A scheme of the five single product (SP) value chains is presented in **Figure 1**. For each of these products a process chain was designed and these designs were applied to all four microalgal strains, resulting in 20 possible production scenarios. Two cultivation conditions have been addressed in order to optimize the content of the main product to be extracted and purified: (1) nutrient replete cultivation conditions ('N^+-biomass') and, (2) cultivation under nutrient limitation by nitrogen starvation to enhance the TAG content ('N^--biomass').

Each process chain starts with harvesting by microfiltration and centrifugation. In SP-I the biomass is dried to obtain the main product of whole microalgae. For the other SP chains cell disruption by high pressure homogenization is applied, followed by a drying step for SP-II, SP-IV, and SP-V. SP-III continues after disruption with two–step centrifugation with resuspension in water for separating the supernatant from cell debris, followed by UF/DF at 300 kDa (separation of polysaccharides from soluble proteins) and at 8 kDa (separation of soluble proteins from monosaccharides and ashes). SP-IV applies high pressure pigment extraction, the procedure is species dependent:

- *I. galbana*, spray drying, SFE→GXL→PLE
- *I. galbana*, no pre-processing, directly the reverse process PLE→GXL→SFE
- *N. gaditana*, disruption → spray drying → SFE→PLE
- *P. tricornutum*, disruption → spray drying → PLE
- *S. obliquus*, disruption → spray drying → SFE→GXL→PLE

Single product SP-V uses solvent extraction by a mixture of hexane with ethanol or isopropanol. Details on each process step are given in the **Supplementary Material.**

[2]The species has recently been renamed to *Acutodesmus obliquus*, but in the remainder of this work *Scenedesmus obliquus* is used.

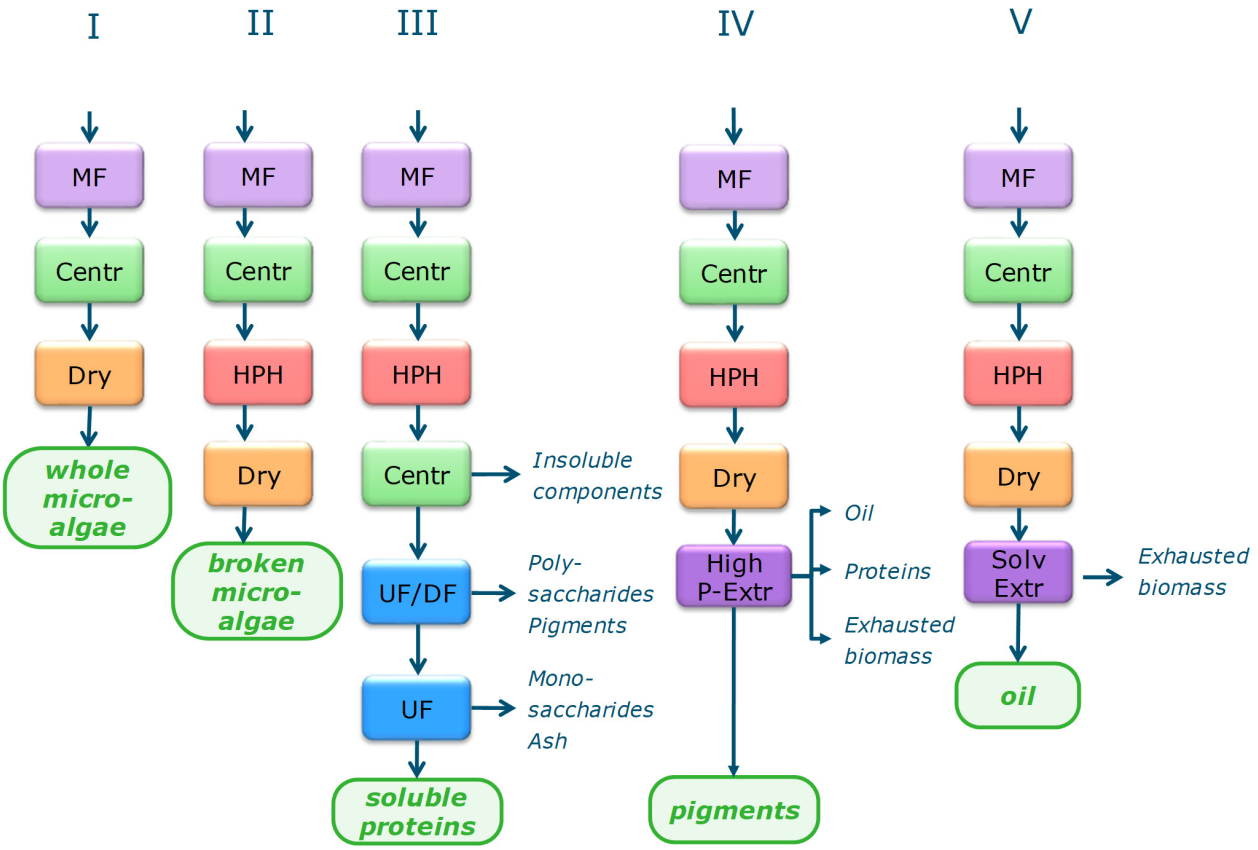

FIGURE 1 | Biorefinery process schemes for single product value chains. MF, microfiltration; Centr, centrifugation; Dry, Spray drying; HPH, high pressure homogenization; UF, ultrafiltration; UF/DF, ultrafiltration/diafiltration; High P–Extr, high pressure extraction (PLE, pressurized liquid extraction; GXL, gas expanded liquid extraction; SFE, supercritical fluid extraction), Alkal Extr, alkaline extraction; Enz Hydr, enzymatic hydrolysis.

Multiproduct Value Chains

The multiproduct chains have multiple valuable marketable products. These multiproduct value chains (MP) were developed on basis of the most promising single product value chain scenarios. The biomass valorization was enhanced by applying a cascade approach to the multiproduct chains. All residue streams were either directly linked to a specific market application or were subjected to further refinery processing. Focus was on the main biomass components in terms of mass and/or product value. **Figures 2A–D** shows the flowsheets of the four selected multiproduct value chains. All MP chains start with harvesting by microfiltration and centrifugation.

The first multiproduct value chain (MP1) uses *N. gaditana* ('N^+-biomass') and focusses on extraction of soluble proteins. The biorefinery processing consists of:

- Cell disruption by high pressure homogenization.
- Two-step centrifugation with resuspension in water for separating the supernatant from cell debris.
- UF/DF at 300 kDa (separation of polysaccharides from soluble proteins) and at 8 kDa (separation of soluble proteins from monosaccharides and ashes).
- Cell debris is dried and high-pressure extraction is applied to yield a pigment containing fraction.
- Alkaline extraction of proteins from the pigment extraction residue followed by enzymatically hydrolysis to obtain mainly peptides.

The second multiproduct value chain (MP2) uses *I. galbana* ('N^+-biomass') and aims at extracting pigments as most valuable product. The process consists of:

- High pressure pigment extraction.
- Alkaline extraction of proteins from the pigment extraction residue.

The third multiproduct value chain (MP3) considers *N. gaditana* cultivated under nutrient limitation to enhance the TAG content ('N^--biomass'). The process chain is mainly based on the single product value chain V for oil extraction (see **Figure 1**). The process consists of the steps:

- Cell disruption by high pressure homogenization.
- Drying.
- Solvent extraction of oil by hexane/isopropanol.

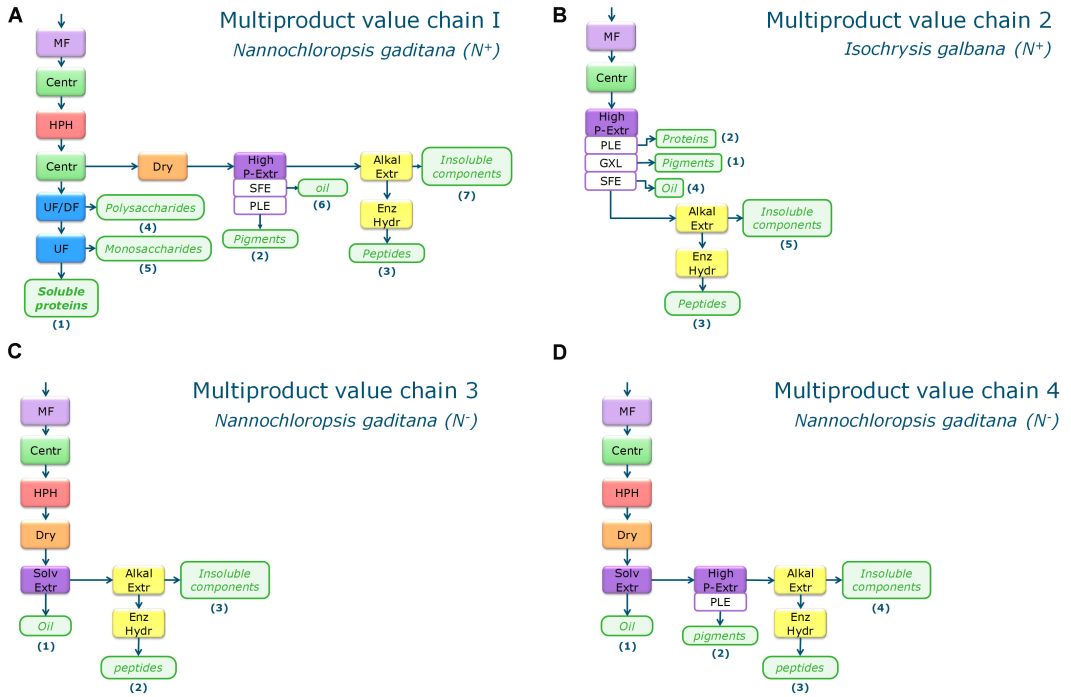

FIGURE 2 | Biorefinery process schemes for the four multiproduct value chains **(A–D)**. MP Chain 1 **(A)** and 2 **(B)** are based on N^+-biomass, MP chain 3 **(C)** and 4 **(D)** are using N^--biomass. MF, microfiltration; Centr, centrifugation; Dry, Spray drying; HPH, high pressure homogenization; UF, ultrafiltration; UF/DF, ultrafiltration/diafiltration; High P–Extr, high pressure extraction (PLE, pressurized liquid extraction; GXL, gas expanded liquid extraction; SFE, supercritical fluid extraction), Alkal Extr, alkaline extraction; Enz Hydr, enzymatic hydrolysis.

– Alkaline extraction of proteins from the pigment extraction residue followed by enzymatic hydrolysis to obtain mainly peptides.

The fourth multiproduct value chain (MP4) considers again *N. gaditana* that was cultivated under nutrient limitation ('N^--biomass'). This chain first aims at extraction of the lipids, then on pigment extraction, and separation of proteins for peptide production. The process consists of the steps:

– Cell disruption by high pressure homogenization.
– Drying.
– Solvent extraction by hexane/isopropanol.
– High pressure pigment extraction from the defatted biomass.
– Alkaline extraction of proteins from the pigment extraction residue followed by enzymatically hydrolysis to obtain mainly peptides.

Approach of Process Design

For each value chain, both single and multiproduct, a specific technical process model has been designed and linked to an economic evaluation. All scenario calculations are based on a microalgae production of 10 kton dry weight y^{-1} in a photobioreactor located in the South of Spain at a benchmark level of 2 g L^{-1} biomass concentration. The physico-chemical properties and composition of the biomass was dependent on species and cultivation conditions, (N^+-biomass and 'N^--biomass'). The biomass composition after cultivation is reported in **Supplementary Table S1** on a dry basis (based on duplicate production data). The production data were provided by Fitoplancton Marino S.L. for N^+-growth conditions (20 ton ha^{-1} $year^{-1}$) and N^--growth conditions (12 ton ha^{-1} $year^{-1}$) at a required 500 and 840 ha scale, respectively. To place this area into perspective, it can be compared to the greenhouse horticulture sector in Netherlands with a total area of 9,300 ha in 2016 (Wageningen University and Research, 2017). Cultivation cost estimate were provided by Fitoplancton Marino S.L. based on their experience at production scale. The estimated cultivation costs on 100 ha basis are a projection compared to cost of current 1 ha production scales. Specifically the cultivation cost at 100 ha scale are 4.5 € kg^{-1} ('N^+-biomass') and 7.5 € kg^{-1} ('N^--biomass'). The latter correspond to an N starvation period up to the point where the further lipid accumulation becomes negligible.

The design and calculations for each processing model at industrial scale of 10 kton microalgal dry weight y^{-1} was performed with the aid of the software SuperPro Designer v10.0b3® from Intelligen, Inc[3]. Data on yields, material and energy consumption were based on pre- and pilot size production plants (TRL 5–6). As far as possible, the processes have been modeled in the software adopting continuous operations. In

[3]www.intelligen.com

case of batch operations (required for pigment extraction) a detailed schedule has been implemented according to the procedure carried out at lab and pilot-scale as reported in previous literature (Gilbert-Lopez et al., 2015, Gilbert-López et al., 2017a; del Pilar Sánchez-Camargo et al., 2017; Ibáñez et al., 2017) and scaled to the analyzed industrial scale of 10 kton y^{-1} of microalgae biomass. In case of multiple batch operations in sequence, the schedule of each operation has been designed integrated with the other in order to have a complete and coherent procedure for each batch. The presence of tanks for intermediate storage has been not taken into account even in case of batch operations. The complete flowsheets developed in SuperPro Designer are reported in the section with **Supplementary Material**, including an overview of the inputs and outputs (**Supplementary Figures S1–S8**). The detailed description of each process step is also given in the **Supplementary Material.**

Economic Evaluation

The cost calculations covered capital investment (CAPEX) and operating expenditures (OPEX). Biorefinery capital investments were calculated from the purchase costs of the main equipment (PC) increased by an overall Lang factor of 3.54 (Harrison et al., 2003; Heinzle et al., 2006; Safi et al., 2014). More details on the calculation of the total CAPEX are provided in **Supplementary Tables S2, S3.** Linear depreciation of the CAPEX over 15 years lifetime with 8% interest rate has been assumed. The working capital is assumed to cover 2 months of OPEX.

Operating expenditures are calculated as the sum of the costs of utilities (electricity, heat, steam, cooling agents), (raw) materials (like solvents), consumables (membranes), wastewater treatment, labor, laboratory costs like quality assurance (Lab/QC/QA), additional facility costs (based on Lang factor), and others (maintenance, operating supplies, overheads, contingencies). Free-on-board costs of raw materials were retrieved from the websites ICIS[4] and IndexMundi[5]. The costs for utilities and raw materials are specified in **Supplementary Table S4**. Wastewater treatment costs were assumed constant at 0.45 € m^{-3}. For location-dependent costs, Spain was assumed as reference. The costs for CO_2 adsorption and cultivation are provided and explained in the **Supplementary Material.** Input of labor was set by considering that an operator can manage up to five continuous process operations simultaneously. In case of batch operations a full-time operator is required per operation. Supervisors and managers were calculated based on three shifts, resulting in a ratio of one manager: three foremen or supervisors: 20 operators (Ruiz et al., 2016). The number of operator workers is calculated on the basis of: (1) the amount of required labor hours per hour of operation; (2) considering three shifts per week. Further information on the assumptions can be found in the **Supplementary Material.** The expected near-future revenues from both commodity and niche products were determined by the end-users partners of the MIRACLES project team based on their experience and market data (Multi-product Integrated bioRefinery of Algae: from Carbon dioxide and Light Energy to high-value SpecialtiesMulti-product Integrated bioRefinery of Algae: from Carbon dioxide and Light Energy to high-value Specialties, 2017). Niche product market prices are sensitive to an increase of production. The expected near-future product market values were therefore based on a confidential market database developed by the company partner Value for Technology in the project with inputs from the other industrial partners. The assumed near-future foreseeable market prices for each of the products are listed in **Supplementary Table S5**.

[4]www.icis.com

[5]www.indexmundi.com

Sensitivity Analysis

Table 1 shows a summary of the operating conditions as adopted in the process models. A linear local sensitivity analysis has been performed, since large parts of the processes are sequential and the interacting effects of the different operating conditions can be neglected. In particular the effects of the adopted strain is also addressed modulating the operating conditions on the basis of the physico-chemical properties of the whole cell (size and density) at the harvesting operations and of the biomass composition at the extraction operations.

RESULTS AND DISCUSSION

Benchmark Performance Single Product Value Chains

For each chain the cultivation costs of 4.50 and 7.50 € kg^{-1} are most of the time the major costs of the value chain. In general, every microalgal chains will benefit from lower cultivation costs. The biorefinery costs (excluding cultivation) per kg product are given in **Figure 3** for each of the microalgae strain-product scenarios. The results specify the contribution of the different cost components to the total biorefinery cost.

For whole microalgae, the biorefinery costs (excluding cultivation) are 0.30–0.35 € kg^{-1}. The range in costs is caused by the difference in cell diameter between the microalgae species. *S. obliquus* is the cheapest to process as result of the large cell diameter. The cost for utilities account for about 50%, the facility costs (related to equipment facilities, installation, piping, etc.) are another significant cost factor. For whole microalgae the majority of capital expenses is due to the membrane facilities. The steam use in the dryer contributes most to the operating expenses, followed by the electricity use of the membrane filtration.

For broken microalgae the utility costs increase as homogenization is energy intense. This leads to biorefinery costs of 0.50–0.65 € kg^{-1} broken microalgae, with a share for utilities above 50% of the costs. The total costs are thus strongly influenced by the ease of cell disruption. In all cases, the overall yield of broken microalgae on the whole process is around 93%, due to the combination of harvesting losses (∼2%) and losses due to incomplete cell disruption (∼5%).

Processing biomass while aiming for soluble proteins results in biorefinery costs (excluding cultivation) of 4.50–12.80 € kg^{-1} soluble purified protein. The lowest biorefinery costs are for

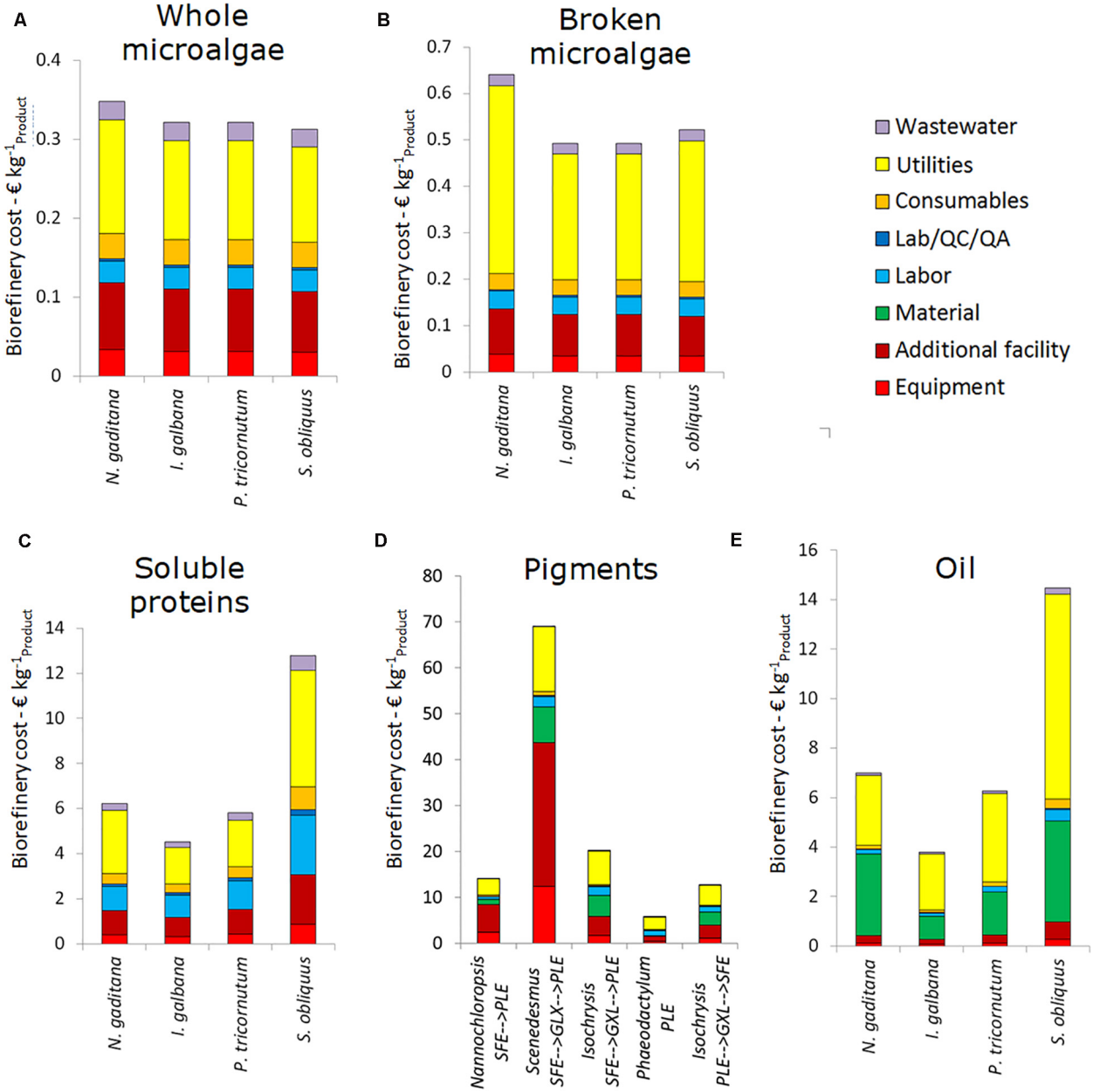

FIGURE 3 | Breakdown of the biorefinery costs (excluding cultivation) for the five single product value chain at 10 ktons y^{-1} scale. **(A)** Whole microalgae, **(B)** Broken microalgae, **(C)** Soluble proteins, **(D)** Pigments, and **(E)** Oil. Data are expressed as costs per unit of main product. SFE, supercritical fluid extraction; GXL, gas expanded liquid extraction; PLE, pressurized liquid extraction.

processing *I. galbana* (high soluble protein content and easy to break) and the highest for *S. obliquus* (low protein content and low disruption and separation yield). The large difference in soluble protein yield and, in general, in cell disruption efficiency among the algal strains is also reported in literature (Safi et al., 2014; Günerken et al., 2015; Show et al., 2015).

The overall protein product yields with respect to the initial amount of biomass are for all microalgae species below 10%. As a result, the biorefinery processing costs per kg of product are significantly higher compared to whole and broken microalgae. The utilities contribute significantly to the costs. Furthermore, the relative contribution of labor to the total costs is higher due to the ultrafiltration and diafiltration processes.

The range of pigment processing cost is quite broad: 5.80–68.95 € kg^{-1} pigment product. It mainly depends on the microalgal species that affects the design of the extraction process in terms of capacity and yield. Utility, materials and equipment (related) costs are most relevant in these chains. For the pigment chains all data are expressed per unit of product in which pigments are dissolved. The reason is

twofold: (1) pigments are never extracted in pure form, and (2) pigments are frequently unstable and to ensure stability at long term storage they are often dissolved in oil. Drying of the biomass is needed when the first extraction step is supercritical fluid extraction (SFE). The product yields with respect to the initial amount of biomass vary from 9.1% for *S. obliquus* to 24.4% for *N. gaditana*. The steps starting with pressurized liquid extraction (PLE) do not require drying and have product yields around 20%. The capital expenses are mainly due to the investment costs for the extraction vessels. The extraction processes also contribute most to the utility and material costs.

The biorefinery costs for oil are lower than for pigment, i.e., 3.80–14.45 € kg^{-1} extracted oil. The solvents and utilities used for lipid extraction contribute most to these costs. Equipment costs only contribute marginally to the costs. The overall product yields vary between 8.3% for *S. obliquus* and 29.1% for *I. galbana*. *N. gaditana* is also promising for lipid production with an overall yield of lipid extraction of 21.9% of the initial biomass.

Process Optimization: Effect of Scale and the Most Relevant Operating Conditions

The results above were based on a facility with 10 kton per year capacity. The biorefinery costs for facilities of 1, 10, and 100 kton capacity per year are shown in **Figure 4**. For all five single product value chains the decrease in biorefinery costs is significant from 1 to 10 kton y^{-1} throughput. For SP value chains I, II, and III cost savings of 50% are feasible. For the other chains the difference in costs is smaller, since their costs are for a large part determined by operating expenses. The cost reduction from 10 to 100 kton y^{-1} is less for all chains and negligible for pigments and lipids. Overall, the results indicate that biorefineries should have a throughput of 10 kton y^{-1} or more to benefit from economy of scale.

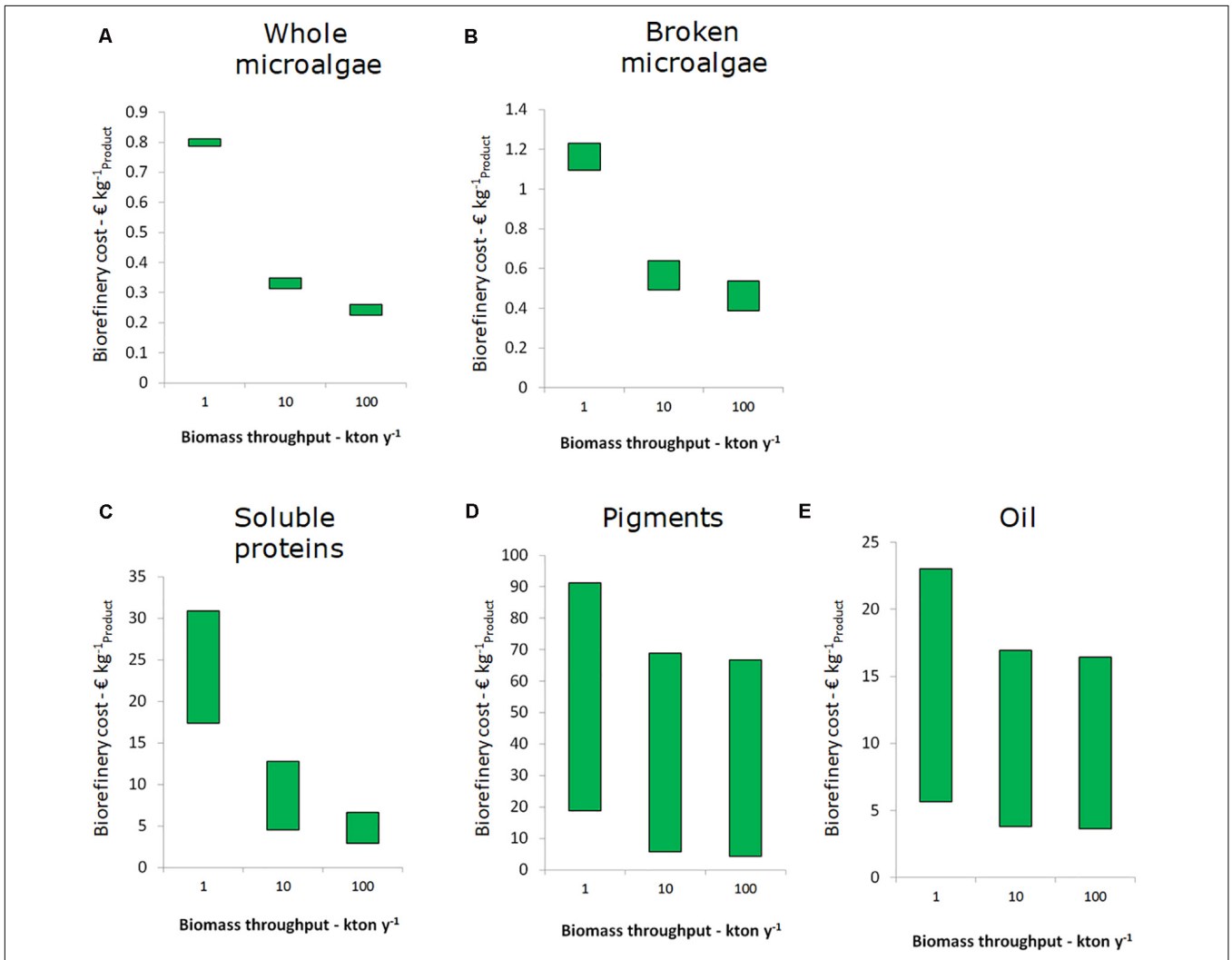

FIGURE 4 | Effect of processing scale on the biorefinery costs (excluding cultivation) for the single product value chain, per unit of main product. **(A)** Whole microalgae, **(B)** Broken microalgae, **(C)** Soluble proteins, **(D)** Pigments, and **(E)** Oil. The bars indicate the range of costs, which is species dependent.

TABLE 1 | Operating conditions for the biorefinery process steps for benchmark conditions and as used in sensitivity analysis.

Process step	Operating Conditions	Benchmark values	Range for sensitivity analysis
Microfiltration	Filtrate flux rate	50	20–100 L m^{-2} h^{-1}
	Power input	0.02	0.01–0.05 kW m^{-2}
	Cleaning time	4	1–4 h over 24 h
	Concentration factor	10	5–20
	Operating temperature	25°C	n.a.
	Biomass recovery	100%	n.a.
Centrifugation (harvesting)	Minimum limiting particle diameter	[A]1–4 μm	n.a.
	Minimum limiting particle density	1,050 kg m^{-3}	1,020–1,100 kg m^{-3}
	Sedimentation efficiency	50%	n.a.
	Power to heat dissipation	50%	n.a.
	Operating temperature	25°C	n.a.
	Biomass recovery	98%	n.a.
	Outlet biomass concentration	[#]100–200 kg m^{-3}	100–200 kg m^{-3}
Spray drying	Final water content	5%	n.a.
	Evaporation rate	30 kg h^{-1} m^{-3}	10–50 kg h^{-1} m^{-3}
	Air/water ratio	35 kg kg^{-1}	n.a.
	Steam/water ratio	1.4 kg kg^{-1}	n.a.
	Steam temperature	160°C	n.a.
	Final solids temperature	60°C	50–70°C
	Biomass recovery	100%	n.a.
High pressure homogenization (disruption)	Inlet pressure	[A]600–1,200 bars	600–1,500 bars
	Number of passes	[A]1–2	1
	Power to heat dissipation	100%	n.a.
	Pumping efficiency	70%	n.a.
	Inlet biomass concentration	100 g L^{-1}	n.a.
	Disruption efficiency	95%	90–95%
Centrifugation (cell debris separation)	Minimum limiting particle diameter	0.5 μm	n.a.
	Minimum limiting particle density	1,500 kg m^{-3}	n.a.
	Sedimentation efficiency	50%	n.a.
	Power to heat dissipation	50%	n.a.
	Operating temperature	25°C	n.a.
	Solids recovery	100%	n.a.
	Solids concentration	300 kg m^{-3}	n.a.
	Liquid viscosity	4 cP	n.a.
Ultrafiltration/Diafiltration	Permeate flux rate	30 L m^{-2} h^{-1}	10–50 L m^{-2} h^{-1}
	Concentration factor	5	n.a.
	Diafiltration volume/liquid volume	2	n.a.
	Filtration time	1 h	n.a.
	Cleaning time	0.5 h	n.a.
	Power input	0.2 kW m^{-2}	n.a.
	Operating temperature	25°C	n.a.
	Membrane cut-off	300 kDa	n.a.
Ultrafiltration (protein concentration)	Permeate flux rate	80 L m^{-2} h^{-1}	60–100 L m^{-2} h^{-1}
	Concentration factor	20	n.a.
	Filtration time	2 h	n.a.
	Cleaning time	0.5 h	n.a.
	Power input	0.2 kW m^{-2}	n.a.

(Continued)

TABLE 1 | Continued

Process step	Operating Conditions	Benchmark values	Range for sensitivity analysis
	Operating temperature	25°C	n.a.
	Membrane cut-off	8 kDa	n.a.
High pressure extraction	Super critical fluid (SFE) extraction time	[A]1–2 h	n.a.
	Gas expanded liquid (GXL) extraction time	[A]0.3–2.5 h	n.a.
	PLE extraction time	[A]0.5–0.75 h	n.a.
	Biomass loading in the extraction chamber	[A]3.3–10%	18.2–33.3%
Solvent extraction	Temperature	50°C	n.a.
	Time	2–3 h	1–1.5 h
	Solvent to biomass ratio (hexane/ethanol)	15 kg kg^{-1}	n.a.
	Solvent to biomass ratio (hexane/isopropanol)	30 kg kg^{-1}	n.a.
	Hexane losses in biomass	1 kg kg^{-1}	0 kg kg^{-1}

Algal species dependent values are indicated with [A]. [#]Value chain dependent. For chains that are directly followed by drying 200 kg m^{-3}, otherwise 100 kg m^{-3}. n.a. means not applicable.

A sensitivity analysis combined with process optimization was made for each single product value chain at the 10 kton y^{-1} scale. This was done by optimizing all the adjustable variables according to the ranges reported in **Table 1**. In **Figure 5** the outcomes of the scenarios of benchmark (Section "Benchmark Performance Single Product Value Chains") and optimized conditions are compared with potential range of revenues from each primary product. Cultivation costs are excluded in this profitability analysis.

For both whole and disrupted microalgae the biorefinery cost are relatively low compared to the potential revenue, as a result of the high product yield and simple structure of harvesting and further biomass processing. By optimizing the operating conditions the biorefinery cost (excluding cultivation) for whole microalgae can be reduced slightly from 0.30–0.35 to 0.20 € kg^{-1} whole microalgae. The potential revenue ranges between 1.5 and 3.0 € kg^{-1}. For disrupted microalgae the costs can be lowered from 0.50–0.65 to 0.25–0.40 € kg^{-1} by optimizing the harvesting and disruption conditions. For soluble purified proteins the optimization reduces the biorefinery costs from 4.5–13 to 3.3–9.2 € kg^{-1}. This reduction, however, does not necessarily lead to a profitable chain; the revenues for proteins are in the same order of magnitude. However, the value of insoluble components is estimated to be 3.00 € kg^{-1}. In the SP protein chain for every kg of soluble protein also 9.68 kg insolubles are produced, thus potentially around 29 € can be gained from these insolubles per kg soluble protein. This is higher than the revenue of the proteins (4.75–8.25 € kg^{-1}), thus the main product here is actually the insoluble fraction. For strains characterized by both high processing costs and low yields, such as *Scenedesmus*, the soluble proteins value chain has a small chance to become profitable in this scenario. Consequently, simplification and further exploitation of the other biomass components will increase the potential revenue.

The pigment chain optimization can decrease the biorefinery costs from 5.8–69 to 4.1–30 € kg^{-1} product. Compared to the range of potential revenue of pigments (14–31 € kg^{-1}) the effect of the optimization is relevant to achieve a profitable process. In particular, the reverse extraction process applied to *Isochrysis* and the single PLE extraction process applied to *Phaeodactylum* (see **Supplementary Material**) appear as most suitable candidates for this single product value chain. In the first case, the absence of a drying step reduces the process cost significantly. In the second case, the combination of high yield obtained in a single step process makes the process competitive. However, also in these chains a large amount of biomass remains unused (75–80%) and it does make sense to sell the biomass residue for (aqua)feed worth 0.50 € kg^{-1} residue. This would generate an additional 2.0–5.0 € for each kg of pigment extract.

Optimization indicates that the oil biorefinery costs can be decreased from 3.8–14 to 1.9–8.8 € kg^{-1} oil, which is significantly lower than the potential revenue of the extracted oil (10–29 € kg^{-1} of oil). Again, the biorefinery process based on *Scenedesmus* shows the most critical situation due to the low extraction yield (8%). The exhausted biomass has, however, a residual value for feed or material applications and is potentially worth up to 2.00 € kg^{-1} residue, leading to 4.8 € additional revenue per kg oil extract. *Isochrysis* and *Nannochloropsis* are the most likely candidates for such a type of biorefinery, due to the high yield (29 and 22%). These yields are achieved with biomass cultivated under nitrogen replete conditions. Microalgal biomass obtained by growth under N-limitation or N-starvation can contain up to 50–65% lipids (Breuer et al., 2012). Especially *Nannochloropsis* is interesting due to the lipid profile (Draaisma et al., 2013). Thus, a suitable strategy could be to produce *Nannochloropsis* biomass under N-limited conditions and to exploit the half of the unused biomass.

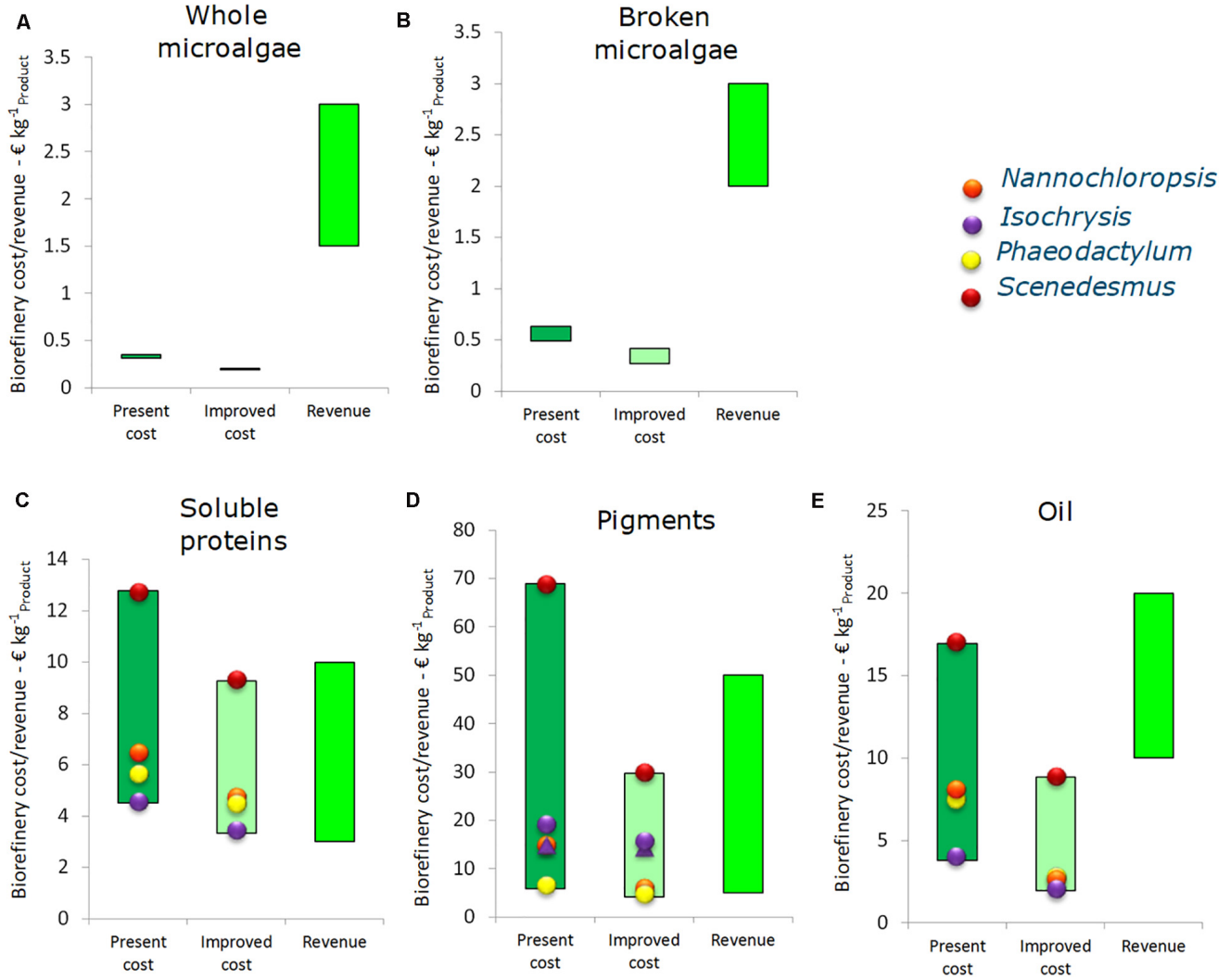

FIGURE 5 | Costs and revenues of the biorefinery process for single product value chain at 10 ktons y^{-1} scale (excluding cultivation), expressed per unit of main product. **(A)** Whole microalgae, **(B)** Broken microalgae, **(C)** Soluble proteins, **(D)** Pigments, and **(E)** Oil. Costs are reported for benchmark scenario (first bar) and for the scenario leading to reduced cost (second bar, results sensitivity analysis and linear optimization). The revenues (third bar) are further specified in **Supplementary Table S5**.

Multiproduct Value Chains

Four multiproduct value chains have been selected based on the results of the single product value chains. The first multiproduct value chain MP1 was designed for *N. gaditana*. Although the single value chain III with *Isochrysis* resulted in slightly higher product yields and lower costs, *Nannochloropsis* was preferred due to its potential product range and opportunities to diversify the multiproduct chains. **Figure 6A** shows the distribution of the microalgal components over the various products for MP1. The potential of enhanced biomass exploitation is clearly shown. In comparison to single product value chain III the biomass exploitation in the form of marketable products with potential increases significantly from 7 to 97%. As expected, the biorefinery costs (without cultivation) increased to 2.8 € kg^{-1} biomass for multiproduct value chain MP1 (**Figure 7**). However, the broader product portfolio also increased the overall revenue to 5.0–12 € kg^{-1} biomass (**Figure 8**). The breakdown of the overall biorefinery costs is shown in **Figure 7A**. Equipment and utilities are the main cost contributors. **Figure 7B** illustrates the contribution of the biorefinery steps, the high pressure extraction is the most costly biorefinery step followed by solvent extraction. The increase of biorefinery costs due to the alkaline extraction and enzymatic hydrolysis is low.

The second multiproduct value chain MP2 (**Figure 2B**) can be compared to the single product value chain IV for pigment extraction. Based on the costs and revenue analysis of the single product chains the reverse extraction process has

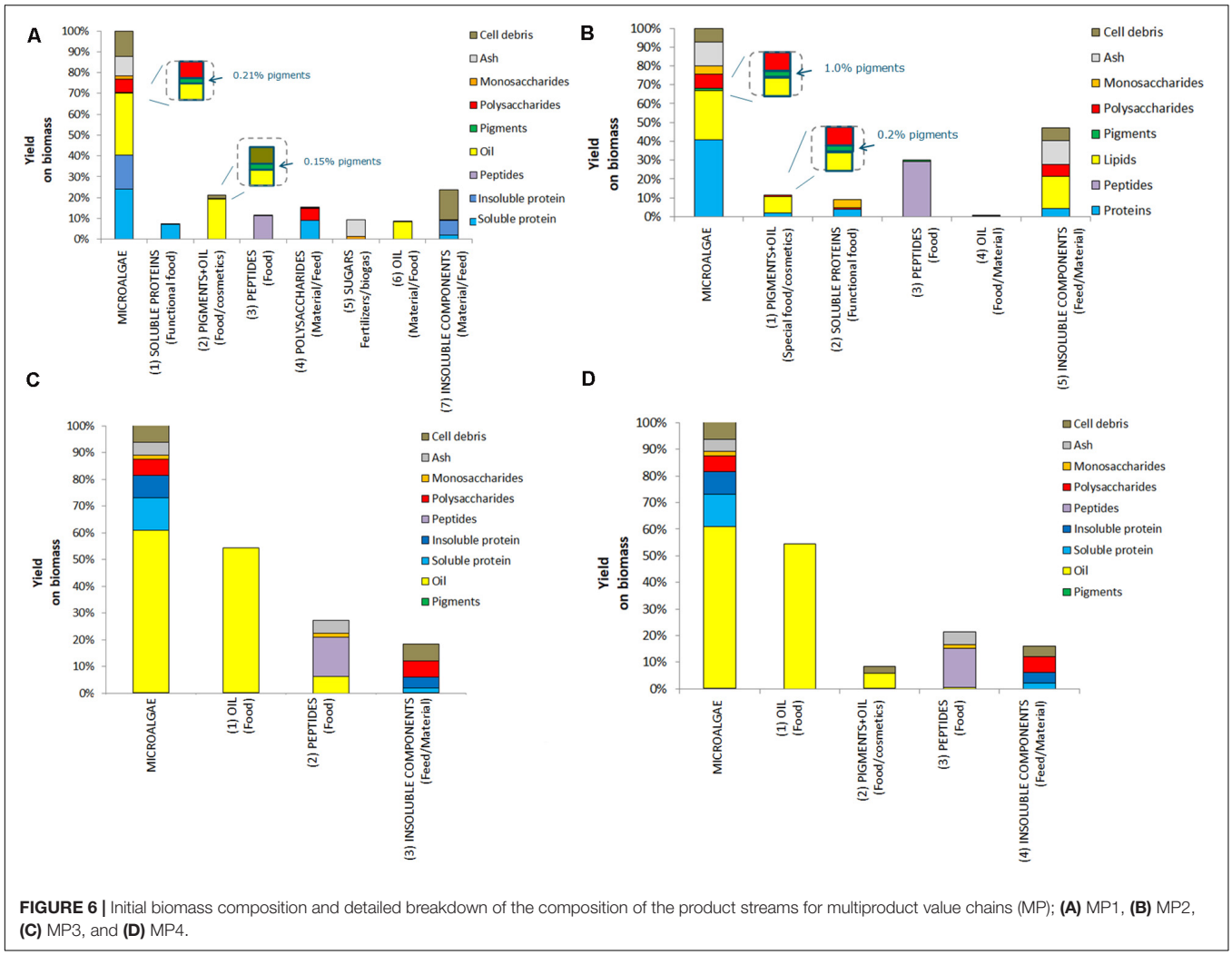

FIGURE 6 | Initial biomass composition and detailed breakdown of the composition of the product streams for multiproduct value chains (MP); **(A)** MP1, **(B)** MP2, **(C)** MP3, and **(D)** MP4.

been chosen as the most suitable technology for extracting the pigments. *I. galbana* appeared the most suitable strain for this process since no cell disruption was needed before the extraction, the high product yield, and low costs compared to the revenue. **Figure 6B** shows the microalgal components in each product for multiproduct value chain MP2. Again the biomass usage potentially increased from an initial 11% (single value chain) to 98%. In this multiproduct chain the biorefinery costs increase slightly to 2.3 € kg^{-1} biomass, with a potential revenue ranging from 3.6 to 8.6 € kg^{-1} biomass (**Figure 8**). In this chain the utilities are the main cost contributor, followed by material use and equipment. This is again due to the high pressure required for pigment extraction, which, although a costly process, also generates a major share of the revenue (**Figure 7B**).

The third multiproduct value chain MP3 (**Figure 2C**) is mainly based on single product value chain V and considers using N^--biomass of *N. gaditana* which contains more TAG-rich oil than N^--grown biomass. According to the costs and revenues of the single product value chain the extraction with a mixture of hexane/isopropanol (3:2) applied to dry biomass has been selected as the most favorable approach. **Figure 6C** shows the overall microalgal components starting with the N^--biomass and a breakdown of the composition and the extracted components. With the multiproduct cascading the biomass use increased from 33% till almost 98%. The biorefinery costs are 1.03 € kg^{-1} biomass, the lowest of all multiproduct chains (**Figure 7A**). Large part of the cost is due to the utilities (**Figure 7A**), whose consumption is quite similar in all the process steps (**Figure 7B**). The revenues range between 6.2 and 16.4 € kg^{-1} biomass (**Figure 8**). Around 60% of the revenue is due to the oil and about 35% due to the peptides product. The fourth multiproduct value chain MP4 also considers N^--biomass of *N. gaditana* In addition to MP3, here also pigments are extracted. **Figure 6D** shows the overall composition of the N^--biomass and a breakdown of the extracted components. In the single product chain only one third of the biomass was exploited. The biorefinery costs (excluding cultivation) are 1.55 € kg^{-1} biomass (**Figure 7A**). The revenue ranges between 6.1–16.5 € kg^{-1} biomass (**Figure 8**) and is thus similar to that of the MP3 chain, despite the additional extraction of pigments (8% of product mass). In MP4 the peptide fraction decreases from 27% (MP3) to 21% (MP4). In this chain

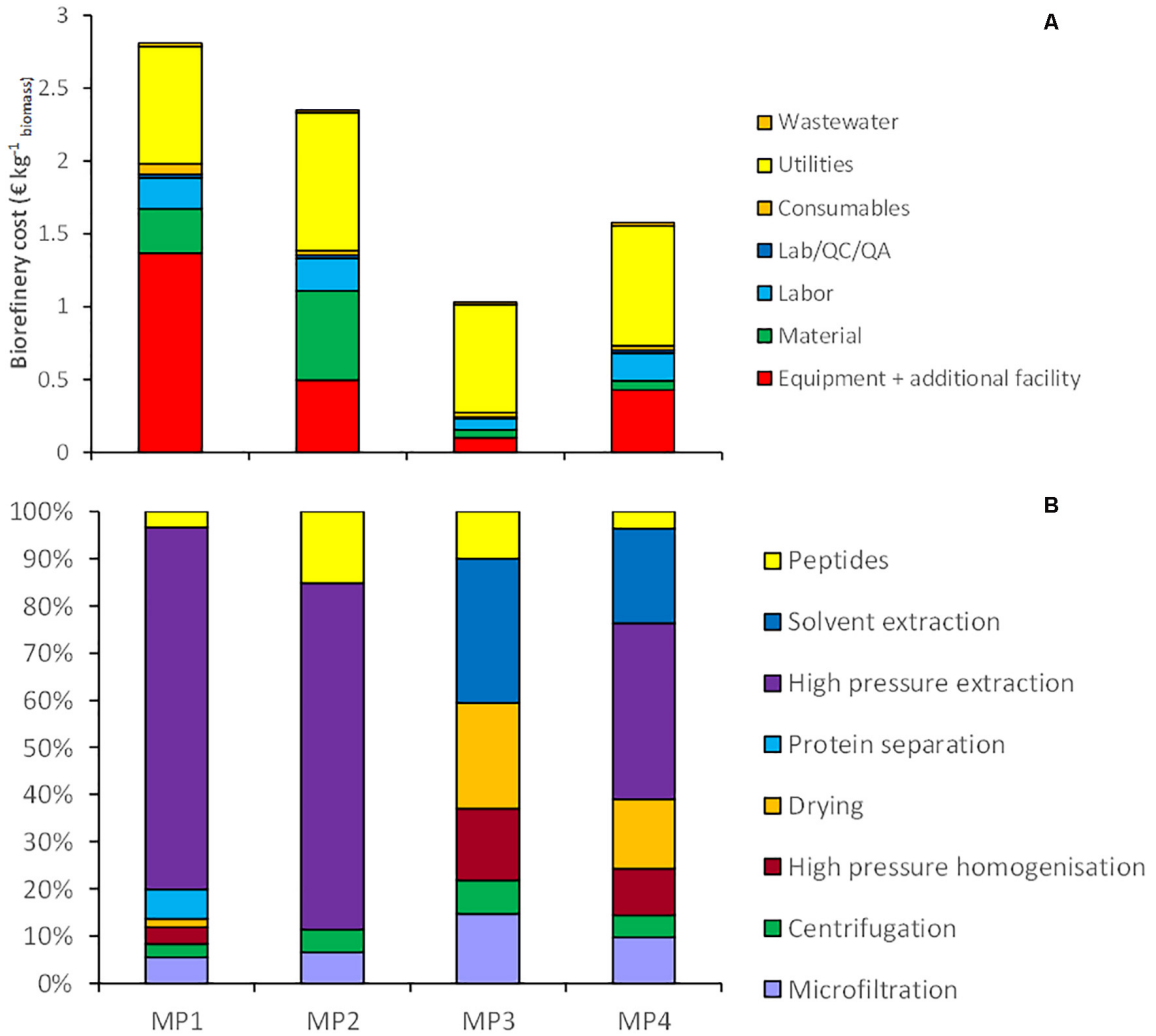

FIGURE 7 | (A) Breakdown of the biorefinery costs (excluding cultivation) for the multiproduct value (MP) chains at 10 ktons y^{-1} scale, expressed per unit of initial biomass, **(B)** contribution of each biorefinery step to total biorefinery costs. Protein separation = Centrifugation + UF/DF + UF; Peptides = alkaline extraction + enzymatic hydrolysis.

the remaining insoluble fraction is 18% of the starting biomass (**Figure 6D**), but with a lower value than in MP3 due to the extracted oil and pigments.

Discussion: Profitability Analysis

The potential profit ranges of the five single product and four multiproduct value chains at 10 kton y^{-1} scale are shown in **Figure 9**. For each single product value chain, the data for the strains with the highest and lowest costs are shown. The profit range was calculated based on the revenues (worst and best case estimates) and cost (including CO_2 capture and cultivation). The center points of the profit ranges are used to evaluate the profitability of the value chains. A positive center point indicates that the estimated revenue is sufficient to balance the costs, a negative center point suggests that the estimated revenue is unlikely to be sufficient to balance the cost. No cash flow analysis was performed. Below the results are discussed together with other proposed value chains in literature.

The results show that for each chain the cultivation costs (4.50 € kg^{-1} for N^+-biomass and 7.50 € kg^{-1} for N^--biomass) are most of the time the major production costs. One should realize that the used estimates of cultivation costs are already a projection compared to the current 1 ha production. In general, all SP and MP chains will benefit from lower cultivation costs, as also indicated previously (Laurens et al., 2017). The benchmark size of the production facility reported here as well as in literature (100 ha; Beal et al., 2015; Ruiz et al., 2016) can affect the market equilibrium, maybe ending in the demand saturation for some high value products.

The scenarios for whole and broken microalgae, as well as for soluble proteins (including the residue as co-product) always lead to a negative potential profit at 10 kton y^{-1}

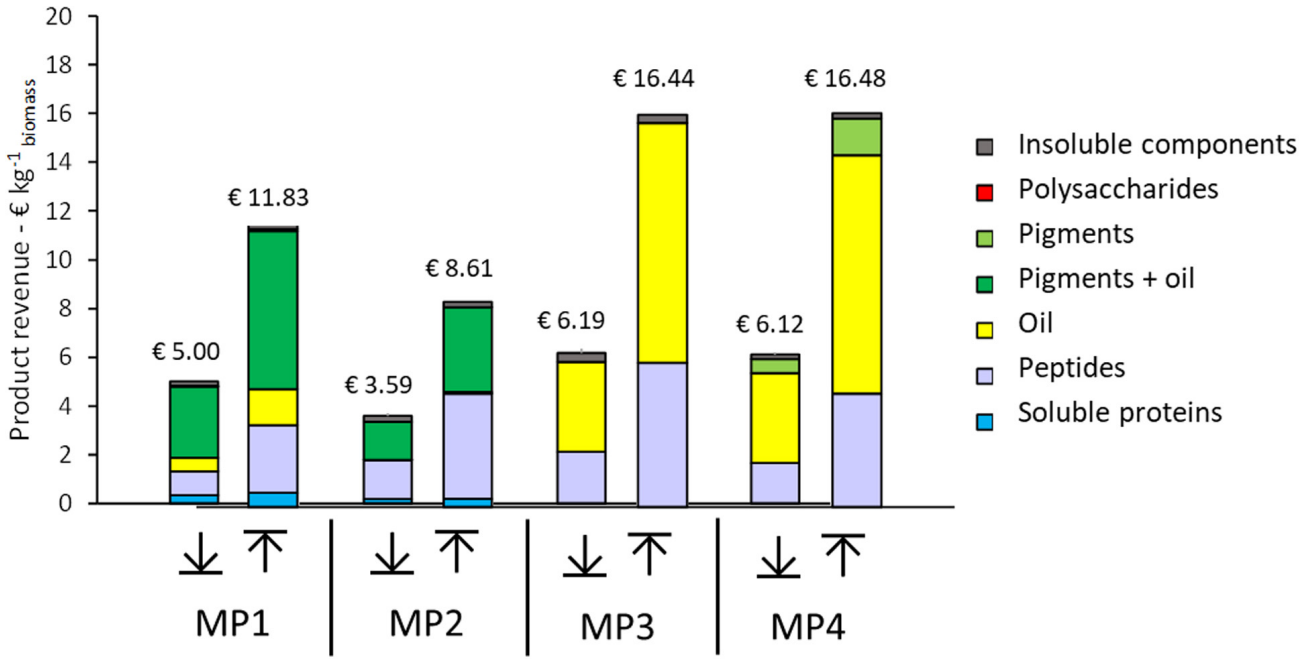

FIGURE 8 | Range of potential product revenue expressed per unit of initial biomass for each multiproduct (MP) value chain. (↓) worst case revenue estimates, (↑) best case revenue estimates.

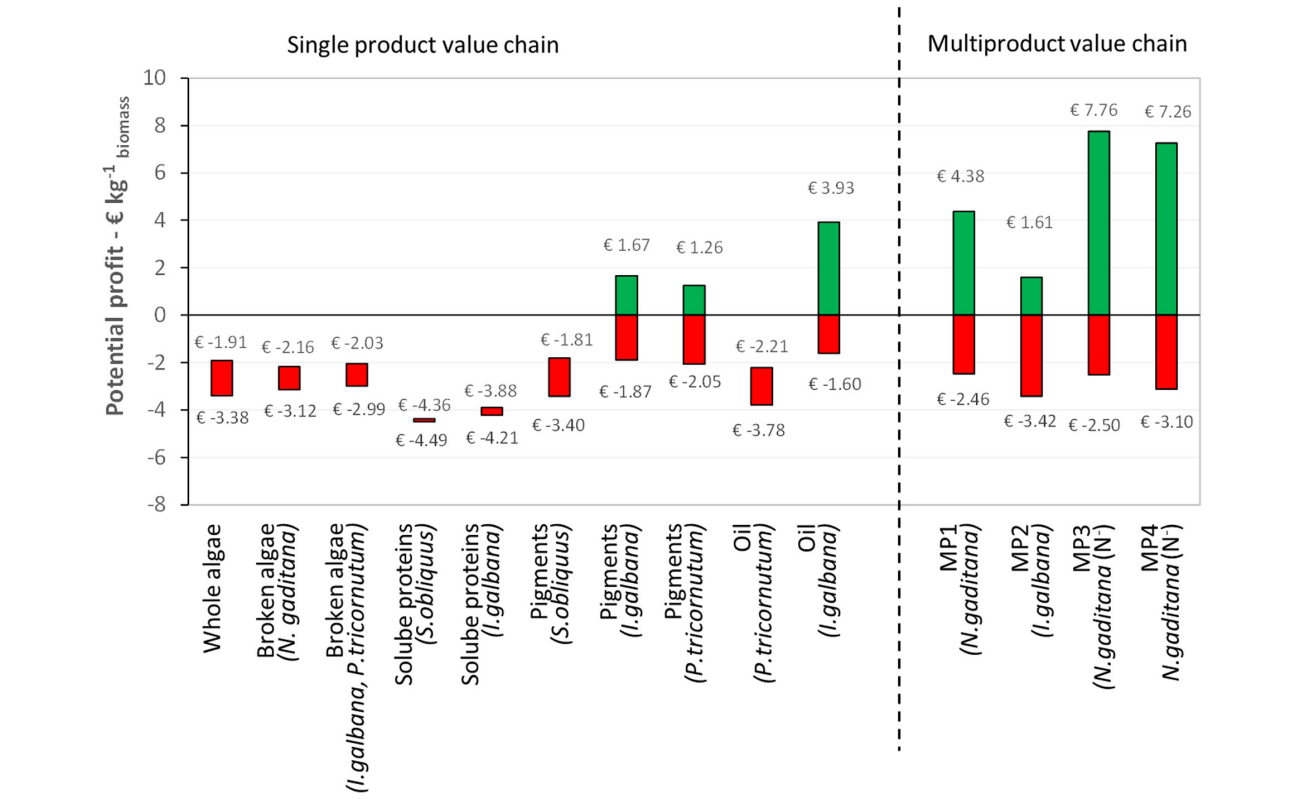

FIGURE 9 | Potential profit expressed per unit of initial biomass for the single and multiproduct value chains at 10 ktons y^{-1} scale, based on the total production costs (including CO_2 capture, cultivation, and biorefinery) and the potential revenues. MP, multiproduct value chain.

scale. This means that the combination of cultivation and biorefinery costs are higher than the generated revenues. The soluble protein value chain is also least investigated in literature in terms of process design and economic evaluation. Asiedu et al. (2018) provided a TEA for production of a dry protein hydrolysate powder (amino-acid and peptides) produced via flash hydrolysis from *S. obliquus* cultivated in open ponds. Assuming 81% of protein extraction and conversion, they ended with production cost of 2.99 € kg^{-1} protein and a minimum selling price of 4.31 € kg^{-1} protein (Asiedu et al., 2018).

For pigments and oil, the profit of the process depends on: (I) the oil and pigments content of the microalgal strain; (II) the efficiency of high pressure extraction; (III) the selling price of the pigments or oil. These figures are also confirmed in literature. Quinn and Davis (2015) have reviewed more than 20 techno-economic analysis for biodiesel production, which is a single product chain based on oil. In that work they showed that the large variety in costs (0.27–9.7 € kg^{-1} biofuel) is mainly related to the cultivation technology (open pond vs. closed photobioreactor) and on the lipid yield from cultivation (Quinn and Davis, 2015). Thomassen et al. (2016) have analyzed several scenarios of beta-carotene and astaxanthin production, confirming that the pigment content and extraction efficiency mainly affect the process profitability (Thomassen et al., 2016). In contrast to our work (range of 13.75–31.25 € kg^{-1} pigment), they consider a small market for their product and assume higher pigment selling prices, i.e., for beta-carotene 1180 € kg^{-1} and for astaxanthin 5113 € kg^{-1}.

For the multiproduct chains the profit range increases, with a positive center point (average) for MP1, 3, and 4. For these chains the worst-case estimate of revenue is thus not sufficient to balance the cultivation and biorefinery costs. For MP1 and MP2, large part of the revenue comes from pigments and peptides, while for MP3 and MP4 significant revenues are obtained from the oil and peptide products (**Figure 8**). Therefore, the efficiencies of the process steps related to those pigment, peptide and oil extraction and purification are the main factors affecting the process profitability. In contrast at this stage, the contribution of the additional co-products such as soluble proteins to the whole process economy seems not relevant. Additional insights in the product functionality, quality and their market size are needed to narrow down the wide range of foreseen product revenues and resulting profits.

To develop a profitable micro-algae production chain a combination is required of (1) technological innovations enabling cost reductions, especially in micro-algae production, (2) developing multiproduct biorefinery concepts aimed at valorizing the full biomass through the cascading principle, and (3) deriving a range of new specialty products with applications in food, aquaculture and non-food. Cascading increases the biorefinery costs significantly, but this is compensated by the enhanced overall biomass revenue, provided that the sequence of operations does not affect the yield and properties of the final products. When these conditions are met the achieved overall biomass revenues of the integrated, multiproduct chains enable an economically competitive microalgae biorefinery.

DATA AVAILABILITY STATEMENT

The raw data supporting the conclusions of this article will be made available by the authors, without undue reservation.

AUTHOR CONTRIBUTIONS

PS and GO performed TE evaluation and interpretation, drafted the manuscript, and took the responsibility for the integrity of the work as a whole, i.e., from conception until the finished article. PS coordinated data acquisition. GO developed and optimized the flow sheets. PS, GO, EB, LS, and JR conceived and designed the study. ME, RW, and JR obtained funding. All authors contributed to the selection of the single value chains, have critically reviewed the proposed multiproduct chains and results, and have critically revised the manuscript, read, and approved the submitted version.

FUNDING

The MIRACLES-project has received funding from the European Union's Seventh Framework Programme for research, technological development and demonstration under grant agreement no. 613588[6].

ACKNOWLEDGMENTS

The authors recognize the precious support of the other partners involved in the projects in providing data on the operating conditions and results from the biorefinery operations described in the manuscript: Antonius J. B. van Boxtel, Lambertus A. M. van den Broek, Corjan van den Berg, and Carl Safi (Wageningen University & Research), Bienvenida Gilbert-Lopez and Elena Ibanez (UAM-CSIC), Marina de Filette and Kris Schatteman (Eco Treasures), Philippe Willems (Value for Technology), Lalia Mantecon and Carlos Unamunzaga (Fitoplancton Marino S.L.), Leen Bastiaens (Vlaamse Instelling voor Technologisch Onderzoek NV), Bertus van den Burg (ImEnz), D. Wim, F. Brilman, and Qian Yu (University of Twente).

SUPPLEMENTARY MATERIAL

The Supplementary Material for this article can be found online at: https://www.frontiersin.org/articles/10.3389/fbioe.2020.550758/full#supplementary-material

[6]http://miraclesproject.eu/

REFERENCES

Asiedu, A., Ben, S., Resurreccion, E., and Kumar, S. (2018). Techno-economic analysis of protein concentrate produced by flash hydrolysis of microalgae. *Environ. Prog. Sustain. Energy* 37, 881–890. doi: 10.1002/ep.12722

Beal, C. M., Gerber, L. N., Sills, D. L., Huntley, M. E., Machesky, S. C., Walsh, M. J., et al. (2015). Algal biofuel production for fuels and feed in a 100-ha facility: a comprehensive techno-economic analysis and life cycle assessment. *Algal Res.* 10, 266–279. doi: 10.1016/j.algal.2015.04.017

Beal, C. M., Gerber, L. N., Thongrod, S., Phromkunthong, W., Kiron, V., Granados, J., et al. (2018). Marine microalgae commercial production improves sustainability of global fisheries and aquaculture. *Sci. Rep.* 8:15064. doi: 10.1038/s41598-018-33504-w

Breuer, G., Lamers, P. P., Martens, D. E., Draaisma, R. B., and Wijffels, R. H. (2012). The impact of nitrogen starvation on the dynamics of triacylglycerol accumulation in nine microalgae strains. *Bioresour. Technol.* 124, 217–226. doi: 10.1016/j.biortech.2012.08.003

Buono, S., Langellotti, A. L., Martello, A., Rinna, F., and Fogliano, V. (2014). Functional ingredients from microalgae. *Food Funct.* 5, 1669–1685. doi: 10.1039/c4fo00125g

Chandra, R., Iqbal, H. M. N., Vishal, G., Lee, H.-S., and Nagra, S. (2019). Algal biorefinery: a sustainable approach to valorize algal-based biomass towards multiple product recovery. *Bioresour. Technol.* 278, 346–359. doi: 10.1016/j.biortech.2019.01.104

Chauton, M. S., Reitan, K. I., Norsker, N. H., Tveterås, R., and Kleivdal, H. T. (2015). A techno-economic analysis of industrial production of marine microalgae as a source of EPA and DHA-rich raw material for aquafeed: research challenges and possibilities. *Aquaculture* 436, 95–103. doi: 10.1016/j.aquaculture.2014.10.038

Chew, K. W., Yap, J. Y., Show, P. L., Suan, N. H., Juan, J. C., Ling, T. C., et al. (2017). Microalgae biorefinery: high value products perspectives. *Bioresour. Technol.* 229, 53–62. doi: 10.1016/j.biortech.2017.01.006

Davis, R., Kinchin, C., Markham, J., Tan, E., Laurens, L., Sexton, D., et al. (2014). *Process Design and Economics for the Conversion of Algal Biomass to Biofuels: Algal Biomass Fractionation to Lipid- and Carbohydrate-Derived Fuel Products*. Golden, CO: National Renewable Energy Lab (NREL).

de Carvalho, J. C., Magalhães, A. I., de Melo Pereira, G. V., Medeiros, A. B. P., Sydney, E. B., Rodrigues, C., et al. (2020). Microalgal biomass pretreatment for integrated processing into biofuels, food, and feed. *Bioresour. Technol.* 300:122719. doi: 10.1016/j.biortech.2019.122719

de la Noue, J., and de Pauw, N. (1988). The potential of microalgal biotechnology: a review of production and uses of microalgae. *Biotechnol. Adv.* 6, 725–770. doi: 10.1016/0734-9750(88)91921-0

del Pilar Sánchez-Camargo, A., Pleite, N., Herrero, M., Cifuentes, A., Ibáñez, E., and Gilbert-López, B. (2017). New approaches for the selective extraction of bioactive compounds employing bio-based solvents and pressurized green processes. *J. Supercrit. Fluids* 128, 112–120. doi: 10.1016/j.supflu.2017.05.016

Delrue, F., Li-Beisson, Y., Setier, P. A., Sahut, C., Roubaud, A., Froment, A. K., et al. (2013). Comparison of various microalgae liquid biofuel production pathways based on energetic, economic and environmental criteria. *Bioresour. Technol.* 136, 205–212. doi: 10.1016/j.biortech.2013.02.091

DeRose, K., DeMill, C., Davis, R. W., and Quinn, J. C. (2019). Integrated techno economic and life cycle assessment of the conversion of high productivity, low lipid algae to renewable fuels. *Algal Res.* 38:101412. doi: 10.1016/j.algal.2019.101412

Dong, T., Knoshaug, E. P., Davis, R., Laurens, L. M. L., Van Wychen, S., Pienkos, P. T., et al. (2016). Combined algal processing: a novel integrated biorefinery process to produce algal biofuels and bioproducts. *Algal Res.* 19, 316–323. doi: 10.1016/j.algal.2015.12.021

Draaisma, R. B., Wijffels, R. H., Slegers, P. M., Brentner, L. B., Roy, A., and Barbosa, M. J. (2013). Food commodities from microalgae. *Curr. Opin. Biotechnol.* 24, 169–177. doi: 10.1016/j.copbio.2012.09.012

Eppink, M. H. M., Olivieri, G., Reith, H., van den Berg, C., Barbosa, M. J., and Wijffels, R. H. (2019). "From current algae products to future biorefinery practices: a review," in *Biorefineries*, eds K. Wagemann and N. Tippkötter (Cham: Springer International Publishing), 99–123. doi: 10.1007/10_2016_64

Gilbert-López, B., Barranco, A., Herrero, M., Cifuentes, A., and Ibáñez, E. (2017a). Development of new green processes for the recovery of bioactives from *Phaeodactylum tricornutum*. *Food Res. Intern.* 99, 1056–1065. doi: 10.1016/j.foodres.2016.04.022

Gilbert-López, B., Mendiola, J. A., van den Broek, L. A. M., Houweling-Tan, B., Sijtsma, L., Cifuentes, A., et al. (2017b). Green compressed fluid technologies for downstream processing of *Scenedesmus obliquus* in a biorefinery approach. *Algal Res.* 24, 111–121. doi: 10.1016/j.algal.2017.03.011

Gilbert-Lopez, B., Mendiola, J. A., Fontecha, J., van den Broek, L. A. M., Sijtsma, L., Cifuentes, A., et al. (2015). Downstream processing of *Isochrysis galbana*: a step towards microalgal biorefinery. *Green Chem.* 17, 4599–4609. doi: 10.1039/c5gc01256b

Gong, J., and You, F. (2015). Value-added chemicals from microalgae: greener, more economical, or both? *ACS Sustain. Chem. Eng.* 3, 82–96. doi: 10.1021/sc500683w

Günerken, E., D'Hondt, E., Eppink, M. H. M., Garcia-Gonzalez, L., Elst, K., and Wijffels, R. H. (2015). Cell disruption for microalgae biorefineries. *Biotechnol. Adv.* 33, 243–260. doi: 10.1016/j.biotechadv.2015.01.008

Gupta, S. S., Shastri, Y., and Bhartiya, S. (2017). Optimization of integrated microalgal biorefinery producing fuel and value-added products. *Biofuels Bioprod. Biorefin.* 11, 1030–1050. doi: 10.1002/bbb.1805

Harrison, R. G., Todd, P., Rudge, S. R., and Petrides, D. P. (2003). *Bioseparations; Science And Engineering*. Oxford: Oxford University Press.

Heinzle, E., Biwer, A. P., and Cooney, C. L. (2006). *Development of Sustainable Bioprocesses: Modelling and Assessment*. Chirchester: John Wiley and Sons.

Ibáñez, E., Gilbert-López, B., Mendiola, J. A., Cifuentes, A., and Herrero, M. (2017). *Integrated Green Extraction Processes for Downstream Processing of Microalgae Wet Biomass (GREENμWETBIO)*. Spanish patent No. ES1641.1286.

International Energy Agency [IEA] (2009). *Task 42 Biorefineries*. Available online at: http://www.iea-bioenergy.task42-biorefineries.com/en/ieabiorefinery/Activities-1.htm (accessed October 30, 2019).

Laurens, L. M. L., Markham, J., Templeton, D. W., Christensen, E. D., Van Wychen, S., Vadelius, E. W., et al. (2017). Development of algae biorefinery concepts for biofuels and bioproducts; a perspective on process-compatible products and their impact on cost-reduction. *Energy Environ. Sci.* 10, 1716–1738. doi: 10.1039/C7EE01306J

Milledge, J. J. (2011). Commercial application of microalgae other than as biofuels: a brief review. *Rev. Environ. Sci. Biol. Technol.* 10, 31–41. doi: 10.1007/s11157-010-9214-9217

Multi-product Integrated bioRefinery of Algae: from Carbon dioxide and Light Energy to high-value Specialties [MIRACLES] (2017). *Project Final Report*. Available online at: http://miraclesproject.eu/publications.php (accessed April 19, 2019).

Norsker, N.-H., Barbosa, M. J., Vermuë, M. H., and Wijffels, R. H. (2011). Microalgal production - A close look at the economics. *Biotechnol. Adv.* 29, 24–27. doi: 10.1016/j.biotechadv.2010.08.005

Pulz, O., and Gross, W. (2004). Valuable products from biotechnology of microalgae. *Appl. Microbiol. Biotechnol.* 65, 635–648. doi: 10.1007/s00253-004-1647-x

Quinn, J. C., and Davis, R. (2015). The potentials and challenges of algae based biofuels: a review of the techno-economic, life cycle, and resource assessment modeling. *Bioresour. Technol.* 184, 444–452. doi: 10.1016/j.biortech.2014.10.075

Rajesh Banu, J., Preethi, K. S., Gunasekaran, M., and Kumar, G. (2020). Microalgae based biorefinery promoting circular bioeconomy-techno economic and life-cycle analysis. *Bioresour. Technol.* 302:122822. doi: 10.1016/j.biortech.2020.122822

Ruiz, J., Olivieri, G., de Vree, J., Bosma, R., Willems, P., Reith, J. H., et al. (2016). Towards industrial products from microalgae. *Energy Environ. Sci.* 9, 3036–3043. doi: 10.1039/c6ee01493c

Sadhukhan, J., Ng, K. S., and Martinez, E. (2013). *Biorefineries and Chemical Processes*. Chirchester: John Wiley & Sons Ltd.

Safi, C., Liu, D., Yap, B. J., Martin, G. O., Vaca-Garcia, C., and Pontalier, P.-Y. (2014). A two-stage ultrafiltration process for separating multiple components of Tetraselmis suecica after cell disruption. *J. Appl. Phycol.* 26, 2379–2387. doi: 10.1007/s10811-014-0271-0

Show, K.-Y., Lee, D.-J., Tay, J.-H., Lee, T.-M., and Chang, J.-S. (2015). Microalgal drying and cell disruption – Recent advances. *Bioresour. Technol.* 184, 258–266. doi: 10.1016/j.biortech.2014.10.139

Thomassen, G., Egiguren Vila, U., Van Dael, M., Lemmens, B., and Van Passel, S. (2016). A techno-economic assessment of an algal-based biorefinery.

Clean Technol. Environ. Policy 18, 1849–1862. doi: 10.1007/s10098-016-1159-2

Vandermeulen, V., Van der Steen, M., Stevens, C. V., and Van Huylenbroeck, G. (2012). Industry expectations regarding the transition toward a biobased economy. *Biofuels Bioprod. Biorefin.* 6, 453–464. doi: 10.1002/bbb.1333

Vigani, M., Parisi, C., Rodríguez-Cerezo, E., Barbosa, M. J., Sijtsma, L., Ploeg, M., et al. (2015). Food and feed products from micro-algae: market opportunities and challenges for the EU. *Trends Food Sci. Technol.* 42, 81–92. doi: 10.1016/j.tifs.2014.12.004

Wageningen University and Research (2017). *Areaal Tuinbouw Onder Glas en Aantal Bedrijven*. Available online at: http://www.agrimatie.nl/SectorResultaat.aspx?subpubID=2290&sectorID=2240&themaID=2286&indicatorID=2014 (accessed March 2018).

Wijffels, R. H., and Barbosa, M. J. (2010). An outlook on microalgal biofuels. *Science* 329, 796–799. doi: 10.1126/science.1189003

Wijffels, R. H., Barbosa, M. J., and Eppink, M. H. M. (2010). Microalgae for the production of bulk chemicals and biofuels. *Biofuels Bioprod. Biorefin.* 4, 287–295. doi: 10.1002/bbb.215

Conflict of Interest: The authors declare that the research was conducted in the absence of any commercial or financial relationships that could be construed as a potential conflict of interest.

frontiers in Bioengineering and Biotechnology

ORIGINAL RESEARCH
published: 15 September 2020
doi: 10.3389/fbioe.2020.564667

Chlorella vulgaris Extract as a Serum Replacement That Enhances Mammalian Cell Growth and Protein Expression

*Jian Yao Ng[1], Mei Ling Chua[1], Chi Zhang[2], Shiqi Hong[2], Yogesh Kumar[2], Rajeev Gokhale[2] and Pui Lai Rachel Ee[1,3]**

[1] Department of Pharmacy, Faculty of Science, National University of Singapore, Singapore, Singapore, [2] Roquette Innovation Center, Helios, Singapore, Singapore, [3] National University of Singapore (NUS) Graduate School for Integrative Sciences and Engineering, Singapore, Singapore

The global cell culture market is experiencing significant growth due to the rapid advancement in antibody-based and cell-based therapies. Both rely on the capacity of different living factories, namely prokaryotic and eukaryotic cells, plants or animals for reliable and mass production. The ability to improve production yield is of important concern. Among many strategies pursued, optimizing the complex nutritional requirements for cell growth and protein production has been frequently performed via culture media component titration and serum replacement. The addition of specific ingredients into culture media to modulate host cells' metabolism has also recently been explored. In this study, we examined the use of extracted bioactive components of the microalgae *Chlorella vulgaris*, termed chlorella growth factor (CGF), as a cell culture additive for serum replacement and protein expression induction. We first established a chemical fingerprint of CGF using ultraviolet-visible spectroscopy and liquid chromatography-mass spectrometry and evaluated its ability to enhance cell proliferation in mammalian host cells. CGF successfully promoted the growth of Chinese hamster ovary (CHO) and mesenchymal stem cells (MSC), in both 2D and 3D cell cultures under reduced serum conditions for up to 21 days. In addition, CGF preserved cell functions as evident by an increase in protein expression in CHO cells and the maintenance of stem cell phenotype in MSC. Taken together, our results suggest that CGF is a viable culture media additive and growth matrix component, with wide ranging applications in biotechnology and tissue engineering.

Keywords: *Chlorella vulgaris*, algae extract, serum replacement, 3D cell culture, CHO cells, bioprocess engineering, protein expression, tissue engineering and regenerative medicine

OPEN ACCESS

Edited by:
Norio Nagao, Independent Researcher, Nagasaki, Japan

Reviewed by:
Swee Keong Yeap, Xiamen University, Malaysia, Malaysia
Chou Min Chong, Putra Malaysia University, Malaysia

****Correspondence:***
Pui Lai Rachel Ee
phaeplr@nus.edu.sg

Specialty section:
This article was submitted to Bioprocess Engineering, a section of the journal Frontiers in Bioengineering and Biotechnology

Received: *22 May 2020*
Accepted: *20 August 2020*
Published: *15 September 2020*

Citation:
Ng JY, Chua ML, Zhang C, Hong S, Kumar Y, Gokhale R and Ee PLR (2020) Chlorella vulgaris Extract as a Serum Replacement That Enhances Mammalian Cell Growth and Protein Expression. Front. Bioeng. Biotechnol. 8:564667. doi: 10.3389/fbioe.2020.564667

INTRODUCTION

Therapeutic proteins are an important class of medications for the treatment of complex diseases such as diabetes and immunological defects. The advent of recombinant DNA technology has enabled the production of these proteins in industrial-scale bioreactors. The process involves upstream genetic engineering of host systems, such as bacterial, yeast, insect, or transgenic plant and mammalian cells, along with downstream purification of extracted proteins

(Tripathi and Shrivastava, 2019). In recent years, mammalian cells have become the main host systems for recombinant protein production (Walsh, 2014). This is due to their innate membranous organelles allowing post-translational modification (PTM) of the expressed proteins, which is critical for certain proteins to fold properly and/or exert its biological activity (Amann et al., 2019). In particular, given their ease of *in vitro* cell culture and ability to adapt to selection pressure, Chinese hamster ovary (CHO) cells are established as the workhorse for industrial protein production (Berger et al., 2020).

Commercial CHO cell lines (e.g., CHO-K1 and CHO-DG44) and their corresponding established transfection protocols have facilitated successful cell line development (Elshereef et al., 2019). However, the challenge of a cost-effective production lies in the costly and time-consuming upstream process development. Notably, tremendous research efforts are required for media composition optimization (Hunter et al., 2019). The conventional approach is focused on the development of an optimized cultivation media via component titration using the "one factor at a time" (OFAT) method (Ritacco et al., 2018). Recently, by understanding how certain intracellular anabolic pathways contribute to protein expression, there is considerable interest in improving protein production efficiency by tuning host cell metabolism via incorporation of expression pathway inducers into the cultivation media (Huang et al., 2017).

Substantial emphasis has also been placed on fetal bovine serum (FBS) replacement. The main components of FBS are proteins; and they include growth factors, hormones, and other functional proteins that are essential for cell growth and protein production (Gstraunthaler, 2003; Brunner et al., 2010). Despite the importance of FBS, several disadvantages in terms of batch-to-batch variations, risk of zoonosis, and high protein content complicating downstream purification process have motivated the search for serum-free medium formulations (van der Valk et al., 2018).

Chlorella vulgaris (*C. vulgaris*) is a unicellular microalgae discovered in 1890 by Martinus Willem Beijerinck (Krienitz et al., 2015). It is highly nutritious in nature and thus various forms of *C. vulgaris* extract are often consumed as a health supplement in some countries, notably Japan. Given *C. vulgaris*' nutritious profile, some literatures have reported its potential use as an FBS alternative for *in vitro* cell culture. For example, Song et al. (2012) demonstrated that their hot water *C. vulgaris* extract stimulated proliferation of rat intestinal epithelial (IEC-6) cells after 24 h of incubation at serum-free conditions, via activation of the mitogen-activated protein kinase (MAPK), phosphoinositide-3-kinase–protein kinase B (PI3K/Akt), and canonical wingless-related integration site (Wnt) pathways. This study iterated that water extracts of *C. vulgaris* contained bioactive polysaccharides, that exerted important cell proliferative effects through gene induction pathways. These polysaccharides were later identified as phenolic compounds, which are usually found in algal or plant extracts bound to carbohydrates as glycosides (Safafar et al., 2015). *C. vulgaris* derived phenolic compounds possess potent antioxidative properties (Diaz-Vivancos et al., 2015), which may protect cells from serum deprivation-induced injury (Jung et al., 2017). Of interest, MAPK, PI3K/Akt and canonical Wnt are cross-species conserved signaling pathways that regulate protein expression (Proud, 2007), and manipulation thereof may potentially improve protein production yield (Chevallier et al., 2019). There is, however, to date no report that systematically evaluate the potential of *C. vulgaris* extract as a cell culture additive that could act as both a serum replacement and an inducer of protein expression.

In this report, we present the characterization of extracted bioactive components of *C. vulgaris*, termed chlorella growth factor (CGF), and demonstrate their ability to support cell growth in low serum conditions using high utility mammalian cell lines, such as CHO and mesenchymal stem cells (MSCs). The enhanced proliferative capacity in turn led to induced protein expression in CHO cells as measured by GFP protein marker expression. On the other hand, when used with MSCs, CGF stimulated their growth in both 2D and 3D cultures, while preserving their stem-like phenotype. Our results not only present an exciting opportunity for commercial protein production, but also for the development of novel MSC-based therapeutic strategies for tissue engineering and regenerative medicine (TERM).

MATERIALS AND METHODS

Materials

Puromycin dihydrochloride (P8833), bovine serum albumin (BSA) lyophilized powder (A2153-10G), low-glucose (D5523), and high-glucose (D1152) Dulbecco's Modified Eagle's medium (DMEM), DMEM/Nutrient Mixture F-12 Ham, 1:1 mixture (D2906), Accutase solution (A6964), penicillin/streptomycin (P4333), paraformaldehyde (PFA, P6148), DAPI readymade solution (MBD0015-5ML), CelLytic^{TM} M (C2976-50ML), and Whatman® 0.45 μm nylon membrane filters (WHA7404004) were purchased from Sigma-Aldrich (St Louis, MO, United States). All salts were received in anhydrous form. Fetal Bovine Serum (FBS) was obtained from Hyclone (South Logan, UT, United States). Ultrapure grade phosphate buffered saline (10× PBS) was procured from Vivantis Technologies Sdn Bhd (Subang Jaya, Selangor Darul Ehsan, Malaysia). Triton-X was obtained from Bio-Rad Laboratories (Hercules, CA, United States). CellTiter 96 AQueous One Solution Cell Proliferation Assay (MTS) was purchased from Promega (Madison, WI, United States). 0.22 μm polyethersulfone (PES) filters were acquired from sartorius stedim (Göttingen, Germany). Franz diffusion cells and Franz cell incubator, as well as HaCaT keratinocytes were kindly sponsored by Professor Paul Ho Chi Lui (NUS, Singapore). Human dermal fibroblasts (HDF), human Mesenchymal Stem Cells (hMSC, PT-2501) and Adipose-derived Stem Cells (ADSC, PT-5006) were purchased from Lonza Bioscience (Basel, Switzerland). Both GFP-transfected (puromycin) and native CHO-K1 cells were obtained from Accegen Biotech (Fairfield, NJ, United States). All other materials obtained are of research grade and used as received.

CGF Extraction Method

Aqueous extraction of *C. vulgaris* biomass was performed at Roquette Singapore Innovation Center. *C. vulgaris* biomass

harvest was first grinded into a powder form and suspended in deionized water to a concentration of 10% (w/v). The suspension was left to boil at 100°C for 20 min. After cooling down to room temperature, the suspension was centrifuged at 8,000 g for 30 min. Water-soluble bioactive components of *C. vulgaris*, termed as CGF, were harvested from the supernatant. This aqueous extract of CGF was sterile filtered through a 0.22 μm syringe filter prior to use for all studies.

Characterization of CGF

Determination of Proximate Crude Composition of CGF

Direct protein quantification methods such as Bradford and Lowry assays are inaccurate for plant-based extracts (Biancarosa et al., 2017). Therefore, to determine the protein content of biomass extracts, a majority of studies employed an indirect nitrogen-protein (N-protein) conversion factor. By using HPLC (method described below) to measure N and Kjeldahl's N-protein factor of 6.25, we determined the crude protein content of CGF and subsequently, calculated its carbohydrate content (Kjeldahl, 1883). Next, standardized methods of atomic absorption spectroscopy (AAS) and plate counting were used to determine the ash/trace metal and microbial contents of CGF respectively (Feldsine et al., 2002). The results were compared against prescribed limits for human use.

UV-Vis Spectroscopy

UV-Vis spectroscopy was used to quantify the amount of functional phenolic compounds in CGF. UV absorbance were measured at a wavelength of 260 nm (OD_{260}) using Ultrospec 2100 pro UV-Vis spectrophotometer (Little Chalfont, United Kingdom). Briefly, 1 mL of diluted CGF samples were added into separate Starna quartz spectrophotometer cells (Ilford, United Kingdom) ($n = 3$). The solvent, either deionized water or 1× PBS, was used as blank. Linear calibration curves of blank corrected-OD_{260} against concentration of CGF were constructed for both solvents (**Supplementary Figure S1**). R^2-values with weighted observation at $1/X^2$ for CGF concentration were computed to show a linear relationship between absorbance and the range of CGF concentration used.

LC-MS

The chemical composition of CGF was determined by high-performance liquid chromatography (HPLC) with mass selective detection, using Agilent 1200 series LC (Santa Clara, CA, United States) coupled with Bruker electrospray ionization (ESI) tandem mass spectrometer (micrOTOF-Q II) (Billerica, MA, United States). Components were separated using Merck Chromolith Performance RP-18 endcapped 100-3 HPLC column, 130 Å, 2 × 100 mm, 2.0 μm column (Kenilworth, NJ, United States), held at room temperature. Mobile phase consists of 1% (v/v) aqueous formic acid (A) and acetonitrile (ACN) (B), and was used with a discontinuous gradient; 0 min 5% B, to 40% B in 22 min, to 100% B in the next 15 min until the 62nd min, B decreased to 5% by the 63rd min, until the run ended on the 70th min, all at the flow rate of 0.2 mL/min. Chromatographic profiles were acquired in the wavelength at 260 nm. Injection volume was 20 μL ($n = 3$). Eluted components were ionized by ESI source, using N_2 for nebulization (pressure of 2.0 bar) and drying (flow of 6 L/min, temperature of 200°C). Set capillary voltage was 3,500 V, end plate offset −500°V, collision cell RF 250.0 Vpp. Data were acquired in MS (auto) scanning mode between 50 to 2,000 mass-to-charge ratio (m/z). The entire LCMS experiment was repeated for three separate batches of CGF ($n = 3$), statistical comparison of characteristics peak areas was then performed with one-way ANOVA using GraphPad Prism v8.4.3.

Cell Culture

In vitro Expansion of Mammalian Cell Lines

All mammalian cells received in cryovials were thawed and cultured on Nunc T-75 cell culture flasks (Roskilde, Denmark), according to the manufacturer's protocol. HDF and HaCaT cells were expanded using high-glucose DMEM, while hMSC and ADSC were expanded using low-glucose DMEM. GFP-transfected and native CHO-K1 cells were expanded in DMEM/Nutrient Mixture F-12 Ham 1:1 mixture media, with or without 20 mg/mL of puromycin (selection pressure) respectively. All culture media were supplemented with 10% (v/v) FBS and 1% (v/v) penicillin-streptomycin. HDF, HaCaT, and CHO-K1 cells were used between passage 3–20. The stem cells were used between passages 3–5. All cells were harvested between 80 and 90% confluency.

Cell Encapsulation Into Hydrogel Matrix for *in vitro* 3D Cell Culture

A cell-adhesive gellan gum-collagen hydrogel scaffold was used for *in vitro* 3D cell culture. The hydrogel matrix was prepared as previously reported (Ng et al., 2019). Briefly, 60 μL of cell-laden hydrogels were formed in each well of 96-well plate (HDF) or 48-well plate (hMSC or ADSC), and supplemented with 200 and 600 μL of culture media respectively. All cultured cells were incubated at 37°C in a humidified atmosphere of 5% CO_2 in air. The culture media were replaced every 2–3 days (Mon, Wed and Fri).

Cytotoxicity Assay

The effect of CGF on cell viability was examined using the colorimetric MTS assay, according to the manufacturer's protocol. Mammalian cells were harvested using Accutase solution and seeded at 5,000 cells per well of 96-well plates ($n = 3$ per concentration of CGF). The plates were incubated for 24 h to allow cell adhesion. After which, the spent media were replaced with fresh media containing varying final concentrations (w/v) of CGF and further incubated for 72 h. Next, 10 μL of MTS was incubated with the cells per 100 μL of culture media for another 3 h to allow the conversion of MTS into a brown formazan product. Then, 100 μL of the supernatant of each well was transferred to a new well in a 96-well plate. The measurement of total metabolic activity was done on Hidex Sense microplate reader (Turku, Finland) at OD_{490}.

Cell-free wells were used as blank controls, untreated cells were used as negative controls. Relative cell viability was determined when blank-corrected OD_{490} values of cells exposed

to different concentrations of CGF were expressed against blank-corrected OD_{490} of negative controls. The concentration of CGF that induced highest cell viability (E_{max}) and killed 50% of the cell population (CC_{50}) were tabulated. For 3D cell culture, cell-free hydrogels were used as blank controls and untreated encapsulated HDF were used as negative controls instead.

Serum Replacement Assay

At their respective E_{max} concentrations, the effect of CGF on proliferation of mammalian cells cultured in serum-reduced conditions was examined using the colorimetric MTS assay as described above. Cells were seeded in either serum-free (0% FBS), low serum (2% for HDF, HaCaT and CHO-K1, or 5% for hMSC and ADSC) or full serum (10% FBS) culture media [n = 3 (2D cell culture) and = 9 (3D cell culture) per concentration of serum, per time point]. MTS assays were performed on day 0 (6 h after seeding) to determine the cells' initial viability, and on days 1, 3, and 7 of incubation, as well as days 14 and 21 for encapsulated stem cells. Cell proliferation was determined by expressing the blank-corrected OD_{490} values obtained from each time points against that of day 0's.

Flow Cytometry Analysis

After 21 days of incubation with CGF at serum-reduced conditions, multipotency of ADSC was assessed via flow cytometry analysis of cell surface protein markers, using the CytoFLEX LX flow cytometer (Beckman Coulter, CA, United States). Briefly, ADSC was first harvested using Accutase solution and resuspended in 0.1% BSA in 1× PBS at the cell density of 1×10^6 cells/mL. The cells were then stained with FITC anti-human CD105 (Clone MEM-229), CD73 (Clone AD2), and CD90 (Clone 5E10), as well as PE/Cy5.5 anti-human CD45 (all Abcam, Cambridge, United Kingdom), at 4°C for 30 min in the dark, according to the manufacturer's protocol. Untreated and unstained ADSC was assessed in the same manner for the quadrants to be drawn. Percentage of positive cells for each marker was calculated from three independent experiments (n = 3).

Protein Expression via GFP-Transfected CHO Cell Line

GFP-transfected or native CHO-K1 cells were seeded separately with 1 mL of 10% FBS puromycin-free culture media at the cell density of 5×10^4 cells/mL, in each Ibidi 35 mm glass bottom dish (n = 3 per group) (Martinsried, Germany), overnight for the cells to attach. After which, the cells were first rinsed with sterile 1× PBS, then exposed to 0% FBS (serum-free) puromycin-free culture media supplemented either with or without 0.001 g/L of CGF for 72 h. The four groups were labeled as GFP-transfected CHO-K1 "GFP (+)" or native CHO-K1 cells "GFP (−),"supplemented with "CGF (+)" or without "CGF (−)" CGF.

Enzyme-Linked Immunosorbent Assay (ELISA)

Quantification of intracellular GFP was conducted with Abcam GFP SimpleStep ELISA kit (ab171581, Cambridge, United Kingdom) on cell lysates that were harvested using CelLytic M, according to the manufacturer's protocol. Using GFP standards provided in the kit and Tecan Infinite M Plex plate reader (Männedorf, Switzerland), a calibration curve of blank-corrected absorbance intensity against the concentration range of GFP was drawn. The concentration of GFP from the four different experimental groups were calculated from the calibration curve.

Confocal Microscopy

Green fluorescence emitted from GFP was observed with confocal laser scanning microscopy (CLSM). Briefly, cells were fixed with 1 mL of 4% PFA for 10 min, and subsequently permeabilized with 1 mL of 0.1% triton-x for 3 min. After which, cells' nuclei were counter-stained with 1,000× -diluted DAPI readymade solution for 20 min. Cell fixation, permeabilization and staining were all conducted at room temperature in dark. Confocal images were captured with Zeiss LSM710 (Oberkochen, Germany) using the 20×/0.8 objectives, with 405 nm diode and 488 nm argon laser as the excitation sources. Images were processed and exported using ZEN lite 2.3 (Carl Zeiss). The GFP intensity of each sample (n = 3 per group) was normalized against its own DAPI intensity using the ImageJ software. The average normalized GFP intensities of all groups were then statistically analyzed and compared.

Statistical Analysis

Statistical analysis was performed using GraphPad Prism v7.0.3. Data are presented as mean ± SD. One-way ANOVA was calculated between different experimental groups, with subsequent Bonferroni *post-hoc* tests performed to determine statistically significant differences ($^*p < 0.05$, $^{**}p < 0.005$, $^{***}p < 0.0005$, $^{****}p < 0.0001$) against controls.

RESULTS AND DISCUSSION

Chemical Fingerprint of CGF

Table 1 shows the proximate crude composition of CGF. The soluble extract contained approximately 67.1% crude protein, 27.4% carbohydrate, and 5.7% crude ash, which is in good agreement with a previous study (Song et al., 2012). In addition, the trace metals and microbial contents of CGF were found to be within the prescribed limits according to Singapore Medicines Act for human usage (Koh and Woo, 2000). Next, to establish the chemical fingerprint of CGF, phenolic compounds within CGF were separated by liquid chromatography, and the precursor ions present in each peak were subjected to collision-induced associated (CID) mass spectrometry analysis. The base peak chromatograms (BPC) for three separate batches of CGF are shown in **Figure 1**. The representative retention time (t_R) and area under curve (AUC) of each peak of CGF are presented in **Supplementary Table S1**. A total of 44 peaks were identified in the chromatogram and the major phenolic component of CGF was eluted at the 41st min. Characteristics peak areas were compared between the chromatograms of three separate batches of CGF (**Supplementary Figure S2**) and were not found to be statistically different (P = 0.9885). Our results indicate that our

TABLE 1 | Proximate crude composition of *C. vulgaris* extract, CGF.

Moisture (%)	Crude protein† (%)	Crude carbohydrate‡ (%)	Crude ash (%)	Trace metals§ (mg/kg)	Microbial content¶ (CFU/g)
Chlorella growth factor (CGF)					
5.5	67.1	27.4	5.7	Arsenic < 0.20	Total aerobic microbe < 110
				Mercury < 0.02	*E. Coli* undetectable
				Cadmium < 0.10	Salmonella species undetectable
				Lead < 0.20	

†*Crude protein composition = expressed as percentage of dry base.* ‡*% carbohydrate = 100% - % moisture - % protein - % lipid (assumed to be 0% in aqueous extract of C. vulgaris).* §*Trace element content complied with Singapore Medicines Act, under Medicines (Prohibition of Sale and Supply) Order for prohibition of sales or supply of medicinal products containing excessive levels of toxic heavy metals -p3 (1) (c).* ¶*Microbial content complied with Singapore Medicines Act, under Medicines (Prohibition of Sale and Supply) Order for prohibition of import, sale or supply of Chinese proprietary medicine containing excessive microbial contamination -p4.*

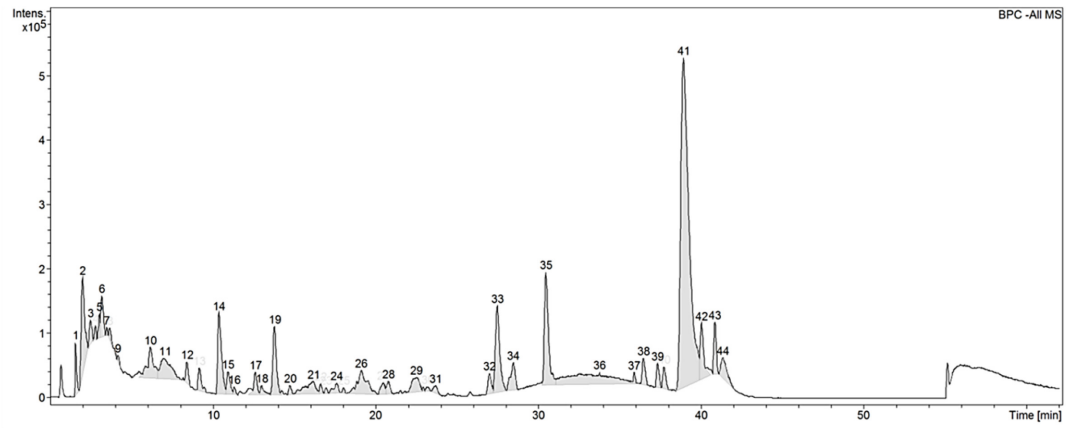

FIGURE 1 | Base peak chromatogram (BPC) of CGF analyzed with HPLC on Agilent 1200 series LC. Mobile phase consists of 1% (v/v) aqueous formic acid and acetonitrile (ACN) and, they were used with a discontinuous gradient. Flow rate was 0.2 mL/min. UV detection was set at the wavelength of 260 nm and, 20 μL of 10% (w/v) CGF was injected each run. The ordinate and abscissa are UV absorbance intensity (mAU) and retention time (t_R) respectively.

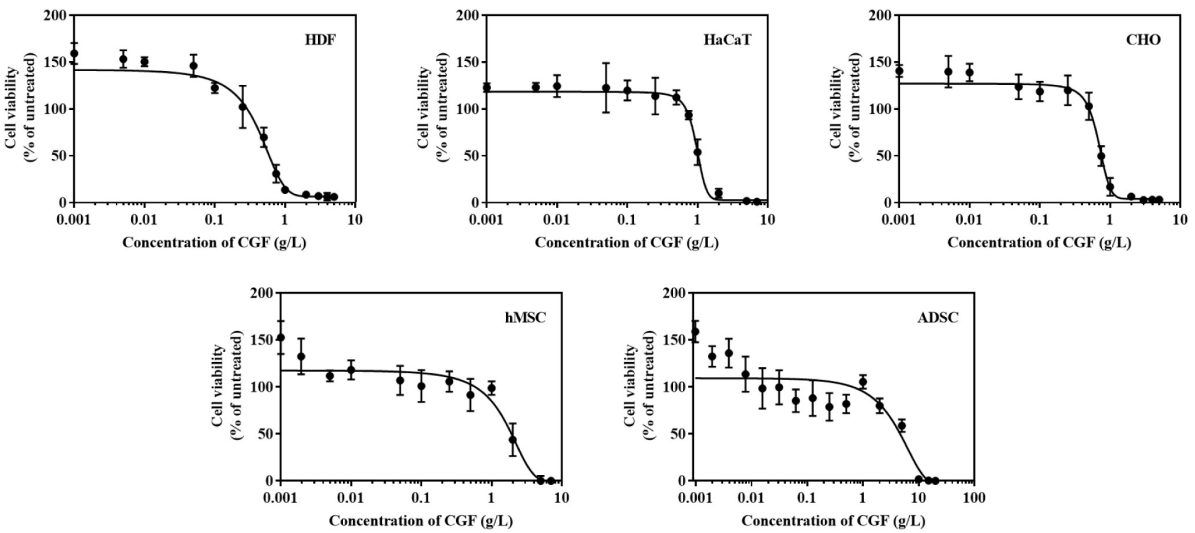

FIGURE 2 | Effect of various concentrations of CGF on the cell viability of HDF, HaCaT, CHO, hMSC, and ADSC (2D cell culture). Cells were cultured on 96-well plates with increasing concentrations of CGF for 72 h. Their cell viability was determined via MTS assay. For each concentration of CGF, the cell viability was expressed against untreated cells to obtain a percentage cell viability value. The resultant percentages of cell viability were plotted against concentrations of CGF. E_{max} and CC_{50} values of CGF for each cell lines were interpolated from the graphs. The mean (n = 3) ± SD are shown.

method of extracting CGF from different *C. vulgaris* harvests have minimal batch-to-batch variation.

Preliminary full scan mode yielded mass spectra with signal between 50 and 2,000 m/z, hence for increased sensitivity, subsequent scans were limited to this mass range. Using Bruker's SmartFormula structure elucidation algorithm, the most probable molecular formulae of 39 precursor ions were deduced. The major phenolic component of CGF has the molecular formula of $C_{16}H_{31}O_2$. For all proposed molecular formulae, their molecular weights were concluded on the basis of their

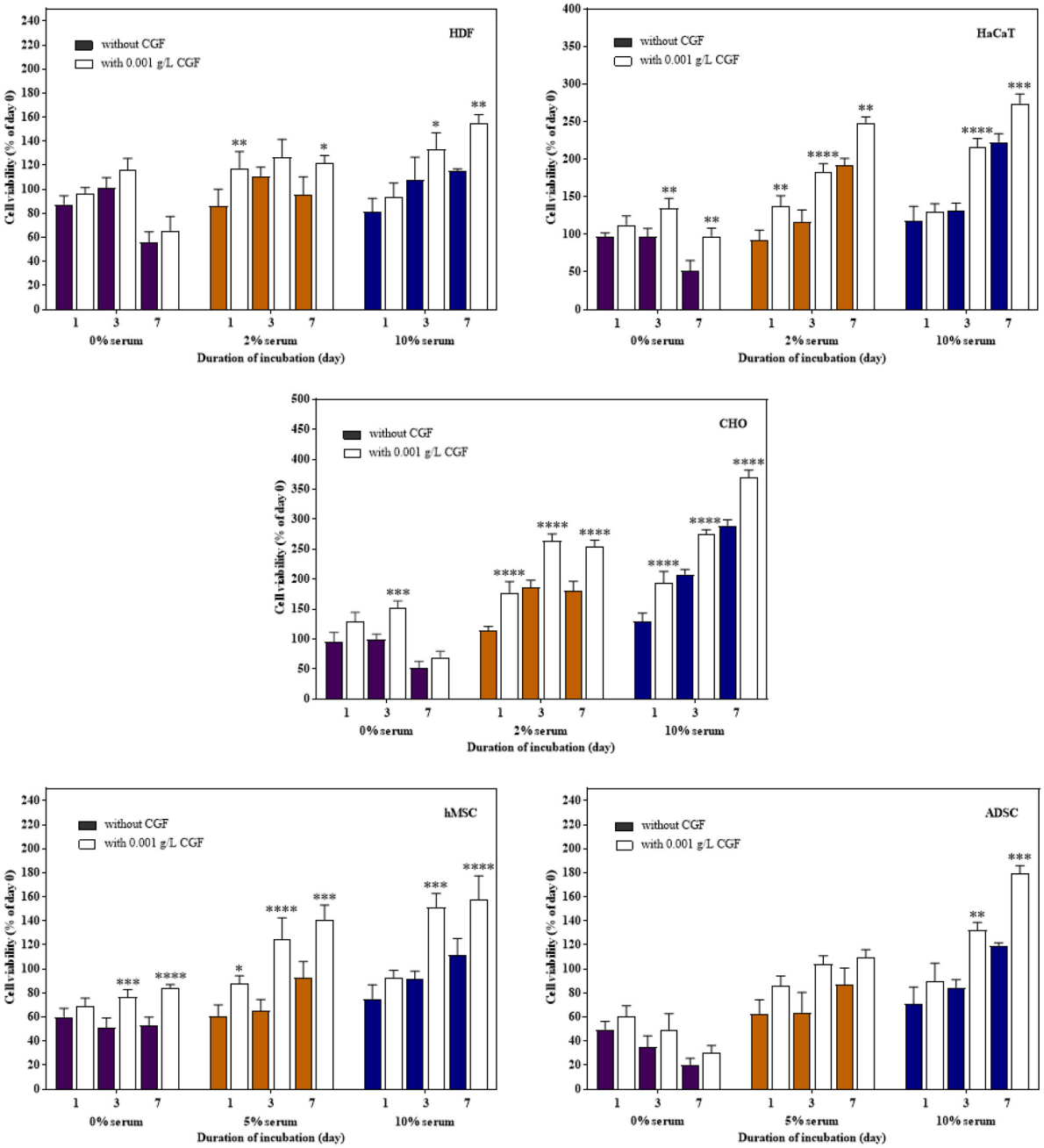

FIGURE 3 | Effect of CGF at its E_{max} concentration on the cell viability of HDF, HaCaT, CHO, hMSC, and ADSC at varying serum concentrations (2D cell culture). Cells were cultured on 96-well plates with no serum (0%), low serum (2% for HDF, HaCaT, CHO, and 5% for hMSC and ADSC), or full serum (10%) culture media, supplemented with or without CGF, for 7 days. Cell viability was determined at referred time points via MTS assay. The cell viability was then expressed against cells seeded for 6 h on day 0 to obtain a percentage cell viability value. The resultant percentages of cell viability were plotted against duration of incubation. The mean (n = 3) ± SD are shown. Statistical comparisons were made between cells incubated with CGF against cells incubated without CGF of the same duration of incubation (*$p < 0.05$, **$p < 0.005$, ***$p < 0.0005$, ****$p < 0.0001$).

negative ion ESI mass spectra, which showed precursor ions as $[M - H]^-$. A full list of possible molecular formulae as well as their calculated exact masses are presented in **Supplementary Table S1**. For accurate mass reporting, the tolerance for maximum mass deviations (measurement errors) of identified precursor ions were kept to less than ±0.001 Da. Standardization of aqueous extractions of *C. vulgaris* to obtain CGF are based on identical BPC and mass spectra for all our subsequent studies.

CGF Promoted Cell Proliferation at Serum-Reduced Conditions in Mammalian Cell Types of Industry Significance

Cytotoxicity Assay

C. vulgaris extracts have been shown to induce cell proliferation in cell lines such as IEC-6, HepG2, and MOLT-4 cells (Saad et al., 2006; An et al., 2010; Yusof et al., 2010). These evaluations are however limited in cells directly relevant to the medical and biotech industry. To address this gap, we thus selected 5 mammalian cell lines of industry significance and performed cytotoxic assays over a range of CGF concentrations (**Figure 2**). At low concentrations, CGF induced cell proliferation with a maximum increase in cell viabilities at E_{max} of 0.001 g/L for all cell types. This is in good agreement with previous studies which have shown that extracts of *C. vulgaris* are cell proliferative at lower concentrations while being cytotoxic at high concentrations (Yusof et al., 2010; Song et al., 2012). In addition, our study revealed that variable cytotoxicity was observed amongst mammalian cell lines, with HDF displaying the highest sensitivity with an average CC_{50} value of 0.597 g/L (95% CI: 0.508–0.710) and ADSC displaying the lowest sensitivity at CC_{50} value of 4.645 g/L (95% CI: 2.932–7.172) (**Supplementary Table S2**).

Serum Replacement Assay

Therapeutic proteins are produced through cell fermentation in a culture media that generally consists of growth factors derived from serum of an animal origin. To avoid complications associated with animal blood-derived ingredients, animal component-free chemically defined media are currently gold-standard alternatives (Schnellbaecher et al., 2019). However, these cell-line and cell-clone specific formulations often require extensive optimization before the ideal composition could be identified (Lakshmanan et al., 2019; Marigliani et al., 2019). In another approach, from the classic example of Advate and Recombinate, cell lines could also be adapted to serum-free culture (Négrier et al., 2008). Unfortunately, this method can only be applied to a very limited number of cell types without deleterious phenotypic alterations (van der Valk et al., 2018). To investigate the role of CGF as an alternative cell growth additive, we herein subjected mammalian cells to growth supplementation with CGF at full serum and serum-reduced conditions. As shown in **Figure 3**, significant increase in cell proliferation with CGF supplementation at E_{max} of 0.001 g/L was observed for all cell types at both conditions as compared to those cultured without CGF. Specifically, after 7 days of culture, mammalian cells exposed to CGF in low serum conditions exhibited between 30 and 70% increase in cell viabilities. Given that stem cells are notoriously sensitive to culture media composition, we made significant observations when their cell viabilities recovered from 85 to 140% upon CGF treatment at serum reduced conditions. However, in the complete absence of serum, CGF displayed only limited effect in reversing cell death over a period of 7 days. Taken together, our results suggest that CGF-enriched media enables a wide range of previously non-adapted high-utility mammalian cells, such as CHO and stem cells, to grow in serum-reduced conditions without disadvantages associated with conventional strategies.

CGF Supplementation Preserved Mammalian Cell Function and Phenotype

To show that CGF not only enhance cell growth but also preserve their function, we quantified GFP production using the stably transfected GFP reporter-producing cell line, CHO-K1, in the absence and presence of CGF (Lo et al., 2015). GFP is constitutively expressed in the presence of 20 mg/mL of puromycin in CHO-K1 but intracellular GFP degrades rapidly when protein synthesis is inhibited (Halter et al., 2007). As shown in **Figure 4** and **Supplementary Figure S3**, at serum-free conditions, CGF supplementation resulted in ∼5.6-fold increase in GFP expression as compared to that without CGF treatment. As expected, GFP could not be detected from the cell lysates of wild-type CHO-K1 cells with or without CGF supplementation, indicating that increased GFP expression was a result of activation of protein expression pathways by CGF in transfected CHO cells. Confocal images supported our observations and showed visually that the fluorescence intensities correlated with CGF supplementation in the cells (**Figure 5**). Similarly,

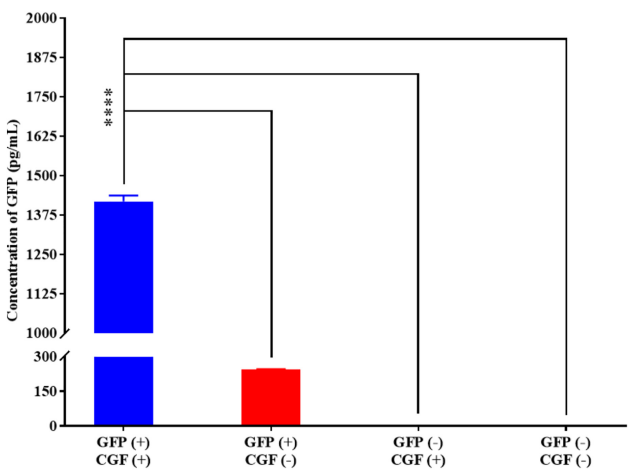

FIGURE 4 | Quantification of GFP expressed by CHO-K1 cells upon exposure to CGF as determined from ELISA. Significantly higher concentration (∼5.60-fold) of GFP could be detected in GFP-transfected CHO cells treated with CGF "GFP (+), CGF (+)" as compared to GFP-transfected CHO cells not treated with CGF "GFP (+), CGF (–)" as well as native CHO cells treated with CGF "GFP (–), CGF (+)" or without CGF "GFP (–), CGF (–)" (*$p < 0.05$, **$p < 0.005$, ***$p < 0.0005$, ****$p < 0.0001$).

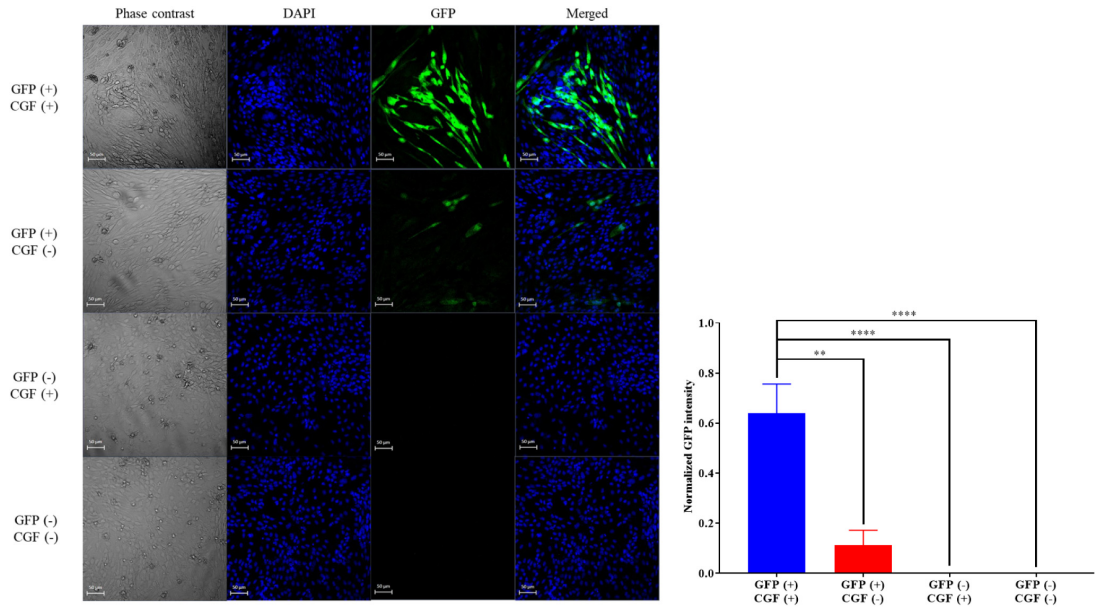

FIGURE 5 | Confocal images of GFP-transfected and native CHO cells with or without exposure to CGF. Visualization of intracellular GFP fluorescence via CLSM was performed at 20× zoom. Cells' nuclei were counter-stained with DAPI. Phase contrast images were taken for reference to cell boundaries. Images of GFP and DAPI were merged for co-localization purposes. Visually, the GFP fluorescence intensities are significantly higher in GFP-transfected CHO cells treated with CGF "GFP (+), CGF (+)" as compared to GFP-transfected CHO cells not treated with CGF "GFP (+), CGF (−)" as well as native CHO cells treated with CGF "GFP (−), CGF (+)" or without CGF "GFP (−), CGF (−)". Normalized GFP intensity of GFP (+), CGF (+) CHO cells were statistically significantly higher than the other groups (*$p < 0.05$, **$p < 0.005$, ***$p < 0.0005$, ****$p < 0.0001$).

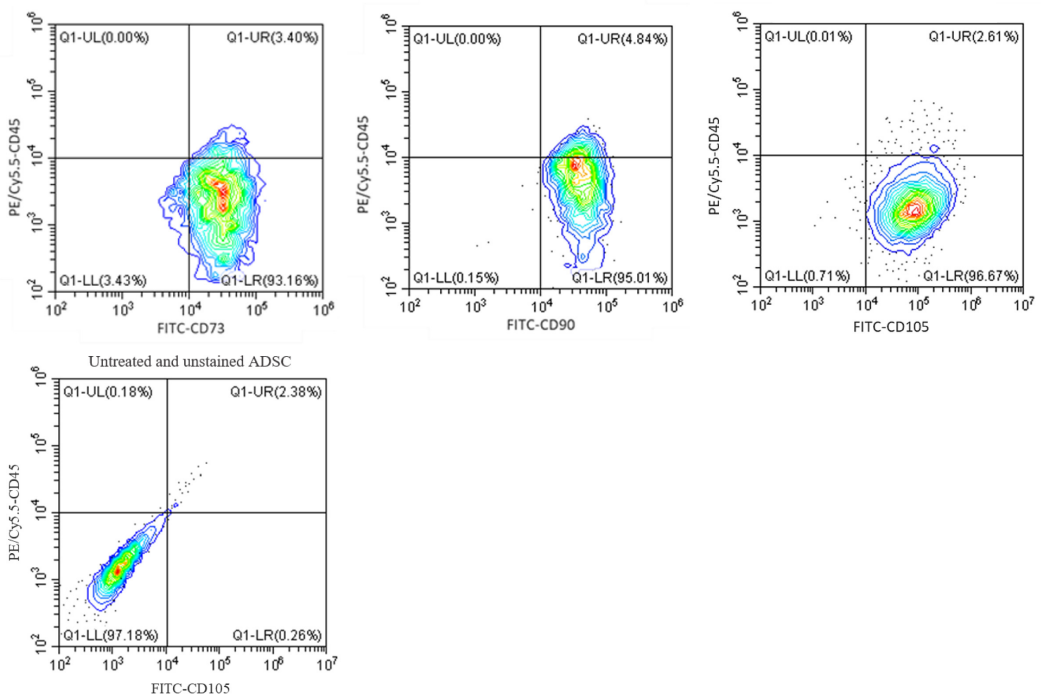

FIGURE 6 | Flow cytometry analysis of ADSC exposed to CGF for 21 days. The analysis was performed with gates set on CD73/90/105 + CD45- cell population. Representative flow cytometry contour-plots showed that a majority of the cell population (>95%) exhibited canonical CD73, CD90, and CD105 mesenchymal stem cell surface markers. Whereas, only a small population (<5%) of cell population was positive for the hemopoietic stem cell surface marker, CD45. This indicated that multipotency of ADSC was retained after culture with CGF. A contour plot of unstained ADSC below denotes how the quadrants were drawn. The data represent analyzed cultures in triplicates.

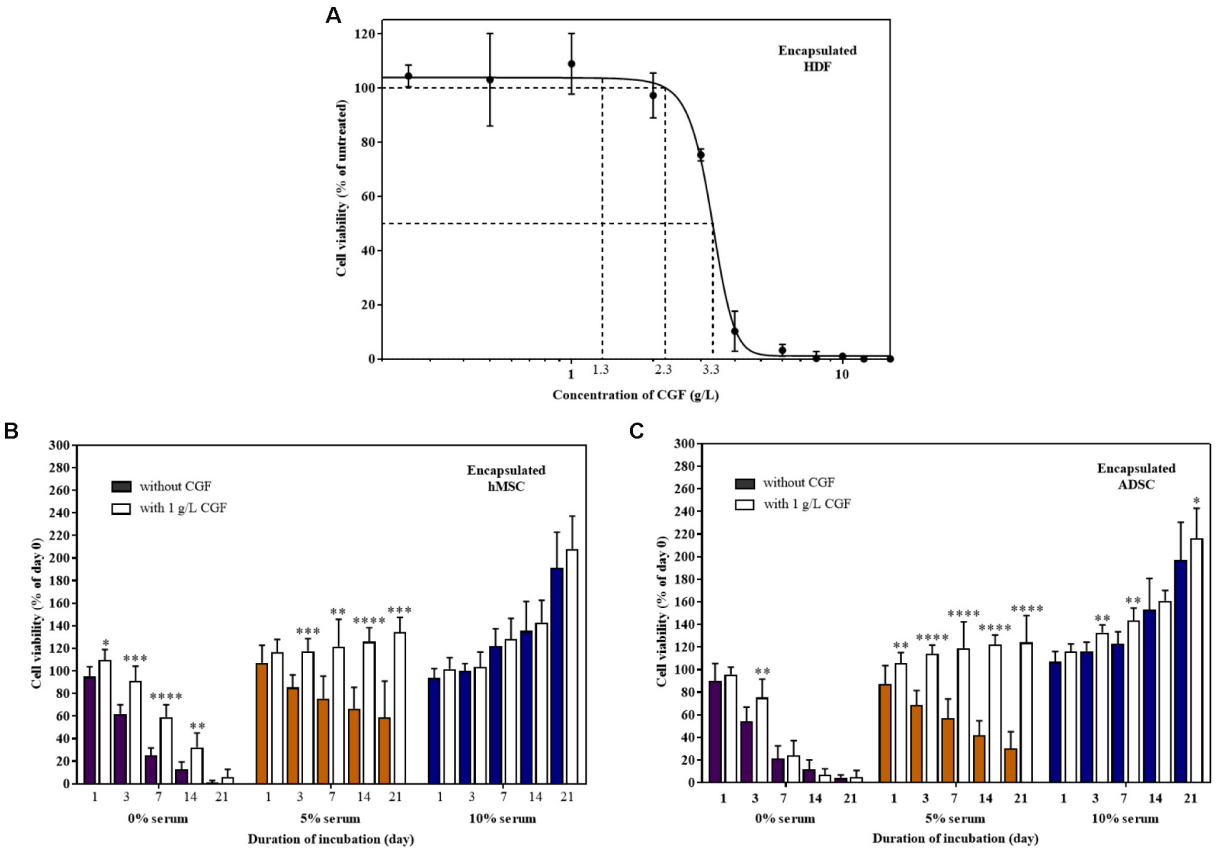

FIGURE 7 | Effect of CGF on HDF, hMSC, and ADSC cultured in 3D hydrogel scaffolds. **(A)** Effect of various concentrations of CGF on the cell viability of encapsulated HDF. Cells were encapsulated and cultured on 48-well plates with increasing concentrations of CGF for 72 h. Their cell viability was determined via MTS assay. For each concentration of CGF, the cell viability was expressed against untreated cells to obtain a percentage cell viability value. The resultant percentages of cell viability were plotted against concentrations of CGF. The mean (n = 3) ± SD are shown. Effect of CGF at its E_{max} concentration on the cell viability of encapsulated **(B)** hMSC and **(C)** ADSC. Cells were encapsulated and cultured on 48-well plates with no serum (0%), low serum (5%), or full serum (10%) culture media, supplemented with or without CGF, for 21 days. The cell viability was then expressed against cells seeded for 6 h on day 0 to obtain a percentage cell viability value. The resultant percentages of cell viability were plotted against the duration of incubation. The mean (n = 9) ± SD are shown. Statistical comparisons were made between cells incubated with CGF against cells incubated without CGF of the same duration of incubation (*$p < 0.05$, **$p < 0.005$, ***$p < 0.0005$, ****$p < 0.0001$).

normalized GFP intensity of the confocal images showed ∼5.7-fold increase when GFP CHO cells were supplemented with CGF. Hence. our data presents an exciting opportunity for bioprocess re-engineering via CGF supplementation for enhanced commercial protein production.

Next, to confirm that CGF does not affect the maintenance of cell phenotype with continuous expansion, we performed flow cytometry using specific antibodies against canonical cell surface markers in ADSC through five passages. **Figure 6** shows that ADSC maintained a stem-like phenotype with multiple passages under CGF supplementation. The majority of ADSC (>95%) was shown to express MSC markers CD73, CD 90 and CD105, while a negligible population (<5%) expressed the hematopoietic marker CD45. This gives confidence to the use of CGF in cell expansion designated for TERM applications. Given prior studies have shown that plant extracts are capable of stimulating differentiation in MSC, it is important to conduct future complementary investigations to understand the effect of CGF on the differentiation potential of 3D-cultuired ADSC (Zhang et al., 2015; Imran et al., 2017; Saud et al., 2019).

CGF Supports 3D Cell Culture for TERM Applications

TERM is concerned with the replacement of damaged tissues with *in vitro* created tissues (Gomes et al., 2017; Liu et al., 2017). For the artificial construction of living tissues, the tri-component recipe of a tissue scaffold, stem cells, and animal-derived growth factors are quintessential (Ng et al., 2020). To replicate 3D cell culture, MSCs encapsulated in a previously reported hybrid gellan gum-collagen hydrogel (Ng et al., 2019) were grown with and without CGF in both full and reduced serum conditions. The hydrogels exhibited consistent high degree of porosity (**Supplementary Figure S4**) with a maximal pore diameter of 150 μm and did not impede the effective movement of relatively smaller sized bioactive components of CGF

(**Supplementary Table S3**) in the matrix to reach the encapsulated mammalian cells according to the Franz cell diffusion assay (**Supplementary Figure S5**). First, we determined the E_{max} and CC_{50} of CGF to be 1 and 3.314 g/L (95% CI: 3.150–3.489 g/L) respectively, using hydrogel encapsulated HDF (**Figure 7A**). Next, at this E_{max} concentration, CGF exerted the most significant effect at reduced serum conditions (5%) by increasing stem cell viabilities beyond 120% after 3 weeks of culture (**Figures 7B,C**). This is a 2- to 4-fold increase in enhancement as compared to cells grown in the absence of CGF.

However, similar to 2D cell culture, in the complete absence of serum, CGF could not reverse cell death, although it could potentially delay the process as shown with encapsulated MSCs. Expectedly, CGF did not make any difference in full serum conditions, given the supraphysiological levels of growth factors present. Nonetheless, partial serum replacement with the use of algal-derived CGF as a growth matrix component in TERM may in part circumvent pertinent biosafety concerns associated with animal-derived serum for artificial tissue implantation such as xeno-immunization and zoonosis.

CONCLUSION

We have shown that CGF, an aqueous extract of *C. vulgaris*, was able to enhance cell proliferation in mammalian cell lines of biomedical significance in both *in vitro* 2D and 3D cell culture, with the subsequent increase in protein production yield and maintenance of stem cell phenotype. This highlights the exciting use of CGF as an industry-relevant biocatalyst for increasing therapeutic protein production yield, as well as a cell growth component for TERM applications.

DATA AVAILABILITY STATEMENT

All datasets generated for this study are included in the article/**Supplementary Material**.

AUTHOR CONTRIBUTIONS

JN, RG, and PE conceived the direction of the research work. CZ and SH extracted *C. vulgaris* into CGF. MC conducted the 2D cell culture studies. JN conducted the other experiments. JN and PE analyzed the data and wrote the manuscript. CZ, SH, and YK reviewed and edited the manuscript. RG and PE provided technical guidance and edited the manuscript drafts. All authors contributed to the article and approved the submitted version.

FUNDING

We would like to acknowledge research funding and facilities provided by the National University of Singapore, Ministry of Education Academic Research Fund (R148000287114) and Roquette Asia Pacific Pte Ltd. (R148000251592) awarded to PE and NUS-IRP Scholarship to JN.

ACKNOWLEDGMENTS

We thank Dr. Yuan Cheng-hui and his colleagues at Chemical, Molecular and Materials Analysis Centre (CMMAC) at NUS department of chemistry for their help with the liquid chromatography high-resolution mass spectrometry (LCHRMS). We express our gratitude to Dr. Lim Seng Han, from Prof. Paul Ho Chi Lui lab, for his help with the Franz diffusion cell experiments. We also thank Lee Shuying from the confocal microscopy unit of Yong Loo Ling School of Medicine (YLLSOM) for her help with the CLSM imaging.

SUPPLEMENTARY MATERIAL

The Supplementary Material for this article can be found online at: https://www.frontiersin.org/articles/10.3389/fbioe.2020.564667/full#supplementary-material

REFERENCES

Amann, T., Schmieder, V., Faustrup Kildegaard, H., Borth, N., and Andersen, M. R. (2019). Genetic engineering approaches to improve posttranslational modification of biopharmaceuticals in different production platforms. *Biotechnol. Bioeng.* 116, 2778–2796. doi: 10.1002/bit.27101

An, H. J., Rim, H. K., Jeong, H. J., Hong, S. H., Um, J. Y., and Kim, H. M. (2010). Hot water extracts of Chlorella vulgaris improve immune function in protein-deficient weanling mice and immune cells. *Immunopharmacol. Immunotoxicol.* 32, 585–592. doi: 10.3109/08923971003604778

Berger, A., Le Fourn, V., Masternak, J., Regamey, A., Bodenmann, I., Girod, P. A., et al. (2020). Overexpression of transcription factor Foxa1 and target genes remediate therapeutic protein production bottlenecks in Chinese hamster ovary cells. *Biotechnol.Bioeng.* 117, 1101–1116. doi: 10.1002/bit.27274

Biancarosa, I., Espe, M., Bruckner, C., Heesch, S., Liland, N., Waagbø, R., et al. (2017). Amino acid composition, protein content, and nitrogen-to-protein conversion factors of 21 seaweed species from Norwegian waters. *J. Appl. Phycol.* 29, 1001–1009. doi: 10.1007/s10811-016-0984-3

Brunner, D., Frank, J., Appl, H., Schöffl, H., Pfaller, W., and Gstraunthaler, G. (2010). The serum-free media interactive online database. *ALTEX-Altern. Anim. Exp.* 27, 53–62. doi: 10.14573/altex.2010.1.53

Chevallier, V., Andersen, M. R., and Malphettes, L. (2019). Oxidative stress-alleviating strategies to improve recombinant protein production in CHO cells. *Biotechnol. Bioeng.* 117, 1172–1186. doi: 10.1002/bit.27247

Diaz-Vivancos, P., de Simone, A., Kiddle, G., and Foyer, C. H. (2015). Glutathione–linking cell proliferation to oxidative stress. *Free Radic. Biol. Med.* 89, 1154–1164. doi: 10.1016/j.freeradbiomed.2015.09.023

Elshereef, A. A., Jochums, A., Lavrentieva, A., Stuckenberg, L., Scheper, T., and Solle, D. (2019). High cell density transient transfection of CHO cells for TGF-β1 expression. *Eng. Life Sci.* 19, 730–740. doi: 10.1002/elsc.201800174

Feldsine, P., Abeyta, C., and Andrews, W. H. (2002). AOAC International methods committee guidelines for validation of qualitative and quantitative food microbiological official methods of analysis. *J. AOAC Int.* 85, 1187–1200. doi: 10.1093/jaoac/85.5.1187

Gomes, M. E., Rodrigues, M. T., Domingues, R. M., and Reis, R. L. (2017). Tissue engineering and regenerative medicine: new trends and directions—a year in review. *Tissue Eng. Part B Rev.* 23, 211–224. doi: 10.1089/ten.teb.2017.0081

Gstraunthaler, G. (2003). Alternatives to the use of fetal bovine serum: serum-free cell culture. *ALTEX-Altern. Anim. Exp.* 20, 275–281.

Halter, M., Tona, A., Bhadriraju, K., Plant, A. L., and Elliott, J. T. (2007). Automated live cell imaging of green fluorescent protein degradation in individual fibroblasts. *Cytometry Part A* 71, 827–834. doi: 10.1002/cyto.a.20461

Huang, M., Bao, J., Hallström, B. M., Petranovic, D., and Nielsen, J. (2017). Efficient protein production by yeast requires global tuning of metabolism. *Nat. Commun.* 8, 1–12. doi: 10.1007/978-1-61779-770-5_1

Hunter, M., Yuan, P., Vavilala, D., and Fox, M. (2019). Optimization of protein expression in mammalian cells. *Curr. Protoc. Protein Sci.* 95:e77. doi: 10.1002/cpps.77

Imran, K. M., Rahman, N., Yoon, D., Jeon, M., Lee, B.-T., and Kim, Y.-S. (2017). Cryptotanshinone promotes commitment to the brown adipocyte lineage and mitochondrial biogenesis in C3H10T1/2 mesenchymal stem cells via AMPK and p38-MAPK signaling. *Biochim. Biophys. Acta Mol. Cell Biol. Lipids* 1862, 1110–1120. doi: 10.1016/j.bbalip.2017.08.001

Jung, E. H., Lee, J.-H., Kim, S. C., and Kim, Y. W. (2017). AMPK activation by liquiritigenin inhibited oxidative hepatic injury and mitochondrial dysfunction induced by nutrition deprivation as mediated with induction of farnesoid X receptor. *Eur. J. Nutr.* 56, 635–647. doi: 10.1007/s00394-015-1107-7

Kjeldahl, J. (1883). Neue methode zur bestimmung des stickstoffs in organischen körpern. *Z. Anal. Chem.* 22, 366–382. doi: 10.1007/bf01338151

Koh, H.-L., and Woo, S.-O. (2000). Chinese proprietary medicine in Singapore. *Drug Saf.* 23, 351–362. doi: 10.2165/00002018-200023050-00001

Krienitz, L., Huss, V. A., and Bock, C. (2015). Chlorella: 125 years of the green survivalist. *Trends Plant Sci.* 20, 67–69. doi: 10.1016/j.tplants.2014.11.005

Lakshmanan, M., Kok, Y. J., Lee, A. P., Kyriakopoulos, S., Lim, H. L., Teo, G., et al. (2019). Multi-omics profiling of CHO parental hosts reveals cell line-specific variations in bioprocessing traits. *Biotechnol. Bioeng.* 116, 2117–2129. doi: 10.1002/bit.27014

Liu, M., Zeng, X., Ma, C., Yi, H., Ali, Z., Mou, X., et al. (2017). Injectable hydrogels for cartilage and bone tissue engineering. *Bone Res.* 5, 1–20.

Lo, C.-A., Kays, I., Emran, F., Lin, T.-J., Cvetkovska, V., and Chen, B. E. (2015). Quantification of protein levels in single living cells. *Cell Rep.* 13, 2634–2644. doi: 10.1016/j.celrep.2015.11.048

Marigliani, B., Balottin, L. B. L., and Augusto, E. D. F. P. (2019). Adaptation of mammalian cells to chemically defined media. *Curr. Protoc. Toxicol.* 82:e88.

Négrier, C., Shapiro, A., Berntorp, E., Pabinger, I., Tarantino, M., Retzios, A., et al. (2008). Surgical evaluation of a recombinant factor VIII prepared using a plasma/albumin-free method: efficacy and safety of Advate in previously treated patients. *Thromb. Haemost.* 100, 217–223. doi: 10.1160/th08-02-0117

Ng, J. Y., Obuobi, S., Chua, M. L., Zhang, C., Hong, S., Kumar, Y., et al. (2020). Biomimicry of microbial polysaccharide hydrogels for tissue engineering and regenerative medicine–A review. *Carbohydr. Polym.* 241:116345. doi: 10.1016/j.carbpol.2020.116345

Ng, J. Y., Zhang, C., Hong, S., Gokhale, R., and Ee, P. L. R. (2019). *FR Patent No. BEP180943. E. P. Office*. Munich, Germany. doi: 10.1016/j.carbpol.2020.116345

Proud, C. G. (2007). Signalling to translation: how signal transduction pathways control the protein synthetic machinery. *Biochem. J.* 403, 217–234. doi: 10.1042/bj20070024

Ritacco, F. V., Wu, Y., and Khetan, A. (2018). Cell culture media for recombinant protein expression in Chinese hamster ovary (CHO) cells: history, key components, and optimization strategies. *Biotechnol. Prog.* 34, 1407–1426. doi: 10.1002/btpr.2706

Saad, S. M., Yusof, Y. A. M., and Ngah, W. Z. W. (2006). Comparison between locally produced Chlorella vulgaris and Chlorella vulgaris from Japan on proliferation and apoptosis of liver cancer cell line, HepG2. *Malays J. Biochem. Mol. Biol.* 13, 32–36. doi: 10.1002/j.1537-2197.1943.tb14728.x

Safafar, H., Van Wagenen, J., Møller, P., and Jacobsen, C. (2015). Carotenoids, phenolic compounds and tocopherols contribute to the antioxidative properties of some microalgae species grown on industrial wastewater. *Mar. Drugs* 13, 7339–7356. doi: 10.3390/md13127069

Saud, B., Malla, R., and Shrestha, K. (2019). A review on the effect of plant extract on mesenchymal stem cell proliferation and differentiation. *Stem Cells Int.* 2019, 7513404.

Schnellbaecher, A., Binder, D., Bellmaine, S., and Zimmer, A. (2019). Vitamins in cell culture media: stability and stabilization strategies. *Biotechnol. Bioeng.* 116, 1537–1555. doi: 10.1002/bit.26942

Song, S. H., Kim, I. H., and Nam, T. J. (2012). Effect of a hot water extract of Chlorella vulgaris on proliferation of IEC-6 cells. *Int. J. Mol. Med.* 29, 741–746.

Tripathi, N. K., and Shrivastava, A. (2019). Recent developments in bioprocessing of recombinant proteins: expression hosts and process development. *Front. Bioeng. Biotechnol.* 7:420. doi: 10.3389/fbioe.2019.00420

van der Valk, J., Bieback, K., Buta, C., Cochrane, B., Dirks, W. G., Fu, J., et al. (2018). Fetal bovine serum (FBS): past–present–future. *ALTEX Altern. Anim. Exp.* 35, 99–118. doi: 10.14573/altex.1705101

Walsh, G. (2014). Biopharmaceutical benchmarks 2014. *Nat. Biotechnol.* 32, 992–1000. doi: 10.1038/nbt.3040

Yusof, Y. A., Saad, S. M., Makpol, S., Shamaan, N. A., and Ngah, W. Z. (2010). Hot water extract of Chlorella vulgaris induced DNA damage and apoptosis. *Clinics* 65, 1371–1377. doi: 10.1590/s1807-59322010001200023

Zhang, X., Zhou, C., Zha, X., Xu, Z., Li, L., Liu, Y., et al. (2015). Apigenin promotes osteogenic differentiation of human mesenchymal stem cells through JNK and p38 MAPK pathways. *Mol. Cell. Biochem.* 407, 41–50. doi: 10.1007/s11010-015-2452-9

Conflict of Interest: CZ, SH, YK, and RG were employed by the company Roquette Asia Pacific Pte Ltd., Singapore.

The remaining authors declare that the research was conducted in the absence of any commercial or financial relationships that could be construed as a potential conflict of interest.

frontiers in Bioengineering and Biotechnology

ORIGINAL RESEARCH
published: 22 September 2020
doi: 10.3389/fbioe.2020.557572

Chlorella vulgaris and Its Phycosphere in Wastewater: Microalgae-Bacteria Interactions During Nutrient Removal

*Roland Wirth[1,2], Bernadett Pap[1], Tamás Böjti[2], Prateek Shetty[1], Gergely Lakatos[1], Zoltán Bagi[2], Kornél L. Kovács[2,3] and Gergely Maróti[1,4]**

[1] Institute of Plant Biology, Biological Research Centre, Szeged, Hungary, [2] Department of Biotechnology, University of Szeged, Szeged, Hungary, [3] Department of Oral Biology and Experimental Dental Research, Faculty of Dentistry, University of Szeged, Szeged, Hungary, [4] Faculty of Water Sciences, National University of Public Service, Baja, Hungary

OPEN ACCESS

Edited by:
Raul Muñoz,
University of Valladolid, Spain

Reviewed by:
Peter J. Lammers,
Arizona State University, United States
José Carlos Pires,
University of Porto, Portugal

***Correspondence:**
Gergely Maróti
maroti.gergely@brc.hu;
maroti.gergely@brc.mta.hu

Specialty section:
This article was submitted to Bioprocess Engineering, a section of the journal Frontiers in Bioengineering and Biotechnology

Received: 30 April 2020
Accepted: 28 August 2020
Published: 22 September 2020

Citation:
Wirth R, Pap B, Böjti T, Shetty P, Lakatos G, Bagi Z, Kovács KL and Maróti G (2020) Chlorella vulgaris and Its Phycosphere in Wastewater: Microalgae-Bacteria Interactions During Nutrient Removal. Front. Bioeng. Biotechnol. 8:557572. doi: 10.3389/fbioe.2020.557572

Microalgae-based bioenergy production is a promising field with regard to the wide variety of algal species and metabolic potential. The use of liquid wastes as nutrient clearly improves the sustainability of microalgal biofuel production. Microalgae and bacteria have an ecological inter-kingdom relationship. This microenvironment called phycosphere has a major role in the ecosystem productivity and can be utilized both in bioremediation and biomass production. However, knowledge on the effects of indigenous bacteria on microalgal growth and the characteristics of bacterial communities associated with microalgae are limited. In this study municipal, industrial and agricultural liquid waste derivatives were used as cultivation media. *Chlorella vulgaris* green microalgae and its bacterial partners efficiently metabolized the carbon, nitrogen and phosphorous content available in these wastes. The read-based metagenomics approach revealed a diverse microbial composition at the start point of cultivations in the different types of liquid wastes. The relative abundance of the observed taxa significantly changed over the cultivation period. The genome-centric reconstruction of phycospheric bacteria further explained the observed correlations between the taxonomic composition and biomass yield of the various waste-based biodegradation systems. Functional profile investigation of the reconstructed microbes revealed a variety of relevant biological processes like organic acid oxidation and vitamin B synthesis. Thus, liquid wastes were shown to serve as valuable resources of nutrients as well as of growth promoting bacteria enabling increased microalgal biomass production.

Keywords: wastewater, green algae, phycosphere, algal-bacterial interactions, metagenomics

Abbreviations: BMP, biochemical methane potential (test); BOD, biological oxygene demand (test); C/N, carbon to nitrogen ratio; CMS, chicken manure supernatant (medium); DM and oDM: dry mass and organic dry mass; FE, anaerobe fermentation effluent (medium); GHG, Green house gas (emission); MAGs, metagenome assembled genomes; MCR, module completion ratio; MW, municipal wastewater (medium); PCA, principal component analysis; PGPB, plant growth promoting bacteria; TAP, tris-acetate-phosphate (medium); TC and TN, total carbon and total nitrogen; VOAs, volatile organic acids.

INTRODUCTION

Biofuels derived from microalgae are alternative second-generation biofuels having no significant impact on agriculture (Klassen et al., 2016; Rizwan et al., 2018; Wirth et al., 2018). Microalgae have a higher biomass productivity than that of terrestrial crops and can be cultivated on marginal land area all year round. Additionally, the use of microalgae have the potential to directly reduce greenhouse gas emissions (GHG) through the replacement of fossil fuels and by photosynthetic CO_2 fixation in their biomass (Lam and Lee, 2012; Yen et al., 2013). Water and nutrients are identified as important limiting resources for microalgae production. The nutrients for microalgae cultivation are readily available in various types of wastewater. Using photoheterotrophic microalgae in biological wastewater treatment represents a dual exploitation of green algae, removing dissolved organic and inorganic pollutants is combined with the production of sustainable bioresource for biofuel production (Mujtaba et al., 2015; Guldhe et al., 2017; Cheah et al., 2018; Vo Hoang Nhat et al., 2018; Li et al., 2019; Shetty et al., 2019). Microalgae have an evolutionary determined ecological relationship with bacteria in natural aquatic environments representing an important interkingdom association (Fuentes et al., 2016). These interactions are strongly influenced by nutrient cycling which regulates the productivity and stability of natural aquatic food webs. The intimate relationship between microalgae and bacteria represents the phycosphere, a key microenvironment ultimately mediating the ecosystem productivity (Cho et al., 2015; Seymour et al., 2017). The exchange of micro- and macronutrients defines the relationship of the interactive partners, which are influenced by a number of key aspects. Firstly, the pH level and the available nutrients determine the surrounding chemical environment, which has a central role in chemotaxis, the motility of bacteria, which enables microbial colonization (Medipally et al., 2015). Secondly, the bacterial communities in the specific ecosystem have important roles in shaping the phycosphere. The most frequently observed bacteria in wastewaters are affiliated with the phyla of the *Bacteroidetes* and *Alpha-*, *Beta-*, and *Gammaproteobacteria* (with Plant Growth Promoting Bacteria (PGPB) among them) (Guo and Tong, 2014; Kouzuma and Watanabe, 2015; Calatrava et al., 2018). Thirdly, the available microalgae and bacteria synergistically affect each other's physiology and metabolism. Microalgae produce O_2 through photosynthesis for consumption by the actively respiring aerobic bacteria, while bacteria release CO_2, which improves the photosynthetic efficiency of green microalgae (Mouget et al., 1995). Another important interkingdom interaction is observed between vitamin-synthetizing bacteria and vitamin auxotrophic microalgae. Most microalgae are auxotrophic for vitamin B derivatives, which are essential for growth and provided by bacteria in exchange for organic carbon (Croft et al., 2005, 2006). Fourthly, the competition for available nutrients, algicidal activities or related defense mechanisms of microalgae are important factors in phycosphere development. Similarly to other natural symbiotic settings, there is only a thin line separating mutualistic and antagonistic associations between microalgae and bacteria (Santos and Reis, 2014; Ramanan et al., 2016).

There are three main sources of wastewater intensively studied in alternative microalgal cultivation; municipal, industrial and agricultural wastewater (Chiu et al., 2015; Guldhe et al., 2017). Utilization of natural microalgal-bacterial communities is a highly promising recycle solution for liquid wastes. This inexpensive and environment-friendly system can contribute to the sustainable management of water resources (Liu J. et al., 2017; Qi et al., 2018). The green microalgae *Chlorella vulgaris* is the most investigated eukaryotic algae species in wastewater treatment (Chiu et al., 2015; Otondo et al., 2018; Shetty et al., 2019). *C. vulgaris* is a common eukaryotic microalgae species found in various natural and engineered freshwater and soil habitats. *C. vulgaris* has a relatively small cell size, thin cell wall, fast growth rate and short reproduction time. This alga is a robust strain that can easily accommodate to changing physico-chemical conditions. Under nutrient limitation and stress *C. vulgaris* often accumulate high amount of lipids as store materials. These features make this microalgae suitable to cultivate in wastewater, thereby using it for combined wastewater treatment and bioenergy generation (Mussgnug et al., 2010; Collet et al., 2011; Mahdy et al., 2014; Klassen et al., 2016, 2017). It was observed that high nitrogen and phosphorus removal efficiency can be reached with *Chlorella* species (Chiu et al., 2015; Guldhe et al., 2017; Chen et al., 2018).

A number of studies examined municipal wastewater treatment efficiency using *Chlorella*-bacteria mixed cultures (Mujtaba et al., 2015; Otondo et al., 2018). More efficient nutrient removal was observed from settled domestic wastewater compared to the commonly used activated sewage process, which indicated the potential of microalgae in the activated sludge process potentially as a secondary step for further nutrient reduction and concomitant biomass production (Otondo et al., 2018). Besides, CO_2 originated from the degradation of carbonaceous matter in an activated sludge process is released freely into the atmosphere, thus promoting GHG accumulation. In contrast, microalgae can assimilate CO_2 into cellular components such as lipid and carbohydrate, thus achieving pollutant reduction in a more environmental-friendly way (Santos and Reis, 2014; Gonçalves et al., 2017).

In the bioenergy industry biogas is used as a source for generation of heat and/or electricity (Mao et al., 2015; Ullah Khan et al., 2017). Besides biogas, digestate is another important byproduct of anaerobic degradation of organic wastes. Digestate processing is a major bottleneck in the development of the biogas industry. Digestate can be separated into solid (10–20%) and liquid (80–90%) fractions (Xia and Murphy, 2016). Solid digestate is easily stored and transported, and can be used as an agricultural biofertilizer. However, liquid phase processing is more difficult mostly due to its relatively high ammonia content (Uggetti et al., 2014). Digestate is continuously produced, while land application is dependent on the growth stage of the crop and the period of the year. Therefore, digestate needs to be stored, which can increase GHG emission and the general costs as well (Xia and Murphy, 2016; Zhu et al., 2016). Previous studies reported that *Chlorella* species can be applied to treat liquid

digestate (Collet et al., 2011; Skorupskaite et al., 2015; Uggetti et al., 2016). The performance of treatment is dependent on the algae access to carbon, nitrogen and phosphorous as well as on the availability of photosynthetically active light, which indicates a mixotrophic algae growth (Skorupskaite et al., 2015; Zhu et al., 2016).

The rapid growth of the poultry industry in agriculture has raised the need for poultry waste treatment (Sakar et al., 2009). The runoff coming from the chicken farms is highly harmful for the environment through altering the nitrogen and phosphorus balance (Liu Q. et al., 2017). One possible treatment of chicken manure is the anaerobic degradation (Anjum et al., 2017). Chicken manure can be used in small quantities in biogas producing anaerobic fermenters. High dosage of chicken manure cause ammonia accumulation and process failure (Nie et al., 2015; Sun et al., 2016). Water extraction is one possible solution for this problem (Böjti et al., 2017). The supernatant liquid waste still contains high amount of nitrogen and phosphorus, thereby represents suitable medium for microalgal biomass production (Han et al., 2017).

From the biotechnological process point of view the goal is to strengthen the mutually beneficial algal-bacterial interactions to achieve higher biomass growth (beside the bioremediation of liquid wastes). The present study examined and compared different types of wastewater recycling processes using microalgae and their specific bacterial partners. This investigation mainly focused on the interacting bacterial members in specific liquid wastes. The ubiquitous relationship between eukaryotic microalgae and bacteria should be taken into account when designing innovations in microalgal biotechnology (Cooper and Smith, 2015; Gonçalves et al., 2017; Quijano et al., 2017; Lian et al., 2018).

MATERIALS AND METHODS

Algal-Bacterial Biomass Cultivation on Different Types of Wastewaters

The *Chlorella vulgaris* MACC-360 microalgae was obtained from the Mosonmagyaróvár Algal Culture Collection (MACC) of Hungary. *C. vulgaris* was maintained and cultivated on TAP (Tris-acetate-phosphate) plates, then TAP liquid medium (500 mL) was used for the pre-growth of microalgal biomass. The TAP plates and liquid media were incubated at 50 μmol m^{-2} s^{-1} light intensity at 25°C for 4 days (OD_{750}: 4.00 ± 0.20). The microalgal stock solution was equally distributed in 17–17 mL portions into 50 mL Falcon tubes with a final optical density (OD_{750}) of 0.70 ± 0.10. Microalgal biomass was separated by centrifugation from the medium and used for inoculation (microalgal dry mass content: ∼100 mg/L). TAP medium was an internal control during the experiment. Different wastewater types were prepared as follows:

Chicken Manure Supernatant (CMS)

Chicken manure (CM) was collected from a commercial broiler poultry farm (Hungerit Corp.) located at Csengele, Hungary. The free-range poultry houses use wheat straw bedding. Water extraction comprised of soaking 2,5 g; 5 g; 10 g and 20 g CM in 100 mL distilled water (v/v %: 2,5; 5; 10 and 20) at room temperature followed by separation of the liquid (CMS: chicken manure supernatant) and solid phases by centrifugation (10,000 rpm for 8 min).

Anaerobic Fermentation Effluent (FE)

Inoculum sludge was obtained from an operating biogas plant (Zöldforrás Ltd) using pig manure and maize silage mixture as feedstock. The liquid and solid phases were separated by centrifugation (10,000 rpm for 8 min). Distilled water was used to dilute FE (2, 5, 10 and 20 mL effluent in 100 mL distilled water, respectively), to the final concentrations of 2; 5; 10 and 20% (v/v %), respectively.

Municipal Wastewater (MW)

The municipal wastewater was originated from the Municipal Wastewater Plant of Szeged, Hungary and sampled from the secondary settling tank. The liquid phase was separated from the solid phase by centrifugation (10,000 rpm 8 min). Final concentrations were set at 20 and 50 v/v % using distilled water. Non-diluted (100 v/v %) MW was also used for cultivation.

Cultivation was performed in 250 mL serum bottles (Wheaton glass serum bottle, WH223950) with liquid volume of 200 mL and stirred on a magnetic stirrer tray. Cultivation time was 4 days. Bottles were sealed with paper plugs. Different media were incubated at 50 μmol m^{-2} s^{-1} light intensity at 25°C. The OD_{750} values of the different wastewater media were summarized in **Supplementary Information**.

Determination of Cultivation Parameters

DM/oDM Measurements

The dry matter (DM) content was quantified by drying the biomass at 105°C overnight and weighing the residue. Further heating of this residue at 550°C for 1 h provided the organic dry mass (oDM) content.

C/N Ratio

To determine C/N (both liquid and biomass), an Elementar Analyzer Vario MAX CN (Elementar Group, Hanau, Germany) was employed. The approach is based on the principle of catalytic tube combustion under O_2 supply at high temperatures (combustion temperature: 900°C, post-combustion temperature: 900°C, reduction temperature: 830°C, column temperature: 250°C). The desired components were separated from each other using specific adsorption columns (containing Sicapent (Merck, Billerica, MA, United States), in C/N mode) and were determined in succession with a thermal conductivity detector. Helium served as flushing and carrier gas.

NH_4^+-N

For the determination of NH_4^+ ion content, the Merck Spectroquant Ammonium test (1.00683.0001) (Merck, Billerica, MA, United States) was used.

Total Phosphate Measurement

Total phosphate content of the different types of wastewater were measured by the standard 4500-PE ascorbic acid, molybdenum blue method (APHA-AWWA-WPCF, 1998).

VOAs (Volatile Organic Acids)

The VOAs measurement process was carried out using a Pronova FOS/TAC 2000 Version 812-09.2008 automatic titrator (Pronova, Berlin, Germany).

Acetate Concentration

The samples were centrifuged (13,000 rpm for 10 min) and the supernatant was filtered through polyethersulfone (PES) centrifugal filter (PES 516-0228, VWR) at 16,000 g for 20 min. The concentrations of volatile organic acids were measured with HPLC (Hitachi LaChrome Elite) equipped with refractive index detector L2490. The separation was performed on an ICSep ICE-COREGEL—64H column. The temperature of the column and detector was 50 and 41°C, respectively. 0.01 M H_2SO_4 (0.8 mL min^{-1}) was used as eluent. Acetate, propionate, and butyrate were determined in a detection range of 0.01–10 g L^{-1}. Propionate and butyrate were present in traces relative to acetate and therefore these are not reported in the results section.

BOD (Biological Oxygen Demand) Test

To measure the biochemical oxygen demand of the wastewater samples a 5-day BOD test was applied (OxiTop OC 110, Wissenschaftlich-Technische Werkstätten GmbH). In the parallel 500 mL BOD-sample bottles 43 mL of wastewater solution were placed. The results were read after 5 days in mg O_2/L.

BMP (Biochemical Methane Potential) Test

Experiments were carried out in 160 mL reactor vessels (Wheaton glass serum bottle, Z114014 Aldrich) containing 60 mL liquid phase at mesophilic temperature (37 ± 0.50°C). All fermentations were done in triplicates. The inoculum sludge was filtered to remove particles larger than 1 mm and was used according to the VDI 4630 protocol (Vereins Deutscher Ingenieure 4630, 2006). Each batch fermentation experiment lasted for 30 days in triplicates.

Gas Chromatographic Analysis

The CH_4 content was determined with an Agilent 6890N GC (Agilent Technologies) equipped with an HP Molesive 5 Å (30 m × 0.53 mm × 25 μm) column and a TCD detector. The temperature of the injector was 150°C and split mode 0.2:1 was applied. The column temperature was maintained at 60°C. The carrier gas was Linde HQ argon 5.0 with the flow rate set at 16.80 mL/min. The temperature of TCD detectore was set to 150°C.

In this study data originated from the most effective cultivations under illumination are summarized and highlighted (MW: 100 v/v %, FE: 10 v/v % and CMS: 5 v/v %). All data collected under the various dilution parameters are shown in **Supplementary Information**.

Total DNA Isolation for Metagenomics

The composition of the microbial community was investigated two times during the experimental period from each wastewater type and control (TAP), i.e., at the starting point (inoculation) and at the end of cultivation. For total community DNA isolation 2 mL of samples were used from each cultivation media type. DNA extraction and quality estimation were performed according Wirth et al. (2019).

Shotgun Sequencing

The Ion Torrent PGM™ platform was used for shotgun sequencing, the manufacturer's recommendations were followed (Life Technologies, United States). Sample preparation, quantification and barcoding were described previously (Wirth et al., 2019). Sequencing was performed with Ion PGM 200 Sequencing kit (4474004) on Ion Torrent PGM 316 chip. The characteristic fragment parameters are summarized in **Supplementary Table 1**. Raw sequences are available on NCBI Sequence Read Archive (SRA) under the submission number: PRJNA625695.

Raw Sequence Filtering

Galaxy Europe server was employed to pre-process the raw sequences (i.e., sequence filtering, mapping, quality checking) (Afgan et al., 2016). Low-quality reads were filtered by Prinseq (Schmieder and Edwards, 2011) (min. length: 60; min. score: 15; quality score threshold to trim positions: 20; sliding window used to calculated quality score:1). Filtered sequences were checked with FastQC (**Supplementary Table 1**).

Read-Based Metagenome Data Processing and Statistical Analysis

After filtering and checking the passed sequences were further analized by Kaiju applying default greedy run mode on Progenomes2 database (Menzel et al., 2016; Mende et al., 2017). MEGAN6 was used to investigate microbial communities and export data for statistical calculation (Huson et al., 2016). Statistical Analysis of Metagenomic Profiles (STAMP) was used to calculate principal component analysis (PCA) employing ANOVA statistical test (Parks and Beiko, 2010). The distribution of abundant microbial classes between cultivation media were presented with Circos (Krzywinski et al., 2009).

Metagenome Co-assembly, Gene Calling and Binning

The filtered sequences produced by Prinseq were co-assembled with Megahit (Li et al., 2015) (min. contig length: 2000; min k-mer size: 21; max k-mer size: 141). Bowtie 2 was equipped to mapped back the original sequences to the contigs (Langmead and Salzberg, 2012). Then Anvi'o V5 was used following the "metagenomics" workflow (Eren et al., 2015). Briefly, during contig database generation GC content, k-mer frequencies were computed, open reading frames were identified by Prodigal (Hyatt et al., 2010) and Hidden Markov Modell (HMM) of single-copy genes were aligned by HMMER on each contig (Finn et al., 2011; Campbell et al., 2013; Rinke et al., 2013; Simão et al., 2015). InterProScan v5.31-70 was used on Pfam and Kaiju on NCBInr database for the functional and taxonomic annotation of contigs (Finn et al., 2014, 2017; Jones et al., 2014; Menzel et al., 2016). The taxonomic and functional data were imported into the contig database. BAM files made by Bowtie2 were used to profile contig database, in this way sample-specific information was obtained about the contigs (i.e., mean coverage of contigs) (Langmead and Salzberg, 2012). Three automated binning programs, namely CONCOCT, METABAT2 and MAXBIN2 were employed to

reconstruct microbial genomes from the contigs (Alneberg et al., 2013; Kang et al., 2015; Wu et al., 2015). The Anvi'o human-guided binning option was used to refine MAGs Anvi'o interactive interface was employed to visualize and summarize the data. Binning statistics is summarized in **Supplementary Table 1**. Figure finalization was made by open-source vector graphics editor Gimp 2.10.8[1]. Prokka was employed to translate and map protein sequences (create protein FASTA file of the translated protein coding sequences) (Seemann, 2014). For the calculation of module completion ratio (MCR) MAPLE 2.3.2 (Metabolic And Physiological potentiaL Evaluator) was used (Arai et al., 2018). This automatic system is mapping genes on an individual genome and calculating the MCR in each functional module defined by Kyoto Encyclopedia of Genes and Genomes (KEGG) (Kanehisa and Guto, 2000) (**Supplementary Table 2**).

RESULTS

Bioremediation Efficiency and Biochemical Methane Potential (BMP) of the Cultivated Algal-Bacterial Biomass

The bioremediation efficiency of *Chlorella vulgaris* microalgae and its phycosphere was characterized through the assessment of carbon, nitrogen, phosphate and BOD removal capability of the algal-bacterial biomass (**Figure 1**). The performance of microalgal-bacterial dry biomass was monitored in three liquid waste types i.e., municipal wastewater (MW), fermentation effluent (FE) and chicken manure supernatant (CMS) over 4 days. The light conditions in the cultivating media are of key importance for microalgal biomass generation. The applied wastewater types are typically dark liquids; therefore, different dilutions with distilled water were prepared in order to increase light penetration to the cultures. Only the experimental data of the most effective dilutions (non-diluted MW, 10 v/v % FE and 5 v/v % CMS) are shown and discussed in the main text of the article (efficiency was defined by the obtained yield of microalgal biomass). However, the nutrient composition of all dilutions for each liquid waste were measured and detailed in **Supplementary Information**. TAP medium was used as control during the experiments. Significant nutrient removal was observed in all three types of investigated wastewater indicating an active metabolism of the *C. vulgaris* microalgae and its bacterial partners. However, due to the specific features of the various liquid wastes serving as growth media the algal-bacterial nutrient removal and bioremediation capability was strongly varying. There is a clear correlation between the available nutrients (phosphate, nitrogen and acetate) and the algal-bacterial biomass yield.

The non-diluted municipal wastewater (MW) originated from the second settling tank of a wastewater plant contained the lowest amount of nutrients (acetate and nitrogen) and had the lowest optical density (OD_{750}: 0.02) compared to the 10 v/v % fermentation effluent (FE) originated from a production scale biogas digester (OD_{750}: 0.72) and to the 5 v/v % chicken manure supernatant (CMS: OD_{750}: 0.25) (**Supplementary Information**). The nutrient removal rate of phosphate and total nitrogen (mostly ammonium) was also shown to be dependent on the light penetration. The highest phosphate removal rate was observed in CMS (0.20 mM day^{-1}), while only 0.02 mM day^{-1} and 0.01 mM day^{-1} phosphate uptake were monitored in MW and in FE, respectively (**Figure 1C**). The monitored phosphate consumption in CMS were comparable to that of measured in TAP medium (0.20 mM day^{-1}). Moreover, in all tested media the microalgal-bacterial consortia removed nitrogen more effectively than phosphate. Total nitrogen removal rate was 0.32 mM day^{-1} in MW, 0.78 mM day^{-1} in FE and 2.46 mM day^{-1} in CMS, respectively (**Figure 1E**). Similar values were observed for the ammonium content (MW: 0.31 mM day^{-1}, FE: 0.77 mM day^{-1}) and CMS: 2.44 mM day^{-1}) (**Figure 1D**). Significant organic carbon utilization was observed in all types of liquid wastes. The observed total nitrogen (and ammonium) removal rate were higher in CMS compared to TAP medium (CMS: 2.46 mM day^{-1} and in TAP: 1.31 mM day^{-1}, respectively). Carbon removal rate was around 82% in all liquid wastes (CMS: 2.20 mM day^{-1}, FE: 1.51 mM day^{-1}, MW: 0.38 mM day^{-1}) (**Figure 1E**). Likewise, considerable decrease in total VOAs (and acetic acid) was monitored through the experiment (FE: 2 mM day^{-1}, MW and CMS: 3 and 108 mg L^{-1} day^{-1}) (**Figure 1F**). As expected, the high C utilization capability of *C. vulgaris* and its phycosphere is in strong correlation with the BOD consumption (CMS: 78%, FE: 77% and MW: 88%) (**Figure 1B**). During cultivation pH increase was observed (**Figure 1A**). The increased pH correlated with the degradation of the organic substrates. The dry mass of the co-cultivated *C. vulgaris* biomass was the highest in CMS with 0.70–0.90 g DM L^{-1} day^{-1}, while in FE it was 0.30–0.60 g DM L^{-1} day^{-1}. The lowest microalgal-bacterial biomass was measured in MW with a value of 0.10–0.20 g DM L^{-1} day^{-1}. The bacterial biomass was only ∼10% of the total biomass in MW, while these values were ∼38 and ∼27% in FE and CMS, respectively (**Supplementary Information** and **Figure 1G**). Highest biomass production was observed in CMS followed by TAP, FE and MW (**Figure 1G**). The cultivated total algal-bacterial biomass carbon to nitrogen ratio in MW, FE and CMS was 9:1, 7:1 and 6:1, respectively. The higher C/N ratio of MW compared to the TAP control (5:1) might indicate nitrogen limitation in MW. The biochemical methane potential (BMP) of the cultivated mixed biomasses show negligible differences compared to the TAP control (TAP: 249 ± 15 CH_4 mL_N g oDM^{-1}; MW:236 ± 14 CH_4 mL_N g oDM^{-1}; FE: 238 ± 14 CH_4 mL_N g oDM^{-1} and CMS: 241 ± 15 CH_4 mL_N g oDM^{-1}) (**Figure 1H**).

Read-Based Metagenomics Analysis of the Phycosphere

An average of 271,721 sequence reads were generated for each sample, with a mean read length of 231 nucleotides using an Ion Torrent PGM sequencing platform. Sequence reads were quality filtered by Prinseq, this resulted in an average of 266,119 reads with a mean length of 232 nucleotides (**Supplementary Table 1**). The sequences were analyzed and bacterial partners of *C. vulgaris* were identified using the Kaiju software on

[1]https://www.gimp.org/

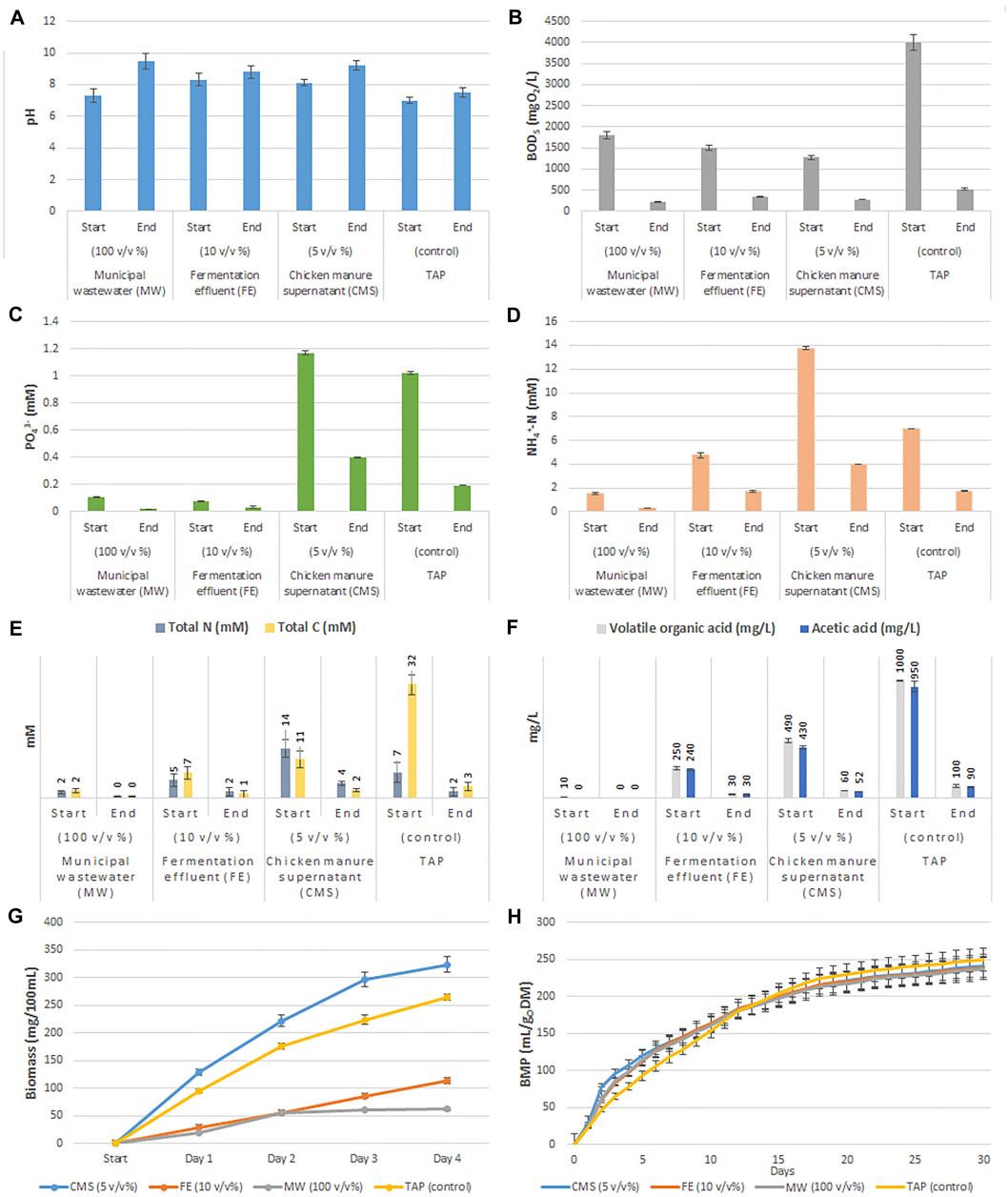

FIGURE 1 | Summary of microalgal-bacterial bioremediation and cultivation efficiency on different types of wastewater. **(A)** Results of pH measurements. **(B)** Results of biological oxygen demand calculations. **(C)** Total phosphate measurements. **(D)** Ammonium ion measurement data. **(E)** Total carbon and nitrogen contents. **(F)** Volatile organic acid (VOAs) and acetic acid concentrations. **(G)** Biomass growth dynamics over time (days). **(H)** Cumulative biological methane potential of cultivated biomasses.

Progenomes2 database. The comparison of the prokaryotic microbes using PCA showed significant community shifts between the different wastewater samples over cultivation time (**Figure 2A**). At the start point (T0) the CMS, FE and MW liquid wastes have diverse microbial community (**Figure 2B**). The most abundant classes in CMS were *Actinobacteria* (55%), *Bacilli* (27%) and *Gammaproteobacteria* (7%), while in FE *Clostridia* (33%), *Bacteroidia* (27%), *Bacilli* (8%), and in MW *Beta-* and *Gammaproteobacteria* (23–23%) as well as *Actinobacteria* (13%) dominated. The relative abundance of the observed taxa significantly changed over the cultivation period. The *Alpha-*, *Beta-* and *Gammaproteobacteria* and *Bacilli* classes dominated the prokaryotic community at the end point of the experiments (CMS: *Gammaproteobacteria* 74%, *Alphaproteobacteria* 11%, *Betaproteobacteria* 7%; FE: *Alphaproteobacteria* 60%, *Gammaproteobacteria* 17%, *Betaproteobacteria* 16%; MW: *Alphaproteobacteria* 52%, *Bacilli* 40%, *Gammaproteobacteria* 4%, respectively). The control TAP media showed the least microbial

shift between the start and the end of the cultivation, where representatives of the *Gammaproteobacteria* class (T0: 100%; end: 95%, respectively), were the most abundant (**Figures 2A,B**).

Genome-Centric Analysis of the Phycosphere

Metagenome assembly was carried out by Megahit. A total of 6,148 contigs with a minimum length of 2,000 nucleotides were generated. The contigs were then binned together using MAXBIN2, METABAT2 and CONCOCT automated binning programs. The generated bins were further refined by human guided binning process based on automated binning results with Anvi'o. The 7 bins accounted for a total of 20,038,573 nucleotides. Bins were checked for completion and contamination using CheckM.

Seven metagenome assembled genomes (MAGs) were generated by Anvi'o (**Figure 3**). Bin 1 contained the *C. vulgaris* genome fragments. Beside Bin 1 six bacterial MAGs were detected. From these six MAGs five belonged to partly unknown taxa, namely *Pseudomonas*, *Exiguobacterium*, *Acinetobacter*, *Enterobacteriaceae* and *Bacteroidetes*. The *unknown Pseudomonas* (Bin 2) showed a high degree of genome completeness (95%). This MAG included ribosomal maturation proteins (**Supplementary Table 2**), however, 16S rRNA sequences were not found by HMMER (Bowers et al., 2017). One species level bin (Bin 6) belonged to the *Bacteroidetes bacterium 4484_276*. By mapping back the original reads to the *unknown Pseudomonas* (Bin 2) and *unknown Acinetobacter* (Bin 3) bins it was observed, that these microbes were detected in all cultivation media at each time point. The *unknown Enterobacteriaceae* (Bin 5) was found in all liquid waste cultivations (i.e., MW, FE, CMS), while the *unknown Exiguobacterium* (Bin 4) occurred only in MW. The low quality *Bacteroidetes bacterium 4484_276* (Bin 6) and the *unknown Bacteroidetes* (Bin 7) bins were detected only in FE.

To predict protein pathways, the translated protein coding sequences created by Prokka were further analyzed to calculate module completion ratio (MCR) by MAPLE 2.3.2 using the Kegg database (Kanehisa and Guto, 2000; Seemann, 2014; Arai et al., 2018). The *unknown Pseudomonas* (Bin 2) bin genom harbored complete pathways of gluconeogenesis, Entner-Doudoroff pathway, pyruvate-oxidation, beta-oxidation, sulphate reduction, pentose phosphate pathway, fatty acid, amino acid, cofactor and vitamin metabolism (**Supplementary Table 2**). The MCR of vitamin B biosynthesis was also found at high percentage in the *unknown Pseudomonas* MAG. Among vitamin B variants, the complete biotin (B_7) biosynthesis pathway was detected (100%) in Bin 2, while the completeness of cobalamin (B_{12}) and thiamin (B_1) biosynthesis pathways were 86% and 60%, respectively. Between the MAGs showing low degree of genome completeness the *unknown Acinetobacter* (Bin 3) and the *unknown Enterobacteriaceae* bin (Bin 5) had complete MCRs for acetate kinase pathway, while the *unknown Exiguobacterium* (Bin 4) and *Bacteroidetes bacterium 4484_276* (bin 6) bins had complete phospho-ribose-diphosphate pathway. The *unknown Bacteroidetes* (Bin 7) had the lowest genome completeness among the detected MAGs, therefore complete pathways could not be detected in this bin (**Supplementary Table 2**).

DISCUSSION

Microalgae and their phycosphere represent powerful natural associations, which can be exploited in bioremediation and biofuel production (Gonçalves et al., 2017; Guldhe et al., 2017). Using liquid wastes for alternative algae cultivation has emerged as a potential cost effective strategy to make microalgae biotechnology more sustainable and economically feasible. It is essential to understand the nature of microalgal-bacterial relationships in order to develop combined bioremediation and biofuel production systems. Therefore, the main objective in this study was the assessment of nutrient removal and microalgal-bacterial biomass production efficiency using different types of wastewater sources (i.e., chicken manure supernatant, fermentation effluent and municipal wastewater). Furthermore, bioremediation and production efficiency data were supported by applying read-based and novel genome-centric approach for the identification of the phycosphere components and their functional profiles.

Chlorella Vulgaris and Its Phycosphere Is Effective in Bioremediation of Liquid Wastes

THE following major bioremediation process parameters were measured during the experiments: pH, biomass yield, carbon, nitrogen and phosphorous content. The biomass' carbon/nitrogen ratio and biochemical methane potential were also characterized. The experiments were designed for 4 days, since previous literature data indicated that *C. vulgaris* entered stationary growth phase by the 4th–5th day, no significant biomass production could be observed thereafter (Mujtaba et al., 2015, 2017; Otondo et al., 2018; Qi et al., 2018) (**Supplementary Information**).

The total carbon (TC), total nitrogen (TN) and phosphate (PO_4^{3-}) concentrations of the applied liquid wastes substantially varied (**Figures 1E,C** and **Supplementary Information**). The major nutrients required for microalgal growth are nitrogen and phosphorus incorporated to the cells via active transport. Ammonium is among the most common forms of nitrogen that can easily be utilized by most microalgal species (Gonçalves et al., 2017). Thus, liquid wastes represent a cheap source of nitrogen for microalgal cultivation (Razzak et al., 2013). Previously it was observed, that the optimal ammonium concentration for microalgal cultivation was around 8–10 mM (Uggetti et al., 2014; Chen et al., 2018), higher concentration might inhibit microalgal growth (Källqvist and Svenson, 2003). Another important element required for microalgae growth and metabolism is phosphorus primarily occurring in the form of phosphate (PO_4^{3-}) in wastewater. Phosphorus is an essential ingredient of ATP and nucleic acids in the cells. Phosphate availability has a large impact on microalgal photosynthesis as well (Razzak et al., 2013). Optimal phosphate concentration was found around ∼1 mM (Chiu et al., 2015). The concentration of ammonium

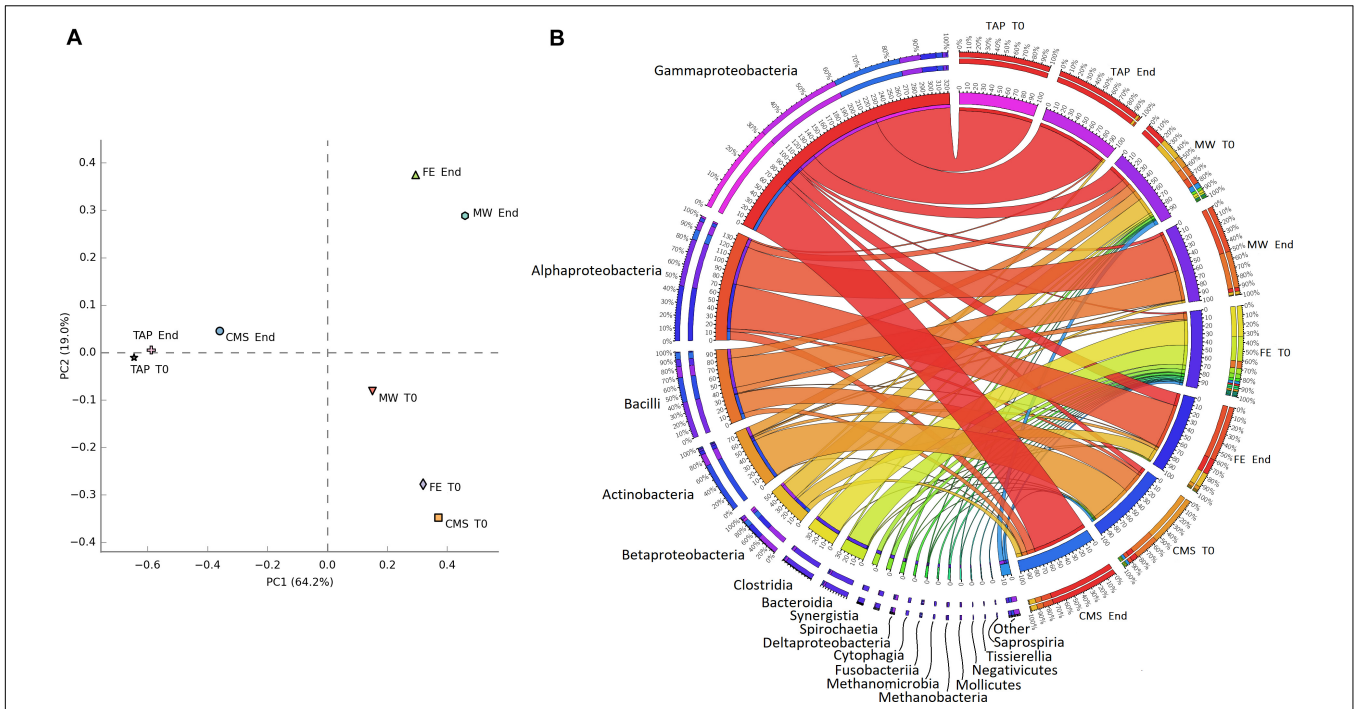

FIGURE 2 | (A) PCA of prokaryotic communities in various cultivation media. The variation represented by the first axis (PC1, 64% of overall variation) and the second axis (PC2, 19% of overall variation) indicating diverse phylogenetic structures. **(B)** Relative distribution of abundant microbial classes in different media (left side: classes, right side: cultivation media).

and phosphate were relatively low in the applied non-diluted MW (NH_4^+-N: 1.6 mM; PO_4^{3-}: 0.1 mM) (**Figures 1C,D** and **Supplementary Information**). In the diluted FE (10 v/v%) the amount phosphate was low (PO_4^{3-}: 0.1 mM), while the ammonium content was approximately half of the optimum (NH_4^+-N: 4.8 mM). The diluted CMS (5 v/v%) contained high amount of both nutrients (NH_4^+-N: 13.7 mM; PO_4^{3-}: 1.2 mM) (**Figures 1C,D** and **Supplementary Information**). The ammonium and phosphate removal rates were also high in CMS (NH_4^+-N: 2,44 mM day^{-1}; PO_4^{3-}: 0.20 mM day^{-1}), while lower in FE (NH_4^+-N: 0.77 mM day^{-1}; PO_4^{3-}: 0.01 mM day^{-1}) and MW (NH_4^+-N: 0.31 mM day^{-1}; PO_4^{3-}: 0.02 mM day^{-1}). The experimental data indicated that mostly *C. vulgaris* was responsible for the removal of ammonium and phosphate, and the biomass yield strongly correlated with the removal efficiencies. The results also implied to the dependency of microalgae growth on the available nitrogen sources, which is in good correlation with previous studies (Chiu et al., 2015). The observed low nitrogen content of the biomass generated on MW compared to the TAP control might be explained by the nitrogen limitation (Klassen et al., 2015; Seger et al., 2019).

Microalgae can fix CO_2 derived from flue gas emission through photosynthesis (Sayre, 2010; Pires et al., 2012). Additionally, microalgae are able to uptake soluble carbonates as a source of CO_2 (Thomas et al., 2016; Sydney et al., 2019). This uptake depends on the environmental pH. At low pH values the CO_2 uptake occurs through diffusion (pH 7 ± 1), while in the case of bicarbonate, which is the common form of inorganic carbon under high pH (10 ± 1), the microalgal cells use active transport (Gonçalves et al., 2017). Microalgal photosynthesis raises pH by consumption of CO_2 and HCO_3^-. It was observed that microalgal growth rate is affected by the pH as pH affects the availability of inorganic carbon. When pH is around or over 10, CO_2 is limiting and bicarbonate is used as a carbon source (Otondo et al., 2018). The pH is slightly increased during the microalgal-bacterial biomass generation in all type of liquid wastes indicating effective photosynthetic activity of microalgae. At the end point of the biomass production in MW the pH was high, this might have been an inhibitory on microalgal biomass growth beside the limited nutrient source (**Figure 1**).

Although microalgae are mainly autotrophic, *C. vulgaris* is able to grow in a mixotrophic/photoheterotrophic way using organic carbon source (e.g., acetate, glucose) in addition to CO_2 (Skorupskaite et al., 2015; Zuñiga et al., 2016). Typically both respiratory and photosynthetic processes occur in darkish wastewater (Morales-Sánchez et al., 2015; Skorupskaite et al., 2015; Zuñiga et al., 2016). Microalgae also consume the CO_2 released from bacterial respiration, in turn the algae provide the O_2 necessary for the phycospheric bacteria to degrade organic carbon sources (Fuentes et al., 2016; Liu J. et al., 2017). Therefore, organic carbon source of liquid wastes is readily reduced by both microalgal and bacterial metabolic activities. Furthermore, it was observed earlier that microalgae could improve the energy efficiency of BOD removal (Mujtaba and Lee, 2016). These observations were confirmed,

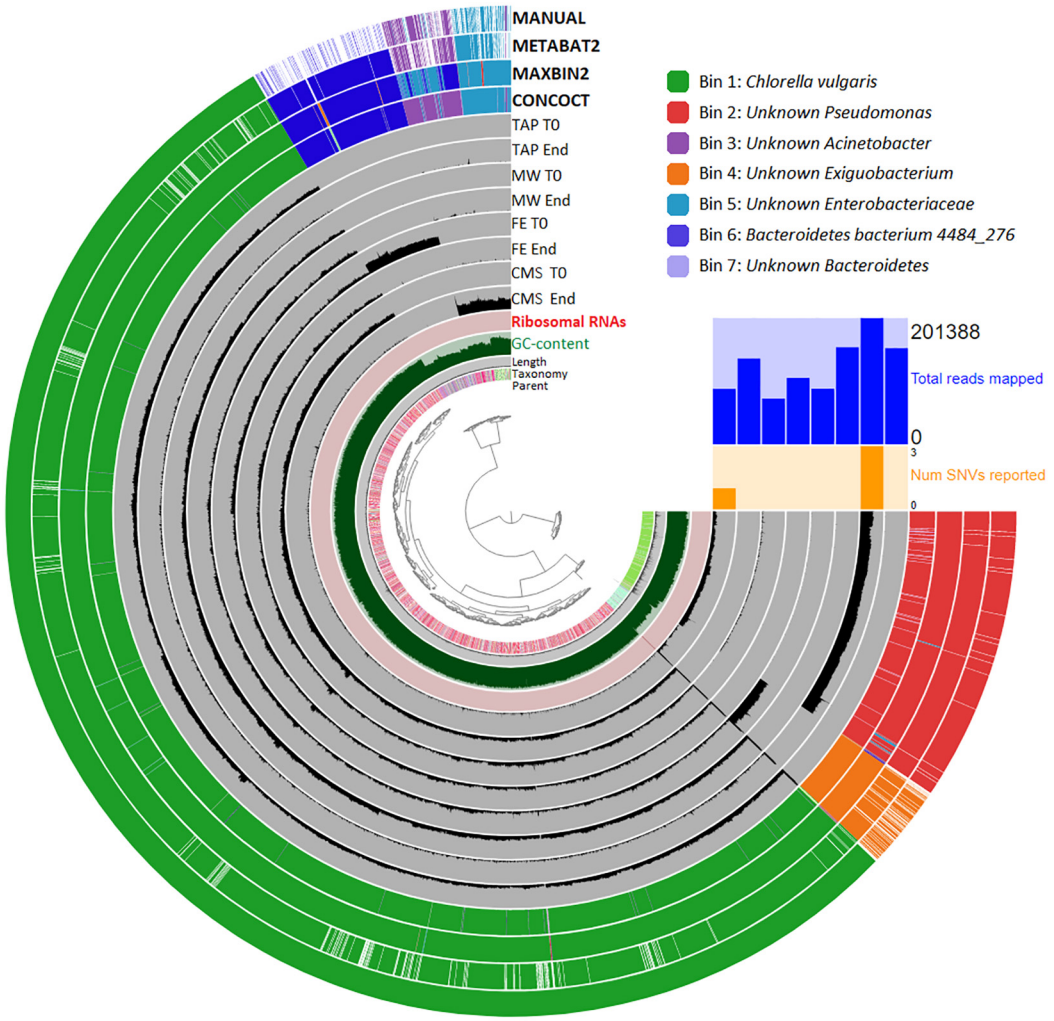

FIGURE 3 | Visualization of the genome-centric metagenomics data. The hierarchical dendrogram of the contigs based on its tetra-nucleotide frequency is in the center of the picture. The taxonomy of the individual contigs is color-coded. The length, GC content, and the presence of ribosomal RNAs of contigs is displayed at the next level. The inner circles show the frequency of the contigs in each wastewater type (CMS: chicken manure supernatant, FE: fermentation effluent, MW: municipal wastewater) in time (T0: start point, End: end point). The outer layer shows the CONCOCT, MAXBIN2, METABAT2 and manual binning results (color-code: upper right corner).

significant carbon loss was detected in all type of applied wastewaters (over 80%), which was in clear correlation with the BOD removal rate.

Using microalgae and its phycosphere to utilize nutrients from wastewater for biomass production and the combined use of the generated biomass for biofuel generation is a promising and promoted way to build circular economy (Chiu et al., 2015; Zhu et al., 2016). The advantage of the algal biomass-based biogas production is that the microalgal-bacterial biomass can be directly applied in the biogas reactor, the total biomass is degraded and converted to methane and CO_2 by a complex microbial community in a well-controlled manner (Guldhe et al., 2017). Microalgal dry biomass productivity was found to be the most effective in CMS (18% higher compared to TAP) followed by FE (CMS: 0.70–0.90 g DM/L/day; FE: 0.30–0.60 g DM/L/day), while the lowest biomass was detected when using MW (0.10–0.20 g DM/L/day) (**Supplementary Information** and **Figure 1G**). Similarly, bacterial content was found to be higher in biomass generated in CMS and FE (27 and 38%), while only 10% in MW. The high nutrient content (including acetate, phosphate and ammonium) of CMS explains its effectiveness in biomass production. The biochemical methane potential (BMP) of the biomass generated in the alternative media were comparable to the methane potential of the biomass produced on TAP control (ranging from 236 to 241 CH_4 mL_N/g oDM in CMS, FE, and MW, while 249 ± 15 CH_4 mL_N/g oDM in TAP). Differences in BMP might be caused by the biomass carbon to nitrogen ratio and by bacterial content of the biomass (Arcila and Buitrón, 2016; Molinuevo-Salces et al., 2016; Jankowska et al., 2017). The presence of bacteria also explains the relatively higher C/N

ratio of biomass cultivated in FE and CMS compared to that of TAP. However, in the aspect of anaerobic digestion this ratios are far from the optimal range (C/N: 20–30:1) (Ward et al., 2014). Thus, the long-term effects of the low C/N ratio and the bacterial content of the biomass on the anaerobic digestion and on the decomposing microbial community need to be further investigated (Wirth et al., 2015a,b, 2018).

Revealing the Phycosphere of Microalgae Cultivated on Liquid Wastes by Read-Based and Genome-Centric Approach

The read-based metagenomics approach revealed a diverse microbial composition at the start point of cultivations in different type of liquid wastes (**Supplementary Information**). The PCA of the prokaryotic communities showed significant alterations during the cultivation period (**Figure 2A**). At the starting point the highest diversity was observed in FE, where *Clostridia*, *Bacteroidia* and *Bacilli* were the most abundant classes. *Beta*,- *Gammaproteobacteria* and *Bacilli* dominated the microbial communities in MW. *Actinobacteria*, *Bacilli* and *Gammaproteobacteria* were the most abundant classes in CMS (**Figure 2B**). The observed microbial classes are typical for chicken manure, municipal wastewater and anaerobic digesters (Lu et al., 2007; Ju et al., 2014; Campanaro et al., 2020). The starting communities were significantly altered by the end of the cultivation period. Mainly *Alpha*-, *Beta*-, *Gammaproteobacteria* and *Bacilli* became the most dominant classes (**Figure 2B**). In previous studies similar changes were observed in the prokaryotic microbial community composition in microalgal-seeded systems (Krustok et al., 2015; Chen et al., 2019; Paquette et al., 2020). The TAP medium (control) showed the lowest composition change, in this medium the representatives of *Gammaproteobacteria* class were the dominant bacterial partners of *C. vulgaris* microalgae throughout the cultivation. Two further interesting aspects were observed in the microbial communities. On one hand the prokaryotic community of CMS at the end point was the most similar to that of the TAP medium (**Figure 2A**). On the other hand the dominance of the class *Gammaproteobacteria* is in close correlation with the biomass yield (**Figures 1**, **2B**).

The genome-centric metagenomics results further explain these interesting observations. The human-guided binning approach resulted one medium (Bin 2) and six low quality (Bin 1, 3–7) Metagenome-Assembled Genomes (MAGs) (Bowers et al., 2017). These bins are identified as one eukaryotic algae MAG (Bin 1) and six bacterial MAGs (Bin 2–7). The *unknown Pseudomonas* (Bin 2), *unknown Acinetobacter* (Bin 3) and *unknown Enterobacteriaceae* (Bin 5) belong to the class *Gammaproteobacteria* within the phylum *Proteobacteria*. Two bins were found as representatives of the phylum *Bacteroidetes*, these are the *Bacteroidetes bacterium 4484-246* MAG (Bin 6) and an *unknown Bacteroidetes* MAG (Bin 7), while the *unknown Exiguobacterium* MAG (Bin 4) belongs to the phylum *Firmicutes* (**Figure 3**).

Multiple members of the class *Gammaproteobacteria* and the phylum *Bacteroidetes* are considered as Plant Growth Promoting Bacteria (PGPB) interacting with microalgae trough metabolite exchange and by enhancing the microalgal biomass yield and lipid production (Seymour et al., 2017; Calatrava et al., 2018; Cho et al., 2019). The representatives of class *Gammaproteobacteria*, the phylum *Bacteroidetes* and the genus *Exiguobacterium* are commonly found in the phycosphere of *C. vulgaris* cultivated on liquid wastes strengthening the hypothesis, that there are a specific interactions between microalgae and bacteria (Guo and Tong, 2014; Kouzuma and Watanabe, 2015; Mujtaba et al., 2017; Cheah et al., 2018; Qi et al., 2018). It was reported that the representatives of the genus *Pseudomonas* are capable of increasing the growth rate of *Chlorella* microalgae species through the reduction of photosynthetic oxygen tension (Berthold et al., 2019) beside their decomposing activities (Mujtaba et al., 2017; Cheah et al., 2018). The presence of *Pseudomonas* sp. resulted higher *Chlorella* cell concentrations in a given period compared to that observed in axenic microalgae culture (Guo and Tong, 2014; Mujtaba and Lee, 2016). Certain *Pseudomonas* and *Acinetobacter sp.* also promoted the *Chlorella* microalgae growth when cultivated on palm oil mill effluent (Cheah et al., 2018). A symbiotic relationship between *Chlorella* and *Bacteroidetes* species was described recently, the abundance of *Bacteroidetes* specifically increased during pre-treatment of dairy-derived liquid digestate (Zhu et al., 2019). In another study *Proteobacteria* and *Bacteroidetes* induced growth promotion of three microalgae, *Chlamydomonas reinhardtii*, *C. vulgaris* and *Euglena gracilis* in wastewater and swine manure effluent (Toyama et al., 2018). The genus *Exiguobacterium* was previously described among the dominant bacteria during domestic wastewater treatment, this specific bacterium was shown to promote *Chlorella* biomass accumulation and chlorophyll synthesis (Qi et al., 2018; Ren et al., 2019).

The read coverage of bins indicated that the *unknown Pseudomonas* (Bin 2) and *unknown Acinetobacter* (Bin 3) were presented in all types of wastewater media. The *unknown Enterobacteriaceae* (Bin 5) was detected in CMS, FE and MW, while *Bacteroidetes bacterium 4484_276* (Bin 6) and the *unknown Bacteroidetes* (Bin 7) were present only in FE. These data indicated that some of the bacteria were in strong interaction with the *Chlorella* algae while the others were specific to the applied wastewater type. It was reported that many bacteria are able to survive together with microalgae in algae culture collections for long term (Krohn-Molt et al., 2017). The *unknown Pseudomonas* (Bin 2) and the *unknown Acinetobacter* (Bin 3) seem to belong this category, they had a strong interaction with *Chlorella* and might have been inoculated together into the examined waste liquids. The *unknown Enterobacteriaceae* and *Exiguobacterium*, furthermore the representatives of *Bacteroidetes* are likely to be wastewater-specific bacterial strains (Toyama et al., 2018).

Multiple factors influence the presence of bacterial partners of eukaryotic microalgae. A highly important factor is the algal photosynthesis, through which microalgae can increase the dissolved oxygen concentration and the pH of the medium (Seymour et al., 2017). Also the microalgal products having bactericidal effect are important in shaping the phycosphere. The *C. vulgaris* are able to produce a mixture of polyunsaturated fatty acids exhibiting antibiotic activity, i.e., chlorellin (Fergola

et al., 2007). Chlorellin is produced in small amount in stationary growth phase, and it exerts different inhibitory effects on different bacteria (DellaGreca et al., 2010; Alwathnani and Perveen, 2017). The effect of chlorellin might have been limited on the development of the phycosphere due to the applied short cultivation time (4 days). Nevertheless, bacteria are also able to influence microalgal growth through nutrient competition (Guldhe et al., 2017). Based on the measurement of the key nutrients and binning results, microalgae and bacteria are competing for VOAs (i.e., acetate). *C. vulgaris* is able to use acetate in photoheterotrophic cultivation mode via active transport (Zuñiga et al., 2016; Huang et al., 2017; Cecchin et al., 2018). The functional profiling of the *unknown Pseudomonas* (Bin 2), *unknown Acinetobacter* (Bin 3) and *unknown Enterobacteriaceae* (Bin 5) resulted in pathways with complete module completion ratio (MCR). These pathways are linked to fatty acid metabolism (**Supplementary Table 2**). Therefore, it is assumed that these bacteria were mainly responsible for the fatty acid consumption, while the microalgae had only minor role in this metabolic activity. They degrade the fatty acids and release CO_2 during their metabolic activity, this CO_2 is consumed by microalgae which in turn produce photosynthetic oxygen essential for the bacteria for fatty acid oxidation. According to MCR calculations the *unknown Exiguobacterium* (Bin 4) and the *Bacteroidetes bacterium 4484-246* (Bin 6) have complete phospho-ribo-biphosphate biosynthesis pathway indicating their carbohydrate metabolic activity. It is not clear, whether these bacteria use the microalgal carbohydrate by-products or possibly degrade algal cell wall components. However, it is very likely that these bacteria also produce CO_2, thereby increase microalgal photosynthetic activity and growth. Since the genome completeness of these bacteria is low, similarly to the *unknown Acinetobacter* (Bin 3) and the *unknown Enterobacteriaceae* (Bin 5), the knowledge on their detailed roles in the phycosphere is limited.

Vitamins like cobalamin, thiamin, biotin are needed in the lipid biosynthesis pathway in microalgae and higher plants (Croft et al., 2006; Smith et al., 2007). Although *C. vulgaris* is not auxotroph for vitamin B derivatives, the addition of these ingredients still have a positive effect for *Chlorella* growth (Croft et al., 2005). Previous studies involving 306 microalgal species showed that more than half of the examined species (51%) required exogenous cobalamin (vitamin B_{12}), 22% required thiamin (vitamin B_1) and 5% required biotin (vitamin B_7) for better growth (Croft et al., 2006). It was reported that vitamin supplementation increased the lipid production and intracellular vitamin concentration of the *Chlorella* species, which ultimately resulted in increased growth rate and biomass yield (Fazeli Danesh et al., 2018). It is possible to supply these vitamins by the addition of bacterial partners. It is especially beneficial at industrial scale algae farms to increase sustainability and economic feasibilty. The genome-centric binning results showed that the *unknown Pseudomonas* (Bin 2) showed high MCR for biotin (100%), cobalamin (80%) and thiamin (60%) biosynthesis. The capability of this specific MAG to synthesize these important vitamin B derivatives further supports the close relationship between this bacterium and the *C. vulgaris* microalgae.

CONCLUSION

The applied microalgae and its phycosphere effectively reduced the carbon, nitrogen and phosphorus content as well as decreased the BOD of the applied liquid wastes. The nitrogen and phosphorus losses were predominantly caused by the microalgal activity. Nitrogen had the greatest effect on the growth of microalgae, however, the algal consumption of this nutrient depended on the transparency of the medium (light penetration) implying to the significance of the photosynthetic algae growth. The fatty acid content of the liquid wastes was used by both the microalgae and the bacterial partners, however, microalgae had limited importance in this activity. The CO_2 produced by the phycospheric bacteria was consumed by microalgae and in exchange the photosynthetically produced oxygen was respired by the phycospheric bacteria during the oxidation of organic acids. CMS proved to be the most efficient for microalgal dry mass production, while FE and MW had medium and low efficiency in this term, respectively. However, the lowest bacterial content was detected in the dry biomass grown in MW. Diverse prokaryotic microbial community featured the used liquid wastes at the start point of cultivation, which compositions are typical to the given wastewater type. These were significantly changed at the endpoint. The genom-centric approach revealed that the *unknown Pseudomonas* (Bin 2) and the *unknown Acinetobacter* (Bin 3) strongly interacted with *Chlorella.* Such genome-level investigations may reveal bacterial indicators of culture status, which could be useful for monitoring the health of microalgae in complex bioremediating communities (Seger et al., 2019). The explorations on microalgae-bacteria associations in wastewater contribute to the better understanding of phycosphere activities and help their applications in bioremediation and combined next-generation biofuel production.

DATA AVAILABILITY STATEMENT

The datasets presented in this study can be found in online repositories. The names of the repository/repositories and accession number (s) can be found in the article/ **Supplementary Material**.

AUTHOR CONTRIBUTIONS

RW designed and performed the bioinformatics analyses and composed the manuscript. BP, TB, GL, and ZB performed the wastewater cultivation experiments and analytical measurements. PS contributed to the metagenome analyses. KK and GM designed the study, composed the

manuscript and thoroughly discussed the relevant literature. All authors read and approved the final manuscript.

FUNDING

This study has been supported in part by the Hungarian National Research, Development and Innovation Fund projects GINOP-2.2.1-15-2017-00081, GINOP-2.2.1-15-2017-00033, and EFOP-3.6.2-16-2017-00010. RW and GM received support from the Hungarian NKFIH fund projects PD121085 and FK123899. This work was also supported by the János Bolyai Research Scholarship (GM) of the Hungarian Academy of Sciences and by a Bolyai+ Grant UNKP-19-4-SZTE-70 (GM) and by the Lendület-Programme (GM) of the Hungarian Academy of Sciences (LP2020-5/2020).

SUPPLEMENTARY MATERIAL

The Supplementary Material for this article can be found online at: https://www.frontiersin.org/articles/10.3389/fbioe.2020.557572/full#supplementary-material

SUPPLEMENTARY INFORMATION | Bioremediation data, biomass production and biochemical methane production (BMP) measurements.

TABLE S1 | Sequence statistics, read-based and genome-centric data.

TABLE S2 | Results of module completion ratio (MCR) calculations.

REFERENCES

Afgan, E., Baker, D., van den Beek, M., Blankenberg, D., Bouvier, D., Čech, M., et al. (2016). The Galaxy platform for accessible, reproducible and collaborative biomedical analyses: 2016 update. *Nucleic Acids Res.* 44, W3–W10. doi: 10.1093/nar/gkw343

Alneberg, J., Bjarnason, B. S., de Bruijn, I., Schirmer, M., Quick, J., Ijaz, U. Z., et al. (2013). CONCOCT: clustering contigs on coverage and composition. *arXiv* 1–28. doi: 10.1371/journal.pone.0005299

Alwathnani, H., and Perveen, K. (2017). Antibacterial activity and morphological changes in human pathogenic bacteria caused by chlorella vulgaris extracts. *Biomed. Res.* 28, 1610–1614.

Anjum, R., Grohmann, E., and Krakat, N. (2017). Anaerobic digestion of nitrogen rich poultry manure: impact of thermophilic biogas process on metal release and microbial resistances. *Chemosphere* 168, 1637–1647. doi: 10.1016/j.chemosphere.2016.11.132

APHA-AWWA-WPCF (1998). *Standard Methods for the Examination of Water and Wastewater*, 20th Edn. Washington, DC: American Public Health Association.

Arai, W., Taniguchi, T., Goto, S., Moriya, Y., Uehara, H., Takemoto, K., et al. (2018). MAPLE 2.3.0: an improved system for evaluating the functionomes of genomes and metagenomes. *Biosci. Biotechnol. Biochem.* 82, 1515–1517. doi: 10.1080/09168451.2018.1476122

Arcila, J. S., and Buitrón, G. (2016). Microalgae–bacteria aggregates: effect of the hydraulic retention time on the municipal wastewater treatment, biomass settleability and methane potential. *J. Chem. Technol. Biotechnol.* 91, 2862–2870. doi: 10.1002/jctb.4901

Berthold, D. E., Shetty, K. G., Jayachandran, K., Laughinghouse, H. D., and Gantar, M. (2019). Enhancing algal biomass and lipid production through bacterial co-culture. *Biomass Bioenergy* 122, 280–289. doi: 10.1016/j.biombioe.2019.01.033

Böjti, T., Kovács, K. L., Kakuk, B., Wirth, R., Rákhely, G., and Bagi, Z. (2017). Pretreatment of poultry manure for efficient biogas production as monosubstrate or co-fermentation with maize silage and corn stover. *Anaerobe* 46, 138–145. doi: 10.1016/j.anaerobe.2017.03.017

Bowers, R. M., Kyrpides, N. C., Stepanauskas, R., Harmon-Smith, M., Doud, D., Reddy, T. B. K., et al. (2017). Minimum information about a single amplified genome (MISAG) and a metagenome-assembled genome (MIMAG) of bacteria and archaea. *Nat. Biotechnol.* 35, 725–731. doi: 10.1038/nbt.3893

Calatrava, V., Hom, E. F. Y., Llamas, Á, Fernández, E., and Galván, A. (2018). Ok, thanks! A new mutualism between chlamydomonas and methylobacteria facilitates growth on amino acids and peptides. *FEMS Microbiol. Lett.* 365:fny021. doi: 10.1093/femsle/fny021/4828328

Campanaro, S., Treu, L., Rodriguez-R, L. M., Kovalovszki, A., Ziels, R. M., Maus, I., et al. (2020). New insights from the biogas microbiome by comprehensive genome-resolved metagenomics of nearly 1600 species originating from multiple anaerobic digesters. *Biotechnol. Biofuels* 13, 1–18. doi: 10.1186/s13068-020-01679-y

Campbell, J. H., O'Donoghue, P., Campbell, A. G., Schwientek, P., Sczyrba, A., Woyke, T., et al. (2013). UGA is an additional glycine codon in uncultured SR1 bacteria from the human microbiota. *Proc. Natl. Acad. Sci. U.S.A.* 110, 5540–5545. doi: 10.1073/pnas.1303090110

Cecchin, M., Benfatto, S., Griggio, F., Mori, A., Cazzaniga, S., Vitulo, N., et al. (2018). Molecular basis of autotrophic vs mixotrophic growth in *Chlorella sorokiniana*. *Sci. Rep.* 8:6465. doi: 10.1038/s41598-018-24979-8

Cheah, W. Y., Show, P. L., Juan, J. C., Chang, J. S., and Ling, T. C. (2018). Waste to energy: the effects of *Pseudomonas* sp. on Chlorella sorokiniana biomass and lipid productions in palm oil mill effluent. *Clean Technol. Environ. Policy* 20, 2037–2045. doi: 10.1007/s10098-018-1505-7

Chen, X., Hu, Z., Qi, Y., Song, C., and Chen, G. (2019). The interactions of algae-activated sludge symbiotic system and its effects on wastewater treatment and lipid accumulation. *Bioresour. Technol.* 292:122017. doi: 10.1016/j.biortech.2019.122017

Chen, X., Li, Z., He, N., Zheng, Y., Li, H., Wang, H., et al. (2018). Nitrogen and phosphorus removal from anaerobically digested wastewater by microalgae cultured in a novel membrane photobioreactor. *Biotechnol. Biofuels* 11:190. doi: 10.1186/s13068-018-1190-0

Chiu, S. Y., Kao, C. Y., Chen, T. Y., Chang, Y., Bin, Kuo, C. M., et al. (2015). Cultivation of microalgal Chlorella for biomass and lipid production using wastewater as nutrient resource. *Bioresour. Technol.* 184, 179–189. doi: 10.1016/j.biortech.2014.11.080

Cho, D. H., Ramanan, R., Heo, J., Lee, J., Kim, B. H., Oh, H. M., et al. (2015). Enhancing microalgal biomass productivity by engineering a microalgal-bacterial community. *Bioresour. Technol.* 175, 578–585. doi: 10.1016/j.biortech.2014.10.159

Cho, K., Heo, J., Cho, D.-H., Tran, Q.-G., Yun, J.-H., Lee, S.-M., et al. (2019). Enhancing algal biomass and lipid production by phycospheric bacterial volatiles and possible growth enhancing factor. *Algal Res.* 37, 186–194. doi: 10.1016/j.algal.2018.11.011

Collet, P., Hélias Arnaud, A., Lardon, L., Ras, M., Goy, R. A., and Steyer, J. P. (2011). Life-cycle assessment of microalgae culture coupled to biogas production. *Bioresour. Technol.* 102, 207–214. doi: 10.1016/j.biortech.2010.06.154

Cooper, M. B., and Smith, A. G. (2015). Exploring mutualistic interactions between microalgae and bacteria in the omics age. *Curr. Opin. Plant Biol.* 26, 147–153. doi: 10.1016/j.pbi.2015.07.003

Croft, M. T., Lawrence, A. D., Raux-Deery, E., Warren, M. J., and Smith, A. G. (2005). Algae acquire vitamin B12 through a symbiotic relationship with bacteria. *Nature* 438, 90–93. doi: 10.1038/nature04056

Croft, M. T., Warren, M. J., and Smith, A. G. (2006). Algae need their vitamins. *Eukaryot. Cell* 5, 1175–1183. doi: 10.1128/ec.00097-06

DellaGreca, M., Zarrelli, A., Fergola, P., Cerasuolo, M., Pollio, A., and Pinto, G. (2010). Fatty acids released by *Chlorella vulgaris* and their role in interference with Pseudokirchneriella subcapitata: experiments and modelling. *J. Chem. Ecol.* 36, 339–349. doi: 10.1007/s10886-010-9753-y

Eren, A. M., Esen, ÖC., Quince, C., Vineis, J. H., Morrison, H. G., Sogin, M. L., et al. (2015). Anvi'o: an advanced analysis and visualization platform for 'omics data. *PeerJ* 3:e1319. doi: 10.7717/peerj.1319

Fazeli Danesh, A., Mooij, P., Ebrahimi, S., Kleerebezem, R., and van Loosdrecht, M. (2018). Effective role of medium supplementation in microalgal lipid accumulation. *Biotechnol. Bioeng.* 115, 1152–1160. doi: 10.1002/bit.26548

Fergola, P., Cerasuolo, M., Pollio, A., Pinto, G., and DellaGreca, M. (2007). Allelopathy and competition between *Chlorella vulgaris* and *Pseudokirchneriella subcapitata*: experiments and mathematical model. *Ecol. Modell.* 208, 205–214. doi: 10.1016/j.ecolmodel.2007.05.024

Finn, D. R., Clements, J., and Eddy, R. S. (2011). HMMER web server: interactive sequence similarity searching. *Nucleic Acids Res.* 39, W29–W37.

Finn, R. D., Attwood, T. K., Babbitt, P. C., Bateman, A., Bork, P., Bridge, A. J., et al. (2017). InterPro in 2017-beyond protein family and domain annotations. *Nucleic Acids Res.* 45, D190–D199. doi: 10.1093/nar/gkw1107

Finn, R. D., Bateman, A., Clements, J., Coggill, P., Eberhardt, R. Y., Eddy, S. R., et al. (2014). Pfam: the protein families database. *Nucleic Acids Res.* 42, 222–230. doi: 10.1093/nar/gkt1223

Fuentes, J. L., Garbayo, I., Cuaresma, M., Montero, Z., González-Del-Valle, M., and Vílchez, C. (2016). Impact of microalgae-bacteria interactions on the production of algal biomass and associated compounds. *Mar. Drugs* 14:100. doi: 10.3390/md14050100

Gonçalves, A. L., Pires, J. C. M., and Simões, M. (2017). A review on the use of microalgal consortia for wastewater treatment. *Algal Res.* 24, 403–415. doi: 10.1016/j.algal.2016.11.008

Guldhe, A., Kumari, S., Ramanna, L., Ramsundar, P., Singh, P., Rawat, I., et al. (2017). Prospects, recent advancements and challenges of different wastewater streams for microalgal cultivation. *J. Environ. Manage.* 203, 299–315. doi: 10.1016/j.jenvman.2017.08.012

Guo, Z., and Tong, Y. W. (2014). The interactions between *Chlorella vulgaris* and algal symbiotic bacteria under photoautotrophic and photoheterotrophic conditions. *J. Appl. Phycol.* 26, 1483–1492. doi: 10.1007/s10811-013-0186-1

Han, X., Rusconi, N., Ali, P., Pagkatipunan, K., and Chen, F. (2017). Nutrients extracted from chicken manure accelerate growth of microalga *Scenedesmus obliquus* HTB1. *Green Sustain. Chem.* 07, 101–113. doi: 10.4236/gsc.2017.72009

Huang, A., Sun, L., Wu, S., Liu, C., Zhao, P., Xie, X., et al. (2017). Utilization of glucose and acetate by Chlorella and the effect of multiple factors on cell composition. *J. Appl. Phycol.* 29, 23–33. doi: 10.1007/s10811-016-0920-6

Huson, D. H., Beier, S., Flade, I., Górska, A., El-Hadidi, M., Mitra, S., et al. (2016). MEGAN community edition - interactive exploration and analysis of large-scale microbiome sequencing data. *PLoS Comput. Biol.* 12:e1004957. doi: 10.1371/journal.pcbi.1004957

Hyatt, D., Chen, G. L., LoCascio, P. F., Land, M. L., Larimer, F. W., and Hauser, L. J. (2010). Prodigal: prokaryotic gene recognition and translation initiation site identification. *BMC Bioinform.* 11:119. doi: 10.1186/1471-2105-11-119

Jankowska, E., Sahu, A. K., and Oleskowicz-Popiel, P. (2017). Biogas from microalgae: review on microalgae's cultivation, harvesting and pretreatment for anaerobic digestion. *Renew. Sustain. Energy Rev.* 75, 692–709. doi: 10.1016/j.rser.2016.11.045

Jones, P., Binns, D., Chang, H. Y., Fraser, M., Li, W., McAnulla, C., et al. (2014). InterProScan 5: genome-scale protein function classification. *Bioinformatics* 30, 1236–1240. doi: 10.1093/bioinformatics/btu031

Ju, F., Guo, F., Ye, L., Xia, Y., and Zhang, T. (2014). Metagenomic analysis on seasonal microbial variations of activated sludge from a full-scale wastewater treatment plant over 4 years. *Environ. Microbiol. Rep.* 6, 80–89. doi: 10.1111/1758-2229.12110

Källqvist, T., and Svenson, A. (2003). Assessment of ammonia toxicity in tests with the microalga, *Nephroselmis pyriformis*, Chlorophyta. *Water Res.* 37, 477–484. doi: 10.1016/S0043-1354(02)00361-5

Kanehisa, M., and Guto, S. (2000). Kegg: kyoto encyclopedia of genes and genomes. *Infect. Genet. Evol.* 44, 313–317. doi: 10.1016/j.meegid.2016.07.022

Kang, D. D., Froula, J., Egan, R., and Wang, Z. (2015). MetaBAT, an efficient tool for accurately reconstructing single genomes from complex microbial communities. *PeerJ* 3:e1165. doi: 10.7717/peerj.1165

Klassen, V., Blifernez-Klassen, O., Hoekzema, Y., Mussgnug, J. H., and Kruse, O. (2015). A novel one-stage cultivation/fermentation strategy for improved biogas production with microalgal biomass. *J. Biotechnol.* 215, 44–51. doi: 10.1016/j.jbiotec.2015.05.008

Klassen, V., Blifernez-Klassen, O., Wibberg, D., Winkler, A., Kalinowski, J., Posten, C., et al. (2017). Highly efficient methane generation from untreated microalgae biomass. *Biotechnol. Biofuels* 10:186. doi: 10.1186/s13068-017-0871-4

Klassen, V., Blifernez-Klassen, O., Wobbe, L., Schlüter, A., Kruse, O., and Mussgnug, J. H. (2016). Efficiency and biotechnological aspects of biogas production from microalgal substrates. *J. Biotechnol.* 234, 7–26. doi: 10.1016/j.jbiotec.2016.07.015

Kouzuma, A., and Watanabe, K. (2015). Exploring the potential of algae/bacteria interactions. *Curr. Opin. Biotechnol.* 33, 125–129. doi: 10.1016/j.copbio.2015.02.007

Krohn-Molt, I., Alawi, M., Förstner, K. U., Wiegandt, A., Burkhardt, L., Indenbirken, D., et al. (2017). Insights into microalga and bacteria interactions of selected phycosphere biofilms using metagenomic, transcriptomic, and proteomic approaches. *Front. Microbiol.* 8:1941. doi: 10.3389/fmicb.2017.01941

Krustok, I., Truu, J., Odlare, M., Truu, M., Ligi, T., Tiirik, K., et al. (2015). Effect of lake water on algal biomass and microbial community structure in municipal wastewater-based lab-scale photobioreactors. *Appl. Microbiol. Biotechnol.* 99, 6537–6549. doi: 10.1007/s00253-015-6580-7

Krzywinski, M., Schein, J., Birol, I., Connors, J., Jones, S. J., Gascoyne, R., et al. (2009). Circos: an information aesthetic for comparative genomics. *Genome Res.* 19, 1639–1645. doi: 10.1101/gr.092759.109

Lam, M. K., and Lee, K. T. (2012). Microalgae biofuels: a critical review of issues, problems and the way forward. *Biotechnol. Adv.* 30, 673–690. doi: 10.1016/j.biotechadv.2011.11.008

Langmead, B., and Salzberg, S. L. (2012). Fast gapped-read alignment with Bowtie 2. *Nat. Methods* 9, 357–359. doi: 10.1038/nmeth.1923

Li, D., Liu, C. M., Luo, R., Sadakane, K., and Lam, T. W. (2015). MEGAHIT: an ultra-fast single-node solution for large and complex metagenomics assembly via succinct de Bruijn graph. *Bioinformatics* 31, 1674–1676. doi: 10.1093/bioinformatics/btv033

Li, K., Liu, Q., Fang, F., Luo, R., Lu, Q., Zhou, W., et al. (2019). Microalgae-based wastewater treatment for nutrients recovery: a review. *Bioresour. Technol.* 291:121934. doi: 10.1016/j.biortech.2019.121934

Lian, J., Wijffels, R. H., Smidt, H., and Sipkema, D. (2018). The effect of the algal microbiome on industrial production of microalgae. *Microb. Biotechnol.* 11, 806–818. doi: 10.1111/1751-7915.13296

Liu, J., Wu, Y., Wu, C., Muylaert, K., Vyverman, W., Yu, H. Q., et al. (2017). Advanced nutrient removal from surface water by a consortium of attached microalgae and bacteria: a review. *Bioresour. Technol.* 241, 1127–1137. doi: 10.1016/j.biortech.2017.06.054

Liu, Q., Wang, J., Bai, Z., Ma, L., and Oenema, O. (2017). Global animal production and nitrogen and phosphorus flows. *Soil Res.* 55:451. doi: 10.1071/sr17031

Lu, J., Santo Domingo, J., and Shanks, O. C. (2007). Identification of chicken-specific fecal microbial sequences using a metagenomic approach. *Water Res.* 41, 3561–3574. doi: 10.1016/j.watres.2007.05.033

Mahdy, A., Mendez, L., Ballesteros, M., and González-Fernández, C. (2014). Algaculture integration in conventional wastewater treatment plants: anaerobic digestion comparison of primary and secondary sludge with microalgae biomass. *Bioresour. Technol.* 184, 236–244. doi: 10.1016/j.biortech.2014.09.145

Mao, C., Feng, Y., Wang, X., and Ren, G. (2015). Review on research achievements of biogas from anaerobic digestion. *Renew. Sustain. Energy Rev.* 45, 540–555. doi: 10.1016/j.rser.2015.02.032

Medipally, S. R., Yusoff, F. M., Banerjee, S., Shariff, M., Medipally, S. R., Yusoff, F. M., et al. (2015). Microalgae as sustainable renewable energy feedstock for biofuel production. *Biomed Res. Int.* 2015:519513. doi: 10.1155/2015/519513

Mende, D. R., Letunic, I., Huerta-Cepas, J., Li, S. S., Forslund, K., Sunagawa, S., et al. (2017). ProGenomes: a resource for consistent functional and taxonomic annotations of prokaryotic genomes. *Nucleic Acids Res.* 45, D529–D534. doi: 10.1093/nar/gkw989

Menzel, P., Ng, K. L., and Krogh, A. (2016). Fast and sensitive taxonomic classification for metagenomics with Kaiju. *Nat. Commun.* 7:11257. doi: 10.1038/ncomms11257

Molinuevo-Salces, B., Mahdy, A., Ballesteros, M., and González-Fernández, C. (2016). From piggery wastewater nutrients to biogas: microalgae biomass revalorization through anaerobic digestion. *Renew. Energy* 96, 1103–1110. doi: 10.1016/j.renene.2016.01.090

Morales-Sánchez, D., Martinez-Rodriguez, O. A., Kyndt, J., and Martinez, A. (2015). Heterotrophic growth of microalgae: metabolic aspects. *World J. Microbiol. Biotechnol.* 31, 1–9. doi: 10.1007/s11274-014-1773-2

Mouget, J. L., Dakhama, A., Lavoie, M. C., and de la Noüe, J. (1995). Algal growth enhancement by bacteria: is consumption of photosynthetic oxygen involved? *FEMS Microbiol. Ecol.* 18, 35–43. doi: 10.1016/0168-6496(95)00038-C

Mujtaba, G., and Lee, K. (2016). Advanced treatment of wastewater using symbiotic co-culture of microalgae and bacteria. *Appl. Chem. Eng.* 27, 1–9. doi: 10.14478/ace.2016.1002

Mujtaba, G., Rizwan, M., and Lee, K. (2015). Simultaneous removal of inorganic nutrients and organic carbon by symbiotic co-culture of *Chlorella vulgaris* and *Pseudomonas putida*. *Biotechnol. Bioprocess. Eng.* 20, 1114–1122. doi: 10.1007/s12257-015-0421-5

Mujtaba, G., Rizwan, M., and Lee, K. (2017). Removal of nutrients and COD from wastewater using symbiotic co-culture of bacterium *Pseudomonas* putida and immobilized microalga *Chlorella vulgaris*. *J. Ind. Eng. Chem.* 49, 145–151. doi: 10.1016/j.jiec.2017.01.021

Mussgnug, J. H., Klassen, V., Schlüter, A., and Kruse, O. (2010). Microalgae as substrates for fermentative biogas production in a combined biorefinery concept. *J. Biotechnol.* 150, 51–56. doi: 10.1016/j.jbiotec.2010.07.030

Nie, H., Jacobi, H. F., Strach, K., Xu, C., Zhou, H., and Liebetrau, J. (2015). Mono-fermentation of chicken manure: ammonia inhibition and recirculation of the digestate. *Bioresour. Technol.* 178, 238–246. doi: 10.1016/j.biortech.2014.09.029

Otondo, A., Kokabian, B., Stuart-Dahl, S., and Gude, V. G. (2018). Energetic evaluation of wastewater treatment using microalgae, *Chlorella vulgaris*. *J. Environ. Chem. Eng.* 6, 3213–3222. doi: 10.1016/j.jece.2018.04.064

Paquette, A. J., Sharp, C. E., Schnurr, P. J., Allen, D. G., Short, S. M., and Espie, G. S. (2020). Dynamic changes in community composition of Scenedesmus-seeded artificial, engineered microalgal biofilms. *Algal Res.* 46:101805. doi: 10.1016/j.algal.2020.101805

Parks, D. H., and Beiko, R. G. (2010). Identifying biologically relevant differences between metagenomic communities. *Bioinformatics* 26, 715–721. doi: 10.1093/bioinformatics/btq041

Pires, J. C. M., Alvim-Ferraz, M. C. M., Martins, F. G., and Simões, M. (2012). Carbon dioxide capture from flue gases using microalgae: engineering aspects and biorefinery concept. *Renew. Sustain. Energy Rev.* 16, 3043–3053. doi: 10.1016/j.rser.2012.02.055

Qi, W., Mei, S., Yuan, Y., Li, X., Tang, T., Zhao, Q., et al. (2018). Enhancing fermentation wastewater treatment by co-culture of microalgae with volatile fatty acid- and alcohol-degrading bacteria. *Algal Res.* 31, 31–39. doi: 10.1016/j.algal.2018.01.012

Quijano, G., Arcila, J. S., and Buitrón, G. (2017). Microalgal-bacterial aggregates: applications and perspectives for wastewater treatment. *Biotechnol. Adv.* 35, 772–781. doi: 10.1016/j.biotechadv.2017.07.003

Ramanan, R., Kim, B. H., Cho, D. H., Oh, H. M., and Kim, H. S. (2016). Algae-bacteria interactions: evolution, ecology and emerging applications. *Biotechnol. Adv.* 34, 14–29. doi: 10.1016/j.biotechadv.2015.12.003

Razzak, S. A., Hossain, M. M., Lucky, R. A., Bassi, A. S., and De Lasa, H. (2013). Integrated CO2 capture, wastewater treatment and biofuel production by microalgae culturing - a review. *Renew. Sustain. Energy Rev.* 27, 622–653. doi: 10.1016/j.rser.2013.05.063

Ren, H. Y., Zhu, J. N., Kong, F., Xing, D., Zhao, L., Ma, J., et al. (2019). Ultrasonic enhanced simultaneous algal lipid production and nutrients removal from non-sterile domestic wastewater. *Energy Convers. Manag.* 180, 680–688. doi: 10.1016/j.enconman.2018.11.028

Rinke, C., Schwientek, P., Sczyrba, A., Ivanova, N. N., Anderson, I. J., Cheng, J. F., et al. (2013). Insights into the phylogeny and coding potential of microbial dark matter. *Nature* 499, 431–437. doi: 10.1038/nature12352

Rizwan, M., Mujtaba, G., Memon, S. A., Lee, K., and Rashid, N. (2018). Exploring the potential of microalgae for new biotechnology applications and beyond: a review. *Renew. Sustain. Energy Rev.* 92, 394–404. doi: 10.1016/j.rser.2018.04.034

Sakar, S., Yetilmezsoy, K., and Kocak, E. (2009). Anaerobic digestion technology in poultry and livestock waste treatment - a literature review. *Waste Manag. Res.* 27, 3–18. doi: 10.1177/0734242X07079060

Santos, C. A., and Reis, A. (2014). Microalgal symbiosis in biotechnology. *Appl. Microbiol. Biotechnol.* 98, 5839–5846. doi: 10.1007/s00253-014-5764-x

Sayre, R. (2010). Microalgae: the potential for carbon capture. *Bioscience* 60, 722–727. doi: 10.1525/bio.2010.60.9.9

Schmieder, R., and Edwards, R. (2011). Quality control and preprocessing of metagenomic datasets. *Bioinformatics* 27, 863–864. doi: 10.1093/bioinformatics/btr026

Seemann, T. (2014). Prokka: rapid prokaryotic genome annotation. *Bioinformatics* 30, 2068–2069. doi: 10.1093/bioinformatics/btu153

Seger, M., Unc, A., Starkenburg, S. R., Holguin, F. O., and Lammers, P. J. (2019). Nutrient-driven algal-bacterial dynamics in semi-continuous, pilot-scale photobioreactor cultivation of Nannochloropsis salina CCMP1776 with municipal wastewater nutrients. *Algal Res.* 39:101457. doi: 10.1016/j.algal.2019.101457

Seymour, J. R., Amin, S. A., Raina, J. B., and Stocker, R. (2017). Zooming in on the phycosphere: the ecological interface for phytoplankton-bacteria relationships. *Nat. Microbiol.* 2:17065. doi: 10.1038/nmicrobiol.2017.65

Shetty, P., Boboescu, I. Z., Pap, B., Wirth, R., and Kovács, K. L. (2019). Exploitation of algal-bacterial consortia in combined biohydrogen generation and wastewater treatment. *Front. Energy Res.* 7:52. doi: 10.3389/fenrg.2019.00052

Simão, F. A., Waterhouse, R. M., Ioannidis, P., Kriventseva, E. V., and Zdobnov, E. M. (2015). BUSCO: assessing genome assembly and annotation completeness with single-copy orthologs. *Bioinformatics* 31, 3210–3212. doi: 10.1093/bioinformatics/btv351

Skorupskaite, V., Makareviciene, V., and Levisauskas, D. (2015). Optimization of mixotrophic cultivation of microalgae *Chlorella* sp. for biofuel production using response surface methodology. *Algal Res.* 7, 45–50. doi: 10.1016/j.algal.2014.12.001

Smith, A. G., Croft, M. T., Moulin, M., and Webb, M. E. (2007). Plants need their vitamins too. *Curr. Opin. Plant Biol.* 10, 266–275. doi: 10.1016/j.pbi.2007.04.009

Sun, C., Cao, W., Banks, C. J., Heaven, S., and Liu, R. (2016). Biogas production from undiluted chicken manure and maize silage: a study of ammonia inhibition in high solids anaerobic digestion. *Bioresour. Technol.* 218, 1215–1223. doi: 10.1016/j.biortech.2016.07.082

Sydney, E. B., Sydney, A. C. N., de Carvalho, J. C., and Soccol, C. R. (2019). "Potential carbon fixation of industrially important microalgae," in *Biofuels From Algae*, eds A. Pandey, J.-S. Chang, C. R. Soccol, D.-J. Lee, and Y. Chisti, (Amsterdam: Elsevier), 67–88.

Thomas, D. M., Mechery, J., and Paulose, S. V. (2016). Carbon dioxide capture strategies from flue gas using microalgae: a review. *Environ. Sci. Pollut. Res.* 23, 16926–16940. doi: 10.1007/s11356-016-7158-3

Toyama, T., Kasuya, M., Hanaoka, T., Kobayashi, N., Tanaka, Y., Inoue, D., et al. (2018). Growth promotion of three microalgae, *Chlamydomonas reinhardtii*, *Chlorella vulgaris* and *Euglena gracilis*, by in situ indigenous bacteria in wastewater effluent. *Biotechnol. Biofuels* 11:176. doi: 10.1186/s13068-018-1174-0

Uggetti, E., Passos, F., Solé, M., Garfí, M., and Ferrer, I. (2016). Recent achievements in the production of biogas from microalgae. *Waste Biomass Valoriza.* 8, 129–139. doi: 10.1007/s12649-016-9604-3

Uggetti, E., Sialve, B., Latrille, E., and Steyer, J. P. (2014). Anaerobic digestate as substrate for microalgae culture: the role of ammonium concentration on the microalgae productivity. *Bioresour. Technol.* 152, 437–443. doi: 10.1016/j.biortech.2013.11.036

Ullah Khan, I., Hafiz Dzarfan, Othman, M., Hashim, H., Matsuura, T., Ismail, A. F., et al. (2017). Biogas as a renewable energy fuel – a review of biogas upgrading, utilisation and storage. *Energy Convers. Manag.* 150, 277–294. doi: 10.1016/j.enconman.2017.08.035

Vereins Deutscher Ingenieure 4630, (2006). *Fermentation of Organic Materials – Characterisation of the Substrate, Sampling, Collection of Material Data, Fermentation Tests, VDI Guideline 4630*. Düsseldorf: Verein Deutscher Ingenieure.

Vo Hoang Nhat, P., Ngo, H. H., Guo, W. S., Chang, S. W., Nguyen, D. D., Nguyen, P. D., et al. (2018). Can algae-based technologies be an affordable green process for biofuel production and wastewater remediation? *Bioresour. Technol.* 256, 491–501. doi: 10.1016/j.biortech.2018.02.031

Ward, A. J., Lewis, D. M., and Green, F. B. (2014). Anaerobic digestion of algae biomass: a review. *Algal Res.* 5, 204–214. doi: 10.1016/j.algal.2014.02.001

Wirth, R., Böjti, T., Lakatos, G., Maróti, G., Bagi, Z., Rákhely, G., et al. (2019). Characterization of core microbiomes and functional profiles of mesophilic anaerobic digesters fed with *Chlorella vulgaris* green microalgae and maize silage. *Front. Energy Res.* 7:111. doi: 10.3389/fenrg.2019.00111

Wirth, R., Lakatos, G., Böjti, T., Maróti, G., Bagi, Z., Kis, M., et al. (2015a). Metagenome changes in the mesophilic biogas-producing community during fermentation of the green alga *Scenedesmus obliquus*. *J. Biotechnol.* 215, 52–61. doi: 10.1016/j.jbiotec.2015.06.396

Wirth, R., Lakatos, G., Maróti, G., Bagi, Z., Minárovics, J., Nagy, K., et al. (2015b). Exploitation of algal-bacterial associations in a two-stage biohydrogen and biogas generation process. *Biotechnol. Biofuels* 8:59. doi: 10.1186/s13068-015-0243-x

Wirth, R., Lakatos, G., Böjti, T., Maróti, G., Bagi, Z., Rákhely, G., et al. (2018). Anaerobic gaseous biofuel production using microalgal biomass - a review. *Anaerobe* 52, 1–8. doi: 10.1016/j.anaerobe.2018.05.008

Wu, Y. W., Simmons, B. A., and Singer, S. W. (2015). MaxBin 2.0: an automated binning algorithm to recover genomes from multiple metagenomic datasets. *Bioinformatics* 32, 605–607. doi: 10.1093/bioinformatics/btv638

Xia, A., and Murphy, J. D. (2016). Microalgal cultivation in treating liquid digestate from biogas systems. *Trends Biotechnol.* 34, 264–275. doi: 10.1016/j.tibtech.2015.12.010

Yen, H. W., Hu, I. C., Chen, C. Y., Ho, S. H., Lee, D. J., and Chang, J. S. (2013). Microalgae-based biorefinery - from biofuels to natural products. *Bioresour. Technol.* 135, 166–174. doi: 10.1016/j.biortech.2012.10.099

Zhu, L., Yan, C., and Li, Z. (2016). Microalgal cultivation with biogas slurry for biofuel production. *Bioresour. Technol.* 220, 629–636. doi: 10.1016/j.biortech.2016.08.111

Zhu, S., Feng, S., Xu, Z., Qin, L., Shang, C., Feng, P., et al. (2019). Cultivation of *Chlorella vulgaris* on unsterilized dairy-derived liquid digestate for simultaneous biofuels feedstock production and pollutant removal. *Bioresour. Technol.* 285:121353. doi: 10.1016/j.biortech.2019.121353

Zuñiga, C., Li, C.-T., Huelsman, T., Levering, J., Zielinski, D. C., McConnell, B. O., et al. (2016). Genome-Scale metabolic model for the green alga *Chlorella vulgaris* UTEX 395 accurately predicts phenotypes under autotrophic, heterotrophic, and mixotrophic growth conditions. *Plant Physiol.* 172, 589–602. doi: 10.1104/pp.16.00593

Conflict of Interest: The authors declare that the research was conducted in the absence of any commercial or financial relationships that could be construed as a potential conflict of interest.

frontiers in Bioengineering and Biotechnology

ORIGINAL RESEARCH
published: 23 November 2020
doi: 10.3389/fbioe.2020.581628

Taxon- and Growth Phase-Specific Antioxidant Production by Chlorophyte, Bacillariophyte, and Haptophyte Strains Isolated From Tropical Waters

*Norazira Abdu Rahman[1], Tomoyo Katayama[1], Mohd Effendy Abd Wahid[2,3], Nor Azman Kasan[4], Helena Khatoon[5], Yuichiro Yamada[6] and Kazutaka Takahashi[1]**

[1] Department of Aquatic Bioscience, Graduate School of Agricultural and Life Sciences, The University of Tokyo, Tokyo, Japan, [2] Institute of Marine Biotechnology, Universiti Malaysia Terengganu, Kuala Terengganu, Malaysia, [3] School of Fisheries and Aquaculture Sciences, Universiti Malaysia Terengganu, Kuala Terengganu, Malaysia, [4] Institute of Tropical Aquaculture and Fisheries, Universiti Malaysia Terengganu, Kuala Terengganu, Malaysia, [5] Department of Aquaculture, Faculty of Fisheries, Chittagong Veterinary and Animal Sciences University, Chittagong, Bangladesh, [6] School of Marine Biosciences, Kitasato University, Kanagawa, Japan

OPEN ACCESS

Edited by:
Norio Nagao, Independent Researcher, Nagasaki, Japan

Reviewed by:
Hazel Monica Matias Peralta, Central Luzon State University, Philippines
Natrah Fatin Mohd Ikhsan, Putra Malaysia University, Malaysia

***Correspondence:**
Kazutaka Takahashi
kazutakahashi@g.ecc.u-tokyo.ac.jp

Specialty section:
This article was submitted to Bioprocess Engineering, a section of the journal Frontiers in Bioengineering and Biotechnology

Received: *09 July 2020*
Accepted: *23 October 2020*
Published: *23 November 2020*

Citation:
Rahman NA, Katayama T, Wahid MEA, Kasan NA, Khatoon H, Yamada Y and Takahashi K (2020) Taxon- and Growth Phase-Specific Antioxidant Production by Chlorophyte, Bacillariophyte, and Haptophyte Strains Isolated From Tropical Waters. Front. Bioeng. Biotechnol. 8:581628. doi: 10.3389/fbioe.2020.581628

Antioxidants found in microalgae play an essential role in both animals and humans, against various diseases and aging processes by protecting cells from oxidative damage. In this study, 26 indigenous tropical marine microalgae were screened. Out of the 26 screened strains, 10 were selected and were further investigated for their natural antioxidant compounds which include carotenoids, phenolics, and fatty acids collected in their exponential and stationary phases. The antioxidant capacity was also evaluated by a total of four assays, which include ABTS, DPPH, superoxide radical ($O_2^{\bullet-}$) scavenging capacity, and nitric oxide ($\bullet NO^-$) scavenging capacity. This study revealed that the antioxidant capacity of the microalgae varied between divisions, strains, and growth phase and was also related to the content of antioxidant compounds present in the cells. Carotenoids and phenolics were found to be the major contributors to the antioxidant capacity, followed by polyunsaturated fatty acids linoleic acid (LA), eicosapentaenoic acid (EPA), arachidonic acid (ARA), and docosahexaenoic acid (DHA) compared to other fatty acids. The antioxidant capacity of the selected bacillariophytes and haptophytes was found to be positively correlated to phenolic (R^2-value = 0.623, 0.714, and 0.786 with ABTS, DPPH, and $\bullet NO^-$) under exponential phase, and to carotenoid fucoxanthin and β-carotene (R^2 value = 0.530, 0.581 with ABTS, and 0.710, 0.795 with $O_2^{\bullet-}$) under stationary phase. Meanwhile, antioxidant capacity of chlorophyte strains was positively correlated with lutein, β-carotene and zeaxanthin under the exponential phase (R^2 value = 0.615, 0.615, 0.507 with ABTS, and R^2 value = 0.794, 0.659, and 0.509 with $\bullet NO^-$). In the stationary phase, chlorophyte strains were positively correlated with violaxanthin (0.755 with $\bullet NO^-$), neoxanthin (0.623 with DPPH, 0.610 with $\bullet NO^-$), and lutein (0.582 with $\bullet NO^-$). This study showed

that antioxidant capacity and related antioxidant compound production of tropical microalgae strains are growth phase-dependent. The results can be used to improve the microalgal antioxidant compound production for application in pharmaceutical, nutraceutical, food, and feed industry.

Keywords: phenolic, carotenoid, fatty acids, growth phase, antioxidant capacity, micro algae

INTRODUCTION

Highly reactive free radicals, including reactive oxygen species (ROS) and reactive nitrogen species (RNS), such as hydroxyl radicals (•OH), superoxide anions ($O_2^{\bullet-}$), and hydrogen peroxides (H_2O_2), are generated as a part of normal cellular metabolism in both humans and animals. Under normal conditions, these radicals are part of the cellular redox signaling and immune function and are readily converted into a safer intermediate (Pham-Huy et al., 2008). However, under abiotic or biotic stress, the imbalance between the rate of radical production and antioxidant defense may induce oxidative stress, leading to the oxidation of proteins, lipids, DNA, and eventually, cell death (Halliwell, 2007). An organism can counteract this situation by various enzymatic and non-enzymatic mechanisms, including antioxidant compounds such as carotenoids and polyphenols (Oroian and Escriche, 2015). An antioxidant is defined as any substance that delays or inhibits the oxidation of substrates even when present at low concentrations compared to the oxidizable substrate (Gutteridge, 1995). Butylated hydroxyanisole (BHA) and butylated hydroxytoluene (BHT) are two widely used synthetic antioxidants in the food and feed industry. However, increasing concerns about their potential carcinogenic and toxic effects have led to a broader search for a natural and sustainable source of antioxidants (Shebis et al., 2013).

Microalgae are natural sources of antioxidants, which have an excellent ability to accumulate various intracellular valuable bioactive compounds (Venkatesan et al., 2015; Sansone and Brunet, 2019). In particular, their fast growth rate and high productivity under normal or stressful conditions make them an attractive candidate for the sustainable alternative of antioxidant sources with high nutritional value (Bulut et al., 2019). It is well-known that the concentrations of microalgal bioactive compounds vary widely depending on the original habitat, species, strains, and growth phases, which may influence the differences in the antioxidant properties of certain microalgae. Microalgal flora in tropical waters has a high potential to accommodate natural antioxidants because their habitat is characterized by high temperature, light, and ultraviolet radiation almost all year round, creating harsh environmental conditions that require defense mechanisms to survive against oxidative stress. Therefore, screening for indigenous tropical microalgae, which have adapted to the harsh environment, would be beneficial in the search for new strains having high antioxidant properties.

Various bioactive compounds found in microalgae play an essential role in protection against oxidative stress and damage. Some of the most important and well-known antioxidants from microalgae include carotenoids and phenolics (Safafar et al., 2015). Both compounds are considered as potent non-enzymatic antioxidants capable of protecting against oxidative damage by converting the radical into a safer by-product. The complex ringed chain molecules of carotenoids enable them to absorb the energy of singlet oxygen radicals and delay the propagation of lipid peroxidation chain reactions, which can disintegrate the lipid membrane (Takaichi, 2011). Meanwhile, a phenolic compound may act as an antioxidant by single electron transfer (SAT) or hydrogen atom transfer (HAT) (Goiris et al., 2012). Recently, fatty acids, especially one with a high degree of unsaturation, have been shown to contribute to the antioxidant activity of various microalgae (Banskota et al., 2018). Nevertheless, very few studies have evaluated the correlation between the antioxidant activity and lipid or fatty acid composition of microalgal strains. According to Lavens and Sorgeloos (1996), microalgae growth phase is characterized into five phases which include lag (initial cell metabolism adaptation to growth), exponential (increased growth), declining growth rate (cell division slows down due to physical or chemical limitation), stationary (constant cell density) and death phase (due to depleted nutrient). Optimal harvesting of microalgae biomass for various industries is usually conducted at an exponential or stationary phase as these are the two phases with high cell biomass and overall compound productivity. However, so far, the antioxidant capacity of microalgae is usually determined using samples taken at either exponential or stationary phase. Thus, the results mostly represent a particular growth phase, without considering the differences in the antioxidant compound constitution among phases.

In this study, the results of the screening of 26 indigenous marine microalgae isolated from Malaysian water bodies for antioxidant production were presented. Being a country with high biodiversity and various unique water bodies, Malaysia is a promising habitat for millions of phytoplankton (Mazlan et al., 2005). However, only a few strains have been isolated and screened for antioxidant production (Natrah et al., 2007). As microalgal antioxidant production could vary depending on the locality, species, strains, and culture conditions, the antioxidant capacity of the microalgae was screened and compared between different taxonomic groups (Bacillariophyta, Chlorophyta, and Haptophyta) at different growth phases in relation to their bioactive compounds.

MATERIALS AND METHODS

Molecular Identification

In this study, twenty-three strains newly isolated from several Malaysian water bodies were identified by molecular

identification. The strains were originated from (1) Remis Beach, Selangor (N03°12′ E101°18′), (2) Teluk Ketapang Beach, Terengganu (N05°23′ E103°06′), and (3) Shrimp pond, Terengganu (N05°38′ E102°45′). For molecular identification, DNA was extracted from the microalgae cells using the DNeasy Plant Mini Kit (Qiagen, Germany). Prior to extraction, microalgal cell disruption was carried out using zirconium beads (EZ-Beads, AMR, Japan) to ensure the release of intracellular contents (especially DNA) into the medium. One milliliter of microalgal cells was bead-beaten for 2 min, centrifuged at 14,000 rpm for 1 min, and the supernatant was used for PCR amplification. For amplification of the SSU region of chlorophytes, the primer combinations used were NS1F-1650R, NS1F-1150R, 1170F-1650R, or PRIMER A-PRIMER B as described previously by Medlin et al. (1988) and Štenclová et al. (2017). For the amplification of the ITS region for the chlorophytes, the primers ITS1 and Pico-ITS4 adapted from Hadi et al. (2016) were used. For the bacillariophyte strain, the primer combination used for amplification of the SSU rDNA region was 1-F-1528-R (Medlin et al., 1988). All primer information are listed in **Table 1**. The amplicon, as determined by gel electrophoresis, was purified using the QIAquick PCR Purification Kit (Qiagen Genomics, United States) and then sequenced by Eurofins Genomics Inc. (Tokyo, Japan). For the microalgae species identification, the resulting SSU ITS rDNA sequences were aligned and analyzed using the BLAST algorithm at the National Centre for Biotechnology Information. Despite of its high antioxidant capacity, one of the screened bacillariophyte strain TRG8-01 was not included in further analysis as it was not successful to be identified even at genus level. The detail of the unidentified strain is shown in the **Supplementary Materials**.

Microalgae Strains and Screening Experiments

A total of 26 indigenous marine microalgae strains, including 22 of newly isolated strains and 4 established strains belonging to six algal classes, namely, Trebouxiophyceae, Chlorophyceae, Prasinophyceae, Bacillariophyceae, Mediophyceae, and Coccolithophyceae, were screened for their antioxidant capacity. Established strains of *Chaetoceros gracilis*, *Isochrysis galbana,* and *Chlorella vulgaris* were obtained from Universiti Putra Malaysia (Natrah et al., 2007; Goh et al., 2010). *Tetraselmis suecica* were obtained from the University Malaysia Terengganu. *Phaeodactylum tricornutum* (CCMP1327) was obtained from the Provosoli-Guillard National Center for Culture of Marine Phytoplankton, United States, and used as the control strain. This strain is known to be rich in fucoxanthin, a carotenoid known for its antioxidant activity (Goiris et al., 2012; Guo et al., 2016).

A pre-inoculum was cultivated for 4 days to ensure that the cells are in the exponential phase by the time of inoculation in 100 mL of Conway medium (Tompkins et al., 1995) containing 1 mL L^{-1} of micronutrients (100 g L^{-1} $NaNO_3$, 45 g L^{-1} EDTA, 33.6 g L^{-1} H_3BO_3, 20 g L^{-1} NaH_2PO_4, 1.30 g L^{-1} $FeCL_3$, 0.36 g L^{-1} $MnCL_2$), 0.1 mL L^{-1} of trace metals (2.10 g L^{-1} $ZnCL_2$, 2 g L^{-1} $CoCL_3$, 0.90 g L^{-1} $(NH_4)_6MO_7O_2$, 2 g L^{-1} $CuSO_4.5H_2O$), 2 mL of silicate solution (15 g L^{-1} Na_2SiO_3) and 0.1 mL L^{-1} of vitamins solution. The pre-inoculum was then inoculated at an initial optical density of 0.001 into 250 mL of fresh medium in 300 mL Erlenmeyer flasks (triplicate). Each algal culture was maintained at 25°C and salinity of 30 ppt under an illumination intensity of 150 μmol m^{-2} s^{-1} under a 12:12 h light/dark photoperiod until the exponential phase. Daily growth was monitored by optical density measurement at 750 nm (OD_{750}) using a microplate reader (Varioskan LUX, Thermo, Japan). On day 7, all cells were harvested by centrifugation at 3,500 rpm for 10 min, freeze-dried, and then kept at −20°C before analysis. As a first screening process, the total antioxidant capacity of all strains was spectrophotometrically determined by their scavenging capacity using 2,2'-azino-bis(3-ethylbenzothiazoline-6-sulfonicacid) (ABTS) and 2,2-diphenyl-1-picrylhydrazyl (DPPH) total antioxidant capacity assay (the analytical method has been described in the antioxidant measurement section below).

Antioxidant Compound Characterization of the Selected Strains

Based on the first screening of their antioxidant capacity, 10 potential microalgal species which produced high antioxidant were selected. The selected species are comprised of bacillariophytes, chlorophytes, and haptophytes. For further experiments involving antioxidant compound characterization, each potential strain was cultivated in triplicate in a 4L Nalgene polycarbonate bottle until the stationary phase, which varied

TABLE 1 | List of primers used for PCR amplification in the present study.

Gene	Name	Sequence	F/R	References
SSU	NS1F	GTAGTCATATGCTTGTCTC	F	Štenclová et al., 2017
	1150R	ACGCCTGGTGGTGCCCTTCCGT	R	Štenclová et al., 2017
	1170F	CTGTGGCTTAATTTGACTCAACACG	F	Štenclová et al., 2017
	1650R	TCACCAGCACACCCAAT	R	Štenclová et al., 2017
	PRIMER A	AACCTGGTTGATCCTGCCAGT	F	Aburai et al., 2013
	PRIMER B	TGATCCTTCTGCAGGTTCACCTAC	R	Aburai et al., 2013
	1-F	AACCTGGTTGATCCTGCCAGTA	F	Rimet et al., 2011
	1528-R	CTTCTGCAGGTTCACCTAC	R	Rimet et al., 2011
ITS	Fw_ITS1Pico	GGAAGGAGAAGTCGTAACAA	F	Hadi et al., 2016
	Rv_ITS4	TCCTCCGCTTATTGATATGC	R	Hadi et al., 2016

among strains. Aeration was supplied for the whole culture period to provide mixing and equal light and nutrient exposure of the algal cells. The number of days for the exponential and stationary phase of each algal strains was determined based on a preliminary growth curve experiment conducted prior using similar initial cell density and culture conditions. All strains were inoculated at an initial optical density of 0.010, and the growth of each strain was monitored by determining optical density at 750 nm (OD_{750}) and dry weight (DW). The optical density was measured daily using a 96-well microplate. Briefly, 200 μL algae sample was added into each well, and OD_{750} was measured using a microplate reader. The total biomass dry weight (g DW L^{-1}) of each strain was obtained according to Zhu and Lee (1997) by filtering a known volume of algal suspension using a pre-weighed Whatman GF/F filter, dried for 24 h in an oven and weighed. Using the DW data, the specific growth rate (SGR) for each strain was calculated according to Levasseur et al. (1993). Each algal biomass during both exponential and stationary phases was collected, centrifuged, and freeze-dried to evaluate antioxidant activity, as described in the next section.

Antioxidant Quantification

The antioxidant capacity was evaluated by a total of four antioxidant assays, including the two radical scavenging assays, ABTS and DPPH, and two other assays that are more specific against the ROS: superoxide radical ($O_2^{\bullet-}$) scavenging capacity and RNS: Nitric oxide ($\bullet NO^-$) scavenging capacity was also analyzed at different growth phases. Details of the measurements are shown below.

First, 2 mL of pure methanol (Wako Chemical, Japan) was added to a tube of 1 mg of finely ground freeze-dried sample and shaken vigorously for 30 s. The sample was sonicated in an ice bath for 45 min (35 kHz, 240 W). The samples were then centrifuged at 5,000 g for 10 min at 4°C and the supernatant was separated. The collected supernatant was combined and used immediately in analysis or purged to dryness using nitrogen gas before it was stored at -20°C.

The total antioxidant radical-scavenging capacities were evaluated using the ABTS radical cation ($ABTS^{\bullet+}$) assay, as originally described by Re et al. (1999). $ABTS^{\bullet+}$ radical cation was prepared by mixing 7 mol m^{-3} ABTS (Wako Chemical, Japan) with 2.45 mol m^{-3} potassium persulfate ($K_2S_8O_4$, Wako Chemical, Japan) for 8 h in the dark at room temperature (21°C). Briefly, 350 μl of the microalgal extract was added to 1 mL of the $ABTS^{\bullet+}$ solution, and the absorbance was measured at 734 nm using a spectrophotometer (Shimadzu UV-1601, Japan) exactly 1 min after initial mixing and up to 6 min. The results were then expressed as micromole Trolox (TE) equivalent per gram of dry algae biomass (μmol TE g^{-1} DW).

The total antioxidant capacity was also measured using the 1,1-diphenyl-2-picrylhydrazyl (DPPH) stable radical, according to Brand-Williams et al. (1995). The sample extract was added to 3.9 mL of 0.06 mM DPPH radicals (Sigma-Aldrich, MO, United States) in methanol solution and then incubated in the dark for 30 min at room temperature. The reduction of the DPPH free radical was measured at 517 nm using a spectrophotometer. The results were also expressed as μmol TE g^{-1} DW.

Meanwhile, superoxide anions were generated in a phenazine methosulphate-NADH system and assayed by reduction of nitro blue tetrazolium (NBT) as described by Robak and Gryglewski (1988) with slight modifications (Abdullah et al., 2017). All reagents were prepared using 0.1 M phosphate-buffered saline. In a 96-well microplate, 50 μL NBT (150 μM), 50 μL algal extract, and 50 μL NADH (468 μM) were mixed with 50 μL phenazine methosulfate (60 μM). Absorbance was read at 570 nm using a microplate reader after incubation in the dark for 10 min at room temperature. The results were expressed as μmol TE g^{-1} DW.

The nitric oxide radical scavenging activity was determined, according to Oliveira et al. (2010). Briefly, 100 μL of the algal extract was incubated with 100 μL of sodium nitroprusside (20 mM) under light at room temperature. After 60 min of incubation, Griess reagent containing 1% sulphanilamide and 0.1% naphthylethylenediamine in 2% phosphoric acid was added to each well. After 10 min incubation, the absorbance of the chromophore formed during the diazotization of nitrite with sulphanilamide and subsequent coupling with naphthylethylenediamine was read at 562 nm, and the results were expressed as μmol TE g^{-1} DW.

Antioxidant Compound Profiling

Carotenoids in each extract were tentatively identified and quantified according to using a reverse-phase gradient elution HPLC system, according to Zapata et al. (2000). The algal methanolic extract was filtered through a 0.2 μm PTFE filter (Whatman) before it was injected into the HPLC system (Shimadzu) equipped with a Symmetry C8 column (Waters). The mobile phase comprised of the following two solvents: (A) methanol: acetonitrile: aqueous 0.25 M pyridine solution (50:25:25 v:v:v), (B) acetonitrile: methanol (80:20 v:v). The solvent gradient was as follows: (1) Solvent A 100% for 18 min; (2) to 60% solvent A, 40% solvent B for 12 min, and (3) to 100% solvent B for 10 min. Carotenoids were identified by comparing their elution order and UV-Vis spectra with chromatographic HPLC-grade standards under identical conditions: diadinoxanthin, fucoxanthin, α- and β-carotene, astaxanthin, antheraxanthin, neoxanthin, violaxanthin, zeaxanthin, lutein, diatoxanthin and Chl *a* were estimated from respective peaks calibrated against pure standards (Danish Hydraulic Institute Water and Environment, Denmark).

Total crude lipids were extracted from the freeze-dried samples with a mixture of chloroform: methanol (1:2, v:v) according to Bligh and Dyer (1959), and fatty acid methyl esters were then produced from the lipid extracts by direct transesterification in methanol containing 5% acetyl chloride at 100°Ñ for 1 h. Fatty acid methyl esters (FAME) were analyzed in a gas chromatograph (GC353, GL-Sciences) using a flame ionization detector and an Agilent DB-FFAP column (30 m length, 0.25 mm inner diameter and 0.25 μm film thickness). The oven heating program comprised a linear increase in column temperature from 160 to 240°C at a rate of 4°C min^{-1}. EZ Chrom Elite software (ver. 3.1.7J, GL-Sciences) was used for recording and integration. Chromatographic grade standards of fatty acids in methyl ester formed from Nu-Check-Prep (GLC-68D,

United States) containing 20 FAME and from Kitasato University containing 13 FAME were used for tentative peak identification.

The total phenolic content was determined using Folin–Ciocalteu reagent described by Singleton and Rossi (1965). One hundred microliters of each methanolic sample extract were mixed with 400 μL of Folin–Ciocalteu reagent and then incubated at room temperature (5 min) before the addition of 500 μL sodium bicarbonate solution (7.5% w/v). After incubation for 90 min in the dark, absorbance was measured at 760 nm using a microplate reader. Gallic acid was used as the standard. The results were then expressed as gallic acid equivalent (GAE) mg g^{-1} dry weight of microalgae.

Statistical Analysis

The experiments were carried out in triplicate, and all results are expressed as mean ± standard error. Data were then analyzed using one-way variance analysis (ANOVA), followed by Tukey's *post-hoc* comparison test to measure differences between data. Statistical significance was determined at $p < 0.05$. Correlations among antioxidant capacities and contents of bioactive compounds were calculated using Pearson's correlation coefficient (r). Statistical analysis was carried out using the statistical software SPPS, version 23 (SPSS Inc., United States).

RESULTS

Selection of Indigenous Microalgae With High Antioxidant Capacity and Growth Capacity

The newly isolated indigenous microalgal strains were identified as *Nanochlorum eucaryotum* (two strains), *Picochlorum maculatum* (two strains), *Chlorella sorokiniana* (two strains), *Oocystis heteromucosa*, *Oocystis marina*, and *Chlamydomonas uva-maris* as chlorophytes, and *Amphora montana* (two strains), *Nitzschia capitellata* (two strains), *Nitzschia palea*, *Psammodictyon pustulatum*, *Pauliella taeniata*, *Navicula arenaria* (three strains), *Navicula radiosa* (two strains) and *Thalassiosira weisflogii* (two strains) as bacillariophytes (see **Supplementary Table 1**).

The 26 indigenous microalgae showed that antioxidant capacity varied among division, class, species, and strain (**Table 2**). Among the chlorophytes, the highest scavenging

TABLE 2 | Antioxidant capacity of tropical microalgal strains from Malaysian waters, assessed by the ABTS and DPPH radical scavenging assay, expressed as micromol equivalent to Trolox per g of biomass dry weight (mean ± SE).

Division	Class	Strain	ABTS (μmol trolox g^{-1} DW)	DPPH (μmol trolox g^{-1} DW)
Chlorophytes (Green algae)	Trebouxiophyceae	*Nanochlorum eucaryotum* SLG4-08	29.08 ± 0.02	8.51 ± 0.28
		Nanochlorum eucaryotum SLG4-11	**26.72 ± 1.67**	**9.23 ± 1.45**
		Picochlorum maculatum TRG9-05	7.69 ± 0.56	**11.76 ± 1.12**
		Picochlorum maculatum TRG9-06	12.71 ± 0.66	5.71 ± 1.80
		Chlorella sorokiniana SLG4-12	**34.16 ± 1.18**	**11.29 ± 0.87**
		Chlorella sorokiniana SLG4-13	**29.68 ± 0.33**	**8.50 ± 0.22**
		Chlorella vulgaris	11.59 ± 1.76	**11.77 ± 0.25**
		Oocystis heteromucosa TRG10-P102	7.37 ± 0.37	2.43 ± 1.21
		Oocystis marina TRG10-P104	10.45 ± 1.45	1.86 ± 0.02
	Chlorophyceae	*Chlamydomonas uva-maris* SLG4-14	4.32 ± 0.02	5.34 ± 0.08
	Prasinophyceae	*Tetraselmis suecica*	**28.29 ± 0.53**	**12.29 ± 0.29**
Bacillariophytes (Diatom)	Bacillariophyceae (pennate diatom)	*Amphora montana* SLG4-03	**30.74 ± 0.05**	**8.50 ± 0.21**
		Amphora montana SLG4-17	13.33 ± 0.18	1.06 ± 0.48
		Nitzschia capitellata TRG9-08	15.99 ± 1.87	2.57 ± 0.22
		Nitzschia capitellata TRG9-09	7.81 ± 1.48	3.49 ± 2.29
		Nitzschia palea SLG4-16	8.66 ± 0.61	6.30 ± 0.20
		Psammodictyon pustulatum TRG9-10	10.99 ± 0.94	7.05 ± 0.39
		Pauliella taeniata TRG8-02	9.79 ± 0.53	5.24 ± 0.24
		Navicula arenaria SLG4-18	5.33 ± 1.14	0.68 ± 0.36
		Navicula radiosa TRG9-03	9.67 ± 1.41	6.89 ± 0.61
		Navicula arenaria SLG4-01	14.94 ± 0.53	3.28 ± 1.52
		Navicula radiosa SLG4-02	10.16 ± 0.41	**8.77 ± 0.43**
		Phaeodactylum tricornutum	25.23 ± 0.12	6.68 ± 1.09
	Mediophyceae (centric diatom)	*Thalassiosira weissflogii* TRG10-P103	**27.16 ± 0.02**	**9.38 ± 0.43**
		Thalassiosira weissflogii TRG10-P105	**32.49 ± 1.68**	**16.83 ± 1.03**
		Chaetoceros gracilis	**30.46 ± 1.16**	**9.56 ± 0.23**
Haptophytes	Coccolithophyceae	*Isochrysis galbana*	**33.60 ± 0.67**	**19.01 ± 1.34**

Significantly high value among strains are printed in bold ($p < 0.05$).

effect against ABTS was obtained by *Chlorella sorokiniana* (SLG4-12) at 34.16 ± 1.18 μmol TE g^{-1} DW, followed by *Nanochlorum eucaryotum* (SLG4-08, SLG4-11), and *Chlorella sorokiniana* (SLG4-13), and *Tetraselmis suecica.* On the other hand, the lowest ($p < 0.05$) antioxidant capacity among the chlorophyte strains was observed in *Chlamydomonas uva-maris* (SLG4-14) at 4.32 ± 0.02 μmol TE g^{-1} DW. The only haptophyte strain evaluated was *Isochrysis galbana* (33.60 ± 0.67 μmol TE g^{-1} DW), showed higher ($p < 0.05$) antioxidant capacity by ABTS than the bacillariophyte strain *Phaeodactylum tricornutum* (control) at 25.23 ± 0.12 μmol TE g^{-1} DW. Among the 12 pennate diatoms studied, only *Amphora montana* (SLG4-03) showed higher ($p < 0.05$) antioxidant capacity in ABTS than that of the control strain (25.23 ± 0.12 μmol TE g^{-1} DW) at 30.74 ± 0.05 μmol TE g^{-1} DW. The lowest ($p < 0.05$) ABTS scavenging capacity among all diatoms was observed in *Navicula arenaria* (SLG4-18) at only 5.33 ± 1.14 μmol TE g^{-1} DW, respectively. All three centric diatom strains, *Chaetoceros gracilis*, *Thalassiosira weissflogii* (TRG10-P103), and *Thalassiosira weissflogii* (TRG10-P105), indicated a higher ($p < 0.05$) total antioxidant capacity than *Phaeodactylum tricornutum*.

Meanwhile, the total antioxidant capacity, according to the DPPH assay, varied from 0.68 ± 0.36 to 19.01 ± 1.34 μmol TE g^{-1} DW (**Table 2**). The bacillariophytes and haptophytes with significantly higher ($p < 0.05$) antioxidant capacity than the control (6.68 ± 1.09 μmol TE g^{-1} DW) were *Isochrysis galbana* (19.01 ± 1.34 μmol TE g^{-1} DW), *Thalassiosira weissflogii* (TRG10-P105) (16.83 ± 1.03 μmol TE g^{-1} DW), *Chaetoceros gracilis* (9.56 ± 0.23 μmol TE g^{-1} DW), *Amphora montana* (SLG4-03) (8.50 ± 0.21 μmol TE g^{-1} DW) and *Navicula radiosa* (SLG4-02) (6.89 ± 0.61 μmol TE g^{-1} DW), respectively. Among the chlorophytes, high ($p < 0.05$) DPPH scavenging capacity compared to control was observed in *Tetraselmis suecica*, *Chlorella vulgaris*, *Chlorella sorokiniana* (SLG4-12), *Nanochlorum eucaryotum* (SLG4-11), *Chlorella sorokiniana* (SLG4-13), and *Nanochlorum eucaryotum* (SLG4-08) ranging from 12.29 ± 0.29 to 8.51 ± 0.28 μmol TE g^{-1} DW, respectively.

Based on the screening results (**Table 2**), 10 strains were selected for their high antioxidant production and were subjected to further analysis. These include 1. Chlorophyte strains; *Nanochlorum eucaryotum* (SLG4-08), *Nanochlorum eucaryotum* (SLG4-11), *Chlorella sorokiniana* (SLG4-12), *Chlorella sorokiniana* (SLG4-13), and *Tetraselmis suecica*, 2. Bacillariophyte strains; *Amphora montana* (SLG4-03), *Chaetoceros gracilis*, *Thalassiosira weissflogii* (TRG10-P103) and *Thalassiosira weissflogii* (TRG10-P105), and 3. Haptophyte strain; *Isochrysis galbana*.

Growth Characteristics of Selected Microalgae Candidate Strain at Different Growth Phases

Growth characteristics in terms of maximum optical density, maximum dry biomass weight, and specific growth rate were different among the 10 selected potential strains as natural antioxidant producers (**Figure 1**). Under stationary phases, the highest ($p < 0.05$) SGR, OD_{750} and biomass dry weight

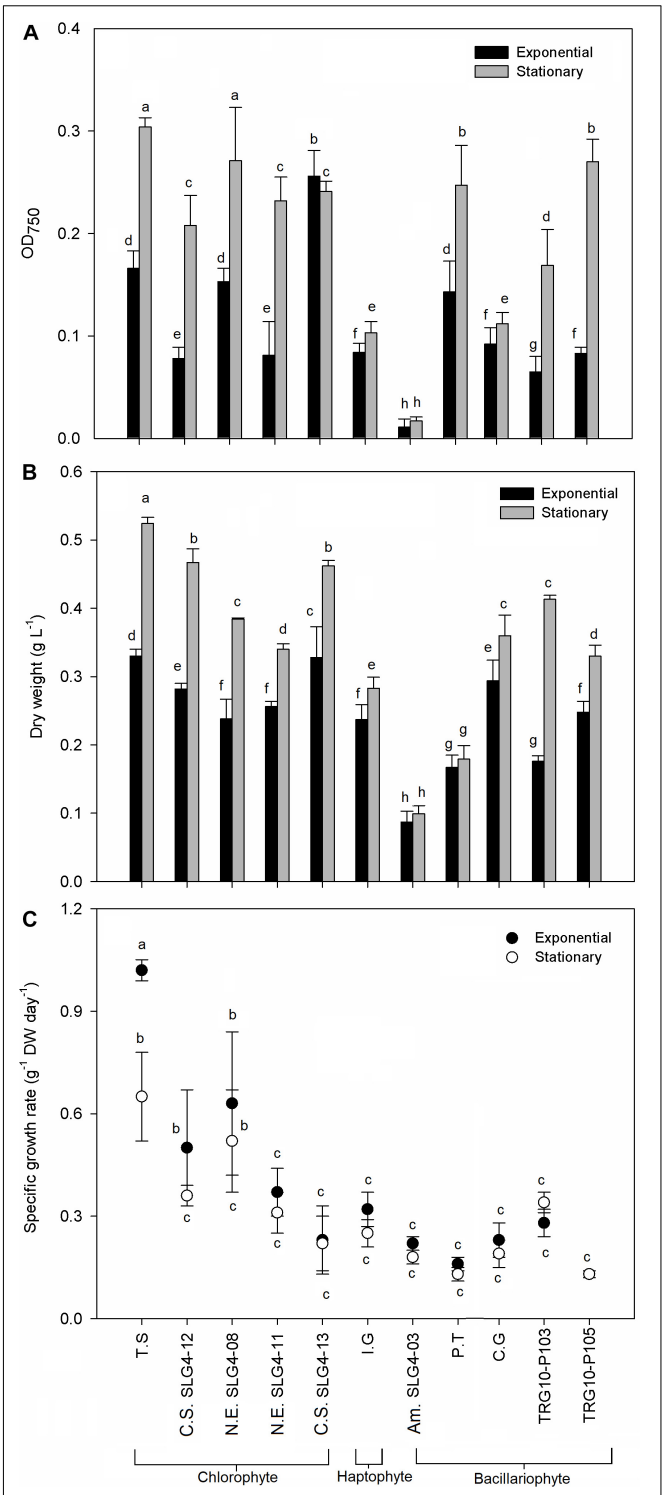

FIGURE 1 | Growth characteristic by **(A)** optical density, **(B)** dry weight, and **(C)** dry weight specific growth rate of selected microalgae strains at exponential and stationary phase. Means denoted by a different letter indicate significant differences between strains ($p < 0.05$); Pico SLG4-12, SLG4-11, SLG4-08, *Picochlorum* sp.; T.S, *Tetraselmis suecica*; C.S. SLG4-13, *Chlorella sorokiniana*; I.G, *I. galbana*; Am. SLG4-03, *Amphora* sp.; P.T, *Phaeodactylum tricornutum*; C.G, *Chaetoceros gracilis*; TRG10-P103, *Thalassiosira* sp.; TRG10-P105, *Thalassiosira weissflogii*.

among all strains were found in the chlorophyte *Tetraselmis suecica* at 1.420 ± 0.31 g^{-1} DW day^{-1}, 0.304 ± 0.009 OD_{750} and 0.524 ± 0.002 g DW L^{-1}. Meanwhile, under the exponential phase, the highest ($p < 0.05$) OD_{750} and biomass dry weight was observed in the *Chlorella sorokiniana* (SLG4-13) at 0.256 ± 0.025 OD_{750} and 0.328 ± 0.045 g DW L^{-1}, respectively. Bacillariophyte, chlorophyte, and haptophyte strains showed relatively higher OD_{750} and biomass dry weight during the stationary phase compared to that during the exponential phase.

Carotenoid Composition at Different Growth Phases

The microalgal biomass showed division and species-specific carotenoid profiles (**Figure 2**). Generally, total carotenoids in bacillariophytes and haptophytes are higher than those in chlorophytes. Total carotenoids in bacillariophytes and haptophytes were consistently higher in the stationary phase than in the exponential phase and could be characterized by the presence of fucoxanthin, diadinoxanthin, and diatoxanthin. In particular, the higher total carotenoid content of bacillariophytes and the haptophyte *Isochrysis galbana* compared to chlorophytes was mainly due to their high fucoxanthin composition. The highest ($p < 0.05$) total carotenoid in the stationary phase was observed in *Amphora montana* (SLG4-03), followed by *Isochrysis galbana* and the control *Phaeodactylum tricornutum* at 18.97 ± 3.12, 15.66 ± 2.13, and 14.37 ± 1.84 mg g^{-1} DW, respectively. Correspondingly, the highest fucoxanthin level under the stationary phase was also observed in *Amphora montana* (SLG4-03) (16.90 ± 2.75 mg g^{-1} DW) followed by *Isochrysis galbana*, *Phaeodactylum tricornutum*, *Chaetoceros gracilis*, and *Thalassiosira weissflogii* (TRG10-P105) at 13.96 ± 1.91, 12.34 ± 1.65, 11.37 ± 2.11, and 10.29 ± 0.17 mg g^{-1} DW, respectively. Dry weight-specific fucoxanthin content was generally higher during the early stationary phase than in the exponential phase. Meanwhile, total carotenoids of

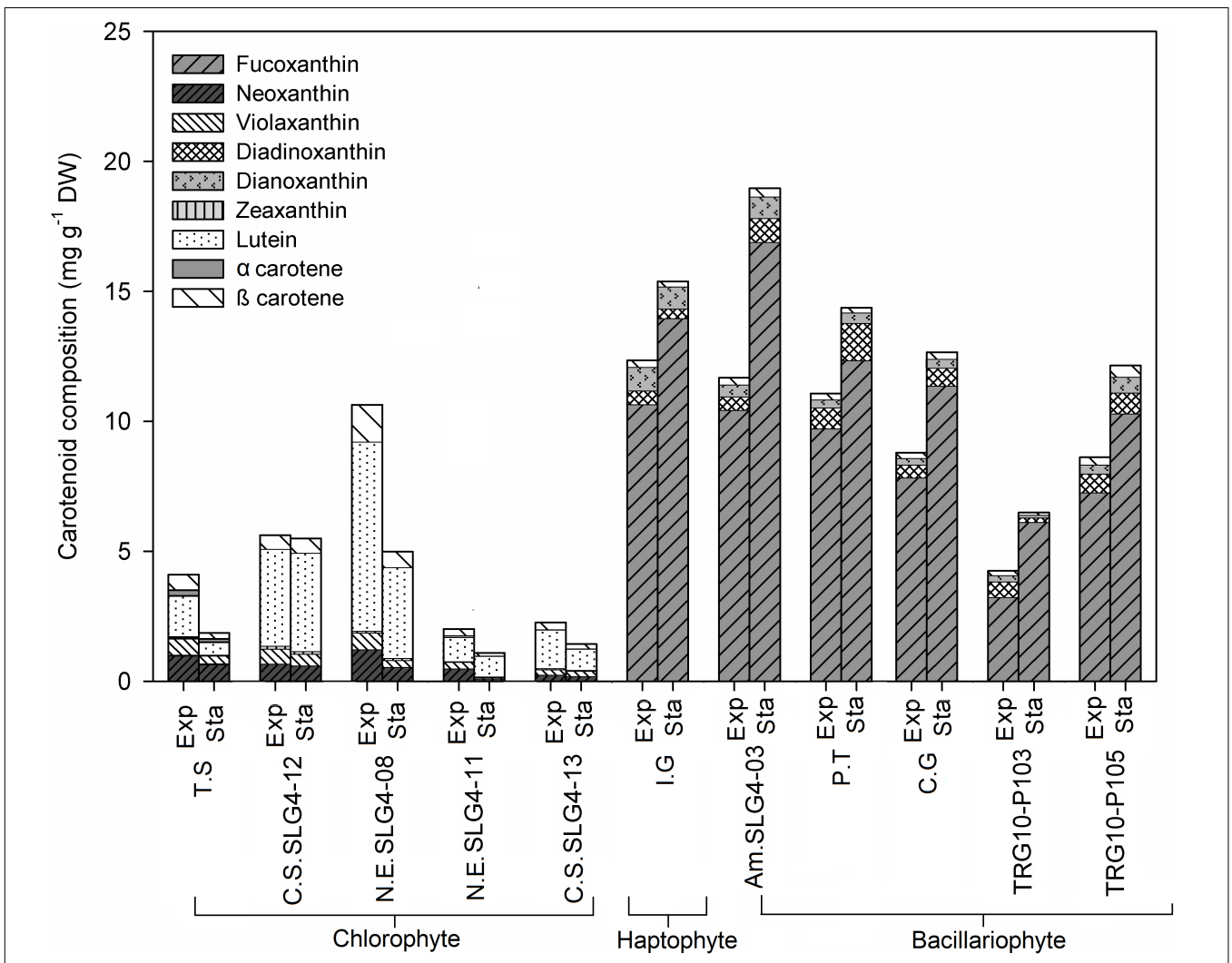

FIGURE 2 | Carotenoid content and composition (mg g^{-1} DW) of selected microalgae strains at exponential (Exp) and stationary phase (Sta). Abbreviations of the strains as for **Figure 1**.

chlorophytes tended to be higher in the exponential phase than in the early stationary phase and can be characterized by the presence of lutein, neoxanthin, violaxanthin, and zeaxanthin. Total carotenoid content (10.68 ± 4.09) was higher in the chlorophyte strain *Nanochlorum eucaryotum* (SLG4-08), in the exponential phase, as compared to the other chlorophyte strains with relatively rich contents of β-carotene, neoxanthin, violaxanthin, and zeaxanthin.

Fatty Acid Composition at Different Growth Phases

The highest fatty acid content was found in *Isochrysis galbana* under exponential phase at 749.25 μg g^{-1} DW, followed by *Thalassiosira weissflogii* (TRG10-P103) (495.46 ± 60.32 μg g^{-1} DW: exponential phase) and *Chaetoceros gracilis* (433.64 ± 220.34 μg g^{-1} DW: exponential phase) (**Figure 3**). Fatty acids with various degrees of saturation were detected, including saturated (SFA) and monounsaturated and polyunsaturated fatty acids (MUFA, PUFA), while their relative importance was differed depending on the strain. *Isochrysis galbana* and *Chlorella sorokiniana* (SLG4-12) contained the highest amount of PUFA compared to other strains during the exponential phase at 364.33 ± 73.43 and 343.45 ± 52.69 μg g^{-1} DW, respectively. High PUFA composition observed in chlorophytes is contributed mainly by their α-linoleic acid (ALA) and linoleic acid (LA) content. Whereas, for bacillariophytes, PUFA was mainly contributed by their eicosapentaenoic acid (EPA) content. Among the bacillariophytes, *Chaetoceros gracilis, Phaeodactylum tricornutum*, and *Thalassiosira weissflogii* (TRG10-P103), the high EPA content was observed during the exponential phase at 94.93 ± 39.89, 82.29 ± 8.34, and 78.62 ± 1.06 μg g^{-1} DW, respectively.

Meanwhile, the highest ALA was observed during the exponential phase in *Nanochlorum eucaryotum* (SLG4-11) (91.02 ± 6.26 μg g^{-1} DW), followed by *Tetraselmis suecica* (87.38 ± 15.17 μg g^{-1} DW). Likewise, *Nanochlorum eucaryotum* (SLG4-08) under the exponential phase showed the highest LA

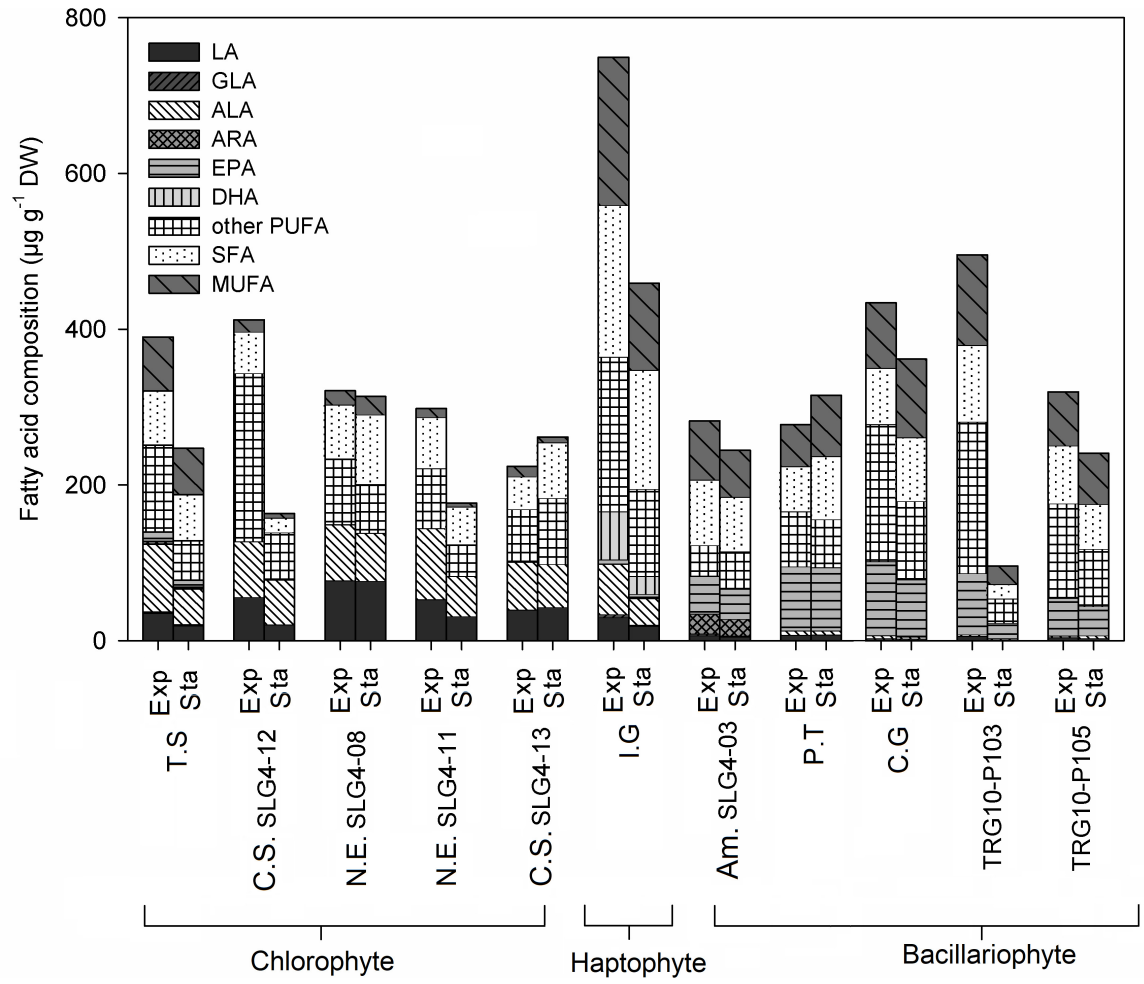

FIGURE 3 | Fatty acid (FA) composition (μg g^{-1} DW) of selected microalgae strains at exponential (Exp) and stationary (Sta) phase. Abbreviations of the strains as for **Figure 1**. ALA, α- linolenic acid; LA, Linoleic acid; ARA, Arachidonic acid; EPA, Eicosapentaenoic acid; GLA, γ-Linolenic acid; DHA, Docosahexaenoic acid; PUFA, Polyunsaturated fatty acid; SFA, Saturated fatty acid; MUFA, Monounsaturated fatty acid.

content at 77.21 ± 7.08 μg g^{-1} DW compared to other strains. Among the 10 strains analyzed, only *Isochrysis galbana* contained docosahexaenoic acid (DHA) at 61.76 ± 9.37 μg g^{-1} DW during the exponential phase and 23.00 ± 4.30 μg g^{-1} DW during the stationary phase, respectively. Meanwhile, γ-linolenic acid (GLA) was only detected at low concentrations in *Tetraselmis suecica* (exponential: 1.35 ± 0.20; stationary phase: 0.95 ± 0.16 μg g^{-1} DW), *Isochrysis galbana* (exponential: 3.81 ± 1.27; stationary phase: 1.47 ± 0.69 μg g^{-1} DW), *Amphora montana* (SLG4-03) (exponential: 2.34 ± 0.83; stationary phase: 1.28 ± 0.88 μg g^{-1} DW), and *Chaetoceros gracilis* (exponential:1.81 ± 1.04; stationary phase 2.23 ± 0.63 μg g^{-1} DW). The highest ARA was observed in *Amphora montana* (SLG4-03) at 25.08 ± 7.06 μg g^{-1} DW at the exponential phase.

Total Phenolic Content at Different Growth Phases

The phenolic content of the 10 strains ranged from 0.53 to 15.54 mg GAE g^{-1} DW under the exponential phase and from 0.79 to 11.80 mg GAE g^{-1} DW under the stationary phase (**Table 3**). The phenolic content varied among species, although generally higher content was observed in the exponential phase, except for *Amphora montana* (SLG4-03) and *Phaeodactylum tricornutum* (**Table 3**). The highest phenolic content was found under the exponential phase in *Tetraselmis suecica* at 15.54 ± 2.22 mg GAE g^{-1} DW, followed by *Isochrysis galbana* and *Thalassiosira weissflogii* (TRG10-P105) at 14.53 ± 2.04 and 12.46 ± 1.55 mg GAE g^{-1} DW, respectively (**Table 3**).

Interrelationship of Microalgae Antioxidant Capacity With Carotenoid, Fatty Acid, and Phenolic Contents at Different Growth Phases

The total antioxidant capacity (by ABTS and DPPH assays) showed a group-specific variation (**Figures 4A,B**). Higher ($p > 0.05$) total antioxidant capacity among the bacillariophyte and haptophyte strains compared to chlorophyte was found in *Thalassiosira weissflogii* (TRG10-P105) with ABTS and DPPH scavenging at 73.8 ± 1.94 (stationary phase) and 31.42 ± 0.80 (exponential phase) μmol TE g^{-1} DW, respectively. ABTS scavenging activity was also high in *Chaetoceros gracilis* (67.79 ± 7.45 μmol TE g^{-1} DW) and *Isochrysis galbana* (63.12 ± 6.51 μmol TE g^{-1} DW) during the stationary phase compared to the chlorophyte strains. Meanwhile, among the chlorophyte strains, the highest ($p > 0.05$) total antioxidant capacity was found in *Nanochlorum eucaryotum* (SLG4-08) under the exponential phase with ABTS scavenging at 40.11 ± 1.11 μmol TE g^{-1} DW. As for DPPH, *Isochrysis galbana* at the exponential phase showed a scavenging capacity at 32.11 ± 0.89 μmol TE g^{-1} DW. The highest $O_2^{\bullet-}$ scavenging capacity was observed in *Chaetoceros gracilis* and *Thalassiosira weissflogii* (TRG10-P105) under the early stationary phase at 30.4 ± 3.66 and 30.94 ± 3.15 μmol TE g^{-1} DW, respectively (**Figure 4C**). Similarly, the highest NO^- scavenging capacity was also observed in both strains during the early stationary phase (**Figure 4D**).

The results of the Parsons correlation indicated that carotenoids and phenolic compounds were significant contributors to the antioxidant scavenging capacity of the microalgae methanol extracts (**Table 4**). Meanwhile, a low influence with antioxidant capacity was observed for total fatty acid and PUFA compared to total carotenoid and total phenolic content. The variation in the antioxidant capacities of the bacillariophytes, chlorophytes, and haptophytes under different growth phases was closely related to the differences in the production of the bioactive compounds, especially carotenoids and phenolic compounds. In particular, for the selected bacillariophyte and haptophyte strains, the relatively higher R^2-values of the correlation analysis for ABTS (0.623), DPPH (0.714), and $\bullet NO^-$ (0.786) compared to total carotenoid, total fatty acid, and PUFA, suggest that their antioxidant capacity was significantly influenced by the phenolic content during the exponential phase ($p < 0.05$). Meanwhile, during the stationary phase, their antioxidant capacity was significantly contributed by carotenoids, as observed with ABTS (0.565), $\bullet NO^-$ (0.466),

TABLE 3 | Total phenolic content in the selected microalgae biomass for antioxidant compound production.

Division	Class	Strain	Total phenolic (mg GAE g^{-1} DW)	
			Exponential phase	Stationary phase
Chlorophytes (Green algae)	Trebouxiophyceae	*Nanochlorum eucaryotum* SLG4-08	**6.80 ± 1.68**	0.79 ± 0.11
		Nanochlorum eucaryotum SLG4-11	**7.27 ± 1.41**	5.97 ± 1.03
		Chlorella sorokiniana SLG4-12	**10.17 ± 1.44**	6.79 ± 1.76
		Chlorella sorokiniana SLG4-13	**5.34 ± 1.26**	3.11 ± 1.08
	Prasinophyceae	*Tetraselmis suecica*	**15.54 ± 2.22**	11.80 ± 0.60
Bacillariophytes (Diatom)	Bacillariophyceae (pennate diatom)	*Amphora montana* SLG4-03	0.53 ± 1.03	**5.97 ± 1.05**
		Phaeodoctylum tricornutum	10.64 ± 1.03	11.09 ± 1.55
	Mediophyceae (centric diatom)	*Thalassiosira weissflogii* TRG10-P103	**7.04 ± 1.67**	2.32 ± 1.82
		Thalassiosira weisflogii TRG10-P105	**12.46 ± 1.55**	9.38 ± 2.41
		Chaetoceros gracilis	**10.97 ± 1.21**	4.50 ± 1.24
Haptophytes	Coccolithophyceae	*Isochrysis galbana*	**14.53 ± 2.04**	7.32 ± 0.27

Significantly high value among growth phases are printed in bold ($p < 0.05$).

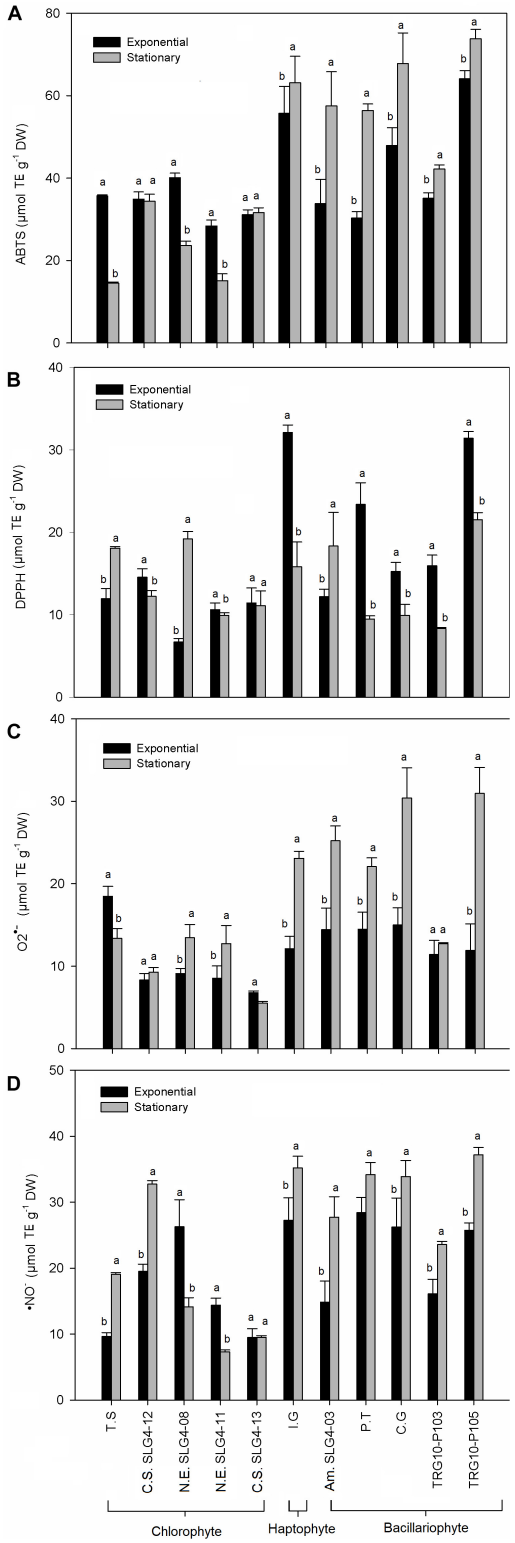

FIGURE 4 | Antioxidant activity obtained for the total antioxidant capacity and biological radical scavenging assay performed **(A)** $ABTS^{\bullet+}$, **(B)** DPPH•, **(C)** $O_2^{\bullet-}$, and **(D)** NO^-. Means denoted by a different letter indicate significant differences between growth phase ($p < 0.05$); Abbreviations of the strains as for **Figure 1**.

and $O_2^{\bullet-}$ (0.657). As for the chlorophyte strains, significant correlations with antioxidant capacity were observed in carotenoids (ABTS and $\bullet NO^-$) and phenolic ($\bullet NO^-$ and $O_2^{\bullet-}$) during both the exponential and stationary phases (**Table 4**).

Detailed analysis of the correlation with each carotenoid showed that their antioxidant capacity (ABTS and $O_2^{\bullet-}$) was significantly ($p < 0.05$) influenced by their fucoxanthin, diadinoxanthin, and β-carotene content for bacillariophytes and haptophytes (**Table 5**). For the chlorophyte strains during the exponential phase, ABTS showed a significant correlation with β-carotene (R^2-value = 0.615), lutein (0.615), and zeaxanthin (0.507). Similarly, $\bullet NO^-$ was also largely contributed by lutein (0.794), β-carotene (0.659), and neoxanthin (0.509). Meanwhile, a significant influence of α-carotene was observed for $O_2^{\bullet-}$ (0.534). In the stationary phase, chlorophytes were significantly influenced ($p < 0.05$) by the presence of violaxanthin (0.755 with $\bullet NO^-$), neoxanthin (0.623 with DPPH, 0.610 with $\bullet NO^-$), and lutein (0.582 with $\bullet NO^-$).

Some essential fatty acids also showed a significant correlation with antioxidant capacity, especially during the exponential phase. For bacillariophytes and haptophytes (**Table 6**), the contribution of LA (R^2 value = 0.559), ALA (0.510), and DHA (0.536) toward antioxidant capacity was observed for DPPH, while they were lower than the R^2 value of total phenolic (0.714) (**Table 4**). No significant relationships with essential fatty acids were found in the stationary phase of bacillariophytes and haptophytes strains. Meanwhile, for the chlorophytes, the highest influence on antioxidant capacity ($O_2^{\bullet-}$) was observed for ARA (0.923) and EPA (0.947). In addition, LA also showed a significant contribution toward ABTS (0.566) and $\bullet NO^-$(0.781). Significant relationships were also observed under the stationary phases of the chlorophytes for DPPH with ARA (0.503) and EPA (0.517).

DISCUSSION

In the present study, 26 indigenous tropical marine tropical microalgae from Malaysian waters were screened for their antioxidant capacity by ABTS and DPPH radical scavenging assays. Both assays measure the total antioxidant capacity through HAT and SET mechanisms of the polar and non-polar compounds present in the extract (Prior et al., 2005). Due to the varying nature and polarity of these compounds, the choice of solvents used during extraction determines its composition and effect on the biological activity. Methanolic solvent has been widely known to have an affinity for a wide range of bioactive compounds, mainly carotenoids and phenolics, as well as high antioxidative properties than extract obtained from other common solvents (Pereira et al., 2015; Safafar et al., 2015). In addition, the different antioxidant molecules in the microalgal methanolic extracts may also act through different mechanisms, which highlights the importance of using at least two assays for the evaluation of antioxidant capacity in natural extracts (Gülçin et al., 2011; Assunção et al., 2017). The results from the methanolic algal extract have often shown considerable variation even between species of the same genus or among multiple isolates of the same species (Safafar et al., 2015). Thus,

TABLE 4 | Parsons correlation, between antioxidant capacity and total carotenoid, total phenolic, total fatty acid (FAs), and total polyunsaturated fatty acid (PUFAs) in different algal group analyzed in this study.

Division	Growth stage	Antioxidant capacity	Total carotenoid	Total phenolic	Total FAs	Total PUFA
Bacillariophytes (Diatom) and haptophyte*	Exponential	ABTS	0.104	**0.623**	0.350	−0.142
		DPPH	0.275	**0.714**	0.324	0.188
		•NO⁻	0.141	**0.786**	0.141	0.403
		$O_2^{\bullet-}$	0.267	−0.255	0.267	0.069
	Stationary	ABTS	**0.565**	−0.027	0.117	0.064
		DPPH	−0.225	0.104	−0.074	−0.129
		•NO⁻	**0.466**	0.297	0.149	0.072
		$O_2^{\bullet-}$	**0.657**	0.082	0.175	0.121
Chlorophytes (Green algae)	Exponential	ABTS	**0.591**	0.023	0.486	0.399
		DPPH	−0.081	0.089	0.243	0.356
		•NO⁻	**0.655**	−0.271	0.027	0.168
		$O_2^{\bullet-}$	−0.222	**0.669**	0.437	0.173
	Stationary	ABTS	**0.517**	−0.283	−0.227	0.030
		DPPH	0.350	0.125	0.441	0.256
		•NO⁻	**0.642**	**0.505**	−0.226	−0.148
		$O_2^{\bullet-}$	0.135	0.168	−0.080	−0.260

*Significant correlations among growth phases are printed in bold ($p < 0.05$), $O_2^{\bullet-}$, Superoxide radical scavenging capacity; •NO⁻, Nitric oxide radical scavenging capacity. *Haptophyte (Isochrysis galbana) was analyzed with strains belonging to Bacillariophytes due to its similarity in carotenoid composition (see **Figure 2**).*

TABLE 5 | Parsons correlation between antioxidant capacity and each carotenoid compounds in different algal group analyzed in this study.

Division	Growth stage	Antioxidant capacity	Fuco	Diadino	Diato	β-caro	Neo	Viola	Zea	Lutein	α-caro
Bacillariophytes (Diatom) and haptophyte*	Exponential	ABTS	**0.530**	0.220	0.184	**0.581**	–	–	–	–	–
		DPPH	0.107	0.103	0.071	0.351	–	–	–	–	–
		•NO⁻	0.179	0.192	0.236	0.193	–	–	–	–	–
		$O_2^{\bullet-}$	−0.093	−0.112	−0.311	−0.584	–	–	–	–	–
	Stationary	ABTS	**0.609**	**0.472**	0.372	**0.689**	–	–	–	–	–
		DPPH	−0.211	−0.338	−0.229	−0.046	–	–	–	–	–
		•NO⁻	0.405	0.492	0.291	0.408	–	–	–	–	–
		$O_2^{\bullet-}$	**0.710**	**0.631**	0.523	**0.795**	–	–	–	–	–
Chlorophytes (Green algae)	Exponential	ABTS	–	–	–	**0.615**	0.434	0.466	**0.507**	**0.615**	−0.060
		DPPH	–	–	–	−0.400	−0.040	0.059	0.300	−0.374	0.304
		•NO⁻	–	–	–	**0.695**	**0.509**	0.412	0.270	**0.794**	−0.182
		$O_2^{\bullet-}$	–	–	–	0.146	0.373	0.475	0.190	−0.087	**0.534**
	Stationary	ABTS	–	–	–	0.390	0.108	0.446	0.421	0.487	−0.423
		DPPH	–	–	–	0.403	**0.623**	0.339	0.210	0.263	0.456
		•NO⁻	–	–	–	0.499	**0.610**	**0.755**	0.483	**0.582**	0.065
		$O_2^{\bullet-}$	–	–	–	0.178	0.387	−0.006	−0.242	0.099	0.342

*Significant correlations among growth phases are printed in bold ($p < 0.05$). Fuco, Fucoxanthin; Diadino, Diadinoxanthin; Diato, Diatoxanthin; β-caro, β carotene; Neo, Neoxanthin; Viola, Violaxanthin; Zea, Zeaxanthin; α-caro, α carotene; $O_2^{\bullet-}$, Superoxide radical scavenging capacity; •NO⁻, Nitric oxide radical scavenging capacity. *Haptophyte (Isochrysis galbana) was analyzed with strains belonging to Bacillariophytes due to its similarity in carotenoid composition (see **Figure 2**). -: not detected.*

when dealing with a large number of samples available with the nature of the compounds present in those extracts is unknown, screening by evaluating the antioxidant capacity of the entire extract adopted in this study is more appropriate.

DPPH scavenging assay has been described as less sensitive for samples with high carotenoids, but more sensitive with high phenolic sample (Amaro et al., 2015; Assunção et al., 2017). Meanwhile, ABTS assay is considered as highly sensitive on both carotenoid and phenolic rich sample in the measurement of antioxidant scavenging capacity (Safafar et al., 2015; Assunção et al., 2017). Thus, candidate strain selection was based on strain showing both higher ABTS and DPPH than the control. These selection criteria allowed a more consistent confirmation of the high antioxidant capacity species/strain selection. Based on overall comparisons of the results from the first screening, 10 indigenous tropical microalgal strains comprising several chlorophytes, bacillariophytes, and haptophytes strains were selected as potential candidates showing high total antioxidant capacity. The selected strains were *Nanochlorum eucaryotum* (SLG4-08), *Nanochlorum eucaryotum* (SLG4-11), *Chlorella*

TABLE 6 | Parsons correlation between antioxidant capacity and each essential fatty acid compounds in different algal group analyzed in this study.

Division	Growth stage	Antioxidant capacity	LA (C18:2 n-6)	GLA (C18:3 n-6)	ALA (C18:3 n-3)	ARA (C20:4 n-6)	EPA (C20:5 n-3)	DHA (C22:6 n-3)	Total PUFA	Total fatty acid
Bacillariophytes	Exponential	ABTS	0.332	−0.318	0.324	−0.100	−0.404	0.356	−0.142	0.350
(Diatom) and		DPPH	**0.559**	−0.142	**0.510**	−0.284	−0.349	**0.536**	0.188	0.324
haptophyte*		•NO$^-$	0.343	0.173	0.361	−0.440	−0.024	0.350	0.403	0.141
		$O_2^{\bullet-}$	−0.306	−0.018	−0.207	0.030	0.318	−0.202	0.069	0.267
	Stationary	ABTS	−0.041	0.048	−0.062	0.187	0.321	−0.106	0.064	0.117
		DPPH	0.034	−0.336	−0.103	0.188	−0.050	−0.106	−0.129	−0.074
		•NO$^-$	0.174	−0.193	0.186	−0.126	0.021	0.244	0.072	0.149
		$O_2^{\bullet-}$	0.033	−0.057	−0.018	0.301	0.336	0.006	0.121	0.175
Chlorophytes	Exponential	ABTS	**0.566**	−0.18	0.145	0.227	0.218	–	0.399	0.458
(Green algae)		DPPH	−0.538	0.015	**0.517**	0.036	0.135	–	0.356	0.243
		•NO$^-$	**0.781**	−0.251	0.056	−0.457	−0.487	–	0.168	0.027
		$O_2^{\bullet-}$	−0.357	−0.242	0.068	**0.923**	**0.947**	–	0.173	0.437
	Stationary	ABTS	−0.027	−0.053	0.019	−0.507	−0.545	–	0.03	−0.227
		DPPH	0.352	0.310	0.047	**0.503**	**0.517**	–	0.256	0.441
		•NO$^-$	−0.341	−0.076	0.021	0.117	0.112	–	−0.148	−0.226
		$O_2^{\bullet-}$	−0.045	0.349	−0.206	0.347	0.318	–	−0.026	−0.08

*Significant correlations among growth phases are printed in bold ($p < 0.05$). ALA, α- linolenic acid; LA, Linoleic acid; ARA, Arachidonic acid; EPA, Eicosapentaenoic acid; GLA, γ-Linolenic acid; DHA, Docosahexaenoic acid; $O_2^{\bullet-}$, Superoxide radical scavenging capacity; •NO$^-$, Nitric oxide radical scavenging capacity. *Haptophyte (Isochrysis galbana) was analyzed with strains belonging to Bacillariophytes due to its similarity in fatty acid composition (see **Figure 3**). –: not detected.*

sorokiniana (SLG4-12), *Chlorella sorokiniana* (SLG4-13), *Tetraselmis suecica*, *Amphora montana* (SLG4-03), *Chaetoceros gracilis*, *Thalassiosira weissflogii* (TRG10-P103), *Thalassiosira weisflogii* (TRG10-P105) and *Isochrysis galbana*. Among them, eight strains, except for *Chaetoceros gracilis* and *Isochrysis galbana,* which were previously isolated by Natrah et al. (2007), were newly established in this study, indicating that microalgal flora in Malaysian water bodies is a highly promising habitat for antioxidant producers. It was found that several strains, especially *Amphora montana* (SLG4-03), *Thalassiosira weisflogii* (TRG10-P105), *Chaetoceros gracilis*, and *Isochrysis galbana*, were two to three times better in scavenging ABTS radical in comparison to the value reported by Li et al. (2007); Goiris et al. (2012), Safafar et al. (2015), and Agregán et al. (2018) as shown in **Table 7**. In addition, the carotenoid content in most selected strains in this study showed higher value compared to that in the previously reported algal strains (**Table 7**). This includes *Isochrysis galbana* with 15.66 ± 2.13 mg g^{-1} DW carotenoid content compared to 4.33 ± 0.04 mg g^{-1} DW and 7.75 ± 0.13 mg g^{-1} DW as reported by Goiris et al. (2012) and Foo et al. (2017). *Chaetoceros gracilis* also showed 12.66 ± 2.45 mg g^{-1} DW of total carotenoid compared to the previously reported *Chaetoceros calcitrans* at 2.33 ± 0.14 (Goh et al., 2010) and 6.13 ± 0.25 mg g^{-1} DW (Foo et al., 2017), respectively. Some other selected species with high total carotenoid content compared to the previously reported one also includes the *Nanochlorum eucaryotum* (SLG4-08), *Amphora montana* (SLG4-03) and *Thalassiosira weissflogii* (TRG10-P105) as shown in **Table 7**. Our data also showed that bacillariophytes and haptophytes tended to show higher antioxidant capacities than chlorophytes. Although there are previous studies on the screening of antioxidants among different microalgae (Natrah et al., 2007; Goiris et al., 2012; Lauritano et al., 2016; Morowvat and Ghasemi, 2016; Assunção et al., 2017), this is the first thorough comparison across different divisions among the phyla Bacillariophyta, Chlorophyta and Haptophyta, for their antioxidant capacities and bioactive compositions, using the same experimental protocol. This is also the first study to compare the effects of compounds on antioxidants across the three divisions under different growth phases using a standardized unit for better comparison. These results clearly show that the variations in the antioxidant compounds and growth phase influence the antioxidant capacity across the taxonomical group (i.e., fucoxanthin in Bacillariophyta and lutein in Chlorophyta). The effect of the growth phase is mainly due to the nutrient availability factor, which affects the composition of the antioxidant compounds and, thus, the total antioxidant capacity of each algal strains, as we have discussed in detail below.

Our results showed that carotenoids contribute significantly to the antioxidant properties of the selected potential strains. A similar contribution has been reported in previous studies (Goiris et al., 2012; Safafar et al., 2015). It is known that although carotenoids play an important role in quenching reactive oxygen species, different carotenoid compounds exhibit different antioxidative power or action mechanisms (Young and Lowe, 2018). Each carotenoid antioxidant activity depends on the presence of the electron-rich conjugated system of the polyene and functional cyclic end groups, which enables them to scavenge harmful radicals either by electron transfer, radical adduct formation, or hydrogen atom transfer (Chen et al., 2014). For the selected bacillariophyte and haptophyte strains, under both exponential and early stationary phases, their high antioxidant capacity by carotenoids was significantly influenced by the presence of fucoxanthin and β-carotene. Fucoxanthin has higher antioxidant activity and sensitivity toward radicals than other carotenoids owing to the presence of the unique allenic

TABLE 7 | Comparison of antioxidant capacity and bioactive compounds in high potential Bacillariophyte, Haptophyte, and Chlorophyte strains.

Division	Microalgae strain	Antioxidant capacity		Carotenoid (mg g^{-1} DW)	Phenolic (mg GAE g^{-1} DW)	Growth phase	References
		ABTS (μmol TE g^{-1} DW)	DPPH (μmol TE g^{-1} DW)				
Chloro-phytes	*Nanochlorum eucaryotum* SLG4-08	40.11 ± 1.11	6.73 ± 0.39	10.68 ± 4.09	6.80 ± 1.68	Exp	This study
		23.60 ± 1.10	19.21 ± 0.90	5.01 ± 1.39	0.79 ± 0.11	Sta	
	Chlorella sorokiniana SLG4-12	34.88 ± 1.70	14.58 ± 0.97	5.70 ± 0.13	10.17 ± 1.44	Exp	
		34.3 ± 1.72	12.24 ± 0.70	5.59 ± 0.55	6.79 ± 1.76	Sta	
	Chlorella sorokiniana SLG4-13	31.13 ± 1.22	11.45 ± 1.79	2.27 ± 0.67	5.34 ± 1.26	Exp	
		31.62 ± 1.22	11.11 ± 1.60	1.45 ± 0.26	3.11 ± 1.08	Sta	
	Tetraselmis suecica	35.7 ± 0.27	11.96 ± 1.23	3.94 ± 0.63	15.54 ± 2.22	Exp	
		14.5 ± 0.30	18.09 ± 0.19	1.76 ± 0.24	11.80 ± 0.60	Sta	
	Nannochloropsis sp.	–	23.18 ± 0.55	–	–	Sta	Goh et al., 2010
	Scenedesmus sp. ME02*	–	3.71	0.61 ± 0.05	5.40 ± 0.28	Exp	Bulut et al., 2019
	*Chlamydomonas nivalis***	24.13 ± 0.47	–	–	15.07 ± 0.26	nd	Li et al., 2007
	Desmodesmus sp.	24.26 ± 0.60	*29.11%	6.70 ± 0.01	7.72 ± 0.08	Sta	Safafar et al., 2015
	*Scenedesmus rubescens***	–	68.68 ± 5.95	–	48.57 ± 3.99	Sta	Morowvat and Ghasemi, 2016
	*Chlorella vulgaris**	15.64	0.86	–	–	nd	Agregán et al., 2018
Bacillario-phytes	*Amphora montana* SLG4-03	33.79 ± 5.91	12.20 ± 0.94	11.66 ± 3.17	0.53 ± 1.03	Exp	This study
		57.46 ± 8.27	18.34 ± 4.09	18.97 ± 3.12	5.97 ± 1.05	Sta	
	Thalassiosira weissflogii TRG10-P103	35.10 ± 1.31	15.94 ± 1.26	7.14 ± 2.24	7.04 ± 1.67	Exp	
		42.18 ± 1.00	8.33 ± 0.15	3.60 ± 0.49	2.32 ± 1.82	Sta	
	Thalassiosira weisflogii TRG10-P105	64.12 ± 1.94	31.42 ± 0.14	8.63 ± 1.04	12.46 ± 1.55	Exp	
		73.78 ± 2.31	21.53 ± 0.84	12.15 ± 0.12	9.38 ± 2.41	Sta	
	Chaetoceros gracilis	47.88 ± 4.35	15.24 ± 2.31	8.80 ± 4.43	10.97 ± 1.21	Exp	
		67.79 ± 7.45	9.92 ± 0.79	12.66 ± 2.45	4.50 ± 1.24	Sta	
	Chaetoceros calcitrans	0.068	–	6.13 ± 0.25	12.24 ± 1.61	nd	Foo et al., 2017
	Chaetoceros sp.	–	39.22 ± 2.52	–	–	Sta	Goh et al., 2010
	*Chaetoceros calcitrans**	24.24 ± 1.64	–	2.33 ± 0.14	1.84 ± 0.11	nd	Goiris et al., 2012
Hapto-phytes	*Isochrysis galbana*	55.68 ± 6.51	32.11 ± 0.89	12.08 ± 1.80	14.53 ± 2.04	Exp	This study
		63.12 ± 6.51	15.83 ± 3.00	15.66 ± 2.13	7.32 ± 0.27	Sta	This study
	Isochrysis galbana	21.55 ± 1.58	–	4.33 ± 0.04	3.68 ± 0.39	nd	Foo et al., 2017
	Isochrysis sp.*	22.50 ± 0.93	–	7.75 ± 0.13	4.57 ± 0.18	Exp	Goiris et al., 2012

*All data were from algal methanolic extract, otherwise noted. Exp, Exponential phase; Sta, Stationary phase. *Ethanol/water mixture extract. **Hexane/ethyl acetate/water sequential extract. –: not determined.*

carbon bond (C-7') 5,6-monoepoxide, two hydroxyl groups, a carbonyl group, an acetyl group in the terminal ring, and six oxygen atoms in its molecular structure (Sachindra et al., 2007; Peng et al., 2011). Meanwhile, the antioxidant capacity of the chlorophyte strains was highly correlated with lutein and β-carotene, followed by neoxanthin and zeaxanthin content. In the stationary phase, their antioxidant capacity was largely influenced by violaxanthin, neoxanthin, and lutein, respectively. Similarly, the presence of the conjugated double bond in xanthophyll and carotenes such as β-carotene, vioxanthin, zeaxanthin, and other structurally related carotenoids enables them to be highly effective quenchers of singlet oxygen, which in algae, serves as part of their active defense mechanism against photooxidation (Stahl and Sies, 2003; Faraloni and Torzillo, 2017). While carotenoid compound accumulation is generally related to environmental conditions (i.e., light intensity), it has also been shown to be growth stage-dependent, mainly due to the effect of nutrient depletion on the later growth stages (Campo et al., 2007; McClure et al., 2018). Guo et al. (2016) reported an increase in fucoxanthin content at the beginning of cell growth and a decline in accumulation toward the end of the stationary phase due to nitrate depletion. Although the differences in carotenoid composition across division and growth phases have been previously reported, this study showed in detail what specific carotenoids are correlated with the antioxidant capacity under different growth phases.

Significant effects of phenolic compounds on the antioxidant activities of bacillariophytes and haptophytes were observed during the exponential phase, and for chlorophytes, during the exponential and stationary phases. Phenolic compounds have been linked to the antioxidative action in the biological system in several ways: as hydrogen-donating antioxidants reacting with RNS or ROS, breaking the cycle of new radical generation in the termination reaction, and also by chelating metal ions involved in free radical production (Pereira et al., 2009). It has been widely associated as one of the potential antioxidants in terrestrial plants for many years (Klejdus et al., 2010). However, its presence and contribution to the antioxidant capacity of microalgae have only recently been acknowledged; thus, data on this are still limited. Most previous studies focussed on chlorophytes, and there are still very few data available on bacillariophytes. Pereira et al. (2015) have reported the phenolic composition of several *Picochlorum* sp., *Desmochloris* sp., and *Nannochloris* sp. as being higher than that observed in several other species (5.8–114 mg GAE g^{-1} DW), except than *Picochlorum* sp., which has the highest phenolic content, specifically three phenolic acids (gallic, coumaric, and salicylic acids). Jerez-Martel et al. (2017) also observed high antioxidant activity in microalgal extracts rich in phenolic compounds, especially with high gallic and protocatechuic acid composition. Bulut et al. (2019) also found a significant correlation between antioxidant capacity and phenolic-rich *Scenedesmus* sp. ME02 extract (high in quercetin and rutin). In this study, we showed that phenolic compounds also contribute to the antioxidant activities of bacillariophytes and haptophytes. In addition, the contribution of phenolic content to the antioxidant capacity is particularly significant during the exponential phase. Because the phenolic compound accumulation is known to be growth-dependent, where their content is reduced under nutrient-limiting conditions (Goiris et al., 2012), the relative importance of phenolic content in antioxidant capacity in bacillariophytes and haptophytes may become higher during the exponential phase when carotenoid production decreases.

In the present study, the total fatty acid content, including PUFA, had little influence on the antioxidative capacity compared to carotenoid and phenolic content. This is contradictory to the reports that fatty acids and especially those with a high degree of unsaturation have been known to contribute to the antioxidant activity of various microalgae (de la Vega et al., 2011; Pereira et al., 2015; Banskota et al., 2018). However, when comparing each specific fatty acid compound, some significant relationships can be observed, especially during the exponential phase DPPH and $O_2^{\bullet-}$, which are known to be effective in measuring the antioxidant capacity of PUFA, especially for the conjugated LA (Fagali and Catalá, 2008; Amaro et al., 2015). For bacillariophyte strains, high influence by LA, ALA, and DHA was observed toward the antioxidant capacity. Meanwhile, for chlorophyte strains, ARA, EPA, and LA had the highest influence on antioxidant capacity than other fatty acids. The differences in the influence of specific PUFAs on antioxidant capacity are highly dependent on the PUFA composition of each strain, which changes under different growth phases and has also been shown to be species-dependent (Mansour et al., 2005; Schwarzhans et al., 2015). To our knowledge, there are no other studies to investigate the PUFA composition and their relation to antioxidant capacity in detail under different growth phases. Our results clearly showed that the contribution of fatty acid to the antioxidant capacity in microalgae should be evaluated with each specific fatty acid compound but not a combined component like total PUFA or total fatty acids.

This study showed that the selected 10 tropical microalgal strains belonging to Bacillariophyta, Chlorophyta, and Haptophyta, have potential as a new source of natural antioxidants, along with a substantial amount of carotenoids, fatty acids, and phenolic compounds. In particular, carotenoid and phenolic content significantly influenced the antioxidant capacity of the selected strains. This study also suggests that the antioxidant capacity and related bioactive compound production of these strains are growth phase-dependent. The higher antioxidant capacity observed in the bacillariophytes and the haptophyte was majorly influenced by their phenolic content (in the exponential phase) and their dominant carotenoid, fucoxanthin, and β-carotene (under stationary phase), which may have been acting synergistically or antagonistically with other compounds. Meanwhile, the antioxidant capacity of chlorophytes during the exponential phase is largely influenced by the presence of the carotenoid lutein and β-carotene, and during the stationary phase, by violaxanthin, neoxanthin, and lutein. The high carotenoid, phenolic, and fatty acid contents still have the potential to be enhanced further for commercial purposes by cultivation under certain environmental or abiotic stressors. Moreover, our results revealed several high antioxidants producing candidate strains that can be exploited as feedstocks for various other applications, such as pharmaceutical, aquaculture, and biofuels, with their high nutritional value. These potential strains include *Thalassiosira weissflogii* (TRG10-P105) (high fucoxanthin), *Isochrysis galbana* (high fucoxanthin, fatty acid, and DHA content), *Amphora montana* (SLG4-03) (high fucoxanthin and ARA), *Chlorella sorokiniana* (SLG4-12) (high total PUFA), and *Tetraselmis suecica* (high phenolic, ALA).

DATA AVAILABILITY STATEMENT

The raw data supporting the conclusions of this article will be made available by the authors, without undue reservation.

AUTHOR CONTRIBUTIONS

NR, KT, and TK conceived and designed the experiments. NR collected and analyzed data, prepared the manuscript, and participated in the assembly and editing of the final manuscript. KT and TK supervised and assisted in the interpretation of data, assembly, and editing of the manuscript. TK, MW, NK, and HK assisted in collecting algal material and editing of the manuscript. YY assisted in the fatty acid analysis and the

interpretation of the data. All authors contributed to the article and approved the submitted version.

FUNDING

This research was supported by the Japan Science and Technology Agency (JST)/Japan International Cooperation Agency (JICA), Science and Technology Research Partnership for Sustainable Development (SATREPS) through the project for Continuous Operation System for Microalgae Production Optimised for Sustainable Tropical Aquaculture (COSMOS) (Grant No. JPMJSA1509), and the SATREPS-COSMOS Matching Fund from the Ministry of Higher Education Malaysia. In addition, NR was also supported by the Japanese Government (Monbukagakusho: MEXT) doctoral scholarship.

ACKNOWLEDGMENTS

We wish to thank Mitsunori Iwataki, Kazuya Takahashi, and Lum Wai Mun of the University of Tokyo for their assistance with the molecular and morphological identification. We would also like to acknowledge Sanjoy Banerjee of Universiti Putra Malaysia for providing the microalgae strain *Chaetoceros gracilis* and *Isochrysis galbana*.

SUPPLEMENTARY MATERIAL

The Supplementary Material for this article can be found online at: https://www.frontiersin.org/articles/10.3389/fbioe.2020.581628/full#supplementary-material

REFERENCES

Abdullah, M. Z., Ali, J. M., Abolmaesoomi, M., Abdul-Rahman, S., and Hashim, O. H. (2017). Anti-proliferative, in vitro antioxidant, and cellular antioxidant activities of the leaf extracts from Polygonum minus Huds: effects of solvent polarity. *Int. J. Food. Prop.* 20, 846–862. doi: 10.1080/10942912.2017.1315591

Aburai, N., Ohkubo, S., Miyashita, H., and Abe, K. (2013). Composition of carotenoids and identification of aerial microalgae isolated from the surface of rocks in mountainous districts of Japan. *Algal Res.* 2, 237–243. doi: 10.1016/j.algal.2013.03.001

Agregán, R., Munekata, P. E. S., Franco, D., Carballo, J., Barba, F. J., Lorenzo, J. M., et al. (2018). Antioxidant potential of extracts obtained from Macro- (*Ascophyllum nodosum*, *Fucus vesiculosus* and *Bifurcaria bifurcata*) and Micro-Algae (*Chlorella vulgaris and Spirulina platensis*) assisted by ultrasound. *Medicines* 5:33. doi: 10.3390/medicines5020033

Amaro, H. M., Fernandes, F., Valentão, P., Andrade, P. B., Sousa-Pinto, I., Malcata, F. X., et al. (2015). Effect of solvent system on extractability of lipidic components of *Scenedesmus* obliquus (M2-1) and *Gloeothece* sp. on antioxidant scavenging capacity thereof. *Mar. Drugs.* 13, 6453–6471. doi: 10.3390/md13106453

Assunção, M. F. G., Amaral, R., Martins, C. B., Ferreira, J. D., Ressurreição, S., and Santos, S. D. (2017). Screening microalgae as potential sources of antioxidants. *J. Appl. Phycol.* 29, 865–877. doi: 10.1007/s10811-016-0980-7

Banskota, A. H., Sperker, S., Stefanova, R., McGinn, P. J., and O'Leary, S. J. B. (2018). Antioxidant properties and lipid composition of selected microalgae. *J. Appl. Phycol.* 31, 309–318. doi: 10.1007/s10811-018-1523-1

Bligh, E. G., and Dyer, W. J. (1959). A rapid method of total lipid extraction and purification. *Can. J. Biochem. Physiol.* 37, 911–917. doi: 10.1016/j.algal.2014.11.011

Brand-Williams, W., Cuvelier, M. E., and Berset, C. (1995). Use of a free radical method to evaluate antioxidant activity. *Food Sci. Technol.* 28, 25–30. doi: 10.1016/S0023-6438(95)80008-5

Bulut, O., Akın, D., Sönmez, Ç, Öktem, A., Yücel, M., and Öktem, H. A. (2019). Phenolic compounds, carotenoids, and antioxidant capacities of a thermotolerant *Scenedesmus* sp. (*Chlorophyta*) extracted with different solvents. *J. Appl. Phycol.* 31, 1675–1683. doi: 10.1007/s10811-018-1726-5

Campo, J., García-González, M., and Guerrero, M. (2007). Outdoor cultivation of microalgae for carotenoid production: current state and perspectives. *Appl. Microbiol. Biotechnol.* 74, 1163–1174. doi: 10.1007/s00253-007-0844-9

Chen, F., Sun, Z., Sun, P., Chen, T., and Zhang, J. (2014). Microalgal carotenoids: beneficial effects and potential in human health. *Food Funct.* 5, 413–415. doi: 10.1039/c3fo60607d

de la Vega, M., Díaz, E., Vila, M., and León, R. (2011). Isolation of a new strain of *Picochlorum* sp. and characterization of its potential biotechnological applications. *Biotechnol. Prog.* 27, 1535–1543. doi: 10.1002/btpr.686

Fagali, N., and Catalá, A. (2008). Antioxidant activity of conjugated linoleic acid isomers, linoleic acid and its methyl ester determined by photoemission and DPPH radical dot techniques. *Biophys. Chem.* 137, 56–62. doi: 10.1016/j.bpc.2008.07.001

Faraloni, C., and Torzillo, G. (2017). "Synthesis of antioxidant carotenoids in microalgae in response to physiological stress," in *Carotenoids*, eds D. J. Cvetkovic and G. S. Nikolic (London: IntechOpen), 143–157. doi: 10.5772/67843

Foo, S. C., Yusoff, F. M., Ismail, M., Basri, M., Yau, S. K., Khong, N. M. H., et al. (2017). Antioxidant capacities of fucoxanthin-producing algae as influenced by their carotenoid and phenolic contents. *J. Biotechnol.* 241, 175–183. doi: 10.1016/j.jbiotec.2016.11.026

Goh, S., Yusoff, F. M., and Loh, S. P. (2010). A comparison of the antioxidant properties and total phenolic content in a diatom, *Chaetoceros* sp. and a green microalga, *Nannochloropsis* sp. *J. Agr. Sci.* 2, 123–130. doi: 10.5539/jas.v2n3p123

Goiris, K., Muylaert, K., Fraeye, I., Foubert, I., De Brabanter, J., and De Cooman, L. (2012). Antioxidant potential of microalgae in relation to their phenolic and carotenoid content. *J. Appl. Phycol.* 24, 1477–1486. doi: 10.1007/s10811-012-9804-6

Gülçin, I., Topal, F., Çakmakçl, R., Bilsel, M., Gören, A. C., and Erdogan, U. (2011). Pomological features, nutritional quality, polyphenol content analysis, and antioxidant properties of domesticated and 3 wild ecotype forms of raspberries (*Rubus idaeus* L.). *J. Food Sci.* 76, 585–593. doi: 10.1111/j.1750-3841.2011.02142.x

Guo, B., Liu, B., Yang, B., Sun, P., Lu, X., Liu, J., et al. (2016). Screening of diatom strains and characterization of *Cyclotella cryptica* as a potential fucoxanthin producer. *Mar. Drugs* 14, 1–14. doi: 10.3390/md14070125

Gutteridge, J. M. C. (1995). Lipid peroxidation and antioxidants as bio-markers of tissue damage. *Clin. Chem.* 41, 1819–1828. doi: 10.1093/clinchem/41.12.1819

Hadi, S. I. I. A., Santana, H., Brunale, P. P. M., Gomes, T. G., Oliveira, M. D., and Matthiensen, A. (2016). DNA barcoding green microalgae isolated from neotropical inland waters. *PLoS One* 11:e0149284. doi: 10.1371/journal.pone.0149284

Halliwell, B. (2007). Biochemistry of oxidative stress. *Biochem. Soc. Trans.* 35, 1147–1150. doi: 10.1042/BST0351147

Jerez-Martel, I., García-Poza, S., Rodríguez-Martel, G., Rico, M., Afonso-Olivares, C., and Gómez-Pinchetti, J. (2017). Phenolic profile and antioxidant activity of crude extracts from microalgae and cyanobacteria strains. *J. Food. Qual.* 4, 1–8. doi: 10.1155/2017/2924508

Klejdus, B., Lojková, L., Plaza, M., Snóblová, M., and Stìrbová, D. (2010). Hyphenated technique for the extraction and determination of isoflavones in algae: ultrasound-assisted supercritical fluid extraction followed by fast chromatography with tandem mass spectrometry. *J. Chromatogr. A* 1217, 7956–7965. doi: 10.1016/j.chroma.2010.07.020

Lauritano, C., Andersen, J. H., Hansen, E., Albrigtsen, M., Escalera, L., Esposito, F., et al. (2016). Bioactivity screening of microalgae for antioxidant, anti-inflammatory, anticancer, anti-diabetes, and antibacterial activities. *Front. Mar. Sci.* 3:68. doi: 10.3389/fmars.2016.00068

Lavens, P., and Sorgeloos, P. (1996). *Manual on the Production and use of Live Food for Aquaculture*. FAO Fisheries Technical Paper. No. 361. Rome: FAO, 295.

Levasseur, M., Thompson, P. A., and Harrison, P. J. (1993). Physiological acclimation of marine phytoplankton to different nitrogen sources. *J. Phycol.* 29, 587–595. doi: 10.1111/j.0022-3646.1993.00587.x

Li, H. B., Cheng, K. W., Wong, C. C., Fan, K. W., Chen, F., and Jiang, Y. (2007). Evaluation of antioxidant capacity and total phenolic content of different fractions of selected microalgae. *Food Chem.* 102, 771–776. doi: 10.1016/j.foodchem.2006.06.022

Mansour, M. P., Frampton, D. M. F., Nichols, P. D., Volkman, J. K., and Blackburn, S. I. (2005). Lipid and fatty acid yield of nine stationary-phase microalgae: applications and unusual C24-C28 polyunsaturated fatty acids. *J. Appl. Phycol.* 17, 287–300. doi: 10.1007/s10811-005-6625-x

Mazlan, A. G., Zaidi, C. C., Wan-Lotfi, W. M., and Othman, B. H. R. (2005). On the current status of coastal marine biodiversity in Malaysia. *Indian J. Mar. Sci.* 34, 76–87.

McClure, D. D., Luiz, A., Gerber, B., Barton, G. W., and Kavanagh, J. M. (2018). An investigation into the effect of culture conditions on fucoxanthin production using the marine microalgae Phaeodactylum tricornutum. *Algal Res.* 29, 41–48. doi: 10.1016/j.algal.2017.11.015

Medlin, L. K., Elwood, H. J., Stickels, S., and Sogin, M. L. (1988). The characterization of enzymatically amplified eukaryotic 16S-like rRNA coding regions. *Gene* 71, 491–499. doi: 10.1016/0378-1119(88)90066-2

Morowvat, M. H., and Ghasemi, Y. (2016). Evaluation of antioxidant properties of some naturally isolated microalgae: identification and characterization of the most efficient strain. *Biocatal. Agric. Biotechnol.* 8, 263–269. doi: 10.1016/j.bcab.2016.09.010

Natrah, F. M. I., Yusoff, F. M., Shariff, M., Abas, F., and Mariana, N. S. (2007). Screening of Malaysian indigenous microalgae for antioxidant properties and nutritional value. *J. Appl. Phycol.* 19, 711–718. doi: 10.1007/s10811-007-9192-5

Oliveira, A. P., Silva, L. R., Ferreres, F., Guedes de Pinho, P., Valentão, P., Silva, B. M., et al. (2010). Chemical assessment and in vitro antioxidant capacity of *Ficus carica* latex. *J. Agr. Food Chem.* 58, 3393–3398. doi: 10.1021/jf9039759

Oroian, M., and Escriche, I. (2015). Antioxidants: characterization, natural sources, extraction and analysis. *Food Res. Int.* 47, 10–36. doi: 10.1016/j.foodres.2015.04.018

Peng, J., Yuan, J. P., Wu, C. F., and Wang, J. H. (2011). Fucoxanthin, a marine carotenoid present in brown seaweeds and diatoms: metabolism and bioactivities relevant to human health. *Mar. Drugs* 9, 1806–1828. doi: 10.3390/md9101806

Pereira, D. M., Valentão, P., Pereira, J. A., and Andrade, P. B. (2009). Phenolics: from chemistry to biology. *Molecules* 14, 2202–2211. doi: 10.3390/molecules14062202

Pereira, H., Custódio, L., and Rodrigues, M. J. (2015). Biological activities and chemical composition of Methanolic extracts of selected autochthonous microalgae strains from the Red Sea. *Mar. Drugs* 13, 3531–3549. doi: 10.3390/md13063531

Pham-Huy, L. A., He, H., and Pham-Huy, C. (2008). Free radicals, antioxidants in disease and health. *Int. J. Biomed. Sci.* 4, 89–95.

Prior, R. L., Wu, X., and Schaich, K. (2005). Standardized methods for the determination of antioxidant capacity and phenolics in foods and dietary supplements. *J. Agric. Food Chem.* 53, 4290–4302. doi: 10.1021/jf0502698

Re, R., Pellegrini, N., Proteggente, A., Pannala, A., Yang, M., and Rice-Evans, C. (1999). Antioxidant activity applying an improved ABTS radical cation decolorization assay. *Free Radic. Biol. Med.* 26, 1231–1237. doi: 10.1016/S0891-5849(98)00315-3

Rimet, F., Kermarrec, L., Bouchez, A., Hoffmann, L., Ector, L., and Medlin, L. K. (2011). Molecular phylogeny of the family Bacillariaceae based on 18s rDNA sequences: focus on freshwater *Nitzschia* of the section *Lanceolatae*. *Diatom. Res.* 26, 273–291. doi: 10.1080/0269249X.2011.597988

Robak, J., and Gryglewski, R. J. (1988). Flavonoids are scavengers of superoxide anions. *Biochem. Pharmacol.* 37, 837–841. doi: 10.1016/0006-2952(88)90169-4

Sachindra, N. M., Sato, E., Maeda, H., Hosokawa, M., Niwano, Y., and Kohno, M. (2007). Radical scavenging and singlet oxygen quenching activity of marine carotenoid fucoxanthin and its metabolites. *J. Agr. Food Chem.* 55, 8516–8522. doi: 10.1021/jf071848a

Safafar, H., van Wagenen, J., and Møller, P. (2015). Carotenoids, phenolic compounds and tocopherols contribute to the antioxidative properties of some microalgae species grown on industrial wastewater. *Mar. Drugs* 13, 7339–7356. doi: 10.3390/md13127069

Sansone, C., and Brunet, C. (2019). Promises and challenges of microalgal antioxidant production. *Antioxidants* 8:199. doi: 10.3390/antiox8070199

Schwarzhans, J. P., Cholewa, D., Grimm, P., Beshay, U., Risse, J. M., Friehs, K., et al. (2015). Dependency of the fatty acid composition of Euglena gracilis on growth phase and culture conditions. *J. Appl. Phycol.* 27, 1389–1399. doi: 10.1007/s10811-014-0458-4

Shebis, Y., Iluz, D., Kinel-Tahan, Y., Dubinsky, Z., and Yehoshua, Y. (2013). Natural antioxidants: function and sources. *Food Nutr. Sci.* 4, 643–649. doi: 10.4236/fns.2013.46083

Singleton, V. L., and Rossi, J. A. (1965). Colorimetry of total phenolics with phosphomolybdic phosphotungstic acid reagents. *Am. J. Enol. Vitic.* 16, 144–158.

Stahl, W., and Sies, H. (2003). Antioxidant activity of carotenoids. *Mol. Aspects Med.* 24, 345–351. doi: 10.1016/S0098-2997(03)00030-X

Štenclová, L., Fuèíková, K., Kaštovskı, J., and Pažoutová, M. (2017). Molecular and morphological delimitation and generic classification of the family Oocystaceae (*Trebouxiophyceae*. *Chlorophyta*). *J. Phycol.* 53, 1263–1282. doi: 10.1111/jpy.12581

Takaichi, S. (2011). Carotenoids in algae: distributions, biosynthesis and functions. *Mar. Drugs* 9, 1101–1118. doi: 10.3390/md9061101

Tompkins, Z. J., DeVille, M. M., Day, J. G., and Turner, M. F. (1995). *Catalogue of Strains. Culture Collection of Algae and Protozoa*. Kendal: Titus Wilson and Sons Ltd.

Venkatesan, J., Manivasagan, P., and Kim, S. (2015). "Marine microalgae biotechnology: present trends and future advances," in *Handbook of Marine microalgae*, ed. S. K. Kim (Cambridge, MA: Academic Press), 1–9. doi: 10.1016/b978-0-12-800776-1.00001-7

Young, A. J., and Lowe, G. L. (2018). Carotenoids–antioxidant properties. *Antioxidants* 7, 10–13. doi: 10.3390/antiox7020028

Zapata, M., Rodriguez, F., and Garrido, J. L. (2000). Separation of chlorophylls and carotenoids from marine phytoplankton: a new HPLC method using a reversed phase C8 column and pyridine-containing mobile phases. *Mar. Ecol. Prog. Ser.* 195, 29–45. doi: 10.3354/meps195029

Zhu, C. J., and Lee, Y. K. (1997). Determination of biomass dry weight of marine microalgae. *J. Appl. Phycol.* 9, 189–194. doi: 10.1023/A:1007914806640

Conflict of Interest: The authors declare that the research was conducted in the absence of any commercial or financial relationships that could be construed as a potential conflict of interest.

frontiers in Bioengineering and Biotechnology

ORIGINAL RESEARCH
published: 11 December 2020
doi: 10.3389/fbioe.2020.602721

High Productivity of Eicosapentaenoic Acid and Fucoxanthin by a Marine Diatom *Chaetoceros gracilis* in a Semi-Continuous Culture

Saki Tachihana[1], Norio Nagao[2†], Tomoyo Katayama[3], Minamo Hirahara[1], Fatimah Md. Yusoff[4], Sanjoy Banerjee[2], Mohamed Shariff[5], Norio Kurosawa[1], Tatsuki Toda[1] and Ken Furuya[1,3]*

[1] Department of Science and Engineering for Sustainable Innovation, Faculty of Science and Engineering, Soka University, Tokyo, Japan, [2] Laboratory of Marine Biotechnology, Institute of Bioscience, Universiti Putra Malaysia, Seri Kembangan, Malaysia, [3] Department of Aquatic Bioscience, Graduate School of Agricultural and Life Sciences, The University of Tokyo, Tokyo, Japan, [4] Department of Aquaculture, Universiti Putra Malaysia, Seri Kembangan, Malaysia, [5] Faculty of Veterinary Medicine, Universiti Putra Malaysia, Seri Kembangan, Malaysia

OPEN ACCESS

Edited by:
Fu-Li Li,
Qingdao Institute of Bioenergy and Bioprocess Technology (CAS), China

Reviewed by:
Jin Liu,
Peking University, China
Xiangzhao Mao,
Ocean University of China, China

***Correspondence:**
Tomoyo Katayama
tkatayama@g.ecc.u-tokyo.ac.jp

†Present address:
Norio Nagao,
Bluescientific Shinkamigoto Co., Ltd., Nagasaki, Japan

Specialty section:
This article was submitted to Bioprocess Engineering, a section of the journal Frontiers in Bioengineering and Biotechnology

Received: *04 September 2020*
Accepted: *23 November 2020*
Published: *11 December 2020*

Citation:
Tachihana S, Nagao N, Katayama T, Hirahara M, Yusoff FM, Banerjee S, Shariff M, Kurosawa N, Toda T and Furuya K (2020) High Productivity of Eicosapentaenoic Acid and Fucoxanthin by a Marine Diatom Chaetoceros gracilis in a Semi-Continuous Culture. Front. Bioeng. Biotechnol. 8:602721. doi: 10.3389/fbioe.2020.602721

Significantly high eicosapentaenoic acid (EPA) and fucoxanthin contents with high production rate were achieved in semi continuous culture of marine diatom. Effects of dilution rate on the production of biomass and high value biocompounds such as EPA and fucoxanthin were evaluated in semi-continuous cultures of *Chaetoceros gracilis* under high light condition. Cellular dry weight increased at lower dilution rate and higher light intensity conditions, and cell size strongly affected EPA and fucoxanthin contents. The smaller microalgae cells showed significantly higher ($p < 0.05$) value of 17.1 mg g-dw^{-1} fucoxanthin and 41.5% EPA content per total fatty acid compared to those observed in the larger cells. *Chaetoceros gracilis* can accumulate relatively higher EPA and fucoxanthin than those reported previously. In addition, maintenance of small cell size by supplying sufficient nutrients and light energy can be the key for the increase production of valuable biocompounds in *C. gracilis*.

Keywords: microalgae production, eicosapentaenoic acid, fucoxanthin, *Chaetoceros gracilis*, dilution rate

INTRODUCTION

Microalgae have been utilized for the production of high value-added compounds such as carotenoids (Foo et al., 2015, 2017) and poly unsaturated fatty acids (PUFA) including eicosapentaenoic acid (EPA) and docosahexaenoic acid (DHA) (Chrismadha and Borowitzka, 1994; Yang et al., 2017). Among different microalgal groups, diatoms are known to be efficient producers of fucoxanthin and EPA, and have been widely used in aquaculture for feeding juvenile fish and shrimp to improve growth rate, survival rate and nutritional value (Enright et al., 1986). In addition to aquaculture, microalgae with high EPA and fucoxanthin contents have the potential to be used in food, cosmetic and pharmaceutical industries. Furthermore, EPA is one of the essential fatty acids which humans are unable to produce, and has both anti-arteriosclerosis (Hata et al., 1983) and anti-inflammation properties (Mickleborough et al., 2009). Fucoxanthin has anti-oxidation

and anti-obesity effects on humans (Kanazawa, 2012). Therefore, there is a need for technological development to enhance valuable compounds production by diatoms to meet high social and economic demands (Krichnavaruk et al., 2007; Monkonsit et al., 2011; Kaspar et al., 2014).

Sufficient light intensity and nutrient supply are required for effective microalgal production. Since algal production is the process whereby light energy is transferred to chemical energy by photosynthesis (Mata et al., 2010), theoretically, high growth rate can be obtained under high light intensity. However, excess light can cause photoinhibition and decrease or impair the growth rate (Imaizumi et al., 2016). Therefore, light intensity should be adjusted to an optimal level, which is determined by the cell density.

Nutrient supply is also critical for effective biomass production. In high cell density culture with sufficient light intensity, nutrients are absorbed rapidly, thus resulting in inadequate nutrients for the cells. Light intensity and nutrient concentration affect not only biomass productivity, but also physiological cell quality. In high-light stress conditions, algal cells tend to lower cell division rate and store excess light energy in the form of starch and/or lipids (Williams and Laurens, 2010; Xin et al., 2010). On the other hand, insufficient nutrient concentration can also decrease biomass yield and alter the cell state. For example, Kaspar et al. (2014) observed that increase in the cell size and morphology transformation of *Chaetoceros calcitrans* cultured in batch mode occurred at the late phase of culture when nutrients were almost exhausted. This observation suggested that morphological change could be caused by nutrient deprivation. However, the relationship between the cell state and the production of biocompounds, such as EPA and fucoxanthin, has not been adequately investigated. Thus, it is necessary to investigate the mechanisms involved in the accumulation of these valuable compounds by a specific diatom at varying cell states under different light intensities and nutrient conditions.

The dilution rate in semi-continuous or continuous cultures can effectively regulate both light intensity and nutrient availability to the microalgal cells, which are the main operational factors for high biomass production, which in turn affect growth, cell composition and production of valuable compounds (Fernández Sevilla et al., 1998). At high dilution rate, high nutrient supply to algal cells can be achieved. However, cell density tends to decline with the high rate of periodical outflow of culture. A decrease in cell density causes an increase in light intensity exposure per cell, and accordingly cause photoinhibition when a photobioreactor receives high light energy. In contrast, at low dilution rate, photoinhibition is prevented for most of the culture period owing to increase of cell density. However, due to high cell density with low nutrient feed rate under sufficient light, rapid intake of nutrients by cells is likely to cause nutrient deficiency. Thus, dilution rate affects both light intensity and nutrient supply rate, and subsequently, affecting biomass production and chemical composition of the cell. Thus, by optimizing dilution rate, there is a potential for high biomass productivity and enhancing cells to contain intended valuable compound. In order to maximize biomass productivity and improve the concentration of EPA and fucoxanthin production by diatoms, optimization of dilution rate is necessary in a continuous culture under high light intensity. Therefore, the objective of this study was to examine the effect of dilution rate on biomass production and accumulation of EPA and fucoxanthin by the marine diatom *Chaetoceros gracilis* in semi-continuous culture under high irradiance.

MATERIALS AND METHODS

Microalga and Culture Medium

Chaetoceros gracilis (UPMC-A0010-2) was isolated from Port Dickson, Malaysia and cultured in modified Conway medium which consisted of (per liter): 200 mg of KNO_3; 20 mg of Na_3PO_4; 45 mg of Na_2EDTA; 33.6 mg of H_3BO_3; 1.3 mg of $FeCl_3{\cdot}6H_2O$; 0.36 mg of $MnCl_2{\cdot}4H_2O$; 2.1 mg of $ZnCl_2$; 2.0 mg of $CoCl_2{\cdot}6H_2O$; 0.9 mg of $(NH4)_6Mo_7O_{24}{\cdot}4H_2O$; 2.0 mg of $CuSO_4{\cdot}5H_2O$; 0.2 mg of Thymine; 0.01 mg of Cyanocobalamin; and 15 mg of $Na_2SiO_3{\cdot}9H_2O$. The pre-culture was grown in a 1 L column reactor at 30°C under light intensity of 300 μmol m^{-2} s^{-1}. The culture was aerated at a rate of 0.2 L min^{-1}.

Culture Conditions

Three different dilution rates of 0.1, 0.2, and 0.4 d^{-1} were applied to the *C. gracilis* culture. The temperature was maintained at 30 ± 1°C and 2% CO_2 gas was added through a 0.2 μm filter at the flow rate of 0.2 L min^{-1}. The volume of fresh medium supplied for dilution rates of 0.1, 0.2, and 0.4 d^{-1} was 100, 200, and 400 mL, respectively. Light intensity of 300 μmol m^{-2} s^{-1} was applied in all dilution rate treatments. In the dilution rates of 0.2 and 0.4 d^{-1}, light intensity increased up to 1,000 μmol m^{-2} s^{-1}. Since nutrient intake increased with the increase in light intensity, 2.5 times higher nutrient concentration than that under 300 μmol m^{-2} s^{-1} was added. The photoperiod was maintained at 12 L:12 D in all experimental conditions.

Photobioreactor Setup

The culture system consisted of three parts: (1) a column reactor with culture medium supplying system, (2) a LED light, and (3) a thermos-regulator with a water bath (**Figure 1**). The column reactor was made of a transparent glass with an inner diameter of 6.0 cm and a height of 52 cm. Working volume and light-receiving area in this reactor were 1.0 L and 0.021 m^2, respectively. The LED light was installed along the reactor. The light intensity was confirmed at the surface of the reactor using a quantum sensor (QSPL-2101, Biospherical Instruments, United States). Carbon dioxide concentration was controlled by a flow meter, and air with 2% CO_2 at a rate of 0.2 L min^{-1} was introduced to the reactor through 0.2 μm filter continuously. The temperature was maintained by a thermos-regulator with a water bath. An electric fan was installed at the back side of LED light to dissipate heat. Sampling was conducted once in a day before the light period, and fresh medium was added until the culture volume reached 1.0 L. All operations were conducted under sterilized conditions.

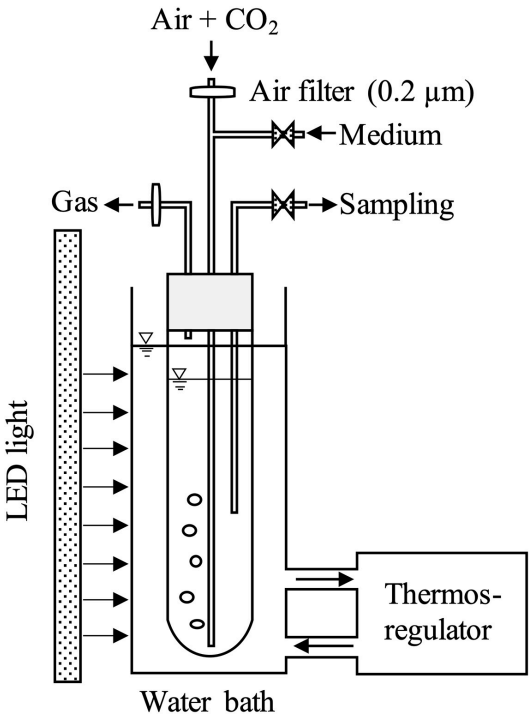

FIGURE 1 | Schematic diagram of the column photobioreactor: inner diameter of 6.0 cm, working volume of 1.0 L. Light was provided to the surface of the water bath at 12L:12D. Filtered air (0.2 μm) was added with 2% CO_2 from the bottom of the column reactor at a flow rate of 0.2 L min^{-1}.

Analytical Methods

Dry weight, cell numbers, nutrient concentration, pigment composition and fatty acid composition were measured in triplicates. Cellular dry weight and areal production rates were calculated.

Biomass concentration was determined by dry weight (g-dw L^{-1}) and cell number (cells mL^{-1}) counts. For dry weight measurement, cell suspensions were filtered through Whatman GF/A filter and rinsed with 0.5 M ammonium formate to remove NaCl. The filters were dried in an oven at 70°C for 24 hrs and cooled down to room temperature in a desiccator before weighing. Cell numbers were counted daily using a hemocytometer. Cellular dry weight (CDW: ng-dw $cell^{-1}$) was calculated using the following equation:

$$CDW = \frac{DW}{N} \quad (1)$$

where DW is dry weight (g-dw L^{-1}) and N is cell numbers (cells mL^{-1}).

Samples for nutrient analyses (NO_3-N, PO_4-P, and SiO_2-Si) were collected from filtrate through Whatman GF/A filters. The aliquots were stored at −20°C and thawed for analysis by an autoanalyzer (QuAAtro 39, BL TEC, Japan).

The dominant pigments for diatoms, chlorophyll *a* and fucoxanthin, were analyzed using a LCMS (liquid chromatography mass spectroscopy, Prominence-i LC-2030 3D, Shimazu Co., Ltd., Kyoto, Japan). Samples were filtered through glass fiber filters (GF/A, Whatman, United States) for the pigment analysis. The filters frozen at −80°C were thawed and soaked with 2 mL methanol, then extracted by ultrasound for 10 min. The samples were stored at 4°C for up to 72 h, and then the pigment analysis was conducted by using the LCMS equipped with a reversed phase column (XBridge, 2.1 × 150 mm i.d., C18, 5 μm, Waters Co., Ltd., Tokyo, Japan) and a photodiode array detector. Aliquots of 10 μL were used for the LCMS analysis. The mobile phase consisted of the eluent A (methanol: 0.5 M ammonium acetate = 8:2, v/v) and eluent B (methanol: ethyl acetate = 7:3, v/v) as described by Wright (1997). The following elution gradient was used: 0% B for 24.9 min, 100% B at 25 min for 9 min, 0% B until the end of the run at 39 min. The flow rate was maintained at 0.5 mL min^{-1}, and the column temperature was 40°C during the analysis. The peaks were identified using standards obtained from the Danish Hydraulic Institute (Denmark).

For the extraction and analysis of fatty acids methyl ester (FAME), aliquots were filtered through a GF/A filter every 3 days and subsequently the filters were kept at −25°C until subjected to fatty acid analysis. The fatty acid composition was analyzed by the modified method of Bligh and Dyer (1959). The filtered samples were soaked in a 3 mL chloroform: methanol (1: 2, v/v) solution and extracted by sonication for 10 min. The extract was centrifuged at 2,000 rpm for 10 min, and the supernatant was collected. Ultrapure water of 10 mL was added to the extract, and then the extract was separated to remove impurities by centrifugation at 2,000 rpm for 10 min.

A known amount of C21 (heneicosane) was added to the extract as the internal standard. Fatty acids in the extract were transmethylated with acetyl chloride: methanol (5:100, v/v) solution at 100°C for 60 min to form FAME. The FAME was immersed in hexane and quantified by a gas chromatograph-mass spectrometer (GC-MS) (6890N GC/5973MS, Agilent Technologies, United States), equipped with a capillary column (30 m DB-5MS, Phenyl-Methyl/Silicone: J&W Scientific Inc., Folsom, CA, United States). Helium was used as a mobile phase at a flow rate of 1 mL min^{-1}. The oven temperature was raised from 60 to 310°C at a rate of 5°C min^{-1}. The injector and ion source temperatures were held at 310 and 230°C, respectively. Data analysis software (Agilent MSD Productivity ChemStation For GC and GC-MS Systems Data Analysis, Agilent Technologies, United States) was used for GC-MS data analysis. Identification of each fatty acid was conducted by comparison between the retention time and the mass spectrum of the standard, and quantified by comparing their peak area with that of the internal standard.

Areal production rate (P_A: g-dw $m^{-2}d^{-1}$) was calculated according to the following equation:

$$P_A = \frac{DW_n \times V - DW_{n-1} \times V \times (1 - R)}{A \times T} \quad (2)$$

Where DW_n is dry weight at day N (g-dw L^{-1}), V is volume of the reactor (L), R is dilution rate (d^{-1}), A is surface area of the reactor (m^2), and T is culturing time (day).

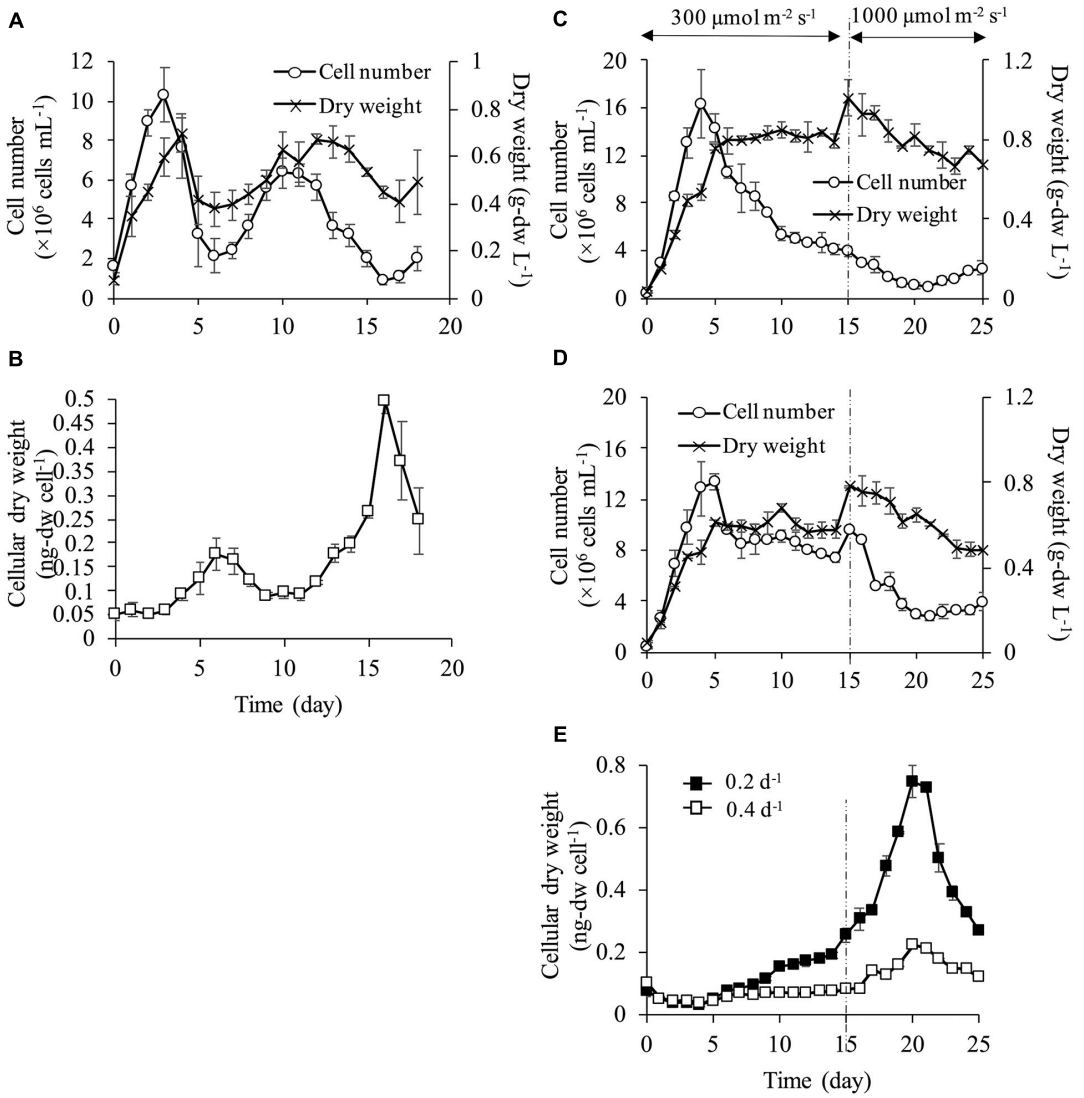

FIGURE 2 | Growth characteristics at each dilution rate. Cell number and dry weight **(A)** and cellular dry weight **(B)** at dilution rate of 0.1 d^{-1} under 300 μmol m^{-2} s^{-1}. At dilution rates of 0.2 and 0.4 d^{-1}, light intensity was set at 300 μmol m^{-2} s^{-1} during days 0–14, and at 1,000 μmol m^{-2} s^{-1} during days 15–25. Cell number and dry weight at dilution rate of 0.2 d^{-1} **(C)** and dilution rate of 0.4 d^{-1} **(D)**. Cellular dry weight of dilution rates of 0.2 d^{-1} and 0.4 d^{-1} **(E)**.

Statistical Analysis

All data were tested for normality before being analyzed using a two-way ANOVA to assess the impacts of dilution rates, light intensity and their interactions at $p < 0.05$.

RESULTS AND DISCUSSION

Cell Density and Cellular Dry Weight

Cell density fluctuated and did not reach a steady state at the dilution rate of 0.1 d^{-1} (**Figure 2A**). The cell numbers on day 0 was 1.56 ± 0.26 × 10^6 cells mL^{-1}, and then sharply increased up to 10.3 ± 1.3 × 10^6 cells mL^{-1} on day 3. However, the cells decreased to 2.15 ± 0.87 × 10^6 cells mL^{-1} on day 6 and fluctuated subsequently. Dry weight exhibited a similar trend of fluctuation as the cell numbers, but the was not exactly in the same proportion. The difference in the proportion of the change between the cell numbers and dry weight indicated that the dry weight per single cell changed during the experimental period. Cellular dry weight was approximately 0.05 ng-dw $cell^{-1}$ until day 4 when the cell numbers reached the maximum values (**Figure 2B**). However, cellular dry weight increased up to 0.180 ng-dw $cell^{-1}$ on day 7 with the decrease in cell numbers. During day 7–11, when the second increase in cell numbers occurred, cellular dry weight decreased again. On day 16 when cell numbers reached the minimum, cellular dry weight increased up to the maximum of 0.50 ng-dw $cell^{-1}$ which corresponded to the 10-fold increase of cellular dry weight at the beginning of the culture. The dilution rate of 0.1 d^{-1}, which provided the lowest nutrient supply and the lowest discharge of culture medium

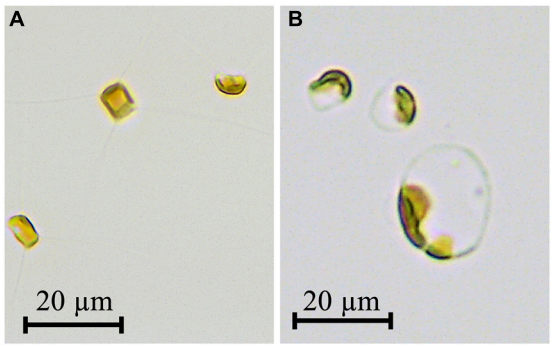

FIGURE 3 | Photomicrographs of *Chaetoceros gracilis* grown at dilution rate of 0.2 d^{-1} under 300 μmol m^{-2} s^{-1} **(A)** and dilution rate of 0.2 d^{-1} under 1,000 μmol m^{-2} s^{-1} **(B)**. Scale bar = 20 μm.

did not show a steady state of cell density and cellular dry weight in a semi-continuous culture. This result showed that cell physiological condition changed possibly due to insufficient nutrient or other stress factors, and thus stable cell division rate could not be maintained. The steady state of both cell density and cell physiology could not be attained at a dilution rate of 0.1 d^{-1} suggesting that both consistent cell quality and stable biomass production rate could not be achieved in the actual production process for commercialization.

At a dilution rate of 0.2 d^{-1}, dry weight increased until day 5 and it reached a steady state at approximately 0.8 g L^{-1} during the light intensity of 300 μmol m^{-2} s^{-1}. However, the cell numbers showed different behavior from the dry weight under the same light condition. The cell numbers increased rapidly from the onset of the culture and reached the maximum of $16.4 \pm 2.9 \times 10^6$ cells mL^{-1} on day 4. Then, the cell numbers continued decreasing after day 4, although the dry weight was maintained (**Figure 2C**). After increasing the light intensity up to 1,000 μmol m^{-2} s^{-1}, the cell numbers continued decreasing and dry weight surpassed 0.8 g L^{-1} for a few days. However, dry weight gradually decreased after that and was stable at a lower level compared to values under 300 μmol m^{-2} s^{-1}. This result showed that a stable dry weight under 300 μmol m^{-2} s^{-1} could be achieved due to the increase in cellular dry weight, suggesting that cell physiological condition could be changed in the process.

During the late phase of the culture at a dilution rate of 0.2 d^{-1}, unusually large cells of about 20 μm in diameter were observed (**Figure 3B**). Compared to cells in the initial phase (**Figure 3A**), their appearance changed from typical rectangular to round-shape with an increase in cell size. Furthermore, a brown plastid only occupied up to a small portion of the large round cell, although the plastid completely filled up the small rectangular cell. This indicated that pigment contents per dry weight decreased in large round-shaped cells.

At a dilution rate of 0.4 d^{-1} under 300 μmol m^{-2} s^{-1}, both the cell density and dry weight reached a steady state after day 6 (**Figure 2D**) and cellular the dry weight was stable at low values of <0.1 ng-dw $cell^{-1}$ (**Figure 2E**). Increases in cell numbers and dry weight were observed temporally after day 15 with increasing light intensity but cell numbers decreased after a few days. While only dry weight reached a steady state at a dilution rate of 0.2 d^{-1} under 300 μmol m^{-2} s^{-1}, both cell numbers and dry weight were maintained at a dilution rate of 0.4 d^{-1}. Cellular dry weight at a dilution rate of 0.4 d^{-1} was maintained by small-sized cells ranging from 0.04 to 0.07 ng-dw $cell^{-1}$ under a light intensity of 300 μmol m^{-2} s^{-1}. However, the cell size increased resulting in a maximum cellular dry weight of 0.22 ng-dw $cell^{-1}$ on day 20 under 1,000 μmol m^{-2} s^{-1} even at the highest dilution rate (i.e., the highest nutrient supplying rate). At dilution rates of 0.2 and 0.4 d^{-1}, the cell numbers slightly increased from day 20 and cellular dry weight decreased under a light intensity of 1,000 μmol m^{-2} s^{-1}. This result indicated that cell division started again from day 20 as seen by the smaller cell size (**Figure 2E**).

Generally, in semi-continuous and continuous cultures, nutrients are introduced in a reactor periodically or continuously, and microalgae use the nutrients for their growth. Therefore, biomass production increases with increasing nutrient availability if sufficient light energy and carbon dioxide are provided (Ruiz-marin et al., 2010; Mcginn et al., 2012; Imaizumi et al., 2014). However, interestingly this general phenomenon was not observed in the current study. It was illustrated that under a relatively high light intensity of 300 μmol m^{-2} s^{-1}, *C. gracilis* did not maintain its cell numbers and dry weight at a low dilution rate of 0.1 and 0.2 d^{-1} even under continuous nutrient supply. The phenomenon of increase in cellular dry weight was observed (1) at lower dilution rate, which was low flow rate of culture media and (2) at higher light intensity, where cells consumed high amount of nutrient to grow. This suggested that stress factors such as nutrient deprivation, accumulation of inhibitor in the medium and excess light intensity would attribute to the decrease in cell numbers and enlargement of cell size.

Nutrient Concentration

Concentrations of nitrogen (NO_3-N), phosphorus (PO_4-P) and silicon (SiO_2-Si) in the culture media showed their decreased concentrations with time indicating their uptake by the microalgae (**Figure 4**). At every dilution rate, nitrogen and phosphorus decreased during the culture, yet they did not become depleted. In the case of high light intensity of 1,000 μmol m^{-2} s^{-1} at dilution rates of 0.2 and 0.4 d^{-1}, nitrogen and phosphorus concentrations were at least more than 3.60 and 0.35 mM, respectively. In contrast, the silicon concentration was significantly low during the culture period. The ratio of silicon concentration in the reactor to an input concentration of 1.88 mM was low, and 95.5 and 96.3% of silicon were absorbed at dilution rates of 0.2 and 0.4 d^{-1}, respectively. A considerable increase in cellular dry weight was observed in a dilution rate of 0.2 d^{-1} under a light intensity of 1,000 μmol m^{-2} s^{-1} as mentioned above, and this phenomenon was possibly attributed to the depletion of silicon. Kaspar et al. (2014) reported that change in cell morphology and enlargement of cell size of *C. calcitrans* could be caused by nutrient depletion. In the current study, more silicon supply might be necessary to avoid the cell enlargement.

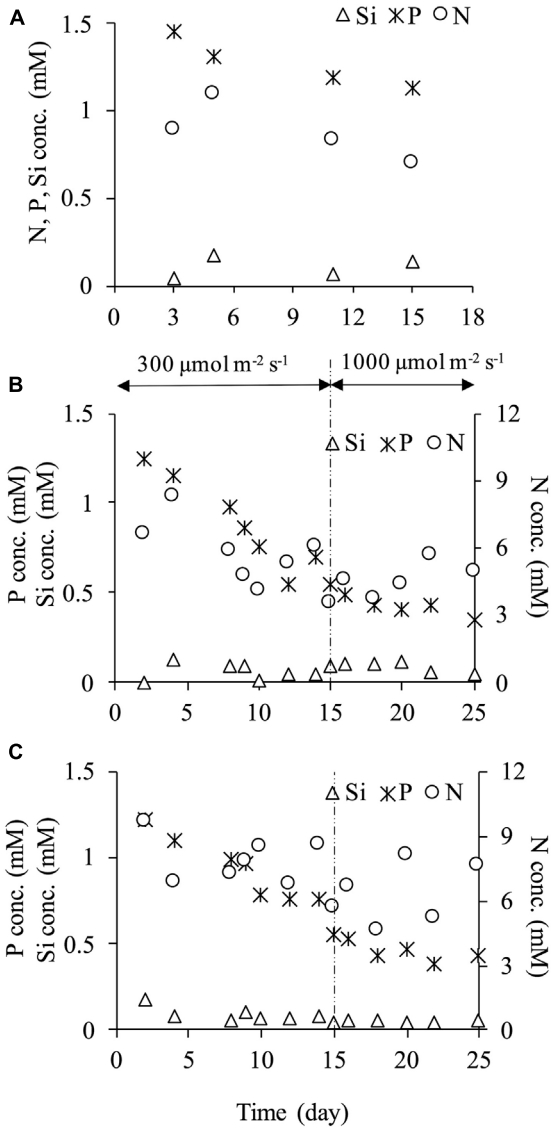

FIGURE 4 | Nutrients concentration (NO_3-N, PO_4-P, SiO_2-Si) at dilution rate of 0.1 d^{-1} **(A)**, 0.2 d^{-1} **(B)** and 0.4 d^{-1} **(C)**.

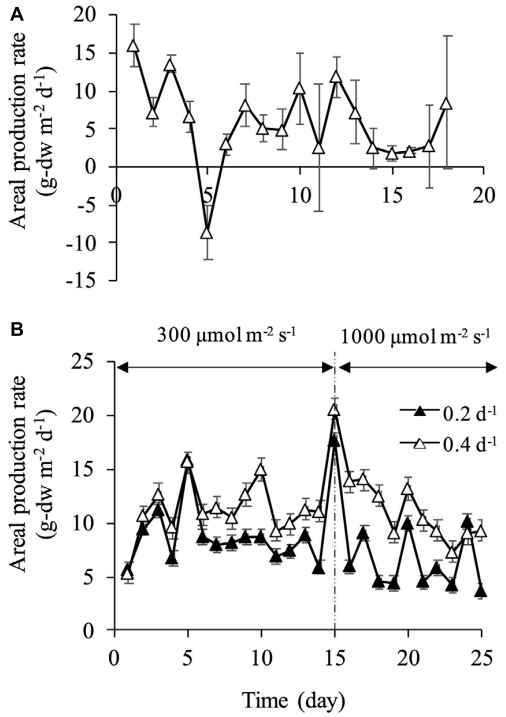

FIGURE 5 | Areal and volumetric production rates at dilution rate of 0.1 d^{-1} **(A)** and dilution rates of 0.2 and 0.4 d^{-1} **(B)**.

The high silicon uptake was also observed even at the dilution rate of 0.4 d^{-1} under 300 µmol m^{-2} s^{-1} (**Figure 4C**). Tantanasarit et al. (2013) examined nutrient uptake kinetics by *C. calcitrans* in high nutrient concentrations, and they showed that this species could absorb nutrient beyond its requirement level and accumulated it in its vacuoles. In *C. gracilis* cells cultured in the present study, a similar phenomenon may have occurred. In other words, *C. gracilis* possibly absorbed more silicon than was needed and accumulated it in its vacuoles. Cell enlargement might have occurred due to silicon deficiency as the diatom has a high demand for silicon, resulting in unsustainable growth.

Production Rate

At a dilution rate of 0.1 d^{-1}, areal production rate became negative value on day 5 due to the fluctuation of cell density and dry weight (**Figure 5A**). Overall, aerial production rate varied significantly in the range of −8.61 to 16.1 g-dw m^{-2} d^{-1}. The relatively stable production rate was attained at dilution rates of 0.2 and 0.4 d^{-1}, which ranged from 7 to 9 g-dw m^{-2} d^{-1} and from 10 to 14 g-dw m^{-2} d^{-1}, respectively (**Figure 5B**). The production rate increased instantaneously on day 15 when light intensity was increased to 1,000 µmol m^{-2} s^{-1}, and the maximum production rate of 17.7 g-dw m^{-2} d^{-1} at a dilution rate of 0.2 d^{-1} and 20.6 g-dw m^{-2} d^{-1} at a dilution rate of 0.4 d^{-1} were observed, corresponding to volumetric production rate of 0.372 and 0.433 g-dw L^{-2} d^{-1}, respectively. In previous studies of biomass production by diatoms, areal production of 2.24 g-dw m^{-2} d^{-1} by *C. gracilis* (Hatate et al., 1998), 10.1 g-dw m^{-2} d^{-1} by *Nitzschia* sp. (Silva-Aciares and Riquelme, 2008), 13.1 g-dw m^{-2} d^{-1} by *Fistulifera* sp. (Satoh et al., 2013), and 15.4 g-dw m^{-2} d^{-1} by *C. muelleri* (Zhang and Richmond, 2003) were reported. In the current study, similar results of 15–20 g-dw m^{-2} d^{-1} were observed at the dilution rate of 0.4 d^{-1}. However, production rate decreased after a few days under 1,000 µmol m^{-2} s^{-1}. This result might be attributed to excessive light intensity and/or silicon limitation. After day 15, areal production rates at both dilution rates of 0.2 and 0.4 d^{-1} decreased, but were maintained at approximately 6 and 10 g-dw m^{-2} d^{-1}, respectively. At a dilution rate of 0.2 d^{-1} under 300 µmol m^{-2} s^{-1}, relatively high stable production rate was obtained due to an increase in dry weight with enlargement of the cell. In other words, the cell physiological condition was not stable at the dilution rate of 0.2 d^{-1} under 300 µmol m^{-2} s^{-1}, although the production rate

reached a steady state. These results showed that the biomass production rate in terms of dry weight could be maintained at relatively high values in both dilution rates of 0.2 and 0.4 d^{-1}. However, the stable production of a uniform-size cell was achieved only in the condition of 0.2 d^{-1} under 300 μmol m^{-2} s^{-1}. Therefore, appropriate nutrient supply and optimum light intensity are crucial to secure homogeneity of products and high productivity.

Fatty Acid and Pigment Composition

Cellular content of valuable compounds is quite important in the process of maximizing microalgae productivity. Fatty acid composition (as% total fatty acid) on day 4 showed the minimum cellular dry weight and on day 20 the maximum as shown in **Table 1**. Fatty acids in *C. gracilis* mainly consisted of C16, C16:1n-7, C16:3, C20:5n−3. According to the comparison of fatty acid composition in small cells on day 4 and in large cells on day 20, saturated fatty acid (SFA) contents in small cells at both dilution rates showed significantly ($p < 0.05$) lower percentages of 14.6 and 18.3%, respectively, compared to those of large cells. Monounsaturated fatty acid (MUFA) contents in the small cells were also relatively low. Conversely, polyunsaturated fatty acid (PUFA) content including EPA showed significantly higher values of 60 and 55%, respectively, associated with small cells on day 4, compared to the large cells.

Relationship between cellular dry weight and SFA, MUFA, PUFA, and EPA contents per total fatty acid were evaluated because of the difference between fatty acid composition in different cell sizes (**Figures 6A–D**). Significant positive correlation of SFA ($y = 45.3/(1 + 2.27\ e^{-7.77x})$, $r^2 = 0.748$) and MUFA ($y = 35.9/(1 + 0.549\ e^{-7.74x})$, $r^2 = 0.641$) to cellular dry weight was obtained. On contrary, significant negative

TABLE 1 | Fatty acid composition (as % of total fatty acid) of *C. gracilis* on days 4 and 20 at dilution rates of 0.2 and 0.4 d^{-1}.

	C. gracilis				***C. gracilis***		***C. gracilis***	***T. pseudonana***	***C. sorokiniana***
	Semi-continuous				**Batch**		**Batch**	**Batch**	**Batch**
	0.2 d^{-1}		**0.4 d^{-1}**		**–**	**–**	**–**	**–**	**–**
	Day 4	**Day 20**	**Day 4**	**Day 20**	**Day 3**	**Day 10**			
C14	3.3	11.2	5.9	9.2	15.9	13.0	8.8	14.3	0.1
C15	0.4	0.8	0.5	0.5	0.9	0.9	1.0	0.8	–
C16	10.3	30.7	11.3	23.7	35.8	24.0	23.3	11.2	21.4
C17	–	–	–	–	–	–	0.3	0.1	–
C18	0.7	1.3	0.6	0.9	–	3.2	4.1	0.7	1.2
Other	–	–	–	–	7.0	2.5	1.2	0.1	0.8
ΣSFA	14.6	43.9	18.3	34.3	59.6	43.6	38.7	27.2	23.5
C14:1	–	–	–	–	–	0.7	–	–	–
C16:1	–	–	–	–	–	–	–	–	3.9
C16:1n−9	–	–	–	–	14.4	–	–	–	–
C16:1n−7	25.4	36.9	25.9	37.5	–	–	33.4	18.0	–
C18:1	–	–	–	–	–	–	–	–	32.8
C18:1n−11	–	–	–	–	–	7.5	–	–	–
C18:1n−9	–	0.5	0.7	0.4	20.9	17.4	3.6	0.5	–
C18:1n−7	–	–	–	–	–	–	1.7	0.1	–
Other	–	–	–	–	0.7	5.2	1.3	0.9	0.9
ΣMUFA	25.4	37.4	26.6	38.0	36.0	30.8	40.0	19.5	37.6
C16:2	–	–	–	–	0.5	0.9	–	–	1.5
C16:3	16.1	5.8	17.6	1.3	–	–	–	–	–
C16:3n−4	–	–	–	–	–	–	2.3	12.7	–
C18:2	–	–	–	–	0.7	–	–	–	30.3
C18:2n−9	–	–	–	–	–	–	2.0	–	–
C18:2n−6	–	2.4	1.5	2.4	3.2	0.6	0.5	0.4	–
C18:3	–	–	–	–	–	–	–	–	5.7
C20:2n−6	–	–	–	–	–	21.5	–	–	–
C20:4n−6	2.4	1.9	1.4	16.7	–	0.4	4.5	0.3	–
C20:5n−3	41.5	8.6	34.6	27.8	–	–	4.6	19.3	–
C22:6n−3	–	–	–	–	–	–	0.3	3.9	–
Other	–	–	–	–	–	2.2	5.6	16.0	0.4
ΣPUFA	60.0	18.7	55.0	7.3	4.4	25.6	19.8	52.6	37.9
References	This study				Pratiwi et al., 2009	Pratiwi et al., 2009	Volkman et al., 1989	Volkman et al., 1989	Li et al., 2013

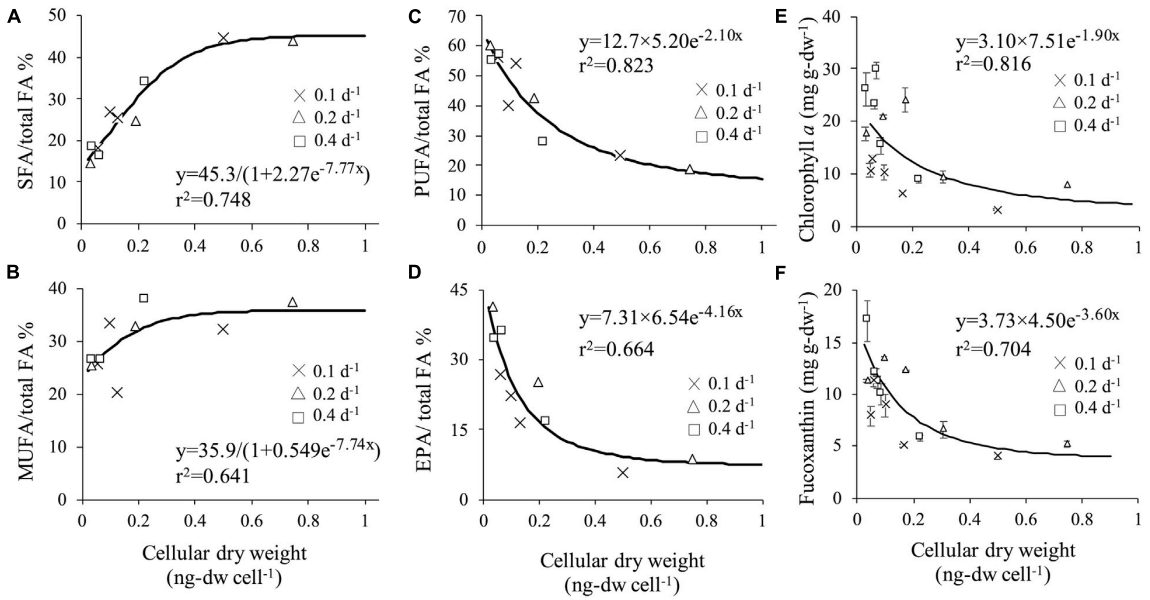

FIGURE 6 | Correlation between cellular dry weight and SFA **(A)**, MUFA **(B)**, PUFA **(C)** and EPA **(D)**. Correlation between cellular dry weight and chlorophyll *a* **(E)** and fucoxanthin **(F)**.

correlation of PUFA ($y = 12.7 \times 5.20\ e^{-2.10x}$, $r^2 = 0.823$) showed that bigger cell size accumulated less PUFA content.

In previous studies using *C. gracilis*, SFA and MUFA in total was 78.7% (Volkman et al., 1989) and 74.4% on day 10 in batch culture (Pratiwi et al., 2009) which were similar to the data on day 20 of the present study. According to Pratiwi et al. (2009), cells on day 3 marked high SFA content of 95.6% and low PUFA content of 4.4%. Volkman et al. (1989) reported a high PUFA content of 52.6% in *Thalassiosira pseudonana*. EPA content was previously reported with 5.0% (Tokushima et al., 2016) and 5.7% (Volkman et al., 1989) in *C. gacilis*. and 10.94% (Foo et al., 2017 and 20.8% (Natrah et al., 2007) in *C. calcitrans* (**Table 2**). Wu et al. (2016) reported EPA content of 25.65% in *Phaeodactylum tricornutum*. In the present study, high PUFA content of 60% and significant high EPA contents of 41.5% in total fatty acid was associated with small cells of *C. gracilis*. These results indicated that cell size affects PUFA, mainly EPA, indicating that maintenance of small cellular dry weight is the key operation factor for effective production of EPA.

Microscopic observation revealed that changes in dilution and light intensity influenced both cell morphology and the amount of plastid (**Figures 3A,B**). Therefore, chlorophyll *a* which is the prime light harvesting pigment for photosynthesis and fucoxanthin which is utilized as valuable compound, were selected to examine for their relationship between cellular dry weight and each related pigment. High correlation with cellular dry weight was observed in chlorophyll *a* ($y = 3.10 \times 7.51e^{-1.90x}$, $r^2 = 0.816$) and fucoxanthin ($y = 3.73 \times 4.50\ e^{-3.60x}$, $r^2 = 0.704$) (**Figures 6E,F**). Pigment per dry weight decreased as cellular dry weight increased. The maximum chlorophyll *a* content of 29.7 mg g-dw^{-1} was obtained at cellular dry weight of 0.071 ng-dw cell^{-1}, and the maximum fucoxanthin content of 17.1 mg g-dw^{-1} at cellular dry weight of 0.037 ng-dw cell^{-1}. It was illustrated that a small cell can accumulate approximately 3.76-fold chlorophyll *a* and 3.30-fold fucoxanthin compared to enlarged cells. Dilution rate represents the amount of nutrient supply, i.e., nutrient input at a dilution rate of 0.4 d^{-1} is four times larger than that at a dilution rate of 0.1 d^{-1}. The fucoxanthin productivity at a dilution rate of 0.2 d^{-1} was half of that at a dilution rate of 0.4 d^{-1}. This indicated that productivity proportionally changed with the input of nutrients. However, the productivity at a dilution rate of 0.1 d^{-1} was lower than a quarter of that at a dilution rate of 0.4 d^{-1}, possibly due to the unstable cell physiological condition under insufficient nutrients. According to Volkman et al. (1989), *C. calcitrans* showed a tendency to contain higher chlorophyll *a* per unit volume in the smaller cell. Although no specific chlorophyll *a* content was stated in their study, the result obtained were similar to the present study.

Fucoxanthin is one of major carotenoid pigments found only in diatoms and brown algae. In previous studies, fucoxanthin contents of 8.55 mg g-dw^{-1} in *Phaeodactylum tricornutum*, 4.92 mg g-dw^{-1} in *Nitzschia* sp. (Kim et al., 2012) and 5.5 mg g-dw^{-1} in *P. tricornutum* were reported (Wu et al., 2016; **Table 2**). The present result was comparable to the values of 18.14 mg g-dw^{-1} reported by Xia et al. (2013) with *Odontella aurita* and 15.8-18.23 mg g-dw^{-1}, obtained with *Isochrysis galbana* by Foo et al. (2017) and Sun et al. (2019). McClure et al. (2018) reported a greater content of 59.2 mg g-dw^{-1} for *P. tricornutum*, however, the areal fucoxanthin productivity is markedly lower (108.0 mg-dw m^{-2} d^{-1}) due to their low biomass production rate. High yields of 189 mg-dw m^{-2} d^{-1} for *P. tricornutum* (Gao et al., 2017) and 187.4 mg-dw m^{-2} d^{-1} for *O. aurita* (Xia et al., 2013) were reported, however, both of these studies conducted in batch culture under continuous

TABLE 2 | Biomass productivity, contents and productivities of fucoxanthin and EPA.

Algae	Type of reactor	Culture mode	Biomass		Fucoxanthin			EPA				References
			Volumetric productivity (g-dw L^{-1} d^{-1})	Areal productivity (g-dw m^{-2} d^{-1})	Content (mg g-dw^{-1})	Volumetric productivity (mg-dw L^{-1} d^{-1})	Areal productivity (mg-dw m^{-2} d^{-1})	Composition (%TFA)	Content (mg g-dw^{-1})	Volumetric productivity (mg-dw L^{-1} d^{-1})	Areal productivity (mg-dw m^{-2} d^{-1})	
Isochrysis galbana (2 strains)	Bubble column	Batch	–	–	6.04-18.23	–	–	–	–	–	–	Kim et al., 2012
Chaetoceros gracilis	Bubble column	Batch	–	–	2.24	–	–	–	–	–	–	
Phaeodactylum tricornutum	Bubble column	Batch	–	–	8.55	–	–	–	–	–	–	
Nitzschia sp.	Bubble column	Batch	–	–	4.92	–	–	–	–	–	–	
Chaetoceros calcitrans	Bubble column	Batch	–	–	5.13	–	–	10.94	–	–	–	Foo et al., 2017
Isochrysis galbana	Bubble column	Batch	–	–	2.19	–	–	0.77	–	–	–	
Skeletonema costatum	Bubble column	Batch	–	–	0.36	–	–	4.19	–	–	–	
Odontella sinensis	Bubble column	Batch	–	–	1.18	–	–	10.46	–	–	–	
Phaeodactylum tricornutum	Bubble column	Batch	–	–	0.07	–	–	19.12	–	–	–	
Isochrysis galbana (14 strains)	Bubble column	Semi-cont. (d = 0.375 d^{-1})	0.14-0.48	2.08-10.02	8.9-15.8	1.07-5.85	25.2-137.8	–	–	–	–	Sun et al., 2019
Odontella aurita	Bubble column	Batch	0.34-0.56	9.4-15.0	4.28-18.14	1.82-7.96	42.9-187.4*	–	–	–	–	Xia et al., 2013
Phaeodactylum tricornutum	Flat plate	Semi-cont. (d = 0.03 d^{-1})	0.018-0.054	0.75-2.28	10.1-59.2	0.44-2.16	22.0-108.0	–	–	–	–	McClure et al., 2018
Phaeodactylum tricornutum	Flat plate	Batch	–	–	8	4.73	189*	15	–	9.58	383*	Gao et al., 2017
Isochrysis sp.	Flat plate	Semi-cont. (d = 0.4 d^{-1})	–	–	17	–	–	–	–	–	–	Crupi et al., 2013
Navicula sp.	Flat plate	Batch	0.56	–	–	–	–	8	56	56	–	Satoh et al., 2013

(Continued)

TABLE 2 | Continued

Algae	Type of reactor	Culture	Biomass		Fucoxanthin			EPA				References
		mode	Volumetric productivity	Areal productivity	Content	Volumetric productivity	Areal productivity	Composition	Content	Volumetric productivity	Areal productivity	
Phaeodactylum tricornutum	Pond	Semi-cont. (d = 0.2-0.4 d^{-1})	–	–	–	–	–	–	–	–	0.15	Veloso et al., 1991
Cylindrotheca closterium	Tubular	Cont.	–	–	5.34	–	–	–	–	–	–	Pasquet et al., 2011
Chaetoceros gracilis	Tube	Batch	–	–	1.0-5.2	0.04-0.68	0.1-1.6	2.8-5.0	–	–	–	Tokushima et al., 2016
Phaeodactylum tricornutum	Tube	Batch	–	–	–	–	–	29.8	62.3	–	–	Yongmanitchai and Ward, 1991
Phaeodactylum tricornutum	Flask	Batch	1.52	–	–	–	–	–	2.83	43.13	–	Cerón García et al., 2005
Phaeodactylum tricornutum (6 strains)	Flask	Batch	0.022-0.031	–	2.14-5.5	0.047-0.17	–	12.43-25.65		–	–	Wu et al., 2016
Cyclotella cryptica	Flask	Batch	0.18-0.25	–	6.5-12.9	1.2-3.4	–	–	–	–	–	Guo et al., 2016
Chrysotila carterae	Flask	Batch	–	–	1.04	0.024	–	–	–	–	–	Ishika et al., 2017
Chaetoceros muelleri	Flask	Batch	0.018	–	2.92	0.072	–	–	–	–	–	
Phaeodactylum tricornutum	Flask	Batch	0.022	–	1.87	0.041	–	–	–	–	–	
Tisochrysis lutea	Flask	Batch	0.027	–	2.05	0.055	–	–	–	–	–	
Navicula sp.	Flask	Batch	0.037	–	1.49	0.054	–	–	–	–	–	
Amphora sp.	Flask	Batch	0.047	–	1.21	0.053	–	–	–	–	–	
Chaetoceros muelleri	–	Batch	–	–	–	–	–	–	10.4	–	–	Martínez-Fernández et al., 2006
Chaetoceros sp.	–	Batch	–	–	–	–	–	–	15.4	–	–	
Pavlova sp.	–	Batch	–	–	–	–	–	–	30.8	–	–	
Micromonas pusilla	–	Batch	–	–	–	–	–	–	35.2	–	–	

(Continued)

TABLE 2 | Continued

Algae	Type of reactor	Culture	Biomass		Fucoxanthin			EPA				References
		mode	Volumetric productivity	Areal productivity	Content	Volumetric productivity	Areal productivity	Composition	Content	Volumetric productivity	Areal productivity	
Chaetoceros calcitrans	Flask	Batch	–	–	–	–	–	11.1	–	–	–	Volkman et al. (1989)
Chaetoceros gracilis (2 strains)	Flask	Batch	–	–	–	–	–	4.6-5.7	–	–	–	
Skeletonema costatum	Flask	Batch	–	–	–	–	–	6	–	–	–	
Thalassiosira pseudonana	Flask	Batch	–	–	–	–	–	19.3	–	–	–	
Pavlova lutheri	Flask	Batch	–	–	–	–	–	19.7	–	–	–	
Chaetoceros calcitrans	Bottle	Batch	–	–	–	–	–	20.8	–	–	–	Natrah et al., 2007
Isochrysis galbana	Bottle	Batch	–	–	–	–	–	8.4	–	–	–	
Chaetoceros gracilis	Bubble column	Semi-cont. (d = 0.1 d^{-1})	0.082	3.89	7.36	0.60	28.6	17.8	8.03	0.66	31.2	This study
Chaetoceros gracilis	Bubble column	Semi-cont. (d = 0.2 d^{-1})	0.168	7.99	11.8	1.98	94.3	25.2	11.07	1.86	88.5	
Chaetoceros gracilis	Bubble column	Semi-cont. (d = 0.4 d^{-1})	0.248	11.8	15.4	3.82	182	29.2	14.11	3.50	167	

**Xia et al. (2013) and Gao et al. (2017) conducted batch culture under continuous illumination condition. Cont., continuous culture; Semi-cont., semicontinuous culture; d, dilution rate; TFA, total fatty acid. The values of this study indicate the averages during the cultivation.*

illumination condition. Meanwhile, the present study operated in semi-continuous culture under 12 h:12 h light-dark cycle. Many previous studies reported fucoxanthin contents in microalgae were conducted in a batch culture which was not supplied with additional nutrient during the culturing process. This study revealed that sufficient nutrient supply, especially silicon is one of the key operational factors to maintain small cells and to gain high fucoxanthin content of *C. gracilis*. These results raised the possibility that the fucoxanthin contents can be improved in other diatom species by maintaining the small-sized cells in a continuous culture with sufficient nutrients.

Furthermore, macroalgae also contain fucoxanthin which has high commercial value potential as a bioresource. Previous studies reported fucoxanthin contents of 4.49 ± 0.60 mg g-dw^{-1} in *Sargassum horneri* (Nomura et al., 2013), 0.2674 mg g-dw^{-1} in *Padina australis*, 0.2134 mg g-dw^{-1} in *Turbinaria conoides* (Zailanie and Purnomo, 2011) and 0.0297 mg g-dw^{-1} in *Laminaria* sp. (Frecha-ferreiro, 2010). Results obtained in the present study showed relatively higher fucoxanthin content of >10 mg g-dw^{-1} and high EPA contents compared to other macro- and microalgae reported. Therefore, *C. gracilis* can be regarded as a highly prospective species for production of EPA and fucoxanthin by optimizing operation with sufficient nutrient supply and appropriate light intensity.

CONCLUSION

High biomass production, EPA and Fucoxanthin contents were achieved in semi-continuous culture of marine diatom, *C. gracilis*. At low dilution rate of 0.1 and 0.2, the cell weight increased and both EPA and fucoxanthin contents significantly decreased due to deficiency of nutrients, especially silicon. In order to obtain high biomass production and valuable biocompounds contents, it is important to keep cells small by providing sufficient nutrients for *C. gracilis*. Further studies should focus on perfusion culture which provides sufficient nutrients to further increase biomass and valuable biocompounds production in diatom culture.

DATA AVAILABILITY STATEMENT

The original contributions presented in the study are included in the article/supplementary material, further inquiries can be directed to the corresponding author.

AUTHOR CONTRIBUTIONS

ST contributed to the collection and analyzing of the data and the writing of the manuscript. NN, TK, and KF contributed to the conception and design of experimental work, supervised the project, reviewed, and edited the draft prior to the submission. SB and MS contributed to the writing of the manuscript. FY, KF, and TT contributed to the funding acquisition of the research. MH and NK contributed to the analysis of the samples and the interpretation of the data. All authors read and approved the submitted manuscript.

FUNDING

This research was supported by the Japan Science and Technology Agency (JST)/Japan International Cooperation Agency (JICA), Science and Technology Research Partnership for Sustainable Development (SATREPS) through the project for Continuous Operation System for Microalgae Production Optimized for Sustainable Tropical Aquaculture (COSMOS) (Grant No. JPMJSA1509), and the SATREPS-COSMOS Matching Fund from the Ministry of Education Malaysia (MOE).

REFERENCES

Bligh, E. G., and Dyer, W. J. (1959). A rapid method of total lipid extraction and purification. *Can. J. Biochem. Physiol.* 37, 911–917.

Cerón García, M. C., Sánchez Mirón, A., Fernández Sevilla, J. M., Molina Grima, E., and García Camacho, F. (2005). Mixotrophic growth of the microalga *Phaeodactylum tricornutum* influence of different nitrogen and organic carbon sources on productivity and biomass composition. *Process Biochem.* 40, 297–305. doi: 10.1016/j.procbio.2004.01.016

Chrismadha, T., and Borowitzka, M. A. (1994). Effect of cell density and irradiance on growth, proximate composition and eicosapentaenoic acid production of *Phaeodactylum tricornutum* grown in a tubular photobioreactor. *J. Appl. Phycol.* 6, 67–74. doi: 10.1007/BF02185906

Crupi, P., Toci, A. T., Mangini, S., Wrubl, F., Rodolfi, L., Tredici, M. R., et al. (2013). Determination of fucoxanthin isomers in microalgae (*Isochrysis* sp.) by high-performance liquid chromatography coupled with diode-array detector multistage mass spectrometry coupled with positive electrospray ionization. *Rapid. Commun. Mass Spectrom.* 27, 1027–1035. doi: 10.1002/rcm.6531

Enright, C. T., Newkirk, G. F., Craigie, J. S., and Castell, J. D. (1986). Growth of juvenile *Ostrea edulis* L. fed Chaetoceros gracilis Schütt of varied chemical composition. *J. Exp. Mar. Bio. Ecol.* 96, 15–26. doi: 10.1016/0022-0981(86)90010-9

Fernández Sevilla, J. M., Molina Grima, E., García Camacho, F., Acién Fernández, F. G., and Sánchez Pérez, J. A. (1998). Photolimitation and photoinhibition as factors determining optimal dilution rate to produce eicosapentaenoic acid from cultures of the microalga *Isochrysis galbana*. *Appl. Microbiol. Biotechnol.* 50, 199–205. doi: 10.1007/s002530051277

Foo, S. C., Yusoff, F. M., Ismail, M., Basri, M., Khong, N. M. H., Chan, K. W., et al. (2015). Efficient solvent extraction of antioxidant-rich extract from a tropical diatom, *Chaetoceros calcitrans* (Paulsen) Takano 1968. *Asian Pac. J. Trop. Biomed.* 5, 834–840. doi: 10.1016/j.apjtb.2015.06.003

Foo, S. C., Yusoff, F. M., Ismail, M., Basri, M., Yau, S. K., Khong, N. M. H., et al. (2017). Antioxidant capacities of fucoxanthin-producing algae as influenced by their carotenoid and phenolic contents. *J. Biotechnol.* 241, 175–183. doi: 10.1016/j.jbiotec.2016.11.026

Frecha-ferreiro, S. (2010). Antioxidant compounds in edible brown seaweeds. *Eur. Food Res. Technol.* 231, 495–498. doi: 10.1007/s00217-010-1295-6

Gao, B., Chen, A., Zhang, W., Li, A., and Zhang, C. (2017). Co-production of lipids, eicosapentaenoic acid, fucoxanthin, and chrysolaminarin by *Phaeodactylum tricornutum* cultured in a flat-plate photobioreactor under varying nitrogen conditions. *J. Ocean Univ. China* 16, 916–924. doi: 10.1007/s11802-017-3174-2

Guo, B., Liu, B., Yang, B., Sun, P., Lu, X., Liu, J., et al. (2016). Screening of diatom strains and characterization of *Cyclotella cryptica* as a potential fucoxanthin producer. *Mar. Drugs* 14:125. doi: 10.3390/md14070125

Hata, K., Mikajiri, A., and Hujita, T. (1983). Aozakana to EPA (Blue-fish and EPA). *Cho Ri kagaku* 16, 155–160. doi: 10.11402/cookeryscience1968.16.3_155

Hatate, H., Ohgai, M., Murase, N., Miyake, N., and Suzuki, N. (1998). Accumulation of fatty acids in *Chaetoceros gracilis* (*Bacillariophyceae*) during stationary growth phase. *Fish. Sci.* 64, 578–581. doi: 10.2331/fishsci.64.578

Imaizumi, Y., Nagao, N., Yusoff, F. M., Kurosawa, N., Kawasaki, N., and Toda, T. (2016). Lumostatic operation controlled by the optimum light intensity per dry weight for the effective production of *Chlorella zofingiensis* in the high cell density continuous culture. *Algal Res.* 20, 110–117. doi: 10.1016/j.algal.2016.09.015

Imaizumi, Y., Nagao, N., Yusoff, F. M., Taguchi, S., and Toda, T. (2014). Estimation of optimum specific light intensity per cell on a high-cell-density continuous culture of *Chlorella zofingiensis* not limited by nutrients or CO2. *Bioresour. Technol.* 162, 53–59. doi: 10.1016/j.biortech.2014.03.123

Ishika, T., Moheimani, N. R., Bahri, P. A., Laird, D. W., Blair, S., and Parlevliet, D. (2017). Halo-adapted microalgae for fucoxanthin production: effect of incremental increase in salinity. *Algal Res.* 28, 66–73. doi: 10.1016/j.algal.2017.10.002

Kanazawa, K. (2012). High bioavailability and diverse biofunctions of fucoxanthin in brown algae. *Nippon Shokuhin Kagaku Kogaku Kaishi* 59, 49–55. doi: 10.3136/nskkk.59.49

Kaspar, H. F., Keys, E. F., King, N., Smith, K. F., Kesarcodi-Watson, A., and Miller, M. R. (2014). Continuous production of *Chaetoceros calcitrans* in a system suitable for commercial hatcheries. *Aquaculture* 42, 1–9. doi: 10.1016/j.aquaculture.2013.10.021

Kim, S. M., Kang, S., Kwon, O., Donghwa, C., and Pan, C. (2012). Fucoxanthin as a major carotenoid in *Isochrysis* aff. galbana: characterization of extraction for commercial applicationfFucoxanthin as a major carotenoid in Isochrysis aff . galbana: characterization of eExtraction for commercial application. *J. Korean Soc. Appl. Biol. Chem.* 55, 477–483. doi: 10.1007/s13765-012-2108-3

Krichnavaruk, S., Powtongsook, S., and Pavasant, P. (2007). Enhanced productivity of *Chaetoceros calcitrans* in airlift photobioreactors. *Bioresour. Technol.* 98, 2123–2130. doi: 10.1016/j.biortech.2006.08.010

Li, T., Zheng, Y., Yu, L., and Chen, S. (2013). High productivity cultivation of a heat-resistant microalga *Chlorella sorokiniana* for biofuel production. *Bioresour. Technol.* 131, 60–67. doi: 10.1016/j.biortech.2012.11.121

Martínez-Fernández, E., Acosta-Salmón, H., and Southgate, P. C. (2006). The nutritional value of seven species of tropical microalgae for black-lip pearl oyster (*Pinctada margaritifera*. L.). larvae. *Aquaculture* 257, 491–503. doi: 10.1016/j.aquaculture.2006.03.022

Mata, T. M., Martins, A. A., and Caetano, N. S. (2010). Microalgae for biodiesel production and other applications: a review. *Renew. Sustain. Energy Rev.* 14, 217–232. doi: 10.1016/j.rser.2009.07.020

McClure, D. D., Luiz, A., Gerver, B., Barton, G. W., and Kavanagh, J. M. (2018). An investigation into the effect of culture conditions on fucoxanthin production using the marine microalgae *Phaeodactylum tricornutum*. *Algal Res.* 29, 41–48. doi: 10.1016/j.algal.2017.11.015

Mcginn, P. J., Dickinson, K. E., Park, K. C., Whitney, C. G., Macquarrie, S. P., Black, F. J., et al. (2012). Assessment of the bioenergy and bioremediation potentials of the microalga *Scenedesmus* sp . AMDD cultivated in municipal wastewater ef fl uent in batch and continuous mode. *Algal Res.* 1, 155–165. doi: 10.1016/j.algal.2012.05.001

Mickleborough, T. D., Tecklenburg, S. L., Montgomery, G. S., and Lindley, M. R. (2009). Eicosapentaenoic acid is more effective than docosahexaenoic acid in inhibiting proinflammatory mediator production and transcription from LPS-induced human asthmatic alveolar macrophage cells. *Clin. Nutr.* 28, 71–77. doi: 10.1016/j.clnu.2008.10.012

Monkonsit, S., Powtongsook, S., and Pavasant, P. (2011). Comparison between airlift photobioreactor and bubble column for *Skeletonema costatum* cultivation. *Eng. J.* 15, 53–64. doi: 10.4186/ej.2011.15.4.53

Natrah, F. M. I., Yusoff, F. M., Shariff, M., Abas, F., and Mariana, N. S. (2007). Screening of Malaysian indigenous microalgae for antioxidant properties and nutritional value. *J. Appl. Phycol.* 19, 711–718. doi: 10.1007/s10811-007-9192-5

Nomura, M., Kamogawa, H., Susanto, E., Kawagoe, C., Yasui, H., Saga, N., et al. (2013). Seasonal variations of total lipids, fatty acid composition, and fucoxanthin contents of *Sargassum horneri* (Turner) and *Cystoseira hakodatensis* (Yendo) from the northern seashore of Japan. *J. Appl. Phycol.* 25, 1159–1169. doi: 10.1007/s10811-012-9934-x

Pasquet, V., Chérouvrier, J. R., Farhat, F., Thiéry, V., Piot, J. M., Bérard, J. B., et al. (2011). Study on the microalgal pigments extraction process: performance of microwave assisted extraction. *Process Biochem.* 46, 59–67. doi: 10.1016/j.procbio.2010.07.009

Pratiwi, A. R., Syah, D., Hardjito, L., Panggabean, L. M. G., and Suhartono, M. T. J. (2009). Fatty acid synthesis by Indonesian marine diatom, *Chaetoceros gracilis*. *HAYATI J. Biosci.* 16, 151–156. doi: 10.4308/hjb.16.4.151

Ruiz-marin, A., Mendoza-espinosa, L. G., and Stephenson, T. (2010). Growth and nutrient removal in free and immobilized green algae in batch and semi-continuous cultures treating real wastewater. *Bioresour. Technol.* 101, 58–64. doi: 10.1016/j.biortech.2009.02.076

Satoh, A., Ichii, K., Matsumoto, M., Kubota, C., Nemoto, M., Tanaka, M., et al. (2013). A process design and productivity evaluation for oil production by indoor mass cultivation of a marine diatom, *Fistulifera* sp. JPCC DA0580. *Bioresour. Technol.* 137, 132–138. doi: 10.1016/j.biortech.2013.03.087

Silva-Aciares, F. R., and Riquelme, C. E. (2008). Comparisons of the growth of six diatom species between two configurations of photobioreactors. *Aquac. Eng.* 38, 26–35. doi: 10.1016/j.aquaeng.2007.10.005

Sun, Z., Wang, X., and Liu, J. (2019). Screening of *Isochrysis* strains for simultaneous production of docosahexaenoic acid and fucoxanthin. *Algal Res.* 41:101545. doi: 10.1016/j.algal.2019.101545

Tantanasarit, C., Englande, A. J., and Babel, S. (2013). Nitrogen, phosphorus and silicon uptake kinetics by marine diatom *Chaetoceros calcitrans* under high nutrient concentrations. *J. Exp. Mar. Bio. Ecol.* 446, 67–75. doi: 10.1016/j.jembe.2013.05.004

Tokushima, H., Inoue-Kashino, N., Nakazato, Y., Masuda, A., Ifuku, K., and Kashino, Y. (2016). Advantageous characteristics of the diatom *Chaetoceros gracilis* as a sustainable biofuel producer. *Biotechnol. Biofuels* 9:235. doi: 10.1186/s13068-016-0649-0

Veloso, V., Reis, A., Gouveia, L., Fernandes, H. L., Empis, J. A., and Novais, J. M. (1991). Lipid production by *Phaeodactylum tricornutum*. *Bioresour. Technol.* 38, 115–119.

Volkman, J. K., Jeffrey, S. W., Nichols, P. D., and Rogers, G. I. (1989). Fatty acid and lipid composition of 10 species of microalgae used in mariculture. *Jounal Exp. Mar. Biol. Ecol.* 128, 219–240.

Williams, P. J. L. B., and Laurens, L. M. L. (2010). Microalgae as biodiesel & biomass feedstocks: review & analysis of the biochemistry, energetics & economics. *Energy Environ. Sci.* 3, 554–590. doi: 10.1039/b924978h

Wright, S. W. (1997). "Evaluation of methods and solvents for pigment extraction," in *Phytoplankton Pigments in Oceanography*, eds S. W. Jeffrey, R. F. C. Mantoura, and S. W. Wright (Paris: UNESCO Publishing), 261–282.

Wu, H., Li, T., Wang, G., Dai, S., He, H., and Xiang, W. (2016). A comparative analysis of fatty acid composition and fucoxanthin content in six *Phaeodactylum tricornutum* strains from different origins. *Chin. J. Oceanol. Limnol.* 34, 391–398. doi: 10.1007/s00343-015-4325-1

Xia, S., Wang, K., Wan, L., Li, A., Hu, Q., and Zhang, C. (2013). Production, characterization, and antioxidant activity of fucoxanthin from the marine diatom *Odontella aurita*. *Mar. Drugs.* 11, 2667–2681. doi: 10.3390/md11072667

Xin, L., Hong-ying, H., Ke, G., and Ying-xue, S. (2010). Effects of different nitrogen and phosphorus concentrations on the growth, nutrient uptake, and lipid accumulation of a freshwater microalga *Scenedesmus* sp. *Bioresour. Technol.* 101, 5494–5500. doi: 10.1016/j.biortech.2010.02.016

Yang, Y., Du, L., Hosokawa, M., Miyashita, K., Kokubun, Y., Arai, H., et al. (2017). Fatty acid and lipid class composition of the microalga *Phaeodactylum tricornutum*. *J. Oleo Sci.* 66, 363–368. doi: 10.5650/jos.ess16205

Yongmanitchai, W., and Ward, P. (1991). Growth ofand omega-3 fatty acid production by *Phaeodactylum tricornutum* under different culture conditions. *Appl. Environ. Microbiol.* 57, 419–425.

Zailanie, K., and Purnomo, H. (2011). Fucoxanthin Content of Five Species Brown Seaweed from Talango District, Madura Island. *J. Agric. Sci. Technol.* 1, 1103–1105.

Zhang, C. W., and Richmond, A. (2003). Sustainable, high-yielding outdoor mass cultures of *Chaetoceros muelleri* var. subsalsum and Isochrysis galbana in vertical plate reactors. *Mar. Biotechnol.* 5, 302–310.

Conflict of Interest: The authors declare that the research was conducted in the absence of any commercial or financial relationships that could be construed as a potential conflict of interest.

frontiers in Bioengineering and Biotechnology

REVIEW
published: 04 January 2021
doi: 10.3389/fbioe.2020.546067

Meeting Sustainable Development Goals: Alternative Extraction Processes for Fucoxanthin in Algae

Su Chern Foo[1], Kuan Shiong Khoo[2], Chien Wei Ooi[3], Pau Loke Show[2], Nicholas M. H. Khong[4] and Fatimah Md. Yusoff[5,6]*

[1] School of Science, Monash University Malaysia, Subang Jaya, Malaysia, [2] Department of Chemical and Environmental Engineering, Faculty of Science and Engineering, University of Nottingham Malaysia, Semenyih, Malaysia, [3] School of Engineering, Monash University Malaysia, Subang Jaya, Malaysia, [4] School of Pharmacy, Monash University Malaysia, Subang Jaya, Malaysia, [5] Department of Aquaculture, Faculty of Agriculture, Universiti Putra Malaysia, Selangor, Malaysia, [6] International Institute of Aquaculture and Aquatic Sciences (I-AQUAS), Universiti Putra Malaysia, Port Dickson, Malaysia

The ever-expanding human population puts tremendous pressure on global food security. With climate change threats lowering crop productivity and food nutritional quality, it is important to search for alternative and sustainable food sources. Microalgae are a promising carbon-neutral biomass with fast growth rate and do not compete with terrestrial crops for land use. More so, microalgae synthesize exclusive marine carotenoids shown to not only exert antioxidant activities but also anti-cancer properties. Unfortunately, the conventional method for fucoxanthin extraction is mainly based on solvent extraction, which is cheap but less environmentally friendly. With the emergence of greener extraction techniques, the extraction of fucoxanthin could adopt these strategies aligned to UN Sustainable Development Goals (SDGs). This is a timely review with a focus on existing fucoxanthin extraction processes, complemented with future outlook on the potential and limitations in alternative fucoxanthin extraction technologies. This review will serve as an important guide to the sustainable and environmentally friendly extraction of fucoxanthin and other carotenoids including but not limited to astaxanthin, lutein or zeaxanthin. This is aligned to the SDGs wherein it is envisaged that this review becomes an antecedent to further research work in extract standardization with the goal of meeting quality control and quality assurance benchmarks for future commercialization purposes.

Keywords: carotenoids, fucoxanthin, algae, health benefits, solvent extraction, alternative extraction processes, sustainability, environmentally friendly

OPEN ACCESS

Edited by:
Caixia Wan,
University of Missouri, United States

Reviewed by:
Changhong Yao,
Sichuan University, China
Héctor A. Ruiz,
Universidad Autónoma de Coahuila, Mexico

****Correspondence:***
Su Chern Foo
suchern@gmail.com;
foo.suchern@monash.edu

Specialty section:
This article was submitted to Bioprocess Engineering, a section of the journal Frontiers in Bioengineering and Biotechnology

Received: *27 March 2020*
Accepted: *09 November 2020*
Published: *04 January 2021*

Citation:
Foo SC, Khoo KS, Ooi CW, Show PL, Khong NMH and Yusoff FM (2021) Meeting Sustainable Development Goals: Alternative Extraction Processes for Fucoxanthin in Algae. Front. Bioeng. Biotechnol. 8:546067. doi: 10.3389/fbioe.2020.546067

THE NEED FOR MICROALGAE TO MEET SUSTAINABLE DEVELOPMENT GOALS

A rich biodiversity at the hierarchical levels of ecosystem, species, and genetics (Mace et al., 2012) is the key to sustainable development of humanity (Toledo and Burlingame, 2006). Microalgae represent untapped resources with its biodiversity ranging from 200,000 species to several million species (Norton et al., 1996), as compared to only about 250,000 species in higher plants (Pulz and Gross, 2004). Microalgae provide crucial ecosystem services under their roles in provision

(as raw materials for consumption and use), support (as primary producers in aquatic ecosystems), regulation (supplying more than 80% of world oxygen), and food culture (e.g., spirulina was a food source for the Aztecs until the 16th century). The rich taxonomic diversity of microalgae is attractive not only for bioprospecting but also to produce valuable and diverse bioactive compounds such as carotenoids, proteins, enzymes, polyunsaturated fatty acids (PUFAs), lipids, or exopolysaccharides (EPS). Microalgae are photosynthetic and can be found in extreme ecosystems including polar regions, hot springs, deserts, ocean, and micro-aerobic environments. The versatility of microalgae makes them very promising candidates as crops for the future. Combining the latest cultivation and harvesting technologies for improvements in resource efficiency, microalgae could be a new impetus to the current lag in global economic growth.

Sustainable development goals (SDGs; 2015–2030), an extension of millennium development goals (MDGs; 2000–2015), were adopted by all United Nations Member States as a universal call to action for poverty eradication, global prosperity and, protection of the environment (Sachs, 2012). Microalgae, as a carbon-neutral resource, have directly contributed to three out of the eight MDGs (i.e., reducing poverty and hunger, promoting environmental sustainability, and developing global partnerships). Further to this, the application of microalgae in biotechnological platforms could contribute to sixteen out of the seventeen SDGs, detailed in **Table 1**.

THE POTENTIAL OF FUCOXANTHIN

Introduction to Fucoxanthin: Structure and Function

Fucoxanthin is a xanthophyll with an unusual epoxide group, allenic bond and, conjugated carbonyl group on the polyene molecule that sets it apart from the other carotenoids (Peng et al., 2011). The major structure responsible for the antioxidant and light-harvesting properties in carotenoids is the conjugated double-bond system in the chromophore (**Figure 1**). Carotenoids in microalgae are efficient scavengers for singlet molecular oxygen ($^1O_2$) and peroxyl radicals (ROO) (Stahl and Sies, 2012). In radical scavenging, carotenoids act as a radical trap and add electrons to their conjugated double-bond, yielding a ground-state oxygen and a triplet-state carotenoid. Subsequently, the excited carotenoid structure dissipates the excess energy to the surrounding environment by returning to its ground state (Takashima et al., 2012).

The antioxidant activities of fucoxanthin have been well characterized in the past. Fucoxanthin demonstrated proton-donative activities in the 1,1-diphenyl-2-picrylhydrazyl (DPPH) assay (Nomura et al., 1997). Moreover, fucoxanthin and its metabolites (fucoxanthinol and halocynthiaxanthin) exhibited radical scavenging activity and singlet oxygen quenching activity (Sachindra et al., 2007). Similarly, research in the last few years showed that fucoxanthin not only could scavenging radicals but also was effective in chelating iron (Foo et al., 2015b) and slowing down the bleaching of β-carotene in linoleic acid emulsion systems (Foo et al., 2015a).

Fucoxanthin Sources

Unlike β-carotene and lutein that are found ubiquitously in terrestrial crops, fucoxanthin is obtained exclusively from the aquatic environment. Fucoxanthin is the signature pigment markers for macroalgae and microalgae species listed in **Table 2**. This includes Phaeophyceae (e.g., *Laminaria japonica, Sargassum fulvellum, Undaria pinnatifida*), Bacillariophyceae (e.g., *Odontella aurita, Chaetoceros* sp., *Phaeodactylum tricornutum, Cylindrotheca closterium*), Prymnesiophyceae (e.g., *Isochrysis galbana, Pavlova lutheri*), Chrysophycea (e.g., *Pelagococcus subviridis*), Raphidophyceae (e.g., *Psammamonas australis*) and Dinophyceae (e.g., *Kryptoperidinium foliaceum*) (Wright and Jeffrey, 1987; Stauber and Jeffrey, 1988; Bjornland and Liaeen-Jensen, 1989; Grant et al., 2013). The annual production of microalgae biomass in 2000–2004 was at 5000–10000 tons (Van Harmelen and Oonk, 2006). Due to increasing market demand, this number has almost doubled to 20000 tons (Tredici et al., 2016) in the last 10 years or so. Whilst in 2003, the world production of macroalgae or seaweed reached 8 million tons and was valued at US$ 5.5–6 billion (McHugh, 2003). A report by Roesijadi et al. (2010) showed global monetary value of seaweeds to have reached over US$ 7 billion and was projected to continue with increasing human population growth. From here, microalgae and macroalgae biomass are the prospective and sustainable feedstock of the future.

There has been an increasing number of scientific reports showing the potential of fucoxanthin to improve the nutritional quality of food, which in turn benefits the health and well-being of consumers. This shows great opportunities for fucoxanthin from both microalgae and macroalgae to be commercialized and made available on food shelves. Intriguingly, the ultimate nutraceutical sources are mainly derived from producers at the beginning of the food chain (Shahidi and Alasalvar, 2010). By careful control of nutrients, a wide spectrum of biochemicals can be synthesized by algae and be used as safe and value-adding ingredients in food and nutraceutical sectors. Not only can algae act as suitable nutrition cell factories to meet food demand, but they could also be a healthy, *halal* and clean plant source for vegetarians and vegans. It would thus be encouraging to make fucoxanthin more accessible to consumers.

Fucoxanthin Applications

In the last decade, fucoxanthin has found applications as nutraceuticals and more recently in nutricosmetics. Fucoxanthin is classified as a type of nutraceutical because it exerts therapeutic effects (e.g., anti-inflammatory, anti-obesity, anti-diabetic, and anti-cancer) as presented in **Table 3**. Fucoxanthin can be incorporated into conventional food (e.g., milk, rice, bread, and pasta) as a bioactive ingredient to increase the nutritional value and enhance the sensory qualities (Prabhasankar et al., 2009; Abu-Ghannam and Shannon, 2017). Besides that, fucoxanthin has found application in nutricosmetics as anti-obesity pills or "oral cosmetics" (Agatonovic-Kustrin and Morton, 2013; Couteau and Coiffard, 2016). Fucoxanthin is a good ingredient

TABLE 1 | Summary of the roles of microalgae in achieving SDGs.

SDG	Main targets	Microalgae applications	References
(1) No poverty	Wealth creation	Aside from using terrestrial biomass like barley or hop, alternative aquatic biomass from *Chlorella vulgaris* could be opted for energy and revenue creation	Kusin and Horan, 2015
(2) Zero hunger	• End hunger • Achieve food security and improved nutrition • Promote sustainable agriculture	Microalgae is a cell factory for essential nutrients to support human health. Nutrients from microalgae has been used in the past as a diet supplement for undernourished children. Whereas microalgae by-products can be used as feed additives in poultry and aquaculture	Matondo et al., 2016; García et al., 2017; Kwon et al., 2019
(3) Good health and well being	• Ensure healthy lives • Promote well-being for all at all ages	Microalgae extracts are found to be effective in preventing and treating both communicable and non-communicable diseases	Yan et al., 2016; Foo et al., 2017, 2019; Kawee-Ai et al., 2019
(4) Quality education	• Ensure inclusive and equitable quality education for all • Promote life-long learning opportunities	The availability of microalgae in culture collections enables for worldwide accessibility in different forms of teaching, research, or industrial training. This in turn promotes an inclusive and equitable education to all	Blackburn et al., 1997, 2005
(5) Gender equality	Gender equality and empowerment of women and girls	Empowerment and scholarship opportunity for women in science, technology, engineering, and mathematics (STEM) industries especially for those working in the fields of agricultural and blue biotechnology involving microalgae	Jelić and Jovanović, 2013
(6) Clean water and sanitation	Ensure availability and sustainable management of water and sanitation for all	Microalgae-bacteria symbiosis improves water quality by removing organic matter, excessive nutrients, hazardous contaminants and heavy metals	Abdel-Raouf et al., 2012; Kumar et al., 2015
(7) Affordable and clean energy	Ensure access to affordable, reliable, sustainable, and modern energy for all	Microalgae are the fastest growing aquatic plant and they have the potential to yield more oil or biomass per ha when compared to terrestrial crops and plants. For example, hydrocarbons from *Botryococcus braunii* can replace fossil fuels	Banerjee et al., 2002; Bayro-Kaiser and Nelson, 2017; Moriarty and Honnery, 2019
(8) Decent work and economic growth	Promote sustained, inclusive, and sustainable economic growth, full and productive employment, and decent work for all	Microalgae can improve sustainability practices of existing industrial activities, including wastewater treatment and the production of pharmaceuticals, cosmetics, feed, food, and biofuel	Simas-Rodrigues et al., 2015; Richmond, 2017
(9) Industry, innovation and infrastructure	Build resilient infrastructure, promote inclusive and sustainable industrialization and foster innovation	Microalgae are used as an innovative greening component in future buildings. For example, microalgae were cultured in photobioreactors that were retrofitted or architecturally planned as bio-facades of buildings to harvest solar energy for electricity conversion	Mohseniazar et al., 2011; Qiu, 2014; Dahoumane et al., 2016; Elrayies, 2018; Kashyap et al., 2019
(10) Reduced inequalities	Reduce inequality within and among countries	More development interventions (e.g., equal access to credit and information for women) should be implemented for example, development policies like "Kenya Vision 2030" with the goal of using algae biomass as a source of food, feed and biofuel for the country, recognizes the role of women in policy implementation	Derun, 2009; Moejes and Moejes, 2017
(11) Sustainable cities and communities	Make cities and human settlements inclusive, safe, resilient, and sustainable	Sustainable architecture is one of the approaches to energy conservation in view of the increasing human population. A cost-benefit analysis from an environmental perspective showed that the closed tubular microalgae photobioreactor system has more benefits as compared to solar panel system	Biloria and Thakkar, 2020; Talebi et al., 2020
(12) Responsible consumption and production	Ensure sustainable consumption and production patterns	A circular approach was demonstrated using *Spirulina* as a bio-template in the synthesis of photocatalysts for water decontamination, and at the same time, the remaining biomass was used for the bioethanol production. Similarly, microalgae-based biorefinery can promote circular economy based on techno-economic and life-cycle analyses	Kavitha and Gunasekaran, 2020; Serrà et al., 2020
(13) Climate action	Take urgent action to combat climate change and its impacts	Microalgae are effective in capturing carbon dioxide, a greenhouse gas that contributes to climate change	Singh et al., 2019
(14) Life below water	Conserve and sustainably use the oceans, seas and marine resources for sustainable development	Microalgae could be a bioindicator for assessing the climate change as well as the terrestrial influences on marine health and ecology of coral reefs. If microalgae were used to replace fishmeal and fish oil globally, the effect would be equivalent to 30% of reduction in fishing pressure at the lower end of the food web; this would contribute to restoration of the marine ecosystem	Blanco et al., 2008; Hemaiswarya et al., 2011; Beal et al., 2018; Gaignard et al., 2019

(Continued)

TABLE 1 | Continued

SDG	Main targets	Microalgae applications	References
(15) Life on land	Protect, restore and promote sustainable use of terrestrial ecosystems, sustainably manage forests, combat desertification, and halt and reverse land degradation and halt biodiversity loss	Microalgae are an effective pioneer microorganism in the restoration of acrid soil and the desertification where several successful cases of implementations have been reported	Lababpour, 2016
(16) Peace, justice and strong institution	Promote peaceful and inclusive societies for sustainable development, provide access to justice for all and build effective, accountable and inclusive institutions at all levels	n/a	n/a
(17) Partnerships for the goals	Strengthen the means of implementation and revitalize the global partnership for sustainable development	CyanoFactory is a R&D project focusing on the design and construction of novel photosynthetic cell factories for solar biofuel production. Such examples of "purpose driven" research that are supported by the scientific goals and the need for creation of new technologies requires more interdisciplinary partnerships to promote the application of microalgae to a greater level	Akinsemolu, 2018; Lindblad et al., 2019

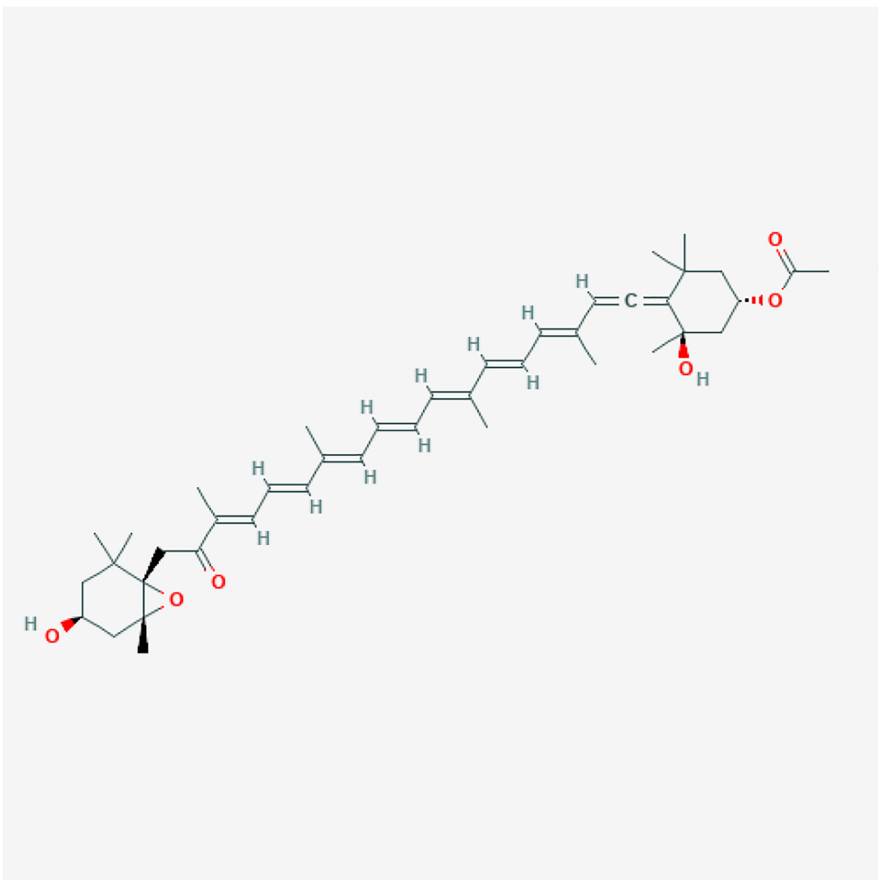

FIGURE 1 | The 2D structure image of CID 5281239 (fucoxanthin). Source: https://pubchem.ncbi.nlm.nih.gov/compound/5281239#section=2D-Structure.

of nutricosmetics because it has demonstrated slimming effects by inhibiting fat absorption (Muradian et al., 2015).

In the present market, microalgae cosmetic products from carotenoids are mainly extracted from the chlorophycean, *Nannochloropsis oculata* (Shen et al., 2011). As microalgae are considered "superfoods," they are composed of amino acids, essential fatty acids, vitamins, key minerals, trace elements, antioxidants, electrolytes, nucleic acids and, enzymes that play important roles in cellular regeneration. Urikura et al. (2011) demonstrated the protective effects of fucoxanthin

TABLE 2 | Fucoxanthin in microalgae and macroalgae.

Type	Class	Species	Fucoxanthin quantity ($mg.g^{-1}$ DW)	References
Microalgae	Bacillariophyceae	*Phaeodactylum tricornutum*	15.42–16.51	Kim et al., 2012
		Chaetoceros calcitrans	2.33 ± 0.14	Goiris et al., 2012
		Chaetoceros calcitrans (Paulsen) Takano 1968	5.25 ± 0.03	Foo et al., 2015b
		Phaeodactylum tricornutum SCSIO828	5.50	Wu et al., 2015
Microalgae	Prymnesiophyceae	*Isochrysis galbana*	7.75 ± 0.13 18.23	Goiris et al., 2012; Kim et al., 2012
		Pavlova lutheri	17.9	Griffiths and Harrison, 2009
Microalgae	Chrysophyceae	*Dinobryon cylindrical*	n.d	Withers et al., 1981
		Ochromonas sp.	0.03–0.12	Withers et al., 1981
Macroalgae	Phaeophyceae	*Laminaria japonica*	1.85	Xiao et al., 2012
		Laminaria digitata	0.468	Holdt and Kraan, 2011
		Undaria pinnatifida (Harv.) Sur.	0.727	Xiao et al., 2012
		Sargassum fusiforme	0.0133	Xiao et al., 2012
		Sargassum duplicatum	1.01 ± 0.10	Noviendri et al., 2011
		Sargassum binderi	0.73 ± 0.39	Noviendri et al., 2011
		Myagropsis myagroides	9.01	Heo and Jeon, 2009
		Dictyota coriacea	6.42	Heo and Jeon, 2009
		Eisenia bicyclis	0.109	Airanthi et al., 2011
		Kjellmaniella crassifolia	0.152	Airanthi et al., 2011
		Alaria crassifolia	0.041	Airanthi et al., 2011
		Sargassum horneri	0.020	Airanthi et al., 2011
		Cystoseira hakodatensis	0.0041	Airanthi et al., 2011
		Turbinaria turbinata	0.59 ± 0.08	Jaswir et al., 2013
		Sargassum plagiophyllum	0.71 ± 0.08	Jaswir et al., 2013

against UVB-induced skin photoaging as evidenced in hairless mice. Compounds responsible for such activity included phlorotannins, polysaccharides, carotenoid pigments (fucoxanthin), and fucosterol in brown algae (Kim, 2011). With more focus on natural carotenoids, there is a huge market of opportunity for the incorporation of these bioactive ingredients to replace synthetic colorings in food and nutricosmetics.

FUCOXANTHIN EXTRACTION PROCESSES

The isolation of fucoxanthin from microalgae feedstock can be attained by various extraction methods. The selection of extraction techniques is driven by the cost of operation, the complexity of feedstock, demand for the quality and the yield of final bioproducts. For example, to commercialize fucoxanthin in the fields of pharmaceutical, cosmetics, food or analytical testing, the bioactivity and purity of fucoxanthin must be well preserved. The characteristics of microalgae biomass possess a challenge to the extraction of fucoxanthin (Abu-Ghannam and Shannon, 2017) and one of them is the type of cell wall (e.g., cellulosic or siliceous). Hence, the extraction parameters influencing the performance of extraction need to be identified and optimized for maximizing the product yield while minimizing the operation time, chemical consumption, utility cost and waste generation. In the past, fucoxanthin extraction from microalgae feedstock was achieved by organic-solvent-based extraction with the aid of maceration or Soxhlet extraction. To date, alternative extraction techniques have been adopted as an environmentally friendly route to extract fucoxanthin. In the following sections, the conventional and alternative methods for extraction of fucoxanthin were reviewed and compared in the aspects of working principle, extraction performance, strength, and weakness of the method.

Conventional Solvent Extraction Methods for Fucoxanthin

The common techniques for extraction of carotenoids include maceration (soaking or direct organic-solvent extraction), Soxhlet extraction, or steam/hydro distillation (Kadam et al., 2013; Khoo et al., 2019). In general, the selection of organic solvent and the operation cost must be taken into consideration (Zarekarizi et al., 2019) when treating different types of macroalgae or microalgae for carotenoid extraction (**Table 4**). In addition, the operation involving organic solvents must be handled with care because of the highly volatile and flammable characteristics of these solvents. Examples of organic solvents used in the solvent extraction of fucoxanthin are acetone, methanol, ethanol, n-hexane, dimethyl sulfoxide, dichloromethane, tetrahydrofuran and ethyl acetate. The properties of solvent systems, including dielectric constant and polarity index, affect the extraction yield of carotenoids. Fucoxanthin can be dissolved in mid-polar solvent systems because of the semi-polar characteristic of fucoxanthin and the oxygen molecule in the fucoxanthin structure, but water was

TABLE 3 | Therapeutic effect and toxicity studies of fucoxanthin.

Activity(s)	Models	Results	Mechanism of action	References
Anti-inflammation	RAW 264.7 macrophages	Inhibitory effects on inflammatory cytokines and mediators	Inhibition of nuclear factor-κB gene activation and phosphorylation of mitogen-activated protein kinases	Heo et al., 2012
	Mast cells	Suppression of mast cell degranulation *in vivo*	Suppression of antigen-induced aggregation of high-affinity IgE receptor and activation of degranulating signals of mast cells	Tan and Hou, 2014
Anti-obesity	Wistar rats and KK-Ay mice	A reduction of abdominal white adipose tissue weights in subjects	Inhibition of fat absorption and decreased serum triglyceride level by induction of uncoupling protein-1 (UCP-1)	Maeda et al., 2007
Anti-diabetic	Diabetic/obese mice	Fucoxanthin decreased the blood glucose and plasma insulin levels thereby improving alterations in lipid metabolism and insulin resistance induced by a high-fat diet via reduction of visceral fat mass, hyperinsulinemia, hepatic glucose production, and hepatic lipogenesis	Via downregulation of adipokines like tumor necrosis factor-α, monocyte chemoattractant protein-1, interleukin-6 and, plasminogen activator inhibitor-1	Miyashita et al., 2012
Anti-cancer	MCF-7 breast cancer cell line	*Chaetoceros calcitrans* extracts were able to induce apoptosis at a concentration as low as 3 ppm	Fucoxanthin increased the expression of apoptotic genes, resulting in an increase in BAX/Bcl-2 ratio and activation of caspase 7 mRNA expression	Ebrahimi Nigjeh et al., 2013
	HepG2 cancer cell line	*Chaetoceros calcitrans* extracts induced cytotoxicity to HepG2 cells following concentration and time-dependent pattern	Modulation of numerous genes involved in cell signaling (AKT1, ERK1/2, and JNK), apoptosis (BAX, BID, Bcl-2, APAF, and CYCS), and oxidative stress (SOD1, SOD2, and CAT)	Foo et al., 2019
	BNL CL.2 transformed murine liver cells	Fucoxanthin acted as a cell signaling inhibitor at 12 h incubation (5 μM) of *Undaria pinnatifida* extracts	Fucoxanthin activated the Nrf2/ARE pathway by increasing the expressions of HO-1 and NQO-1 expression primarily through the ERK/P38 pathway	Liu et al., 2011
Anti-aging	Topical application on HOS: HR-1 hairless mice	Suppression of UVB-induced wrinkle formation	Fucoxanthin prevents skin photoaging via antioxidant and antiangiogenic effects	Urikura et al., 2011
Toxicity and safety evaluation	Single and repeated oral dose toxicity studies	No fatalities or abnormalities reported in both studies	Low toxicity and safe for consumption. Normal histology and no abnormal changes in liver, kidney, spleen, and gonadal tissues	Beppu et al., 2009
Multiple drug resistance (MDR)	Caco-2 and CEM/ADR5000 cells	Fucoxanthin exhibited a chemosensitizers role to alleviate MDR	By acting as competitive inhibitors of ATP-binding cassette (ABC)	Batista et al., 2012
Metabolism, bioavailability, and safety	Oral administration to mice	Results demonstrated dietary fucoxanthin accumulates in the heart and liver as fucoxanthinol and in adipose tissue as amarouciaxanthin A	This indicates that the bioavailability of fucoxanthin (and its metabolites) may be higher than that of other xanthophylls, at least of astaxanthin	Hashimoto et al., 2009
	13 groups of C57BL/6J mice	No toxicological effects were observed. Neither histological nor serum analyses revealed any heart, kidney, or liver toxicity induced by algae diets	Algae-rich diets were thus well accepted, well-tolerated and suitable for the maintenance of body weight and normal organ function	Neumann et al., 2018

found to be ineffective in solubilizing fucoxanthin (Aslanbay Guler et al., 2020). Although acetone was commonly used in the direct solvent extraction of fucoxanthin (Abu-Ghannam and Shannon, 2017), the yield of extraction was typically lesser than that by ethanol due to the lack of hydroxyl functional group for better hydrophilic interaction. Tetrahydrofuran was found to be less efficient in extracting fucoxanthin because it generates peroxides that degrade fucoxanthin (Aslanbay Guler et al., 2020). A previous study showed that the ethanolic extraction of fucoxanthin from diatom *P. tricornutum* yielded 15.71 mg/g dried weight (Kim et al., 2012). Similarly, a recent study found that the extraction of fucoxanthin from *P. tricornutum* was governed by the type of solvent used; the selectivity of solvent for fucoxanthin was in the descending order of d-limonene > ethyl acetate > ethyl lactate > ethanol (del Pilar Sánchez-Camargo et al., 2017).

Moreover, the extraction of fucoxanthin from *P. tricornutum* can be improved by the application of a hot soaking process with acetone (Pasquet et al., 2011). However, this approach caused the degradation of chlorophyll *a* from diatom *C. closterium*, while the cold soaking process rendered the chlorophyll *a* to be partially decomposed after 60 min. Similarly, the extraction efficiency of fucoxanthin from *P. tricornutum* was improved when the temperature of ethanol (50%) increased from 30 to 70°C (Kim et al., 2012). Nonetheless, an extremely high temperature condition of solvent extraction (e.g., above the boiling point of solvent) could cause the localized overheating effects on the fucoxanthin that render its degradation and low recovery.

Soxhlet extraction is a solid-liquid extraction approach that involves the continuous mass transfer of non-volatile target compounds via reflux of organic solvents. The efficiency of extraction depends on the selectivity of solvents for the compounds, the diffusion rate of solvents, and the solubility of target compounds in the solvents (Kim, 2012). Although Soxhlet extraction is a simple diffusion process without applying shear stress to the biomass, it is unsuitable for the extraction of temperature-sensitive carotenoids as their bioactivity will be degraded during the heating cycles (Kim et al., 2012).

Although the maximum yield of the product remains a priority, the selection of solvents should thoroughly consider other criteria such as environmental impact, toxicity and sustainability of the selected solvent (**Table 4**). For instance, in the extraction of fucoxanthin from *P. tricornutum*, the extraction efficiency of methanol was higher than that of ethanol (Aslanbay Guler et al., 2020). However, by considering the toxicity of solvents, methanol is relatively hazardous to both environment and human use. Other alternative organic solvents such as petroleum ether and n-hexane are typically incompatible with the extraction of fucoxanthin because of their hydrophobic properties. Moreover, solvent extraction often suffers from the large consumption of organic solvent (Khoo et al., 2019). Nonetheless, the feasibility of recycling solvents via distillation and evaporation under vacuum could mitigate the chemical consumption and waste generation. More importantly, the extracted fucoxanthin must be depleted of organic solvents used in the solvent extraction process if the final product is used as a functional ingredient in food or supplements.

Alternative Fucoxanthin Extraction Methods

The importance of SDG no. 12 (i.e., responsible consumption and production) has become more prominent as the world faces challenges in coping with pollution problems and food demand. The sustainability in the food supply chain and the low-carbon footprint of the commercial food products should begin with the growth of sustainable crops as well as the greener extraction methods in processing of bioproducts. The emergence of alternative extraction methods has opened new avenues to the sustainable extraction of fucoxanthin from algal sources. **Table 5** shows the emerging methods for extraction of fucoxanthin from macro- and microalgae.

Supercritical Fluid Extraction (SFE)

Supercritical fluid extraction (SFE) utilizes carbon dioxide (CO_2) at high pressure and constant temperature to extract bioactive components from feedstock (Kanda et al., 2014). Supercritical fluids had a better transport performance than liquid because of its low viscosity and high diffusivity (Kadam et al., 2013). Moreover, the dissolving power of supercritical fluid is dependent on its density, which is regulated by temperature and pressure (Kadam et al., 2013). The physical appearance of the final product is typically in oily and concentrated forms. This extraction method is deemed to be a sustainable processing method as it aligns with SDGs via the usage of environmentally benign solvents (Ramsey et al., 2009). The utilization of CO_2 in its supercritical fluid state (SC-CO_2) as an extraction solvent reduces the reliance on organic solvents and minimizes the generation of hazardous waste during processing. The low viscosity of SC-CO_2 ensures a more efficient mass transfer for rapid penetration of solid matrices and extraction of compounds (Ramsey et al., 2009). More importantly, the solvating strength and polarity of SC-CO_2 can be manipulated by controlling the density of SC-CO_2, which can be regulated by the temperature and pressure (Kadam et al., 2013). The low critical temperature of CO_2 (31°C) allows the extraction of carotenoid at a relatively lower temperature as compared to other traditional extraction methods involving high temperature (Ramsey et al., 2009).

A SFE study performed by Kanda et al. (2014) showed that the extraction of fucoxanthin from *Undaria pinnatifida* by SC-CO_2 increased at least 16-fold in the presence of ethanol as an entrainer (3.23%). Similarly, the addition of entrainer (15% ethanol) was effective in the extraction of fucoxanthin from *Sargassum muticum* and the yield of fucoxanthin was improved marginally (Conde et al., 2014). Ethanol was commonly used as an entrainer in SC-CO_2 extraction to increase the polarity of CO_2; this effect is beneficial to the performance of fucoxanthin extraction. A recent work by Aslanbay Guler et al. (2020) showed that the yield of fucoxanthin extracted from *P. tricornutum* using SC-CO_2 was 0.69 mg/g, which was comparable to the yield of fucoxanthin (0.57 mg/g) obtained by the conventional solvent extraction with methanol.

Yet, there are limitations in SFE of fucoxanthin because the optimal extraction conditions are dependent on the characteristics of algae species and fucoxanthin. For example,

TABLE 4 | Conventional extraction methods and fucoxanthin yield from microalgae and macroalgae.

Extraction methods	Type of solvent	Species	Class	Temperature (°C)	Fucoxanthin yield	References
Solvent extraction or maceration	Ethanol	*Phaeodactylum tricornutum*	Bacillariophyceae	30	15.71 mg/g	Kim et al., 2012
	Ethanol	*Odontella aurita*	Bacillariophyceae	45	17.20 mg/g	Xia et al., 2013
	Ethanol (96%)	*Sargassum muticum*	Phaeophyceae	40	0.55 mg/g	Conde et al., 2014
	Methanol	*Chaetoceros calcitrans*	Bacillariophyceae	25	22.71%	Foo et al., 2015a
	Acetone	*Phaeodactylum tricornutum*	Bacillariophyceae	25	4.60 mg/g	Kim et al., 2012
	Ethyl acetate	*Phaeodactylum tricornutum*	Bacillariophyceae	25	2.26 mg/g	Kim et al., 2012
	Dimethyl sulfoxide	*Laminaria japonica*	Phaeophyceae	25	122.10 μg/g	Wang et al., 2005
	Acetone	*Fucus vesiculosus*	Phaeophyceae	30	0.70 mg/g	Shannon and Abu-Ghannam, 2017
	Tetrahydrofuran	*Phaeodactylum tricornutum*	Bacillariophyceae	35	1.28 mg/g	Aslanbay Guler et al., 2020
	Dichloromethane	*Phaeodactylum tricornutum*	Bacillariophyceae	35	1.28 mg/g	Aslanbay Guler et al., 2020
	Methanol	*Phaeodactylum tricornutum*	Bacillariophyceae	35	0.57 mg/g	Aslanbay Guler et al., 2020
	Acetone + methanol (1:1, v/v)	*Saccharina japonica*	Phaeophyceae	25	0.48 mg/g	Sivagnanam et al., 2015
	Acetone + methanol (1:1, v/v)	*Sargassum horneri*	Phaeophyceae	25	0.71 mg/g	Sivagnanam et al., 2015
	Hexane	*Saccharina japonica*	Phaeophyceae	25	0.16 mg/g	Sivagnanam et al., 2015
	Hexane	*Sargassum horneri*	Phaeophyceae	25	0.05 mg/g	Sivagnanam et al., 2015
	Ethanol	*Saccharina japonica*	Phaeophyceae	25	0.12 mg/g	Sivagnanam et al., 2015
	Ethanol	*Sargassum horneri*	Phaeophyceae	25	0.08 mg/g	Sivagnanam et al., 2015
	Cold acetone-methanol (7:3 v/v)	*Sargassum binderi*	Phaeophyceae	25	0.73 mg/g	Noviendri et al., 2011
	Cold acetone-methanol (7:3 v/v)	*Sargassum duplicatum*	Phaeophyceae	25	1.01 mg/g	Noviendri et al., 2011
	Acetone, 120 min	*Cylindrotheca closterium*	Bacillariophyceae	20	5.34 μg/mg	Pasquet et al., 2011
	Acetone, 60 min	*Cylindrotheca closterium*	Bacillariophyceae	56	5.23 μg/mg	Pasquet et al., 2011
Soxhlet extraction	Ethanol (80%)	*Phaeodactylum tricornutum*	Bacillariophyceae	80	15.42 mg/g	Kim et al., 2012
	Ethanol	*Laminaria japonica*	Phaeophyceae	40	191 μg/g	Kanazawa et al., 2008
	Ethanol	*Undaria pinnatifida*	Phaeophyceae	78	50 μg/g	Kanda et al., 2014

the vapor pressure of fucoxanthin is an important factor influencing the extraction efficiency; the high vapor pressure of fucoxanthin at a higher temperature enhances its diffusion from the solid matrices (Quitain et al., 2013). In addition, the algae biomass subjected to SFE must undergo an energy-intensive drying step because the water layers on wet biomass obstruct the penetration of SC-CO_2 (Derwenskus et al., 2019). Therefore, the implementation of SFE for industrial applications may face some challenges. For example, the requirement of pressurized gas and the expensive equipment may impose greater operational and investment costs. Nonetheless, CO_2 could be easily recycled by separating the gas stream during the process depressurization. The application of entrainer or co-solvents can improve the extraction efficiency of SFE but an additional step of solvent separation from the extract is required (Quitain et al., 2013). Moreover, polar impurities such as pigments may be co-extracted because the entrainer tends to enhance the polarity of SC-CO_2.

Pressurised Liquid Extraction (PLE)

Pressurised liquid extraction (PLE) is an extraction technique utilizing high temperature (50–200°C) and pressure (3.5–20 MPa) to improve solubility and diffusion rate of biomolecules from complex crude extracts to the solvent phase (Kadam et al., 2013; Derwenskus et al., 2019). In PLE, the high-pressure condition increases the fluid density and maintains the solvent in the liquid (subcritical) state above their boiling point, while the high-temperature condition accelerates the penetration of solvents by lowering the viscosity and surface tension of solvents (Gilbert-López et al., 2017). The major advantages of PLE over the direct solvent extraction and Soxhlet extraction techniques include the rapid extraction process and the lower consumption of solvent. Ethanol was commonly used in the extraction of fucoxanthin via PLE. Although the high-temperature condition of PLE enhances the solubility and diffusivity characteristics of compounds, it was not favorable for the extraction of fucoxanthin from *Eisenia bicyclis* because of the yield of fucoxanthin

TABLE 5 | Emerging methods for extraction of fucoxanthin from macro- and microalgae.

Extraction method	Extractive solvents	Operating conditions	Algae strains	Yield of fucoxanthin	References
SFE	SC-CO_2	70°C, 40 MPa, 3 h	*Undaria pinnatifida* (seaweed)	59.51 μg/g	Kanda et al., 2014
	SC-CO_2 + ethanol (3.23%)	60°C, 40 MPa, 3 h	*Undaria pinnatifida* (seaweed)	994.53 μg/g	Kanda et al., 2014
	SC-CO_2	50°C, 30 MPa, 1 h	*Sargassum muticum* (seaweed)	1.5 mg/100 g	Conde et al., 2014
	SC-CO_2 + ethanol (10%)	50°C, 20 MPa, 40 min	*Sargassum muticum* (seaweed)	12 mg/100 g	Conde et al., 2014
	SC-CO_2	40°C, 40 MPa, 3 h	*Undaria pinnatifida* (seaweed)	1.22 g/100 g	Quitain et al., 2013
	SC-CO_2	60°C, 40 MPa, 150 min	*Undaria pinnatifida* (seaweed)	58 μg/g	Goto et al., 2015
	SC-CO_2	40°C, 30 MPa, 3 h	*Saccharina japonica* (seaweed)	2.08 mg/g	Getachew et al., 2018
	SC-CO_2 + methanol	30°C, 20 MPa, 1 h	*Phaeodactylum tricornutum* (diatom)	0.69 mg/g	Aslanbay Guler et al., 2020
	SC-CO_2 + ethanol (10%)	45°C, 25 MPa, 2 h	*Saccharina japonica* (seaweed)	0.41 mg/g	Sivagnanam et al., 2015
	SC-CO_2 + ethanol (10%)	45°C, 25 MPa, 2 h	*Sargassum horneri* (seaweed)	0.77 mg/g	Sivagnanam et al., 2015
	SC-CO_2 + ethanol (10%, v/v)	50°C, 20 MPa, 2 h	*Undaria pinnatifida* (seaweed)	0.00753 μg/g	Roh et al., 2008
PLE	Ethanol: water (9:1)	110°C, 10.3 MPa	*Eisenia bicyclis* (brown algae)	0.42 mg/g	Shang et al., 2011
	Ethanol	100°C, 10.3 MPa	*Phaeodactylum tricornutum* (diatom)	16.51 mg/g	Kim et al., 2012
	Dimethyl ether	25°C, 10.3 MPa	*Undaria pinnatifida* (seaweed)	390 μg/g	Kanda et al., 2014
	Ethanol	100°C, 10.3 MPa	*Phaeodactylum tricornutum* (diatom)	7.73 mg/g	Gilbert-López et al., 2017
	Ethanol	170°C, 10.3 MPa	*Phaeodactylum tricornutum* (diatom)	5.81 mg/g	Gilbert-López et al., 2017
	Ethanol	100°C, 10.3 MPa	*Phaeodactylum tricornutum* (diatom)	26.1 mg/g	Derwenskus et al., 2019
UAE	Ethanol	25°C, 70 KHz, 30 min	*Phaeodactylum tricornutum* (diatom)	15.96 mg/g	Kim et al., 2012
	Acetone	8.5°C, 12.2 W, 10 min	*Cylindrotheca closterium* (diatom)	4.49 μg/g	Pasquet et al., 2011
	Coconut oil	450 W, 25 KHz, 15 min (bath)	*Phaeodactylum tricornutum* (diatom)	0.97 mg/mL	Papadaki et al., 2017
	Ethanol (80%, v/v)	230 W, 50 Hz, 30 min (bath)	*Padina tetrastromatica* (seaweed)	0.75 mg/g	Raguraman et al., 2018
MAE	Acetone	50 W, 5 min	*Cylindrotheca closterium* (diatom)	4.24 μg/mg	Pasquet et al., 2011
	Ethanol (50%)	300 W, 60°C, 10 min	*Laminaria japonica* (seaweed)	5.13 mg/100 g	Xiao et al., 2012
	Ethanol (50%)	300 W, 60°C, 10 min	*Undaria pinnatifida* (seaweed)	109.3 mg/100 g	Xiao et al., 2012
	Ethanol (50%)	300 W, 60°C, 10 min	*Sargassum fusiforme* (seaweed)	2.12 mg/100 g	Xiao et al., 2012
	Ethanol (50%)	300 W, 60°C, 5 min	*Undaria pinnatifida* (seaweed)	0.73 mg/g	Xiao et al., 2012
	Ethanol	850 W, 2455 MHz, 2 min	*Phaeodactylum tricornutum* (diatom)	4.59 mg/g	Gilbert-López et al., 2017
	Ethanol	700 W, 2450 MHz, 1 min	*Phaeodactylum tricornutum* (diatom)	58.07%	Zhang et al., 2018
EAE	Sodium buffer, Cellulase:pectinase	50°C, 80 min	*Laminaria japonica* (seaweed)	18.3 mg/100 g	Qin et al., 2013
	Sodium acetate buffer (0.1M), Viscozyme (100 fungal β-glucanase units/g)	50°C, 100 rpm, 12 h	*Fucus vesiculosus* (seaweed)	0.657 mg/g	Shannon and Abu-Ghannam, 2018

was only about 0.42 mg/g (Shang et al., 2011). A similar observation was also reported by Gilbert-López et al. (2017), who discovered that the yield of fucoxanthin dropped by 25% when the operating temperature of PLE increased from 50 to 170°C. Fucoxanthin, which is a temperature-sensitive bioactive compound, can undergo oxidation process at high-temperature conditions and result in the poor yield of extraction. Therefore, it is envisaged that optimal operating temperature for the extraction of fucoxanthin is to be used to preserve the extracted fucoxanthin and subsequently its bioactivities. Furthermore, the safety of PLE operation must be considered because of the high pressure used. The operation period needs to be optimized for ensuring a sufficient contact time between fucoxanthin and solvents until the concentration gradient of fucoxanthin between solvent phase

and plant matrix reached a balance. However, a prolonged period of PLE was not encouraged because fucoxanthin could undergo isomerization under the extreme physical conditions of PLE (Aslanbay Guler et al., 2020).

Ultrasound-Assisted Extraction (UAE)

Ultrasound-assisted extraction (UAE) has proven useful in overcoming the bottlenecks of conventional solvent extraction processes such as extraction duration and solvent consumption (Papadaki et al., 2017). This approach has been widely used for the extraction of various carotenoids and high-value bioactive compounds (e.g., lutein, astaxanthin, canthaxanthin, β-carotenes, docosahexaenoic acid, eicosapentaenoic acid) from complex feedstock (Cravotto et al., 2008; Dey and Rathod, 2013; Taghi Gharibzahedi et al., 2015; Goula et al., 2017; Chew et al., 2018; Sankaran et al., 2018). The ultrasound technology induces cavitation bubbles that collapse and produce heat energy along with ultrasonic waves (Chemat et al., 2017). These generated mechanical shear forces are responsible for disrupting the cell wall of algae, thereby releasing the target compounds into the solvent phase. The advantage of UAE lies in the disruptive-extractive forces that facilitate the extraction of target compounds from complex feedstock (e.g., algae with thick cell wall) in a single-step approach within a shorter period of extraction. Moreover, the mixing effect caused by acoustic streaming enhances the contact between solvents and target compounds. In conjunction with SDGs, ultrasound technology has been a potential extraction method for the green and sustainable processing of bioactive compounds from natural resources (Tiwari, 2015).

The UAE can be achieved with either an ultrasound bath or an ultrasound probe. It is recommended to adopt a probe instrument due to its effectiveness in cell disruption and energy efficiency. However, the drawback of the ultrasound probe is the overheating of the tip of ultrasound probe that could damage the heat-labile compounds. To overcome the overheating issue, the sample is usually chilled in an ice bath prior to the ultrasonic treatment. In general, UAE with an ultrasound probe gave a higher yield of fucoxanthin (15.96 mg/g), as compared to the ultrasound bath yielding only 0.75–0.97 mg/g of extracted fucoxanthin (Kim et al., 2012; Papadaki et al., 2017; Raguraman et al., 2018). To date, there is still insufficient literature reporting the application of UAE of fucoxanthin from diatom species.

Microwave-Assisted Extraction (MAE)

Microwave-assisted extraction (MAE) is a rapid and efficient extraction process for the recovery of bioactive compounds. The heating of the sample by microwave can be typically done in less than a minute, and the homogenous heating of the sample by microwave irradiation ensures no hot spots or limitations in heat transfer (Pasquet et al., 2011). Microwave irradiation induces heat energy through molecular interaction between solid and liquid (Chew et al., 2019). The heating effect generated from the incident electromagnetic waves promote the rapid dissolution of photosynthetic membranes by selective heating of the more polar part of cellulose (Banik et al., 2003). This heating effect is useful for releasing fucoxanthin from the fucoxanthin-chl *a*/*c*-protein complexes (Halim et al., 2012; Xia et al., 2013). Besides, the microwave facilitates an efficient release of intracellular bioactive compounds by improving the penetration of solvent into the matrix (Kadam et al., 2013). In aligning to the principles of green chemistry, microwave technology is favored for a green and clean process of extraction without the need for high-pressure conditions.

Ethanol has been commonly chosen as the solvent for MAE of fucoxanthin. This bio-based solvent favorably interacts with membrane-related lipid complexes. MAE of fucoxanthin in ethanol has been applied to macroalgae such as *L. japonica, Undaria pinnatifida,* and *Sargassum fusiforme* under the operating conditions of 300 W, 60°C, and 10 min. Among the tested macroalgae strains, the yield of fucoxanthin obtained from brown seaweed *S. fusiforme* was the least, which might be due to the rigidity of the cellular wall structure of algae. On the other hand, there are two separate studies demonstrating the rapid extraction of fucoxanthin from microalgae *P. tricornutum* via MAE in ethanol, which could be completed within 1–2 min (del Pilar Sánchez-Camargo et al., 2017; Zhang et al., 2018). The higher yield of fucoxanthin extracted from microalgae was attributed to the fact that cell wall of microalgae is less recalcitrant than that of macroalgae. To date, the scaling-up of MAE operation remains a challenge and the operating parameters such as temperature and duration of treatment must be optimized systematically. Preferably, the MAE of carotenoid should not exceed 60°C (Pasquet et al., 2011). The pulsed microwave processing or the continuous interval microwave processing with a short period of treatment time could circumvent the over-heating of sample, which effectively reduces the rate of fucoxanthin degradation during the MAE process.

Enzymatic-Assisted Extraction (EAE)

Enzymatic-assisted extraction (EAE) involves the use of hydrolytic enzymes such as pectinase and cellulase to hydrolyze algal cell walls. Algal cell walls mainly consist of cellulose (Domozych, 2001). The enzymatic treatment of algae is effective in hydrolyzing the cell wall to release the intracellular components into the extraction medium. Furthermore, EAE can be considered as a relatively low-cost technology if common food-grade enzymes including amylase, cellulose, pectinase, or β-galactosidase are used. In comparison to other alternative extraction techniques, EAE does not depend on energy-intensive equipment and it can be applied for large-scale extraction of algal bioactive compounds. However, EAE can be inadequate for large-scale applications due to the main drawbacks such as long enzymatic process, low selectivity, and poor yield. Apart from the duration of enzymatic treatment, the temperature condition of EAE must be optimized to maximize the extraction yield.

A recent work by Shannon and Abu−Ghannam (2018) demonstrated the applicability of EAE of fucoxanthin in brown seaweeds pre-treated at low temperature followed by drying and mechanical blending. A commercial enzyme cocktail, Viscozyme, was found to be effective not only in hydrolyzing the cellulose in the cell wall of seaweeds but also in reducing the viscosity of mixture. However, the efficiency of EAE was dependent on the physical texture and the target part (e.g., blade, stipe

or holdfast) of seaweed. EAE could also be used as a pre-treatment step to improve the yield of fucoxanthin obtained from solvent extraction (dimethyl ether and ethanol); a 9.3% increase in fucoxanthin yield was obtained from *Undaria pinnatifida* biomass that was pre-treated by alginate lyase (Billakanti et al., 2013). EAE of fucoxanthin from microalgae was feasible, although the yield was lower as compared to that from the conventional extraction approaches.

FUTURE PERSPECTIVES: POTENTIAL AND LIMITATION OF EXTRACTION TECHNIQUES

Conventional solid-liquid extraction has always been the dominant method used in the extraction of carotenoids from natural sources. Likewise, fucoxanthin is no exception, as evidenced by this review. Although solvents used in solid-liquid extraction could be recovered by evaporation or steam distillation processes for the economical consideration, it is desirable to minimize the usage of chemicals in the extraction process due to the inherent concerns over the toxicity of chemical solvents and the stricter regulations on food and environment. Moreover, increasing consumer awareness, as well as the urge for sustainable and responsible production, have put pressure on the search for cleaner and greener extraction processes. Considering the rising demand for bioactive compounds, the efforts in developing more efficient extraction technologies are underway. Irrespective of the extraction methods, it is crucial to ensure that the bioactivity of fucoxanthin is not compromised during the extraction.

The major challenge in fucoxanthin extraction is the potential degradation of fucoxanthin during the extraction process. Fortunately, it is apparent that the emerging extraction methods can be a good substitute to conventional extraction techniques, although none of them can be regarded as the prime method for the extraction of fucoxanthin from algal sources. In general, these alternative and emerging extraction methods have been proven effective in reducing the total volume of solvent consumed. Except for EAE, these extraction methods are energy-intensive, and their instrumentation and setup costs could be exorbitant to small and medium-sized enterprises. PLE and MAE methods are restricted by the high-temperature conditions used, and the optimization of extraction parameters are required for different algal species. EAE can mitigate the reliance on solvent, but the major obstacle to its application is the high cost of enzymes as compared to solvents and CO_2. SFE and UAE methods are increasingly viewed as viable methods for the extraction of fucoxanthin. UAE is a versatile extraction method that can be integrated with other novel extraction methods such as SFE, MAE, and PLE. The integrative extraction method exploits the advantages of both discrete methods for a more satisfactory extraction performance.

SC-CO_2 has gained popularity as a suitable solvent for the extraction of plant-based biomolecules because it is inexpensive, non-toxic, chemically inert, non-flammable, and readily available (Roh et al., 2008). Aside from that, an ongoing research effort has been devoted to the microalgae biorefinery by using green solvents like ionic liquids (ILs) and deep eutectic solvents (DESs). ILs have distinctive characteristics such as tunable properties, low melting point, low vapor pressure, and resistance toward high thermal stability. Surface-active ILs and tensioactive compounds have a high affinity to the hydrophobic carotenoid or pigments present in algal biomass (Vieira et al., 2018). They are miscible with water, making them suitable for extraction of fucoxanthin from wet algal biomass. The extractive capability of the anionic surfactant sodium dodecyl sulfate (SDS) was more superior than that of ethanol in the extraction of carotenoid (fucoxanthin included) from wet or dried biomass of *Sargassum muticum* (Vieira et al., 2018). It was postulated that SDS promoted cell disruption, facilitating the solubilization of hydrophobic compounds. However, the sustainable extraction of fucoxanthin using ILs still requires more in-depth studies as the concern for IL application is mainly on the hazardous raw materials involved in the synthesis of certain types of ILs. Alternative solvents such as using choline-based DESs have yet to be fully explored for fucoxanthin extraction, but the high viscosity of DESs may obstruct the mass transfer during extraction. Ideally, the recyclability of these alternative solvents should be adequately addressed to meet the sustainability criteria in the water-based extraction of fucoxanthin.

The extraction of fucoxanthin at a commercial scale is viable, as evidenced by a past study by Kanazawa et al. (2008). It was reported that the extraction of fucoxanthin from the waste part of brown macroalgae, *L. japonica* via a conventional extraction approach (i.e., ethanol along with silica gel column separation). The extracted fucoxanthin was estimated to be 149 g of fucoxanthin per ton of waste part of *L. japonica.* This biorefinery process is a good example of circular economy and it fulfills the SDGs by utilizing waste as a raw material of bioproduct. Liquefied dimethyl ether was also proposed as a suitable solvent for extraction for fucoxanthin due to its low boiling point for easy removal of solvent from the final product (Zarekarizi et al., 2019) as well as lower energy consumption. Moreover, liquefied dimethyl ether was regarded as a safe extraction solvent by food safety authorities from various countries (Zarekarizi et al., 2019). Aside from these, the scaling-up of extraction process must also consider the safety of operation at industrial level.

The biorefinery of microalgae for fucoxanthin extraction must be thoroughly considered in terms of techno-economic analysis (assessing economic feasibility) and life-cycle analysis (assessing potential environmental impacts). In particular, the de-watering step of microalgae biomass from culture (via energy-intensive centrifugation) prior to the extraction step is the major contributor to energy consumption and eventually increases total production cost. Therefore, direct extraction of fucoxanthin or other carotenoids from the wet microalgae biomass could overcome this concern. For example, fucoxanthin was extracted from wet *P. tricornutum* by subcritical fluid extraction, or known as PLE (Derwenskus et al., 2019; Aslanbay Guler et al., 2020). The optimal yield of fucoxanthin was attained by using methanol at solvent-to-solid ratio of 200:1, 200 MPa pressure and 35°C (Aslanbay Guler et al., 2020). The residual carbon-rich biomass obtained after the extraction could be prospectively used in other

applications including livestock feed and fodder, making the extraction method a sustainable platform for biorefinery.

Furthermore, the isolation of fucoxanthin from algal sources could be accompanied by a step of purification to improve the purity of fucoxanthin. The conventional solvent extraction of fucoxanthin from brown algae could be non-selective and would co-extract chlorophylls during the extraction process. Fucoxanthin is often associated with the chlorophyll in the assembly of fucoxanthin-chlorophyll-protein complexes (Wang et al., 2005). This phenomenon renders a complex mixture for the downstream processing of fucoxanthin. Therefore, the ability of a solvent to specifically target fucoxanthin instead of other pigments from algal sources should be considered in these alternative and emerging extraction processes. Chromatographic separation techniques such as silica gel column chromatography, preparative thin-layer chromatography, high-performance liquid chromatography and liquid-liquid partition chromatography have been commonly used in the purification of fucoxanthin (Xiao et al., 2012). To improve the overall efficiency of downstream processing, the extraction techniques can be coupled with the separation techniques. The fucoxanthin-containing solvent fraction retrieved from the solvent extraction (e.g., ethanolic stream) could be directly subjected to the liquid-liquid separation systems like aqueous two-phase system (Gómez-Loredo et al., 2014, 2015) or high-speed countercurrent chromatography (Xiao et al., 2012). Prospectively, the simultaneous extraction and purification of fucoxanthin can be accomplished by integrating biphasic separation techniques with the emerging extraction techniques assisted by ultrasound, electricity, microwave, magnetic field and bubbles (Zhao et al., 2016; Sankaran et al., 2018; Chew et al., 2019; Khoo et al., 2019; Leong et al., 2019).

CONCLUSION

With the inevitable increase in the human population, it is pertinent to ensure food security by seeking alternative and sustainable food sources. Microalgae stand out as a promising candidate as the next generation feedstock that contributes to 16 out of 17 SDGs. One of the most important microalgal biomolecules is fucoxanthin, which has powerful antioxidant properties due to its radical scavenging and singlet oxygen quenching activities. However, the apparent energy-intensive nature of emerging extraction methods can be prohibitive to the commercial production of fucoxanthin and counter-productive to the objectives of SDGs. From here, this review provides an updated understanding of existing and alternative green extraction technologies for fucoxanthin extraction. This enables stakeholders to make informed decisions which is an important milestone for biorefineries, propelling industries toward sustainable development.

The green extraction strategy is one of the many processing stages for sustainable supplies of bioactive ingredients. Other processing stages like extract separation and purification or upstream work (e.g., microalgae cultivation, biomass harvesting, transportation, and storage as well as a fair trade for workers) should also be aligned to SDGs. Further optimization of extraction technologies should focus on the minimization of energy consumption and the integration of different extraction methods to improve the efficiency of fucoxanthin extraction. In the long term, the gradual adoption and advocacy of sustainable strategies in microalgae biorefinery will ultimately close the loop for a circular bioeconomy.

AUTHOR CONTRIBUTIONS

SF conceptualized, wrote a section, and led the project. KK, CO, and PS contributed to the extraction processes section. NK contributed the section "Introduction." FY completed the section "Conclusion." All authors critically reviewed, edited, and approved the final manuscript.

FUNDING

The authors acknowledge the financial support of the Monash University Malaysia Sustainable Community Grant Scheme (SDG-2018-04-SCI), Malaysia-Japan collaborative research fund for the SATREPS–COSMOS (project no. JPMJSA 1509) project, and the Ministry of Higher Education for Fundamental Research Grant Scheme (FRGS/1/2019/STG05/MUSM/03/2).

REFERENCES

Abdel-Raouf, N., Al-Homaidan, A., and Ibraheem, I. (2012). Microalgae and wastewater treatment. *Saudi J. Biol. Sci.* 19, 257–275. doi: 10.1016/j.sjbs.2012.04.005

Abu-Ghannam, N., and Shannon, E. (2017). "Seaweed carotenoid, fucoxanthin, as functional food," in *Microbial Functional Foods and Nutraceuticals*, eds V. K. Gupta, H. Treichel, V. O. Shapaval, L. Antoniode Oliveira and M. G. Tuohy (Chichester: John Wiley & Sons Ltd), 39–64. doi: 10.1002/9781119048961.ch3

Agatonovic-Kustrin, S., and Morton, D. (2013). Cosmeceuticals derived from bioactive substances found in marine algae. *Oceanography* 1:106.

Airanthi, M. W., Hosokawa, M., and Miyashita, K. (2011). Comparative antioxidant activity of edible japanese brown seaweeds. *J. Food Sci.* 76, C104–C111. doi: 10.1111/j.1750-3841.2010.01915.x

Akinsemolu, A. A. (2018). The role of microorganisms in achieving the sustainable development goals. *J. Cleaner Prod.* 182, 139–155. doi: 10.1016/j.jclepro.2018.02.081

Aslanbay Guler, B., Deniz, I., Demirel, Z., Yesil-Celiktas, O., and Imamoglu, E. (2020). A novel subcritical fucoxanthin extraction with a biorefinery approach. *Biochem. Eng. J.* 153:107403. doi: 10.1016/j.bej.2019.107403

Banerjee, A., Sharma, R., Chisti, Y., and Banerjee, U. C. (2002). *Botryococcus braunii*: a renewable source of hydrocarbons and other chemicals. *Crit. Rev. Biotechnol.* 22, 245–279. doi: 10.1080/07388550290789513

Banik, S., Bandyopadhyay, S., and Ganguly, S. (2003). Bioeffects of microwave—-a brief review. *Bioresour. Technol.* 87, 155–159. doi: 10.1016/S0960-8524(02)00169-4

Batista, A. P., Nunes, M. C., Fradinho, P., Gouveia, L., Sousa, I., Raymundo, A., et al. (2012). Novel foods with microalgal ingredients – Effect of gel setting conditions on the linear viscoelasticity of Spirulina and Haematococcus gels. *J. Food Eng.* 110, 182–189. doi: 10.1016/j.jfoodeng.2011.05.044

Bayro-Kaiser, V., and Nelson, N. (2017). Microalgal hydrogen production: prospects of an essential technology for a clean and sustainable energy economy. *Photosynthesis Res.* 133, 49–62. doi: 10.1007/s11120-017-0350-6

Beal, C. M., Gerber, L. N., Thongrod, S., Phromkunthong, W., Kiron, V., Granados, J., et al. (2018). Marine microalgae commercial production improves sustainability of global fisheries and aquaculture. *Sci. Rep.* 8:15064. doi: 10.1038/s41598-018-33504-w

Beppu, F., Niwano, Y., Tsukui, T., Hosokawa, M., and Miyashita, K. (2009). Single and repeated oral dose toxicity study of fucoxanthin (FX), a marine carotenoid, in mice. *J. Toxicol. Sci.* 34, 501–510. doi: 10.2131/jts.34.501

Billakanti, J. M., Catchpole, O. J., Fenton, T. A., Mitchell, K. A., and Mackenzie, A. D. (2013). Enzyme-assisted extraction of fucoxanthin and lipids containing polyunsaturated fatty acids from *Undaria pinnatifida* using dimethyl ether and ethanol. *Process Biochem.* 48, 1999–2008. doi: 10.1016/j.procbio.2013.09.015

Biloria, N., and Thakkar, Y. (2020). Integrating algae building technology in the built environment: a cost and benefit perspective. *Front. Architect. Res.* 9, 370–384. doi: 10.1016/j.foar.2019.12.004

Bjornland, T., and Liaeen-Jensen, S. (1989). "Distribution patterns of carotenoids in relation to chromophyte phylogeny and systematics," in *The Chromophyte Algae: Problems and Perspectives*, eds J. C. Green, B. S. C. Leadbeater, and W. L. Diver (Oxford: Clarendon Press), 37–61.

Blackburn, S., Bolch, C., Brown, M., Leroi, J.-M., and Volkman, J. (1997). *The CSIRO Collection of Living Microalgae: The Importance of Culture Collections and Microalgal Biodiversity to Aquaculture and Biotehcnology*. (Plouzane: IFREMER).

Blackburn, S., Frampton, D., Jameson, I., Brown, M., Mansour, M., Negri, A., et al. (2005). "The CSIRO collection of living microalgae: an australian perspective on microalgal biodiversity and applications," in *Algal Culture Collections and the Environment*, eds F. Kasai, K. Kaya, and M. M. Watanabe (Hadano: Tokai University Press), 29–63.

Blanco, A. C., Nadaoka, K., and Yamamoto, T. (2008). Planktonic and benthic microalgal community composition as indicators of terrestrial influence on a fringing reef in Ishigaki Island, Southwest Japan. *Mar. Environ. Res.* 66, 520–535. doi: 10.1016/j.marenvres.2008.08.005

Chemat, F., Rombaut, N., Sicaire, A.-G., Meullemiestre, A., Fabiano-Tixier, A.-S., and Abert-Vian, M. (2017). Ultrasound assisted extraction of food and natural products. Mechanisms, techniques, combinations, protocols and applications. A review. *Ultrason. Sonochem.* 34, 540–560. doi: 10.1016/j.ultsonch.2016.06.035

Chew, K. W., Chia, S. R., Lee, S. Y., Zhu, L., and Show, P. L. (2019). Enhanced microalgal protein extraction and purification using sustainable microwave-assisted multiphase partitioning technique. *Chem. Eng. J.* 367, 1–8. doi: 10.1016/j.cej.2019.02.131

Chew, K. W., Show, P. L., Yap, Y. J., Juan, J. C., Phang, S. M., Ling, T. C., et al. (2018). Sonication and grinding pre-treatments on *Gelidium amansii* seaweed for the extraction and characterization of agarose. *Front. Environ. Sci. Eng.* 12:2. doi: 10.1007/s11783-018-1040-0

Conde, E., Moure, A., and Domínguez, H. (2014). Supercritical CO2 extraction of fatty acids, phenolics and fucoxanthin from freeze-dried *Sargassum muticum*. *J. Appl. Phycol.* 27, 957–964. doi: 10.1007/s10811-014-0389-0

Couteau, C., and Coiffard, L. (2016). "Seaweed application in cosmetics," in *Seaweed in Health and Disease Prevention*, eds J. Fleurence and I. Levine (Amsterdam: Elsevier), 423–441. doi: 10.1016/B978-0-12-802772-1.00014-2

Cravotto, G., Boffa, L., Mantegna, S., Perego, P., Avogadro, M., and Cintas, P. (2008). Improved extraction of vegetable oils under high-intensity ultrasound and/or microwaves. *Ultrason. Sonochem.* 15, 898–902. doi: 10.1016/j.ultsonch.2007.10.009

Dahoumane, S. A., Mechouet, M., Alvarez, F. J., Agathos, S. N., and Jeffryes, C. (2016). Microalgae: an outstanding tool in nanotechnology. *Bionatura* 1, 196–201. doi: 10.21931/RB/2016.01.04.7

del Pilar Sánchez-Camargo, A., Pleite, N., Herrero, M., Cifuentes, A., Ibáñez, E., and Gilbert-López, B. (2017). New approaches for the selective extraction of bioactive compounds employing bio-based solvents and pressurized green processes. *J. Supercrit. Fluids* 128, 112–120. doi: 10.1016/j.supflu.2017.05.016

Derun, Y. (2009). "Training of trainers programme: strengthening capacity of small holder ASEAN aquaculture farmers for competitive and sustainable aquaculture," *Proceedings of a 3–7 August 2009 Conference* (Bangkok: NACA Secretariat), Available online at: http://library.enaca.org/inland/reports/training-oftrainers-report.pdf

Derwenskus, F., Metz, F., Gille, A., Schmid-Staiger, U., Briviba, K., Schließmann, U., et al. (2019). Pressurized extraction of unsaturated fatty acids and carotenoids from wet *Chlorella vulgaris* and *Phaeodactylum tricornutum* biomass using subcritical liquids. *GCB Bioenergy* 11, 335–344. doi: 10.1111/gcbb.12563

Dey, S., and Rathod, V. K. (2013). Ultrasound assisted extraction of β-carotene from *Spirulina platensis*. *Ultrason. Sonochem.* 20, 271–276. doi: 10.1016/j.ultsonch.2012.05.010

Domozych, D. S. (2001). "Algal cell walls," in *eLS*, ed. P. Gregg (Hoboken, NJ: Wiley). doi: 10.1038/npg.els.0000315

Ebrahimi Nigjeh, S., Yusoff, F. M., Mohamed Alitheen, N. B., Rasoli, M., Keong, Y. S., and Omar, A. R. B. (2013). Cytotoxic effect of ethanol extract of microalga, Chaetoceros calcitrans, and its mechanisms in inducing apoptosis in human breast cancer cell line. *Biomed Res. Int.* 2013:783690. doi: 10.1155/2013/783690

Elrayies, G. M. (2018). Microalgae: prospects for greener future buildings. *Renew. Sustain. Energy Rev.* 81, 1175–1191. doi: 10.1016/j.rser.2017.08.032

Foo, S. C., Yusoff, F. M., Imam, M. U., Foo, J. B., Ismail, N., Azmi, N. H., et al. (2019). Increased fucoxanthin in *Chaetoceros calcitrans* extract exacerbates apoptosis in liver cancer cells via multiple targeted cellular pathways. *Biotechnol. Rep.* 21:e00296. doi: 10.1016/j.btre.2018.e00296

Foo, S. C., Yusoff, F. M., Ismail, M., Basri, M., Chan, K. W., Khong, N. M. H., et al. (2015a). Production of fucoxanthin-rich fraction (FxRF) from a diatom, Chaetoceros calcitrans (Paulsen) Takano 1968. *Algal Res.* 12, 26–32. doi: 10.1016/j.algal.2015.08.004

Foo, S. C., Yusoff, F. M., Ismail, M., Basri, M., Khong, N. M. H., Chan, K. W., et al. (2015b). Efficient solvent extraction of antioxidant-rich extract from a tropical diatom, *Chaetoceros calcitrans* (Paulsen) Takano 1968. *Asian Pac. J. Trop. Biomed.* 5, 834–840. doi: 10.1016/j.apjtb.2015.06.003

Foo, S. C., Yusoff, F. M., Ismail, M., Basri, M., Yau, S. K., Khong, N. M., et al. (2017). Antioxidant capacities of fucoxanthin-producing algae as influenced by their carotenoid and phenolic contents. *J. Biotechnol.* 241, 175–183. doi: 10.1016/j.jbiotec.2016.11.026

Gaignard, C., Laroche, C., Pierre, G., Dubessay, P., Delattre, C., Gardarin, C., et al. (2019). Screening of marine microalgae: investigation of new exopolysaccharide producers. *Algal Res.* 44, 101711. doi: 10.1016/j.algal.2019.101711

García, J. L., De Vicente, M., and Galán, B. (2017). Microalgae, old sustainable food and fashion nutraceuticals. *Microb. Biotechnol.* 10, 1017–1024. doi: 10.1111/1751-7915.12800

Getachew, A. T., Saravana, P. S., Cho, Y. J., Woo, H. C., and Chun, B. S. (2018). Concurrent extraction of oil from roasted coffee (*Coffea arabica*) and fucoxanthin from brown seaweed (*Saccharina japonica*) using supercritical carbon dioxide. *J. CO2 Util.* 25, 137–146. doi: 10.1016/j.jcou.2018.03.018

Gilbert-López, B., Barranco, A., Herrero, M., Cifuentes, A., and Ibáñez, E. (2017). Development of new green processes for the recovery of bioactives from *Phaeodactylum tricornutum*. *Food Res. Int.* 99, 1056–1065. doi: 10.1016/j.foodres.2016.04.022

Goiris, K., Muylaert, K., Fraeye, I., Foubert, I., De Brabanter, J., and De Cooman, L. (2012). Antioxidant potential of microalgae in relation to their phenolic and carotenoid content. *J. Appl. Phycol.* 24, 1477–1486. doi: 10.1007/s10811-012-9804-6

Gómez-Loredo, A., Benavides, J., and Rito-Palomares, M. (2014). Partition behavior of fucoxanthin in ethanol-potassium phosphate two-phase systems. *J. Chem. Technol. Biotechnol.* 89, 1637–1645. doi: 10.1002/jctb.4514

Gómez-Loredo, A., González-Valdez, J., and Rito-Palomares, M. (2015). Insights on the downstream purification of fucoxanthin, a microalgal carotenoid, from an aqueous two-phase system stream exploiting ultrafiltration. *J. Appl. Phycol.* 27, 1517–1523. doi: 10.1007/s10811-014-0443-y

Goto, M., Kanda, H., and Machmudah, S. (2015). Extraction of carotenoids and lipids from algae by supercritical CO2 and subcritical dimethyl ether. *J. Supercrit. Fluids* 96, 245–251. doi: 10.1016/j.supflu.2014.10.003

Goula, A. M., Ververi, M., Adamopoulou, A., and Kaderides, K. (2017). Green ultrasound-assisted extraction of carotenoids from pomegranate wastes using vegetable oils. *Ultrason. Sonochem.* 34, 821–830. doi: 10.1016/j.ultsonch.2016.07.022

Grant, B., Waller, R. F., Clementson, L. A., and Wetherbee, R. (2013). Psammamonas australis gen. et sp. nov.(Raphidophyceae), a new dimorphic, sand-dwelling alga. *Phycologia* 52, 57–64. doi: 10.2216/12-070.1

Griffiths, M. J., and Harrison, S. T. L. (2009). Lipid productivity as a key characteristic for choosing algal species for biodiesel production. *J. Appl. Phycol.* 21, 493–507. doi: 10.1007/s10811-008-9392-7

Halim, R., Danquah, M. K., and Webley, P. A. (2012). Extraction of oil from microalgae for biodiesel production: a review. *Biotechnol. Adv.* 30, 709–732. doi: 10.1016/j.biotechadv.2012.01.001

Hashimoto, T., Ozaki, Y., Taminato, M., Das, S. K., Mizuno, M., Yoshimura, K., et al. (2009). The distribution and accumulation of fucoxanthin and its metabolites after oral administration in mice. *Br. J. Nutr.* 102, 242–248. doi: 10.1017/S0007114508199007

Hemaiswarya, S., Raja, R., Kumar, R. R., Ganesan, V., and Anbazhagan, C. (2011). Microalgae: a sustainable feed source for aquaculture. *World J. Microbiol. Biotechnol.* 27, 1737–1746. doi: 10.1007/s11274-010-0632-z

Heo, S. J., and Jeon, Y. J. (2009). Protective effect of fucoxanthin isolated from *Sargassum siliquastrum* on UV-B induced cell damage. *J. Photochem. Photobiol. B Biol.* 95, 101–107. doi: 10.1016/j.jphotobiol.2008.11.011

Heo, S. J., Yoon, W. J., Kim, K. N., Oh, C., Choi, Y. U., Yoon, K. T., et al. (2012). Anti-inflammatory effect of fucoxanthin derivatives isolated from *Sargassum siliquastrum* in lipopolysaccharide-stimulated RAW 264.7 macrophage. *Food Chem. Toxicol.* 50, 3336–3342. doi: 10.1016/j.fct.2012.06.025

Holdt, S. L., and Kraan, S. (2011). Bioactive compounds in seaweed: functional food applications and legislation. *J. Appl. Phycol.* 23, 543–597. doi: 10.1007/s10811-010-9632-5

Jaswir, I., Noviendri, D., Salleh, H. M., Taher, M., Miyashita, K., and Ramli, N. (2013). Analysis of fucoxanthin content and purification of all-trans-fucoxanthin from *Turbinaria turbinata* and *Sargassum plagyophyllum* by SiO2 open column chromatography and reversed phase-HPLC. *J. Liquid Chromatogr. Relat. Technol.* 36, 1340–1354. doi: 10.1080/10826076.2012.691435

Jelić, S., and Jovanović, T. (2013). "Education in transition," in *Terms Of The Development Of Agriculture And Rural Development*. ed. N. Bogdanov (Belgrade: University of Belgrada).

Kadam, S. U., Tiwari, B. K., and O'donnell, C. P. (2013). Application of novel extraction technologies for bioactives from marine algae. *J. Agric. Food Chem.* 61, 4667–4675. doi: 10.1021/jf400819p

Kanazawa, K., Ozaki, Y., Hashimoto, T., Das, S. K., Matsushita, S., Hirano, M., et al. (2008). Commercial-scale preparation of biofunctional fucoxanthin from waste parts of brown sea algae *Laminalia japonica*. *Food Sci. Technol. Res.* 14, 573–582. doi: 10.3136/fstr.14.573

Kanda, H., Kamo, Y., Machmudah, S., and Goto, M. (2014). Extraction of fucoxanthin from raw macroalgae excluding drying and cell wall disruption by liquefied dimethyl ether. *Mar. Drugs* 12, 2383–2396. doi: 10.3390/md12052383

Kashyap, M., Samadhiya, K., Ghosh, A., Anand, V., Shirage, P. M., and Bala, K. (2019). Screening of microalgae for biosynthesis and optimization of Ag/AgCl nano hybrids having antibacterial effect. *RSC Adv.* 9, 25583–25591. doi: 10.1039/C9RA04451E

Kavitha, S., and Gunasekaran, M. (2020). Microalgae based biorefinery promoting circular bioeconomy-Techno economic and life-cycle analysis. *Bioresour. Technol.* 302:122822. doi: 10.1016/j.biortech.2020.122822

Kawee-Ai, A., Kim, A. T., and Kim, S. M. (2019). Inhibitory activities of microalgal fucoxanthin against α-amylase, α-glucosidase, and glucose oxidase in 3T3-L1 cells linked to type 2 diabetes. *J. Oceanol. Limnol.* 37, 928–937. doi: 10.1007/s00343-019-8098-9

Khoo, K. S., Chew, K. W., Ooi, C. W., Ong, H. C., Ling, T. C., and Show, P. L. (2019). Extraction of natural astaxanthin from *Haematococcus pluvialis* using liquid biphasic flotation system. *Bioresour. Technol.* 290:121794. doi: 10.1016/j.biortech.2019.121794

Kim, S.-K. (2011). *Marine Cosmeceuticals: Trends and Prospects*. Boca Raton, FL: CRC Press.

Kim, S. K. (2012). *Handbook of Marine Macroalgae*. West Sussex: John Wiley & Sons Ltd.

Kim, S. M., Jung, Y.-J., Kwon, O.-N., Cha, K. H., Um, B.-H., Chung, D., et al. (2012). A potential commercial source of fucoxanthin extracted from the microalga *Phaeodactylum tricornutum*. *Appl. Biochem. Biotechnol.* 166, 1843–1855. doi: 10.1007/s12010-012-9602-2

Kumar, K. S., Dahms, H.-U., Won, E.-J., Lee, J.-S., and Shin, K.-H. (2015). Microalgae–a promising tool for heavy metal remediation. *Ecotoxicol. Environ. Saf.* 113, 329–352. doi: 10.1016/j.ecoenv.2014.12.019

Kusin, O.-S. C., and Horan, N. (2015). Energy and revenue creation from the anaerobic digestion of *Chlorella vulgaris* cultivated in liquor from chemically treated sewage sludge. *Int. J. Tech. Res. Appl.* 32, 49–55.

Kwon, K.-C., Lamb, A., Fox, D., and Jegathese, S. J. P. (2019). An evaluation of microalgae as a recombinant protein oral delivery platform for fish using green fluorescent protein (GFP). *Fish Shellfish Immunol.* 87, 414–420. doi: 10.1016/j.fsi.2019.01.038

Lababpour, A. (2016). Potentials of the microalgae inoculant in restoration of biological soil crusts to combat desertification. *Int. J. Environ. Sci. Technol.* 13, 2521–2532. doi: 10.1007/s13762-016-1074-4

Leong, H. Y., Ooi, C. W., Law, C. L., Julkifle, A. L., Katsuda, T., and Show, P. L. (2019). Integration process for betacyanins extraction from peel and flesh of Hylocereus polyrhizus using liquid biphasic electric flotation system and antioxidant activity evaluation. *Sep. Purif. Technol.* 209, 193–201. doi: 10.1016/j.seppur.2018.07.040

Lindblad, P., Fuente, D., Borbe, F., Cicchi, B., Conejero, J. A., Couto, N., et al. (2019). CyanoFactory, a European consortium to develop technologies needed to advance cyanobacteria as chassis for production of chemicals and fuels. *Algal Res.* 41:101510. doi: 10.1016/j.algal.2019.101510

Liu, C. L., Chiu, Y. T., and Hu, M. L. (2011). Fucoxanthin enhances HO-1 and NQO1 expression in murine hepatic BNL CL. 2 cells through activation of the Nrf2/ARE system partially by its pro-oxidant activity. *J. Agric. Food Chem.* 59, 11344–11351. doi: 10.1021/jf2029785

Mace, G. M., Norris, K., and Fitter, A. H. (2012). Biodiversity and ecosystem services: a multilayered relationship. *Trends Ecol. Evol.* 27, 19–26. doi: 10.1016/j.tree.2011.08.006

Maeda, H., Hosokawa, M., Sashima, T., Funayama, K., and Miyashita, K. (2007). Effect of medium-chain triacylglycerols on anti-obesity effect of fucoxanthin. *J. Oleo Sci.* 56, 615–621. doi: 10.5650/jos.56.615

Matondo, F. K., Takaisi, K., Nkuadiolandu, A. B., Kazadi Lukusa, A., and Aloni, M. N. (2016). Spirulina supplements improved the nutritional status of undernourished children quickly and significantly: experience from kisantu, the Democratic Republic of the Congo. *Int. J. Pediatr.* 2016:1296414. doi: 10.1155/2016/1296414

McHugh, D. J. (2003). *A Guide to the Seaweed Industry*. Rome: FAO.

Miyashita, K., Nishikawa, S., and Hosokawa, M. (2012). Therapeutic effect of fucoxanthin on metabolic syndrome and type 2 diabetes. *Nutr. Ther. Interv. Diabetes Metab. Syndr.* 3, 367–379. doi: 10.1016/B978-0-12-385083-6.00029-2

Moejes, F. W., and Moejes, K. B. (2017). Algae for Africa: microalgae as a source of food, feed and fuel in Kenya. *Afr. J. Biotechnol.* 16, 288–301. doi: 10.5897/AJB2016.15721

Mohseniazar, M., Barin, M., Zarredar, H., Alizadeh, S., and Shanehbandi, D. (2011). Potential of microalgae and lactobacilli in biosynthesis of silver nanoparticles. *Bioimpacts* 1, 149–152.

Moriarty, P., and Honnery, D. (2019). New energy technologies: microalgae, photolysis and airborne wind turbines. *Sci* 1:43. doi: 10.3390/sci1020043

Muradian, K., Vaiserman, A., Min, K.-J., and Fraifeld, V. (2015). Fucoxanthin and lipid metabolism: a minireview. *Nutr. Metab. Cardiovasc. Dis.* 25, 891–897. doi: 10.1016/j.numecd.2015.05.010

Neumann, U., Derwenskus, F., Gille, A., Louis, S., Schmid-Staiger, U., Briviba, K., et al. (2018). Bioavailability and Safety of Nutrients from the Microalgae *Chlorella vulgaris*, *Nannochloropsis oceanica* and *Phaeodactylum tricornutum* in C57BL/6 Mice. *Nutrients* 10:965. doi: 10.3390/nu10080965

Nomura, T., Kikuchi, M., Kubodera, A., and Kawakami, Y. (1997). Proton-donative antioxidant activity of fucoxanthin with 1,1-diphenyl-2-picrylhydrazyl (DPPH). *Biochem. Mol. Biol. Int.* 42, 361–370. doi: 10.1080/15216549700202761

Norton, T. A., Melkonian, M., and Andersen, R. A. (1996). Algal biodiversity*. *Phycologia* 35, 308–326. doi: 10.2216/i0031-8884-35-4-308.1

Noviendri, D., Jaswir, I., Salleh, H. M., Taher, M., Miyashita, K., and Ramli, N. (2011). Fucoxanthin extraction and fatty acid analysis of *Sargassum binderi* and *Sargassum duplicatum*. *J. Med. Plants Res.* 5, 2405–2412.

Papadaki, S., Kyriakopoulou, K., and Krokida, M. (2017). Recovery and encapsualtion of bioactive extracts from *Haematococcus pluvialis* and *Phaedodactylum tricornutum* for food applications. *IOSR J. Environ. Sci. Toxicol. Food Technol.* 10, 53–58.

Pasquet, V., Chérouvrier, J.-R., Farhat, F., Thiéry, V., Piot, J.-M., Bérard, J.-B., et al. (2011). Study on the microalgal pigments extraction process: performance

of microwave assisted extraction. *Process Biochem.* 46, 59–67. doi: 10.1016/j.procbio.2010.07.009

Peng, J., Yuan, J.-P., Wu, C.-F., and Wang, J.-H. (2011). Fucoxanthin, a marine carotenoid present in brown seaweeds and diatoms: metabolism and bioactivities relevant to human health. *Mar. Drugs* 9, 1806–1828. doi: 10.3390/md9101806

Prabhasankar, P., Ganesan, P., Bhaskar, N., Hirose, A., Stephen, N., Gowda, L. R., et al. (2009). Edible Japanese seaweed, wakame (*Undaria pinnatifida*) as an ingredient in pasta: chemical, functional and structural evaluation. *Food Chem.* 115, 501–508. doi: 10.1016/j.foodchem.2008.12.047

Pulz, O., and Gross, W. (2004). Valuable products from biotechnology of microalgae. *Appl. Microbiol. Biotechnol.* 65, 635–648. doi: 10.1007/s00253-004-1647-x

Qin, Y., Meng, L.-Y., and Wang, F.-W. (2013). Extraction and antioxidant activity of fucoxanthin from *Laminaria japonica*. *Food Sci.* 34, 279–283.

Qiu, F. (2014). *Algae Architecture*. Delft: Delft University of Technology.

Quitain, A. T., Kai, T., Sasaki, M., and Goto, M. (2013). Supercritical carbon dioxide extraction of fucoxanthin from *Undaria pinnatifida*. *J. Agric. Food Chem.* 61, 5792–5797. doi: 10.1021/jf400740p

Raguraman, V., Mubarakali, D., Narendrakumar, G., Thirugnanasambandam, R., Kirubagaran, R., and Thajuddin, N. (2018). Unraveling rapid extraction of fucoxanthin from *Padina tetrastromatica*: purification, characterization and biomedical application. *Process Biochem.* 73, 211–219. doi: 10.1016/j.procbio.2018.08.006

Ramsey, E., Sun, Q., Zhang, Z., Zhang, C., and Gou, W. (2009). Mini-review: green sustainable processes using supercritical fluid carbon dioxide. *J. Environ. Sci.* 21, 720–726. doi: 10.1016/S1001-0742(08)62330-X

Richmond, A. (2017). "Microalgae of economic potential," in *Handbook of Microalgal Mass Culture*, ed. A. Richmond (Boca Raton, FL: CRC Press), 199–244.

Roesijadi, G., Jones, S. B., Snowden-Swan, L. J., and Zhu, Y. (2010). *Macroalgae as a Biomass Feedstock: A Preliminary Analysis*. Richland, WA: Pacific Northwest National Lab.(PNNL). doi: 10.2172/1006310

Roh, M.-K., Uddin, M. S., and Chun, B.-S. (2008). Extraction of fucoxanthin and polyphenol from *Undaria pinnatifida* using supercritical carbon dioxide with co-solvent. *Biotechnol. Bioprocess Eng.* 13, 724–729. doi: 10.1007/s12257-008-0104-6

Sachindra, N. M., Sato, E., Maeda, H., Hosokawa, M., Niwano, Y., Kohno, M., et al. (2007). Radical scavenging and singlet oxygen quenching activity of marine carotenoid fucoxanthin and its metabolites. *J. Agric. Food Chem.* 55, 8516–8522. doi: 10.1021/jf071848a

Sachs, J. D. (2012). From millennium development goals to sustainable development goals. *Lancet* 379, 2206–2211. doi: 10.1016/S0140-6736(12)60685-0

Sankaran, R., Manickam, S., Yap, Y. J., Ling, T. C., Chang, J.-S., and Show, P. L. (2018). Extraction of proteins from microalgae using integrated method of sugaring-out assisted liquid biphasic flotation (LBF) and ultrasound. *Ultrason. Sonochem.* 48, 231–239. doi: 10.1016/j.ultsonch.2018.06.002

Serrà, A., Artal, R., García-Amorós, J., Sepúlveda, B., Gómez, E., Nogués, J., et al. (2020). Hybrid Ni@ ZnO@ ZnS-Microalgae for Circular economy: a smart route to the efficient integration of solar photocatalytic water decontamination and bioethanol production. *Adv. Sci.* 7:1902447. doi: 10.1002/advs.201902447

Shahidi, F., and Alasalvar, C. (2010). "Marine Oils and other Marine Nutraceuticals," in *Handbook of Seafood Quality, Safety and Health Applications*, eds C. Alasalvar, F. Shahidi, K. Miyashita and U. Wanasundara (Hoboken, NJ: Wiley), 444–454. doi: 10.1002/9781444325546.ch36

Shang, Y. F., Kim, S. M., Lee, W. J., and Um, B.-H. (2011). Pressurized liquid method for fucoxanthin extraction from *Eisenia bicyclis* (Kjellman) Setchell. *J. Biosci. Bioeng.* 111, 237–241. doi: 10.1016/j.jbiosc.2010.10.008

Shannon, E., and Abu-Ghannam, N. (2017). Optimisation of fucoxanthin extraction from Irish seaweeds by response surface methodology. *J. Appl. Phycol.* 29, 1027–1036. doi: 10.1007/s10811-016-0983-4

Shannon, E., and Abu-Ghannam, N. (2018). Enzymatic extraction of fucoxanthin from brown seaweeds. *Int. J. Food Sci. Technol.* 53, 2195–2204. doi: 10.1111/ijfs.13808

Shen, C.-T., Chen, P.-Y., Wu, J.-J., Lee, T.-M., Hsu, S.-L., Chang, C.-M. J., et al. (2011). Purification of algal anti-tyrosinase zeaxanthin from Nannochloropsis oculata using supercritical anti-solvent precipitation. *J. Supercrit. Fluids* 55, 955–962. doi: 10.1016/j.supflu.2010.10.003

Simas-Rodrigues, C., Villela, H. D., Martins, A. P., Marques, L. G., Colepicolo, P., and Tonon, A. P. (2015). Microalgae for economic applications: advantages and perspectives for bioethanol. *J. Exp. Bot.* 66, 4097–4108. doi: 10.1093/jxb/erv130

Singh, J., Tiwari, O. N., and Dhar, D. W. (2019). Overview of carbon capture technology: microalgal biorefinery concept and state-of-the-art. *Front. Mar. Sci.* 6:29. doi: 10.3389/fmars.2019.00029

Sivagnanam, S. P., Yin, S., Choi, J. H., Park, Y. B., Woo, H. C., and Chun, B. S. (2015). Biological properties of fucoxanthin in oil recovered from two brown seaweeds using supercritical CO2 extraction. *Mar. Drugs* 13, 3422–3442. doi: 10.3390/md13063422

Stahl, W., and Sies, H. (2012). ß-Carotene and other carotenoids in protection from sunlight. *Am. J. Clin. Nutr.* 96, 1179S–1184S. doi: 10.3945/ajcn.112.034819

Stauber, J. L., and Jeffrey, S. W. (1988). Photosynthetic pigments in fifty-one species of marine diatoms. *J. Phycol.* 24, 158–172. doi: 10.1111/j.1529-8817.1988.tb04230.x

Taghi Gharibzahedi, S. M., Razavi, S. H., and Mousavi, M. (2015). Optimal development of a new stable nutraceutical nanoemulsion based on the inclusion complex of 2-hydroxypropyl-β-cyclodextrin with canthaxanthin accumulated by *Dietzia natronolimnaea* HS-1 using ultrasound-assisted emulsification. *J. Dispers. Sci. Technol.* 36, 614–625. doi: 10.1080/01932691.2014.921188

Takashima, M., Shichiri, M., Hagihara, Y., Yoshida, Y., and Niki, E. (2012). Capacity of fucoxanthin for scavenging peroxyl radicals and inhibition of lipid peroxidation in model systems. *Free Radic. Res.* 46, 1406–1412. doi: 10.3109/10715762.2012.721542

Talebi, A. F., Tabatabaei, M., Aghbashlo, M., Movahed, S., Hajjari, M., and Golabchi, M. (2020). "Algae-powered buildings: a strategy to mitigate climate change and move toward circular economy," in *Smart Village Technology*, eds S. Patnaik et al. (Cham: Springer), 353–365. doi: 10.1007/978-3-030-37794-6_18

Tan, C. P., and Hou, Y. H. (2014). First evidence for the anti-inflammatory activity of fucoxanthin in high-fat-diet-induced obesity in mice and the antioxidant functions in PC12 cells. *Inflammation* 37, 443–450. doi: 10.1007/s10753-013-9757-1

Tiwari, B. K. (2015). Ultrasound: a clean, green extraction technology. *Trends Analyt. Chem.* 71, 100–109. doi: 10.1016/j.trac.2015.04.013

Toledo, Á., and Burlingame, B. (2006). Biodiversity and nutrition: a common path toward global food security and sustainable development. *J. Food Composit. Anal.* 19, 477–483. doi: 10.1016/j.jfca.2006.05.001

Tredici, M. R., Rodolfi, L., Biondi, N., Bassi, N., and Sampietro, G. (2016). Techno-economic analysis of microalgal biomass production in a 1-ha Green Wall Panel (GWP®) plant. *Algal Res.* 19, 253–263. doi: 10.1016/j.algal.2016.09.005

Urikura, I., Sugawara, T., and Hirata, T. (2011). Protective effect of fucoxanthin against UVB-induced skin photoaging in hairless mice. *Biosci. Biotechnol. Biochem.* 75, 757–760. doi: 10.1271/bbb.110040

Van Harmelen, T., and Oonk, H. (2006). *Microalgae Biofixation Processes: Applications and Potential Contributions to Greenhouse Gas Mitigation Options*. Apeldoorn: TNO Built Environmental Geosciences.

Vieira, F. A., Guilherme, R. J. R., Neves, M. C., Rego, A., Abreu, M. H., Coutinho, J. A. P., et al. (2018). Recovery of carotenoids from brown seaweeds using aqueous solutions of surface-active ionic liquids and anionic surfactants. *Sep. Purif. Technol.* 196, 300–308. doi: 10.1016/j.seppur.2017.05.006

Wang, W.-J., Wang, G.-C., Zhang, M., and Tseng, C. K. (2005). Isolation of fucoxanthin from the rhizoid of *Laminaria japonica* Aresch. *J. Integr. Plant Biol.* 47, 1009–1015. doi: 10.1111/j.1744-7909.2005.00054.x

Withers, N. W., Fiksdahl, A., Tuttle, R. C., and Liaaen-Jensen, S. (1981). Carotenoids of the Chrysophyceae. *Comp. Biochem. Physiol. B* 68, 345–349. doi: 10.1016/0305-0491(81)90110-3

Wright, S. W., and Jeffrey, S. W. (1987). Fucoxanthin pigment markers of marine phytoplankton analysed by HPLC and HPTLC. *Mar. Ecol. Prog. Ser.* 38, 259–266. doi: 10.3354/meps038259

Wu, H., Li, T., Wang, G., Dai, S., He, H., and Xiang, W. (2015). A comparative analysis of fatty acid composition and fucoxanthin content in six *Phaeodactylum tricornutum* strains from different origins. *Chin. J. Oceanol. Limnol.* 38, 391–398. doi: 10.1007/s00343-015-4325-1

Xia, S., Wang, K., Wan, L., Li, A., Hu, Q., and Zhang, C. (2013). Production, characterization, and antioxidant activity of fucoxanthin from the marine diatom *Odontella aurita*. *Mar. Drugs* 11, 2667–2681. doi: 10.3390/md11072667

Xiao, X., Si, X., Yuan, Z., Xu, X., and Li, G. (2012). Isolation of fucoxanthin from edible brown algae by microwave-assisted extraction coupled with high-speed countercurrent chromatography. *J. Sep. Sci.* 35, 2313–2317. doi: 10.1002/jssc.201200231

Yan, N., Fan, C., Chen, Y., and Hu, Z. (2016). The potential for microalgae as bioreactors to produce pharmaceuticals. *Int. J. Mol. Sci.* 17:962. doi: 10.3390/ijms17060962

Zarekarizi, A., Hoffmann, L., and Burritt, D. (2019). Approaches for the sustainable production of fucoxanthin, a xanthophyll with potential health benefits. *J. Appl. Phycol.* 31, 281–299. doi: 10.1007/s10811-018-1558-3

Zhang, W., Wang, F., Gao, B., Huang, L., and Zhang, C. (2018). An integrated biorefinery process: stepwise extraction of fucoxanthin, eicosapentaenoic acid and chrysolaminarin from the same *Phaeodactylum tricornutum* biomass. *Algal Res.* 32, 193–200. doi: 10.1016/j.algal.2018.04.002

Zhao, X., Fu, L., Liu, D., Zhu, H., Wang, X., and Bi, Y. (2016). Magnetic-field-assisted extraction of astaxanthin from *Haematococcus pluvialis*. *J. Food Process. Preserv.* 40, 463–472. doi: 10.1111/jfpp.12624

Conflict of Interest: The authors declare that the research was conducted in the absence of any commercial or financial relationships that could be construed as a potential conflict of interest.

frontiers in Bioengineering and Biotechnology

ORIGINAL RESEARCH
published: 28 January 2021
doi: 10.3389/fbioe.2021.568776

Tolerance of *Tetraselmis tetrathele* to High Ammonium Nitrogen and Its Effect on Growth Rate, Carotenoid, and Fatty Acids Productivity

Abd Wahab Farahin[1], Ikhsan Natrah[1,2,3], Norio Nagao[4], Fatimah Md. Yusoff[1,2,3], Mohamed Shariff[1,5], Sanjoy Banerjee[1], Tomoyo Katayama[6], Masatoshi Nakakuni[7], Mitsuhiko Koyama[8], Kiyohiko Nakasaki[8] and Tatsuki Toda[9]*

[1] *Laboratory of Marine Biotechnology, Institute of Bioscience, Universiti Putra Malaysia, Serdang, Malaysia,* [2] *Department of Aquaculture, Faculty of Agriculture, Universiti Putra Malaysia, Serdang, Malaysia,* [3] *International Institute of Aquaculture and Aquatic Sciences, Universiti Putra Malaysia, Serdang, Malaysia,* [4] *Bluescientific Shinkamigoto Co. Ltd., Nagasaki, Japan,* [5] *Department of Veterinary Clinical Studies, Faculty of Veterinary Medicines, Universiti Putra Malaysia, Serdang, Malaysia,* [6] *Graduate School of Agricultural and Life Sciences, The University of Tokyo, Bunkyo, Japan,* [7] *Faculty of Agriculture, Kagawa University, Miki, Japan,* [8] *School of Environment and Society, Tokyo Institute of Technology, Ookayama, Japan,* [9] *Department of Environmental Engineering for Symbiosis, Faculty of Engineering, Soka Meguro University, Hachioji, Japan*

OPEN ACCESS

Edited by:
Joseph Boudrant, Centre National de la Recherche Scientifique (CNRS), France

Reviewed by:
Noppol Leksawasdi, Chiang Mai University, Thailand
Jose Maria Vega, Sevilla University, Spain

***Correspondence:**
Ikhsan Natrah
natrah@upm.edu.my

Specialty section:
This article was submitted to Bioprocess Engineering, a section of the journal Frontiers in Bioengineering and Biotechnology

Received: *02 June 2020*
Accepted: *06 January 2021*
Published: *28 January 2021*

Citation:
Farahin AW, Natrah I, Nagao N, Yusoff FM, Shariff M, Banerjee S, Katayama T, Nakakuni M, Koyama M, Nakasaki K and Toda T (2021) Tolerance of Tetraselmis tetrathele to High Ammonium Nitrogen and Its Effect on Growth Rate, Carotenoid, and Fatty Acids Productivity. Front. Bioeng. Biotechnol. 9:568776. doi: 10.3389/fbioe.2021.568776

Microalgae can use either ammonium or nitrate for its growth and vitality. However, at a certain level of concentration, ammonium nitrogen exhibits toxicity which consequently can inhibit microalgae productivity. Therefore, this study is aimed to investigate the tolerance of *Tetraselmis tetrathele* to high ammonium nitrogen concentrations and its effects on growth rate, photosynthetic efficiency (F_v/F_m), pigment contents (chlorophyll *a*, lutein, neoxanthin, and β-carotene), and fatty acids production. Experiments were performed at different ammonium nitrogen concentrations (0.31–0.87 gL^{-1}) for 6 days under a light source with an intensity of 300 μmol photons m^{-2} s^{-1} and nitrate-nitrogen source as the experimental control. The findings indicated no apparent enhancement of photosynthetic efficiency (F_v/F_m) at high levels of ammonium nitrogen (NH_4^+-N) for *T. tetrathele* within 24 h. However, after 24 h, the photosynthetic efficiency of *T. tetrathele* increased significantly ($p < 0.05$) in high concentration of NH_4^+-N. Chlorophyll *a* content in *T. tetrathele* grown in all of the different NH_4^+-N levels increased significantly compared to nitrate-nitrogen (NO_3-N) treatment ($p < 0.05$); which supported that this microalgal could grow even in high level of NH_4^+-N concentrations. The findings also indicated that *T. tetrathele* is highly resistant to high ammonium nitrogen which suggests *T. tetrathele* to be used in the aquaculture industry for bioremediation purpose to remove ammonium nitrogen, thus reducing the production cost while improving the water quality.

Keywords: ammonium nitrogen tolerance, microalgae, photosynthetic efficiency, chlorophyll *a*, *Tetraselmis tetrathele*

INTRODUCTION

In recent years, the rising growth and life expectancy of the global population had resulted in increased demand in energy, healthy food, water, drugs, and other resources. This has caught the attention of researchers worldwide to study the use of microalgae as a goal toward sustainable development. According to Rahman (2020), there is an increasing demand of microalgae-based products, as the global market for microalgae is projected USD 53.43 billion in the year 2026 as compared to USD 32.60 billion in 2017. These figures show that the microalgae industry is steadily growing and gaining more attention for extensive use in various sectors in the future. Research to identify inexpensive sources of nutrients element to mass culture microalgae is needed to reduce its cost of production to meet the increasing global market demand.

The enhancement of cultivation conditions through various techniques helps to contribute to the growth and production of numerous compounds in microalgae. Nitrogen, in the form of either ammonium (NH_4^+) or nitrate (NO_3^-), is an essential nutrient required for microalgae growth which subsequently contributes to the biomass produced. Ammonium is the most predominant source of nitrogen that exists in urban, agricultural and aerobic digested effluents with a wide variation in its concentrations, ranging from low (10 mgL^{-1}-N) to high concentrations (2,000 mgL^{-1}-N) (Cai et al., 2013; Krishna Reddy et al., 2017). It is also documented that certain level of ammonium nitrogen concentration is toxic and can inhibit microalgae productivity. Thus, further elucidation of microalgae ammonium nitrogen tolerance is needed, as some previous studies had pointed out that different strains of microalgae require different levels of nitrogen uptake (Raven et al., 1992; Feng et al., 2020).

Besides, Collos and Harrison (2014) reported that ammonium has both long-term (over days) and short-term (over minutes to hours) physiological effects on microalgae, such as growth rate, the efficiency of photosynthesis and other responses. Generally, these short-term responses could translate into long-term effects during the transient lag or induction phase, which subsequently impacts the expected outcomes of competition among species over a growth period of several days. Since the high concentration of ammonium can affect the physiological processes within the cell, therefore, continuous time-based monitoring should be conducted either in short-term or long-term period culture to evaluate the photosynthetic efficiency of the cells. Thus, the inhibition or tolerance effect of microalgae to the ammonium present in its growth medium should be investigated thoroughly for an initial, short-term physiological response, especially in terms of photosynthesis efficiency, after the microalgae are abruptly exposed to ammonium effluent sources either for a few hours (during lag phase) until several days of growth.

Tetraselmis tetrathele, which belong to the Chlorophyta phylum, is a green marine microalga widely used in aquaculture as feeds for marine lives, such as molluscs (Blanchard et al., 2008; Lu et al., 2017), crustacean larvae (Magnotti et al., 2016) and as a probiotic in fish (Grotkjær et al., 2016; Dittmann et al., 2020). The wide application of *T. tetrathele* could be attributed to the presence of numerous bioactive, biochemical compounds, such as polyunsaturated fatty acids (PUFA), polysaccharides, lipids, protein, enzymes and carotenoids in the microalgae cells (Tsai et al., 2016; Di Lena et al., 2019; Farahin et al., 2019; Schüler et al., 2020). From the culturing perspective, Chlorophyceae was noted to exhibit significant tolerance to high ammonium nitrogen concentration compared to other algae phylum, such as Cyanophyceae, Diatomophyceae, Dinophyceae, Prymnesiophyceae, and Raphidophyceae (Collos and Harrison, 2014).

Generally, there are four major research fields in microalgae biotechnology which consist of wastewater treatment, carbon dioxide sequestration, biofuel production and high value-added molecules production (Levasseur et al., 2020). However, to date, limited studies in the above mentioned research areas resulted in a distinct knowledge gap in understanding the effects of high ammonium nitrogen on *Tetraselmis* sp. algal growth, physiological responses and metabolites production. Therefore, this study was conducted with two aims: (1) to examine the growth rate and the photosynthesis efficiency (F_v/F_m) of *T. tetrathele* species at high concentrations of NH_4^+ medium and (2) to quantify the production of pigments and PUFA profile with NH_4^+ and NO_3^- as nitrogen sources.

MATERIALS AND METHODS

Microalgal Culture and Media Preparation

Tetraselmis tetrathele (West) Butcher (UPMC-A0011) was isolated from Port Dickson, Malaysia and cultured in natural seawater enriched with modified f/2 media (Guillard and Ryther, 1962; Guillard, 1975) which consisted of (per liter): 75 mg $NaNO_3$; 5 mg of $NaH_2PO_4{\cdot}H_2O$; 3.15 mg $FeCl_3{\cdot}6H_2O$; 4.36 mg $Na_2EDTA{\cdot}2H_2O$; 0.18 mg $MnCl_2{\cdot}4H_2O$; 0.22 μg $ZnSO_4{\cdot}7H_2O$; 0.01 mg $CoCl_2{\cdot}6H_2O$; 9.8 μg $CuSO_4{\cdot}5H_2O$; 6.3 μg $Na_2MoO_4{\cdot}2H_2O$; 0.1 mg thiamine.HCl; 0.5 μg biotin; 0.5 μg cyanocobalamin. The pre-culture was grown in 1 L column reactor under 300 μmol photons m^{-2} s^{-1} of light intensity, aerated with 0.2 L min^{-1} air and 1–2% CO_2 at 25°C. Three batch series of pre-culture were done by sub-culturing every week and samples were taken daily to monitor the F_v/F_mvalues of inoculated culture with optimum condition. Values between 0.6 and 0.8 indicate high potential photosynthetic performances which represent chlorophyll production in actively growing cells (Geel et al., 1997). After pre-culture in the exponential phase, the culture was sub-cultured with the initial cell density to ∼0.1 gL^{-1} dry weight.

Experimental Design on Growth Conditions With High Level of Nitrogen Sources

A schematic diagram of the cultivation systems used in this experiment is shown in **Supplementary Figure 1**. The nitrogen source of modified f/2 media was replaced by ammonium chloride (NH_4Cl) with different concentrations of 0.31, 0.61, and 0.87 gL^{-1}-N which initial concentrations of free ammonia were 0.77, 1.50, and 2.08 mM, respectively and 0.31 gL^{-1} of NO_3^--N was used as the control (see **Supplementary Table 1**). Experiments were conducted with

triplicate each. Treatments with ammonium were conducted with Tricine (N-[Tris(hydroxymethyl)-methyl]-glycine) buffer solution to maintain the concentration of free ammonia (NH_3). During the initial growth, pH was maintained to 7.8 ± 0.1 throughout the experiment. Tricine and no Tricine controls were also tested with *T. tetrathele* and no growth inhibition due to Tricine was observed. Microalgae cultures were grown at 12:12 light/dark cycle (300 μmol photons m^{-2} s^{-1}) in room temperature (25 ± 1°C). The aeration and the ventilation ports were equipped with 0.2 μm filters (Millipore) to prevent contamination or release of algae. The reactors were sparged with 0.2 L min^{-1} air with 1–2% CO_2.

Growth Parameter Analysis

The pH of the samples was closely monitored daily to ensure system stability and constant free ammonia concentration by using pH meter (B-712, HORIBA, Japan). Total ammonia concentration for each culture condition was measured using colorimetric method (APHA, 2012). To estimate the content of free ammonia concentration, ratio of free ammonia to total ammonia (NH_3 %) was calculated according to Equation (1):

$$NH_3\ (\%) = \frac{100}{1 + \left[H^+\right]} \times K_a \quad (1)$$

Where K_a is the dissociation constant of ammonia, 4.36×10^{-10} at 25°C and 35 PSU (Khoo et al., 1977).

A cell suspension sample was filtered through a combusted glass fiber filter (GF/A, Whatman, UK) to determine the dry-cell weight. The cell pellet was washed three times with 0.5 M ammonium formate to remove soluble salts, dried at 60°C for 24 h and subsequently cooled to room temperature in a desiccator before weighing. Microalgae cells density were counted using light microscopy and haemacytometer-based counting. The optical density was measured using a spectrophotometer (DR 1900-01, Hach) at the wavelength 530 nm. Dry-cell weight, cell number, and optical density were measured daily and all the analyses were conducted in triplicate.

Chlorophyll Fluorescence Analysis

A variable chlorophyll fluorescence was measured outside the bioreactor with a pulse amplitude modulated fluorometer (PAM, Walz, Water-Pam, Germany) to determine the effect of high ammonium concentration on the photosynthesis performance to the microalgal cells. The maximum photosynthetic efficiency (F_v/F_m) was obtained under actinic light. Subsamples for fluorescence analysis were taken and put in dark condition for 30 min at 25°C. After acclimatization, 3 mL of the samples were immediately transferred into 15 mm diameter quartz cuvette as described by Obata et al. (2009). Once stable maximum fluorescence yield in the dark-adapted state (F_o) was reached, a saturating pulse of 1,200 μmol photons at 655 nm m^{-2} s^{-1} for 0.8 s was supplied to determine the maximum fluorescence yield (F_m) after dark acclimation. The maximum photosynthetic efficiency of PS II (F_v/F_m) was calculated using Equation (2) as described by Schreiber et al. (1986):

$$\frac{F_v}{F_m} = \frac{(F_m - F_o)}{F_m} \quad (2)$$

The monitoring process was done at 0, 1, 3, 6, 24 until 144 h.

Cellular Photosynthethic Pigment Contents Quantification

Samples for analysis of the pigment were filtered through GF/A glass fiber filters (Whatman, UK) and stored at −20°C until further use. Cells collected on the filters (0.1–1.0 g-dw L^{-1}) were extracted with 3 mL methanol, sonicated to break the cell walls and then kept in −4°C in darkness for 48 h. Cell extracts were filtered through a 0.22 μm filter (diameter 13 mm, Nylon, Thermo Scientific, USA) to eliminate glass fibers and cellular debris. All procedures for the extraction were conducted under subdued light to prevent photodegradation of the pigments. Tenth microliters of standards and samples were injected into Shimadzu Prominence-i high-performance liquid chromatography (LC 2030) using reversed phase column (2.1 × 150 mm inner diameter, 5 μm, C18, XBridge, Ireland). The HPLC flow rate was 0.5 mL/min; column temperature 40°C.

The HPLC conditions were performed using 80:20 (v/v) methanol and 0.5 M ammonium acetate as an eluent A and 70:30 (v/v) methanol and ethyl acetate as an eluent B. The gradient elution was performed as follows: initial conditions were 0% of eluent B until 24.9 min, followed by 100% of eluent B at 25 min, this proportion was maintained for 9 min. The column was then returned to the initial condition at 34.01 min and maintained the initial mobile phase until the end of the run at 39 min. Detection and identification were performed using a photodiode array detector (λ detection = 440, 450, 460, 465, 478, and 665 nm). The injection volume was 10 μL: two injections were performed for each sample and standard. The standard curve and the retention times were calibrated using chlorophyll *a*, neoxanthin, lutein and β-carotene standards in methanol at four different concentrations (500, 250, 100, 50 mg/mL). All samples were analyzed in triplicates and the results were expressed as milligram per gram dry weight biomass (mg/g-dw).

Fatty Acid Methyl Ester (FAME)

Samples were filtered through GF/A, washed with 0.5 ammonium formate, lyophilised and kept in −20°C until subjected to fatty acid analysis. Preparation of fatty acid methyl ester from total lipid was performed according to the modified method of Bligh and Dyer (1959). Filtered samples were extracted in 3 mL chloroform: methanol (1:2, v/v) solution and sonicated for 15 min at 15°C. The extract was centrifuged at 4,000 × g for 8 min, and the supernatant was transferred into a new glass tube. The remaining residue was re-extracted three times and obtained extracts were pooled. Ultrapure water of 10 mL was added to remove impurities in the extract and separated by centrifugation for 10 min at 3,000 × g. One hundred microliters of and internal standard of heneicosane (C21) was added into the extract and dried up completely under nitrogen gas at 35°C. For transesterification, 1 mL of methylation mixture

(methanol: acetyl chloride, 100:5, v/v) were added to the dry lipid fraction and heated at 100°C for 60 min. After cooling to room temperature, 2 mL of hexane was added and shaken for 5 s. The upper hexane phase was collected and dried up at 45°C under steam of nitrogen gas.

Then, the FAME was immersed in hexane quantified by an Agilent 6890 gas chromatograph-mass spectrometer (GCMS) (6890N GC/5973MS, Agilent Technologies, USA) equipped with a capillary column 30 m × 0.25 mm ID × 0.25 μm (Zebron ZB-Wax, USA). Helium was used as a carrier gas at a flow rate of 1.3 mL min^{-1} at 75.7 kPa head pressure. The injector temperature was programmed at 250°C and detector temperature at 255°C. The column temperature was initially set at 50°C for 1 min, then programmed to increase to 100°C at 10°C min^{-1}, held for 5 min, and set at 240°C at 4°C min^{-1} for 15 min. Identification of the individual spectrum obtained was performed by comparison of mass spectra with the NIST libraries using data analysis software (Agilent MSD Productivity ChemStation). Identification of each fatty acid was conducted by comparison between the retention time and the mass spectrum of the standard, and quantified by comparing their peak area with that of the internal standard.

Data Handling and Statistical Analysis

All data are shown as mean ± standard deviation (SD) of three determinations which $n = 3$. For dry weight, cell number, F_v/F_m and pigments, repeated-measure one-way ANOVA followed by Tukey multiple comparison tests were used to compare between treatments (NO_3^--N and NH_4^+-N) during the study period. FAME percentages were arcsine transformed before the statistical analysis. A one-way ANOVA followed by a multiple comparison *post-hoc* test (Tukey) was used for FAME in order to compare between treatments. Statistical software SPSS (IBM SPSS Statistics, version 20) was used for the analysis. *P*-values <0.05 were considered to be significant.

RESULTS AND DISCUSSION

Growth Performance of *Tetraselmis tetrathele* Under Different Concentrations of Ammonium

The growth performance of *T. tetrathele* at different ammonium concentrations are shown in **Figure 1**. The algal dry-cell weight and cell number were increased with culturing time for NH_4^+-N conditions which were 0.31, 0.61, and 0.87 gL^{-1}. Even though tested at the same nitrogen concentration (0.31 gL^{-1}), the highest dry-cell weight and cell number with no significant differences to control ($p > 0.05$) were observed in NH_4^+-N condition with 1.25 ± 0.02 g-dw L^{-1} and 3.38 × 10^6 cells mL^{-1}, respectively. Meanwhile, the values of dry-cell weight and cell number under higher NH_4^+-N concentrations (0.61 and 0.87 gL^{-1}) on day 6 were 1.1 and 1.2 times lower than those control conditions, 0.31 gL^{-1} NO_3^--N ($p < 0.05$). From the representative results, although this microalgal tested in high concentrations, the cells were able to grow without inhibiting the growth.

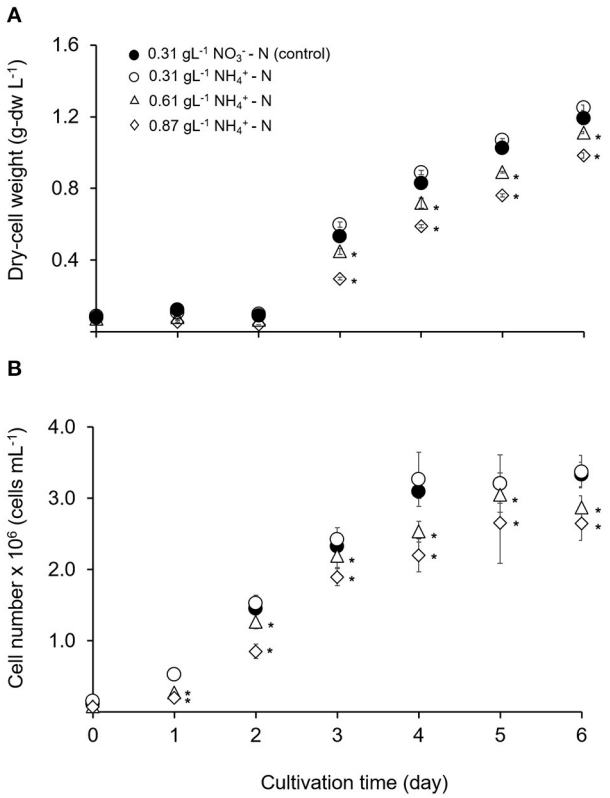

FIGURE 1 | Time course of growth performance for *T. tetrathele* in different concentrations of ammonium nitrogen. **(A)** Dry-cell weight (g-dw L^{-1}), and **(B)** cell number (cells mL^{-1}). Points marked with an asterisk indicate significant differences between treatments on that specific day, $p < 0.05$. Values are means ± SD ($n = 3$).

Nitrogen is one of the primary essential nutrients required for algal growth and amino acids synthesis which is are the building blocks of proteins, beneficial in the formation of chlorophylls quintessential cellular machinery performing survival tasks, such as photosynthesis, light harvesting, and energy generation in microalgae (Grobbelaar, 2007). The inorganic nitrogen sources in microalgal cultivations are nitrate salts, nitrite salts and ammonium. Nitrate and nitrite salts are eventually converted to ammonium before being assimilated into amino acids via the glutamine synthetase/glutamate synthase pathway or the glutamate dehydrogenase pathway (Ramanna et al., 2014). This could be the reason that this microalgal showed higher dry-cell weight and cell number in 0.31 gL^{-1} NH_4^+-N condition compared to 0.31 gL^{-1} NO_3^--N. Shi et al. (2000) reported similar result where *Chlorella protothecoides* absorbed ammonium and higher algal yields were obtained when nitrate was replaced by ammonium. Several other authors mentioned that ammonium was an excellent nitrogen source for certain strain of marine and freshwater algae (Dortch, 1990; Raven et al., 1992). Conversely, Feng et al. (2020) found that *Chlorella* sp. GN1 favored NO_3^- where 11-fold significantly enhanced the growth rate compared to NH_4^+ as a nitrogen source. Thus, different algae species have

TABLE 1 | Evaluation of ammonium nitrogen activities from microalgae.

Species	Source of NH_4^+-N	NH_4^+-N Con. (gL^{-1})	Light ($\mu mol\ m^{-2}s^{-1}$)	Temp. (°C)	pH		Buffer/ pH adjust	CO_2	Culture period	Max. dry-cell weight (gL^{-1})	Major observations	Study on lag phase	Photosynthesis efficiency (Yes/No)	References
					Initial	Final								
Chlorella FACHB-1563 (Chlorophyceae)	Synthetic NH_4Cl	0.26	70	25	9.25	10.5	–	○	5 h	–	- F_v/F_m dropped to 0.	Yes	Yes	Wang et al., 2019
Chlorella FACHB-1216 (Chlorophyceae)	Synthetic NH_4Cl	0.26	70	25	9.25	10.5	–	○	5 h	–	- F_v/F_m dropped to 0.6 at 3 h cultivation and maintained until 5 h culture period.	Yes	Yes	Wang et al., 2019
Nostoc sp. strain H (Ge-Xian-Mi) (Cyanophyceae)	Synthetic NH_4Cl	0.001	70	25	8.3 ± 0.2	8.3 ± 0.2	TAPS	○	4 days	–	- Chl *a* was 0.29 ± 0.07 mgL^{-1} - Value of F_v/F_m on day 4 was 0.31 ± 0.03 - Phycobiliprotein was 0.61 ± 0.07 mgL^{-1} - Saturating irradiance for photosynthesis and PS II activity decreased - Rapid fluorescence rise kinetics indicated oxygen-evolving complex of PS II was inhibitory site of NH_4^+	No	Yes	Dai et al., 2008
Nostoc sp. strain H (Ge-Xian-Mi) (Cyanophyceae)	Synthetic NH_4Cl	0.003	70	25	8.3 ± 0.2	8.3 ± 0.2	TAPS	○	4 days	–	- Chl *a* was 0.07 ± 0.01 mgL^{-1} - Value of F_v/F_m on day 4 was 0.09 ± 0.03 - Phycobiliprotein was 0.16 ± 0.03 mgL^{-1} - Saturating irradiance for photosynthesis and PS II activity decreased - Rapid fluorescence rise kinetics indicated oxygen-evolving complex of PS II was inhibitory site of NH_4^+	No	Yes	Dai et al., 2008
Nostoc sp. strain H (Ge-Xian-Mi) (Cyanophyceae)	Synthetic NH_4Cl	0.005	70	25	8.3 ± 0.2	8.3 ± 0.2	TAPS	○	4 days	–	- Chl *a* was 0.06 ± 0.01 mgL^{-1} - Value of F_v/F_m on day 4 was 0.04 ± 0.03 - Phycobiliprotein was 0.12 ± 0.07 mgL^{-1} - Saturating irradiance for photosynthesis and PS II activity decreased	No	Yes	Dai et al., 2008

(Continued)

TABLE 1 | Continued

Species	Source of NH_4^+-N	NH_4^+-N Con. (gL^{-1})	Light ($\mu mol\ m^{-2}s^{-1}$)	Temp. (°C)	pH		Buffer/ pH adjust	CO_2	Culture period	Max. dry-cell weight (gL^{-1})	Major observations	Study on lag phase	Photosynthesis efficiency (Yes/No)	References
					Initial	Final								
											- Rapid fluorescence rise kinetics indicated oxygen-evolving complex of PS II was inhibitory site of NH_4^+			
Nostoc sp. strain H (Ge-Xian-Mi) (Cyanophyceae)	Synthetic NH_4Cl	0.01	70	25	8.3 ± 0.2	8.3 ± 0.2	TAPS	○	4 days	–	- Chl *a* was 0.03 ± 0.01 mgL^{-1} - Value of F_v/F_m on day 4 was 0.06 ± 0.05 - Phycobiliprotein was 0.05 ± 0.02 mgL^{-1} - Saturating irradiance for photosynthesis and PS II activity decreased - Rapid fluorescence rise kinetics indicated oxygen-evolving complex of PS II was inhibitory site of NH_4^+	No	Yes	Dai et al., 2008
TRG10-p102 *Oocystis heteromucosa* (Chlorophyceae)	Synthetic NH_4Cl	0.0196	150	25	8.0 ± 0.1	8.0 ± 0.1	HEPES	○	6 days	–	- The specific growth rate was not significantly different to control 0.0196 gL^{-1} NO_3^--N	No	No	Katayama et al., 2020
TRG10-p102 *Oocystis heteromucosa* (Chlorophyceae)	Synthetic NH_4Cl	0.042	150	25	8.0 ± 0.1	8.0 ± 0.1	HEPES	○	6 days	–	- The specific growth rate was not significantly different to control 0.0196 gL^{-1} NO_3^--N	No	No	Katayama et al., 2020
TRG10-p102 *Oocystis heteromucosa* (Chlorophyceae)	Synthetic NH_4Cl	0.084	150	25	8.0 ± 0.1	8.0 ± 0.1	HEPES	○	6 days	–	- The specific growth rate was not significantly different to control 0.0196 gL^{-1} NO_3^--N	No	No	Katayama et al., 2020
TRG10-p102 *Oocystis heteromucosa* (Chlorophyceae)	Synthetic NH_4Cl	0.140	150	25	8.0 ± 0.1	8.0 ± 0.1	HEPES	○	6 days	–	- The specific growth rate was not significantly different to control 0.0196 gL^{-1} NO_3^--N	No	No	Katayama et al., 2020
TRG10-p103 *Thalassiosira weissflogii* (Diatomophyceae)	Synthetic NH_4Cl	0.0196–0.140	150	25	8.0 ± 0.1	8.0 ± 0.1	HEPES	○	6 days	–	- The growth rate was inhibited cultured in >0.0196 gL^{-1} NH_4^+-N	No	No	Katayama et al., 2020
TRG10-p103 *Thalassiosira weissflogii* (Diatomophyceae)	Synthetic NH_4Cl	0.0196–0.210	150	25	8.0 ± 0.1	8.0 ± 0.1	HEPES	○	6 days	–	- After acclimatized experiments were carried out, microalagal was able to grow even in 0.14 gL^{-1} NH_4^+-N	No	No	Katayama et al., 2020

(Continued)

TABLE 1 | Continued

Species	Source of NH_4^+-N	NH_4^+-N Con. (gL^{-1})	Light ($\mu mol\ m^{-2}s^{-1}$)	Temp. (°C)	pH		Buffer/ pH adjust	CO_2	Culture period	Max. dry-cell weight (gL^{-1})	Major observations	Study on lag phase	Photosynthesis efficiency (Yes/No)	References
					Initial	Final								
TRG10-p105 *Thalassiosira weissflogii* (Diatomophyceae)	Synthetic NH_4Cl	0.0196–0.140	150	25	8.0 ± 0.1	8.0 ± 0.1	HEPES	○	6 days	–	- The growth rate was inhibited, cultured in >0.0196 gL^{-1} NH_4^+-N	No	No	Katayama et al., 2020
TRG10-p105 *Thalassiosira weissflogii* (Diatomophyceae)	Synthetic NH_4Cl	0.0196 –0.210	150	25	8.0 ± 0.1	8.0 ± 0.1	HEPES	○	6 days	–	- After acclimatized experiments were carried out, microalagal was e were able to grow even in 0.14 gL^{-1} NH_4^+-N	No	No	Katayama et al., 2020
TRG10-p201 *Amphora coffeiformis* (Diatomophyceae)	Synthetic NH_4Cl	0.0196–0.140	150	25	8.0 ± 0.1	8.0 ± 0.1	HEPES	○	6 days	–	- The growth rate was inhibited, cultured in >0.0196 gL^{-1} NH_4^+-N	No	No	Katayama et al., 2020
Chlorella vulgaris (Chlorophyceae)	Synthetic NH_4Cl	0.32	300	25	7.8 ± 0.1	7.8 ± 0.1	Tricine	○	25 days	4.2	- V/V_{max} almost 1.0 indicated microalgal high tolerance to ammonium nitrogen concentration. - Higher dry-cell weight and maximum area productivity was observed compared to NO_3^--N	No	No	Goto et al., 2018
Chlorella vulgaris (Chlorophyceae)	Synthetic NH_4Cl	0.64	300	25	7.8 ± 0.1	7.8 ± 0.1	Tricine	○	22 days	4.0	- V/V_{max} almost 1.0 indicated microalgal high tolerance to ammonium nitrogen concentration. - Higher dry-cell weight and maximum area productivity was observed compared NO_3^--N	No	No	Goto et al., 2018
Chlorella vulgaris (Chlorophyceae)	Synthetic NH_4Cl	0.96	300	25	7.8 ± 0.1	7.8 ± 0.1	Tricine	○	22 days	4.0	- V/V_{max} almost 1.0 indicated microalgal high tolerance to ammonium nitrogen concentration. - Higher dry-cell weight and maximum area productivity was observed compared NO_3^--N	No	No	Goto et al., 2018

(Continued)

TABLE 1 | Continued

Species	Source of NH_4^+-N	NH_4^+-N Con. (gL^{-1})	Light ($\mu mol\ m^{-2}s^{-1}$)	Temp. (°C)	pH		Buffer/ pH adjust	CO_2	Culture period	Max. dry-cell weight (gL^{-1})	Major observations	Study on lag phase	Photosynthesis efficiency (Yes/No)	References
					Initial	Final								
Chlorella vulgaris (Chlorophyceae)	Synthetic NH_4Cl	1.60	300	25	7.8 ± 0.1	7.8 ± 0.1	Tricine	○	22 days	4.0	- V/V_{max} was decreased when free ammonia concentration >1.80 mM. - Higher dry-cell weight and maximum area productivity was observed compared NO_3^--N	No	No	Goto et al., 2018
Chlorella vulgaris (Chlorophyceae)	Synthetic NH_4Cl	1.60	300	25	8.4 ± 0.1	8.4 ± 0.1	Tricine	○	14 days	2.8	- V/V_{max} was decreased when free ammonia concentration >1.80mM. - Low dry-cell weight and maximum area productivity was observed compared to NO_3^--N due to high pH.	No	No	Goto et al., 2018
Spirulina platensis (Cyanophyceae)	Synthetic NH_4Cl	0.02	55	30	7.0	n.m	n.m	○	18 days	0.75	- Showed the most efficient nutrient removal within 6 days	No	No	Converti et al., 2006
Spirulina platensis (Cyanophyceae)	Synthetic NH_4Cl	0.03	55	30	7.0	n.m	n.m	○	18 days	0.73	- Showed slow rate of nutrient removal (12 days)	No	No	Converti et al., 2006
Spirulina platensis (Cyanophyceae)	Synthetic NH_4Cl	0.04	55	30	7.0	n.m	n.m	○	18 days	0.73	- Showed slow rate of nutrient removal (16 days)	No	No	Converti et al., 2006
Monoraphidium spp. SDEC-17 (Chlorophyceae)	Complex wastewater (CW)	0.173	90	25	8.52	9.0	n.m	○	16 days	1.29	- Removal efficiency of ammonium nitrogen in CW was 99.75% - CW not significantly influenced to lipid accumulation - Fatty acids profile quite similar that seen in biodiesel from palm oil resembles biodiesel from palm oil	No	No	Jiang et al., 2016
Monoraphidium spp. SDEC-17 (Chlorophyceae)	Complex wastewater (CW) + BG11	0.173	90	25	8.41	9.0	n.m	○	16 days	1.04	- Removal efficiency of ammonium nitrogen in CW + BG11 was 99.72% - Fatty acids profile quite similar seen in biodiesel from palm oil resembles biodiesel from palm oil - Showed efficient nutrient removal from CW + BG11	No	No	Jiang et al., 2016

(Continued)

TABLE 1 | Continued

Species	Source of NH_4^+-N	NH_4^+-N Con. (gL^{-1})	Light ($\mu mol\ m^{-2}s^{-1}$)	Temp. (°C)	pH		Buffer/ pH adjust	CO_2	Culture period	Max. dry-cell weight (gL^{-1})	Major observations	Study on lag phase	Photosynthesis efficiency (Yes/No)	References
					Initial	Final								
Scenedesmus obliquus (Chlorophyceae)	Domestic wastewater	0.013	107.94	25	n.m	n.m	n.m	○	10 days	0.38	- Based on response surface methodology (RSM) under optimized conditions of light intensity, microalgal showed better nutrient removal and high growth with high chlorophyll and lipid compared to *Spirulina platensis*	No	No	Fan et al., 2020
Spirulina platensis (Cyanophyceae)	Domestic wastewater	0.013	53.97	25	n.m	n.m	n.m	○	10 days	0.33	- Based on response surface methodology (RSM) under optimized conditions of light intensity, microalgal showed rich in protein and carbohydrate compared to *Scenedesmus obliquus*	No	No	Fan et al., 2020
Chlorella vulgaris (Chlorophyceae)	Activated wastewater	0.04	60–70	n.m	7.1	n.m	HCl/NaOH	○	14 days	0.76	- Ratio of activated wastewater to microalgal (1:0.75) was optimum symbiotic algal-bacterial interactions. - This ratio showed the highest efficient nutrient removal from wastewater - The highest lipid yield and flocculation efficiency was observed.	No	No	Leong et al., 2018
Chlorella sorokiniana UKM2 (Chlorophyceae)	POME	0.05	269.86	25	7.0	6.8	–	○	7 days	1.10	- Potential microalgal-assimilable organic carbon source in POME - Achieved maximum CO_2 uptake rate - Showed efficient nutrient removal from POME	No	No	Ding et al., 2020
Coelastrella sp. UKM4 (Chlorophyceae)	POME	0.05	269.86	25	7.0	6.8	–	○	7 days	0.92	- Potential microalgal-assimilable organic carbon source in POME - Showed efficient nutrient removal from POME	No	No	Ding et al., 2020

(Continued)

TABLE 1 | Continued

Species	Source of NH_4^+-N	NH_4^+-N Con. (gL^{-1})	Light ($\mu mol\ m^{-2}s^{-1}$)	Temp. (°C)	pH		Buffer/ pH adjust	CO_2	Culture period	Max. dry-cell weight (gL^{-1})	Major observations	Study on lag phase	Photosynthesis efficiency (Yes/No)	References
					Initial	Final								
Chlorella pyrenoidosa UKM7 (Chlorophyceae)	POME	0.05	269.86	25	7.0	6.8	–	○	7 days	1.10	- Potential microalgal-assimilable organic carbon source in POME - Showed efficient nutrient removal from POME	No	No	Ding et al., 2020
Tetraselmis tetrathele (Chlorophyceae)	Synthetic NH_4Cl	0.31	300	25	7.8 ± 0.1	7.8 ± 0.1	Tricine	○	6 days	1.25	- Through acclimation in high NH_4^+-N, F_v/F_m value of *T. tetrathele*'s cell increased significantly after 24 h ($p < 0.05$) - Chl *a* increased significantly compared 0.31 gL^{-1} NO_3^--N	Yes	Yes	This study
Tetraselmis tetrathele (Chlorophyceae)	Synthetic NH_4Cl	0.61	300	25	7.8 ± 0.1	7.8 ± 0.1	Tricine	○	6 days	1.11	- Through acclimation in high NH_4^+-N, F_v/F_m value of *T. tetrathele*'s cell increased significantly after 24 h ($p < 0.05$) - Chl *a* increased significantly compared 0.31 gL^{-1} NO_3^--N	Yes	Yes	This study
Tetraselmis tetrathele (Chlorophyceae)	Synthetic NH_4Cl	0.87	300	25	7.8 ± 0.1	7.8 ± 0.1	Tricine	○	6 days	0.98	- Through acclimation in high NH_4^+-N, F_v/F_m value of *T. tetrathele*'s cell increased significantly after 24 h ($p < 0.05$) - Chl *a* increased significantly compared 0.31 gL^{-1} NO_3^--N	Yes	Yes	This study

Temp., temperature; Max. dry-cell weight, maximum dry-cell weight; TAPS, N-[tris(hydroxymethyl)methyl-3-amino]propanesulfonic acid; HEPES, N-2-hydroxyethylpiperazine-N-2′-ethanesulfonic acid; Tricine, N-[Tris(hydroxymethyl)-methyl]-glycine; Con., concentration; POME, palm oil mill effluent; n.m., not mentioned.

different preference on type and level of concentration for the nitrogen sources (Zhuang et al., 2018).

However, ammonium nitrogen presents in two types: protonated cation NH_4^+ and gaseous form NH_3 in aqueous solutions where the pH dictates the equilibrium between these two forms. Ammonium ion (NH_4^+) dominates at pH < 9.25 meanwhile free NH_3 (considered to be the most toxic form to the microorganisms) dominates above this pH, since the pK_a of ion equilibrium of NH_4^+/NH_3 is 9.25 (Belkin and Boussiba, 1991; Drath et al., 2008). In the present study, the pH values were stable and maintained at 7.8 ± 0.1 due to the addition of Tricine buffer. This low pH values convert the free ammonia to the non-toxic ammonium ion and also considered 5% of free ammonia of the total ammonia concentration (Hargreaves and Tucker, 2004; Markou et al., 2014). Therefore, the possibility of change in free ammonia was very low since the pH, the temperature and the light intensity values were controlled.

Table 1 shows comparative studies on the evaluation of ammonium nitrogen activities cultivation in different strains of microalgae. Generally, Chlorophyceae showed high tolerant to high ammonium nitrogen concentration compared to other class, such as Cyanophyceae and Diatomophyceae and these findings were consistent with the conclusion of Collos and Harrison (2014). Besides that, Goto et al. (2018) studied on *Chlorella vulgaris* autotrophically grown in batch cultures of Walne's medium and tested the effect of ammonium on growth. It was found that the dry weight of *C. vulgaris* increased even under extreme high ammonium concentration of 0.96 g-N L^{-1} and reached around 4 g-dw L^{-1} of dry weight. In other situation, Katayama et al. (2020) found that after acclimatized in high ammonium concentration for a week, the two strains of *T. weissflogii* (TRG10-p103 and TRG10-p105) which belong to Diatomophyceae class, were able to grow up to 0.14 gL^{-1} NH_4^+-N. This could be the microalgae were responding to the stress and acclimatized, then successfully adapted to these conditions over the time (Borowitzka, 2018).

In respect to upscaling and future utilization in microalgae-based technologies, such as microalgae based wastewater treatment process, selection of suitable microalgal strain are required in order to tolerate in extreme conditions (aerobic digested effluents and agro-industrial wastewater) up to 2 gL^{-1}-N (Cai et al., 2013; Krishna Reddy et al., 2017). Therefore, further elucidation on the physiological effect of this microalgal in ammonium nitrogen tolerance is needed and is discussed in the next section.

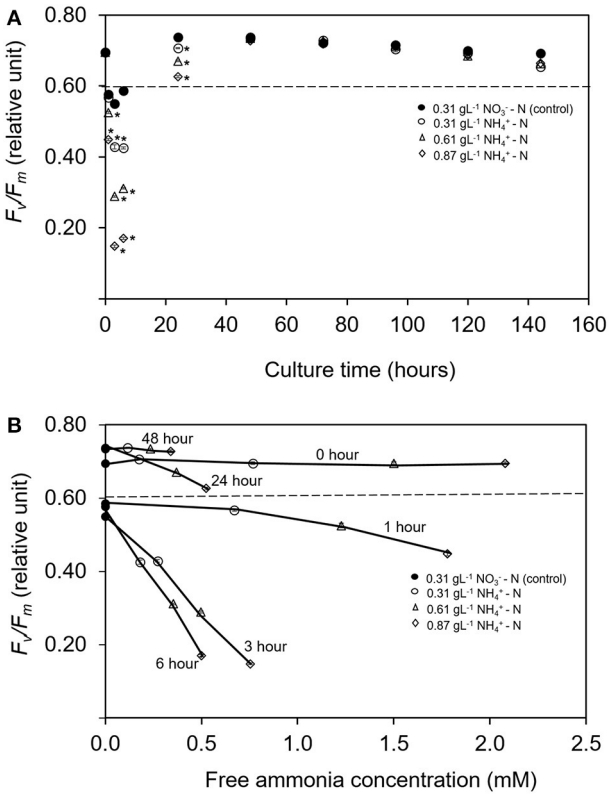

FIGURE 2 | (A) Time course of maximum quantum yield of PS II (F_v/F_m) for *Tetraselmis tetrathele* during culturing period 144 h. **(B)** Relationship between relative F_v/F_m with the ratio of free ammonia concentration for *T. terathele* within 48 h. Dotted lines indicate minimum value of healthy cell condition; F_v/F_m (Geel et al., 1997; Masojídek et al., 2000). Points marked with an asterisk indicate significant differences between treatments on that specific day, $p < 0.05$. Values are means ± SD ($n = 3$).

Maximum Photosynthetic Efficiency (F_v/F_m)

Changes in F_v/F_m is used as the diagnostic of photosynthetic health in microalgal cells (Geel et al., 1997; Cullen and Davis, 2003). **Figure 2A** illustrates the maximum photosynthetic efficiency (F_v/F_m) within 144 h in different ammonium nitrogen concentrations under experimental conditions. The value of F_v/F_m sharply decreased in all treatments as early as hours. After 24 h, the value F_v/F_m gradually increased to a stable condition with no significant differences for all treatments ($p > 0.05$). The relationship between F_v/F_m and free ammonia to total ammonia concentration calculated from the pH and the total nitrogen under different time of culture period are shown in **Figure 2B**. Introduction of *Tetraselmis* in the column reactor at 0 h showed high value of F_v/F_m ($p < 0.05$) even in high ammonium concentration (0.87 gL^{-1} NH_4^+-N). Nevertheless, at 1 h, the value of F_v/F_m was the lowest ($p < 0.005$) at 0.4483, compared to the treatment of 0.61 and 0.31 gL^{-1} NH_4^+-N; with values at 0.5250 and 0.5670, respectively. After 3 h, the values of F_v/F_m was again the lowest in the 0.87 gL^{-1} NH_4^+-N treatment with value of 0.1480 where the stress condition was maintained until 6 h. After 24 h of culture period, the cells were recovered where the value of F_v/F_m increased higher than 0.6 and remained constant after 48 h with F_v/F_m value at 0.730 ± 0.001. No significant difference was found among all treatments ($p > 0.05$). As mentioned by Gorai et al. (2014), the physiological health of microalgal cells can be diagnosed by changes in F_v/F_m. Values lower than 0.65 indicate that the cells are in physiological stress (Masojídek et al., 2000; Cullen and Davis, 2003) while higher values of F_v/F_m indicate high potential photosynthetic performance for

photosystem II (PS II) which represent chlorophyll production in actively growing cells.

Most of the previous studies focused on the interaction effect between microalgae growth and the addition of different ammonium dose exposure over certain time period, such as within a few minutes (Azov and Goldman, 1982), within a few hours (Collos and Slawyk, 2008) or effects in days after the addition of ammonium (Belkin and Boussiba, 1991; Tam and Wong, 1996). Nevertheless, no study has been reported on the intensive measurement on the growth rate reduction due to ammonium inhibition, especially in the first hours of cultivation. In the present study, the continuous decrease in F_v/F_m was detected in the early stage of ammonium-enriched conditions. However, the cell was able to grow at a slow rate in lag-phase even though ammonium was used as nitrogen source in high concentration which was toxic. This slow/inhibition process was probably due to physiological change in nitrogen metabolism (Belkin and Boussiba, 1991; Vonshak and Torzillo, 2004; Drath et al., 2008; Markou et al., 2014). This process might suggest the ability to recover from PS II damage and was reflected in the increase of F_v/F_m value leading to tolerance of *T. tetrathele*'s cell in high ammonium nitrogen concentration. Apart from that, modification in nitrogen metabolic pathway also affected the production of fatty acids as well as pigment production (Paliwal et al., 2017; Nayak et al., 2019) that will be discussed in the next section.

Influence of Ammonium Nitrogen Availability on Pigments and Fatty Acid Profiles

The effects of ammonium nitrogen in different concentration on pigments and fatty acids productivity were analyzed in this study. After day 2, the chlorophyll *a* content in all treatments was significantly higher compared to the control condition ($p < 0.05$) (**Figure 3A**). The dominant carotenoid contents were neoxanthin, lutein, and β-carotene. However, the concentration of these pigments was significantly lower compared to the control ($p < 0.05$) (**Figures 3B–D**). Chlorophyll *a* content is a good indicator for assessing the health of photosynthetic cells and is influenced by the type and the concentration of nitrogen sources (Piorreck et al., 1984; Baker and Oxborough, 2004). Meanwhile, carotenoids play fundamental roles as accessory pigments to protect themselves from photodamage and to aid photosynthesis (Nobel, 2009). Various environmental stresses make microalgae continuously tune their cellular mechanisms to cope with them. The accumulation of the stress metabolites is closely related to the changes occurring in their metabolic pathways (Ramos et al., 2008). Conversely in this study, the physiological activity and carotenoid compositions of *T. tetrathele* were not affected even in high ammonium concentrations.

Fatty acid methyl esters (FAME) profile of *T. tetrathele* grown in different concentration of ammonium nitrogen was analyzed to verify the quality of microalgae biomass (**Table 2**).

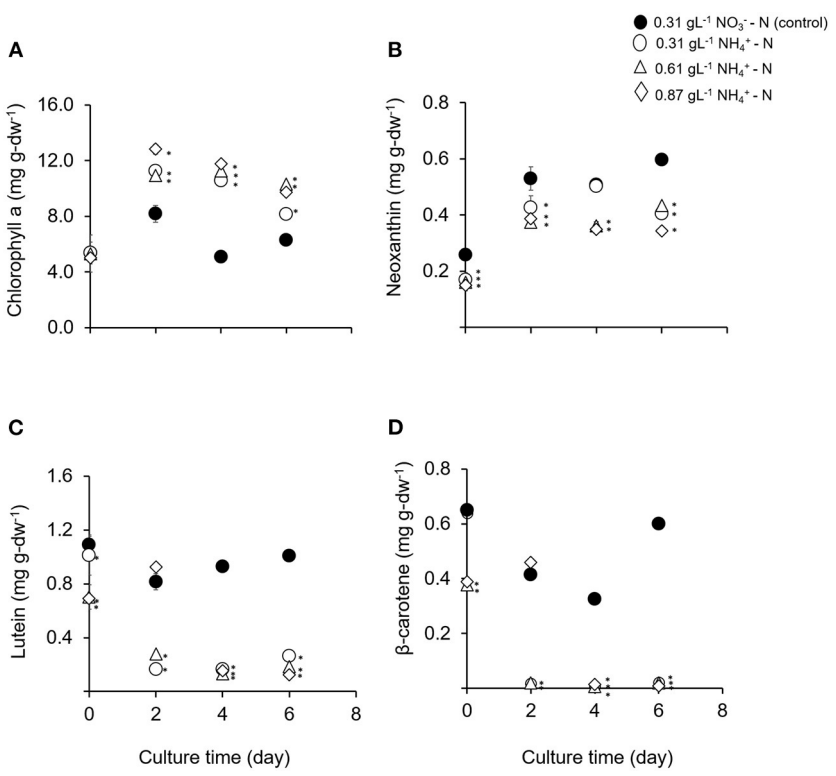

FIGURE 3 | (A–D) Means and standard deviations of phototrophic pigment production in *T. tetrathele* by using different concentrations of ammonia as nitrate act as the control. Points marked with an asterisk indicate significant difference between treatments on that specific day, $p < 0.05$. Values are means ± SD ($n = 3$).

TABLE 2 | Fatty acid composition (% of total fatty acids) of *Tetraselmis tetrathele* grown at day 6 in different concentration of nitrogen sources and review on two marine microalgae species.

Lipid class	0.31 gL^{-1} NO_3^--N (control)	0.31 gL^{-1} NH_4^+-N	0.61 gL^{-1} NH_4^+-N	0.87 gL^{-1} NH_4^+-N	*Tetraselmis suecica*	*Tetraselmis* sp.
C12:0	0.19 ± 0.10^a	0.09 ± 0.00^c	0.06 ± 0.00^d	0.17 ± 0.00^b	–	–
C14:0	0.46 ± 0.01^c	0.63 ± 0.00^b	0.38 ± 0.00^d	1.17 ± 0.00^a	0.49 ± 0.13	1.29 ± 1.03
C15:0	0.08 ± 0.00^c	0.10 ± 0.00^b	0.07 ± 0.00^d	0.37 ± 0.00^a	–	–
C16:0	36.60 ± 0.60^b	31.92 ± 0.25^c	19.29 ± 0.08^d	47.85 ± 0.13^a	16.39 ± 1.09	24.29 ± 0.33
C16:1n-7	4.32 ± 0.07^a	0.42 ± 0.00^d	2.35 ± 0.01^c	2.46 ± 0.01^b	–	1.70 ± 0.07
C16:2	1.04 ± 0.02^c	1.32 ± 0.01^b	0.87 ± 0.00^d	1.79 ± 0.00^a	0.87 ± 0.06	–
C16:3	0.58 ± 0.01^d	4.23 ± 0.03^a	1.30 ± 0.01^c	2.51 ± 0.01^b	3.93 ± 0.15	–
C17:0	0.12 ± 0.00^c	0.25 ± 0.00^b	0.10 ± 0.00^d	0.59 ± 0.00^a	–	4.36 ± 0.08
C17:1	n.d	n.d	0.04 ± 0.00	n.d	–	–
C17:3	n.d	0.20 ± 0.00	n.d	n.d	–	–
C18:0	0.83 ± 0.01^d	1.34 ± 0.01^b	1.09 ± 0.00^c	2.76 ± 0.01^a	–	0.43 ± 0.05
C18:1n-9	21.00 ± 0.34^d	26.95 ± 0.21^c	50.77 ± 0.21^a	40.30 ± 0.11^b	16.13 ± 0.56	18.00 ± 0.22
C18:2n-6	5.50 ± 0.09^a	5.44 ± 0.04^b	2.13 ± 0.01^c	$<0.001^d$	7.57 ± 0.11	11.39 ± 0.20
C18:3n-6	11.56 ± 0.19^b	20.18 ± 0.16^a	11.54 ± 0.05^b	$<0.001^c$	–	18.54 ± 0.21
C20:1n-9	2.09 ± 0.03^b	2.14 ± 0.02^a	1.10 ± 0.00^c	n.d	–	–
C20:3n-3	3.00 ± 0.05	n.d	n.d	n.d	–	–
C20:4n-6	2.59 ± 0.04	n.d	n.d	n.d	1.48 ± 0.05	–
C20:5n-3	10.05 ± 0.16^a	4.48 ± 0.03^c	8.89 ± 0.04^b	$<0.001^d$	4.24 ± 0.06	–
C21:4	n.d	0.33 ± 0.00	n.d	n.d	–	–
C22:6n-3	$<0.001^a$	$<0.001^a$	$<0.001^a$	$<0.001^a$	–	–
Σ SFA	38.3 ± 0.25^b	34.3 ± 0.20^c	21.0 ± 0.04^d	53.2 ± 0.04^a	16.88 ± 0.22	37.00 ± 0.00
Σ UFA	61.7 ± 0.16^c	65.7 ± 0.08^b	79.0 ± 0.05^a	47.0 ± 0.02^d	86.52 ± 0.00	63.00 ± 0.00
Σ MUFA	44.4 ± 0.05^d	44.9 ± 0.05^c	68.7 ± 0.07^b	90.8 ± 0.01^a	25.89 ± 0.57	19.70 ± 0.00
Σ PUFA	55.6 ± 0.10^a	55.1 ± 0.10^b	31.3 ± 0.15^c	9.2 ± 0.05^d	57.23 ± 0.39	43.30 ± 0.00
Σ omega 6	19.65 ± 0.04^b	25.62 ± 0.05^a	13.67 ± 0.11^c	0.03 ± 0.01^d	9.05 ± 0.00	11.39 ± 0.20
Σ omega 3	13.04 ± 0.05^a	4.48 ± 0.04^c	8.89 ± 0.08^b	0.01 ± 0.00^d	4.24 ± 0.06	18.54 ± 0.29
ω6/ω3	1.51 ± 0.06^d	5.72 ± 0.06^a	1.54 ± 0.02^c	1.90 ± 0.17^b	2.13 ± 0.00	0.61 ± 0.00
References	This study	This study	This study	This study	[a]	[b]

n.d., not detected. Data refer to the end of culture period.

$^{a-d}$Results presented as mean ± SD (n = 3). Different letters within the same row indicates significant difference ($p < 0.05$). Σ SFA = total saturated fatty acid, Σ UFA = total unsaturated fatty acid, Σ MUFA = total mono-unsaturated fatty acid, Σ PUFA = total polyunsaturated fatty acid, ω is omega. [a] Abiusi et al. (2014), [b] Kim et al. (2016).

The major fatty acids were C16:0 (palmitic acid), C18:1n-9 (oleic acid), C18:3n-6 (γ-linolenic acid, GLA), and C20:5n-3 (eicosapentaenoic acid, EPA), which comprised of 79–90% fatty acids. Similar results were obtained for *Tetraselmis* sp. by Abiusi et al. (2014), Das et al. (2016), Kim et al. (2016), and Tsai et al. (2016). This present study reported that treatment of 0.61 gL^{-1} NH_4^+-N contained the highest C_{18} fatty acids which was 65.5% followed by 0.31, 0.87 gL^{-1} NH_4^+-N, and control treatments. In addition, it was observed that *T. tetrathele* also produced 31.3% of PUFA even in 0.61 gL^{-1} NH_4^+-N. The highest ammonium concentration in this study resulted in the lowest concentration of PUFA ($p < 0.05$). On the other hands, 0.87 gL^{-1} NH_4^+-N conditions showed high MUFA contents compared to 0.31 and 0.61 gL^{-1} NH_4^+-N treatments ($p < 0.05$).

The variation of fatty acid profile indicated microalgae accumulated lipids or starch as a crucial part of their survival mechanisms which was also reported by Paliwal et al. (2017). In this regards, 0.87 gL^{-1} NH_4^+-N had 53.2% of saturated fatty acids which was the highest compared to other treatments ($p < 0.05$). When the microalga was exposed to extreme stress level conditions, as in 0.87 gL^{-1} NH_4^+-N, the unsaturated fatty acids tend to undergo oxidative cleavage resulting to higher degree of saturation in the microalgae lipids. Similar results were observed in nitrogen depletion conditions of *Chlorella vulgaris* and *Dunaliella tertiolecta* which led to increased degree of saturation (Stephenson et al., 2010; Lee et al., 2014). PUFA are the predominant fatty acids in the composition of structures in chloroplast membranes. PUFA play important roles to maintain the membrane functions including thermal adaptation, regulation of membrane fluidity and permeability, and also oxygen and electron transportations in cellular and tissue metabolisms (Chia et al., 2013; Lee et al., 2014). In this study, high concentration of ammonium nitrogen caused metabolic imbalance in the early stage of stress period and different fatty acid compositions were observed in each ammonium conditions. These results suggest that the ammonium stress could change the fatty acids profile and the media composition can control the type of fatty acids in the cell for production

purposes. Stress response and adaptive process are associated with the photosynthetic apparatus. The high degree of saturation indicated the *T. tetrathele*'s cell undergone oxidative cleavage in order to protect themselves as a survival mechanism. As a result, the chlorophyll *a* in all ammonium treatments were high after recovering process and the carotenoid content was low compared to the control condition.

In the present study, the *T. tetrathele* strain rich in total UFA, MUFA, and PUFA could also benefit aquaculture organisms since PUFA provide essential fatty acids for the growth and the development of several species during early developmental stages including larvae, mollusc, and young aquatic organisms (Otero and Fábregas, 1997).

CONCLUSION

This is an elemental work dealing with the adaptation of *T. tetrathele* to three different high level ammonium (NH_4^+) concentrations by using nitrate (NO_3^-) as the control. This microalgal showed the ability to recover from the damage of the photosynthetic apparatus of photosystem II and was able to grow without inhibiting the growth. The results of chlorophyll *a* content showed that all NH_4^+-N treatments were significantly higher compared to nitrate-nitrogen (NO_3-N). Treatment in 0.87 gL^{-1} NH_4^+-N had 53.2% of saturated fatty acids which was the highest compared to other treatments and indicated the microalgal response to environmental conditions, such as media, as a crucial part of their survival mechanisms. This species is a valuable candidate to be used for mass culture for future microalgae-based technologies whereby can stimulate the economic activity toward attaining high income.

DATA AVAILABILITY STATEMENT

The raw data supporting the conclusions of this article will be made available by the authors, without undue reservation.

AUTHOR CONTRIBUTIONS

AF, IN, and NN conceived and designed the experiments, performed the experiments, analyzed the data, wrote the paper, prepared the figures and/or tables, and reviewed the drafts of the paper. MS contributed to the funding acquisition, reviewed, and edited the draft prior to the submission. SB, TK, MN, and MK were involved in the investigation of the study. FY, KN, and TT contributed to the funding acquisition of the research. All authors contributed to the article and approved the submitted version.

FUNDING

This work was financially supported by the Japan Science and Technology Agency (JST)/Japan International Cooperation Agency (JICA), Science and Technology Research Partnership for Sustainable Development (SATREPS) through the project for Continuous Operation System for Microalgae Production Optimized for Sustainable Tropical Aquaculture (COSMOS) (Grant No. JPMJSA1509), and the SATREPS-COSMOS Matching Fund from the Ministry of Education Malaysia (MOE).

ACKNOWLEDGMENTS

We thank Dr. Norulhuda Ramli, Dr. Minamo Hirahara, Ms. Midori Goto, Mr. Yuki Imaizumi, Ms. Nawwar Zawani, and Mr. Muhammad Farhan Nazarudin for their support during the experiment.

SUPPLEMENTARY MATERIAL

The Supplementary Material for this article can be found online at: https://www.frontiersin.org/articles/10.3389/fbioe.2021.568776/full#supplementary-material

REFERENCES

Abiusi, F., Sampietro, G., Marturano, G., Biondi, N., Rodolfi, L., D'Ottavio, M., et al. (2014). Growth, photosynthetic efficiency, and biochemical composition of *Tetraselmis suecica* F&M-M33 grown with LEDs of different colors. *Biotechnol. Bioeng.* 111, 956–964. doi: 10.1002/bit.25014

APHA (2012). *Standard Methods for the Examination of Water and Wastewater, 22nd Edn*. Washington, DC: American Public Health Association.

Azov, Y., and Goldman, J. C. (1982). Free ammonia inhibition of algal photosynthesis in intensive cultures. *Appl. Environ. Microbiol.* 43, 735–739. doi: 10.1128/AEM.43.4.735-739.1982

Baker, N. R., and Oxborough, K. (2004). "Chlorophyll fluorescence as a probe of photosynthetic productivity," in *Chlorophyll a Fluorescence. Advances in Photosynthesis and Respiration*, eds G. C. Papageorgiou and Govindjee (Dordrecht: Springer), 65–82. doi: 10.1007/978-1-4020-3218-9_3

Belkin, S., and Boussiba, S. (1991). Resistance of *Spirulina platensis* to ammonia at high pH values. *Plant Cell Physiol.* 32, 953–958. doi: 10.1093/oxfordjournals.pcp.a078182

Blanchard, M., Pechenik, J. A., Giudicelli, E., Connan, J. P., and Robert, R. (2008). Competition for food in the larvae of two marine molluscs, *Crepidula fornicata* and *Crassostrea gigas*. *Aquat. Living Resour.* 21, 197–205. doi: 10.1051/alr:2008025

Bligh, E. G., and Dyer, W. J. (1959). A rapid method of total lipid extraction and purification. *Can. J. Biochem. Physiol.* 37, 911–917. doi: 10.1139/o59-099

Borowitzka, M. A. (2018). The 'stress' concept in microalgal biology—homeostasis, acclimation and adaptation. *J. Appl. Phycol.* 30, 2815–2825. doi: 10.1007/s10811-018-1399-0

Cai, T., Park, S. Y., Racharaks, R., and Li, Y. (2013). Cultivation of *Nannochloropsis salina* using anaerobic digestion effluent as a nutrient source for biofuel production. *Appl. Energy* 108, 486–492. doi: 10.1016/j.apenergy.2013.03.056

Chia, M. A., Lombardi, A. T., Melão, M. D. G. G., and Parrish, C. C. (2013). Effects of cadmium and nitrogen on lipid composition of *Chlorella vulgaris* (Trebouxiophyceae, Chlorophyta). *Eur. J. Phycol.* 48, 1–11. doi: 10.1080/09670262.2012.750687

Collos, Y., and Harrison, P. J. (2014). Acclimation and toxicity of high ammonium concentrations to unicellular algae. *Mar. Pollut. Bull.* 80, 8–23. doi: 10.1016/j.marpolbul.2014.01.006

Collos, Y., and Slawyk, G. (2008). 13C and 15N uptake by marine phytoplankton. I. Iinfluence of nitrogen source and concentration in laboratory cultures of diatoms. *J. Phycol.* 15, 186–190. doi: 10.1111/j.1529-8817.1979.tb02983.x

Converti, A., Scapazzoni, A. S., Lodi, A. A., and Carvalho, J. C. M. (2006). Ammonium and urea removal by *Spirulina platensis*. 33, 8–16. doi: 10.1007/s10295-005-0025-8

Cullen, J. J., and Davis, R. F. (2003). The blank can make a big difference in oceanographic measurements. *Limnol. Oceanogr. Bull.* 12, 29–35. doi: 10.1002/lob.200312229

Dai, G., Deblois, C., Liu, S., Juneau, P., and Qiu, B. (2008). Differential sensitivity of five cyanobacterial strains to ammonium toxicity and its inhibitory mechanism on the photosynthesis of rice-field cyanobacterium Ge–Xian–Mi (*Nostoc*). *Aquat. Toxicol.* 89, 113–121. doi: 10.1016/j.aquatox.2008.06.007

Das, P., Thaher, M. I., Hakim, M. A. Q. M. A., Al-Jabri, H. M. S. J., and Alghasal, G. S. H. S. (2016). A comparative study of the growth of *Tetraselmis* sp. in large scale fixed depth and decreasing depth raceway ponds. *Bioresour. Technol.* 216, 114–120. doi: 10.1016/j.biortech.2016.05.058

Di Lena, G., Casini, I., Lucarini, M., and Lombardi-Boccia, G. (2019). Carotenoid profiling of five microalgae species from large-scale production. *Food Res. Int.* 120, 810–818. doi: 10.1016/J.FOODRES.2018.11.043

Ding, G. T., Mohd Yasin, N. H., Takriff, M. S., Kamarudin, K. F., Salihon, J., Yaakob, Z., et al. (2020). Phycoremediation of palm oil mill effluent (POME) and CO_2 fixation by locally isolated microalgae: *Chlorella sorokiniana* UKM2, *Coelastrella* sp. UKM4 and *Chlorella pyrenoidosa* UKM7. *J. Water Process Eng.* 35:101202. doi: 10.1016/j.jwpe.2020.101202

Dittmann, K. K., Rasmussen, B. B., Melchiorsen, J., Sonnenschein, E. C., Gram, L., and Bentzon-Tilia, M. (2020). Changes in the microbiome of mariculture feed organisms after treatment with a potentially probiotic strain of *Phaeobacter inhibens*. *Appl. Environ. Microbiol.* 86:20. doi: 10.1128/aem.00499-20

Dortch, Q. (1990). The interaction between ammonium and nitrate uptake in phytoplankton. *Mar. Ecol. Prog. Ser.* 61, 183–201. doi: 10.3354/meps061183

Drath, M., Kloft, N., Batschauer, A., Marin, K., Novak, J., and Forchhammer, K. (2008). Ammonia triggers photodamage of photosystem II in the cyanobacterium *Synechocystis* sp. strain PCC 6803. *Plant Physiol.* 147, 206–215. doi: 10.1104/pp.108.117218

Fan, H., Wang, K., Wang, C., Yu, F., He, X., Ma, J., et al. (2020). A comparative study on growth characters and nutrients removal from wastewater by two microalgae under optimized light regimes. *Environ. Technol. Innov.* 19:100849. doi: 10.1016/j.eti.2020.100849

Farahin, A. W., Yusoff, F. M., Basri, M., Nagao, N., and Shariff, M. (2019). Use of microalgae: *Tetraselmis tetrathele* extract in formulation of nanoemulsions for cosmeceutical application. *J. Appl. Phycol.* 31, 1743–1752. doi: 10.1007/s10811-018-1694-9

Feng, P., Xu, Z., Qin, L., Asraful Alam, M., Wang, Z., and Zhu, S. (2020). Effects of different nitrogen sources and light paths of flat plate photobioreactors on the growth and lipid accumulation of *Chlorella* sp. GN1 outdoors. *Bioresour. Technol.* 301:122762. doi: 10.1016/j.biortech.2020.122762

Geel, C., Versluis, W., and Snel, J. F. H. (1997). Estimation of oxygen evolution by marine phytoplankton from measurement of the efficiency of photosystem II electron flow. *Photosynth. Res.* 51, 61–70. doi: 10.1023/A:1005779112140

Gorai, T., Katayama, T., Obata, M., Murata, A., and Taguchi, S. (2014). Low blue light enhances growth rate, light absorption, and photosynthetic characteristics of four marine phytoplankton species. *J. Exp. Mar. Bio. Ecol.* 459, 87–95. doi: 10.1016/J.JEMBE.2014.05.013

Goto, M., Nagao, N., Yusoff, F. M., Kamarudin, M. S., Katayama, T., Kurosawa, N., et al. (2018). High ammonia tolerance on growth rate of marine microalga *Chlorella vulgaris*. *J. Environ. Biol.* 39, 843–848. doi: 10.22438/jeb/39/5(SI)/4

Grobbelaar, J. U. (2007). "Inorganic algal nutrition–mineral nutrition," in *Handbook of Microalgal Culture*, eds R. Amos and H. Qiang (Oxford: Blackwell Publishing Ltd.), 95–115. doi: 10.1002/9780470995280.ch6

Grotkjær, T., Bentzon-Tilia, M., D'Alvise, P., Dierckens, K., Bossier, P., and Gram, L. (2016). Phaeobacter inhibens as probiotic bacteria in non-axenic Artemia and algae cultures. *Aquaculture* 462, 64–69. doi: 10.1016/j.aquaculture.2016.05.001

Guillard, R. R. L. (1975). "Culture of phytoplankton for feeding marine invertebrates," in *Culture of Marine Invertebrate Animals*, eds W. Smith and M. Chanley (New York, NY: Plenum Press), 26–60.

Guillard, R. R. L., and Ryther, J. H. (1962). Studies of marine planktonic diatoms. I. *Cyclotella nana* Hustedt, and *Detonula confervacea* (cleve) Gran. *Can. J. Microbiol.* 8,229–239. doi: 10.1139/m62-029

Hargreaves, J., and Tucker, C. (2004). *Ammonia Dynamics in Fish Ponds*. Available at: https://sci-hub.si/https://agrilifecdn.tamu.edu/fisheries2/files/2013/09/SRAC-Publication-No.-4603-Managing-Ammonia-in-Fish-Ponds.pdf (accessed August 18, 2020).

Jiang, L., Pei, H., Hu, W., Hou, Q., Han, F., and Nie, C. (2016). Biomass production and nutrient assimilation by a novel microalga, *Monoraphidium* spp. SDEC-17, cultivated in a high-ammonia wastewater. *Energy Convers. Manag.* 123, 423–430. doi: 10.1016/j.enconman.2016.06.060

Katayama, T., Nagao, N., Kasan, N. A., Khatoon, H., Rahman, N. A., Takahashi, K., et al. (2020). Bioprospecting of indigenous marine microalgae with ammonium tolerance from aquaculture ponds for microalgae cultivation with ammonium-rich wastewaters. *J. Biotechnol.* 323, 113–120. doi: 10.1016/j.jbiotec.2020.08.001

Khoo, K. H., Culberson, C. H., and Bates, R. G. (1977). Thermodynamics of the dissociation of ammonium ion in seawater from 5 to 40°C. *J. Sol. Chem.* 6, 281–290. doi: 10.1007/BF00645459

Kim, G., Bae, J., and Lee, K. (2016). Nitrate repletion strategy for enhancing lipid production from marine microalga *Tetraselmis* sp. *Bioresour. Technol.* 205, 274–279. doi: 10.1016/j.biortech.2016.01.045

Krishna Reddy, Y. V., Adamala, S., Levlin, E. K., and Reddy, K. S. (2017). Enhancing nitrogen removal efficiency of domestic wastewater through increased total efficiency in sewage treatment (ITEST) pilot plant in cold climatic regions of Baltic Sea. *Int. J. Sustain. Built Environ.* 6, 351–358. doi: 10.1016/j.ijsbe.2017.05.002

Lee, S. Y., Kim, S. H., Hyun, S. H., Suh, H. W., Hong, S. J., Cho, B. K., et al. (2014). Fatty acids and global metabolites profiling of *Dunaliella tertiolecta* by shifting culture conditions to nitrate deficiency and high light at different growth phases. *Process Biochem.* 49, 996–1004. doi: 10.1016/j.procbio.2014.02.022

Leong, W. H., Lim, J. W., Lam, M. K., Uemura, Y., Ho, C. D., and Ho, Y. C. (2018). Co-cultivation of activated sludge and microalgae for the simultaneous enhancements of nitrogen-rich wastewater bioremediation and lipid production. *J. Taiwan Inst. Chem. Eng.* 87, 216–224. doi: 10.1016/j.jtice.2018.03.038

Levasseur, W., Perré, P., and Pozzobon, V. (2020). A review of high value-added molecules production by microalgae in light of the classification. *Biotechnol. Adv.* 41:107545. doi: 10.1016/j.biotechadv.2020.107545

Lu, L., Wang, J., Yang, G., Zhu, B., and Pan, K. (2017). Heterotrophic growth and nutrient productivities of *Tetraselmis chuii* using glucose as a carbon source under different C/N ratios. *J. Appl. Phycol.* 29, 15–21. doi: 10.1007/s10811-016-0919-z

Magnotti, C., Lopes, R., Derner, R., and Vinatea, L. (2016). Using residual water from a marine shrimp farming BFT system. Part II: artemia franciscana biomass production fed microalgae grown in reused BFT water. *Aquac. Res.* 47, 2716–2722. doi: 10.1111/are.12720

Markou, G., Vandamme, D., and Muylaert, K. (2014). Ammonia inhibition on *Arthrospira platensis* in relation to the initial biomass density and pH. *Bioresour. Technol.* 166, 259–265. doi: 10.1016/J.BIORTECH.2014.05.040

Masojídek, J., Torzillo, G., Kopecký, J., KoblížEk, M., Nidiaci, L., Komenda, J., et al. (2000). Changes in chlorophyll fluorescence quenching and pigment composition in the green alga *Chlorococcum* sp. grown under nitrogen deficiency and salinity stress. *J. Appl. Phycol.* 12, 417–426. doi: 10.1023/A:1008165900780

Nayak, M., Suh, W. I., Chang, Y. K., and Lee, B. (2019). Exploration of two-stage cultivation strategies using nitrogen starvation to maximize the lipid productivity in *Chlorella* sp. HS2. *Bioresour. Technol.* 276, 110–118. doi: 10.1016/j.biortech.2018.12.111

Nobel, P. S. (ed.). (2009). "Photochemistry of photosynthesis," in *Physicochemical Environmental Plant Physiology* (Amsterdam: Academic Press), 228–275. doi: 10.1016/B978-0-12-374143-1.00005-3

Obata, M., Toda, T., and Taguchi, S. (2009). Using chlorophyll fluorescence to monitor yields of microalgal production. *J. Appl. Phycol.* 21, 315–319. doi: 10.1007/s10811-008-9369-6

Otero, A., and Fábregas, J. (1997). Changes in the nutrient composition of *Tetraselmis suecica* cultured semicontinuously with different nutrient concentrations and renewal rates. *Aquaculture* 159, 111–123. doi: 10.1016/S0044-8486(97)00214-7

Paliwal, C., Mitra, M., Bhayani, K., Bharadwaj, S. V. V., Ghosh, T., Dubey, S., et al. (2017). Abiotic stresses as tools for metabolites in microalgae. *Bioresour. Technol.* 244, 1216–1226. doi: 10.1016/J.BIORTECH.2017.05.058

Piorreck, M., Baasch, K. H., and Pohl, P. (1984). Biomass production, total protein, chlorophylls, lipids and fatty acids of freshwater green and blue-green algae under different nitrogen regimes. *Phytochemistry* 23, 207–216. doi: 10.1016/S0031-9422(00)80304-0

Rahman, K. M. (2020). "Food and High Value Products from Microalgae: Market Opportunities and Challenges," in *Microalgae Biotechnology for Food, Health and High Value Products*, eds M. A. Alam, J. L. Xu, and Z. Wang (Singapore: Springer), 3–27. doi: 10.1007/978-981-15-0169-2_1

Ramanna, L., Guldhe, A., Rawat, I., and Bux, F. (2014). The optimization of biomass and lipid yields of *Chlorella sorokiniana* when using wastewater supplemented with different nitrogen sources. *Bioresour. Technol.* 168, 127–135. doi: 10.1016/j.biortech.2014.03.064

Ramos, A., Coesel, S., Marques, A., Rodrigues, M., Baumgartner, A., Noronha, J., et al. (2008). Isolation and characterization of a stress-inducible *Dunaliella salina* Lcy-β gene encoding a functional lycopene β-cyclase. *Appl. Microbiol. Biotechnol.* 79, 819–828. doi: 10.1007/s00253-008-1492-4

Raven, J. A., Wollenweber, B., and Handley, L. L. (1992). A comparison of ammonium and nitrate as nitrogen sources for photolithotrophs. *New Phytol.* 121, 19–32. doi: 10.1111/j.1469-8137.1992.tb01088.x

Schreiber, U., Schliwa, U., and Bilger, W. (1986). Continuous recording of photochemical and non-photochemical chlorophyll fluorescence quenching with a new type of modulation fluorometer. *Photosynth. Res.* 10, 51–62. doi: 10.1007/BF00024185

Schüler, L. M., Santos, T., Pereira, H., Duarte, P., Katkam, N. G., Florindo, C., et al. (2020). Improved production of lutein and β-carotene by thermal and light intensity upshifts in the marine microalga *Tetraselmis* sp. CTP4. *Algal Res.* 45:101732. doi: 10.1016/j.algal.2019.101732

Shi, X. M., Zhang, X. W., and Chen, F. (2000). Heterotrophic production of biomass and lutein by *Chlorella protothecoides* on various nitrogen sources. *Enzyme Microb. Technol.* 27, 312–318. doi: 10.1016/S0141-0229(00)00208-8

Stephenson, A. L., Dennis, J. S., Howe, C. J., Scott, S. A., and Smith, A. G. (2010). Influence of nitrogen-limitation regime on the production by *Chlorella vulgaris* of lipids for biodiesel feedstocks. *Biofuels* 1, 47–58. doi: 10.4155/bfs.09.1

Tam, N. F. Y., and Wong, Y. S. (1996). Effect of ammonia concentrations on growth of *Chlorella vulgaris* and nitrogen removal from media. *Bioresour. Technol.* 57, 45–50. doi: 10.1016/0960-8524(96)00045-4

Tsai, H. P., Chuang, L. Te, and Chen, C. N. N. (2016). Production of long chain omega-3 fatty acids and carotenoids in tropical areas by a new heat-tolerant microalga *Tetraselmis* sp. DS3. *Food Chem.* 192, 682–690. doi: 10.1016/j.foodchem.2015.07.071

Vonshak, A., and Torzillo, G. (2004). "Environmental stress physiology," in *Handbook of Microalgal Culture: Biotechnology and Applied Phycology*, ed A. Richmond (Carlton, VIC: Blackwell Science), 57–82.

Wang, J., Zhou, W., Chen, H., Zhan, J., He, C., and Wang, Q. (2019). Ammonium nitrogen tolerant *Chlorella* strain screening and its damaging effects on photosynthesis. *Front. Microbiol.* 9:3250. doi: 10.3389/fmicb.2018.03250

Zhuang, L. L., Azimi, Y., Yu, D., Wu, Y. H., and Hu, H. Y. (2018). Effects of nitrogen and phosphorus concentrations on the growth of microalgae Scenedesmus. LX1 in suspended-solid phase photobioreactors (ssPBR). *Biomass Bioenergy* 109, 47–53. doi: 10.1016/j.biombioe.2017.12.017

Conflict of Interest: NN was employed by the company Bluescientific Shinkamigoto Co. Ltd.

The remaining authors declare that the research was conducted in the absence of any commercial or financial relationships that could be construed as a potential conflict of interest.

Advantages of publishing in Frontiers

OPEN ACCESS
Articles are free to read for greatest visibility and readership

FAST PUBLICATION
Around 90 days from submission to decision

HIGH QUALITY PEER-REVIEW
Rigorous, collaborative, and constructive peer-review

TRANSPARENT PEER-REVIEW
Editors and reviewers acknowledged by name on published articles

Frontiers
Avenue du Tribunal-Fédéral 34
1005 Lausanne | Switzerland

Visit us: www.frontiersin.org
Contact us: frontiersin.org/about/contact

REPRODUCIBILITY OF RESEARCH
Support open data and methods to enhance research reproducibility

DIGITAL PUBLISHING
Articles designed for optimal readership across devices

FOLLOW US
@frontiersin

IMPACT METRICS
Advanced article metrics track visibility across digital media

EXTENSIVE PROMOTION
Marketing and promotion of impactful research

LOOP RESEARCH NETWORK
Our network increases your article's readership